

Logistics Engineering Institution, CMES

Proceedings of China Modern Logistics Engineering

Inheritance, Wisdom, Innovation and
Cooperation

Lecture Notes in Electrical Engineering

Volume 286

Board of Series editors

Leopoldo Angrisani, Napoli, Italy
Marco Arteaga, Coyoacán, México
Samarjit Chakraborty, München, Germany
Jiming Chen, Hangzhou, P.R. China
Tan Kay Chen, Singapore, Singapore
Rüdiger Dillmann, Karlsruhe, Germany
Haibin Duan, Beijing, China
Gianluigi Ferrari, Parma, Italy
Manuel Ferre, Madrid, Spain
Sandra Hirche, München, Germany
Faryar Jabbari, Irvine, USA
Janusz Kacprzyk, Warsaw, Poland
Alaa Khamis, New Cairo City, Egypt
Torsten Kroeger, Stanford, USA
Tan Cher Ming, Singapore, Singapore
Wolfgang Minker, Ulm, Germany
Pradeep Misra, Dayton, USA
Sebastian Möller, Berlin, Germany
Subhas Mukhopadhyay, Palmerston, New Zealand
Cun-Zheng Ning, Tempe, USA
Toyoaki Nishida, Sakyo-ku, Japan
Federica Pascucci, Roma, Italy
Tariq Samad, Minneapolis, USA
Gan Woon Seng, Nanyang Avenue, Singapore
Germano Veiga, Porto, Portugal
Haitao Wu, Beijing, China
Junjie James Zhang, Charlotte, USA

About this Series

“Lecture Notes in Electrical Engineering (LNEE)” is a book series which reports the latest research and developments in Electrical Engineering, namely:

- Communication, Networks, and Information Theory
- Computer Engineering
- Signal, Image, Speech and Information Processing
- Circuits and Systems
- Bioengineering

LNEE publishes authored monographs and contributed volumes which present cutting edge research information as well as new perspectives on classical fields, while maintaining Springer’s high standards of academic excellence. Also considered for publication are lecture materials, proceedings, and other related materials of exceptionally high quality and interest. The subject matter should be original and timely, reporting the latest research and developments in all areas of electrical engineering.

The audience for the books in LNEE consists of advanced level students, researchers, and industry professionals working at the forefront of their fields. Much like Springer’s other Lecture Notes series, LNEE will be distributed through Springer’s print and electronic publishing channels.

More information about this series at <http://www.springer.com/series/7818>

Logistics Engineering Institution, CMES
Editor

Proceedings of China Modern Logistics Engineering

Inheritance, Wisdom, Innovation
and Cooperation

Editor
Logistics Engineering Institution, CMES
Beijing
China

ISSN 1876-1100 ISSN 1876-1119 (electronic)
ISBN 978-3-662-44673-7 ISBN 978-3-662-44674-4 (eBook)
DOI 10.1007/978-3-662-44674-4

Library of Congress Control Number: 2014948758

Springer Heidelberg New York Dordrecht London

© Springer-Verlag Berlin Heidelberg 2015

This work is subject to copyright. All rights are reserved by the Publisher, whether the whole or part of the material is concerned, specifically the rights of translation, reprinting, reuse of illustrations, recitation, broadcasting, reproduction on microfilms or in any other physical way, and transmission or information storage and retrieval, electronic adaptation, computer software, or by similar or dissimilar methodology now known or hereafter developed. Exempted from this legal reservation are brief excerpts in connection with reviews or scholarly analysis or material supplied specifically for the purpose of being entered and executed on a computer system, for exclusive use by the purchaser of the work. Duplication of this publication or parts thereof is permitted only under the provisions of the Copyright Law of the Publisher's location, in its current version, and permission for use must always be obtained from Springer. Permissions for use may be obtained through RightsLink at the Copyright Clearance Center. Violations are liable to prosecution under the respective Copyright Law. The use of general descriptive names, registered names, trademarks, service marks, etc. in this publication does not imply, even in the absence of a specific statement, that such names are exempt from the relevant protective laws and regulations and therefore free for general use.

While the advice and information in this book are believed to be true and accurate at the date of publication, neither the authors nor the editors nor the publisher can accept any legal responsibility for any errors or omissions that may be made. The publisher makes no warranty, express or implied, with respect to the material contained herein.

Printed on acid-free paper

Springer is part of Springer Science+Business Media (www.springer.com)

Foreword

With the rapid development of Chinese economy and economic globalization, China's logistics industry has connected to the international market at great speed, logistics engineering has made remarkable development, and logistics technology and equipment market have kept growing.

Logistics engineering is an integrated multidisciplinary technology; the technological progress of logistics engineering has undoubtedly promoted the development of modern logistics greatly. In recent years, the Chinese government's enhanced policy of support to the logistics industry, and the activeness of the logistics market has greatly promoted the rapid development of logistics engineering.

Proceedings of China Modern Logistics Engineering was edited by Logistics Engineering Institution, CMES, which collected 44 thesis covering enterprise logistics, logistics systems and management, logistics warehousing and distribution technology and management, lifting machinery technology, conveying machinery technology, and other fields; it reflects the latest research achievement of China's logistics engineering.

This book can serve as a reference book for teachers, graduate students, and undergraduate students from college/university of logistics management, logistics engineering, transportation, business administration, e-commerce, and industrial engineering. The book can also be used as a reference book for logistics professionals, including scholars, researchers from colleges, and technical personnel of enterprises.

Conference Program Committee

Chairs

Mr. Daming Lu

President, Logistics Engineering institution, CMES
Dean, Beijing Materials Handling Research Institute

Mr. Qifan Bao

Vice President, Logistics Engineering institution, CMES

Prof. Guohua Wang

University of Science and Technology Beijing

Prof. Kenneth C. Williams

University of Newcastle, Australia

Members

Prof. Yuqing Guo

Wuhan University of Science and Technology

Prof. Dexin Tao

Wuhan University of Technology

Prof. Weigang Song

Northeastern University

Prof. Changsheng Liu

Central South University of Forestry and Technology

Prof. Linjing Xiao

Shandong University of Science and Technology

Prof. Nianli Lu

Harbin Institute of Technology

Prof. Qicai Zhou

Tongji University

Prof. Shunde Gao

Dalia University of Technology

Prof. Haim Kalman

Ben-Gurion University of the Negey

Prof. V.K. Agarwal

Indian Institute of Technology Industrial Tribology, ITMMEC

Mr. Heqian Yu

Senior Engineer, Beijing Materials Handling Research Institute

Mr. Gening Xu

Doctor/Vice Dean, Taiyuan University of Science and Technology

Mr. Wenjun Meng

Doctor/Dean, Taiyuan University of Science and Technology

Mr. Jianguo Zhang

General manager, Shanghai Zhenhua Heavy Industries Co., Ltd.

Mr. Renhu Pan

Doctor/Vice President, Fujian Longking Co., Ltd.

Mr. Fusheng Qiu

General manager, Shanghai Logiwis Engineering Co., Ltd.

Mr. Deyuan Fu

Senior Engineer, Beijing Materials Handling Research Institute

Mr. Qingmin Qi

Vice Dean, Beijing Materials Handling Research Institute

Mr. Yaping Zheng

Director, Logistics Engineering institution, CMES

Contents

Part I Logistics Systems and Management Research (LSMR)

1	Research on Distribution Center Logistics Equipment Risk Management	3
	Qicai Zhou, Xiaolei Xiong and Hang Fang	
2	Research on Logistics Center Layout Based on SLP	17
	Yannan Liu and Qilan Zhao	
3	System Dynamics Modeling and Simulation of Two-Stage Remanufacturing Reverse Supply Chain	29
	Yiwei Mo, Liwei Li and Wei Huang	
4	Research and Demonstration of Dynamic Intelligent Logistics System of the Collection and Transportation Process of Giant Municipal Garbage	39
	Shuang Xu, Guangming Li, Haitao Ou and Wenqing Wu	
5	Research on the Stairs Evacuation with Fluid Wave Theory	51
	Xun Weng, Zhiyuan Su, Wenshuo Liu and Qianqing Xu	
6	An Approach to Integrated Cellular Layout Design Based on Logistics Cost Optimization	61
	Yongqian Zheng, Kuixue Ding and Kefeng Cen	
7	The Inventory Demand Forecasting Model of the Regional Logistics Network in Supply Chain	73
	An-Quan Zou and Ren-Cun Huang	

8	Research on Logistics Marketing Based on Local Characteristic Economy Industrial Cluster	85
	Xiaoyuan Shi	
9	Based on AHP and Cluster Analysis for Classification Method of Emergency Supplies	95
	Zhiyuan Su, Xun Weng and Lei Zhang	
10	Green Supply Chain Management System of Modern Enterprise Construction Strategy	105
	Xiaoyuan Shi	
11	Based on FCM Disaster Area Management at Different Levels	115
	Chaowei Zheng, Xun Weng, Zhiyuan Su and Zhijun Zhuang	
12	Life Cycle Inventory of Multi-mode Transport System for Designing Green Logistics	125
	Lu Li and Suiran Yu	
 Part II Lifting Machinery Technology Research (LMTR)		
13	Dynamic Reliability of the Weight Index Model Research of Residual Fatigue Life of the Crane Boom	137
	Fuhai Cai, Fuling Zhao, Xin Wang, Shunde Gao and Liming Chen	
14	Study of the Opening Angle Influence of Y-shaped Guying System on the Buckling Stability of Telescopic Boom Crane	155
	Li Chen, Rumin Teng, Yahui Zheng, Haibo Chi, Wei Xu and Na Hou	
15	Design of New Hydraulic Pushing Device	165
	Qicai Zhou, Jiong Zhao, Xiaolei Xiong and Haiyan He	
16	The Improvement of Running Condition on the Crane with the Wheel Flange	173
	Jigui Kuang, Dabao Liu, Xuequan Xiao and Hao Wu	
17	Lightweight Design for the Combinatorial Jib	179
	Jiong Zhao, Qicai Zhou, Wenjun Li and Zailei Zhou	
18	Research on the Overload Protection System of Knuckle Boom Crane	189
	Kun Song, Yaofeng Xue, Lei Xu and Bo Zhang	

19 Research on Energy Consumption of Variable Frequency Control for Portal or Overhead Crane. 199
 Lili Ma and Wenming Cheng

20 User-Oriented and Visualized Optimization for Crane Design. 209
 Yuanfang Tao and Chaofei Hong

21 Design of the Special Spreader of Super-Tonnage Crane 217
 Jiong Zhao, Xiaolei Xiong, Wenjun Li and Yujun Hu

22 Research of Crane Parametric Collaborative Design Platform 229
 Zongyan Wang, Fen Yang, Jian Zhao, Jian Li and Rongbin Zhai

23 Mechanical Performance of Crane’s Main Girders with Corrugated Webs 243
 Guo-qian Wei, Hai-tao Dong, Yue Li and Qin Fan

24 The Electric Control Scheme of 2500t Ring Crane 255
 Xiaolei Xiong, Jiong Zhao, Qicai Zhou and Li Zeng

Part III Logistics Warehousing and Distribution Technology Management (LWDT)

25 Research on Picking Route Optimization for One Stacker in Multiple Aisles Automated Storage and Retrieval System 265
 Ailan Feng, Zhanzhen Di and Wenying Ding

26 A Cellular Ant Algorithm-Based Method for Solving Stereo Warehouse Slotting Optimization Problem 273
 Meng Jin, Xihui Mu, Fengpo Du and Lei Luo

27 Research on Process Optimization of Automated Warehouse 283
 Wei Yang, Dan Li, Chen Yan and Yuxiao Du

28 Research and Implementation of Condition-Based Maintenance System for Stack Crane in Automatic Storage and Retrieval System 291
 Sixia Fan, Qicai Zhou, Jiong Zhao and Xiaolei Xiong

Part IV Conveying Machinery Technology Research (CMTR)

29 The Research of Integrated Supply Chain Model Rested on Joint Ordering 303
Wenxue Ran and Yang Yu

30 The Necessity of Construction of the Three Gorges Emergency Logistics Base and Its Measures 313
Juan Wang, Weijun He and Yasan Fu

31 Resistance Analysis for Bulk Materials in the Vertical Section of Pipe Scraper Conveyor 327
Yanping Yao, Wenjun Meng, Ziming Kou and Zhicheng Liao

32 Material Uninterrupted Feeding Technology and Feeding Speed Control Research of Large Electroslag Remelting Furnace 337
C.Z. Wang and J.C. Song

33 Structure Weight Reduction of Ship Unloader Based on the Orthogonal Experiment Method 347
Suiran Yu, Jingxing Qian and Jianguo Zhang

Part V Enterprise Logistics (EL)

34 Given Target Position Path Planning of Concrete Pump Vehicle 361
Xin Wang, Hui Jin, Xuyang Cao, Shunde Gao and Shujun Ming

35 A New Hybrid Topology Optimization Method Coupling ESO and SIMP Method 373
Hongyu Jiao, Qicai Zhou, Sixia Fan and Ying Li

36 An Integrated Conceptual Design Calculation Method for Logistics Machinery Based on Working Condition and Load Combination 385
Zhiyi Pan, Shunde Gao, Xin Wang and Xuyang Cao

37 Improved Heuristic Procedure for Mixed-Model U-line Balancing Problem with Fuzzy Times 395
Zeqiang Zhang and Wenming Cheng

38 Research and Building of Database Model of Logistics Business Platform 407
Li Li, Gaoyuan Meng, Xiaoping Liao and Wengui Su

39 Research on Multi-service Demand Path Planning Based on Continuous Hopfield Neural Network 417
Yitong Zhang and Gang Zhao

40 A Graded Optimization-Based Approach to Remanufacturing Production Decision 431
Yiwei Mo, Zhili Huang and Wei Huang

41 Research About Slider Nonlinear Contact Analysis of the Telescopic Boom with Cylinder Supporting 441
Shilin Shen, Zhongpeng Zhang and Bin Gu

42 Research on Automatic Layout Planning and Performance Analysis System of Production Line Based on Simulation 455
Lv Chao, Liu Shuang, Shiming Wang and bei Cai

43 Optimization Study Based on Lean Logistics in Manufacturing Enterprises 463
Xiaoyan Wang

44 Power Assembly and Monitoring Management System of Lithium Ion Battery in Mine 473
Zhihao Yu, Chuanyu Sun, Jiancheng Fang and Linjing Xiao

About the Editors

Mr. Daming Lu

President, Logistics Engineering institution, CMES
Dean, Beijing Materials Handling Research Institute

Personal Profile

Since the early 1980s, Daming Lu mainly engaged in the development of material handling equipment and logistics systems for automatic control research, and started to focus on large logistics system planning since the 1990s. He has successfully hosted more than 10 large logistics system and distribution center projects, and won many awards, such as: the third prize for progress of National Science and Technology, first prize for progress of China Machinery Industry Science and Technology, second prize for progress of Beijing Science and Technology, and so on.

Main Works

1. “The Application of Automated High-rise Warehouse in Light Sensitive Substance Industry” ISBN 7-111-04388-X/TH.
2. “The status and development of our material handling technology and equipment” Published in: (Journal of Modern manufacturing).
3. “Bulk handling system in Cargo Department of Air China” Published in: (Journal of Logistics & Material Handling).

e-mail: ludaming118@vip.sina.com

Phone: 0086-10-64031452

Prof. Wang Guohua

Beijing University of Science and Technology

Personal Profile

Professor Wang Guohua is a famous Chinese logistics expert, who began to engage in the Chinese logistics industry education, publicity, development and research work since the late 1970s, mainly related to “logistics management”, “manufacturing logistics,” “supply chain management” and other aspects of the research. He presided over and carried out more than 30 Chinese key projects and enterprises on logistics projects, and received a number of scientific and technological progress awards. He has published 80 dissertations, was chief editor in participation compilation discussing many state-level, bureau-level scientific research topics, and also responsible for participates.

Main Works

1. “Supply Chain Management of Coal Enterprises and its Performance Evaluation” Published in: (Journal of Logistics & Material Handling)
2. “Logistics Engineering and technological innovation”
Published in: (Journal of Shandong University of Sciences and Technology), Volume 24, 2005
3. “Based on the three-phase simulation method AS/RS logistics system planning”
Published in: (Journal of University of Science and Technology Beijing), Volume 29, 2007
4. “Vehicle distribution system in the LNG supply”
Published in: (Journal of Logistics Technology), Volume 10, 2008

e-mail: bkdwgh@263.net

Phone: 0086-10-62332121

Part I
Logistics Systems and Management
Research (LSMR)

Chapter 1

Research on Distribution Center Logistics Equipment Risk Management

Qicai Zhou, Xiaolei Xiong and Hang Fang

Abstract In view of the problem of the operational risk on distribution center, a technical framework of logistics equipments that adapted to the risk-based maintenance decision making is proposed. The frame includes three modules: risk analysis, risk evaluation, and risk control. The reliability of equipment and consequence of malfunction are considered. The risk is quantitatively analyzed, by which maintenance strategy is built for decision objective, so that we can build the management system of logistics equipment. An instance is taken to explain how to use the risk-based maintenance decision technique to logistics equipment.

Keywords Risk-based maintenance · Risk evaluation · Logistics equipments · Risk management · Fault tree

1.1 Introduction

Since the development of distribution center in the early 1990s in China, there has been extensive application of distribution center. In recent years, along with the utilization of novel technologies, such as logistics information technology, networked objects, and radio frequency identification in logistics, distribution center has been widely used in food, clothing, medicine, tobacco, motorcar, retail, railway, electronics and electrical, chemical industries, etc.

However, with the considerable application of distribution center, accidents happen occasionally during the usage of distribution center and the equipment maintenance and management tasks we are confronted with become more prominent day by day. The whole process that distribution center from accepting goods provided by the suppliers, taking a series of processes such as storage, safekeeping,

Q. Zhou · X. Xiong · H. Fang (✉)
College of Mechanical Engineering, Tongji University, Cao'an Road,
Shanghai 201804, China
e-mail: fanghang716@163.com

sorting, circulation processing and information processing, and so on, and delivering to the particular customers require the participation of lots of modern logistics equipment.

Modern logistics distribution center general is equipped with highly automated and intelligent automatic storage retrieval system (AS/RS). AS/RS is a new type of storage system that features a complicated system configuration, which consists of multitudinous subsystems and components. The operation of AS/RS not only requires enormous capital investment and high operating cost, but also needs constant updates and maintenance after being put into use. Thus, the cost of equipment maintenance accounts for a large proportion in the total cost of enterprise operation. The stacker crane, as the core component of AS/RS, is composed of a great number of mechanical devices and electrical control components and has the important functions of cargo lifting, handling, and access. The operation process of stacker cranes may be affected by many factors such as environment, operation, and maintenance; hence, equipment failures feature uncertainty and fuzziness. Once a system failure happens, it is difficult to identify the source of failure in time, which can greatly affect the normal operation of AS/RS as a whole and in severe situations may cause the breakdown of the entire distribution center. Hence, it is urgent to build up a feasible and economical maintaining strategy to strengthen equipment maintenance management and thus to reduce the probability of malfunction and improve the reliability and stability of AS/RS.

Although risk-based maintenance (RBM) method is a new research area and a trend of future development in the field of equipment maintenance management, but this study is developing quickly. At present, RBM has been successfully adopted in petrochemical plants, power plants, offshore facilities, etc., which can cut down enterprises' cost of maintenance and service by 15–40 % [1]. However, RBM is seldom used in logistics and has not yet formed the complete theoretical frame. The American Society of Mechanical Engineers has already begun to develop a risk evaluation and management model for logistics equipment.

The proposed risk-based maintenance method aims at reducing the operating system's overall risk of failure and optimizing the total life cycle cost. This paper first introduces a methodology of risk-based maintenance and then illustrates how to apply this method to the analysis of AS/RS's maintenance decision making.

1.2 Equipment Risk Management and Risk-Based Maintenance

1.2.1 Equipment Risk Management

A widely accepted definition of risk in the field of risk management is: the overall estimate of the probability of uncertain adverse events and the severity of possible loss. In the risk-based maintenance, risk can be expressed as

$$\text{Risk} = \text{Probability of failure} \times \text{Consequence of failure} \quad (1.1)$$

Risk exists during the equipment's entire life cycle. At different stages, risk types vary. Risk can be caused either by material properties or equipment attrition's influence on the system's reliability, potential unreasonable design or wrong manufacturing, and also improper installation or maintenance management.

On the basis of identifying potential risk, equipment risk management is a process of assessing both the probability of risk and the consequence of failure so as to measure the severity of the risk. Also, equipment risk management serves to judge whether the maintenance measure should be optimized or improved, which focus the attention and resources on the most significant maintenance activities and ensure the equipment's safe operation to the largest extent while helping the maintenance section to control the cost of maintenance within a reasonable range.

The operation of distribution center is affected by many inner and external factors and is full of uncertainty, especially in high-risk chemical industry. The objective of applying the risk-based approach to AS/RS is to conduct a qualitative or quantitative risk assessment of the uncertainty in the operational process so as to control risk scientifically.

1.2.2 Risk-Based Maintenance Methodology

Compared with traditional maintenance method, RBM is a maintenance theory based on risk identification and views risk assessment as its core component and the purpose of risk control as its pursuit. More than simply a maintenance strategy, RBM is an approach or a process to formulate the optimized maintenance strategy for the object of maintenance and is carried out in the maintenance decision-making process. The RBM methodology is broken down into three main modules.

1. Risk analysis, which consists of risk identification and estimation. Based on a comprehensive identification of the system's potential risk, equipment risk analysis is an analytical process integrating failure probability and its resulting consequence. Risk analysis is the most crucial part. This module comprises four steps:
 - (a) To fully identify risk events affecting the equipment's normal operation, the system is divided into subsystems or unit components to develop failure scenario according to operational characteristics of the system; physical conditions under which operation occur; geometry of the system, safety arrangement, etc. [2]. The analysis of failure scenarios is the fundamental of equipment risk management, which details a series of events that may lead to a system failure.

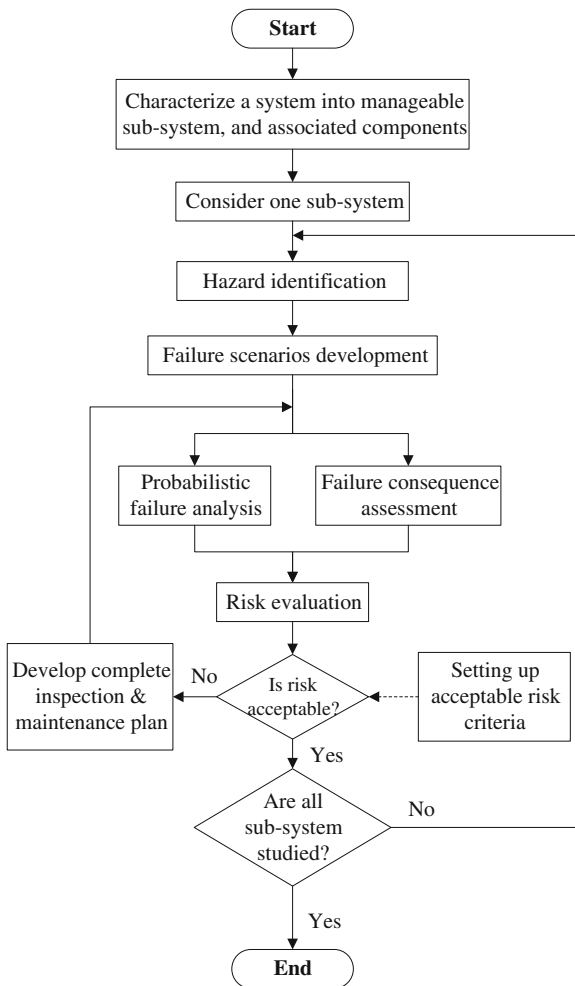
- (b) Fault tree analysis (FTA) [3] is used to establish the logical relationship between malfunctioning components and system failure. The minimum cutsets leading to the system failure can be accurately determined, which in turns helps calculate the probability of the system's ultimate failure.
 - (c) The consequence of the most probable failure scenarios is estimated. Failure consequence assessment includes system performance loss, financial loss, and human health loss. The worst-case consequence should be considered to obtain a relatively conservative result.
 - (d) Combine failure consequence and failure probability to approximate the risk of failure units, which may induce any system failure as well as the system's total risk.
2. Risk evaluation establishes the acceptance criteria of risk and evaluates the result of risk assessment so as to judge whether the estimated risk of the system or its subsystems exceeds the acceptable level. The evaluation provides a scientific foundation for making strict risk control measures. Risk evaluation plays an important role in bridging the identification of systemic risk and the formulation of reasonable risk control measures.
 3. Risk control focuses on systems or faulty units whose level of estimated risk exceeds the acceptance criteria and sets up corresponding maintenance strategies so as to reduce the total systemic risk. The processes of re-estimating and re-evaluating of risk are repeated until the total systemic risk can be kept below the acceptable level. The operational flow chart of RBM in equipment risk management is showed in Fig. 1.1.

The advantages of risk-based maintenance approach are as follows: The risk of all equipment can be identified and distinguished in the process of maintenance; unnecessary inspection and maintenance can be avoided to ensure the effectiveness maintenance activities.

1.3 Application of Risk-Based Maintenance in AS/RS

Automated storage and retrieval system is the principal part of distribution center and has a complicated system configuration. The stacker crane is the core component in AS/RS and has a higher probability and a greater variety of failures than any other component. Hence, the stacker crane becomes a part of relatively high risk in distribution center for its exceptional complexity and seriousness of failure consequence. This paper takes the laneway stacker crane as an example to expound the application of risk-based maintenance approach to equipment management in distribution center.

Fig. 1.1 Framework of RBM methodology



1.3.1 Risk Analysis

1.3.1.1 Failure Scenarios

The stacker crane is divided into mechanical execution system and electrical control system according to operational characteristics, the functional properties of components and control principles. The stacker crane achieves the inbound, outbound, and shift functions via handling, transferring and accessing operations; therefore, its mechanical execution system is subdivided into three mechanisms: a traveling mechanism, a lifting mechanism, and a telescoping fork mechanism. The traveling mechanism is mainly composed of subparts including motor (with brake), reducer,

traveling wheel, and track; the lifting mechanism consists of loading shelf, motor, transmission, brake, steel rope or chain, drum or sprocket, pulley and fall-proof machine, etc., and the telescoping fork mechanism is made up of fork, reducer, clutch, pinion and rack or chain and sprockets, etc. The stacker crane runs to the designated locations through the cooperation of the traveling mechanism and the lifting mechanism. And the cooperation of the telescoping fork mechanism and the lifting mechanism can achieved the functions of cargo deposit and withdrawal. Electrical control system comprises electric drive, control, signal detection, electro-safety protection, and other electrical equipment and is divided into two sub-mechanisms: the main circuit mechanism and the control mechanism. The main circuit mechanism consists of power supply, capacitor, frequency converter, contactor, electric transmission line, over flow protective apparatus, etc., and serves to provide strong electric drive for the above three mechanical mechanisms. The electrical control mechanism mainly performs functions such as automatic location identification, speed control, position detecting, telescoping direction and speed control of fork, etc. [4].

Faulted systems are distinguished according to the aforementioned five mechanisms, and combining with failure symptoms of the stacker crane [5], the most probable failure scenarios for each faulted system are listed as in Fig. 1.2. Finally, the most probable failure scenario is divided into several subfailure scenarios step by step until primary events as listed in Table 1.1.

1.3.1.2 Building Fault Tree

A fault tree with ‘stacker crane is not functioning normally’ as the top event first branches into ‘mechanical system fault’ and ‘electrical control system fault.’ Then, the node ‘mechanical system fault’ is further split into three branches: ‘traveling mechanism is not functioning properly,’ ‘lifting mechanism is not functioning properly,’ ‘telescoping fork mechanism is not functioning properly.’ Meanwhile, the mother node ‘electrical control system fault’ forks into two branches, ‘main circuit mechanism fault,’ and ‘control mechanism fault.’ Finally, the fault tree continues to develop from the bottom events described above until the primary events. The fault tree for ‘stacker crane is not functioning normally’ is shown in Fig. 1.3.

1.3.1.3 Finding of Minimum Cutsets and Optimization

To analyze the fault tree shown in Fig. 1.3, the Boolean algebra simplifying method is adopted to represent the system failures as a single or a combination of indispensable component failure; that is, all minimum cutsets are obtained through fault tree qualitative analysis. Minimum cutsets are all possible unique combinations of component failures that cause a system failure (top event). Therefore, the optimized minimum cutsets can be used to estimate the system’s probability of failure. In this

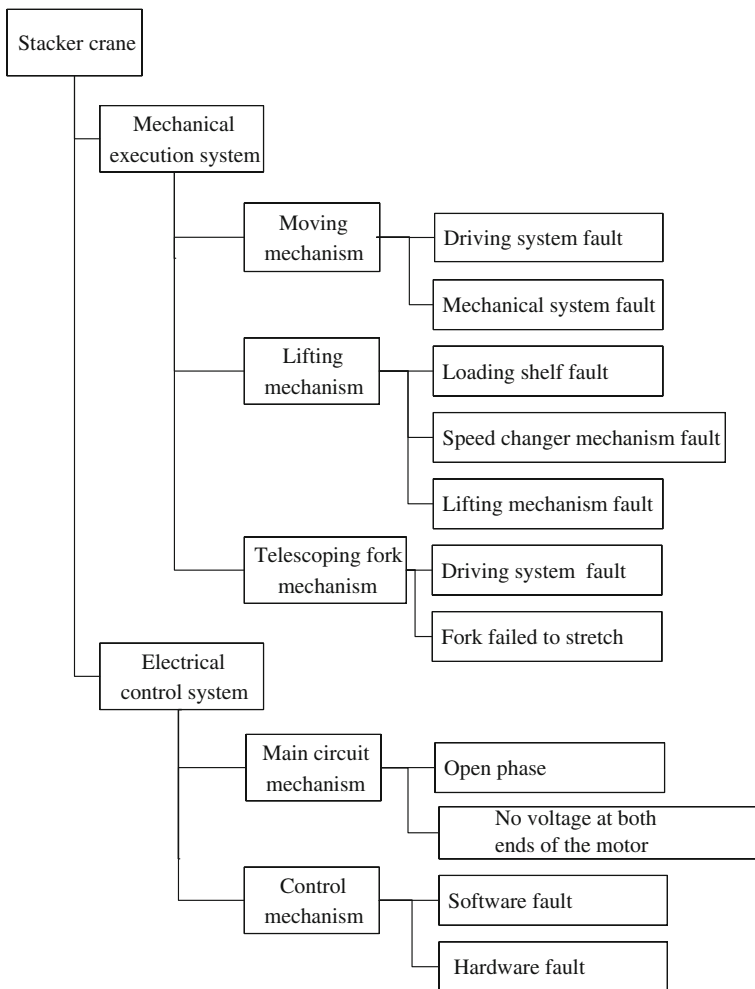


Fig. 1.2 Fault system of stacking crane

paper, the downlink method is adopted to calculate the minimum cutsets. According to Fig. 1.3, the minimum cutsets for ‘mechanical execution system fault’ are:

{X1}, {X2}, {X3}, {X4}, {X5}, {X6, X21}, {X6, X22}, {X6, X23}, {X12, X22}, {X12, X26}, {X13}, {X14}, {X15}, {X16}, {X17}, {X18}, {X19}, {X20};

The minimum cutsets for ‘electrical control system fault’ are:

Table 1.1 Results of consequence analysis for most probable failure scenarios of stacking crane

Failure systems	Most probable failure scenarios	Consequence analysis
Driving system of traveling mechanism fault	Motor fault	6
	Speed changer mechanism fault	4
Mechanical system of traveling mechanism fault	Skew traveling of crane’s running gears	5
	Stacker crane running unstable	5
Loading shelf fault	Loading shelf running unstable	6
	Loading shelf falling	9
Speed changer mechanism of lifting mechanism fault	Motor fault	6
	Transmission fault	6
Lifting mechanism fault	Tilt wheel	7
	Roller failure	6
	Wire rope breaking	8
Driving system of telescoping fork mechanism fault	Motor fault	6
	Gearbox failure	5
Fork failed to stretch	Clutch fault	4
	Obstruction in the movement of fork	4
Open phase	Capacitor failure	5
	Power failure	6
No voltage at both ends of the motor	Frequency converter fault	6
	Electric transmission line fault	5
Software fault	Human error in operation	5
	Faulty data communication	4
Hardware fault	Unable to locate accurately	7
	Frequency conversion fault	5
	Fork is out of control	5

{X7}, {X8}, {X9}, {X10}, {X11}, {X21}, {X24}, {X25},
 {X27}, {X28}, {X29}, {X30}, {X31}, {X32}, {X33};

The minimum cutsets for ‘stacker crane is not functioning normally’ are:

{X1}, {X2}, {X3}, {X4}, {X5}, {X6, X22}, {X6, X23}, {X7}, {X8},
 {X9}, {X10}, {X11}, {X12, X22}, {X12, X26}, {X13}, {X14}, {X15},
 {X16}, {X17}, {X18}, {X19}, {X20}, {X21}, {X24}, {X25}, {X27},
 {X28}, {X29}, {X30}, {X31}, {X32}, {X33}.

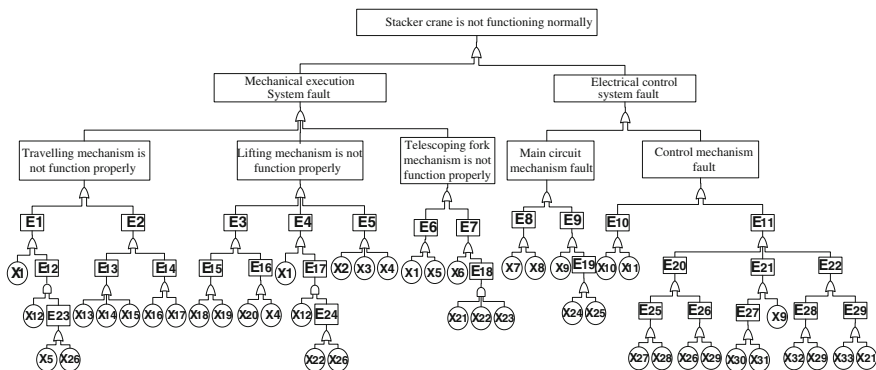


Fig. 1.3 Fault tree for stacking crane failure scenarios, *Note* E1 driving system of traveling mechanism fault; E2 mechanical system of traveling mechanism fault; E3 loading shelf fault; E4 speed changer mechanism of lifting mechanism fault; E5 lifting mechanism fault; E6 driving system of telescoping fork mechanism fault; E7 fork failed to stretch; E8 open phase; E9 no voltage at both ends of the motor; E10 software fault; E11 hardware fault; E12 speed changer mechanism fault; E13 skew traveling of crane’s running gears; E14 stacker crane running unstable; E15 loading shelf running unstable; E16 loading shelf falling; E17 transmission fault; E18 obstruction in the movement of fork; E19 electric transmission line fault; E20 unable to locate accurately; E21 frequency conversion fault; E22 fork is out of control; E23 reduction gear fault; E24 speed changer box fault; E25 error positioning; E26 positioning in the wrong location; E27 no variable speed control signal; E28 location failed to store cargo; E29 fork failed to moving; X1 motor fault; X2 tilt wheel; X3 roller failure; X4 wire rope breaking; X5 gearbox failure; X6 clutch fault; X7 capacitor failure; X8 power failure; X9 frequency converter fault; X10 human error in operation; X11 faulty data communication; X12 motor running normally; X13 track installation error; X14 traveling wheel deviation; X15 track under poor maintenance; X16 track existing a certain slope; X17 brake fault; X18 columns deformation; X19 track supporting wheels wearing down; X20 fall-proof machine fault; X21 fork failed to stretch; X22 pinion and rack fault; X23 chain and sprockets fault; X24 cable fault; X25 sliding contact device fault; X26 coupling fault; X27 address identification device fault; X28 identification bar loosen or migrated; X29 other failures; X30 arithmetic unit of control system fault; X31 counter fault; X32 sensor faults; X33 fork stretching out overtime

1.3.1.4 Probabilistic Failure Analysis

By referring to the literature, analyzing experimental data, and consulting experts and technicians, we can calculate the probability of each faulted system based on the suggested values of the probability of primary events. Taking the fault tree with ‘control mechanism fault’ as the top event as an example, Table 1.2 lists the failure probability of each primary event in the control mechanism.

Using the downlink method, we get: the minimum cutsets of ‘software fault E10,’ $E10 = X10 + X11$; the minimum cutsets of ‘hardware fault E11’ is $E11 = X9 + X21 + X26 + X27 + X28 + 29 + X30 + X31 + X32 + X33$. The minimum cutsets can be regarded as independent events, so we formulate the probability of ‘software fault E10’ and ‘hardware fault E11’ as in (1.2),

Table 1.2 Cumulative failure probability of equipment in control mechanism

No.	Primary event	Probability
X9	Frequency converter fault	0.00020
X10	Human error in operation	0.00010
X11	Faulty data communication	0.00014
X21	Fork failed to stretch	0.00050
X26	Coupling fault	0.00110
X27	Address identification device fault	0.00020
X28	Identification bar loosen or migrated	0.00180
X29	Other failures	0.00030
X30	Arithmetic unit of control system fault	0.00010
X31	Counter fault	0.00020
X32	Sensor faults	0.00030
X33	Fork stretching out overtime	0.00030

$$G = 1 - \prod_{i=1}^N [1 - P(X_i)] \quad (1.2)$$

where N denotes the number of minimum cutsets, $P(X_i)$ signifies the probability of minimum cutsets.

$$P(E10) = 1 - (1 - 0.0001) \times (1 - 0.00014) = 0.00024 \quad (1.3)$$

$$\begin{aligned} P(E11) = & 1 - \{1 - [1 - (1 - P(X27))(1 - P(X28))][1 - (1 - P(X26)) \times (1 - P(X29))]\} \\ & \times \{1 - [1 - (1 - P(X30))(1 - P(X31))] \times (1 - P(X9))\} \\ & \times 1 - [1 - (1 - P(X32))(1 - P(X29))] \\ & \times [1 - (1 - P(X33))(1 - P(X21))] = 0.00529. \end{aligned} \quad (1.4)$$

We can also calculate the probability of all other faulted systems in the same way. The results are presented in the third column of Table 1.3. Finally, the probability of ‘stacker crane is not functioning normally’ can be obtained.

1.3.1.5 Consequence Assessment

The consequence of a stacker crane breakdown involves system performance loss, financial loss, and human health loss. It is so complicated to quantify different kinds of losses accurately that we use a hierarchical approach to rank the seriousness of failure consequences and thus conduct a semi-quantitative analysis. System performance loss L_F accounts for the performance loss due to components’ failures and

Table 1.3 Results of risk estimation for all fault systems

No.	Failure system	Probability	Consequence	Risk factor	Risk ranking
E1	Drive system of traveling mechanism failure	0.00359	6	0.0215	2
E2	Mechanical system of traveling mechanism failure	0.00150	6	0.0090	8
E3	Loading shelf failure	0.00180	9	0.0162	5
E4	Speed shifting mechanism failure	0.00339	6	0.0203	3
E5	Lifting mechanism failure	0.00170	8	0.0136	7
E6	Drive system of telescoping fork mechanism failure	0.00250	6	0.0150	6
E7	Fork failed to stretch	0.00379	5	0.0190	4
E8	Open phase	0.00069	7	0.0048	10
E9	No voltage at both ends of the motor	0.00090	7	0.0063	9
E10	Software fault	0.00024	6	0.0014	11
E11	Hardware fault	0.00529	8	0.0423	1
The stacker crane system failure		0.02511	7	0.1758	

takes as its value an integer ranged from 0 to 10, which denotes the degree of loss from low to high based on experts’ opinions. Financial loss L_A defines the damage to assets or properties, outage losses, and loss of goods in storage. The evaluative method of financial loss is similar to that of system performance loss. Human health loss L_H assesses the severity of personal injury caused by accidents.

According to the specifications in China, human health loss can be subcategorized into light injury, serious injury, heavy casualties, and serious casualties [6], which correspond, respectively, to values 2, 4, 6, and 8, while $L_H = 0$ indicates no fatality. Combining the three types of losses, we can obtain the total failure loss L .

$$L = [(L_F^2 + L_A^2 + L_H^2)/3]^{0.5}. \tag{1.5}$$

It is evident from Table 1.1 that ‘loading shelf falling E16’ and ‘the fracture of steel wire rope X4’ led to the most serious consequence among all failure scenarios in each faulted system. Taking ‘hardware fault E11,’ for example, it consists of three failure scenarios: ‘unable to locate accurately E20,’ ‘frequency conversion fault E21,’ and ‘fork control fault E22.’ ‘Unable to locate accurately E20’ induces a moderate loss of system performance with $L_F = 6$, a significant financial loss with $L_A = 9$ and a serious injury impact on human health with $L_H = 4$; hence, the failure consequence of L_{E20} is determined as in (1.6):

$$L_{E20} = [(7^2 + 9^2 + 7^2)/3]^{0.5} = 7.7244 \approx 8. \quad (1.6)$$

We can also calculate in the same fashion the failure consequence of ‘frequency conversion fault E21’ and ‘fork control fault E22,’ respectively, as in (1.7) and (1.8):

$$L_{E21} = [(6^2 + 6^2 + 0^2)/3]^{0.5} = 4.8990 \approx 5 \quad (1.7)$$

$$L_{E22} = [(6^2 + 7^2 + 2^2)/3]^{0.5} = 5.4467 \approx 5. \quad (1.8)$$

The failure consequence of ‘Hardware fault E11’ is the maximum value of the failure consequence of the three failure scenarios as illustrated in (1.9).

$$L_{E11} = \text{MAX}(L_{E20}, L_{E21}, L_{E22}) = 7 \quad (1.9)$$

The analytical result of failure consequence for different faulted systems is listed in the fourth column of Table 1.3.

1.3.1.6 Risk Estimation

The result of failure probability and the failure consequence are combined to determine the risk value of different faulted systems. The fifth column of Table 1.3 provides the values estimated for the risk of different faulted systems.

The failure probability of the top event ‘stacker crane is not functioning normally’ is 0.02511, while the failure consequence is the mean value of failure consequence of all faulted systems; thus, the total risk of the stacker crane failure is estimated at 10.1758.

1.3.2 Risk Evaluation

There always exists high risk for equipment owing to the uncertainty of risk, and it is difficult to eliminate the risk by taking precautionary measures. The lower the system’s level of risk is, the more difficult it gets to further bring down the level, the more rapidly the maintenance cost increases. The risk must be reduced until the benefit brought by the risk-reducing measures is out of proportion to the cost invested to lower the risk. The risk can be deemed as reasonable only at this point. ‘As Low As Reasonable Practicable’[7] Principle can be used to evaluate the equipment risk comprehensively.

In accordance with the ALARP principle, the risk map can be divided into several regions in equipment risk management with regard to the characteristics of various industries. In this paper, the risk map is partitioned into three quite distinct

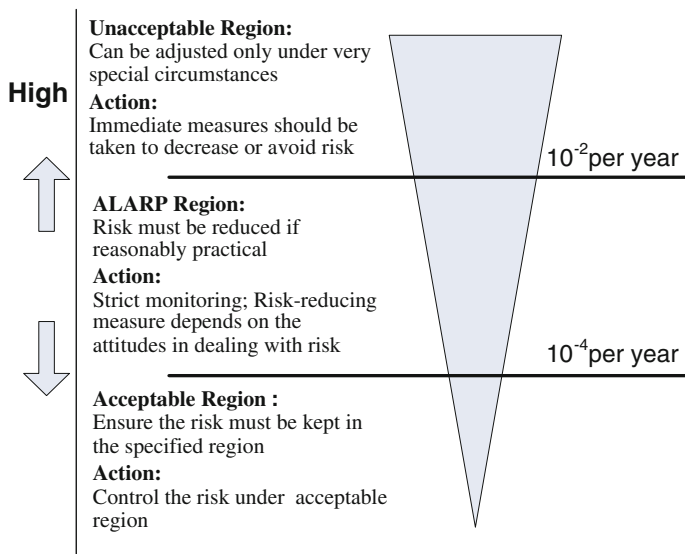


Fig. 1.4 ALARP and (un)acceptable risk level

regions as in Fig. 1.4, the unacceptable risk level is 1.0×10^{-2} per year. If the estimated risk value is greater than the unacceptable risk level, then it falls into the unacceptable region and we should take effective measures to lower the risk as soon as possible.

The total risk of the stacker crane is 0.1758, which is far beyond the unacceptable level of 1.0×10^{-2} . There is a strong correlation between the failure probability of a system and that of its components, so it is feasible to lower the total risk of the system by reducing the failure probability of the components. In this way can the excess risk be distributed over the critical components and can it be ensured that the overall risk is kept within the acceptable range. The results in Table 1.3 show that to reduce the risk of stacker crane failure, we need to cut down the failure probability of ‘hardware fault,’ ‘drive system of traveling mechanism fault,’ and ‘speed changer mechanism fault’ by establishing an appropriate and effective maintenance strategy.

1.3.3 Maintenance Planning

The failure consequence of the equipment is intimately interconnected with the running environment and is identified when it was put into operation. So, we can only control the risk of equipment through reducing its failure probability. The aforementioned equipment with a higher risk should be taken of preventive maintenance measures and be increased the maintenance frequency to improve the

efficiency and quality of maintenance, but breakdown maintenance is applied to equipment with a lower risk. A maintenance or inspection plan has been worked for all high-risk components. The specific implementation of maintenance plan will be elaborated in the further research.

1.4 Conclusion

The objective of risk-based maintenance approach is to develop a technique to build up maintenance program for reducing the total risk caused by system failures and optimizing the total life cycle cost. This paper illustrates that the risk-based maintenance method is a powerful decision-making tool to optimize maintenance programs and can be applied to AS/RS. Analytical results demonstrate that this maintenance strategy can be used to improve the efficiency and cost effectiveness of existing maintenance policies by optimal decision-making procedures at various stages of the life cycle. The greatest advantage of RBM is that it can prevent unexpected damage by assessing the risks of all equipment, and it is remarkably quantitative and comprehensible so as to be operated by technicians and maintenance workers.

References

1. Kaplan Stan (2000) The words of risk analysis. *Risk Anal* 17(4):407–417
2. Khan FI, Haddara M (2003) Risk-based maintenance (RBM): a quantitative approach for maintenance /inspection scheduling and planning. *J Loss Prev Process Ind* 16:561–573
3. Vesely WE, Goldberg FF, Roberts NH (1987) *Fault tree handbook*. Government Printing Office
4. Zhou Q (2002) Study on control and management technique of automated storage and retrieval system (AS/RS) basing on modern logistics. Southwest Jiaotong University, Chengdu
5. Xiong X, Zhao J, Zhou Q (2002) Research on the abnormal state detection and self-recover ability of stacker crane machine. *Hoisting and Conveying Machinery*, (9):1–4
6. National Bureau of Standards (1986) GB6441-86 Classification standard of injured and fatal accident of staffer. China Standards Press, Beijing
7. Melchers RE (2001) On the ALARP approach to risk management. *Reliab Eng Syst Saf* 71 (2):201–208

Chapter 2

Research on Logistics Center Layout Based on SLP

Yannan Liu and Qilan Zhao

Abstract Systematic layout planning (SLP) has been widely applied to the production system, but not to the service system. Combined with the goals, influencing factors, and conditions of logistics center layout, this paper probes into the application of SLP to the layout of the rapidly increasing logistics centers in large- and medium-sized cities in recent years. According to the logistics relationship and non-logistics relationship between work units in the logistics center, the author decides the position of work units and maps out the initial position relationship chart. Through further amendments and adjustment based on the move line and other factors, the author gets the feasible layout plan. Finally, this paper uses a medicine logistics center in Jiangsu Province as an example to design, analyze, and evaluate for the purpose of providing some theoretical basis and method for reference in the service system layout.

Keywords SLP · Logistics center · Layout · Design

2.1 Introduction

Since entering the twenty-first century, the logistic industry in China has been rapidly growing up and the number of logistics centers has increased dramatically. Many large- and medium-sized cities across the country are planning to set up logistics centers. Logistics center is a comprehensive, regional concentration of large quantities of materials, and it is an intermediary between production and marketing enterprises, integrating commodity flow, logistics, information flow, and cash flow [1]. The reasonable layout of logistics centers has taken more and more attention, and it is also the research focus of many scholars.

Y. Liu (✉) · Q. Zhao
School of Economics and Management, Beijing Jiaotong University, Beijing 100044,
People's Republic of China
e-mail: 912688323@qq.com

© Springer-Verlag Berlin Heidelberg 2015
Logistics Engineering Institution, CMES (ed.),
Proceedings of China Modern Logistics Engineering,
Lecture Notes in Electrical Engineering 286, DOI 10.1007/978-3-662-44674-4_2

At first, people use their experience and feeling to design the logistics centers. In the 1950s, developed from the traditional small systems to big and complex systems, it is difficult to design the logistics centers only with experience. And so, with the integration development of the diverse discipline, the system engineering concept and system analysis method have been used in layout planning [2], and some more advanced design methods have gradually emerged. One of the most representative methods is systematic layout planning (SLP) proposed by American R. Muther in 1961. Study on facilities layout problem is developed from qualitative stage to quantitative stage on the basis of SLP [3]. SLP is also widely applied to various production systems and service systems [4]. Finally, it improves to move line SLP.

2.2 The Goals, Influencing Factors, and Conditions of Logistics Center Layout

2.2.1 The Goals of Logistics Center Layout

After determining the location of a logistics center, the overall goal of logistics center layout is to make the personnel, equipment, and material space in the logistics activity process be in the most appropriate allocation and the most effective combination [5]. The specific goals can be the minimum total cost of material flow, work units¹ of high relationship close degree close to each other, simplifying transport routes, shortening the distance between similar work units, avoiding roundabout transport, etc.

2.2.2 Influencing Factors of Logistics Center Layout

Layout design has a significant effect on a production performance or service system performance [6]. For a logistics center, its layout has direct influence on logistics, information flow, the logistics operation efficiency, cost, and safety of the whole system. So the influencing factors of logistics center layout are as follows:

1. The nature and function of a logistics center. Because the nature and function of the logistics centers is different, it is different to choose equipment type and quantity. The size and layout of logistics centers are also not the same. According to its core function, the logistics center has three types: transit logistics center, storage logistics center, and distribution logistics center.

¹ The sectors at all levels in a logistics center are called work units.

2. The basic operation process of a logistics center. The main activities of the logistics center are purchasing, warehousing, distribution, circulation processing, packing, returning, and so on [5]. The operation process has an influence on the move line of personnel, equipment, and material. To realize the efficient logistics, the basic operation process of a logistics center should be in consideration when layout designing.
3. Logistics relationship and non-logistics relationship between work units. Logistics relationship is that there is logistics contact between work units. And interpersonal contact, administrative affairs, and other activities can be expressed as non-logistics relationship between work units. Work units of high relationship close degree should be close to each other.

2.2.3 Application Conditions of SLP in the Layout of Logistics Center

It is necessary to specify five basic elements, namely P (logistics products), Q (logistics quantity), R (logistics routes), S (service sectors), and T (logistics operation time or technology) before applying SLP to logistics center layout. The first two basic elements are the most important. Different logistics products have different demands on storage, loading, and other logistics activities. Ultimately, it leads to different logistics routes. What is more, using different logistics equipment and technology determines logistics operation time. The work quantity of the logistics center reflects the logistics intensity² of all work units; logistics routes, distance, and logistics intensity have an influence on layout, which is reflected in the logistics cost and efficiency [7]. Therefore, SLP can be used in the layout of a logistics center based on logistics product category, logistics quantity, and other factors.

2.3 The Main Steps of Layout Based on SLP

Under the guidance of SLP, the first step is to use quantification method to analyze the logistics relationship and non-logistics relationship between work units and then to get the composite correlation between work units. The close degree relationship between work units determines the distance between work units. According to that, we can arrange its location. Through further amendments and adjustment based on the move line and other factors, we can get the feasible layout plan. The specific layout procedure is as follows.

² The distance of movement of logistics products in a certain time of cycle is called logistics intensity.

2.3.1 Logistics Operation Process and Work Units' Settings

The main activities of the logistics center are purchasing, warehousing, distribution, circulation processing, packing, returning, and so on. It is necessary to make clear the main logistics operation process before layout designing. And then, we analyze the corresponding P, Q, R, S, and T elements. Based on the analysis, we can divide the work units.

2.3.2 Interrelation Analysis Between Work Units

It is reasonable to describe the logistics relationship between work units by logistics intensity. Logistics intensity is divided into five ranks: A, E, I, O, and U [8], as shown in Table 2.1.

We can use relationship close degree proposed by R. Muther to describe the non-logistics relationship between work units. If two work units have frequent activity, their relationship close degree is high and vice versa. First, the relationship close degree is divided into six levels: A, E, I, O, U, and X, as shown in Table 2.2.

Then, list the reason for close relationship (see Table 2.3). Using these two kinds of information, we can determine the correlation between work units. According to the correlation, the higher the degree is, the closer their distance is.

2.3.3 The Composite Correlation Analysis Between Work Units

Integrate the logistics relationship and the non-logistics relationship. According to the certain weight of each relationship, calculate the composite correlation between work unit i and work unit j ($i, j = 1, 2, \dots, n$ and $j \neq i$).

Table 2.1 Logistics intensity rank

Logistics intensity rank	Sign	Logistics routes' proportion (%)	Logistics quantity (%)
Absolutely important	A (4)	10	40
Extremely important	E (3)	20	30
Important	I (2)	30	20
Ordinarily important	O (1)	40	10
Unimportant	U (0)		

Table 2.2 The classification of relationship close degree

Sign	Relationship close degree	Proportion (%)
A	Absolutely important	2–5
E	Extremely important	3–10
I	Important	5–15
O	Ordinarily important	10–25
U	Unimportant	45–80
X	Ignored (or negative close degree)	Discretionary

Table 2.3 The reason for close relationship

Serial number	Reason
1	Using common original records
2	Sharing equipment or site
3	Material handling
4	Frequent contact and file exchange
5	Safety and pollution
6	Continuous work flow
7	Manageable
8	Others

2.3.4 Determine the Relative Position of All the Work Units and Get the Final Feasible Layout Plan

To design a logistics center layout, the first step is not directly considering the floor space and shape of all the work units but the composite correlation between work units. If two work units’ composite correlation is high, their distance is shorter and vice versa. During the layout, according to the composite correlation degree in sequence, we locate different work units. If some work units are at the same level, we determine their relative position by scores.

According to the above steps, we can get the preliminary theory position of all work units, and then, we get the final feasible layout plan through further amendments and adjustment based on the actual area, move line, and other factors.

2.4 Case Analysis

This paper uses a medicine logistics center as an example to design and analyze according to the characteristics of medicine logistics, move line, and the actual ground condition. This paper rationally divides each function areas, solves the evacuating problem, saves land, meets the relevant regulations, and aims to verify the feasibility and rationality SLP.

2.4.1 Business Background

Y medicine logistics center [4] located in Jiangsu Province is a third-party medicine logistics enterprise. It mainly provides a medicine trading platform, stocking, storage, picking, packing, distribution, information processing, and many value-added services for entering enterprises. The logistics center plans to cover 125 units of area. Its construction area is 180,000 m², and its storage area is about 80,000 m².

Medicine logistics center has its own characteristics. Medicines can be divided into three types, namely the normal drugs at room temperature, some medicines requiring refrigeration, and psychiatric drugs. These three types of drugs must be stored separately using different storage facilities and paid different attention to. So this paper divides Y medicine logistics center into several work units as follows.

(1) office area; (2) arrival and sorting area; (3) automatic storage/retrieval system (AS/RS); (4) cold storage; (5) psychiatric drugs storage; (6) picking area; (7) packing and processing area; (8) gathering and distribution; and (9) service sectors.

2.4.2 Application of SLP

1. Analyzing the logistics relationship (see Fig. 2.1) and non-logistics relationship (see Fig. 2.2) between work units.
2. Determining the relative importance of logistics relationship and non-logistics relationship. For Y medicine logistics center, the weight of two relationships is 1:1.
3. Quantifying the logistics intensity rank and the non-logistics relationship close degree. Usually, $A = 4$, $E = 3$, $I = 2$, $O = 1$, $U = 0$, $X = -1$.
4. When the number of work units is N , the total matching number can be calculated using the following equation: $P = N(N - 1)/2$. Here, $N = 9$ so $P = 36$.
5. Calculating the composite correlation between work units (see Table 2.4).
6. Switching the composite correlation scores (see Table 2.4) to the composite correlation close degree rank (see Table 2.5). Then, drawing the composite correlation chart (see Fig. 2.3).
7. Determining the relative position of all the work units. According to Fig. 2.3, the higher the work units' composite correlation is, the shorter their distance is (see Fig. 2.4).
8. Analyzing the move line. The move lines of the logistics centers are different for their different land areas and logistics products. There are five types, namely I, L, U, O, and S. Type I is the most simple, and it is suitable for the rectangular logistics center whose entrance is to the exit. Type S is the most complex, and it is suitable to arrange a long logistics route. Y medicine logistics center is near-rectangular. The main activities of Y medicine logistics center are stocking, storage, picking, packing, distribution, information processing, and many value-

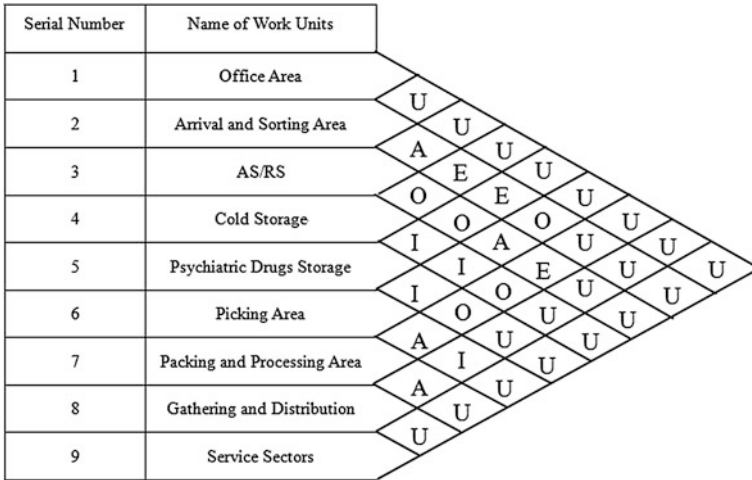


Fig. 2.1 Logistics relationship between work units

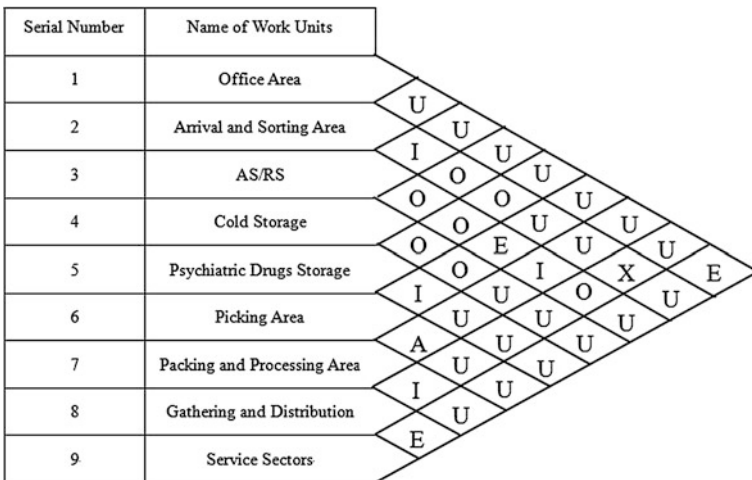


Fig. 2.2 Non-logistics relationship between work units

added services. So this paper intends to design Y medicine logistics center combining type L with type U (see Fig. 2.5).

9. The final feasible layout plan. After adjustment, the final layout plan is shown in Fig. 2.6.

Table 2.4 The composite correlation between work units

Work units' pairing	Relationship close degree				The composite correlation	
	Logistics relationship		Non-logistics relationship			
	Degree	Score	Degree	Score	Score	Degree
1-2	U	0	U	0	0	U
1-3	U	0	U	0	0	U
1-4	U	0	U	0	0	U
1-5	U	0	U	0	0	U
1-6	U	0	U	0	0	U
1-7	U	0	U	0	0	U
1-8	U	0	U	0	0	U
1-9	U	0	E	3	3	O
2-3	A	4	I	2	6	E
2-4	E	3	O	1	4	I
2-5	E	3	O	1	4	I
2-6	O	1	U	0	1	U
2-7	U	0	U	0	0	U
2-8	U	0	X	-1	-1	X
2-9	U	0	U	0	0	U
3-4	O	1	O	1	2	U
3-5	O	1	O	1	2	U
3-6	A	4	E	3	7	E
3-7	E	3	I	2	5	I
3-8	U	0	O	1	1	U
3-9	U	0	U	0	0	U
4-5	I	2	O	1	3	O
4-6	I	2	O	1	3	O
4-7	O	1	U	0	1	U
4-8	U	0	U	0	0	U
4-9	U	0	U	0	0	U
5-6	I	2	I	2	4	I
5-7	O	1	U	0	1	U
5-8	U	0	U	0	0	U
5-9	U	0	U	0	0	U
6-7	A	4	A	4	8	A
6-8	I	2	U	0	2	U

(continued)

Table 2.4 (continued)

Work units' pairing	Relationship close degree				The composite correlation	
	Logistics relationship		Non-logistics relationship			
	Degree	Score	Degree	Score	Score	Degree
6-9	U	0	U	0	0	U
7-8	A	4	I	2	6	E
7-9	U	0	U	0	0	U
8-9	U	0	E	3	3	O
总计					36	100

Table 2.5 The composite correlation close degree rank

Total score	Relationship close degree	Matching number	Proportion (%)
8	A	1	2.8
6-7	E	3	8.3
4-5	I	4	11.1
3	O	4	11.1
0-2	U	23	63.9
-1	X	1	2.8
Total		36	100

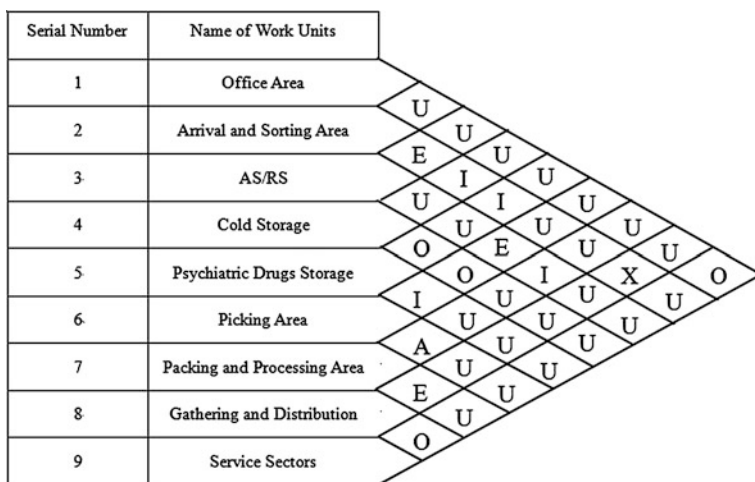
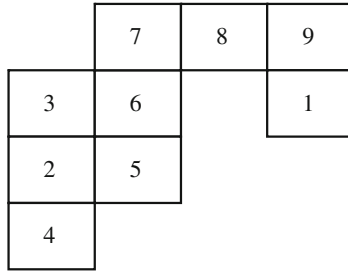
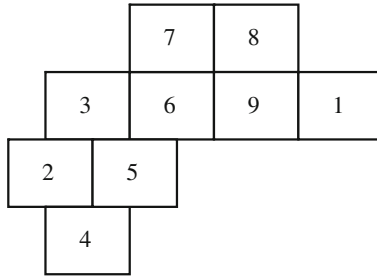


Fig. 2.3 The composite correlation chart



Plan One



Plan Two

Fig. 2.4 The relative position of the work units

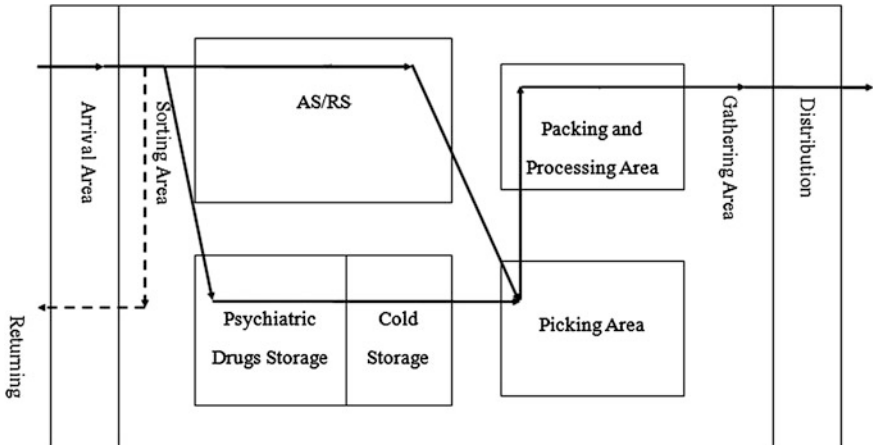


Fig. 2.5 The move line

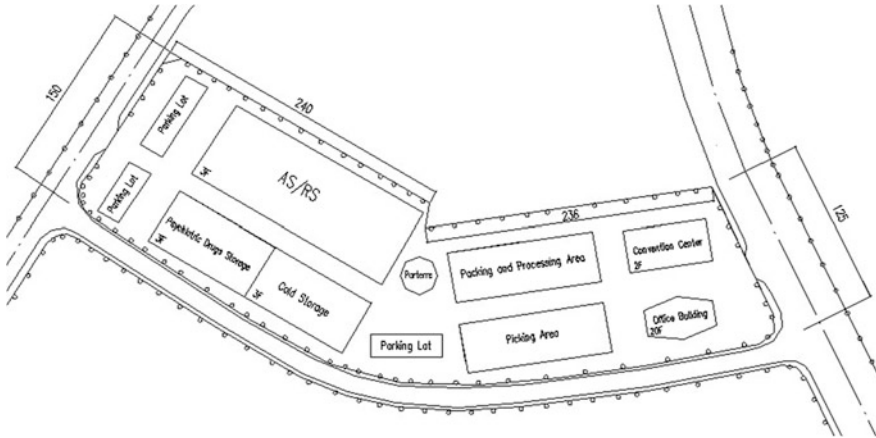


Fig. 2.6 The final layout plan

2.4.3 Evaluation

Through dividing the nine main work units, the paper designs Y medicine logistics center considering the logistics relationship and non-logistics relationship. So the final feasible layout plan is comprehensive. What is more, the main activities of Y medicine logistics center are stocking, storage, picking, packing, distribution, information processing, and many value-added services. Its storage area is about 80,000 m². Therefore, we put the three warehouses nearly in the middle considering the warehouse layout priority principle. This is helpful for the quick contact with the other circumjacent area, and this helps to improve the logistics center's operational efficiency. At the same time, the classification of warehouses contributes to the different storage requirements of different customers. And there is enough space for adjustment, greatly improving the flexibility of the storage system. The designed move line of Y medicine logistics center, combining both the layout of work units and the principle of avoiding circuitous transportation, can well ensure smooth logistics activities. Different storages can also use different move lines.

2.5 Conclusion

This paper focuses on the layout of the logistics center, proposes the use of SLP to design the layout of the logistics center, and adds to the move line analysis. Through the analysis of this paper, the main conclusions are as follows.

The overall goal of logistics center layout is to make the personnel, equipment, and material space in the logistics activity process be in the most appropriate allocation and the most effective combination. At the same time, the main

influencing factors of logistics center layout are the nature, function, basic operation process of a logistics center, logistics relationship, and non-logistics relationship between work units. Through the case analysis, after making clear the P, Q, R, S, and T elements, it is feasible and reasonable to use SLP in the layout of a logistics center.

It provides a good reference for other logistics center layout problem. It is necessary to point out some limitations and shortages. When drawing the relative position of the work units' figure, people have to constantly adjust and amend the plan in order to meet the corresponding condition. What is more, different designers' way of solving conflicts may lead to different design plans. How to use the computer simulation technology to compare SLP layout plan with other plans is one of our future research directions.

References

1. Xue S (2006) Study on medicinal logistic center design and simulation. Huazhong University of Science and Technology, Wuhan
2. Liu W, Lan P (2006) Improvement of systematic layout planning. *Logist Technol* 10: 82–85
3. Shuqin W, Wei L (2008) Layout planning with a controlling structure to logistics parks. In: IEEE international conference on automation and logistics. Qingdao, China, 2039–2043
4. Dong Q (2008) *Logistics engineering*, vol 41, 2nd edn. China Communications Press, Beijing, p 254, 267
5. Zhang J (2008) Study on logistics center facility layout design based on multi-objective programming. Southwest Jiaotong University, Chengdu
6. Yang T, Kuo C (2003) A hierarchical AHP/DEA methodology for the facilities layout design problem. *Eur J Oper Res* 147:128–136
7. Chen J (2009) Steel logistics park layout planning based on SLP. Wuhan University of Technology, Wuhan
8. Li J (2009) The application of SLP in logistics center general layout planning. *Modern Economics*, 8(3):21

Chapter 3

System Dynamics Modeling and Simulation of Two-Stage Remanufacturing Reverse Supply Chain

Yiwei Mo, Liwei Li and Wei Huang

Abstract Remanufacturing is a processing for recycling the availability value of used product; it contains recovery, disassembly, cleaning, overhaul, repair, and replacement operations, and product recovery operations in remanufacturing supply chains face continually changing product demand. In this paper, according to the principle and procedure of system dynamics modeling, system dynamic model of two-stage remanufacturing reverse supply chain including a reproducer and recycler is established. The simulation of model can be used to analyze the remanufacturing supply chain system from the macroscopic qualitative view and microcosmic quantitative view, and to improve the structure and get parameter optimization. As for the purpose of reducing the operation cost and improving the gross profit, this paper analyzes the influence of different factors to the cost and total profit of remanufacturing reverse supply chain through dynamic simulation. Through analyzing and controlling the change of the impact factors, this paper presents the remanufacturing supply chain operation mode with higher benefits.

Keywords Remanufacturing · Supply chain · System dynamics · Simulation · Vensim

3.1 Introduction

Because of the resources shortage, remanufacturing has been an area of increasing attention in recent years. Remanufacturing involved in many fields, such as the car industry, machine tool industry, and household electrical appliance industry. It is different with the traditional production distribution logistics network due to the uncertainty and complexity of recovery time, recovery number, and location. At

Y. Mo (✉) · L. Li · W. Huang
School of Mechanical Engineering College, Guangxi University,
Nanning 530004, Guangxi, People's Republic of China
e-mail: moyw@gxu.edu.cn

present, a few researches refer to the costs and profits of remanufacturing system base on system dynamics [1–6]. And it urgently needs to take the costs and profits into account in modeling and simulations.

According to the system dynamics methodology, we build a system dynamics model of remanufacturing in two-stage supply chain, which consists of recovery dealer and remanufacturer. Remanufacturing logistics activity is analyzed firstly. Secondly, remanufacturing supply chain causal loop diagram and flow diagram is built in Vensim. Then, the proposed system dynamics model is simulated in Vensim and to pursuit higher profits. This research is motivated by the need for the development of methodological tools that would assist the decision-making process to obtain operation mode with higher profit for remanufacturing reverse supply chains, in which some important factors are taken into account. And the operation mode of the high benefit is obtained at last.

3.2 Modeling

In this paper, we focus on the recycled used engineering mechanical transmission in an area. An assumption of our analysis is that this model collects a single type of gearbox, which values 10,000 yuan RMB as new product. Except scraping, all of the collected used products are accepted and transferred for remanufacturing, and the collection capacity of the recovery dealer is infinite. The members of remanufacturing supply chain system are: manufacturers, distributors, remanufacturers, recovery dealers, and customers. Remanufacturing supply chain system contains positive logistics and reverse logistics, as shown in Fig. 3.1. The positive logistics activities include the manufacturing of new products, distribution, and reaching the final customers. And the remanufacturing reverse logistics activities include the recovery of used product, detection, classification, splitting and cleaning, repairing, and redistribution operations [1].

Due to the reciprocal influences of the uncertainty and variety in remanufacturing supply chain, the behavior of the system is analyzed through a simulation model based on the principles of the system dynamics methodology, which is designed for long-term dynamic management problems. It focuses on understanding how the information flows, physical processes, and managerial policies interact. As the modeling foundation, causal loop diagram is used to figure out the system feedback structure [1].

3.2.1 Causal Loop Diagram

Causal loop diagram can reflect the relation between variables in complex system briefly. We will study the causal and effect of recovery dealer subsystem and remanufacturer subsystem. In the sequel, the recovery dealer and remanufacturer

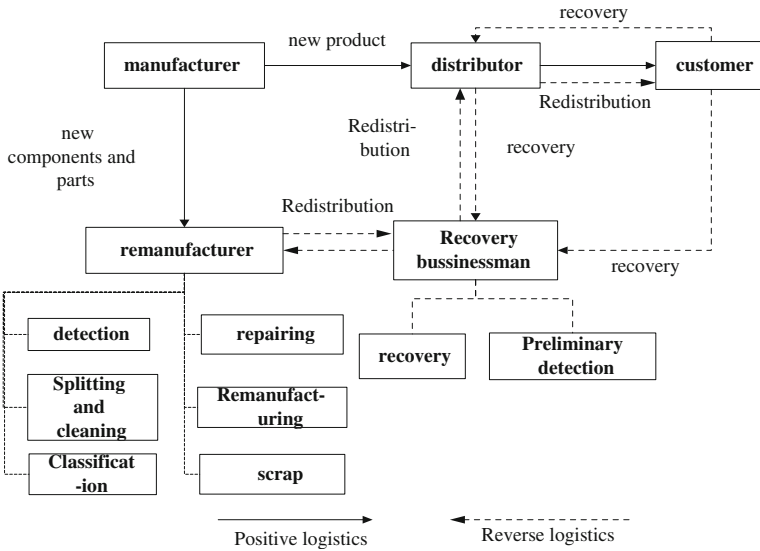


Fig. 3.1 Remanufacturing supply chain system

will be represented by R and H , respectively. The objective of this work is just to study remanufacturing reverse logistics link only.

In the recovery dealer subsystem, the analysis objects are various, such as recovery cost, transportation cost, not reuse rate, resales income, testing time, and error. And in the remanufacturing subsystem, the analysis objects include remanufacturing productivity, remanufacturing products income, scrap rate, remanufacturing production capacity, remanufacturing capacity expansion rate, and remanufacturing capacity adjustment, etc. [2, 3].

Figures 3.2 and 3.3 show the two subsystems, respectively, and embody the causal relationship between the various factors. For example, the increase of R reuse rate causes the remanufacture products increasing, while the increase of scrap rate and testing error will cause remanufacture products decreasing. The important variables will be explained in Sect. 2.2.

3.2.2 Flow Diagram

Although causal feedback loop has analyzed, but it cannot determine the mechanism of how variables work. In the following, we will show the physical structure, behavior, and control laws of these variables through flow diagram. Flow diagram makes up of state variable, rate variables, auxiliary variables, constants, and flow. Then, we build the flow diagram on the basis of causal loop diagram, as shown in Fig. 3.4.

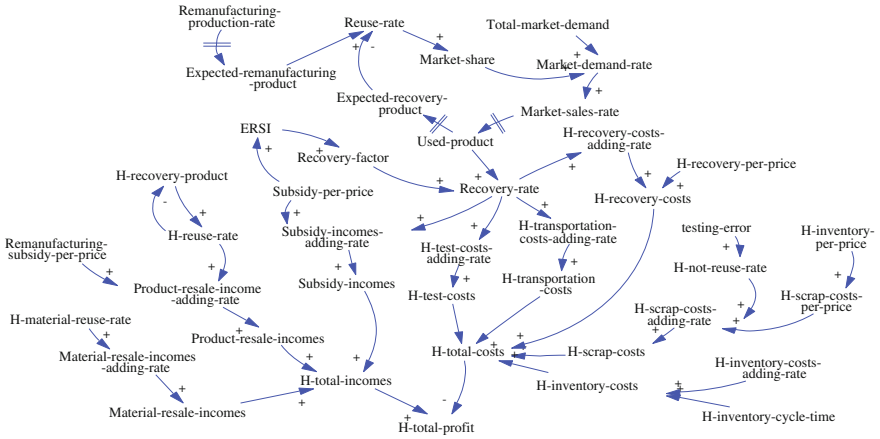


Fig. 3.2 Recovery dealer subsystem causal loop diagram

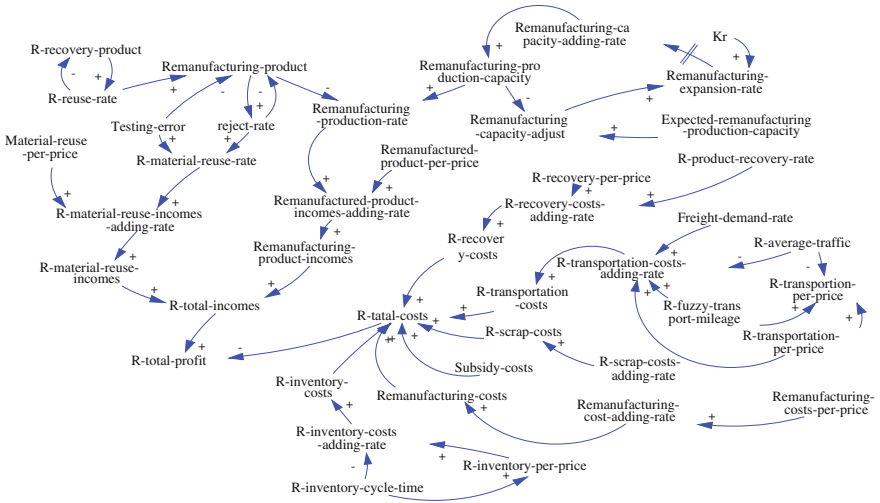


Fig. 3.3 Remanufacturing subsystem causal loop diagram

In order to ensure the validity of parameter and mathematical equations correctly setting, important variables will be stated in the following:

- (1) An assumption of Total_market_demand is that it obeys the random normal distribution, which means for 10,000 and the variance for 500. Total_market_demand = RANDOM NORMAL (1, 200,000, 10,000, 500, 2)
- (2) Hypothesis is to add remanufacturing link to manufacturing enterprise. At the beginning of the remanufacturing system putting into operation, there have

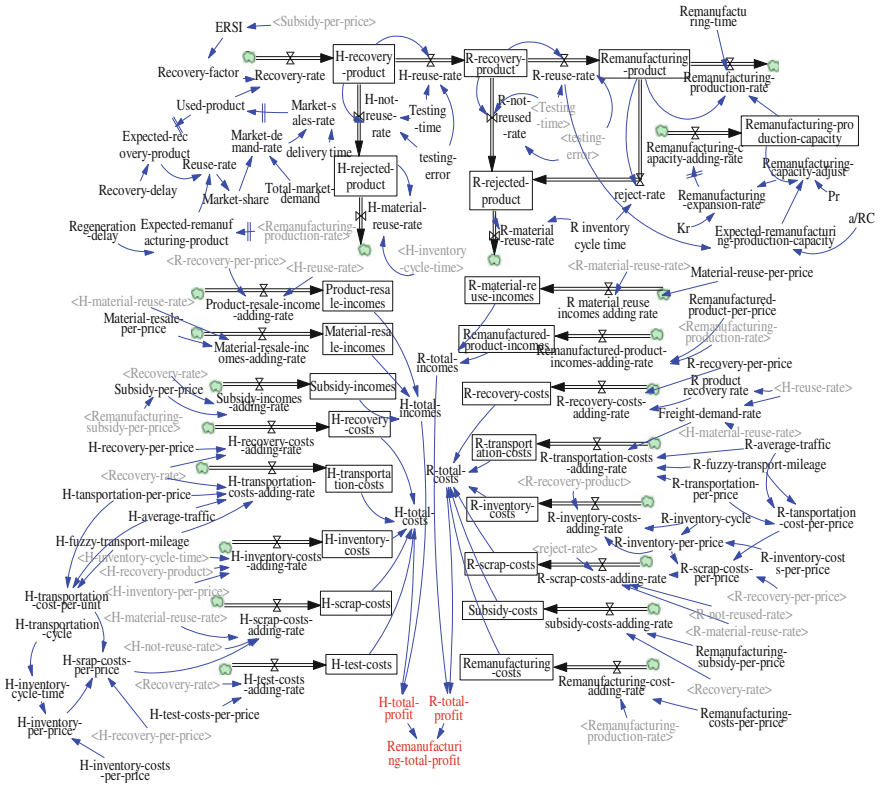


Fig. 3.4 Flow diagram

used products already, the initial value is 3,000. $H_recovery_product = INTEG(Recovery_rate - H_not_reuse_rate - H_reuse_rate, 3,000)$

(3) Expected recovery product is the smooth functions of used product. $Expected_recovery_product = SMOOTH(Used_product, Recovery_delay)$

(4) $Remanufacturing_product = INTEG(R_reuse_rate - Remanufacturing_production_rate - reject_rate, 0)$

(5) $Remanufacturing_production_rate = MIN(Remanufacturing_production_capacity, Remanufacturing_product / Remanufacturing_time)$

(6) Remanufacturing capacity adding rate is the three delay function of Remanufacturing capacity expansion rate; delay time is 15 week. $Remanufacturing_capacity_adding_rate = DELAY3I(Remanufacturing_capacity_expansion_rate, 15, 0)$

(7) $Remanufacturing_capacity_adjust = MAX(Expected_remanufacturing_capacity - Remanufacturing_production_capacity, 0) * PULSE_TRAIN(50, 0, Pr, 300)$; That is the beginning to check whether need to expand capacity after 50 weeks; Pr is the interval for repeated inspection, and the inspection will stop after 300 weeks.

- (8) $\text{Remanufacturing_capacity_expansion_rate} = \text{MAX}(\text{Remanufacturing_capacity_adjust} * \text{Kr}, 0)$
- (9) $\text{R_Transportation_costs_adding_rate} = \text{R_transportation_per_price} * \text{R_fuzzy_transport_mileage} * \text{Freight_demand_rate}/\text{R_average_traffic}$.
- (10) According to the literature [1], Kr is the expansion decision and will be set to 1.5. Pr is the review-check period. Pr = 50 weeks. A/RC is time delay; the value is taken as 12.

3.3 Simulation and Analysis

At the beginning of simulation, the initial value of $H_recovery_product$ is 3,000, all of the other state variables are 0, and product life cycle is 40 weeks. The relations between $Reuse_rate$ and $Market_share$ are showed in tabulate function graph, which can reflect the initial market share is 25 %, and the upper limit is 40 %. The relationship between environmental protection intensity index (ERSI) and $\text{Remanufacturing_subsidy_per_price}$ is also showed in tabulate function graph, and the change range of ERSI is 0.5–0.7. The other parameters are setup as following:

$\text{Remanufactured_product_per_price} = 5,500$ Yuan/unit, $\text{R_recovery_per_price} = 3,000$ Yuan/unit.

$\text{Material_reuse_per_price} = 1,000$ Yuan/unit, $H_average_traffic = 250$, $\text{R_average_traffic} = 300$.

$\text{R_fuzzy_transport_mileage} = 500$ miles, $H_fuzzy_transport_mileage = 600$ miles.

$\text{R_transportation_per_price} = H_transportation_per_price = 6$,

$\text{Remanufacturing_costs_per_price} = 100$ Yuan/unit.

$\text{Material_resale_per_price} = 800$ Yuan/unit, $H_recovery_per_price = 2,500$ Yuan/unit.

$\text{Recovery_delay} = 50 = \text{Regeneration_delay}$.

Setting simulation in length as: INITIAL TIME = 0, FINAL TIME = 300 week.

3.3.1 Model Validation

There are four methods to test the authenticity of the proposed model, which are intuitive inspection, operation test, sensitivity test, and history test [4]. The first two methods have been included in the simulation software, and we cannot carry out history test due to the lack of history data sources, so we just carry out the sensitivity test.

In this research, the price for collecting used product is high, so the scrap cost plays an important role in the whole supply chain. If testing_error increases, the

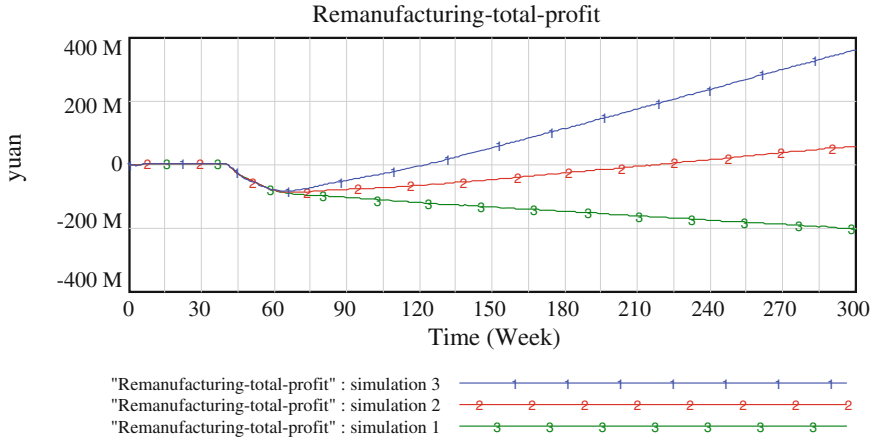


Fig. 3.5 The change of remanufacturing total profit for different testing error

scrap rate increases, and the whole supply chain profits will decrease. The value of testing_error is setup as 0.3, 0.2, and 0.1 in simulation 1, 2, and 3, respectively. The simulation results are given in Fig. 3.5, which shows that it is consistent with the reality. In other words, the proposed model is effective.

3.3.2 Simulation and Results Analysis

There are many factors influencing the profit of remanufacturing reverse supply chain system. In this paper, we focuses on the analysis of testing error, which has the biggest impact on profit and the Remanufacturing_subsidy_per_price that has greater adjustment range.

(1) Testing_error analysis

As shown in Fig. 3.5, it reflects the change of Remanufacturing_total_profit for different testing_error settings. The testing_error influences the quantity of Remanufacturing_product and Remanufacturing_production_rate and then affects the profits of the model. Setting testing_error as same as those in the model validation, the simulation results as shown in Fig. 3.6.

With the testing_error decreasing, the quantity of R_recovery_product, Remanufacturing_total_profit, and Remanufacturing_production_rate increases. When the testing_error is 0.2, the Remanufacturing_total_profit is very low, and it will decrease when testing_error is higher than 0.2. Therefore, the model testing_error must be less than 0.2; according to actual condition, it can be set to 0.1–0.15.

(2) Remanufacturing_subsidy_per_price analysis

ERSI and Recovery_rate increases while the Subsidy_per_price is increasing, and Subsidy_costs of remanufacturer increase while the H_total_incomes

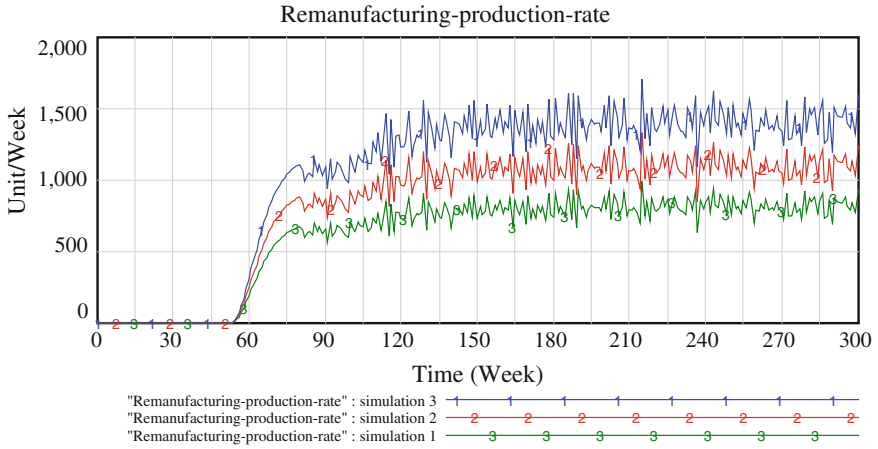


Fig. 3.6 The change of remanufacturing production rate for different testing error

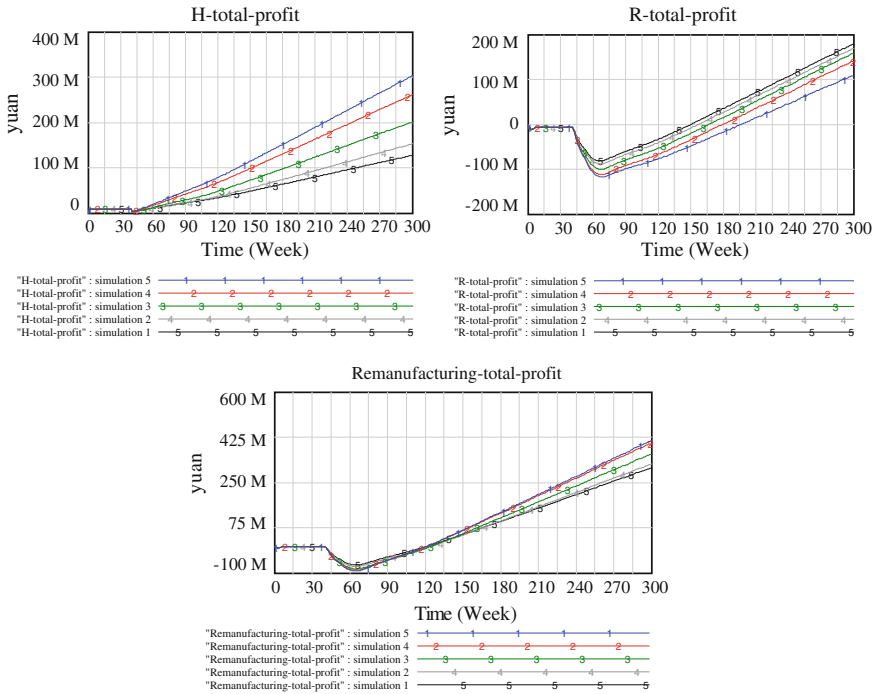


Fig. 3.7 The change of all kinds of profits for different Remanufacturing_subsidy_per_prices

increase. Therefore, we need to balance H_total_profit and R_total_profit under the premise of keeping the $Remanufacturing_total_profit$ increasing.

In the following five simulations, set the $Remanufacturing_subsidy_per_price$ to 10, 50, 100, 150, and 200, respectively. The simulation results as shown in Fig. 3.7. From the simulation results, it can confirm that when the $Remanufacturing_subsidy_per_price$ is improved, $Recovery_rate$, H_total_profit , and $Remanufacturing_total_profit$ will increase naturally, but the R_total_profit will decrease. As shown in Fig. 3.7, the difference of the $Remanufacturing_total_profit$ in simulation1 and simulation2, simulation4 and simulation5 are very small. The profit does not increase obviously. However, the $Remanufacturing_total_profit$ of simulation3 increases obviously. In the meantime, the difference of the R_total_profit in simulation1, simulation2, and simulation3 is very small. Considering about the balance of R_total_profit and H_total_profit , we select the solution of simulation3, which $Remanufacturing_subsidy_per_price$ is 100 yuan.

3.4 Conclusions

This paper establishes a system dynamics model of two-stage remanufacturing supply chain and studies its long-term behaviors based on simulations. Through the simulation analysis, we can find that the affecting the remanufacturing supply chain profits factors include $Remanufacturing_subsidy_per_price$, $transportation_per_price$, $Recovery_rate$, $ERSI$, $Testing_error$, and $Remanufacturing_production_rate$, etc. We not only can adjust the parameters to predict profits and costs of model for a certain point-in-time, but also can use it as the practical decision support. This research is focused on $testing_error$ and $Remanufacturing_subsidy_per_price$. From the simulation results, we can know that the $testing_error$ cannot be more than 0.2, and it is appropriate to set $Remanufacturing_subsidy_per_price$ to 100 yuan. The model can also analysis the other factors to provide effective management decision making. Meanwhile, the model has a certain commonality that it can be used in the other remanufacturing logistics system when change the parameters or take fine tuning.

Acknowledgments This study was supported by the National Key Technology R&D Program of China (Grant No. 2012BAF02B02).

References

1. Zhou H (2008) Simulation of remanufacturing reverse supply chain based on system dynamics. Southeast university, Nanjing
2. Zhou SY, Hu GY (2011) The dynamic behavior analysis of return product recycling. China Bus Mark 1:31–35

3. Wang X (2010) Study on the supply chain simulation based on system dynamics and contract theory. Harbin industrial university
4. Vlachos D, Georgiadis P, Iakovou E (2007) A system dynamics model for dynamic capacity planning of remanufacturing in closed-loop supply chains. *Comput Oper Res* 34:367–394
5. Yan N (2012) Dynamic models and coordination analysis of reverse supply chain with remanufacturing. *Phys Procedia* 24:1357–1363
6. Wen-hui XIA, Dian-yan JIA, Yu-ying HE (2011) The remanufacturing reverse logistics management based on Closed-loop supply chain management processes. *Procedia Environ Sci* 11:351–354

Chapter 4

Research and Demonstration of Dynamic Intelligent Logistics System of the Collection and Transportation Process of Giant Municipal Garbage

Shuang Xu, Guangming Li, Haitao Ou and Wenqing Wu

Abstract Promoting garbage classification and reducing garbage amount are the roots for solving garbage siege problem. Therefore, municipal garbage logistics system can not only collect and transport municipal garbage, but also need to automatically realize precise gathering and managing information of garbage category, garbage producers, collecting spots, capacity, flow rate, and flow direction, which also needs to be blended into traditional garbage collecting and transporting flow. These are all difficulties that municipal garbage logistics system is facing currently. This essay provides a dynamic intelligent logistics system of the collection and transportation process of giant municipal garbage based on questions above. It shows a way of realizing on-car RFID automatically precise position identification and on-car dynamic measurement, which can be perfectly implemented in complicated environment. Besides, RFID precise position and automatic identification, on-car dynamic transduction and measurement, GPS position, GPRS mobile transmission, and other key IOT technologies and information technologies are also integrated, which leads to building up a fine-grained dynamic intelligent logistics system of the collection and transportation process of garbage. It has been successfully implemented in Shanghai and great achievements have also been made. It is a pioneering work of domestic municipal garbage logistics system.

Keywords RFID · IOT · On-car precise identification · On-car dynamic measurement · Garbage logistics

S. Xu · G. Li
College of Mechanical Engineering, Tongji University, Cao'an Road 4800,
Shanghai 201804, China

H. Ou (✉)
Shanghai Refine Information Technology Co., Ltd, Shanghai, China
e-mail: ouhaitao@rfdcn.com

W. Wu
Shanghai Waste Management Office, Shanghai, China

4.1 Overview

Garbage siege has already become an unevadable problem for urbanization process of many developing countries. It deeply restricts development of metropolis such as Shanghai and Beijing. To solve this problem, promoting garbage classification and reduce garbage amount [1] are the root. Nowadays, most cities in China only have a certain numbers of isolated garbage collecting and transporting systems. Even Shanghai initiated primary municipal garbage logistics system [2] recurred to 2010 EXPO. And only intensive management of municipal garbage logistics has been realized. Garbage classification and reducing garbage amount have not been technically supported at angles of logistics engineering and logistics equipment.

As a result, Ministry of Science and Technology and Shanghai decided to build dynamic intelligent logistics system of the collection and transportation process of giant municipal garbage by integrating RFID precise position and automatic identification, on-car dynamic transduction and measurement, GPS position, GPRS mobile transmission, and other key IOT technologies and information technologies. This system is capable of automatically identifying garbage category and garbage weight precisely during the process, while garbage is collected and transported, which lays a very solid technical stone for realizing garbage charge so that things such as garbage classification and reducing garbage amount can be well accomplished. Great effects have been received after demonstrating in 1050 committees in Pudong, Changning, and Minhang in Shanghai.

4.2 System Introduction

Dynamic intelligent logistics system of the collection and transportation process of giant municipal garbage is consisted of three parts: intelligent on-car identification and dynamic measurement system of front-end vehicles, RFID intelligent tag system of user-side, and back-stage intelligent logistics management software of the management side. Please take reference to the system flow chart (Fig. 4.1) as below.

4.2.1 Key Technology of On-car Precise Intelligent Identification System

The purpose of designing on-car intelligent identification system is to achieve the work of automatically identifying different kinds of garbage containers (garbage can, garbage bag, etc.) precisely so that workers who collect and transport garbage can be free from burden of doing such an extra work.

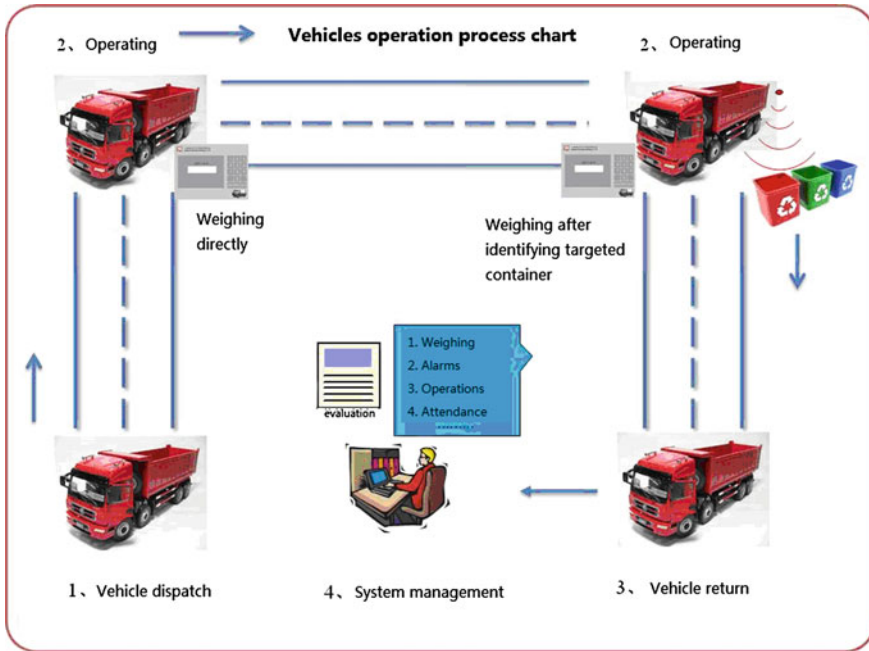


Fig. 4.1 System flow

4.2.1.1 Frequency Simulation of On-car Intelligent Identification System

To identify garbage containers in an on-car environment automatically, we need to work on how to identify different kinds of container materials in certain distance and the unique matching problem between dynamic measurement and automatic identification. Therefore, one of the most important points that can influence automatic identification is the special feature of bidirectional wireless signal transmission in an on-car environment. It makes how to choose wireless frequency for automatic identification system the most important task of all. To choose the best and the most suitable wireless frequency, four kinds of different frequency signals were researched and tested.

According to different working environment of on-car automatic identification system, we did different simulated researches to theoretically analyze features and applicability of different frequencies. The following simulated research results are distribution situations of radio frequency signals analyzed through CTLESS software in on-car environment based on 2.4 GHz, 916, 433 MHz, and 125 kHz. Figure 4.2 shows dissemination and distribution of different radio frequencies on the "Z" axis.

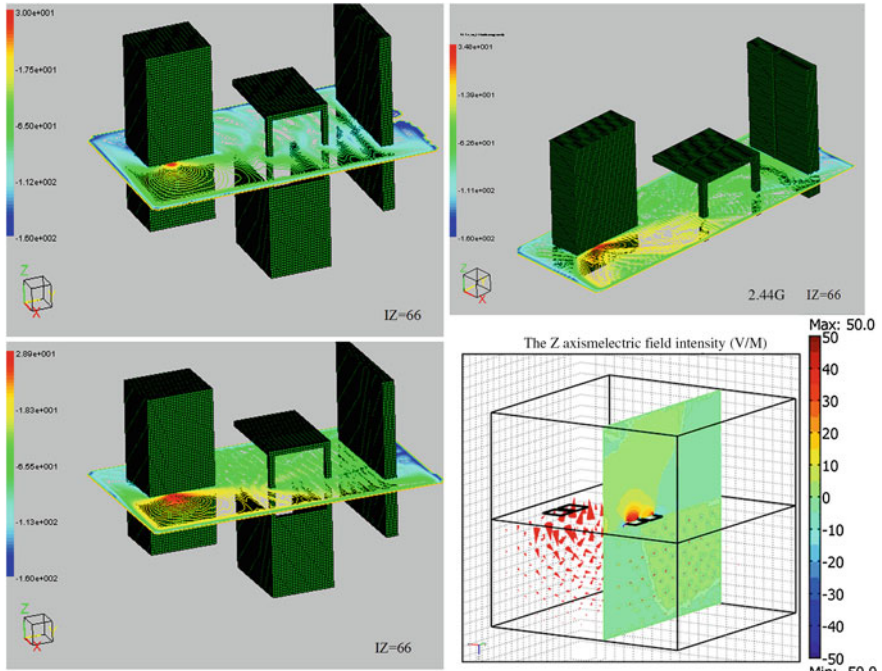


Fig. 4.2 Distribution chart of radio frequency signals in different frequencies on the “Z” axis

By implementing through simulated on-car identification, we found that none of the frequencies (433, 916 MHz and 2.44 GHz) has any advantage particularly. Dissemination efficiency is reduced by from 5 to 10 %, while the frequency is changed from 433 MHz to 2.44 GHz. However, fast-fading feature of 125 kHz has good border effect. Therefore, according to simulation results, we decided to use 2.4 GHz as the main identification frequency of active RFID because it has high speed and low power consumption. On the other hand, as an assisting positioning frequency of dual-mode active RFID, the 125 kHz frequency can satisfy the requirement for precise positioning of automatic identification. We also choose 916 MHz as the main identification frequency [3] of passive RFID, which provides conditions for different garbage containers being able to be compatible with different standards of RFID, especially when it comes to disposable containers such as garbage bag.

4.2.1.2 Design of On-car Precise Automatic Identification System

Dynamic intelligent logistics system of the collection and transportation process of giant municipal garbage requires appropriate RFID automatic identification

technology. However, the key factor to success is to implant this new technology without influencing operation habits of current garbage collecting and transporting workers. Traditional garbage trucks work on garbage cans. They lift and pour them and change for new ones after it is done. This requires unique identification of the garbage can the truck is working on precisely without hitting the other garbage cans. It is only by this way that on-car dynamic weight-measuring result can be precisely matched with practical operative goals. It also solves garbage classification and measurement problems from the origin. This is the key factor for realizing dynamic intelligent logistics system of the collection and transportation process of municipal garbage.

To realize the goal of identifying targeted container automatically in precise distance, we designed a dual-mode frequency RFID precise position identification mechanism, which combines 125 kHz and 2.4 GHz. It fully embodies the fast-fading 3D border feature of low-frequency 125 kHz signal and high-speed low power consumption feature of 2.4 GHz signal, which helps form low-frequency awakening mixing precise identification mode in a passive form.

As what is showing in Fig. 4.3, low-frequency mode under passive mode is activated by locator beacon. Ultrahigh frequency mode sends ultrahigh frequency signal with position information in it after it is activated. A reader catches and reads this signal and sends it to system platform to finish identifying and positioning electronic tag. This mixing precise position mechanism has unparalleled advantage and utility value. It can satisfy the requirement of low power consumption for electronic tag and satisfy the unique requirement for distance identification and garbage identification at the same time.

Please take reference to Fig. 4.4 for information of working mechanism of garbage can RFID tag.

This working mechanism defines four functional modes of tag: sleeping mode, channel inquiry system, semi-sleeping mode, and communication mode. Sleeping mode: A mode that all parts stop working except for timer. Channel inquiry system:

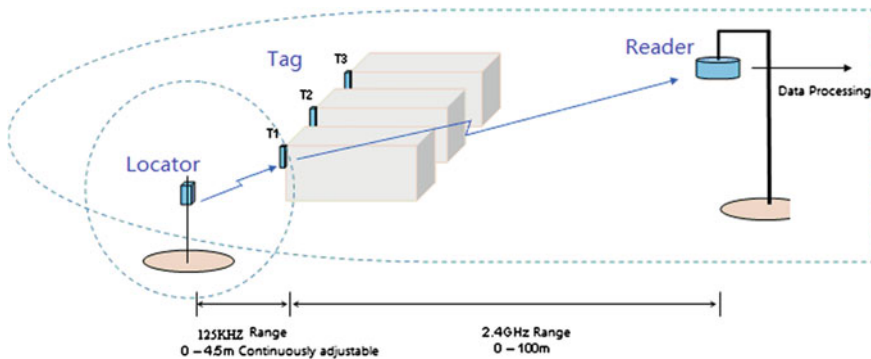
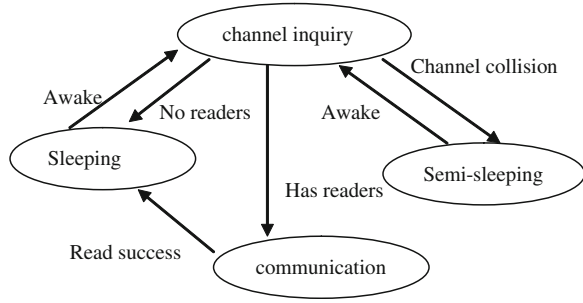


Fig. 4.3 Chart of mixing precise identification mode

Fig. 4.4 Working mechanism of garbage RFID tag



A mode that inquires valid reader signal in the channel after tag is woken up by a certain matter. Semi-sleeping mode: Temporary sleeping mode is activated when hitting another tag. Communication mode: Valid connection to reader is built up to realize data transmission.

Low-frequency radio signal in working mechanism belongs to near-field induction. Getting a long communication distance in near-field induction is a difficulty. Intensive study of main factors that have influence on valid acceptance distance in near-field induction is the key point to design a reasonable optimized 125 kHz low-frequency antenna system. Therefore, we used single-turned large coils with different diameters and receiving coil made by winding 500 turns of multiple-turned small coils around a 0.8-cm-diameter ferrite core to make the simulation and experiment. Coils were all placed horizontally. Output power loaded on transmitting coil is 216 MW. Refer to Fig. 4.5.

According to simulation and test results, we designed two sizes of dipole antenna as what is shown in Fig. 4.6. It realized an adjustable range of 0–4.5 m of 3D valid acceptance distance on small-sized low-frequency antenna, which also satisfied the requirement for mixing precise position identification working mechanism.

Fig. 4.5 Chart of low-frequency coil receiving induction energy

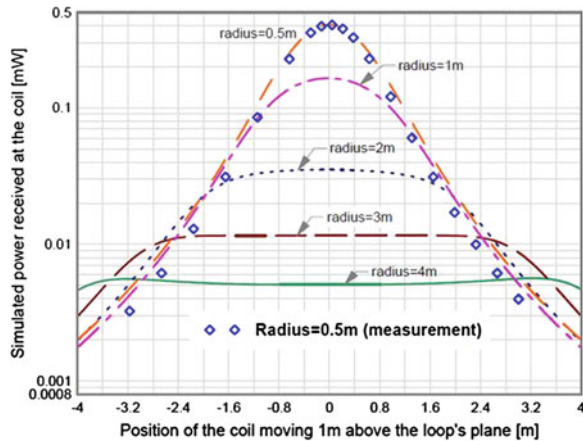
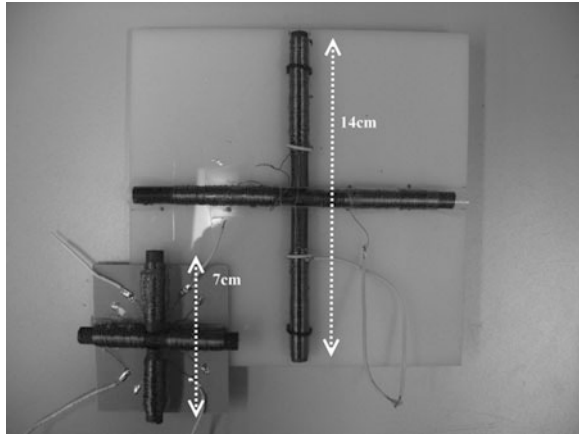


Fig. 4.6 Dipole antenna

4.2.2 Key Technology of On-car Dynamic Measurement System

4.2.2.1 Study of Sensor of On-car Measurement System

Design of on-car measurement sensor is also a difficulty during the whole researching process. It has influence on both measurement accuracy and safety and stability of refitted vehicles.

Traditional sensor is usually bolted on chassis of vehicles, which makes it only be able to support vertical force. As a result, such sensors are not available in many kinds of conditions. When a vehicle runs on a bumpy road or on a slope, traditional sensors cannot receive vertical force but component of forces. As a result, output data is smaller than actual measurement data. This is how error is produced. This error is very difficult to overcome in most situations. Meanwhile, punching on secondary beam has great impact on vehicle intensity, which also reduces safety and stability of vehicles in large scale. Besides, design of traditional sensors also makes vehicles have high requirement for strength of bolts. Vehicles suffer from complicated external forces while they are running, including pressure, pull, and alternating stress and so on. Even the strongest bolts cannot be used for a long time. Once they break, vehicles will become quite dangerous to drive.

We designed a saddle-shaped sensor after repeating tests and researches as what is showed in Fig. 4.7.

Specially designed saddle-shaped sensor has special advantage in both stress and installation:

- a. Saddle-shaped sensor has two radian stress surfaces. Meanwhile, they can produce relatively rotation. It can solve the problem of accurate measurement while vehicles are running on slopes, which also overcomes the influence on measurement system when vehicles work in complicated environments.

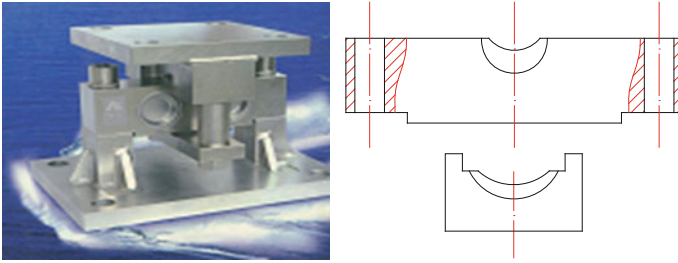


Fig. 4.7 Saddle-shaped sensor

- b. Junction surfaces on top and at bottom are of radian shape, which changes the structure of point-contact or surface-contact of traditional sensors. It is good to increase stress area and enhance stability. The advantage of radian-contact is that junction surface increases or decreases with the change of stress. It can efficiently and randomly change the junction surface area to keep vehicle stable.
- c. We can no longer fasten saddle-shaped sensor on chassis with bolts. Instead, U-bolt is used. It can avoid the influence brought by punching on secondary beam for installing sensors. It can also reduce the blade load created by using bolt, which is also a big influence on vehicle safety.
- d. For garbage trucks that are used for transporting liquid garbage, they have to suffer from big shake during the process of transportation. Shake makes mass transfer, which has big influence on measurement stability. Now, saddle-shaped sensor can well solve this problem. It can overcome the influence created by mass transfer due to its special stress method.

Great amount of experiments prove that this sensor indeed increase safety and stability, which helps the whole test achieve a satisfying result.

4.2.2.2 Research of Refitting Garbage Vehicle Model

Great discover has been found after refitting garbage vehicles (3t, 5t). Ninety percent of domestic garbage vehicles use domestically made ISUZU chassis. Most of them are refitting vehicles, in which self-discharging vehicles have two main types, rear dump, and expadump. Sensor designed by us is qualified for both types of garbage vehicles.

We choose four stress points on the chassis as the supporting point to install our sensor. Measurement method is a traditional paralleled way as shown in Fig. 4.8a. Data is output and collected through quadruple sensor. Final data is gotten after processing. Great amount of tests and experiments have been done based on the model above. However, test result is quite different from result described in this model. Therefore, according to the experiment, general measurement is based on

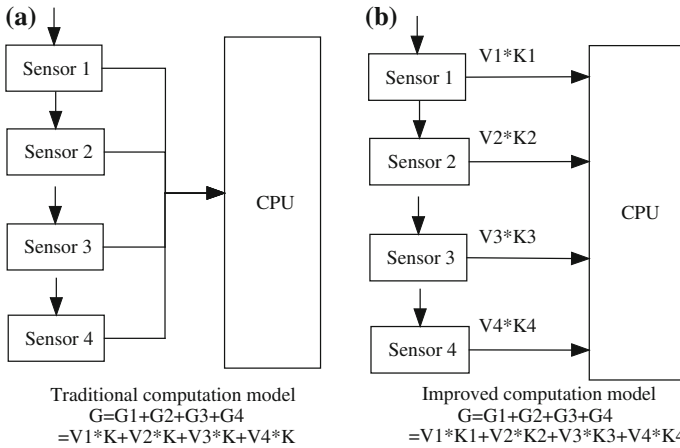


Fig. 4.8 Calculation model of on-car measurement

stress on elastomer. Traditional measurement mode is inadvisable ($G \neq G_1 + G_2 + G_3 + G_4$). This is because traditional mode is a measuring method of rigid theoretical technology. Sensors on vehicles have elastic base. Thus, it is not suitable for traditional theoretical research.

Theoretical model (Fig. 4.8b) is gotten based on above test results and experiment conclusions. The model above shows that each sensor is designed to be an independent magnifying A/D converting unit. Stress of sensor is related to weight of box: $G = G_1 + G_2 + G_3 + G_4$. This model provides supporting base to sensor as a whole elastic unit, which reasonably locates stress sensor in the gravity center position of the model. It breaks through traditional calculation model of rigid supporting base and creates accurate measuring model and calculation method based on elastic base.

Big number of tests has been done to prove the above mechanical part (Installation position as shown in Fig. 4.9), and the theory of how sensor supporting point was chosen. The best condition can be state of the whole system function and structure can be achieved by the research results above.

4.2.2.3 Design of On-car Dynamic Measuring System of Garbage Vehicles

Hardware system needs to be divided into three big units, data acquisition unit, data processing and display unit, and data management unit. Data acquisition model is placed at the bottle of vehicles. Data processing and display unit is installed in the cab. Data management unit is usually placed in vehicle management center. Five independent function modules can be divided as follows: Sensor signal magnifying circuit: magnifying small signal output by sensor and sending A/D port of

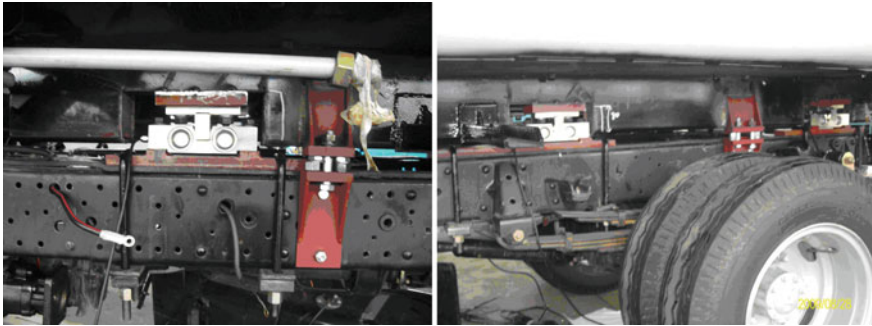


Fig. 4.9 Picture of installation position of sensor

processor. Audible-visual alarm module: this module alarms when vehicles are overloaded. Oil valve control: it is realized by controlling oil channel. Wireless data transferring module: sending weight data processed by processor to main control panel in cab. Processor: collecting magnified sensor signal and converting it into weight data and controlling related peripheral.

Data acquisition unit (Fig. 4.10a) is consisted of processor, sensor, wireless data transferring module, oil valve control, and audible-visual alarm module. Data processing and display unit (Fig. 4.10b) is consisted of main control panel, display screen, ZigBee communication module, GPS module, printer, etc. Data management unit is consisted of servers in each vehicle management station and data transceivers. It can collect vehicle data and transfer it to server in control center through internet to realize data management.

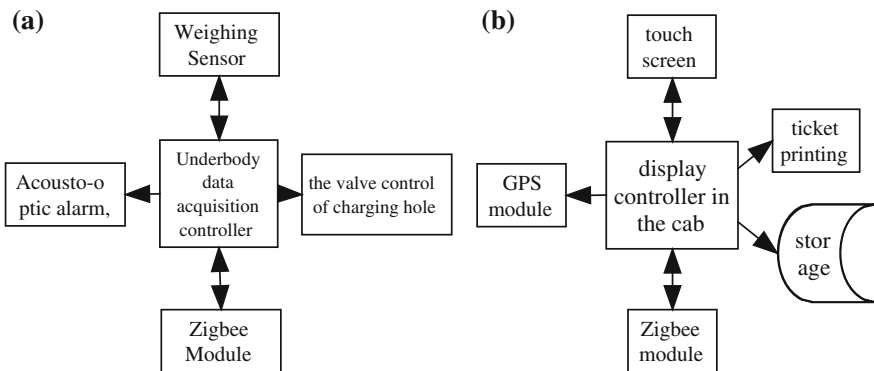


Fig. 4.10 On-car measuring system researching

4.2.3 Municipal Garbage Intelligent Logistics Management Software Platform

Intelligent logistics management software (Fig. 4.11) based on networking garbage electronic declaration uses technical means such as cross-platform open architecture and multilayer system structure. It uses vector-quantized electronic map based on WEB type to display and operate visualized data. It can also automatically produce, import, edit, plan route, page range, and configure map. Municipal garbage real-

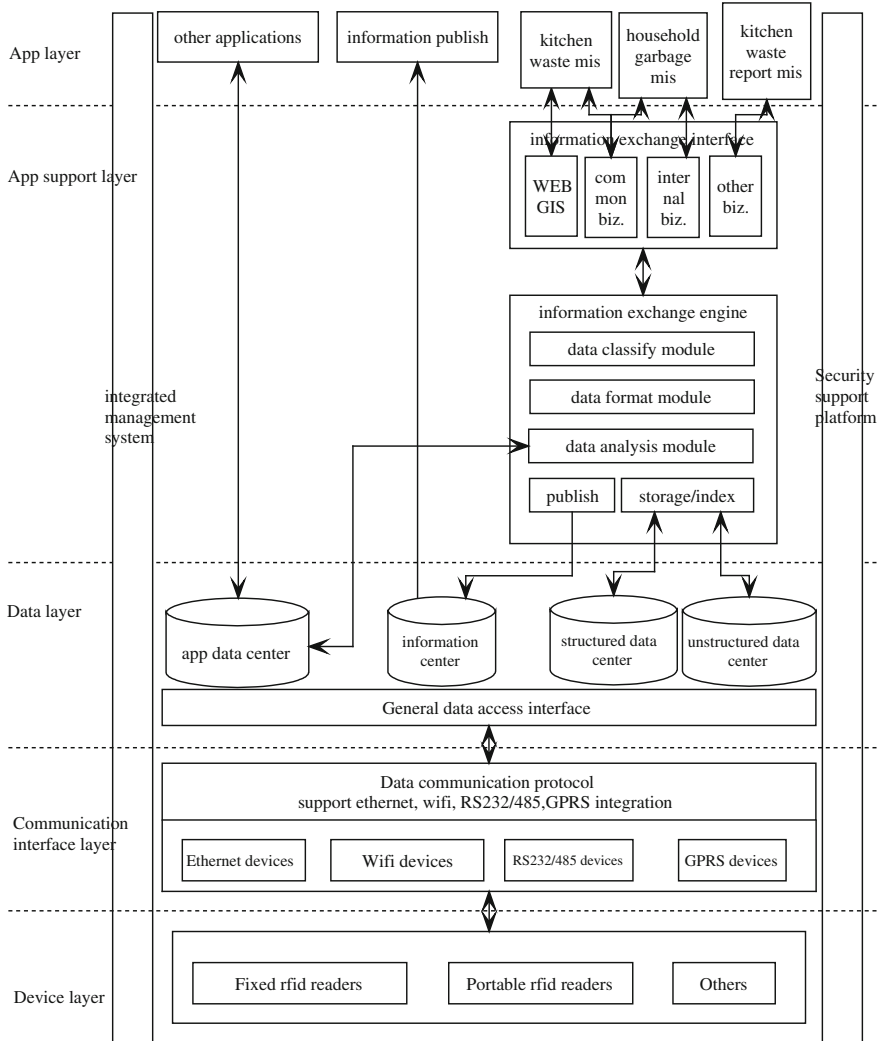


Fig. 4.11 Chart of software platform quantizing structure

time flow fine grit data acquisition unit management and monitoring is realized by integrating information issue, municipal garbage electronic declaration, classified municipal garbage collecting, and transporting management system.

4.3 Conclusion

Giant municipal garbage dynamic intelligent logistics system of the collection and transportation process of giant municipal garbage has on-car intelligent identification and dynamic measuring system as its core, and uses user-side intelligent RFID tag system to achieve automatic precise identification and dynamic weight measuring while collecting garbage. It realizes fine grit garbage logistics origin control and location tracking along the way. It cooperates with backstage logistics management system software based on networking garbage electronic declaration to provide giant municipal garbage charging with fine grit data. It is only by supporting by such a garbage intelligent logistic system with the help of economical management and scientific rewards and punishment can we truly realize garbage classification and the aim of reducing garbage amount. And it will be implemented in the whole Shanghai district gradually based on successful early-stage implementation.

Acknowledgments This task was sponsored by Ministry of Science and Technology project (2010BAK69B24) and Shanghai Commission of Science and Technology project (10DZ0583204).

References

1. Wang YK (2011) Countermeasure of municipal garbage processing methods in china at logistics angle <<Ecological Economy>> (10)
2. Yuan T (2004) Research on urban garbage logistics system <<Environmental Sanitation Engineering>> 12(1)
3. Yu L (2006) IOT Logistics management system based on RFID electronic tag <<Micro Computer Information>> 22(2)

Author Biography

Shuang Xu male, born in 1977, a doctoral candidate from Department of Computer Science and Technology of Tongji University. He majors in IOT service and data processing.

Chapter 5

Research on the Stairs Evacuation with Fluid Wave Theory

Xun Weng, Zhiyuan Su, Wenshuo Liu and Qianqing Xu

Abstract With the point of view that building's structure has different influences on evacuation, and focusing on the structural complexity of the building itself, the paper creatively divides the stairs into three basic areas from the point of architectural construction: step area, bend area, and influx area. Then, basing on the division of the stairs' architectural construction, the paper will build a new and complete evacuation model in stairs by using the theory of fluid mechanics. The fundamentals of fluid mechanics and the ideas of fluid wave will be used to penetratingly analyze the crowd's behaviors in the phases of evacuation in stairs, and the paper will finally put forward the sophisticated evacuation model using stairs in the way that build piecewise models. The new evacuation model using stairs not only can offer facilities for geotechnical analysis, but also can establish the theoretical basis to support studies on the more efficient evacuation strategy in high-rise buildings fire.

Keywords Fluid wave theory · Stairs evacuation · Model research

5.1 Background

In recent years, with rapid economic development, China's urbanization is gathering pace, which the most obvious phenomenon is the height of the buildings in all city of China grow quickly. The spring up of high-rise buildings not only can

X. Weng (✉) · Z. Su · W. Liu

School of Automation, Beijing University of Posts and Telecommunications, No 10, Xitucheng Road, Haidian District, Beijing 100876, People's Republic of China
e-mail: wengxun79@163.com

Q. Xu

School of Information and Communication Engineering, Beijing University of Posts and Telecommunications, No 10, Xitucheng Road, Haidian District, Beijing 100876, People's Republic of China

largely save our resources of urban land, but also provide the modern of urban space and functionality. While, as the high-rise buildings have lots of complexity in construction and functionality, besides of the related technology and the security of support equipment are not excellent enough, once the high-rise buildings catch fire, the fire easily spread widely and stereoscopically, which will cause big trouble in rescue operation of fire departments [1, 2].

So far, the only worldwide accepted way of emergency evacuation is that the affected should evacuate from the building by stairs. But as the stairs have the characteristics of structural complexity and limited space, stairs are considered as the bottleneck of the whole evacuation. How to improve the evacuation’s efficiency of the crowd moving in the stairs has become an important problem worried to be solved. The paper basing on the analyzing the stairs’ architectural construction, the fundamentals of fluid mechanics, and fluid wave will be used to study the evacuation of the crowd’s movement in stairs, offering security to the more efficient and more secure evacuation planning in future.

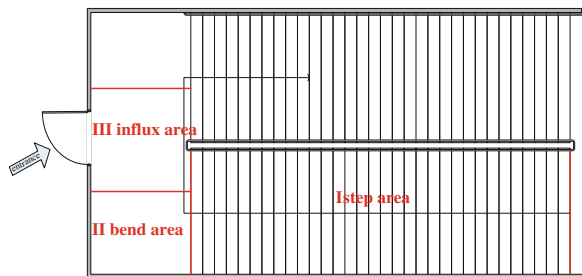
5.2 Evacuation Model Using Stairs

Stairs have the characteristics of structural complexity and limited space, thus not only can impact the crowd’s behavior trajectories in the stage of evacuation by stairs, but also can directly change the moving speed of crowd, even can reduce the efficiency of the evacuation [3]. For these reasons, with the point of view that building’s structure has different influences on evacuation, the paper divides the stairs into three basic areas from the point of architectural construction as follows:

- I. step area
- II. bend area
- III. influx area (Fig. 5.1)

In the stair structure, generally, there are one exit and two entrances. The one exit connects the upper floor to lower floor; the two entrances are that: one entrance connects the upper floor to lower floor and the other entrance is the influx entrance by which people come from this floor to stair hall. The structure schematic above is

Fig. 5.1 The three basic areas of architectural construction



gotten referring to the ordinary buildings; structure schematic about these special structures also is a flexible combination with these three basic areas. As the three basic areas have different influences on evacuation, the paper will further analysis, respectively.

Basing on the stairs' architectural construction, the paper will build a new and complete evacuation model in stairs by using the theory of fluid mechanics. The evacuation model that the paper built not only can offer facilities for geotechnical analysis, but can also establish the theoretical basis to support studies on the more efficient evacuation strategy in high-rise buildings fire.

Studying the observation to real evacuation, we always find that the certain behaviors of the crowd are very similar to the theory of fluid in fluid mechanics. In the real evacuation, each individual needs the necessary space environment for themselves; once arrive to the some structure of the building, the crowd also can generate the phenomenon of lower speed, and the phenomenon will propagate backward soon; in the crowd, one individual cannot climb over the one before him to keep moving forward, and so on. Basing on the many similarities between the crowd in the evacuation and fluid mechanics, the paper will analyze the movement in the evacuation of the crowd referencing the relevant theory of fluid mechanics. Considering the characteristic of three basic areas, on the basis of using theory of fluid mechanics uniformly, the paper will discuss the behavior of the crowd in the evacuation by stairs.

5.2.1 Evacuation in Step Area

The step area of stairs has its unique characteristic in structure: There is not only difference in height between adjacent steps, but also the distance change in the horizontal direction. In order to accurately describe the behavior characteristic of the crowd in this area, the architectural structure must be analyzed first. In this stage, there are not obvious obstructions in front of the crowd, the movement of the crowd is much more regular, the people always move forward at a constant speed. With lots of actual observations and theoretical analysis, the paper put forward that in the step area, a pace-covered one step is the most efficiency and secure way to pass the step area. The reason can be described as follows:

1. For different buildings, the design of the step in the step area is not unique, that means the height and the width of the steps are not same. Even to some building, the dimension of step is not designed reasonable; thus, a pace-covered numbers of steps is so difficulty.
2. In step area, a pace-covered numbers of steps will expend more energy and strength of the individuals in crowd, which can greatly increase the risk of injury in the evacuation. For example, the fault of pace often will cause individual's ankle injury even tumble. So that will bring about a congestion point in stairs, and this will directly reduce efficiency of the whole evacuation.

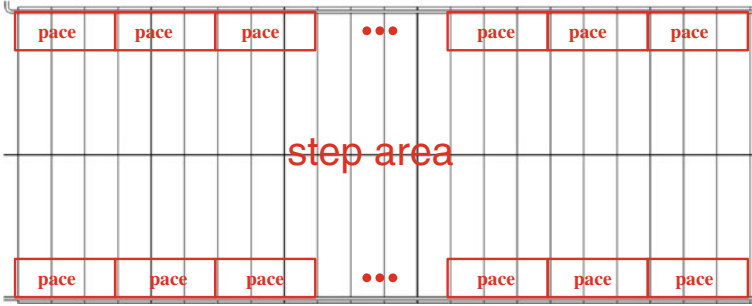


Fig. 5.2 The example of the relationship between movement space and move speed

- 3. In the step stage, as there are the characteristic of laddering structure in this area, the space seems much more limited. If the individual choose a pace-covered numbers of steps, thus will cost more available space in the moving direction. The two problems will be caused as follows:
 - (1) As the individual increase the space needed to move forward, it will reduce the rate of accommodate per unit area for individuals, the number of each stair accommodated will become smaller, and the efficiency of evacuation will be reduced finally. It can be described as Fig. 5.2.
 - (2) In the real evacuation, it is impossible that all the individuals keep the same tempo and frequency; thus, a pace-covered numbers of steps will further reduce the use efficiency of the space in the stairs (Fig. 5.3).

The paper attempts to in macroscopic view discuss the theoretic time for the crowd needed to evacuate using stairs in the case high-rise buildings fire and establishes the theoretical basis to support further studies and engineering practices.

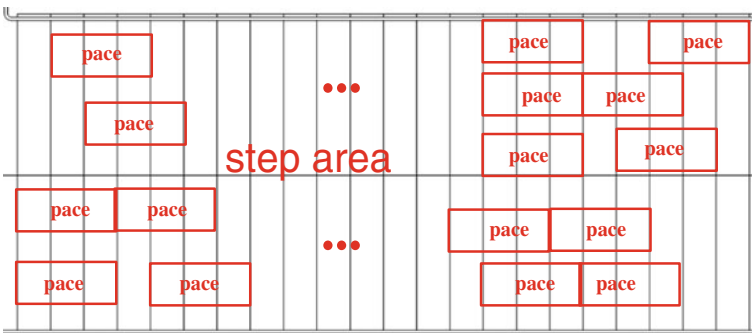


Fig. 5.3 The influence of multi-number steps in stairs evacuation

So, based on the above three reasons, the paper considers that the crowd will choose the way that a pace-covered one step to pass the step area.

Thus, the speed and time formula for the crowd in the step area can be obtained as follows:

$$V_{\text{step}} = B \times f \tag{5.1}$$

$$t_{\text{step}} = N/f \tag{5.2}$$

5.2.2 Evacuation in Bend Area

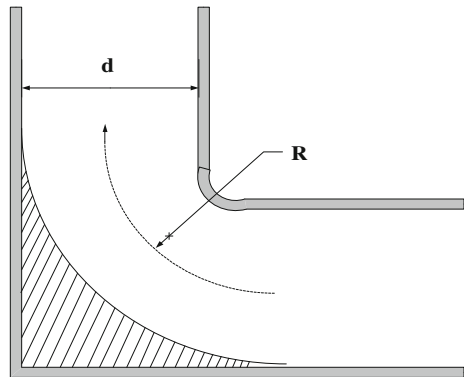
The bend area is a specific area in the evacuation using stairs, once the crowd reach the area will not only change their direction of motion, but also further lower their moving speed because of the right-angle turn in stairs. When the crowd pass the right-angle turn, due to the effect of centrifugal force, also considering the observation of the crowd’s moving law in the real evacuation, the actual evacuation route of the crowd can be described as Fig. 5.4: that means in the real evacuation, the crowd will move along the blank area in Fig. 5.4.

When the crowd passes the bend area, the moving track will change due to the natural instincts that people will avoid impacting to wall and the effect of centrifugal force, which will reduce the speed of the crowd in this area. The phenomenon is much more similar to the theory of head loss in fluid mechanics. When the fluid pass the right-angle turn, much loss of energy will be generated. The reason of loss may be the collision loss, turning loss, eddy current loss, and so on. The paper will study the speed of the crowd in the bend area using the theory of fluid mechanics [4].

$$h = \zeta \frac{v^2}{2g} = k \frac{\theta}{90^\circ} \frac{v^2}{2g} \tag{5.3}$$

In the formula, θ is the turning angle, and when $\theta = 90^\circ$, we can get

Fig. 5.4 The actual evacuation route of the crowd



$$k = \zeta = \left[0.131 + 0.163 \left(\frac{d}{R} \right)^{3.5} \right] \quad (5.4)$$

d is the diameter of the bend, R is curvature radius of the bend's neutral line, then the Formula (5.4) can be changed as follows:

$$h_{\text{bend}} = \zeta \frac{v^2}{2g} = \left[0.131 + 0.163 \left(\frac{d}{R} \right)^{3.5} \right] \frac{v^2}{2g} \quad (5.5)$$

Also the loss of energy in the actual evacuation will directly affect to the loss of speed:

$$\frac{1}{2} m V_{\text{bend}}^2 + h_{\text{bend}} = \frac{1}{2} m V_{\text{step}}^2 \quad (5.6)$$

Then, the Formula (5.6) can be expressed as:

$$V_{\text{bend}} = \sqrt{V_{\text{step}}^2 - \frac{2h_{\text{bend}}}{m}} \quad (5.7)$$

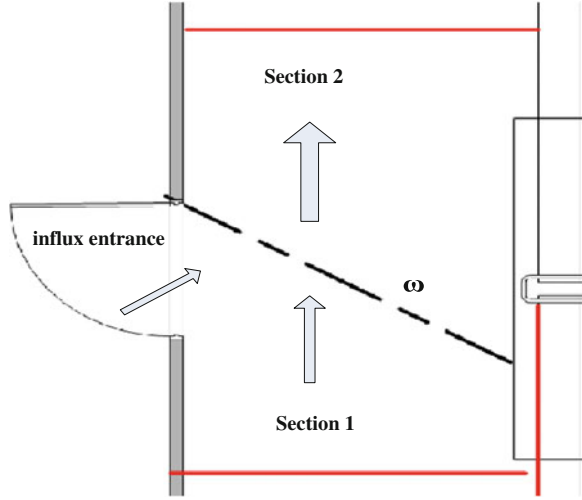
There m is average weight of individual, and the value of it can reference relative standard in the same period.

5.2.3 Evacuation in Influx Area

When the crowd does not reach bottleneck area, the movement of the crowd is much more regular, and the people always move forward at a constant speed. But in the actual evacuation, there is often phenomenon of congestion, chaos even block in the bottleneck area. That is because that as soon as the crowd reach the bottleneck area, a wave that spreads opposite to moving direction of the crowd can be generated, which is similar to phenomenon that sound wave meets an obstacle and reflex or the phenomenon that current meets obstacles and flow backward. The phenomenon in the bottleneck area can be explained by the theory of fluid wave in fluid mechanics. The wave can cause turbulence phenomenon in the area ahead of the bottleneck, and that is wave behavior of the evacuation crowd, which we called the phenomenon of evacuation wave.

When the original crowd reaches the influx area, showed in the Fig. 5.5, a new crowd will join the original crowd, while the density and speed of these two crowds are not same at all. The interface of these two parts whose densities are different is called evacuation wave. This evacuation wave will spread backward one by one, which we called the wave evacuation crowd, and its speed is called wave speed.

Fig. 5.5 Describe the process of evacuation in the influx area



The paper will build a new evacuation model in influx area by using the theory of fluid mechanics in order to describe the process of evacuation in this area. Then, the influx area will be studied separately, as shown in Fig. 5.5.

In the Fig. 5.5, the direction of movement is from below to above, which is considered as positive direction. As this consideration, the number of person per unit distance in evacuation route is considered as linear density of crowd, which is expressed as character ρ .

$$v_{sp1}\rho_1t + v_{spm}\rho_n t = v_{sp2}\rho_2t \tag{5.8}$$

Where v_{sp1} is the speed of crowd in Sect. 5.1 relative to boundary w ; ρ_1 is the linear density of crowd in Sect. 5.1; v_{spn} is the speed of crowd in influx entrance relative to boundary w ; ρ_n is the linear density of crowd in influx entrance; v_{sp2} is the speed of crowd in Sect. 5.2 relative to boundary w ; ρ_2 is the linear density of crowd in Sect. 5.2. Then, the Formula (5.8) can be expressed as:

$$(V_{bend} - V_w)\rho_1 + (V_{inflow} - V_w)\rho_n = (V_{flow} - V_w)\rho \tag{5.9}$$

V_{bend} is the speed when the crowd enter the influx area; V_{inflow} is the speed when the crowd pass the influx entrance; V_{flow} is the speed when the crowd leave the influx area Also get:

$$V_w(\rho_2 - \rho_1 - \rho_n) = V_{flow}\rho_2 - V_{bend}\rho_1 - V_{inflow}\rho_n \tag{5.10}$$

$$V_w = V_{flow}\rho_2 - V_{bend}\rho_1 - V_{inflow}\rho_n / (\rho_2 - \rho_1 - \rho_n) \tag{5.11}$$

Studying the Formula (5.11), the paper finds that in the actual evacuation by stairs, the evacuation wave that is opposite to evacuation direction is not wanted;

thus, some structural characteristics should be improved in order to reduce the possibility of from the evacuation wave. In an ideal world, we can set $V_w = 0$, then

$$V_{\text{flow}} = V_{\text{bend}}\rho_1 + V_{\text{inflow}}\rho_n/\rho_2 \quad (5.12)$$

5.3 Conclusions

Stairs are considered as the most traditional and reliable tool of evacuation and its result is much important to the whole evacuation, relating directly to lives and property of people. According to the influence to crowd, the paper divides the stairs into three basic areas from the point of architectural construction in order to study the crowd's behavior of evacuation in these three areas using the relevant theory of fluid mechanics. Enlightenments can be obtained as follow:

First, in the step area, with the practical observation and theoretical analysis, the paper suggests that the crowd should choose the way that a pace-covered one step to pass the step area. Thus, it not only can reduce the probability of injured in evacuation for individuals to improve the reliability, but also can decrease the space needed for individuals to increase the efficiency of evacuation.

Second, once the crowd reaches bend area in stairs, due to the natural instincts that people will avoid impacting to wall and the practical architecture, the crowd will pass the area along a sector region. Some measures that change the architecture reasonably can at different levels improve the effect of passing this area in evacuation; they amplify turn radius, change inboard wall reasonably, and choose better shape of handrail.

Third, as a new crowd will join the original crowd in the influx area, an evacuation wave that is opposite to evacuation direction will be caused in this area. The evacuation wave may shape congestion in this area, directly reduce the efficiency of the whole evacuation. In practical evacuation, the evacuation wave is not wanted by us. Thus, we can take some measures that design the number of stairs reasonably, scatter the amount of crowd in one stair entrance, and so on, in order to maximum reduce the possibility of formation of the evacuation wave. About the more practical laws of evacuation in this area should be further studied by us.

The paper attempts to deep study the evacuation characteristics of the crowd showed in the evacuation using stairs. It not only helps us to establish more rigorous and efficient evacuation strategy and provided convenience to engineering calculation, but also can put forward renovation projects focusing on the security risk of buildings in evacuation. But as the influences that the crowd suffered in the so narrow stairs are too much miscellaneous, nowadays many knowledge and theory cannot cover and interpret the characteristic of behavior. The relevant research will be continued deep in future.

Acknowledgments This work was supported by the Project of Beijing University of Posts and Telecommunications “Youth Innovative Research Program” (2012RC0502).

References

1. Dan Z (2009) Research on safety evacuation in corridor of fire period. Shanxi Archit 35 (18):33–36
2. Zheng XP, Zhong TK, Liu MT (2008) Review on the simulation approaches of crowd evacuation. J Syst Manage 17(6)
3. Bao QF, Chen J (2010) Macroscopic approach for modeling the effect of obstacles on room evacuation. J Saf Environ 10(6)
4. Mingyuan Z (2010) Fluid mechanics. Higher Education Press, Beijing

Chapter 6

An Approach to Integrated Cellular Layout Design Based on Logistics Cost Optimization

Yongqian Zheng, Kuixue Ding and Kefeng Cen

Abstract Cellular layout includes inter-cell and intra-cell layouts. This paper presented a multi-objective-integrated optimization model that minimizes the total material handling distance and the area of the cellular layout. To avoid the decrease of the solution set of cellular layout problem by solving the inter-cell and intra-cell layouts separately, the proposed model solves the two steps simultaneously. To handle the complexity confronted with the large-scale model, a structured real-code cooperative particle swarm optimization (CPSO) was proposed, the particles were divided into genic particles and non-genic particles, operations of genetic algorithm (GA) were applied on the two kinds of particles, and the performance of the particle swarm optimization was improved largely. Simulation experiment verified the validity of the model and algorithm.

Keywords Cellular layout · Integrated optimization · Multi-objective optimization · Cooperative particle swarm optimization · Co-evolution

6.1 Introduction

As the rapidly increased worldwide competition, the traditional manufacturing systems, such as job-shop and flow-shop, are hard to satisfy the newly emerged needs of manufacturing systems [1]. To meet these challenges, a company must be able to offer perfect quality products at lower cost than competitors and still remain efficient and flexible [2]. To achieve this goal, new manufacturing systems must be designed. In recent years, many advanced manufacturing technology have been proposed. Among them, cellular manufacturing systems (CMSs) combine the advantages of a job-shop's flexibility and a flow-shop's efficiency and are considered one of the manufacturing systems that can meet the above challenges [3].

Y. Zheng (✉) · K. Ding · K. Cen

Department of Industrial Engineering, School of Mechanical Engineering, Tongji University,
Shanghai 200092, People's Republic of China
e-mail: yongqian@tongji.edu.cn

According to Wemmerlov and Johnson [4], the implementation of CMSs provides the opportunity of decreasing material handling cost, work in process, setup time, lead time, and throughput time.

The design for cellular manufacturing involves three stages: (1) grouping of parts and production equipment into cells (cell formation), (2) allocation of the cells within the shop floor (inter-cell layout), and (3) layout of the facilities within each cell (intra-cell layout) [5], while the intra-cell and inter-cell layouts not received attention of researchers in comparison to cell formation in cellular manufacturing systems (CMSs). The purpose of this paper is to solve the facility layout problem in a cellular manufacturing system.

Alfa et al. [6] formulated a model for solving only an intra-cell layout problem. Das [7] formulated a model for solving inter-cell layout problem. Kaebernick [8] proposed a nonlinear goal programming to integrate inter-cell and intra-cell layout problems. Won [9] proposed a linear programming model and minimal backward flow model in order to find an optimal linear machine sequence in a machine cell. A solving method for the model was also proposed.

Wang et al. [10] proposed a new approach based on simulated annealing in order to solve inter-cell and intra-cell layout problems in CMSs. Bazargan-Lari et al. [11] presented the application of an integrated approach to three phases of a design of CMSs to a white-goods manufacturing company in Australia. Sangwan and Kodali [12] formulated the facility layout, both inter-cell and intra-cell as a quadratic assignment problem.

6.2 Problem Formulation

This section formulates the mathematical model for both intra-cell and inter-cell layout problems. The assumptions are described as follows: (1) Cell formation is first completed and known as a prior, i.e., what kinds of facilities belong to which cells are known. (2) The facilities are considered to be rectangular blocks; the orientation of the facility is considered to be horizontal or vertical. (3) Each cell is laid out in U-shape, and the multi-rows strategy is applied on the inter-cell layout. (4) Each cell adds a buffer area to increase the equipment effectiveness. (5) Parts are moved in batches between the equipments, and the flow of materials is static and deterministic.

6.2.1 Variables and Symbols

The variables and symbols used in the model are defined as follows: p is the index for parts ($p = 1, 2, \dots, P$); c is the index for cells ($c = 1, 2, \dots, C$); i, j is the index for facilities ($i, j = 1, 2, \dots, M$); $i \neq j$, (x_i, y_i) is the coordinate of the center of facility i ; (x_{ib}, y_{ib}) is the left-bottom coordinate of the facility i ; (x_{jt}, y_{jt}) is the right-top coordinate

of the facility j ; n_{ij}^p is the number of trips made by material handling between facilities i and j when produce part p ; V_p is the demand of part p ; and H_p is the handling batch size for part p .

6.2.2 Problem Objectives

6.2.2.1 Traveling Distances

In this model, rectilinear distances between centers of the facilities are used to evaluate the traveling distances. In most CMSs, the parts are often moved in batch. The total traveling distance can be described as:

$$\sum_{i=1}^M \sum_{j=1}^M \sum_{p=1}^P n_{ij}^p [V_p/H_p] (|x_i - x_j| + |y_i - y_j|) \quad (6.1)$$

6.2.2.2 Cellular Layout Area

The location of the facilities should consider the principle of closeness, i.e., the high usage of the shop floor is pursued. The shop-floor area utilization rate can be described as:

$$\max \sum_{i=1}^n S_i/S \quad (6.2)$$

S_i , S represent the area of facility i and the total area of final cellular layout, respectively. Due to the area of each facility is constant, so the formula is equal to $\min S$. S can be described as:

$$S = [\max(x_{jt}) - \min(x_{ib})] \cdot [\max(y_{jt}) - \min(y_{ib})]; \quad i, j = 1, 2, \dots, M \quad (6.3)$$

6.2.2.3 Objective Function

To minimize the total material handling distances and the total area of the final layout, a multi-objective optimization is proposed. Consider the two objective functions as only one function, the following measure was adopted:

$$\eta = 1 / \sum_{i=1}^M \sum_{j=1}^M \sum_{p=1}^P n_{ij}^p \cdot l_i \cdot [V_p/H_p] \quad (6.4)$$

$$\mu = 1 / \sum_{i=1}^n S_i \quad (6.5)$$

$$\text{minz} = \alpha \cdot \eta \cdot \sum_{i=1}^M \sum_{j=1}^M \sum_{p=1}^P n_{ij}^p \cdot \text{ceil}(V_p/H_p) \cdot d_{ij} + \beta \cdot \mu \cdot S \quad (6.6)$$

In objective (6.6), η and μ are used to align the range of total material traveling distance with the area of the layout. They are obtained from formula (6.4) and (6.5). At the same time, α and β stand for the weight of the two objectives. They are set by the decision-makers. Here, $\alpha + \beta = 1$.

6.2.3 Problem Constraints

6.2.3.1 Constraints of Intra-cell Layout

The assumptions are described as follows: (1) In each cell, the facilities are laid out in U-shape; (2) There are two kinds of orientation for each facility: horizontal or vertical; (3) The loading point is the same as the unloading point, that is, the center of the facility; (4) The facilities within the same side have the same value of Y-axis.

If the facilities i, j are within the same side, they should meet the constrain:

$$|x_i - x_j| \geq (h_i + h_j)/2 + dh_{ij}, y_i = y_j \quad (6.7)$$

Otherwise, the constrain is changed to

$$|y_i - y_j| \geq (v_i + v_j)/2 + dv_{ij}, y_i \neq y_j \quad (6.8)$$

dh_{ij} and dv_{ij} respectively are referring to as the safety distance in X-axis and Y-axis, respectively; h_i and v_i are defined as follows:

If facility is positioned horizontally, $h_i = l_i$, $v_i = w_i$, if facility is positioned vertically, $h_i = w_i$, $v_i = l_i$. Constrains (6.7) and (6.8) aim to keep the facilities in a safety distance.

6.2.3.2 Constraints of Inter-cell Layout

The multi-rows strategy is applied on the inter-cell layout. The assumptions are described as follows: (1) Each cell is considered to be rectangular blocks; (2) The center of each cell has the same Y-axis value when the cells are located in the same row; (3) If the sum of the safety distance and the length of all cells in the same row exceed the length of shop floor, the last cell in this row will be relocated in the next

row. Here, by introducing the extended cellular model, the original cellular model is stretched longer and wider based on the safety distances in the X-axis and Y-axis. Distance between the centers of the adjacent cells is represented by d , while L_c and W_c , another two parameters of the model, are the length and width of the extended cellular model. For each manufacturing cellular model, the following constrains should be met:

$$S_{cr} = \begin{cases} 1, & \text{cellular } c \text{ is in row } r \\ 0, & \text{otherwise} \end{cases} \quad (6.9)$$

$$\sum_{r=1}^R S_{cr} = 1, \quad c = 1, 2, \dots, C \quad (6.10)$$

$$\sum_{c=1}^C S_{cr} \leq C, \quad r = 1, 2, \dots, R \quad (6.11)$$

$$[x_{cb} - (x_{c'b} + L_{c'b})] \cdot [(x_{cb} + L_{cb}) - x_{c'b}] \geq 0, S_{cr} = S_{c'r} \quad (6.12)$$

$$[y_{cb} - (y_{c'b} + W_{c'b})] \cdot [(y_{cb} + W_{cb}) - y_{c'b}] \geq 0, S_{cr} \neq S_{c'r} \quad (6.13)$$

$$x_{cb} + L_c \leq \max_x \quad (6.14)$$

$$y_{cb} + W_c \leq \max_y \quad (6.15)$$

Constrain (6.10) makes sure that each facility location is assigned only one row; constrain (6.11) ensures the number of cells in each row is less than the total number; constrain (6.12) makes sure the cells c and c' are not overlapped in x-projection if they are in the same row; constrain (6.13) ensures the cells c and c' are not overlapped in y-projection if they are in the different rows; constrains (6.14) and (6.15) make sure the facilities are laid out within the provided area.

6.3 Proposed CPSO Algorithm

6.3.1 Cooperative Particle Swarm Optimization

Basic PSO is easily stuck in local optimal solution. To improve the performance of the basic PSO, this section proposed an improved cooperative particle optimization (CPSO).

In CPSO, the particles are split into several populations, and in each population, the particles evolve as basic PSO. In every iteration, the best solution is selected from all of the particles, the Gbest is updated if the current solution is better than Gbest.

The GA's idea in research literatures [14, 15] is added to the PSO, inspired by them, here absorb the operations of selection and crossover of GA to improve the performance of the CPSO. The algorithm selected the genic particles and the same quantity of non-genic particles into a pool. Here, define $p1$, and $p1$ are parents that are selected from the genic and non-genic particles randomly; q is a constant in intervals (0, 1). For child x_i , the j -dimension x_{ij} is created according to the following rule: if $\text{rand}() < q$, $x_{ij} = p1_j$, else $x_{ij} = p2_j$. The newly created children are used to replace the equal number of non-genic parents, and the genic parents are kept unchanged.

6.3.2 Particles Encoding/Decoding

Here is a structured real-code method of encoding. Figure 6.1 illustrates an example of encoding.

Each part of the encoding is explained as follows:

- (1) Encode the inter-cell layout. This part is a string of real number at the length of C , each of the real number represents a manufacturing cell. When decoding, the number is ranked decreasing, the arrangement of the serial number equates the sequence of the manufacturing cells.
- (2) Encode the intra-cell layout. This part is a string of real number at the length of M ; each of the real number represents a facility. The ranking of the real number represents the sequence of the facilities.
- (3) Encode of the orientation of the facility. This part is a string of integers at the length of M ; the arrangement of the facilities is the result of the encoding of inter-cell and intra-cell layouts, while each integer represents the orientation of the corresponding facility. If the integer is an odd number, then the orientation of the facility is horizontal, otherwise the facility will be placed vertically.

This section illustrated an example of 7 facilities. The cell formation is a known condition. The result of cell formation is as follows: $c1 = \{1, 4, 5\}$, $c2 = \{3, 6\}$, and $c3 = \{2, 7\}$. From Fig. 6.1, the encoding of the inter-cell layout is (10.5, 3.2, 11.6), the ranking of three number is 2-1-3, which equates the arrangement of the manufacturing cells; the encoding of the intra-cell layout is (2.1, 1.3, 13.6, 0.3, 8.2, 3.5, and 1.6), according to the ranking, the arrangement of the facilities is 6-3 |5-1-4|7-2; the encoding of the orientation of facility is (2, 7, 3, 4, 15, 19, and 10), after the identification of the odd number and even number, the orientation of the facilities is decoded as follows: vertical-horizontal- horizontal- vertical- horizontal- horizontal- vertical.

inter-cell	10.5	3.2	11.6				
intra-cell	2.1	1.3	13.6	0.3	8.2	3.5	1.6
orientation	2	7	3	4	15	19	10

Fig. 6.1 Example of the encoding of a particle

6.3.3 The Solution Procedure of the Proposed CPSO

This paper uses the improved CPSO to solve the cellular layout problem; the workflow of the proposed CPSO is as follows.

- Step 1: Parameters Setting and Initialization. Set evolutionary environment, such as pop_size (size of population), max_gen (maximal generation for a run), pop_num (number of population), p (ratio of the genic particle), initiate the position and the velocity of the particles. The number of iterations that Gbest has not been optimized is set by $n = 0$.
- Step 2: Check the total number of iterations, if it reaches the max_gen, output result and stop, else go to step 3.
- Step 3: Check that if the Gbest has not been optimized for N iterations in a row, if yes, then output the result and stop, else go to step 4.
- Step 4: For each population, update the position and velocity of the particles.
- Step 5: For each population, if the current position of the particle is better than the Pbest, reset the Pbest.
- Step 6: Compare the Pbest of each population with the Gbest, once one the Pbest is better than the Gbest, reset the Gbest.
- Step 7: According to the ratio of genic particles, divide the particles into genic particles and non-genic particles.
- Step 8: Operator of GA is applied on genic particles and non-genic particles.
- Step 9: The new-generated offspring is used to replace the equate number of non-genic particles randomly.

6.4 Case Study

The facilities in each manufacturing cell and the size of each facility are described as Table 6.1; the routing of each part is listed in Table 6.2.

Set the max_gen = 1,000, the size of the population = 60, the number of population is 4, the ratio of genic particles is 0.4, the maximal iteration that the Gbest has not been updated in a row is $N = 300$, the velocity constants $c1 = c2 = 2$, inertia weight w_{max} and w_{min} equate 0.9 and 0.4, respectively, the weight of handling distance $\alpha = 0.7$, and the weight of area $\beta = 0.3$. The shop floor can be seen as a rectangle with the area of 25 m \times 20 m; the safety distance between the facilities in the same manufacturing cell is 1.2 m, while the safety distance between the manufacturing cells is 3.0 m, the buffer area in each cell is also seen as a rectangle with the size of 2 m \times 2 m.

The traditional approach is solving the intra-cell layout problem firstly, arranging the facilities of each cell to minimize the handling distance within the cell. Then, the inter-cell layout problem is solved by minimizing the total handling distance. Wang [10] used the simulated annealing to solve the cellular layout problem; the paper did not consider the orientation of the facility and the buffer area. To verify

Table 6.1 Facilities in each manufacturing cell and the size of each facility

Cell	Facilities in cell and the size of facility (m ²)
C1	$m_1 (2.5 \times 1.5), m_2 (3.0 \times 1.6), m_9 (3.5 \times 2.5), m_{13} (2.2 \times 2.0), m_{17} (3.0 \times 1.5)$
C2	$m_3 (2.5 \times 1.5), m_8 (3.0 \times 2.8), m_{10} (3.5 \times 1.5), m_{11} (4.0 \times 3.0), m_{15} (2.2 \times 2.0), m_{18} (2.5 \times 2.0), m_{20} (3.5 \times 2.0)$
C3	$m_4 (3.0 \times 1.5), m_5 (3.0 \times 2.5), m_6 (2.5 \times 1.5), m_7 (2.5 \times 1.5), m_{16} (2.2 \times 2.0)$
C4	$m_{12} (4.0 \times 3.0), m_{14} (2.2 \times 2.2), m_{19} (3.5 \times 2.0)$

Table 6.2 The process paths of the parts

Part	Demand/Handling batch	Routing
A	100/10	$m_3-m_8-m_{20}-m_{11}-m_{15}-m_{18}-m_{19}$
	90/10	$m_4-m_7-m_6-m_{16}-m_5-m_{20}$
	180/15	$m_1-m_2-m_9-m_{13}-m_{17}$
	280/20	$m_3-m_8-m_{20}-m_{11}-m_{15}-m_{18}-m_{10}$
	140/10	$m_1-m_3-m_{14}-m_{19}-m_{12}$
	160/20	$m_1-m_2-m_{17}-m_9-m_{13}$
	200/20	$m_{14}-m_{19}-m_{12}$
	180/15	$m_1-m_2-m_5-m_{17}-m_9-m_{13}$
	220/20	$m_1-m_2-m_{17}-m_9-m_{13}$
	120/10	$m_3-m_{11}-m_8-m_{10}-m_{20}-m_{15}-m_{18}$
	240/10	$m_4-m_5-m_7-m_6-m_{16}$
	150/15	$m_{14}-m_{19}-m_{12}-m_{20}$
	160/20	$m_2-m_5-m_7-m_6-m_{16}$
	220/20	$m_{12}-m_{14}-m_{15}-m_{19}$

the validity of the model and proposed algorithm, here use the basic PSO and improved CPSO to solve the three solutions of cellular layout, respectively. There is one point which should be emphasized, it is the value of the population number n will influence the result. If the value is too small, the communication among the manufacturing will be waken, while if the value is too large, the communication among the particles in the same manufacturing cell will be waken as well. The effective of cooperative will reduced. In this section, set $n = 3, 4, 5$, respectively, to illustrate the impact of the value of n .

Use the basic PSO and improved CPSO to solve three solution of cellular layout problem for 30 times; the results are listed in Table 6.3. Figure 6.2 demonstrates the distribution of the value of objective function when solving the three models under the condition of $n = 3, 4, 5$. Figure 6.3 demonstrates the distribution of the value of objective function when use the basic PSO and improved CPSO ($n = 4$) to solve the proposed model of this paper.

Through Figs. 6.2 and 6.3, three conclusions can be reached.

Table 6.3 Comparison of the algorithms and models

Model	Gen	Size	PSO			CPSO			
			Min	Average	Distance/Area	n	Min	Average	Distance/Area
Traditional model	1000	60	2.442	2.527	4420.3/429.7	3	2.413	2.528	4502.1/404.1
						4	2.412	2.484	4376.4/422.8
						5	2.441	2.523	4518.1/414.3
Literature [10]	1000	60	2.309	2.434	4475.1/360.9	3	2.332	2.420	4389.2/385.1
						4	2.306	2.378	4459.9/362.4
						5	2.303	2.426	4450.3/362.4
Proposed model	1000	60	2.255	2.396	4341.3/357.5	3	2.269	2.388	4339.3/376.2
						4	2.248	2.339	4247.8/368.4
						5	2.249	2.378	4224.7/372.4

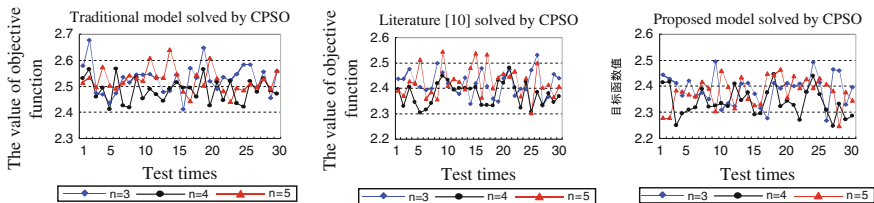


Fig. 6.2 The distribution of the results solved by CPSO ($n = 3, 4, 5$)

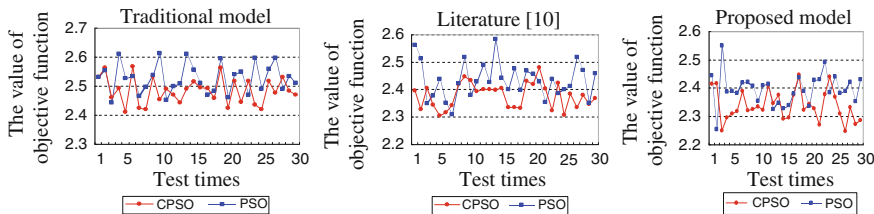
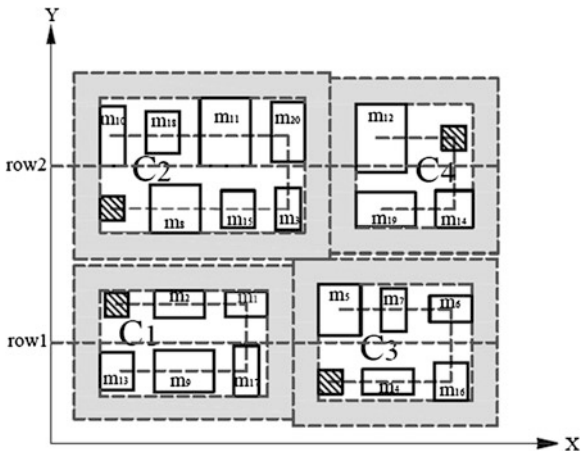


Fig. 6.3 The distribution of the results solved by PSO and CPSO ($n = 4$)

- (1) When use the improved CPSO to solve the case of this paper, the performance of the algorithm reaches best if the number of population $n = 4$. Analyze the CPSO part of the Table 6.3, no matter solve the traditional model, literature [10] or solve the proposed model, the average value of the objective function is best. And from Fig. 6.4, the values of objective function are closer to the optimal solution.
- (2) Compared to basic PSO, the performance of the improved CPSO is better. From Table 6.3, it shows that higher-quality solution can be achieved by improved CPSO.

Fig. 6.4 The final cellular layout



- (3) The proposed model of this paper can achieve high-quality solution. From Table 6.3, the cellular layout solved by the proposed model in this paper is best compared to the other two models. The same conclusion can also be reached from the CPSO part of Table 6.3.

From the results ran by 30 times, the best solution solved by the improved CPSO and the proposed model can be described as follows: $C_1\{m_{13}, m_9, m_{17}, m_1, m_2, m_{21}\}\{0, 1, 0, 1, 1, 0\}$; $C_3\{m_{23}, m_4, m_{16}, m_6, m_7, m_5\}\{1, 1, 0, 1, 0, 0\}$; $C_2\{m_{22}, m_8, m_{15}, m_3, m_{20}, m_{11}, m_{18}, m_{10}\}\{0, 1, 0, 0, 0, 0, 0, 0\}$; $C_4\{m_{19}, m_{14}, m_{24}, m_{12}\}\{1,1,0,0\}$, $m_{21}, m_{22}, m_{23}, m_{24}$ represent the buffer areas. 1 or mean placed horizontally or vertically respectively.

6.5 Conclusion

This paper considers the cellular layout problem in which a multi-objective-integrated optimization model is proposed and the intra-cell and inter-cell layouts are solved simultaneously. To solve the model, an improved cooperative particle swarm optimization was proposed to find near-optimal solutions. The proposed algorithm absorbs the operators of GA and divided the particles into several populations. The particles are evolved through cooperation. According to the case study, the validity of the proposed model and algorithm are verified.

References

1. Kioon SA, Bulgak AA, Bektas T (2009) Integrated cellular manufacturing systems design with production planning and dynamic system reconfiguration. *Eur J Oper Res* 2:192
2. Wang TY, Lin HC, Wu KB (1998) An improved simulated annealing for facility layout problems in cellular manufacturing systems. *J Comput Ind Eng* 2:34
3. Balakrishnan J, Cheng CH (2007) Empirical findings on manufacturing cell design. *Eur J Oper Res* 1:177
4. Wemmerlov U, Johnson DJ (2008) Empirical findings on manufacturing cell design. *Int J Prod Res* 3:38
5. Jajodia S, Minis I, Harhalakis GP, Class JM (1992) Computerized layout solution using simulated annealing. *Int J Prod Res* 1:30
6. Alfa AS, Heragu SS, Chen M (1992) Integrating the grouping and layout problems in cellular manufacturing systems. *J Comput Ind Eng* 23
7. Das SK (1993) A facility layout method for flexible manufacturing systems. *Int J Prod Res* 31
8. Bazargan-Lari M, Kaebnick H (1996) Intra-cell and inter-cell layout designs for cellular manufacturing. *Int J Ind Eng* 3
9. Won YD (1997) A linear programming approach to linear machine layout problem. *J Ind Math* 2:47
10. Tai-Yue W, Her-Chang L, Kudi-Bin W (1998) An improved simulated annealing for facility layout problems in cellular manufacturing systems. *J Comput Ind Eng* 2:34
11. Bazargan-Lari M, Kaebnick H, Harraf A (2000) Cell formation and layout design in a cellular manufacturing. *J Int J Prod Res* 38

12. Sangwan KS, Kodali R (2003) Multicriteria heuristic model for design of layout for cellular manufacturing systems. *J Inst Eng* 3:84
13. Angeline PJ (1998) Evolutionary optimization versus particle swarm optimization: philosophy and performance differences. *Evolutionary programming*, California, USA, 25–27 Mar 1998
14. Fan HY (2002) A modification to particle swarm optimization algorithm. *J Eng Comput* 19 (2002)

Chapter 7

The Inventory Demand Forecasting Model of the Regional Logistics Network in Supply Chain

An-Quan Zou and Ren-Cun Huang

Abstract This article is conducting a study on the demand forecast from the x-retailers, y-distribution centers, and z-suppliers supply chain of logistics area. The supply chain will be divided into upstream and downstream levels. Combined with the characteristics of the supply chain and demand characteristics of the regional logistics network, Dijkstra shortest path algorithm is used and its demand forecast model is constructed based on it to obtain the exact demand of each node enterprises. At last, an example is given to prove it.

Keywords Supply chain · Regional logistics network · Inventory demand · Forecasting

7.1 Introduction

In recent years, logistics has been developing rapidly for enterprise's emphasizes on the third profit source in logistics, huge support to logistics from government, and numerous researches from experts and scholars. However, there is also bottleneck in the process of logistical development [1], such as higher expense and lower level of service. Thus, it is indispensable to solve that how to decrease the expense and increase the service quality. Supply chain [2] is a functional network inventory made up of suppliers, manufacturers, retailers, and clients. The word network inventory is defined as assembly of interrelated organizations and facilities in

This work was supported by the Project of the national social science fund (12BJY020) and soft science of hunan province science and technology department.

A.-Q. Zou (✉)

Department of Business Administration, Changsha University, Changsha 410003, China
e-mail: zaq2833@163.com

A.-Q. Zou · R.-C. Huang

Changsha Institute of Logistics Technology and Application, Changsha University, Changsha 410003, China

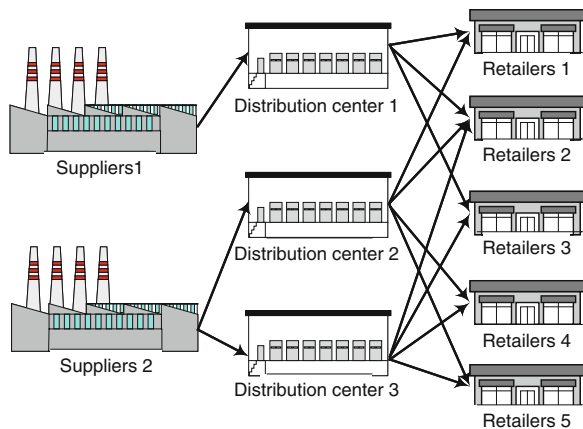
logistical process by the national standard logistic term [3]. Regional logistics network actually, is a complex network system made up of logistical node and interrelated parts in region [4]. So, on account of the regional network inventory in supply chain, enterprises in every node should consider the forecasting problem. Not only the expense and profit of the company but also the expense of the whole supply chain should be considered so that make the mutual benefit and win and decrease the total expense in the society.

Current problem on demand forecasting is the supply period and demand uncertainties [5]. And recently, application of supplier inventory management model (VMI) could eliminate the impact of the supply period uncertainty. But the demand uncertainty remains to solve. Because the demand uncertainty is mainly reflected in huge preference of clients, many enterprises in every node choose the suppliers depending on the shortest distance, for diminishing expense. Whereas, in a certain region, it exist a situation that there are variances in different distances between distribution center and supplier demand, though they are certain and stable that the potential total demand of client and the total demand of distribution center. Main domestic demand forecasting methods are not suitable for this situation currently such as differential equation model [6], time series model [7], gray forecasting theory model [8], and BP neural network model [9]. Therefore, the authors constructed an accurate demand forecasting model [9] combined characteristics of supply chain and network in the situation, for forecasting demand, reducing expense and improving the service level.

7.2 Model Description

In this paper, on the premise of every logistic node fixed, the author researched on the supply chain network is a complex one composed of many retailers, distribution centers, and suppliers. In the network, the nodes stand for retailers, distribution

Fig. 7.1 Supply chain structure diagram



centers, and suppliers, and the edge is the actual road. And every node is inter-dependent [10] (Fig. 7.1).

7.2.1 The Assumptions of the Mode

In a region, retailers have some demands on distribution centers, and they also hold demands on suppliers. Considering the expenses of logistics and transportation, logistics service level, and randomness of shopping, retailers take goods from one or several distribution centers, and the amount of goods that retailers take depends on distance from a distribution center to a retailer that is retailers take more goods from close distribution center and less goods from far distribution center. Similarly, distribution centers chose the closest supplier providing goods, but every distribution center could only chose one supplier, differently. Next, there are such assumptions:

- (1) In a certain region, there are x -retailers r , y -distribution centers d , and z -suppliers s .
- (2) Assumed the locations of retailers, distribution centers, and supplier are defined.
- (3) Demands of every retailers are defined and equal. Let $Q_r = 1$.
- (4) Retailers have a certain demand to distribution centers, let q_r^d .
- (5) Considering the randomness and subjectivity of consumers choosing commodities, assume retailers choose distribution centers only depending on the distance l_{rd} , q_r^d is inversely proportional to l_{rd} .
- (6) Distribution centers have demand on suppliers, let as q_d^s .
- (7) On account of factors, such as expense of transportation, assume that distribution center choose suppliers only depending on distance l_{ds} that is every distribution center only choose one, the closest suppliers (Table 7.1).

Table 7.1 The specific meaning of the symbol

Symbol	Implication
$r(1, \dots, x)$	There are x -retailers
$d(1, \dots, y)$	There are y -distribution centers
$s(1, \dots, z)$	At there are z -suppliers
q_r^d, q_d^s	The amount that retailer demand to distribution center, the amount that distribution center demand to supplier
l_{rd}, l_{ds}	The distance from a retailer to a distribution center, the distance from a distribution center from a supplier
Q_r, Q_d, Q_s	The total demand of retailers, the total demand of distribution centers and the total demand of suppliers

7.2.2 Parameters of Model Contribution

1. Logistics network-weighted matrix

According to graph theory [11], logistics network picture could be described an assembly of a finite number of peaks $V = \{v_1, v_2, \dots, v_n\}$, and an assembly that represents the relationships with these peaks $L = \{l_1, l_2, \dots, l_m\}$. The picture is marked as $G = (V, L)$. And the weights of the side of any two nodes i and j are marked as w_{ij} . And the following network picture is the weighted network one (Fig. 7.2).

Let the weighted network picture be described as a weighted matrix, there are several conditions in the following:

- (1) If there is no side between any two nodes i and j in the picture, $w_{ij} = \infty$.
- (2) If there is side between any two nodes i and j in the picture, w_{ij} is the side weighted value.
- (3) If the two nodes i and j coincided, $w_{ij} = 0$. So, we could conclude a weighted matrix (7.1) as displayed in Fig. 7.2.

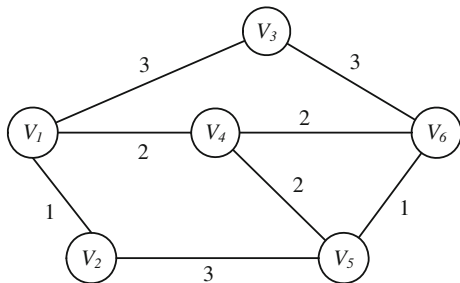
$$W = \begin{bmatrix} 0 & 1 & 3 & 2 & \infty & \infty \\ 1 & 0 & \infty & \infty & 3 & \infty \\ 3 & \infty & 0 & \infty & \infty & 3 \\ 2 & \infty & \infty & 0 & 2 & 2 \\ \infty & 3 & \infty & 2 & 0 & 1 \\ \infty & \infty & 3 & 2 & 1 & 0 \end{bmatrix} \tag{7.1}$$

2. Dijkstra function to find the shortest route matrix

The shortest route problem is started with any node in the network picture, and to find the shortest route from the node to any other node in the network picture. The function proposed by Dijkstra [12], actually and currently, is great function to find the shortest route. The basic steps are in the following:

- (1) Let the first note as i , the shortest distance $D_{ii} = 0$, then let the node i marked by 0 mark in the small square, representing that the node i marked.

Fig. 7.2 Regional network picture



- (2) Start from i and find the point with the shortest distance, and let it as j , and let the symbol $D_{ij} = D_{ii} + w_{ij}$ be marked in the small square, representing that the node j have been marked.
- (3) Start from marked node, and find the several points which have not been marked, marked as p . If there is $D_{ip} = \min\{D_{ii} + w_{ip}, D_{ij} + w_{jp}\}$, then give the p number, and let the D_{ip} be marked beside p .
- (4) Repeat the step 3 again, until the last pointed marked.

Now, we can use these steps above and combine related conditions in order to solve the matrix.

In the shortest route from retailer r to distribution center d , l_{rd} represents the actual distance from r to d , and D_{rd} represents the shortest distance from r to d . According to the steps in Dijkstra function, we could find out the shortest route formula $D_{rd} = \min\{D_{rd}, D_{rd} + l_{rd}\}$, to find out the matrix (7.2) that could conclude the shortest route model.

$$D_{rd} = \begin{bmatrix} D_{11} & D_{12} & \dots & D_{1y} \\ D_{21} & & & \\ \vdots & D_{rd} & & \vdots \\ D_{x1} & \dots & & D_{xy} \end{bmatrix} \quad (7.2)$$

Similarly considered the relevant conditions, we could conclude the matrix to find out the shortest distance from the distribution center and the suppliers, the forecasting model, as (7.3) shows.

$$D_{ds} = \begin{bmatrix} D_{11} & D_{12} & \dots & D_{1z} \\ D_{21} & & & \\ \vdots & D_{ds} & & \vdots \\ D_{y1} & \dots & & D_{yz} \end{bmatrix} \quad (7.3)$$

7.3 Model Construction

We divided the model from upstream and downstream to construct. The upstream is the model forecasting the demand from retailers and distribution centers, and the downstream is the model forecasting the demand from distribution centers and suppliers.

7.3.1 Forecasting Model for the Demand from Retailers and Distribution Centers

The upstream supply chain includes retailers and distribution centers. According to the relevant parametric conditions above, we could construct the forecasting model depending on the demand from retailers and distribution centers.

1. The demand of retailers r

Assumed the demand of every retailer is definite and equal, the total sum of every retailer taking goods from distribution is described as one unit.

$$Q_r = q_1^r + q_2^r + \dots + q_y^r = \sum_{d=1}^y q_d^r = 1 \tag{7.4}$$

2. The demand from distribution centers d

The total sum of the every retailer taking goods from distribution centers are the total demand from distribution centers. The demand function is as (7.5) shows:

$$Q_d = q_1^d + q_2^d + \dots + q_x^d = \sum_{r=1}^x q_r^d \tag{7.5}$$

3. The demand q_d^r is inversely proportional to the distance D_{rd}

The sum that every retailer demands the distribution centers is inversely proportional to the distance from retailers to distribution centers. And the relationship is as (7.6) shows:

$$q_1^r : q_2^r : \dots : q_y^r = \frac{1}{D_{r1}} : \frac{1}{D_{r2}} : \dots : \frac{1}{D_{ry}} \tag{7.6}$$

4. The construction of model

To conclude, we could find out the final forecasting demand model:

$$\begin{aligned}
 & Q_d = q_1^d + q_2^d + \dots + q_x^d = \sum_{r=1}^x q_r^d \\
 & s.t. \left\{ \begin{aligned}
 & D_{rd} = \begin{bmatrix} D_{11} & D_{12} & \dots & D_{1y} \\ D_{21} & & & \\ \vdots & D_{rd} & & \vdots \\ D_{x1} & \dots & & D_{xy} \end{bmatrix} \\
 & Q_r = q_1^r + q_2^r + \dots + q_y^r = \sum_{d=1}^y q_d^r = 1 \\
 & q_1^r : q_2^r : \dots : q_y^r = \frac{1}{D_{r1}} : \frac{1}{D_{r2}} : \dots : \frac{1}{D_{ry}}
 \end{aligned} \right. \tag{7.7}
 \end{aligned}$$

7.3.2 The Model Forecasting Demand that Distribution Centers Demand Suppliers

Similarly, we could find out the model forecasting demand that distribution centers demand suppliers according to several relevant conditions above.

1. To define the relationship that the demand q_d^s is inversely proportional to the distance l_{ds} .

If the distribution choose suitable suppliers, they should consider ability and frequency of the suppliers, and to the most important, they will consider the distance from distribution center to supplier. If so, it is possible to decrease the expense and increase the service level. Thus, in the model, the choice of suppliers should depend on the distance to fix, and every distribution centers choose the shortest distribution center. And the relationship is in the following:

$$q_d^s = \begin{cases} 1 & \min(l_{ds}) \\ 0 & \text{others} \end{cases} \tag{7.8}$$

2. The demand of suppliers s ,

$$Q_s = q_1^s + q_2^s + q_3^s + \dots + q_y^s = \sum_{d=1}^y q_d^s$$

$$s.t. \left\{ \begin{array}{l} D_{ds} = \begin{bmatrix} D_{11} & D_{12} & \dots & D_{1z} \\ D_{21} & & & \\ \vdots & D_{ds} & & \vdots \\ D_{y1} & \dots & & D_{yz} \end{bmatrix} \\ q_d^s = \begin{cases} 1 & \min(l_{ds}) \\ 0 & \text{others} \end{cases} \end{array} \right. \tag{7.9}$$

7.3.3 The Model Forecasting Demand Depending on the Supply Chain

To conclude, in the region that with supply chain, the network model forecasting the demand is shown as the following:

$$\begin{cases}
Q_d = q_1^d + q_2^d + \cdots + q_x^d = \sum_{r=1}^x q_r^d \\
Q_s = q_1^s + q_2^s + \cdots + q_y^s = \sum_{d=1}^y q_d^s \\
s.t. \left\{ \begin{array}{l}
D_{rd} = \begin{bmatrix} D_{11} & D_{12} & \cdots & D_{1y} \\
D_{21} & & & \\
\vdots & D_{rd} & & \vdots \\
D_{x1} & \cdots & & D_{xy} \end{bmatrix} \\
Q_r = q_1^r + q_2^r + \cdots + q_y^r = \sum_{d=1}^y q_d^r = 1 \\
q_1^r : q_2^r : \cdots : q_y^r = \frac{1}{D_{r1}} : \frac{1}{D_{r2}} : \cdots : \frac{1}{D_{ry}} \\
D_{ds} = \begin{bmatrix} D_{11} & D_{12} & \cdots & D_{1z} \\
D_{21} & & & \\
\vdots & D_{ds} & & \vdots \\
D_{y1} & \cdots & & D_{yz} \end{bmatrix} \\
q_d^s = \begin{cases} 1 & \min(l_{ds}) \\ 0 & \text{others} \end{cases}
\end{array} \right.
\end{cases}$$

7.4 An Instance Application

In order to examine the effect of the model, the paper is focused on a logistics network in Xiangtan supermarkets. And we use the model to forecast the demand.

Figure 7.3 is a network of distributing good of the supermarkets. The star nodes s represent the suppliers location. The solid nodes d can be described the location of distribution centers. The hollow nodes r illustrate the retailers. And the sides of the every node stand for the actual distances.

According to the description in the network, we could find out the network matrix, as (7.10) shows:

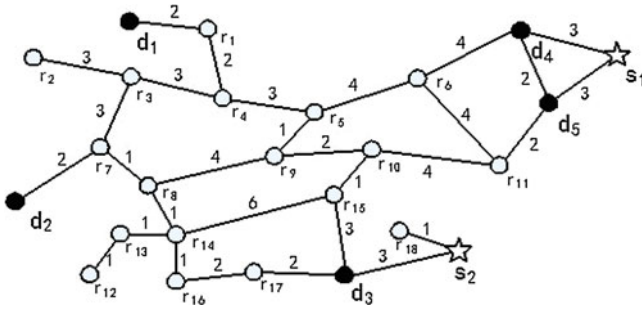


Fig. 7.3 Logistics distribution network diagram

$$A = \begin{bmatrix} 0 & \infty & \infty & 2 & \cdots & \infty & \infty & \infty & \infty & \infty \\ \infty & 0 & 3 & \infty & \cdots & \infty & \infty & \infty & \infty & \infty \\ \infty & 3 & 0 & 3 & \cdots & \infty & \infty & \infty & \infty & \infty \\ 2 & \infty & 3 & 0 & \cdots & \infty & \infty & \infty & \infty & \infty \\ \vdots & \vdots & \vdots & \vdots & \vdots & \vdots & \vdots & \vdots & \vdots & \vdots \\ \infty & \infty & \infty & \infty & \cdots & 0 & 2 & 3 & \infty & \infty \\ \infty & \infty & \infty & \infty & \cdots & 2 & 0 & 3 & \infty & \infty \\ \infty & \infty & \infty & \infty & \cdots & 3 & 3 & 0 & \infty & \infty \\ \infty & \infty & \infty & \infty & \cdots & \infty & \infty & \infty & \infty & 0 \end{bmatrix} \quad (7.10)$$

Using the MATLAB and other programming tools, and combining Dijkstra function to find out the shortest route matrix, and the D_{rd} matrix representing the shortest distance from retailers to distribution centers, as (7.11) shows:

$$D_{rd} = \begin{bmatrix} 2 & 10 & 12 & 13 & 14 \\ 10 & 8 & 13 & 17 & 18 \\ 7 & 5 & 10 & 14 & 15 \\ \vdots & \vdots & \vdots & \vdots & \vdots \\ 15 & 7 & 2 & 14 & 12 \\ 18 & 13 & 4 & 16 & 14 \end{bmatrix} \quad (7.11)$$

Similarly, the D_{ds} matrix standing for the shortest distance from distribution centers to suppliers, as (7.12) shows:

$$D_{ds} = \begin{bmatrix} 18 & 17 \\ 18 & 12 \\ 13 & 3 \\ 3 & 15 \\ 3 & 13 \end{bmatrix} \quad (7.12)$$

Now, we could use the model to find out the sum demand from distribution centers and suppliers, respectively.

1. The total demand from distribution centers:

Combining (7.11) with the matrix Q_d , we could get the (7.13)

$$Q_d = \begin{bmatrix} 0.6012 & 0.1202 & 0.1002 & 0.0925 & 0.0859 \\ 0.2402 & 0.3003 & 0.1848 & 0.1413 & 0.1334 \\ 0.2459 & 0.3443 & 0.1721 & 0.1229 & 0.1148 \\ \vdots & \vdots & \vdots & \vdots & \vdots \\ 0.0771 & 0.1653 & 0.5785 & 0.0826 & 0.0964 \\ 0.1076 & 0.1489 & 0.4841 & 0.1211 & 0.1383 \end{bmatrix} \quad (7.13)$$

Using (7.13), we could find out the final total demand from 5 distribution centers

$$\begin{aligned} Q_{d_1} &= 0.6012 + 0.2402 + \cdots + 0.1076 = 3.2583 \\ Q_{d_2} &= 0.1202 + 0.3003 + \cdots + 0.1489 = 4.4863 \\ Q_{d_3} &= 0.1002 + 0.1848 + \cdots + 0.4841 = 4.7734 \\ Q_{d_4} &= 0.0925 + 0.1413 + \cdots + 0.1211 = 2.6105 \\ Q_{d_5} &= 0.0859 + 0.1334 + \cdots + 0.1383 = 2.8715 \end{aligned} \quad (7.14)$$

And to do a further comparison, we could find out:

$$\begin{aligned} Q'_{d_1} &= \frac{Q_{d_1}}{Q_{d_1} + Q_{d_2} + Q_{d_3}} = \frac{3.2583}{18} = 0.18 \\ Q'_{d_2} &= \frac{Q_{d_2}}{Q_{d_1} + Q_{d_2} + Q_{d_3}} = \frac{4.4863}{18} = 0.25 \\ Q'_{d_3} &= \frac{Q_{d_3}}{Q_{d_1} + Q_{d_2} + Q_{d_3}} = \frac{4.7734}{18} = 0.27 \\ Q'_{d_4} &= \frac{Q_{d_4}}{Q_{d_1} + Q_{d_2} + Q_{d_3}} = \frac{2.6105}{18} = 0.14 \\ Q'_{d_5} &= \frac{Q_{d_5}}{Q_{d_1} + Q_{d_2} + Q_{d_3}} = \frac{2.8715}{18} = 0.16 \end{aligned} \quad (7.15)$$

As (7.15) shows, the demand of distribution centers d_1 account 0.18, and d_2 accounting 0.25, d_3 making up 0.27, d_4 making up 0.14, d_5 making up 0.16. From this, we could know the proportions of the demand of every distribution centers

2. The total demand of suppliers

Combining (7.12) with the model, the total demand of suppliers as (7.16) shows:

$$\begin{aligned} Q_{s_1} &= Q_{d_4} + Q_{d_5} = 5.4820 \\ Q_{s_2} &= Q_{d_1} + Q_{d_2} + Q_{d_3} = 12.5180 \end{aligned} \quad (7.16)$$

And make a further comparison:

$$\begin{aligned} Q'_{s_1} &= \frac{Q_{s_1}}{18} = \frac{5.4820}{18} = 0.3 \\ Q'_{s_2} &= \frac{Q_{s_2}}{18} = \frac{12.5180}{18} = 0.7 \end{aligned} \quad (7.17)$$

The demand of supplier s makes up 0.3 in the whole supply chain, s_2 making up 0.7. Now, the model has calculated the stock sum in suppliers and distribution centers exactly in the network.

7.5 Conclusions

This paper constructs a forecasting model, with graph theory and matrix knowledge, using the Dijkstra function, in the supply chain. And finally, use of MATLAB calculates the accurate demand. And the further research directions are: (1) How to construct a forecasting model considering the randomness, (2) How to let the model become more accurate with accurate expense in the model.

References

1. Christopher M (2005) Logistics and supply chain management: creating value-added networks [M]. Pearson education
2. Ma S, Lin Y (2006) Supply chain management (second edition). Higher Education Press, Beijing
3. GB/T18354-2006 (2006) The standard logistic terms of People's Republic of China. China Standard Press, Beijing
4. Fleischmann M, Bloemhof-Ruwaard JM, Beullens P, Dekker R (2004) Reverse logistics network design. Quantitative approaches to reverse logistics
5. Zhen-Hua Y (2008) Demand forecasting safety stock optimization research based on supply chain. Tianjin University
6. Zill DG (2008) A first course in differential equations: with modeling applications. Brooks/Cole Pub Co
7. Lutkepohl H (2005) New introduction to multiple time series analysis. Springer
8. Ju-Long D (2002) Grey theory basis. Huazhong University of Science Technology Press, Wuhan
9. Ripley BD (2008) Pattern recognition and neural networks. Cambridge University Press, Cambridge
10. Li Y, Chen Y (2004) Research on UML-based ASP business processes modeling. Comput Integr Manuf Syst 10:25–29
11. Zhu DL, Xu Q, Ye YH (2006) Operations research. Higher Education Press, Beijing
12. Chen JC (2003) Dijkstra's shortest path algorithm. J Formalized Math

Chapter 8

Research on Logistics Marketing Based on Local Characteristic Economy Industrial Cluster

Xiaoyuan Shi

Abstract Industrial cluster has become an important phenomenon in the contemporary world economy. For the promotion of regional economic strength, the competitive advantage of its core competitiveness is distinctive day by day through the synergistic effect. Along with the economic globalization, the enterprises gradually transferred from single competition to group competition. And in the modern business environment, the competition among enterprises has replaced by the supply chain and the competition among supply chains. It has brought convenience and opportunities to the development of the logistics industry, based on the regional characteristic industry group formed by local economic traits, the relatively immobilization in the product categories, packaging specifications, logistics modules and standardization, and the shortened geographical restrictions by industry agglomeration. On the basis of this background, logistics enterprises should enhance marketing innovation and service for supply chain. They should carry out targeted marketing strategies based on customer orientation. And also, they should integrate the enterprise service and customer logistics demand and provide their users with integrated, systematic logistics solutions. It will create competitive advantages for the regional industry cluster.

Keywords Industrial cluster · Local economic traits · Competitive advantage · Logistics marketing · Innovation

8.1 Introduction

Industrial cluster has a competitive and scale benefit, by way of an industrial organization form for creating competitive advantages. In today's economic globalization, the enterprises gradually transferred from single competition to group competition. The competition of region economy is also focused on regional

X. Shi (✉)

College of International Business, Zhejiang Yuexiu University of Foreign Languages,
No. 428 Kuaiji Road, Yuecheng District, Shaoxing 312000, Zhejiang, China
e-mail: sxy_008@126.com

industrial competition. From worldwide look, clustering is a very common phenomenon. It becomes new highlight for current world economy and becomes a dominant role in regional economic development, as well a new power for international competitiveness of national industry. Relate to this topic research the domestic scholars mainly concentrated in three aspects. One is focused on the development of the industrial cluster; the two is the logistics of how the market marketing study [1–3]; the three is the logistics industry group studies [4–7]. Comprehensive study of the above, we can see scholars on their respective fields of study are more detailed and thorough, but based on regional characteristic industry group, logistics marketing research rarely mentioned. Along with the economic globalization, the enterprise competition, modern business environment has changed from the supply chain and the competition between supply chains instead of the competition between enterprises. It has become a pressing issue that enterprise how to delivery product to customer high efficiency and low cost and how to improve customer satisfaction.

It has brought convenience and opportunities to the development of the logistics industry, based on the regional characteristic industry group formed by local economic traits, the relatively immobilization in the product categories, packaging specifications, logistics modules and standardization, and the shortened geographical restrictions by industry agglomeration. Logistics enterprises should be based on this background, strengthen supply chain innovation and marketing services, carry out targeted marketing strategies based on customer orientation, through the interaction, communication and other forms of the enterprise customer service and logistics needs of integration, to provide users with an integrated, systematic logistics solutions, and enhance their market competitiveness at the same time as the regional industry cluster development to create competitive advantage.

8.2 The Advantage of the Industrial Cluster in Regional Economy Development

8.2.1 Professionalization Leads to Competitive Advantage

With the global competition, international market has become more and more subdivision, more and more specialization. And industrial cluster is often dominant and leading in industry market. The deep division of industry group is conducive to the formation of the professional market, to improve efficiency and technical innovation. And the formation of professional market will further promote the development of industrial clusters. Cluster industry products generally occupy a large marketing share, so it has a cost advantage in raw materials procurement and sales. Within the industry cluster, all the latest products, technology and information are in this together naturally into competition, and industry healthy competition and further inspire innovative consciousness. If clusters of bibcock enterprise

innovation drive action, then becomes the other enterprises to learn a model, the local industry innovation. In the fierce competition in the market economy society, because of its advanced technology, high market share has formed a certain well-known brands of domestic or international brand, which has the competitive advantage of industry. Let the people mentioned that the household appliances, think of Shunde city; mention lighter, think of Wenzhou city; referred to tie, think of Shengzhou city; mentioned textile, they think of Shaoxing city; mentioned tobacco thought of Yuxi city. Industrial cluster is actually the industry development and regional economic integration, through the professional division of labor and trade convenience, for a kind to promote local economic growth and effective ways of organizing production [8].

8.2.2 Cluster Shows Scale Advantage

Reviewing domestic and international industry group, they are aggregated in space by certain geographical proximity of some enterprises. From the perspective of the mode analysis of industrial cluster, whether by many related small and medium-sized enterprises around the axis of the finished product, forming an oversize wheeled cluster, such as Japan's Toyota motor city; Or small businesses around several large finished products business of multi-core type industrial cluster, such as the United States of Detroit's big three auto company, these have large scale advantage of industrial clusters. "Specialized market + family factory" characteristics of industrial clusters in Zhejiang Province of China are very common. This has obvious local characteristics of regional industry group leading the local economy and social development. It is also known as regional characteristic economy. "Massive economy" the formation of the "agglomeration advantages" often has a great deal of economies of scale advantage. As the Wenzhou lighter accounted for 70 % of world output, Shengzhou tie production accounted for 80 % of domestic market, accounting for 30 % of the global market, these are the spatial agglomeration formation of the economies of scale.

8.3 The Relationship Between Industrial Cluster and Logistics

8.3.1 Industry Group Expedites the Logistics Market

(1) Professional Avails Logistics Market Segmentation

According to different requirements and characteristics of logistics demand, logistics market can be divided into several different small markets. Every little

market logistics requirements in the product transportation, packaging, storage, etc., have similar consumption demand and mode, and the demand characteristics of different markets also have obvious difference. Market segmentation can help decision makers to accurately define the logistics needs of customers, develop marketing objective and reasonable allocation of logistics resources. Logistics enterprises should according to the characteristics of the market of industrial clusters, according to the customer, geographical area, items attributes, customer scale of logistics market segmentation, according to its own conditions and external environment, the size of the market segment and competition situation, as well as the market segment customer service needs, preferences and the enterprise main characteristics to determine the target market, formulate the corresponding marketing strategy.

(2) Cluster is Convenient for Formation of Logistics Scale Economy

“Industrial clusters economy” is a kind of industry concentration of industry. Associated enterprises in industrial cluster and its supporting enterprises gathered in a certain area, easy to form a flexible production complex, constitutes the core of regional competitiveness. These companies are often geographically close local economic pillar industry, also known as regional characteristic economy. Manufacturing of similar products on the space gathered to form brand “location.” With the success of the industry cluster, the product unceasingly to the world of cluster industry formed a kind of regional brand in the world. And this kind of small businesses and large market of agglomeration formed the scale economic advantage, occupying a particular product or one kind of product a large market share. The geographical space gather also provides a lot of logistics demand for logistics enterprises.

(3) Adjacent Regions Provide Convenience for Logistics Enterprises Cooperation

Throughout the home and abroad industrial clusters are almost many enterprises gathered in geographic space. The large and small enterprises from raw material supply to the end product of a series of logistics activities are decentralized and inconsistencies. The scale of logistics demands for logistics facilities, equipment, and logistics cost savings. Due to geographical location, adjacent industry homogeneity, the consistency of its logistics activities for many small businesses had the characteristics of cooperation, facilitating collaboration for both sides, so as to improve the logistics operation mode, save the cost, and improve the efficiency.

8.3.2 Supporting Role of Modern Logistics for Industrial Clusters

With global market many companies realize that profit source from to expand production and reducing consumption has become more and more difficult. Enterprises on the one hand are committed to technology development and improve the quality of

products, on the other hand to seek the cost advantage and value advantage shifts the attention of the logistics field, gradually to the high profits and high returns of marketing, logistics, brand expansion and high added value, etc. Logistics rationalization, modernization, and a series of activities not only make the enterprise reduce the cost and ensure the marketing and procurement activities, but also became enterprise operation profit is the main activity. More important is through the logistics service improve service levels, thus improving the competition ability of the firm. As Michael porter said, the success of the enterprise competition can only be achieved by cost advantage and value advantage. And logistics management not only can reduce business costs, but also can provide customers with quality services; it not only makes the enterprise to obtain cost advantages, but also makes the enterprise gain value advantage. Look around the world well-known multinational enterprises, they not only has the world first-class product research and development, sales and marketing ability, but also has the ability to provide quality logistics services for customers. Through the logistics outsourcing to professional logistics companies, companies can focus on core competence to improve the quality of the product research and development, and manufacture. In this way, companies can provide competitive products to customers, and attract upstream and downstream suppliers and customers [4].

8.4 Logistics Marketing Strategy Based on the Industrial Cluster

8.4.1 Flexibility in the Use of 4P, 4C, and 4R Theory in Logistics Marketing Application

The 4P, 4C, and 4R theories are the three classic marketing combination theories in the history of marketing development. They have their own characteristics and specific. The 4P theory focused on product, price, marketing channel, and promotion, but ignore real object—the customer’s interests. The 4C theory focuses on how to realize the consumer’s needs, pay attention to the two-way exchange and communication with the customer, and focus on the convenience of customers to buy. With the theory development of 4C also shows its limitations, when customer demand conflicts with the social principle, customer strategy is also not adapt. Don E Schultz put forward the relationship, reaction, relevancy, and rewards that is 4R theory. Logistics marketing should be flexibility in the use of marketing theory. Logistics enterprises according to their own strength size, focus on a marketing, differentiation strategy, and benefits with customers as much as possible, cultivate customer loyalty; The services provided by the logistics companies in the customer's consumption process, should be positive and effective to carry on the good communication with customers, as far as possible, provide convenience for the customer; Through its own hardware and software facilities investment, improve service quality and brand awareness. Logistics enterprises should, establish a long-term and win-win strategic cooperative partnership with customers.

8.4.2 Pay Attention to Brand Building

After ten years of development, the whole society and the enterprise all have a more profound understanding of logistics, and realize that the logistics as “the third profit source” can bring wealth to enterprises and society. So lots of enterprises hang “logistics” brand arise all of a sudden. Report statistics show that in 2011, the number of level A logistics enterprises in China has reached 1061. I can see the development of domestic logistics industry is very fast. But very few number is very good in our logistics companies. Many domestic logistics enterprises is committed to the business market development, also want to do business big and strong, but few attention to brand building. Enterprises do not have the brand construction consciousness; the so-called service concept also only stays in oral or some beautiful slogans. They do not know that brand is a kind of intangible assets. The logistics enterprises should, such as DHL, UPS, FedEx, and EXEL, pay attention to brand building. First of all, enterprises should strengthen the brand awareness, integrate internal and external resources from leader to employees, improve the management level and service consciousness, create their own brand, and establish distinctive, domestic well-known international brand. Secondly, establish personality brand. Logistics enterprises should be selectively according to their own strength to provide service for the customer, for example, the powerful integrated logistics services, enterprises can carry out the weaker enterprises can focus on a particular aspect to provide specialized logistics services with high added value. Some powerful enterprise can carry out integrated logistics services, and the weaker enterprises can focus on a particular aspect to provide customers with high value-added logistics services, Brand is a name card, is a kind of trust of customer to you, and is a kind of invisible enterprise core competitiveness. Brand is a name card and a kind of invisible enterprise core competitiveness. Once customers choose a certain brand means the identification of the value of the product. Brand building should not only have a striking image of the “name”, “logo”, also should through the process to establish a good cooperation with the customer. The last is to maintain the brand. Good brand is not stay on the propaganda, but embodied in action. Enterprises should actively improve the service ability and the management level in the face of fierce market competition. Enterprise should do to maintain the brand image and supervision work. Enterprise can shape a brand from some of the details, for example, to participate in public welfare and charity, to help disadvantaged groups, to protect the environment, etc. Logistics enterprises should learn how to fulfill their own responsibility and should not forget their social responsibility, at the same time of gain wealth.

8.4.3 Differentiation Strategy for Market Segments

Differentiation strategy refers to the enterprises on products, service, and corporate image with competitors have obvious differences, so as to gain a competitive advantage and strategy. The strategic emphasis is to create unique products and services for customers. The winner of the logistics enterprises in the future must focus on specialization and market segmentation. A variety of industrial clusters in China, almost every province, has a large and small industrial clusters based on local features. Whether the ship, automobile, engineering machinery, or lighter, tie clip, badges, shoes, hats, socks, ties, lamps and lanterns, lamp decoration, small items such as glass, ceramics, furniture, handicraft, different industries are in an area formed a certain scale of industrial cluster. Products under each kind of industry cluster have its own characteristics in the transportation, storage, packaging, and other logistics link. Logistics industry should be market segmenta. Logistics industry should be based on local flavor characteristics of industrial clusters market segments, positioning target customer, and then concentrated funds, manpower, technology, to provide appropriate to the service. Concentrate funds, man- power, and technology, and good to provide logistics services for the customer. In this way, enterprises can form features and advantages, avoid repeated construction and excessive competition in the industry, and develop their own brands [2]. As Wukuang development company dedicated to domestic comprehensive logistics warehousing, Yiyatong company is supply chain integration services; Pegasus international specialized is engaged in the petrochemical logistics; railway container transport monopolized by Tielong logistics company; Ande logistics company specializing in electrical home appliances; and Anji Tiandi company is committed to automotive logistics.

8.4.4 Establishing Logistics Industrial Clusters Depended on Logistics Park

Gather industry group needs a lot of logistics demand, and these needs to show the multi-level, diversified characteristics. Different logistics companies can provide different logistics service function and level to meet the requirements of enterprise. This kind of space gathered provides the convenience for the coordinated development of logistics enterprise. In dealing with customer demand diversity and ties to reduce enterprise logistics cost, logistics enterprises have more and more difficult to adapt. More and more logistics enterprises come to realize that logistics activity is social, if only from the Angle of supply chain related to the enterprise to improve logistics efficiency, it is difficult to achieve a goal. So, logistics enterprises in the area of the industrial cluster realize efficient and convenient services using of complementary and logistics resources sharing through the synergies and economies of scale and scope economy effect. And this kind of regional brand brought the

accumulation effect of logistics demand with its popularity and the overall marketing strategy to expand, the total demand pull the third party logistics the area [3]. Logistics industry cluster based on logistics parks can provide strong support to enhance the competitiveness of industrial cluster with more effective integration, specialization, and integration services [5, 6].

8.4.5 Collaborative Development of the Third Party Logistics Enterprises and Industry Cluster

Industrial cluster is an important resource of competitive advantage for countries or regions. It has become the important cornerstone of sustained economic growth. The globalization of economy and the shortage of resource lead to new challenges for industrial cluster development. Global manufacturing network accelerates the formation of clusters, requires enterprises to expand their market share, and participates in global division of labor. With the economic globalization, the competition between supply chain and supply chain have taken the place of the competition between individual enterprise. Due to the presence of operations on the interconnection, industry cluster provides market needs for the third party logistics enterprises, and the third party logistics enterprises provide a flow of logistics supply for clusters of enterprise products. Industrial cluster can form strategic cooperation and information sharing with the third party logistics enterprise, has become a tool of cluster enterprise cope with fierce competition. The third party logistics enterprises with professional equipment and technical advantages, in the inventory availability, delivery timeliness, and delivery of the consistency of leader in the same industry, attract more suppliers and the ideal business partners. The enterprise cooperation among the third party logistics enterprise and industry group, not only dispersed logistics business risk, allowed to concentrate resource on their main business, reduced the logistics cost, improved customer satisfaction, remodeled the cost advantage, and enhanced the competitiveness of industrial clusters, but also won the market for the third party logistics enterprises, enhanced its own competitiveness, and achieved a “win-win” result.

8.5 Conclusions

Industrial cluster has shown extraordinary influence and the important status in the economic development of various countries. With global economic competition, the enterprise competition gradually changed to group competition from single competition. And in the modern business environment, the competition among enterprises has replaced by the competition among supply chains. Based on the regional characteristic industry group formed by local economic traits, the geographical

proximity and the products proximity made scale economy easy to form and also brought convenience and opportunities to the development of the logistics industry. Logistics enterprises should conduct effective logistics marketing in the industrial cluster zone. Through providing quality services to the industry, enterprises can obtain the cost advantage and price advantage. Furthermore, they also can create competitive advantage for the regional industry cluster development.

References

1. Xing C, Yufeng M (2009) The third party logistics enterprise marketing mix of 4R + 4Pstrategy [J]. Chinese management informationization 1:78–80
2. Guo F, Hongmei W (2005) “4Rs” theory and the third party logistics enterprise marketing innovation [J]. J Northeast Univ (Social Science Edition) 7(5):346–349
3. Kaixun D (2010) The difference marketing strategy and its application [J]. Logistics Eng Manage 6:158–160
4. Jianhui Ma (2006) To construct modern logistics support system to improve the core competitiveness of industrial clusters in Pearl River Delta [J]. Business Econ Rev 3:29–36
5. Zhilei Y (2007) The competitive advantage of logistics industry cluster analysis [J]. North Econ 6:14–15
6. Hui L (2007) The industrial clusters and the logistics park development [J]. Storage Transp Preserv Commod 3:12–15
7. Chouyong C (2009) The research on the third party logistics and industrial cluster collaborative development [M]. Science Press, Beijing
8. Porter ME (1998) Cluster and the new economics of competition [J]. Harvard Bus Rev, pp 77–90

Chapter 9

Based on AHP and Cluster Analysis for Classification Method of Emergency Supplies

Zhiyuan Su, Xun Weng and Lei Zhang

Abstract This thesis is devoted to the research of emergency material distinction between different levels of reserve and scheduling problems using the combined model of AHP analytical hierarchy process and cluster analysis, AHP analytical hierarch process being both qualitative and quantitative, while the cluster analysis being both clear and concise. Viewing the Features of emergency supplies of scheduling and reserve, two hierarchical models were proposed separately. For the hierarchical model for the emergency supplies scheduling, classification is based on the scheduling characteristics of the emergency materials, defining the emergency materials scheduling as the target layer; the features of the emergency rescue, such as the importance, timeliness and degree of scarcity, as the policy level, and the typical relief supplies to programmers. For the hierarchical process model of the material reserve, classification is based on the reserve characteristics of the emergency material. Set the emergency materials reserve to the target layer in the analytic hierarchy process model of the material reserve. For character of emergency relief set the material costs, management requirements and degree of scarcity to policy makers; For a typical relief supplies set the related material to programmers. Establish a corresponding judgment matrix according to the relevant requirements which is based on reserve and scheduling requirements. The deployment requirements and reserve requirements can be built by using the algorithm of AHP analytical hierarchy process in order to get the weights of 9 kinds of materials. After clustering analysis of these two weighted tables, the correlated classification of the 9 kinds of materials can be obtained finally. The disadvantages of the traditional centralized management can be solved.

This work was supported by the Project of Beijing University of Posts and Telecommunications “Youth Innovative Research Program”(2012RC0502).

Z. Su (✉) · X. Weng
School of Automation, Beijing University of Posts and Telecommunications, Beijing 100876,
China

L. Zhang
National Disaster Reduction Center of China (NDRCC), Beijing 100124, China

Keywords AHP · Cluster analysis · Emergency material

9.1 Introduction

After a natural disaster, a timely and effective distribution of the relief supplies can greatly reduce the loss whi caused by natural hazards, even can save much valuable time, and then numbers of innocent lives can be saved [1]. For now, the classification about emergency materials mostly storage and schedule in uniform management mode, not adequately considering reserve features of materials, causing a series of questions such as high management expense, low efficiency of disaster relief and so on [2]. Focusing on these above problems, the paper mainly researches on how to use AHP and clustering analysis hybrid algorithms, making extensive use of characteristic of analytic hierarchy process (AHP) which combined qualitative and quantitative methods and the advantages of clustering analysis which is concise and brevity [3–5]. Considering the features of scheduling and storing of the reserve materials, two hierarchical process modes were proposed accordingly, to better meet the actual requirements of materials classification.

9.2 Concrete Step of Analytic Hierarchy Process

1. Definitude principle about build index
Before select the appropriate evaluation index, the principle about build index should be confirmed, which can make the selected index more significant.
2. Build hierarchical structure model
The first step of AHP is to build hierarchical structure analysis, which means that they will hierarchical processed according to the interdependency of each main factor which can be referred to the research object
3. Establish judgment matrix
The next step is to determine the weight of each relevant factor in criterion level. In order to determine weight of J which correspond with the n factors, the factors in K need pairwise comparisons separately. The results of comparisons can be indicated as weight ratio of two factors. While these results of comparisons form a judgment matrix.
4. Single-level sort
Single –level sort is a foundation, which the factors of this level comparing with the upper level even the target level are sorted by weight. Eigenvalues and eigenvectors calculated, the consistency inspection of it can be processed.
5. All-levels sort All-levels sort is carried out on the basis of single–level sort. A group of weight of, ..., to the whole J level can be obtained, and it is the basis which the n factors of K level are sorted according to its importance. Finally, consistency inspection is processed.

9.3 Instance Modeling Analysis

9.3.1 Construction of Judgment Matrix

9.3.1.1 Judgment Matrix According to Scheduling Requirements

1. Storing requirements of emergency supplies

According to the pairwise comparisons among the 3 indexes of scheduling requirements of emergency supplies in middle level, judgment matrix is obtained as Fig. 9.1: Consistency ratio of judging matrix: 0.0000; weight to the overall objective: 1.0000.

2. Importance

According to the index importance, pairwise weight comparisons among the 9 emergency supplies are processed, respectively. Judgment matrix is obtained as Fig. 9.2: Consistency ratio of judging matrix: 0.0431; weight to the overall objective: 0.3333.

3. Scarcity

According to the index scarcity, pairwise weight comparisons among the 9 emergency supplies are processed, respectively. Consistency ratio of judging matrix: 0.0889; weight to the overall objective: 0.3333.

4. Timeliness

According to the index timeliness, pairwise weight comparisons among the 9 emergency supplies are processed, respectively. Consistency ratio of judging matrix: 0.0510; weight to the overall objective: 0.3333.

9.3.1.2 Judgment Matrix According to Storing Requirements

1. Storing requirements of emergency supplies

According to the pairwise comparisons among the 3 indexes of storing requirements of emergency supplies in middle level, judgment matrix is obtained as Fig. 9.3: Consistency ratio of judging matrix: 0.0000; weight to the overall objective: 1.0000.

emergency supplies	Importance	Scarcity	Timeliness	WI
Importance\	1	1	1	0.3333
Scarcity	1	1	1	0.3333
Timeliness	1	1	1	0.3333

Fig. 9.1 Scheduling requirements of emergency supplies

Material cost	bottled water	storage battery	tent	searchlight	life detector	cotton-padded clothes	compressed food	emergency medicine	pressure bandage	Wi
bottled water	1.0000	0.1429	0.2000	0.5000	0.1429	0.1429	0.2000	0.1111	0.2000	0.0168
storage battery	7.0000	1.0000	3.0000	7.0000	0.5000	2.0000	4.0000	0.3333	4.0000	0.1593
tent	5.0000	0.3333	1.0000	3.0000	0.2000	1.0000	2.0000	0.2500	2.0000	0.0760
searchlight	2.0000	0.1429	0.3333	1.0000	0.1429	0.2000	0.5000	0.1429	0.3333	0.0260
life detector	7.0000	2.0000	5.0000	7.0000	1.0000	3.0000	5.0000	1.0000	5.0000	0.2443
cotton-padded clothes	7.0000	0.5000	1.0000	5.0000	0.3333	1.0000	2.0000	0.2500	2.0000	0.0924
compressed food	5.0000	0.2500	0.5000	2.0000	0.2000	0.5000	1.0000	0.1429	0.5000	0.0450
emergency medicine	9.0000	3.0000	4.0000	7.0000	1.0000	4.0000	7.0000	1.0000	7.0000	0.2852
pressure bandage	5.0000	0.2500	0.5000	3.0000	0.2000	0.5000	2.0000	0.1429	1.0000	0.0549

Fig. 9.2 Importance

emergency supplies store	Supplies costs	scarcity	managing requirement	WI
Supplies costs	1.0000	0.8187	1.0000	0.3104
scarcity	1.2214	1.0000	1.2214	0.3792
managing requirement	1.0000	0.8187	1.0000	0.3104

Fig. 9.3 Storing requirements of emergency supplies

2. Supplies costs

According to the index supplies costs, pairwise weight comparisons among the 9 emergency supplies are processed, respectively. Consistency ratio of judging matrix: 0.0370; weight to the overall objective: 0.3333.

3. Scarcity

According to the index scarcity, pairwise weight comparisons among the 9 emergency supplies are processed, respectively. Consistency ratio of judging matrix: 0.0582; weight to the overall objective: 0.3333.

4. Managing requirement

According to the index managing requirement, pairwise weight comparisons among the 9 emergency supplies are processed, respectively. Consistency ratio of judging matrix: 0.0381; weight to the overall objective: 0.3333.

Alternatives	weight
bottled water	0.1259
storage battery	0.0568
tent	0.1286
searchlight	0.0629
life detector	0.1780
cotton-padded clothes	0.0791
compressed food	0.0809
emergency medicine	0.1843
pressure bandage	0.1036

Fig. 9.4 Classification weight based on scheduling requirement

9.3.2 Solution of AHP

Calculated by AHP, weights of 9 supplies according to scheduling and storing requirements are presented as follows:

1. Classification weight table based on scheduling requirement is presented in Fig. 9.4
2. Classification weight table based on storing requirement is presented in Fig. 9.5

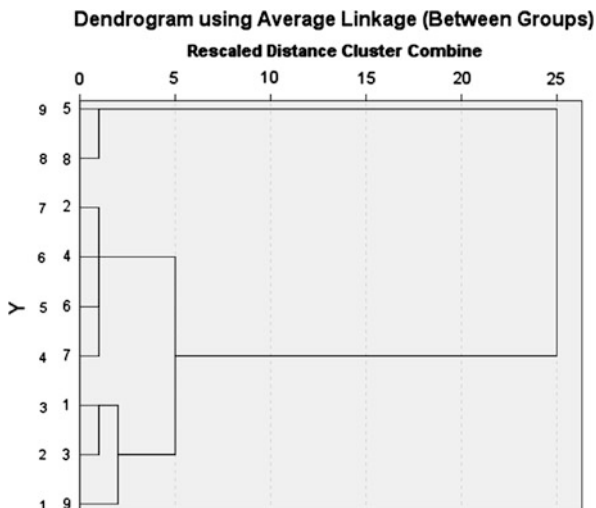
9.3.3 Clustering Analysis

Clustering analysis is processed according to the classification weight table. Clustering variables are processed based on the 3 comprehensive value of the first index in terms of storing requirement. The variables are analyzed with IBM spss

Alternatives	weight
bottled water	0.0813
storage battery	0.0875
tent	0.1392
searchlight	0.0771
life detector	0.1871
cotton-padded clothes	0.0754
compressed food	0.0692
emergency medicine	0.1921
pressure bandage	0.0911

Fig. 9.5 Classification weight based on scheduling requirement

Fig. 9.6 Clustering analysis according to scheduling requirement



statistics 19. Linkage between groups of system clustering is applied in clustering, and square Euclidean distance is applied in measuring distances. In this analysis, supplies are grouped into 9 classes at most, and 1 class at least. However, this classification is obviously unreasonable. So the method is ignored in this study.

Through the final classification and analysis, clustering analysis results are presented as follows:

1. Clustering analysis according to scheduling requirement:

From Fig. 9.6, according to scheduling requirement there are different hierarchy classifications of the nine supplies, the classification is:

The first class: life detector, emergency medicine.

The second class: bottled water, tent, pressure bandage.

The third class: searchlight, compressed food, storage battery, cotton-padded clothes.

2. Clustering analysis according to storing requirement:

there are different hierarchy classifications of the nine supplies, the optimal classification is:

The first class: life detector, emergency medicine.

The second class: tent.

The third class: pressure bandage, searchlight, compressed food, storage battery, cotton-padded clothes.

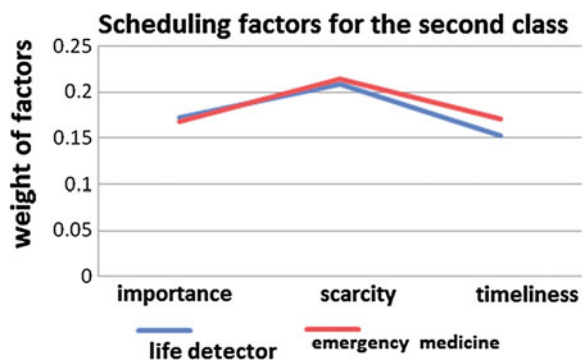
9.3.4 Result Analysis

9.3.4.1 Classification According to the Scheduling Requirements

Detailed analysis for the results of cluster analysis has been achieved in the last paragraph. The first step is to analyze cluster according to scheduling requirements, and the concrete situation are as follows:

1. Figure 9.7 shows the curve evaluation of the first category goods (life detector, emergency medicine) in the respect of importance, scarcity and timeliness. It shows that the trend of these two materials are very similar with each other. The weight of factors are higher, both of them are above 0.15. In particular, the weight of scarcity are higher than 0.2. From the actual demand point of view, these two types of materials are of great importance. Therefore, in the respect of both theory and fact, this classification is reasonable.
2. The second category of materials include bottled water, tent and pressure bandage. The weights of these three types of materials are above the average level. Apart from the scarcity of tent are higher than the other two materials, the overall goodness of fit is very high. Compared with the last figure, if tents are regarded as the first category of materials, the trend of curves is totally feasible. However, compared with life detector and emergency medicine, the importance, scarcity and timeliness of tent is lower. Therefore, the classification of tent is reasonable. From the respect of actual scheduling need, the timeliness weights of bottled water, pressure bandage and tent are above 0.1, which reflects that the timeliness of these materials are fairly high. Therefore, victims should be satisfied within the shortest time in these materials.
3. Finally, the third category of materials includes batteries, searchlights, padded coats and compressed food. The trend of the curves of these types of materials is relatively common. It can be seen that the overall weights of this type are lower than that of the two types mentioned before, no matter in the degree of importance, the degree of scarcity or timeliness. And the distribution of them is above the average level. The distribution of the weights of these types seems

Fig. 9.7 Scheduling factors for the second class

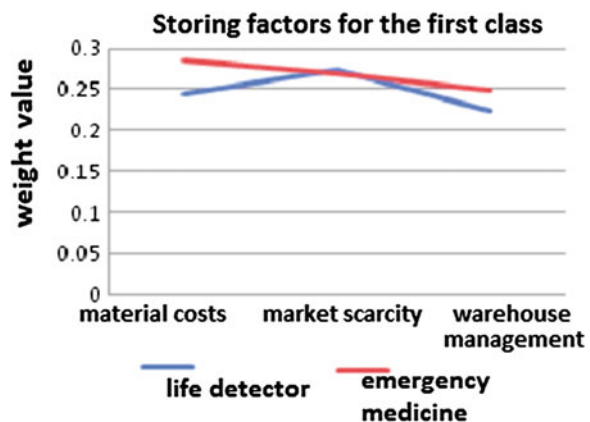


much more concentrated in the degree of scarcity or timeliness. And among them, the scarcity degree of compressed food is the lowest, while the timeliness requirement of batteries is the lowest. In the matter of the degree of importance, the distribution seems not so concentrated. Since the compressed food and padded coats are closely relative to the diet and warming of disaster victims, the importance degree of these to materials are higher. By comparison, batteries and searchlights sorted to auxiliary materials, so the importance degree is the lowest.

9.3.4.2 The Materials Classified Which Based on the Schedule Demands

1. The materials classified which based on the schedule demands, the first category of materials is shown in Fig. 9.8 including life detector and emergency medicine. From the figure we can find these two don't have many difference on the degree of scarcity, but have some differences in the requirement of material costs and warehouse management. The overall level of the weight is in the highest position, and the highest weight value is nearly 0.3. The requirements of these two materials are very high, from the actual reserve requirements. So the materials cost is. But market scarcity are making such material procurement difficult, which is focus on the custody of Class A material. Therefore, these two materials are classified as first category obviously.
2. There is tent that only a kind of materials in the classification of the second category of materials from the point of view of reserve requirement. The overall weight value distribution of it is more extensive. The market scarcity of tents lags far behind the life detector and emergency medicine in the first category of materials. From the view of management requirements, the requirements of tent are not as good as the first category of materials, but the weight of tent is higher than the third category of material. Tents need unbundled storage in the storage process so that the management capability of storehouse is higher. It is reasonable to divide tent into the second category of materials from the view of storage.

Fig. 9.8 Storing factors for the first class



9.4 Conclusion

In this paper, we study the classifications of materials hierarchy, and the algorithm we use is a combined model of AHP and cluster analysis. The combination is first proposed in the study of materials hierarchy, which mainly takes the advantage of AHP's characteristics combining qualitative and quantitative evaluation and the concise advantage of the cluster analysis, to classify the representative materials chosen in this paper and achieved good results.

References

1. Fiedich F, Gehbauer F, Rickers U (2000) Optimized resource allocation for emergency response after earthquake disasters [J]. *Saf Sci* 35:41–57
2. Barbarosoglu G, Ozdamar L, Cevik A (2002) An interactive approach for hierarchical analysis of helicopter logistics in disaster relief operations. *Eur J Oper Res* 140:118–133
3. Santoso T, Ahmed S, Goetschalckx M, Shapiro A (2005) A stochastic programming approach for supply chain network design under uncertainty[J]. *Eur J Oper Res* 167:96–115
4. Kubo S, Akimoto H, Moriwake T (2003) First-aid transportation by hovercraft in a disaster. *Nat Hazards* 29:553–564
5. Chang MS, Tseng YL, Chen JW (2007) A scenario planning approach for the flood emergency logistics preparation problem under uncertainty[J]. *Transp Res* 43E:737–754

Chapter 10

Green Supply Chain Management System of Modern Enterprise Construction Strategy

Xiaoyuan Shi

Abstract With the continuous development of China's logistics industry, green supply chain management is becoming a hot issue for the current research. With the continued enhancement of people's environmental awareness, a growing shift in the mode of economic growth, enterprises cannot succeed in the fierce market competition to occupy a favorable position to achieve long-term survival and development if they do not make innovations in traditional management pattern and adapt to various needs of the changing market. This paper first describes the basic characteristics of the green supply chain management and then analyzes the status quo of green supply chain management in China's enterprises and finally focuses on the strategy for the green supply chain management and the measures.

Keywords Green supply chain · Management system · Modern enterprise · Basic characteristics · Build strategy

10.1 Introduction

At present, the ecological environment of the world is deteriorating, the environment for human survival and life safety is constantly subject to challenges, so sustainable development of the economy has become a hot topic worldwide. As the "green" concept is particularly accepted by people and people have risen their environmental awareness, enterprises also need to assume more social responsibility in the development process. Green supply chain management emphasizes a coordinated development between social economy and ecological environment. Thus, it requires enterprises to pay more attention to environmental protection in product design, packaging, procurement, production, sales, logistics, disposal and

X. Shi (✉)

College of International Business, Zhejiang Yuexiu University of Foreign Languages, No. 428 Kuaiji Road, Yue Cheng District, Shaoxing 312000, Zhejiang, China
e-mail: sxy_008@126.com

recycling, and other sectors and gradually build a scientific system for green supply chain management in modern enterprises, thus achieving harmony and unity between economic and social benefits in the process of enterprise development and promoting the sustainable development of enterprises.

10.2 A Basic Meaning and Features of Green Supply Chain Management of Modern Enterprises

At present, there are many statements about the concept of green supply chain management, but the core concept is the same, referring to a new business management concept in enterprises, namely an effective integration between supply chain management and protection of ecological environment. It means that enterprises should take into account the relationship between effective use of enterprise resources and the protection of ecological environment in the key links of supply chain management in enterprises. By doing so, enterprises may realize economic targets in such fields as supply, production, sales, use and recycling, and the aim of protecting ecosystem. Furthermore, enterprises may improve their ability to make more profits in supply chain management, enhance core competencies to participate in market competition, and ultimately realize a win-win situation between enterprise development and ecological environmental protection.

10.2.1 Concerning About the Environment at Any Time

Modern enterprises should consider the environmental benefits in their operation and management activities so as to avoid negative effects on ecological environment as much as possible when they implement green supply chain management. Therefore, enterprises must take into account the most effective use of management programs to the resources, the lowest emissions of pollutants, or scientific recycling and utilization of waste, and finally, enterprises should make scientific and rational evaluation of the various effects on the ecological environment. If these programs fail to meet relevant requirements, they will not be implemented. The traditional supply chain management is to emphasize a customer-centered method and provide the best quality service, without taking into account environmental factors, and it apparently has been difficult to adapt to the latest requirements of the time.

10.2.2 The Closed-Loop Operation

The factors of production and logistics elements in the implementation process of green supply chain management are not raw materials, but semifinished or final products in the traditional sense, and instead, they emphasize the green movement

and circulation of material elements within the supply chain system. For example, waste generated in the production, or defective products, and expired products in the process of logistics and sales are needed to be recycling and reuse so as to reuse resources or resale products. Modern enterprises implement green supply chain management process, which is a scientific system of closed-loop operation, without a so-called termination point in the green supply chain system.

10.2.3 Emphasis on the Application of Modern Information Network Technology and Data Sharing

With the continuous development and progress of computer technology and network IT, construction and implementation of green supply chain management system become convenient, because modern enterprises can seek a suitable partner in product design and production processes through the computer network to achieve further optimization and sharing of social resources and to achieve expected goals such as resource conservation, inventory savings, and improvement of production efficiency; secondly, enterprises can grasp cutting-edge information about market supply and demand through e-commerce platform, thus achieving the high-quality procurement of raw materials and broadening of sales channels. In this way, enterprises reduce the expenditures in the procurement and marketing chain; thirdly, with the help of modern network technology, companies can also improve the logistics efficiency, reduce waste of logistics resources, and reduce the adverse impact on the surrounding environment in the process of logistics and transport. Meanwhile, data sharing in green supply chain management system is beneficial to optimizing the raw material selection, product design, green production, green logistics, waste recycling, and other aspects.

10.2.4 With the Idea of Concurrent Engineering

Green supply chain management emphasizes its concern about the product life cycle, whether it is the production of raw materials, or manufacturing and recycling of products. All these need “green” concept. Concurrent engineering thinking also attaches importance to the product life cycle. It requires comprehensive consideration of all aspects in the design process and takes into account the recycling and reuse of products and materials. Obviously, the ideal of green supply chain management and concurrent engineering thinking has the same purpose.

10.3 Factors Influencing Green Supply Chain Management Quality

10.3.1 Business Managers Do not Have the Modern Concept of “Green”

Due to the influence of the traditional business management model, many companies blindly pursue the maximization of corporate profits, while ignoring the possible adverse impact on the ecological environment in the process of supply chain management. Many entrepreneurs even believe that only when companies get maximum economic profits, they can in turn make a greater contribution to society. They also think that excessive focus on environmental issues will increase the production and operating costs, which is not conducive to the improvement of economic benefits of enterprises. At the same time, if they want to guarantee the quality of the implementation of green supply chain management, they have to reach consensus among all company members relevant to the whole supply chain and make joint efforts to achieve the desired structure and objectives. If the managers of many companies in China do not have the basic modern concept of green supply chain management, it cannot fully guarantee the effective implementation of green supply chain management.

10.3.2 The Tradition of the Supply Chain Management Has Formed a Barrier

The traditional supply chain management model lays stress on factors such as time, cost, quality, and service, without taking into account the demand of environmental protection. Making suppliers as a starting point and the user as the end point, it is a one-way flow, whether it should be capital flow, information flow, or logistics. It does not pay attention to the closed-loop operation in all sectors of the supply chain management. Obviously, it is in conflict with the green supply chain management in many ways. It is precisely because there are a lot of traditional factors of the supply chain management in modern enterprises and they, to a large extent, hindered the effective implementation of green supply chain management strategies in modern enterprises.

10.3.3 Environmental Policy and Enterprise System Is not Perfect

The government should play a guiding role in the implementation of the green supply chain management, actively carry out and build a sound environmental

policy and system, and do a good job in supervision and management for the implementation of green supply chain to create a favorable policy environment and social environment. However, many local governments lay too much emphasis on economic growth, making inadequate efforts in fighting against environmental pollution. Some even damage the environment to obtain performance, which is shortsighted. Some governments even support the mode of production at the expense of ecological environment by some enterprises, which make many companies ignore the protection of ecological environment and excessively pursue economic interests. Implementation of green supply chain management strategy requires coordination between various links. If there are no sound system and policy measures of environmental protection, it would be difficult to implement the strategy of green supply chain management in a deeper and comprehensive manner.

10.3.4 Consideration of Input and Output by Enterprises

In the process of implementation of green supply chain management strategy, enterprises do not only invest operating costs in the production and management links, such as human resources, information, logistics, and capital, but also require all members to consider the social costs of the entire supply chain, which makes enterprises doubt their proportion of their input and output and fear that they may not have the expected benefits, which to some extent limits the implementation of green supply chain management strategies in modern enterprises.

10.4 Effective Measures to Build Green Supply Chain Management System in Modern Enterprises

If modern enterprises want to truly implement green supply chain management, they need to overcome difficulties, learn successful experience from other enterprises based on their own situation, and gradually build a sound system of green supply chain management.

10.4.1 Green Design System

Researches indicate that the integrated performance of the product depends largely on the product design, which accounts for only a small percentage of the total cost. Therefore, modern enterprises must pay full attention to green design system, giving consideration to the possible impact on the environment by products in the

product life cycle while designing products. Modern enterprises should also ensure the environmental benefits of the product throughout the life cycle, so that they can make full use of social resources to their lowest consumption [1]. First, the modular design can help companies quickly develop products and facilitate the optimization and maintenance of the product structure, conducive to scientific recycling and reuse of products; second, standardized design can reduce the workload of the production and processing and reduce the difficulty of the work and resource consumption; third, removable design and recyclable design are also important methods in green design system, reducing the difficulty of the work and increasing the reuse of parts. In addition, in the process of the product design, enterprises should try to choose green materials and control the quality of green supply chain management from the source, so you can ensure that products can be closely integrated in all aspects of supply chain management of green management objectives.

10.4.2 Green Supply System

In order to ensure the effect of the implementation of the green supply chain management in modern enterprises, enterprises should ensure the supply of raw materials on the one hand, and they also need to build a scientific system of green supply. First is the strict selection of suppliers. In addition to considering the traditional factors in supply chain management, enterprises should look into the efforts made by suppliers in environmental protection, to see whether it can meet the objectives of enterprises in supply chain management to promote the production of green products and energy saving and consumption reduction; second is implementing a green logistics policy [2]. For example, during the packaging process, we should try to choose biodegradable, pollution-free packaging materials; in the handling process, we should reduce the breakage rate of the goods and reduce noise pollution; in the process of transport operations, we should reduce energy consumption and harmful emissions.

10.4.3 Green Production System

In organizing production activities, modern enterprises should fully take into account the adverse effects on ecological environment by raw material input, product output, and a variety of resource consumption. Their aim is to build a scientific production system for environmental protection. First of all, in the choice of production technology and programs, scientific analysis should be given to the factors that may adversely affect the green supply chain management, such as

processing methods, processing machinery efficiency, and resource consumption. Modern enterprises should try to make production technology easier, lower the consumption of resources on the basis of production needs, and reduce pollution caused by production technology. Secondly, with the improvement in production and processing, enterprises should minimize the leftover of processing, which contributes to the conservation of materials and waste generation. Third is the strict production processing machinery and equipment selection and maintenance. Enterprises should try to select those processing machineries with high-performance and lower pollution emissions. And they should also draw up scientific rules about maintenance and repair. Finally, in the production process, more humanized methods should be given consideration and the protection of ecological environment and reduction of the discharge of pollutants should be given more attention.

10.4.4 Construction of Green Marketing and Green Circulation System

First of all, in the sales sector, enterprises should try to choose “green” marketing methods and adopt ecological management method. For example, they can make use of e-commerce platform to carry out online marketing; when choosing sales promotion, enterprises should pay attention to the publicity of the green features of companies and products and select the most economical and most environmentally friendly ways of publicity; in the selection of suppliers or brokers, their green image should also be taken into account [3].

Secondly, in the circulation, it is necessary to select the green, environmentally friendly, and safe packaging materials or forms of packaging, as packaging can easily be discarded by the user, both a waste of resources and also causing damage to the ecology; besides, it is important to select the green mode of transport, such as centralized distribution and optimization of transportation routes; furthermore, a comprehensive evaluation should be given to the service life of products and the extent of their recycling when products are in service.

10.4.5 Green Recycling System

Due to scientific and technological progress, products on the market are not only enriching their functions, but also accelerating the frequency of product replacement and shortening product life cycles, and thus, a large number of obsolete products or waste products are produced. Construction of the green recycling system is to achieve the scientific recycling and reuse of obsolete products or waste products. In this way, enterprises can not only save a lot of resources for themselves but also reduce the damage to ecological environment so as to achieve sustainable development.

10.5 Effective Strategies for the Implementation of Green Supply Chain Management in Modern Enterprises

10.5.1 Create a Strategic Partnership with Green Members

Green supply chain management emphasizes the full attention of the entire product life cycle, requiring the active participation of each member in the supply chain. In view of this, enterprises should actively guide the consumers, encourage the public to actively participate in the process of consumption of green products, and recycle and reuse packaging or old products to achieve the desired objective of protecting the environment. At the same time, in the implementation of green supply chain management strategy, enterprises should develop a strategic partnership with suppliers and partners on the entire supply chain, which is very important. Because only by doing so can they realize sharing of information and resources, improving market competitiveness on the whole and making sure the implementation of management measures on green supply chain.

10.5.2 Making the Building of Green System More Targeted Based on the Actual Situation of Enterprises

Each industry or enterprise has its own characteristics. Therefore, when building a system of green supply chain management, deep analysis should be given to the operating condition and the market environment enterprises live in. And then, scientific management goal can be formulated. What is more, targeted management measures are necessary in the process of product design, supply, packaging, manufacturing, sales, and recycling. All these will make the management system of green supply chain more targeted.

10.5.3 To Build a Good Corporate Green Culture

Modern enterprises can effectively raise green awareness by building the “green culture,” so that all personnel are aware of the importance of environmental protection. Strengthening the guidance of the concept on scientific development and the concept of sustainable development is beneficial to the implementation of green supply chain management [4]. First, enterprises should strengthen in-house promotion and training, improve corporate rules and regulations, strengthen the establishment and penetration of green culture, and gradually build a green culture,

so that completely change the traditional concepts of supply chain management and form green atmosphere within the enterprise; second, companies should carry out a series of forums, lectures, and other activities relevant to green supply chain management in the region or within the industry, sharing green ideas and successful experiences; third, to realize harmony between operating activities and performance appraisal on environment, enterprises should emphasize green business culture and promote the implementation of management thinking about green supply chain.

10.5.4 The Government's Active Participation and Guidance

To get more enterprises to implement green supply chain management strategy, the government and relevant departments must first build sound laws and regulations and policy support system, play a guiding role in helping enterprises implement green supply chain management, and provide a favorable social environment to the implementation of green supply chain management. At the same time, relevant departments should do the monitoring work, punish those who are in violation of the system of relevant laws and regulations or the rules and norms of the enterprise, and ensure the follow-up and implementation of various policies on environmental protection.

10.6 Conclusion

To sum up, there is much room to improve the implementation of the green supply chain management in China's enterprises. Only when environmental awareness is raised among enterprises and the public, relevant laws and regulations and policies are improved and green supply chain management is more recognized and accepted, and enterprises can be more active to implement green chain supply management. Under those circumstances, enterprises are able to build a sound management system of green supply chain, guarantee the implementation of relevant management measures, and finally contribute to the social and economic harmony and sustainable development.

References

1. Gilbert S (2001) Greening supply chain: enhancing competitiveness through green productivity, vol 36. Asian Productivity Organization, Taiwan
2. Tan G, Pan J (2000) Habitual domain analysis based on the rough set theory. *Adv Syst Sci Appl* 02

3. Nie Q, Wang J (2010) The Development of green supply chain in Europe and its implications. *Ecol Econ* 01
4. Hong X (2010) Analysis of green supply chain management in enterprises, vol 27. China Business and Trade

Chapter 11

Based on FCM Disaster Area Management at Different Levels

Chaowei Zheng, Xun Weng, Zhiyuan Su and Zhijun Zhuang

Abstract This chapter mainly researches the classification result of the stricken areas based on the Fuzzy C-mean algorithm. The mortality, building collapse rate, and seismic intensity are considered as the reference factors which need Fuzzy C-Means clustering analysis firstly, and then the reference factors will be converted by nondimensionalizing process in order to compress all the data in the standard interval of [0, 1]. The thresholds of operation will be defined in the process of data initialization, if the condition of thresholds is realized, the operation will be stopped; secondly, iterations of algorithm will be stated. The consequence obtained after the stop of the initialization will be used to calculate the subjection degree of each factor again, and is divided into several intervals in order to construct a matrix set, and then cluster center will be calculated again. After the many steps of repetitive computations, if the cluster center and the matrix set meet the conditions of thresholds and the iterations which are both set by us, and the condition that thresholds is realized means the astringency of algorithm is outstanding enough to meet requirements of relevant target. Besides, the algorithm will be simulation analyzed using MATLAB software, and at last take the some regions such as Qingchuan County, An County and Mianzhu City for example to get the final result. Stricken areas are classified into three categories, and the result will be analyzed in the view of different proportions of all the factors.

Keywords Fuzzy C-Means · Clustering analysis · Classification management

C. Zheng

School of Economics and Management, Beijing University of Posts and Telecommunications, Beijing 100876, China

X. Weng (✉) · Z. Su

School of Automation, Beijing University of Posts and Telecommunications, Beijing 100876, China

e-mail: wengxun79@163.com

Z. Zhuang

School of Computer, Beijing University of Posts and Telecommunications, Beijing 100876, China

© Springer-Verlag Berlin Heidelberg 2015

Logistics Engineering Institution, CMES (ed.),

Proceedings of China Modern Logistics Engineering,

Lecture Notes in Electrical Engineering 286, DOI 10.1007/978-3-662-44674-4_11

11.1 The Disaster Area Classification

In emergency logistics, how to make a reasonable allocation and utilize these materials as much as possible, so that the material needs of the disaster areas to satisfaction optimal is a worthy study in emergency logistics field, we should study how to make a reasonable allocation and utilize these materials as much as possible [1]. There are significant variations, because the disaster area will be based on the different areas and the reserve supplies are limited when it happened in the disaster [2]. In this paper, the concept proposed by analysis of three managements: the hardest disaster areas, moderate disaster areas, and mild disaster areas [2]. We can select the previously mentioned disaster area and classification based on FCM clustering analysis.

11.2 FCM Clustering Algorithm

The hardest disaster areas: natural disasters affected, house severely destroyed, casualties, severe shortage of materials, and in urgent need of aid.

The moderate disaster areas: The condition is better than the hardest disaster areas, moderate housing damage, and casualties in general, the extent of demand for emergency and disaster lower than the hardest disaster area. Such disaster areas should also fully be prepared at allocation.

The mild disaster areas: That is not a very serious disaster, housing only a small part of the damage, lesser casualties and material part of the shortage areas. Such disaster area can be conduct the configuration of materials preparation according to the needs. The urgency and the demand of the priority are lower than the highest disaster area and the moderate disaster area.

A sample object is classified as multiple classes based on the degree of similarity because of large number of samples of traditional clustering algorithms and the difference between the sample object. Based on the above characteristics as the improved C-means algorithm, we named FCM [3].

11.2.1 The Steps of the FCM Clustering Algorithm

FCM operations require the following steps:

1. The original data processing
Define a data range $[0, 1]$, different data with different dimensions, so the first dimensionless, get data range $[A, B]$, all data are normalized in the range, data X into X' , Can put all the data are compressed in the range $[0, 1]$, the step as follow:

(1) Translation-standard deviation conversion:

$$x'_{ik} = \frac{x_{ik} - \bar{x}_k}{S_k} \quad (i = 1, 2, \dots, m) \quad (11.1)$$

in

$$\bar{x}_k = \frac{1}{n} \sum_{i=1}^n x_{ik} \quad (11.2)$$

$$S_k = \sqrt{\frac{1}{n} \sum_{i=1}^n (x_{ik} - \bar{x}_k)^2} \quad (11.3)$$

Get A by a series of variables after standard difference operation, for every factor in A has dimensionless, it is very easy to calculate that mean is 0 and standard deviation is 1, and belongs to the same dimension, can be directly superimposed. There have one problem that is all about the x_{ik} of A range is not necessarily deal with the standard data on the range $[0, 1]$ it also need to standardize conversion factor.

(2) Translation-R conversion

$$x^*_{ik} = \frac{x'_{ik} - \min_{1 \leq i \leq n} \{x'_{ik}\}}{\max_{1 \leq i \leq n} \{x'_{ik}\} - \min_{1 \leq i \leq n} \{x'_{ik}\}} \quad (k = 1, 2, \dots, m) \quad (11.4)$$

Get a new collection B , every x^*_{ik} of B belongs to standard range $[0, 1]$, because x_{ik} is dimensionless, the factor of B is also dimensionless data.

2. Initialization

Defined in the formula, the fuzzy-weighted index of 2, the cluster center value of V , is divided into c categories, C greater than or equal to 2, and less than or equal to the number of samples. We can define as fellow to stop the operator: the first, defined the computing threshold value, the operator stopped when threshold value is satisfied. The second, Making the required number of iterations for the computation stops when the number of iterations is greater than the specified value, to ensure that the entire computation is not unlimited computing down, satisfied the requirements to immediately stop.

3. Re-calculating of each factor to degree membership, for different degrees of membership is divided into various intervals, composed of a matrix set $U(b)$ is as follows:

$$\forall i, k, \begin{cases} u_{ik}^{(b)} = \frac{1}{\sum_{j=1}^c \left(\frac{d_{ik}^{(b)}}{d_{jk}^{(b)}} \right)^{\frac{2}{m-1}}}, & d_{ik} > 0 \\ u_{ik}^{(b)} = 1, & d_{ik} > 0 \end{cases} \quad (11.5)$$

4. Re-computing the cluster centers:

$$v_i^{(b+1)} = \frac{\sum_{k=1}^n (u_{ik}^m)^{(b)} x_k}{\sum_{k=1}^n (u_{ik}^m)^{(b)}} \quad (11.6)$$

5. If $\|v^{(b)} - v^{(b+1)}\| < \varepsilon$, the algorithm satisfies the threshold, stop the calculation; otherwise go to the fourth step, the number of iterations plus 1, if the number of iterations to meet the specified value, and stop counting.
6. The algorithm is constantly calculating and updating the cluster center, as well as material factors attached to the matrix set, after repeating the calculation several times, the cluster center and the matrix set can meet our threshold and the number of iterations. If it is to meet the threshold description in the algorithm, the convergence is good enough to meet the requirements; if it is to meet the number of iterations rather than the threshold, indicating the convergence of the algorithm lack of need to increase the number of iterations or correction algorithm, its nature is a real-time dynamic update process.

11.2.2 FCM Algorithm Characteristics Analysis

FCM is C-means cluster analysis; the algorithm uses a two-tier iterative way to obtain the minimum of the objective function; the algorithm is divided into outer and inner layers: The main of the outer layer is contrast specified threshold to determine whether the algorithm has converged to the corresponding degree; the main of the inner layer is to calculate the new cluster centers and update fuzzy membership matrix. After accomplishing the iterative steps, the matrix will determine the object of vesting conditions in accordance with the degree of a value in the new fuzzy membership matrix and calculate the cluster centers. The weighted index m and the convergence threshold of ε value are more critical.

Weighted index m mainly affects the cluster analysis results of the fuzzy. With the increase of m , the fuzzy classification matrix is also growing. It is lost until the time tends to a certain degree of clustering significance. M parameter is a very important parameter, if is not good that it will have very adverse effects results. Of course, the choice of the m value is not as small as possible m values according to different situations and needs to select the corresponding suitable value.

Convergence threshold the same as the cluster number are related with the clustering accuracy and speed. ε is the greater, and the convergence is the faster. Calculated results may be unsatisfactory. When ε is small, will pay high computational cost and time cost, selecting an appropriate threshold is critical.

11.3 Case Analysis

11.3.1 The Original Data Processing

1. According to Chap. 4, data about the information of disaster areas, to extract useful information to make the disaster area classification required for the management of data, are shown in Table 11.1.

Deaths ratio, rate of housing collapse, and earthquake intensity as the reference for FMC analysis factors where deaths ratio is the ratio of number of deaths and the number of the local population.

2. Data were normalized to get the results as shown in Table 11.2 as before data processing method:

11.3.2 MATLAB Modeling

11.3.2.1 Model Program Design

Based on FCM clustering model algorithm design MATLAB program, the function is:

Function [center, U , O] = Count (data, c , parameter)

Table 11.1 The original data

Area name	Deaths ratio	Rate of housing collapse	Intensity
Mao county	0.038	0.7	8.9
BeiChuan county	0.050	0.8	11.0
Mian Zhu county	0.026	0.7	9.0
Li county	0.003	0.2	8.2
Peng Zhou city	0.001	0.3	7.8
Qing Chuan county	0.020	0.6	9.5
An county	0.008	0.3	9.0

Table 11.2 Standardized

Area name	Deaths ratio	Rate of housing collapse	Earthquake intensity
Mao county	0.0034	0.0635	0.8091
BeiChuan county	0.0048	0.0726	1.0000
Mian Zhu county	0.0018	0.0635	0.8182
Li county	0.0001	0.0181	0.7454
Peng Zhou city	0.0000	0.0272	0.7091
Qing Chuan county	0.0016	0.0544	0.8636
An county	0.0002	0.0272	0.8182

1. Input parameters:

Data are raw data matrix, expressed n samples; each sample has m -dimensional eigenvalue

C is the initial number of aggregation centers as the number of categories represented by the characteristic value of C

Parameter is 4×1 matrix:

$$\text{parameter} = [p_1 \quad p_2 \quad p_3 \quad p_4]$$

In which: p_1, p_2, p_3, p_4 expressed membership matrix U index, >1 (The default value is 2.0), maximum number of iterations (The default value is 100), membership the smallest change, iterative terminate condition (The default value is $1e - 5$), each iteration whether the output message signs (The default value is 1)

2. Output parameters

Center show ultimately obtained the cluster centers; U show membership matrix and O show the end result of the objective function

11.3.2.2 Result

Input parameters data are matrix:

$$A = \begin{bmatrix} 0.0034 & 0.0635 & 0.8091 \\ 0.0048 & 0.0726 & 1.0000 \\ 0.0018 & 0.0635 & 0.8182 \\ 0.0001 & 0.0181 & 0.7454 \\ 0.0000 & 0.0272 & 0.7091 \\ 0.0016 & 0.0544 & 0.8636 \\ 0.0002 & 0.0272 & 0.8182 \end{bmatrix}$$

Num value is 3 that is divided into three categories for the clustering variables C

After MATLAB procedures to obtain, the result is as follows:

$$\text{center} = \begin{bmatrix} 0.0001 & 0.0229 & 0.7276 \\ 0.0018 & 0.0528 & 0.8258 \\ 0.0048 & 0.0725 & 0.9993 \end{bmatrix} \text{obj} = \begin{bmatrix} 0.0194 \\ 0.0166 \\ 0.0136 \\ 0.0117 \\ 0.0097 \\ 0.0055 \\ 0.0031 \\ 0.0031 \\ 0.0031 \end{bmatrix}$$

$$U = \begin{bmatrix} 0.0449 & 0.0000 & 0.0170 & 0.9531 & 0.9713 & 0.0640 & 0.0786 \\ 0.9448 & 0.0000 & 0.9779 & 0.0421 & 0.0246 & 0.8696 & 0.9028 \\ 0.0103 & 1.0000 & 0.0051 & 0.0048 & 0.0041 & 0.0665 & 0.0185 \end{bmatrix}$$

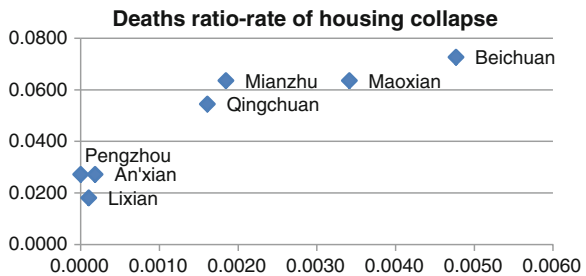
The disaster area clustering is as follows: {Mao county, Beichuan county}, {Mianzhu city, Qingchuan county}, and {Li county, Pengzhou city, An county} Corresponding to the cluster centers: (0.0, 048, 0.0725, 0.9993), (0.0018, 0.0528, 0.8258), and (0.0001, 0.0229, 0.7276).

11.3.2.3 Analysis

According to analysis of these three groups of influencing factors of the deaths ratio and rate of housing collapse, rate of housing collapse and earthquake intensity, and deaths ratio and earthquake intensity in clustering results, the cluster results are verified by FCM and then scatter plots are drawn as follows:

Deaths ratio is X-horizontal coordinate; rate of housing collapse is Y-horizontal coordinate; drawing (deaths ratio, rate of housing collapse) scatter plot is shown in Fig. 11.1. As can be clearly seen from the figure, the seven disaster areas are roughly divided into three parts: as Pengzhou county, An county, and Li county where deaths ratio and rate of housing collapse are very close, so it became a group. Corresponding to point (0.0001, 0.0229) of FCM is very consistent, basically

Fig. 11.1 Deaths ratio–rate of housing collapse



describes the characteristics of the center of this group. Corresponding to point (0.0018, 0.0528) of FCM is very consistent also in Mianzhu city and Qingchuan county. Both of Beichuan County and Mao County in the analysis of the two factors of deaths ratio and rate of housing collapse showed a more serious disaster situation, and it became a group. Basically, in two central locations, corresponding to point (0.0048, 0.0725) of FCM is logical.

Rate of housing collapse is X-horizontal coordinate; earthquake intensity is Y-horizontal coordinate; and drawing (rate of housing collapse, earthquake intensity) scatter plot is shown in Fig. 11.2. As can be clearly seen from the figure, the seven disaster areas are roughly divided into two parts, mainly because Mao and Mianzhu counties' coordinate values are very close. The seven disaster areas can still be divided into three areas virtually.

Pengzhou county, An county, and Li county where earthquake intensity and rate of housing collapse are very close, so it became a group. Corresponding to point (0.0229, 0.7276) of FCM is very consistent, basically describes the characteristics of the center of this group. The upper right of the regional distribution has four disaster areas, Both of Mianzhu city and Mao county have the same intensity values. So there are very difficult to distinct. But, from the cluster analysis point of view, Mianzhu city and Qingchuan county are divided into a group that is very reasonable. Rate of housing collapse is very close; corresponding to point (0.0528, 0.8258) of FCM is very consistent, so it became a group by rate of housing collapse and earthquake intensity. Beichuan County has the highest seismic intensity values and rate of housing collapse into a uniform group with the Mao county, basically in two central locations corresponding to point (0.0725, 0.9993) of FCM is logical

Deaths ratio is X-horizontal coordinate; earthquake intensity is Y-horizontal coordinate; and drawing (deaths ratio, earthquake intensity) scatter plot is shown in Fig. 11.3. As can be clearly seen from the figure, the seven disaster areas are roughly divided into three parts, from (deaths ratio, earthquake intensity) scatter plot, the distribution is the regular at disaster area. Pengzhou county, An county, and Li county, where deaths ratio and earthquake intensity are very close; so, it

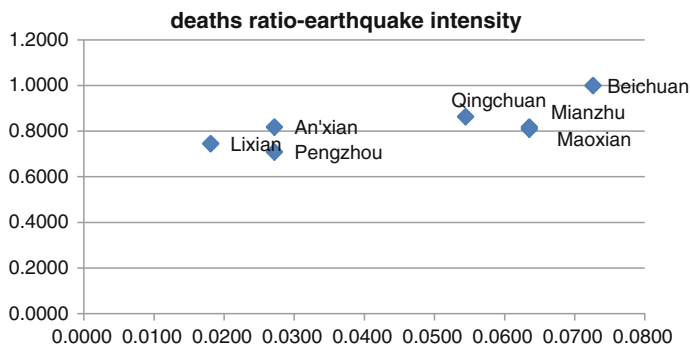
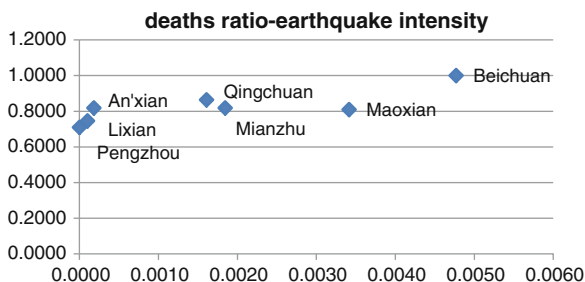


Fig. 11.2 Deaths ratio–earthquake intensity

Fig. 11.3 Deaths ratio–earthquake intensity



became a group. Corresponding to point(0.0001, 0.7276)of FCM is very consistent, which basically describes the characteristics of the center of this group.

Axis in the middle of the first quadrant is the area of Mianzhu city and Qingchuan county; deaths ratio and rate of housing collapse are very close, so it became a group. Corresponding to point (0.0018, 0.8258) of FCM is very consistent.

Finally, it is shown in the upper right part of the areas Beichuan county and Mao county. Deaths ratio and rate of housing collapse are relatively high both in two disaster area than other disaster areas; it became a group. Corresponding to point (0.0048, 0.9993) of FCM is very consistent.

11.4 Summary

This paper mainly studies the disaster area classification based on FMC by taking examples of Qingchuan county, An county, Mianzhu city, and other disaster areas and presents the final results. The paper divided the disaster area into three categories; results were analyzed from the perspective of the ratio of each factor; and the results and the actual situation are consistent. Paper is implemented as proof of algorithm feasibility for disaster management at different levels.

Acknowledgments This work was supported by the Project of Beijing University of Posts and Telecommunications “Youth Innovative Research Program” (2012RC0502).

References

1. Dupuy G, Stransky V (1996) Cities and highway networks in Europe. *J Transp Geogr* 4 (2):107–121
2. Runzhou L (2010) Transportation system connectivity research of earthquake [M]. Institute of Engineering Mechanics, China Earthquake Administration
3. Jin fengjun, Wang J (2004) China’s railway network expansion and spatial accessibility in 20th century. *ActaGeographicaSinica* 59:293–302
4. Song Q, Liu W, Ren Y, Qiao J, Yang X, Xu J (2010) Regional research [M]. Institute of the Ministry of Civil Affairs

Chapter 12

Life Cycle Inventory of Multi-mode Transport System for Designing Green Logistics

Lu Li and Suiran Yu

Abstract Under the background of fact that global environmental crisis is increasingly serious, green logistics issues are gaining interest. As recognized, a good logistics system should be good not only in economy but also in social benefits. Today, the green logistics has already become the trend of the administrative system of logistics. Since transport is the most important function of the system, it becomes the key to lessen environmental pressures caused by logistics activities. The scope of this paper is to summarize a methodology to assess the environmental impact result from transport. The paper focuses on the three main transport modes, i.e., road, rail, and ship, and obtained the whole life cycle inventory (LCI) of the three modes with five main pollutants (CO₂, CO, NO_x, NMVOC, and PM). A case study is given to show the difference between the environmental impacts caused by the three transport modes and how the result changes when different ratios of transport modes were chosen. The obtained inventory can provide the data support for the life cycle inventory analysis of the transport parts of logistics. The results may also be employed to complement global emission inventories and by fleet managers as a green logistics decision-making reference.

Keywords Green logistics · Transport modes · Life cycle inventory (LCI)

12.1 Introduction

Nowadays, the main environmental issues in cities and towns are related to the activities of transport. Increase in environmental concerns boosts the awareness of the importance of finding environmentally friendly ways to reduce emissions and to

L. Li · S. Yu (✉)

School of Mechanical and Power Engineering, Shanghai Jiao Tong University,
800 Dongchuan Road, Shanghai 200240, People's Republic of China
e-mail: sryu@sjtu.edu.cn

© Springer-Verlag Berlin Heidelberg 2015

Logistics Engineering Institution, CMES (ed.),

Proceedings of China Modern Logistics Engineering,

Lecture Notes in Electrical Engineering 286, DOI 10.1007/978-3-662-44674-4_12

save primary energy resources in the transport system. Recently, to better understand and improve the transport system, some researches on the life cycle inventories of different modes of transport were made. Xie et al. [1] found that the emission factors calculated with the COPERT III model are better close to those in the actual emission status in China than with the MOBILE model. Fan et al. [2] have done an estimation on the exhaust emissions from the railway vehicles in Beijing, in which they have studied the locomotive emission factors of the Environmental Protection Agency (EPA) of USA, along with the domestic emission factors in comparison with the emission standards of China, American, and International Union of Railways (IUR). According to the method based on fuel consumption, Jin et al. estimated the emissions from the commercial ships of Tianjin harbor in 2006 [3].

This paper describes a comparative analysis of freight transport alternatives in China under the assessment of their life cycle inventories. A life cycle assessment (LCA) inventory analysis of a multi-mode transport system was undertaken using three main transport modes: road, rail, and inland ship. The inventory analysis followed the guidelines provided by the ISO 14040 and ISO 14044 standards.

12.2 Methods

12.2.1 Goal, Scope, and Functional Unit

The study is focused on a multi-mode transport system. Generic background data have been generated for three modes of transport (road, rail, and inland ship) to account for cumulative exchanges due to the transportation occurring between two process steps of a logistics system. The data represent average transport conditions in China.

In order to quantify environmental exchanges of transport services and to relate transport datasets to other product life cycles, the environmental exchanges are related to the reference unit of 100 ton kilometer ($t \cdot 100 \text{ km}$). A 100 ton kilometer is defined as the transport of one ton of goods by a certain transport service over 100 km.

The system boundary is illustrated in Fig. 12.1. The studied stages are any freight transport occurring between any two process steps of a logistics system. Besides, the extraction, transportation, production, and distribution of the fuel itself are considered. The waste treatment and the production processes of conveyances are excluded.

Transport modes discussed in the paper are as follows:

- Road (gasoline and diesel trucks, freight transport)
- Rail (diesel and electrical trains, freight transport)
- Shipping (inland ship, freight transport)

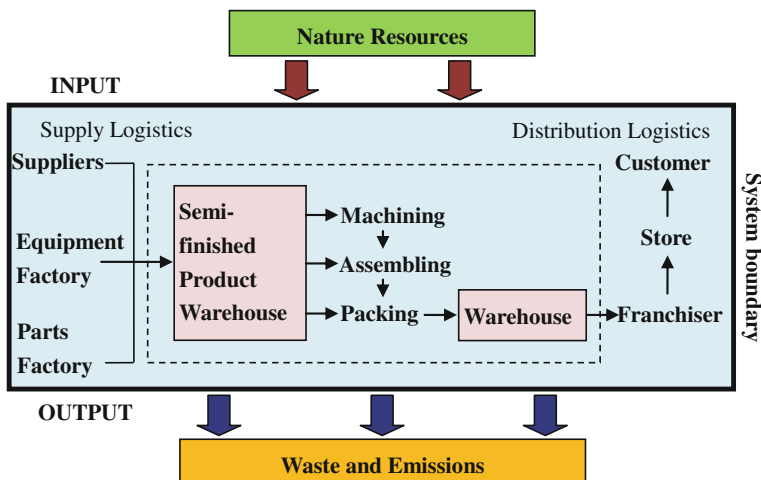


Fig. 12.1 System boundary and transport processes

Pollutants covered: carbon dioxide (CO_2), carbon monoxide (CO), non-methane volatile organic compounds (NMVOC), oxides of nitrogen (NO_x), particulate matter (PM), water pollutants, and solid wastes. These seven kinds of substances are the main items in the output list of transport.

12.2.2 The Inventory Analysis

The environmental pressures considered in the paper are associated with the three main transport modes, i.e., road, rail, and inland ship. The main environmental issues caused by transport are the predominant use of fossil fuel as transport fuel, the combustion of which significantly contributes to air pollution and greenhouse gases. However, emissions result not only from the combustion of fuel, but also as a result of the extraction, transportation, production, and distribution of the fuel itself. Therefore, in the framework of inventory calculation, two related parts are developed for the estimation of emissions and energy consumptions from transport, i.e., conveyance's using stage and energy production stage.

In a LCA study, the data collection has the largest importance for the usefulness of the result, and consumes most of the resources of the study. The reliability of the result of the LCA study is highly dependent on the reliability of the data from which the results are derived, and the data documentation is therefore a crucial issue. Because data collection is such an expensive task, it is more economic to reuse data already collected, and most LCA practitioners do reuse data from previous studies retrieved from LCI databases or other sources.

12.2.2.1 Fuel Production and Electricity Generation Inventories

The inventory analysis started with an estimation of the fuel production and electricity generation stages. The inventory analysis of the life cycle of production of gasoline and diesel as well as the generation of electricity used data from two studies performed by the Key Laboratory for Advanced Functional Materials of the Ministry of State Education, Beijing University of Technology [4, 5].

The input included the consumption of raw coal, crude oil, and natural gas, and the output included water pollutants, solid wastes, and gaseous state pollutants. The life cycle inventories contained the stages of fossil fuels production and transportation. See Table 12.1.

12.2.2.2 Inventories for Road Transport

In China, most of the light vehicles are propelled by gasoline, while heavy vehicles always use diesel as fuel. Under this situation, the studied light vehicles are set to use gasoline and its load is 2t, and the heavy vehicles are set to use diesel and its load is 10t. Based on the report of Ma et al. [6], the energy consumption in a functional unit with light vehicles and heavy vehicles are 6.15 and 3.22 kg, respectively. Emission estimates are produced for three distinct driving modes: urban, rural, and highway driving. Given that the highway driving takes the most place of the logistics processes, only the highway driving mode is considered in this section.

The output list of road transport is built upon existing calculation methods, i.e., the emission factors and combustion equations. In order to evaluate the environmental indicators for road transport, first, the emission factors (g/km) for each vehicle

Table 12.1 Life cycle inventories of fuel and electricity

	Gasoline	Diesel	Electricity
	<i>Input</i>		
Raw coal (kg)	4.7700E-02	4.7300E-02	5.8000E-01
Crude oil (kg)	1.3200E+00	1.3100E+00	1.4400E-02
Natural gas (m ³)	7.9500E-05	7.8700E-05	9.6900E-04
	<i>Output</i>		
Gasoline (kg)	1.0000E+00	0.0000E+00	0.0000E+00
Diesel (kg)	0.0000E+00	1.0000E+00	0.0000E+00
Electricity (kW h)	0.0000E+00	0.0000E+00	1.0000E+00
CO ₂ (g)	2.2000E-01	2.2000E-01	1.0700E+00
CO (g)	1.3500E-04	1.3300E-04	1.5500E-03
NO _x (g)	8.4800E-04	8.4000E-04	6.4600E-03
PM (g)	1.7500E-03	1.7300E-03	4.8700E-04
Water pollutants (g)	7.7000E-01	7.6000E-01	1.7500E-03
Solid wastes (g)	7.7700E-03	7.7000E-03	2.2394E-01

Table 12.2 Emission factors of different transport modes

Transport modes	CO ₂	CO	NO _x	NMVOC	PM
Light vehicle (g/kg gasoline)	2,411.87	365.61	19.11	38.94	9,121.68
Heavy vehicle (g/kg diesel)	3,123.14	14.44	31.40	8.73	3,488.90
Diesel train (g/kg diesel)	3,369.50	4.14	94.34	2.19	1.46
Inland ship (g/kg diesel)	3,161.00	9.16	49.24	4.87	2.43

category and technology class were produced from COPERT III [1]. Then, by using the aforementioned assumed load factors, indicators were calculated for each vehicle category. Emission factors for the five regular air pollutants (CO₂, CO, NO_x, NMVOC, and PM) are expressed as emission per kilogram fuel consumption. The emission factors in this part were all calculated based on the national average in China.

1. CO, NO_x, NMVOC, and PM. The four pollutants' emission factors use the data from a research of Xie et al. [1], which is based on the COPERT model. Compared with MOBILE model, COPERT estimates emissions of all regulated air pollutants and is more suitable for the actual conditions in China [7]. See Table 12.2.
2. CO₂ is calculated on the basis of fuel consumption as follows [6]:

$$f_{\text{CO}_2} = [(C_{\text{fuel}} - f_{\text{THC}}) \times 0.87 - f_{\text{CO}} \times 0.42] / 0.273 \quad (12.1)$$

where C_{fuel} denotes the fuel consumption per kilometer of a certain vehicle category, g/km; f_{THC} and f_{CO} represent the emission factors of THC and CO, respectively, g/km. The CO₂ emission factors can be calculated by using Formula (12.1) (see Table 12.2)

By using the emission factors and corresponding load factors and taking into account each vehicle category's fuel consumption factor, we can get the life cycle inventories of road transport of their usage phase. Additionally, considering about the stages of fossil fuels production and transportation, the LCI for the road transport is obtained and is presented in Table 12.3.

12.2.2.3 Rail Transport

The train is distributed into three classes: steam train, diesel train, and electrical train, which are propelled by coal, diesel, and electricity, respectively. Nowadays, steam trains are no longer working as a means of freight transport. Therefore, Chinese rail transport is a mix of diesel and electric traction. So the diesel trains are the only resources that release pollutants to the environment directly. Although electrical trains do not release emissions directly when being driven, there are emissions due to the electricity generation stages. The emission factors for diesel trains are calculated first.

Table 12.3 Inventories for functional unit of different transport modes

	Light vehicle	Heavy vehicle	Diesel train	Electrical train	Inland ship
<i>Input</i>					
Raw coal (kg)	2.9336E-01	1.5231E-01	1.1920E-02	6.2582E-01	2.6015E-02
Crude oil (kg)	8.1180E+00	4.2182E+00	3.3012E-01	1.5538E-02	7.2050E-01
Natural gas (m ³)	4.8893E-04	2.5341E-04	1.9832E-05	1.0456E-03	4.3285E-05
<i>Output</i>					
CO ₂ (g)	1.6186E+04	1.0765E+04	9.0455E+02	1.1545E+03	1.8596E+03
CO (g)	2.2493E+03	4.6928E+01	1.0768E+00	1.6725E+00	5.1096E+00
NO _x (g)	1.2272E+02	1.0380E+02	2.3985E+01	6.9703E+00	2.7542E+01
NM VOC (g)	2.3950E+02	2.8100E+01	5.5188E-01	5.2547E-01	2.6793E+00
PM (g)	5.6109E+04	1.1240E+04	8.0388E-01	1.8883E+00	2.2872E+00
Water pollutants (g)	4.7355E+03	2.4472E+03	1.9152E+02	2.4163E+02	4.1800E+02
Solid wastes (g)	4.7786E+01	2.4794E+01	1.9404E+00	3.0899E+01	4.2350E+00

The emission factors of CO, NO_x, NMVOC, and PM are provided by the Environmental Protection Agency, USA [8]. See Table 12.2. Based on the Energy Statistical Yearbook of China [9], the emission factor of CO₂ is 73,187 kg/TJ and the heat value of diesel is 46.04 MJ/kg. So the result is 3.3,695 kg/kg diesel.

Inputs and outputs for the operation datasets of rail transport are directly related to the functional unit, i.e., the load factor cannot be adjusted. And according to the Statistical Yearbook of China [10], the fuel consumption factor of diesel train per 10'000 ton kilometer is 25.2 kg as well as the electricity consumption figure of electrical train is 107.9 kW h per 10,000 ton kilometer. By timing the corresponding emission factors with energy consumption figures and taking into account the energy production stages, the inventories of rail transport are obtained and illustrated in Table 12.3. A database is then developed for rail transport consisting of emissions and energy consumption.

12.2.2.4 Ship Transport

In a similar way to rail transport calculation, the life cycle inventory of shipping contains two parts, i.e., the using stage and the fuel production stage. The category of transport considered in this section is only inland ship which traveling in Yangtze River. The results represent the national average condition of inland shipping in China.

According to the database of the Statistical Yearbook of China [10], the average load of inland ship is 844 ton. Then, the indicators of inland ship are set to be 800 ton of load with 360 kW power rating and the average speed is 15 km/h. The emission factors of CO, NO_x, NMVOC, and PM use the data from a study performed in Tianjin [3]. Since the density of diesel is 0.84 kg/L, unit g/L diesel can be turned into g/kg diesel (see Table 12.2). Based on the research of Dolphin and Melcer [11], emission factor of CO₂ is taken as 3,161 g/kg diesel.

Given that the fuel consumption of inland ship is $550 \text{ t}/(10^8 \text{ t km})^3$ and database of emission factors with the definition of functional unit, together with the life cycle inventories of energy production (see Table 12.1), the LCI of ship transport is calculated and shown in Table 12.3.

All the calculative processes presented in this paper are implemented within a PC-based MS Excel 2007 environment, providing detailed pollutant and resource consumption results.

12.3 Results and Discussions

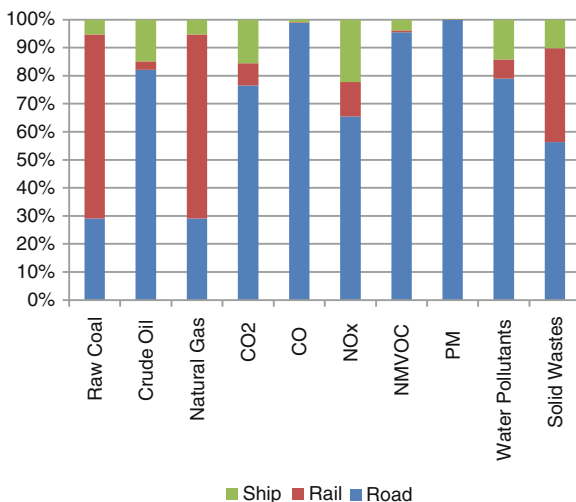
In this section, LCI results are presented and discussed within a certain transport system between Shanghai and Chongqing which represents the average in China. Shanghai is the international economic center and the biggest seaport in China; Chongqing has become the transportation junction of southwest and the economic center in the upper reaches of the Yangtze River with rapid development after Chongqing became municipality since 1997. Extensive and close trade contracts exist between the two modern cities, and transportation plays an important role in their economic cooperation. The implement of greening of logistics activities means much to the two cities.

12.3.1 Inventories of Road, Rail, and Ship Transport

Shanghai and Chongqing are 1,773 miles apart for highway, 2,226 miles for rail, and 2,399 miles for water (inland). Based on the data in the Statistical Yearbook of China [10], the ratios of light vehicles and heavy vehicles are set to be 30 and 70 %; the percentage of diesel and electrical trains in freight transport are 45 and 55 %, respectively. Then, the life cycle inventory of transport system from Shanghai to Chongqing can be calculated with the inventory of the functional unit of different transport modes which was obtained in the paragraph before. To better compare the energy consumption and pollutant emission among different modes, a histogram was drawn to illustrate the percentages of the items in the inventories for road, rail, and ship transport from Shanghai to Chongqing (see Fig. 12.2).

The energy consumption figure for road transport is 3.45 kg raw coal, 95.53 kg crude oil, and $5.75\text{E}-03 \text{ m}^3$ natural gas, and for rail transport is 7.78 kg raw coal,

Fig. 12.2 Percentages of resource consumption and pollutant discharge of a transport system for different modes in LCI results



3.50 kg crude oil, and $1.30E-02 \text{ m}^3$ natural gas, and for ship transport is 0.62 kg raw coal, 17.29 kg crude oil, and $1.04E-03 \text{ m}^3$ natural gas. The road transport consumes the most crude oil, and compared with raw coal and natural gas, crude oil is the predominant energy sources for transport consumption. So based on comprehensive consideration, the road transport is the biggest energy consumer when compared with the other two modes. As clearly shown in Fig. 12.2, road transport discharges most pollutants.

12.3.2 Sensitivity Analysis

The sensitivity analysis is generally used to indicate the impact of changes in the data to the results. Sensitivity analysis can show which influences the results seriously in the system and which slightly. International agreements and scientific assessments call for a social awareness for substantial reductions of global greenhouse gas emissions. In this paper, the environmental load of a multi-mode transport system is represented by its CO₂ emission in the sensitivity analysis section. And improvement suggestions for the system are made according to the results of sensitivity analysis.

Based on the data in the Statistical Yearbook of China [10], the percentages of road, rail, and ship transport are set to be 25, 35 and 40 %, respectively, in the Shanghai–Chongqing transport system. The major parameters are the percentages of the transport modes, energy consumption factors, emission factors, and so on. The results of sensitivity analysis are illustrated in Fig. 12.3. The higher point the graph shows, the more important the item is to the whole system.

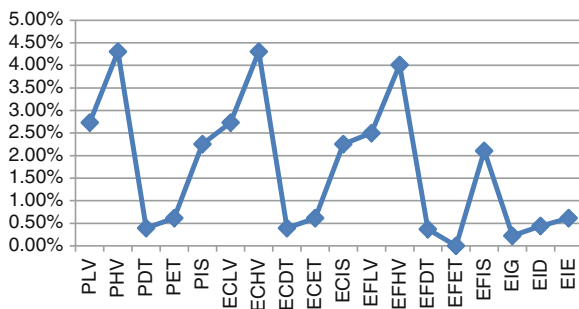


Fig. 12.3 Sensitivity analysis for CO₂ emission of a multi-mode transport system between Shanghai and Chongqing

Where PLV represents the percentage of light vehicle, PHV presents percentage of heavy vehicle, PDT presents percentage of diesel train, PET presents percentage of electrical train, PIS presents percentage of inland ship, ECLV presents energy consumption figure of light vehicle, ECHV presents energy consumption figure of heavy vehicle, ECDT presents energy consumption figure of diesel train, ECET presents energy consumption figure of electrical train, ECIS presents energy consumption of inland ship, EF presents emission factor of CO₂ for different transport modes, EIG means emission intensity of gasoline production, EID means emission intensity of diesel production, and EIE means emission intensity of electricity generation.

It can be easily distinguished that the percentages of road transport, emission factors of road transport, and the fuel consumption figures of vehicles are the most important items in the system for improvement.

12.4 Conclusions

The comparative analysis of different transport modes per ton load of travel in life cycle inventories assessment between Shanghai and Chongqing reveals that road transport consumes most natural resources and discharges most amount of pollutants. Actually, in the Shanghai–Chongqing logistics system, road transport is predominant, ship transport comes next, and rail transport is the least. The result of sensitivity analysis shows that parameters of road transport are the most important impact factors of the whole system. In order to lessen the environmental impact caused by transport activities and assist decision makers in designing a greener logistics system, it is suggested that the rational use of vehicles should be carefully considered, since road transport is not an environmentally friendly alternative compared with the other modes, and the characteristics of vehicles would better be improved.

Acknowledgments This research is financially supported by Natural Science Foundation of China (Project No. 51075275 and 51135004).

References

1. Xie S, Song X, Shen X (2006) Calculating vehicular emission factors with COPERT III mode in China. *Chin J Environ Sci* 27(3):415–419
2. Fan S, Yang T, Tian G (2010) Estimating exhaust emissions from railway vehicles in Beijing. *J Saf Environ* 10(1):90–93. doi:[10.3969/j.issn.1009-6094.2010.01.024](https://doi.org/10.3969/j.issn.1009-6094.2010.01.024)
3. Sheng T, Yin X, Xu J (2009) Air pollutants emission inventory from commercial ships of Tianjin Harbo. *Marin Environ Sci* 28(6):623–625
4. Bao R, Nie Z, Di X, Zuo T (2006) Life cycle inventories of fossil fuels in China (II): final life cycle inventories. *Mod Chem Ind* 27(4):59–61
5. Di X, Nie Z, Zuo T (2005) Life cycle emission inventories for the fuels consumed by thermal power in China. *China Environ Sci* 25(5):632–635
6. Ma L, Hong Z, Gong X (2006) Life cycle inventory analysis of two types of freight transport on city roads. In: Beijing international materials week and China materials seminar, pp 3–8
7. COPERT III: Computer programme to calculate emissions from road transport methodology and emission factors. EEA, Copenhagen (2000)
8. Emission factors for locomotives. Environmental Protection Agency, Washington, USA (1997)
9. State Statistical Energy Bureau, General Affairs Department of the National Energy Board China (2008) Energy statistical yearbook of China 2008. China Statistics Press, Beijing
10. State Statistical Bureau China (2010) Statistical yearbook of China 2010. China Statistics Press, Beijing
11. Dolphin MJ, Melcer M (2008) Estimation of ship dry air emissions. *Am Soc Naval Eng* 3:27–36

Part II
Lifting Machinery Technology
Research (LMTR)

Chapter 13

Dynamic Reliability of the Weight Index Model Research of Residual Fatigue Life of the Crane Boom

Fuhai Cai, Fuling Zhao, Xin Wang, Shunde Gao and Liming Chen

Abstract This paper analyzes the operating characteristics of the crawler crane and summarizes distributed sources in the process of fatigue crack propagation of the boom, makes an introduction of evaluation process of the boom of the remaining life. Three static reliability analysis models are analyzed; the evaluation of reliability indicators do not change over time, and the defect is pointed out that they cannot be satisfied to solve practical engineering problems. This article regards the load and fatigue resistance as a random process and considers the fatigue failure of the randomness in a variety of factors, the concept of dynamic reliability of the weight index is proposed, and models of dynamic reliability of the weight index are built based on the fatigue bearing capacity mode and limit damage degree mode. By computational analysis of the two models and test comparison of the standard welding components, the remaining fatigue life under the dynamic reliability of the weight index model prediction accuracy higher than the static reliability indicators of prediction accuracy. This method provides a new thinking and new methods for the detection and evaluation of the fatigue life of crane booms.

Keywords Crane · Boom crack · Residual fatigue life · Dynamic reliability of the weight index

F. Cai (✉) · F. Zhao · S. Gao
School of Mechanical Engineering, Dalian University of Technology, Dalian 116023, China
e-mail: cfhdlut@163.com

X. Wang
Xuzhou Construction Machinery Research Center of Dalian University of Technology,
Xuzhou 221004, China

L. Chen
Jiangsu Bada Heavy Industry Machinery Co., Ltd., Xuzhou 221400, China

© Springer-Verlag Berlin Heidelberg 2015
Logistics Engineering Institution, CMES (ed.),
Proceedings of China Modern Logistics Engineering,
Lecture Notes in Electrical Engineering 286, DOI 10.1007/978-3-662-44674-4_13

13.1 Introduction

Crawler crane is lifting equipment which is widely used in various fields of the national economy. According to the findings of the accident, serving more than 10 years crawler crane accident in addition to the vehicle overturning, most accidents occurred in the fatigue failure of the boom. It is difficult to detect in advance because there is no obvious plastic deformation harbinger and the fatigue fracture occurred suddenly. So the evaluation of the residual fatigue life of the crane boom is difficult.

Many scholars have proposed the fatigue strength and fatigue life analysis of many systems and made a thorough research on them. However, due to many uncertainties, there is a huge dispersion of the fatigue crack of the boom system in the expansion process.

Dispersion can be divided into three categories according to their sources [1].

1. Intrinsic dispersion: the material itself microstructure heterogeneity, including randomly distributed lattice defects, impurity atoms, dislocations, voids, cracks, manufacturing defects, and so on.
2. External dispersion: Including the external load, specimen geometry, and the work environment uncertainties, all of this dispersion determines the crack extension of the random nature of the process. There are larger deviations between the analysis methods based on deterministic expansion of the fracture crack compared to engineering practice.
3. Evaluation of dispersion: The evaluation of the past is often a definite target. But in the actual process, the safe operation should be dynamic indicators with the time course which the crane is worked after the experience of a variety of loads. The evaluation indicators are gradually reduced to the minimum value. Therefore, the evaluation function for dynamic analysis is necessary on the crack structure of the boom system in order to meet the practical engineering applications.

13.2 Introduction to Residual Fatigue Life Evaluation Methods of Crawler Crane Booms

13.2.1 Working Characteristics

1. The work load is relatively stable, smooth, and small impact
Crawler crane is generally worked with rope, and a smooth lifting and falling is demanded. This job has little impact on the boom. During the working process, the boom will produce a larger elastic deformation to withstand shocks. Boom rods basically belong to the state of compression when the boom is withstanding the load. The boom can be restoring the status quo when the load is gone.

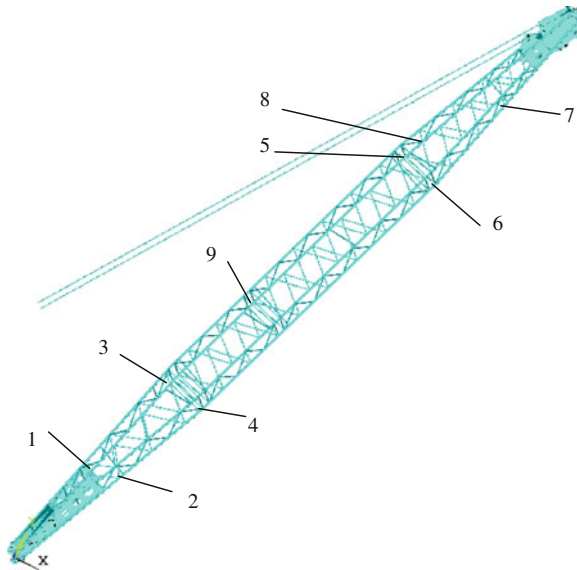


Fig. 13.1 Layout of possible fatigue position. 1 Reinforcing plate of the top chord near the bottom section. 2 Junction of the lower chord and flanks rod of the bottom section. 3 Hinge ears of the top chord of the bottom section. 4 Hinge ears of the lower chord of the bottom section. 5 Hinge ears of the top chord of the top section. 6 Hinge ears of the lower chord of the top section. 7 Abdominal rod and the flanks rod connection at the bottom chord of the top section. 8 Upper chord of the top section and epigastric rod connection. 9 Junction of 3 m section and 6 m boom section

2. The both ends of the boom bear a greater load by force, and the middle bear a small load by force

According to the results of the finite element analysis, there is a larger force in the top section and bottom section of the boom which is shown in Fig. 13.1. We should pay special attention to the weld on the dangerous section, whether or not to bear a greater stress. Truss arm is welded together more than one tube, and the weld is easy to crack damage under alternating load or fluctuating loads. Therefore, the weld initiation, expansion, and the instability of the time course of the model are the focus of life evaluation of the boom system.

3. Boom system under different operating conditions needs to set a different evaluation parameters

The working condition is quite different between different tonnage crawler cranes. Small tonnage crawler cranes loads are generally much smaller than the rated lifting weight. Boom system is working in the elastic range, and the boom plastic deformation is small so it is more suitable for use stress analysis. Large tonnage crawler crane loads are generally close to the rated lifting weight. It means that the work stress is close to the allowable stress value, and the plastic deformation of the boom material is big so it is more suitable for use strain analysis.

13.2.2 Fatigue Life Evaluation Process of Boom

13.2.2.1 Fracture Mechanics Theory

Fracture mechanics theory is the study of crack propagation law of fracture with initial defects in material or structural loads. Complex welded structures are easy to produce a fatigue crack due to the presence of weld defects and crack initiation, and the formation of life is very short. Therefore, the stable propagation life of crack is the main fatigue life of welded structures.

At present, there are several mainstream theories of fatigue crack growth rate model such as the Paris equation, Forman equation, Walker equation, and so on.

The Paris equation has a good accuracy in use with the low stress ratio of fatigue crack growth. The famous Paris equation:

$$da/dN = C(\Delta K)^m \quad (13.1)$$

In the equation: da/dN : the fatigue crack growth rate; ΔK : the stress intensity factor range; $\Delta K = K_{\max} - K_{\min}$; C, m: material constants.

The choice of the stress intensity factor K is critical to calculate in the Paris equation. The degree of the strength of the stress field near the crack tip region can reflect the size of the stress intensity factor and can be an indicator of unstable growth of the crack occurred. Under normal circumstances, the stress intensity factor of a general expression for:

$$K = \alpha\sigma\sqrt{\pi a} \quad (13.2)$$

In the equation: α the coefficient depends on the loading mode, the crack shape, and crack location. α can be a constant or a function about a; σ is the externally imposed stress; a is the crack length.

Paris equation can be integrated under amplitude loads, and the fatigue crack propagation life equation can be obtained from the initial crack length of a_0 to critical crack length of a_c .

$$N = \int_{a_0}^{a_c} \frac{1}{C(\alpha\Delta\sigma\sqrt{\pi a})^m} da \quad (13.3)$$

Analytical solution can be obtained by direct integration when the coefficient α is a constant. It is not easy to calculate the analytical solution when the coefficient α is the function of the crack length of b. Numerical integration methods are commonly used in that way.

13.2.2.2 The Limit Damage Degree Mode

Miner theory is a cumulative damage theory which is proposed in the earliest. It is widely used in engineering of simple. Miner theoretical equation for:

$$D = \sum_{i=1}^m \frac{n_i}{N_i} \quad (13.4)$$

In the equation: D : the damage; m_i : the load level of the variable amplitude loading; n_i : the number of cycles under the i -level load block; N_i : the fatigue cycles under the separate role of the i -level load.

Assume that p_i is the probability under i -class load in the total number of cycles, fatigue life under variable amplitude loading is

$$N = \frac{D}{\sum p_i/N_i} \quad (13.5)$$

Under variable amplitude loading and based on the Paris equation, N_i under each level of load can be calculated using Eq. (13.3). The fatigue life of the structure can be calculated by Eq. (13.5) combined with the Miner theory.

13.3 Study on Fatigue Reliability Analysis Model

13.3.1 Reliability Analysis of Life Cycle

Life cycle of crawler crane begins with design from scrap end. Concurrent design method is used to achieve optimum technical products in the whole life cycle, the most reliable quality, the shortest time and lowest cost, best service, and environmental protection best. Reasonable dynamic adjustment of the safety evaluation indicators is very important. Under normal circumstances, the evaluation indicators should be down to the minimum to meet safety and economy of the most reasonable match with the time history year by year.

Currently, there are three kinds of static reliability analysis model in the engineering on the basis of the difference of the evaluation objectives and evaluation methods:

1. Ultimate stress model

$$\Delta\sigma_R - \Delta\sigma_S \geq 0 \quad (13.6)$$

In the equation:

$\Delta\sigma_R$ the fatigue strength of material or construction details under the amplitude repeated stress effect also named resistance random variables

$\Delta\sigma_S$ equivalent stress amplitude of component or construction details under the amplitude repeated stress effect also named random variable of the load effects

2. Fatigue bearing capacity model

$$R - S \geq 0 \quad (13.7)$$

In the equation:

- S Random variables of structural components to withstand the amplitude of the repeated load effects (bending moments, torque, shear, etc.)
- R Fatigue bearing capacity of structural components under the amplitude repeated load effects

3. The limit damage degree mode

$$D - a \leq 0 \quad (13.8)$$

- D Cumulative damage degree of the material or construction details
- a The limit damage degree index of materials or construction details, general values of 0.8–1.2

If the fatigue performance of materials or construction details to meet the Miner linear cumulative damage rule, assume that a is a variable, then the above equation can be written as:

$$D = \sum \frac{n_i}{N_j} \leq a \quad (13.9)$$

Equation (13.9) is the expression of the linear limit damage model, which is one of the most widely used analytical model. The reliability index obtained does not change over time so it cannot be a satisfactory solution to practical engineering problems.

13.3.2 Building of Dynamic Reliability of the Weight Index Model

The definition of the fatigue dynamic reliability is the functional ability of the structure after the t time. The structure is in a scheduled service time range and under conventional working conditions. In the service time, the fatigue resistance will decrease as the fatigue service cycle increase.

The concept of dynamic weight index is introduced here. The purpose to study these two random variables of load and resistance in the course of time is to

calculate affect of the weights evaluation result. Key factors can be found out through sensitivity analysis of the random variable, then we can find which critical factor has significant impact on the evaluation results.

13.3.2.1 Fatigue Bearing Capacity Model

After the introduction of the time factor, the load and the resistance become random processes. Loading effect of the random process can be expressed by $S(t)$, $t \in T$. Resistance of the random process can be expressed by $R(t)$, $t \in T$. $[0, T]$ is an arbitrary base period which is the specified time defined in the reliability.

$$Z(t) = \frac{\alpha R(t) - \beta S(t)}{\chi} \quad (13.10)$$

In the equation:

- α Value of weighted resistance coefficient, $\alpha \in (0, 1]$
- β Value of weighted load coefficient, $\beta \in (0, 1]$
- χ Value of adjustable reliability coefficient, $\chi \in (0, 1]$

Function of random process $Z(t)$ is a random variable dependent on time t $Z(t_1), Z(t_2), \dots, Z(t_m)$.

In this way, the dynamic reliability can be expressed as:

$$P_Z(t) = P\{Z(t) > 0, \quad t \in [0, t]\} \quad (13.11)$$

Failure probability is expressed as

$$P_f = \frac{\int_0^\infty \beta f_s(s) \left\{ \int_0^S \alpha f_R(R) dR \right\}}{\chi} dS \quad (13.12)$$

$f_R(R)$ is load probability density function and $f_s(s)$ is resistance probability density function. According to the literature [1], they in general obey the normal distribution so the reliable indicator as follows:

$$\lambda = \frac{\mu_R - \mu_S}{\sqrt{\sigma_R^2 + \sigma_S^2}} \quad (13.13)$$

In the equation:

- μ_R the average of the resistance R;
- μ_S the average of the load S;
- σ_R Standard deviation of the resistance R;
- σ_S standard deviation of the load S.

Probability of failure as $P_S = 1 - \phi(\lambda)$

$\phi(\lambda)$ the standard normal distribution function

The number of cycles of fracture reliability in accordance with the theory of fracture mechanics [1] can be expressed:

$$N = \frac{2}{(n-2)CY^n\pi^{n/2}(\Delta\sigma)^n} \left| a_0^{(1-n/2)} - a_c^{(1-n/2)} \right| \quad (13.14)$$

a_0 the original crack length of component present which can be assumed to be 0.25 mm;

a_c the critical size of crack which can be assumed to be 120 mm;

C, n, Y material constants;

$\Delta\sigma$ cycle stress amplitude

13.3.2.2 The Limit Damage Degree Mode

The membership function in fuzzy mathematics can be used to describe the injury fuzziness which we can set the parameter of α (Value of weighted resistance coefficient), β (Value of weighted load coefficient), and χ (Value of adjustable reliability coefficient). For the convenience of expression, the model can be simplified based on the principle:

Value of weighted resistance coefficient α is gradually reduced with the time course which can reflect the aging with the operating process in the base metal and weldments, and the value of weighted load coefficient β and value of adjustable reliability coefficient χ can be set to the initial constant. β and χ can be set to 1. A partial large amendments parabolic distribution function can be used to describe the evolution of α [2].

$$\alpha(x) = \begin{cases} 1, & x \leq a_1 \\ 0.5 - 0.5 \left(\frac{x-a_1}{a_2-a_1} \right)^2, & a_1 < x < a_2 \\ 0.5, & x \geq a_2 \end{cases} \quad (13.15)$$

Fatigue damage degree can be used to describe the membership function which the variable x is used to describe the value of the stress amplitude s . The structural damage degree of membership is $\alpha(x)$ under this stress.

According to the literature [3, 4], the general crane work load stress amplitude is almost more than 20 MPa, the maximum can reach 80 MPa, and therefore, the distribution function of the variable range can be set to 20–80 MPa. So we can set $a_1 = 20$, $a_2 = 80$.

The degree of damage is calculated as follows:

$$D(S_i) = \begin{cases} \frac{\alpha(S_i) \times n_i}{N_0}, & S \leq S_f \\ \frac{\alpha(S_i) \times n_i}{N_i}, & S > S_f \end{cases} \quad (13.16)$$

In the equation

- S_i the i-level stress;
- n_i the number of cycles of S_i ;
- $\alpha(S_i)$ the membership degree of stress S of component damage;
- S_f the fatigue limit of components;
- N_0 the fatigue life under the fatigue limit stress;
- N_i the fatigue life under stress S_i ;

The fatigue failure criterion is:

$$\sum_{i=1}^m \frac{\alpha(S_i) \times n_i}{N_0} + \sum_{i=m+1}^n \frac{\alpha(S_i) \times n_i}{N_i} \geq D_f \quad (13.17)$$

In the equation:

- m the number of stress levels below the fatigue limit;
- n the total number of stress levels;
- S_i the i-level stress;
- D_f the critical damage value.

Equation (13.16) shows the cycle in a load spectrum:

$$N = D_f / \left(\sum_{i=1}^m \frac{\alpha(S_i) \times n_i}{N_0} + \sum_{i=m+1}^n \frac{\alpha(S_i) \times n_i}{N_i} \right) \quad (13.18)$$

13.4 Cases Study

13.4.1 Reliability Evaluation

A domestic 75 tons lattice boom crawler crane booms are detected which is in service for 3 years. The dynamic fatigue reliability analysis model which is discussed in this paper is used to do the evaluation. The failure probability of the crane is 2.3 %, and the actual usage is normal. There is no fatigue crack.

A domestic 160 tons lattice boom crawler crane booms are detected which is in service for 8 years. The failure probability of the crane is 3.5 %, and the actual usage is normal. There is no fatigue crack.

An imported 350 tons lattice boom crawler crane booms are detected which is in service for 16 years. The failure probability of the crane is 38.5 %, and the actual

usage is normal. There are lots of annular circle crack in the boom of the bottom section and top section parts. The maximum length of the crack is 10.0 mm, and the maximum depth is 1.2 mm. Those booms must be recutting and welding or prone to fatigue fracture.

13.4.2 The Load Spectrum and the S–N Curve

In order to research the quantitative analysis of the mode of study fatigue bearing capacity and the limit damage degree mode, a domestic 75 tons crawler crane which is in service and welded joints sample which are under the same load of test is compared with analysis.

According to the literature [5], the S–N curve of 16 Mn material is:

$$\lg N_{99,9} = 18.4403 - 5.57161 gS \quad (13.19)$$

Material S–N curve correction should be done in accordance with the boom welding junction. Usually the fatigue limit stress (The corresponding welded components fatigue limit life $N = 2 \times 10^6$) and the short lifetime stress ($N = 10^4$) are required to correct. The fatigue limit in the post-correction is given by the Eq. (13.20).

$$S'_f = \frac{S_f}{K_f} C_{\text{size}} \beta C_L \quad (13.20)$$

In Eq. (13.20):

S'_f is fatigue limit after correction

S_f is fatigue limit of the standard sample. $S_f = 151$ MPa. It is calculated by the Eq. (13.19)

When the corresponding stress value $S_{10^4} = 390$ MPa when $N = 10^4$.

K_f is fatigue notch factor which is calculated by $q = (K_f - 1)/(K_t - 1)$. q is notch sensitivity coefficient. K_t is theoretical stress concentration factor. According to Refs. [2] and [6], $K_t = 1.96$, $q = 0.5798$, $K_f = 1.56$

C_{size} is size factor. The boom chord size is 76 mm. According to literature [6], alloy steel $C_{\text{size}} = 0.79$

β is coefficient of surface quality. Taking into account the shot peening surface hardening effect, $\beta = 1$;

C_L is load factor. The load of boom is compressive stress, and the S–N curve is obtained by rotating bending conditions, and according to the literature [7], the load factor can be 0.85

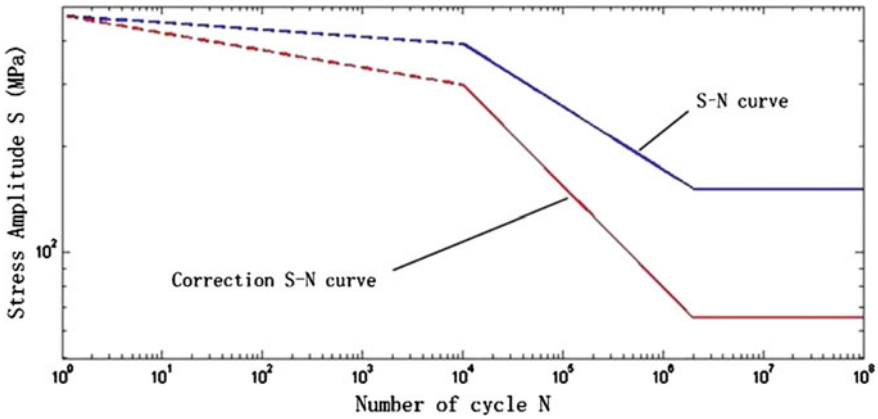


Fig. 13.2 Correction S–N curve

Thus, the fatigue limit in the post-correction can be obtained by Eq. (13.20) that $S'_f = 65$ MPa.

Similarly, in the short lifetime, stress levels are high, and material dispersion and size effect are relative decreased, so they are not considered here. The load factor $C_L = 0.85$. $q \approx 0.2$, $K_f = 1.56$, $K'_f = 1 + 0.2 \times (K_f - 1) = 1.112$.

Corrected stress at the short-lived ($N = 10^4$) $S'_{10^4} = C_L \times S_{10^4} / K'_f = 297$ MPa.

The corrected S–N curve given by the above two endpoints are expressions (65, 2×10^6) and (297, 1×10^4). The corrected S–N curve can be expressed by the Eq. (13.21).

$$\lg N = 12.6078 - 3.4774 \lg S \quad (10^4 \leq N \leq 2 \times 10^6) \quad (13.21)$$

Before and after corrections of the curve are shown in Fig. 13.2.

Fatigue experiment is made by weldments which are made as the crane boom welded joints. The actual crane boom structure of the K type is shown in Fig. 13.3. The test pieces are shown in Fig. 13.4, and PLG-200 high-frequency fatigue testing machine is used to do the experiment.

13.4.3 Result Analysis

By the danger point of the load spectrum and S–N curves of the component, the dynamic reliability of the weight index is used to calculate the fatigue life with two models. The initial crack length can be set to 0.25 mm. Four dangerous point comparison results of the analysis (corresponding to Fig. 13.1 in the dangerous point) are shown in Tables 13.1, 13.2, 13.3, 13.4, and trend analysis is shown in Figs. 13.5, 13.6, 13.7, and 13.8.

Fig. 13.3 The actual crane boom structure of the K type

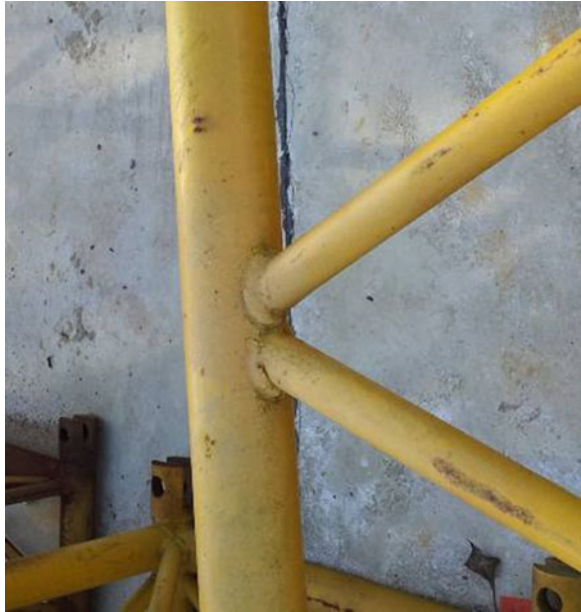


Fig. 13.4 The test piece



The results compared are shown in Table 13.1. It can be seen, when the resistance of the weight coefficient is close to 0.8–0.7, the calculation error compared to the actual sample test life is smaller. Another phenomenon is the polarization. There is an optimal value of the resistance of the weight coefficient.

Table 13.1 Calculated life error analysis of dangerous point 1

The resistance of the weight coefficient α	1	0.9	0.8	0.7	0.6	0.5	0.4
Test life of sample ($\times 10^5$)	5.34	5.34	5.34	5.34	5.34	5.34	5.34
Calculated life of damage degree ($\times 10^5$)	6.17	6.11	5.88	5.66	4.77	4.53	4.43
Calculated life error of damage degree model (%)	15.54	14.42	10.11	5.99	10.67	15.17	17.04
Calculated life of the fatigue bearing capacity model ($\times 10^5$)	6.38	6.22	6.12	5.67	4.98	4.43	4.33
Calculated life error of the fatigue bearing capacity model (%)	19.48	16.48	14.61	6.18	6.74	17.04	18.91

Table 13.2 Calculated life error analysis of dangerous point 2

The resistance of the weight coefficient α	1	0.9	0.8	0.7	0.6	0.5	0.4
Test life of sample ($\times 10^5$)	6.04	6.04	6.04	6.04	6.04	6.04	6.04
Calculated life of damage degree ($\times 10^5$)	7.18	7.11	6.24	5.84	5.43	5.21	5.12
Calculated life error of damage degree model (%)	18.87	17.72	3.31	3.31	10.10	13.74	15.23
Calculated life of the fatigue bearing capacity model ($\times 10^5$)	7.55	7.22	6.98	6.44	5.89	5.44	5.38
Calculated life error of the fatigue bearing capacity model (%)	25.00	19.54	15.56	6.62	2.48	9.93	10.93

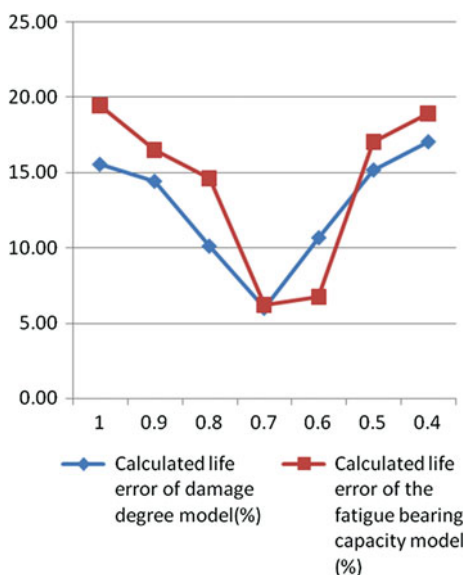
Table 13.3 Calculated life error analysis of dangerous point 3

The resistance of the weight coefficient α	1	0.9	0.8	0.7	0.6	0.5	0.4
Test life of sample ($\times 10^5$)	6.74	6.74	6.74	6.74	6.74	6.74	6.74
Calculated life of damage degree ($\times 10^5$)	7.97	7.44	7.12	6.43	6.44	6.02	5.89
Calculated life error of damage degree model (%)	18.25	10.39	5.64	4.60	4.45	10.68	12.61
Calculated life of the fatigue bearing capacity model ($\times 10^5$)	7.43	7.22	7.01	6.86	6.23	6.02	5.86
Calculated life error of the fatigue bearing capacity model (%)	10.24	7.12	4.01	1.78	7.57	10.68	13.06

Table 13.4 Calculated life error analysis of dangerous point 4

The resistance of the weight coefficient α	1	0.9	0.8	0.7	0.6	0.5	0.4
Test life of sample ($\times 10^5$)	7.45	7.45	7.45	7.45	7.45	7.45	7.45
Calculated life of damage degree ($\times 10^5$)	8.21	7.92	7.7	7.23	7.1	6.94	6.64
Calculated life error of damage degree model (%)	10.20	6.31	3.36	2.95	4.70	6.85	10.87
Calculated life of the fatigue bearing capacity model ($\times 10^5$)	8.45	8.23	6.91	6.67	6.23	6.12	5.87
Calculated life error of the fatigue bearing capacity model (%)	13.42	10.47	7.25	10.47	16.38	17.85	21.21

Fig. 13.5 Trend analysis of point 1



By the above chart analysis, the following conclusions can be drawn:

1. When the resistance of the weight coefficient is close to 0.8–0.7, the calculation error compared to the actual sample test life is smaller. There is an optimal value of the resistance of the weight coefficient.
2. Dangerous points 1 and 2 are under serious regional force in the boom bottom section, and the calculation error is significantly larger. The main reason lies in its part of the plastic deformation zone and is not very suitable for the application of the nominal stress method.

Fig. 13.6 Trend analysis of point 2

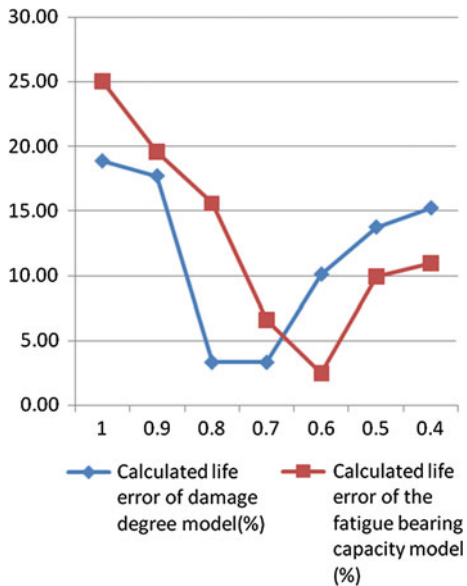


Fig. 13.7 Trend analysis of point 3

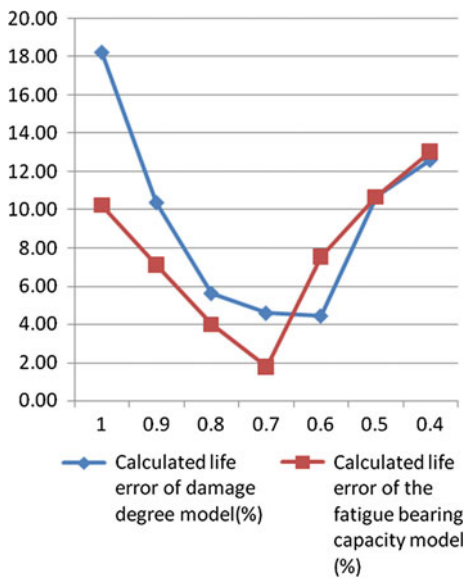
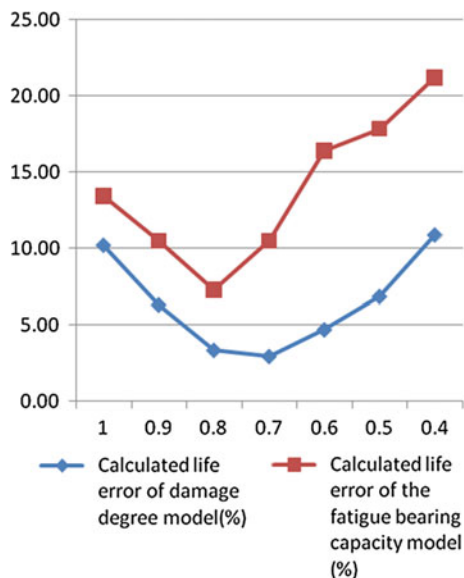


Fig. 13.8 Trend analysis of point 4



13.5 Conclusions

Experimental study based on this article shows that the fatigue life of bottom section is lower than the top section and the middle section. The fatigue dangerous parts are concentrated in the chord and web member welding and the hinge ear welding. Prediction accuracy of dangerous parts is lower than the prediction accuracy of the non-hazardous parts. Dynamic fatigue and fracture reliability analysis methods can be more accurately used in fatigue life analysis of welded structure of the crane boom system, and by adjusting different weight coefficients, the fatigue reliability analysis of error can be reduced. This method offers a new method reference that can predict fatigue life effectively of crane booms through the improvement and optimization.

Acknowledgments This work was financially supported by the national scientific and technological support plan (2011BAF04B01) and Jiangsu Province scientific and technological innovation and technology transfer special support plan (BY2012089).

References

1. Li B, Chen D, Zhao Z, Tao D (2007) Dynamic fatigue reliability analysis of engineering metal structure. *J Mech Strength* 29(3):478–482
2. Yong-Bo S (2007) Analysis of stress concentration factor of welded tubular K-joints subjected to axial loads. *J Ship Mech* 29(3):478–482

3. Xu G, Fan X, Lu F, Yang H (2011) Monte Carlo simulation of fatigue reliabilities and initial cracks for welded box girders of crane. *J Mech Eng* 10:41–44
4. Fan X, Xu G, Wang A (2011) Evaluation method of remaining fatigue life for crane based on the acquisition of the equivalent load spectrum by the artificial neural network. *J Mech Eng* 10:69–74
5. Mechanical Engineering Material Data Sheet. Published by Mechanical Engineering Material Data Sheet. China Machine Press, Beijing
6. Mechanical Design Handbook. Published by Mechanical Engineering Material Data Sheet. China Machine Press, Beijing (2004)
7. Shaobian Z, Zhongbao W (1997) Anti-fatigue design—methods and data. Published by Mechanical Engineering Material Data Sheet. China Machine Press, Beijing (1997)

Chapter 14

Study of the Opening Angle Influence of Y-shaped Guying System on the Buckling Stability of Telescopic Boom Crane

Li Chen, Rumin Teng, Yahui Zheng, Haibo Chi, Wei Xu and Na Hou

Abstract The Y-shaped telescopic boom guying system offers remarkable increases in load capacity of all-terrain crane. However, there are very few articles reporting on this special structure. Because the telescopic boom with Y-shaped guying system is a statically indeterminate space structure of quartic, it cannot be solved by an analytical method and there are no complete qualitative analyses of results. On the one hand, the front guyrope has played a positive role because the pull force partially weakens the bending moment and the deformation of boom head and decreases the stress of the bottom cover plate on the telescopic boom. On the other hand, it has played negative effects due to increasing the axial pressure and the stress of the top cover plate on the telescopic boom. The length and opening angle of guying frame balance the load distributions of working process between the revolution plane and luffing plane. In this paper, the all-terrain crane is simplified as a model which includes the telescopic boom, guying frame, front guyrope and back guyrope in this paper. The eigenvalue buckling analysis of finite element method is used to research the influence of Y-shaped opening angle on the crane maximal lift load decided by buckling stability. The research results show that the critical lifting load determined by stability increases first and then decreases with the increment of the opening angle of guying frame. The bigger of the opening angle, the larger of the pulling force component of guyrope in the revolution, and the better stability in this plane. However, the increasing opening angle will decrease the stability in the luffing plane. The optimal range of the opening angle is between 70° and 100° , which can balance the revolution plane stability and the luffing plane stability. This conclusion might be useful for the design of the Y-shaped guying system of cranes.

L. Chen (✉) · W. Xu · N. Hou
Dalian Yiliya Construction Machinery Co., Ltd., Dalian 116025,
People's Republic of China
e-mail: chenli2yly@163.com

R. Teng · Y. Zheng · H. Chi
School of Mechanical Engineering, Dalian University of Technology, 10F, No. 1,
HuiXianYuan, Hi-tech Zone, Dalian 116023, Liaoning, People's Republic of China

Keywords Crane · Maximal lift load · Y-shaped guying system · Opening angle · Buckling stability

14.1 Introduction

It is obviously that large size crane plays a more and more important role with the development of capital construction of urbanization. In order to meet the requirements, a variety of new components such as guying mast, boom head guyrope are invented. These equipments improve the lifting capacities greatly [1, 2].

Guying system equipments can improve the boom-carrying capacities of all-terrain crane in revolution plane and luffing plane ultimately [3, 4]. These kinds of systems are widely used in the large size products of Liebherr and Terex-Demag, such as LTM1500, LTM11200 and AC1000. The Y-shaped equipment can improve the lifting capacities by 50–200 %. The main parameters of Y-shaped guying system are the length and opening angle of guying frame. The load distribution of the boom system in revolution plane and luffing plane during the process of working is decided by these two parameters. Specially, the opening angle is the more significant factors. The opening angle of guying equipment in Liebherr crane is from 30° to 40° for standard telescopic boom, 20° for lattice fly jib and 84°–90° for luffing lattice jib. However, there are very few studies on the effects of different opening angles about guying system. Because the guyed telescopic boom is a statically indeterminate space structure of quartic, it is difficult to solve with analytical method. Nowadays, some qualitative results cannot be got and the effect of guying system is not clearly. On the one hand, the pull force produced by the guyrope can weaken the bending moment, which reduce the deformation and the bottom cover plate stress of telescopic boom. On the other hand, however, the increasing axial pressure is disadvantageous to the top cover plate.

So far, research on how the parameters of guying system affect the lifting capacities of crane has been elementary stage at home. Shi [5] introduce different kinds of guying systems and make a preliminary analysis on the range of lifting capacities caused by fixing guying system. Teng [6] solve the statically indeterminate problem by energy method of classical mechanics and discuss the influence of boom applied force caused by different length parameters of guying system. Researches on the potential performance of guying system are not enough.

In this paper, the buckling stability influence of crane boom system caused by different opening angles of guying system is studied. The all-terrain crane is simplified as a model which includes the telescopic boom, guying frame, front guyrope and back guyrope. The eigenvalue buckling analysis of finite element method is used to study the influence of opening angle on the telescopic crane maximal lift load decided by buckling stability. The results will give the application of guying system in actual project theoretical guidance.

14.2 Methods

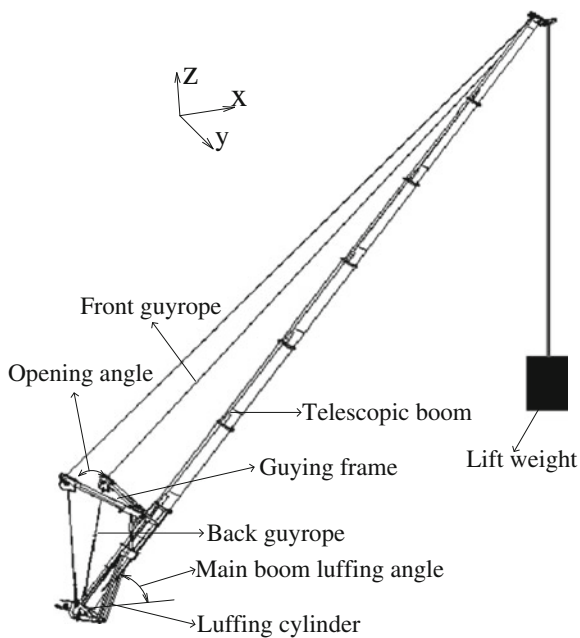
14.2.1 Simplified Model of Telescopic Boom System

This paper takes LTM 11200 for an example and the diagrammatic drawing is shown in Fig. 14.1.

The boom system with guying system is made up of 5 parts, which include telescopic boom, Y-shaped guying frame, front guyrope, back guyrope and luffing cylinder.

The influence of car frame, chassis and telescopic friction are ignored in this paper. The telescopic boom, guying frame, front guyrope, back guyrope and luffing cylinder are modeled by beam element because their slenderness ratios are bigger than 260. All structures are linked through nodes coupling. Three translations degrees of freedom are coupled between front guyrope and guying frame, front guyrope and telescopic boom, back guyrope and guying frame, and back guyrope and telescopic boom. Three translations and rotations degrees of freedom are coupled between guying frame and telescopic boom. The telescopic boom and luffing cylinder are free in the degree of freedom for rotations about the luffing plane, which is also applied on luffing cylinder and rotary tables.

Fig. 14.1 Boom system composition with guying system



14.2.2 Finite Element Method of Buckling Stability [6]

The boom system with guying system instability problem can be treated as an eigenvalue problem that is also called eigenvalue buckling analysis. The instability load is called buckling load that is the maximum critical lift load for the crane.

In the stability balanced state, geometric stiffness matrix $[K_\sigma]$ is used to repress the structure stiffness change in the deformation state considering the structure force influence on the bending deformation. Based on potential energy principle, the balance equation is

$$([K_E] + [K_\sigma])\{U\} = \{P\} \quad (14.1)$$

$[K_E]$ is the elastic stiffness matrix. $[K_\sigma]$ is the geometric stiffness matrix. $\{U\}$ is the nodal displacement vector. $\{P\}$ is the nodal load vector.

When the system is during an equilibrium state, the derivative of the system potential energy Eq. (14.1) should be zero.

$$([K_E] + [K_\sigma])\{\delta U\} = 0 \quad (14.2)$$

That is to say

$$([K_E] + [K_\sigma]) = 0 \quad (14.3)$$

In Eq. (14.3), the elastic stiffness matrix $[K_E]$ is known. The lift load is the buckling load to be solved, so the geometric stiffness matrix $[K_\sigma]$ is unknown. For solving it, we assume that a unit lift load $\{P^0\}$ corresponds with the unit geometric stiffness matrix $[K_\sigma^0]$. The buckling load is $\lambda\{P^0\}$, so $[K_\sigma] = \lambda[K_\sigma^0]$ can be get. The Eq. (14.3) can be conversed as follows:

$$([K_E] + \lambda[K_\sigma^0]) = 0 \quad (14.4)$$

The Eq. (14.4) is conversed to be and eigenvalue equation

$$([K_E] + \lambda_i[K_\sigma^0])\{\phi_i\} = 0 \quad (14.5)$$

λ_i is the i order eigenvalue. $\{\phi_i\}$ is the correspondent eigenvalue vector, which represses the deformation of the structure system, and it also can be called buckling mode shape.

14.3 Examples

There are many work conditions using Y-shaped guying system. In order to investigate the effects of the opening angle on the maximum lift load, three typical cases of shortest, longest and medium boom length are studied here. The range of

Table 14.1 Main finite element parameters of the telescopic crane

	Boom1	Boom2	Boom3	Boom4	Boom5	Boom6	Boom7	Boom8	Cylinder
Length	15.97	15.33	15.20	15.40	15.24	15.08	14.90	15.04	-
Area	1.56e-1	8.70e-2	7.64e-2	1.24e-1	5.68e-2	4.95e-2	4.40e-2	4.30e-2	1.69e-1
Iy	5.84e-2	2.91e-2	2.15e-2	3.04e-2	1.18e-2	8.40e-3	6.60e-3	5.20e-3	5.42e-3
Iz	4.89e-2	2.36e-2	1.76e-2	2.59e-2	9.90e-3	7.40e-3	5.70e-3	4.70e-3	5.42e-3

Length unit is m, section area unit is m^2 , moment of inertia unit is m^4 , Iy is moment of inertia in the luffing plane, and Iz is for the revolution plane

Table 14.2 Main finite element parameters of the Y-shaped guying system

	Guying frame	Front guying rope	Back guying rope
Length	14.50	–	21.30
Area	9.56e-2	2.51e-3	5.76e-3
Iy	6.25e-3	2.50e-7	2.80e-7
Iz	7.84e-3	2.50e-7	2.80e-7

Length unit is m, section area unit is m^2 , moment of inertia unit is m^4 , Iy is moment of inertia in the luffing plane, and Iz is for the revolution plane

luffing angle for telescopic boom is from 20° to 80° with 10° step size and the guying opening angle is from 0° to 180° during the analysis. The opening angle influence of Y-shaped guying system on the lifting buckling stability of telescopic boom crane is studied by compare guying system with non-guying system.

The main finite element parameters of the telescopic crane are shown in Tables 14.1 and 14.2.

The length of telescopic luffing cylinder and front guying rope is a variational value that is determined by the crane luffing angle and telescopic length. The modulus of elasticity of the front guyrope is $1.04e11$ Pa and the others are $2.05e11$ Pa.

14.3.1 Longest Boom Length Case

The crane maximal lift capacity load of the longest boom length (100 m) decided by buckling stability with different opening angles and telescopic boom luffing angle is studied. The result of curves is shown in Fig. 14.2.

As shown in Fig. 14.2, there is an obvious difference on the crane maximal lift load decided by buckling stability between non-guying system and guying system at longest telescopic boom length. The bigger of the telescopic boom luffing angle, the worse of the stability and maximum lift load when there is not guying system. The maximal lift load is 114 t at 20° luffing angle, and the minimum lift load is 25.5 t at 80° . However, the trend is opposite with guying system besides 170° opening angle. During this case, the critical lifting load is better when the range of boom luffing angle is from 20° to 53° and becomes worse when the telescopic boom luffing angle is between 53° and 80° . As we can see, the weakest lift load is at 20° opening angle and the best one is at 80° opening angle. The minimum lift load is 34.5 t at 20° luffing angle and the maximum one is 99 t at 80° luffing angle. Figure 14.3 shows that the potential buckling mode is lateral deformed mode in the revolution plane when the longest length crane luffing angle is 50° with the best guying opening angle of 80° .

Fig. 14.2 Comparative curves of critical lift load by boom luffing angle and different guying opening angle at longest boom length

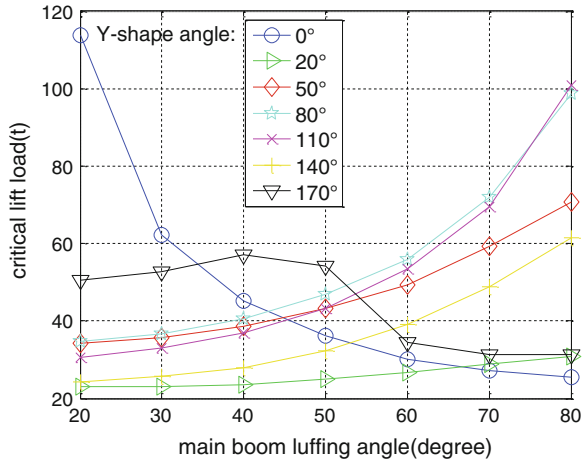
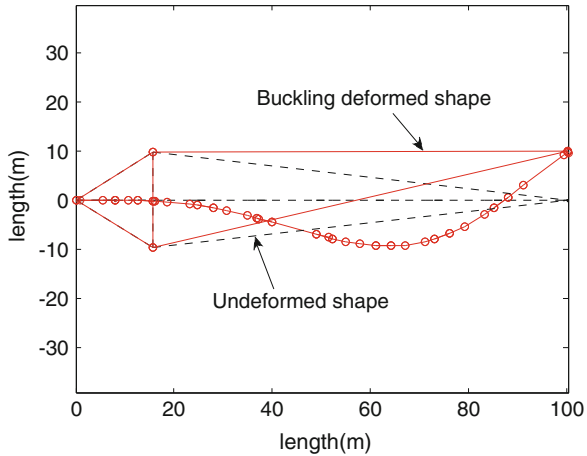


Fig. 14.3 Top view of the finite element buckling mode when boom luffing angle is 80° and guying opening angle is 50° at longest boom length



14.3.2 Medium Boom Length Case

The crane maximal lift capacity load of the medium boom length (65 m) decided by buckling stability with different opening angles and telescopic boom luffing angle is studied, and the result of curves is shown in Fig. 14.4.

As shown in Fig. 14.4, it is also different on the crane maximal lift load decided by buckling stability for non-guying system and guying system at medium telescopic boom length. Without guying system, the bigger of the telescopic boom luffing angle, the worse of the stability and maximum lift load. The maximal lift load is 347 t at 20°, and the minimum lift load is 66 t at 80°. However, the trend is opposite with guying system besides 170° opening angle. As we can see, the minimum lift load is at 20° opening angle and the maximum one is at 80° opening

Fig. 14.4 Comparative curves of critical lift load by boom luffing angle and different guying opening angles at medium boom length

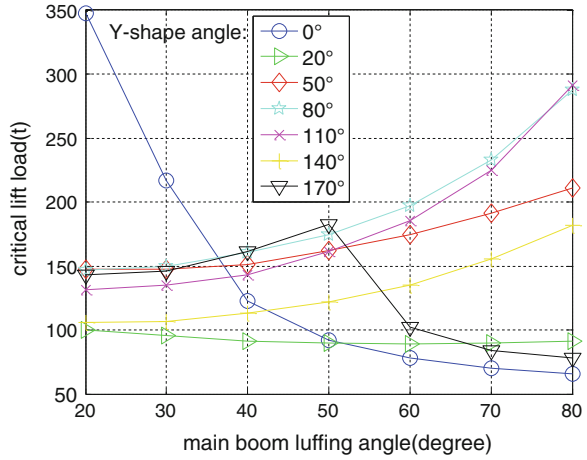
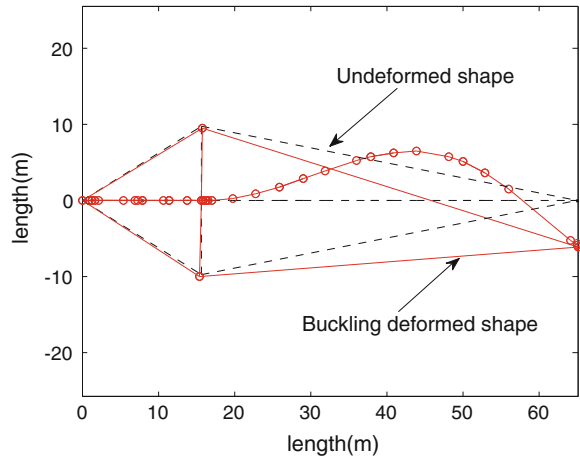


Fig. 14.5 Top view of the finite element buckling mode when boom luffing angle is 80° and guying opening angle is 50° at medium boom length



angle. The minimum lift load is 142 t at 20° luffing angle and the maximum one is 292 t at 80° luffing angle. Figure 14.5 shows that the potential buckling mode is also lateral deformed mode in the revolution plane when the medium boom length crane luffing angle is 50° with the best guying opening angle of 80°.

14.3.3 Shortest Boom Length Case

The crane maximal lift load of the shortest boom length (36.9 m) decided by buckling stability with different opening angles and telescopic boom luffing angle is studied, and the result of curves is shown in Fig. 14.6.

Fig. 14.6 Comparative curves of critical lift load by boom luffing angle and different guying opening angles at shortest boom length

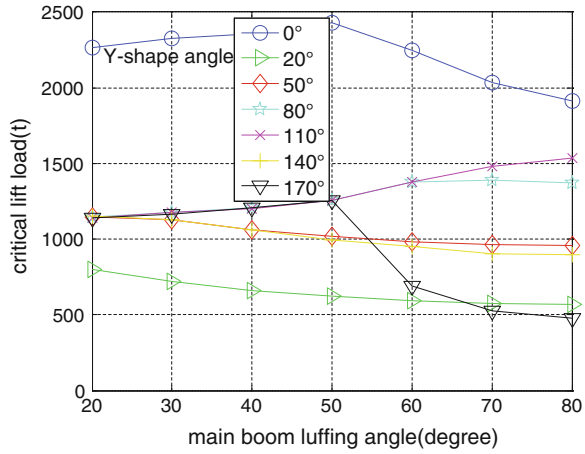
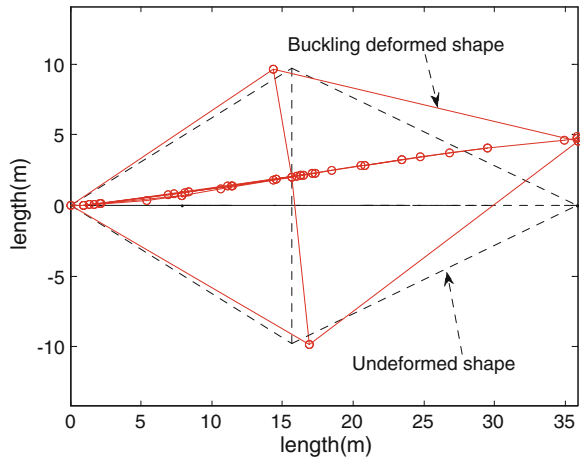


Fig. 14.7 Top view of the finite element buckling mode when boom luffing angle is 80° and guying opening angle is 50° at shortest boom length



As shown in Fig. 14.6, it is also different on the crane maximal lift load decided by buckling stability between non-guying system and guying system at shortest telescopic boom length. With the increasing of the telescopic boom luffing angle, the stability becomes better first and then worse without a guying system. The maximal lift load is 2,430 t at 50° and the minimum lift load is 1,912 t at 80°. However, the lift load is less with guying system than with non-guying system. In a word, the minimum lift load is at 20° opening angle and the maximum one is at 110° opening angle. The minimum lift load is 1,144 t at 20° luffing angle and the maximum one is 1,527 t at 80° luffing angle. Figure 14.7 shows that the potential buckling mode of shortest boom length is the same as that of longest and medium boom length when the crane luffing angle is 50° with the best guying opening angle of 80°.

14.4 Discussion and Conclusion

As shown above, the maximum lift load decreases without a guying system when the boom length increases. Because the stiffness of the longer boom decreases, the stability becomes worse. With the increasing of the telescopic boom luffing angle, the load component along with the boom axis increases, so the maximum lift load decreases.

When there is a guying system, the less of the opening angle, the worse stability in the revolution plane. However, the increasing opening angle of guying equipment will decrease the stability in the luffing plane and the maximum lift load. The instability happens in the revolution plane with a small opening angle. With the increasing of the telescopic boom luffing angle, the boom axial force increases, which makes the stability worse in the revolution plane, but the pulling force component of guyrope in the revolution becomes larger relatively, which makes the stability better in that plane, and it has greater influence than the boom axial force. So, the stability in the revolution plane becomes better. The optimal range of the opening angle is between 80° and 110° . With the increasing of the opening angle, the pulling force component of guyrope in the luffing decreases too quickly relatively, which makes the instability happen in the luffing plane and it becomes worse and worse.

In fact, besides the lifting buckling stability, other factors may affect the crane maximal lift load, such as the stress of the telescopic boom structure, shell buckling stability, overturning stability and luffing cylinder strength, and so on. Only the telescopic boom is longer enough, the crane maximal lift load is decided by the total buckling stability, which can be increased through assembling guying system.

The research results show that the guying system can greatly increase the total buckling stability for the longer boom. The bigger of the opening angle, the greater of the opening angle influence on the total buckling stability. The optimal range of the opening angle is between 80° and 110° , which can balance the revolution plane stability and the luffing plane stability. This conclusion might be useful for the design of the Y-shaped guying system of cranes.

References

1. Zhang M, Wang X, Gao Y (2006) Superlift structure of crawler crane. *Constr Mach Technol Manage* 9:66–68
2. Wang X, Bo J, Teng R (2008) Design and study of compensation waist rope structure for track crane with super lift boom. *Constr Mach* 3:83–86
3. Jia T, Zhang Y (2011) The key technique analysis of all terrain cranes. *Constr Mach* 1(2):54–61
4. Shi Y, Xu H (1997) Superlift structure of telescope crane. *Eng Mach* 12:5–19
5. Teng R, Yao H, Chen L, Long Y, Gao S (2012) Study of influence on boom force by super-lift system for all terrain cranes. *J Mach Des* 29(1):91–96
6. Wang X (2007) ANSYS engineering structure numerical analysis. People Traffic Press, Beijing, p 10

Chapter 15

Design of New Hydraulic Pushing Device

Qicai Zhou, Jiong Zhao, Xiaolei Xiong and Haiyan He

Abstract Hydraulic pushing equipment is widely used to transport the extreme heavy structure and equipment in road and bridge, construction, railway, electric power, metallurgy, petrochemical, etc. In this article, the hydraulic pushing equipment can move with the pushed object along the track, which is mainly composed of hydraulic cylinder and clamping device. The clamping device installed in the back of the hydraulic cylinder mainly consists of a rod and bugles beside the rail. The device can provide reaction force when the piston rod stretches out through the compaction of the rod and bugle. The clamping device follows the movement of the hydraulic cylinder when the piston rod retracted. This paper takes the hydraulic pushing equipment of 2,500-ton ring crane as an example to introduce the specific design, and optimizes the key components and overall structure using ANSYS.

Keywords Hydraulic pushing equipment · Clamping device · Finite element analysis

15.1 Introduction

The hydraulic equipment is widely used due to the smooth, safe, and reliable operation in the field of modern construction. There must be support used to provide anti-force installed behind cylinder when pushing the heavy loads. When the target position is so far, meanwhile the cylinder stroke is fixed, the cylinder would complete the pushing task by accumulation of stroke. It is too tedious, time-consuming, and work-consuming when the anti-force support is dismantled, moved, and reinstalled artificially in traditional construction. Moreover, it would cause

Q. Zhou (✉) · J. Zhao · X. Xiong · H. He
College of Mechanical Engineering, Tongji University, Cao'an Road 4800, Shanghai
201804, China
e-mail: qczhou@tongji.edu.cn

© Springer-Verlag Berlin Heidelberg 2015
Logistics Engineering Institution, CMES (ed.),
Proceedings of China Modern Logistics Engineering,
Lecture Notes in Electrical Engineering 286, DOI 10.1007/978-3-662-44674-4_15

track deformation and wear easily in the process of repeated installation and disassembly [1]. In order to achieve automatic step of anti-force support, this paper presents an automatic hydraulic pushing device.

15.2 Composition and Operating Principle

15.2.1 Composition

The automatic pushing device mainly composes of hydraulic jacking cylinder, anti-force support, existed track and bosses on both sides of track, as shown in Fig. 15.1. Anti-force support is similar to a propeller car, of which the basic frame welded by steel plates is connected to the hydraulic jacking cylinder through bolts. The “L-shaped” rods withstanding the reaction forces are hinged to the frame mainly in this device.

15.2.2 Operating Principle

The anti-force support is located on the track which can move back and forth along the track. There are “L-shaped” rods and corresponding baffle on both sides of the support. During operation, rod 5 can rotate a certain angle about the pin with the piston rod’s retraction. The distance between two adjacent bosses is approximately equal to the cylinder stroke.

This device’s workflow is shown in Fig. 15.2. Figure 15.2a presents the status that when the device just gets started an operating cycle, the “L-shaped” rod fits with the bosses and the baffles. If there is gap between rod and boss when it starts to work, the propellant remains in situ, while the cylinder moves along the track in the

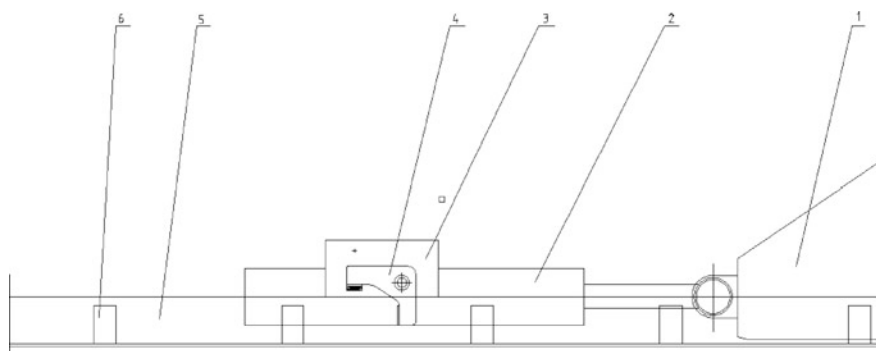


Fig. 15.1 Structure of new hydraulic pushing device. 1 Propellant, 2 cylinder, 3 anti-force support, 4 rod, 5 track, and 6 boss

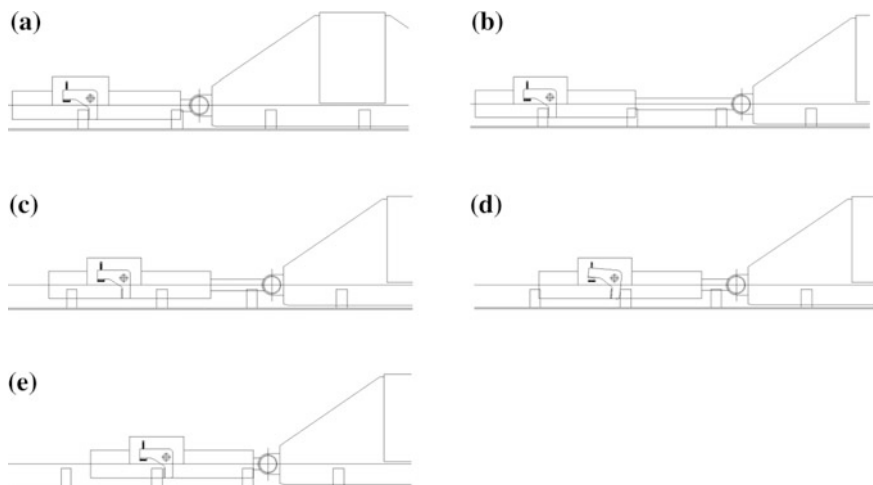


Fig. 15.2 Workflow of the new hydraulic pushing device

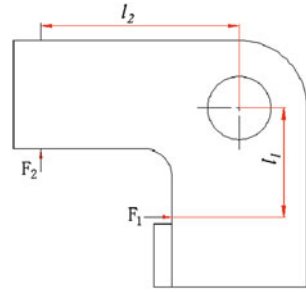
opposite direction, because the propellant's weight is obviously greater than the anti-force generated by hydraulic cylinder. The cylinder stops moving when the rod fits with the boss and baffle. The original still propellant begins to move forward with the stretching of the piston rod till it reached its maximum stroke, and the final position is shown in Fig. 15.2b. Then, the anti-force support moves forward, followed by the cylinder when its piston rod gradually contracts. During the process, the "L-shaped" rod would slide over the boss until the piston rod contracts entirely. At this moment, an operating cycle is completed. The device can start to work immediately after the assembly and commission at the site, and what is more, it does not require repeated disassembly and installation. So not only it is easy and safe to be used, but also it can help save construction time.

15.3 Key Structure Design

Taking the traveling system of 2,500 t ring crane developed by a company for example, the main technical parameters are as follows: pressure: 20 MPa, the maximum thrust: 980.6 kN, the maximum advance speed: 90 m/h, and the maximum stroke: 1,150 mm.

To ensure its reliability and security, the "L-shaped" rod should be designed in detail because it is the main component providing anti-force. There are bosses on the both sides of the track, and with the total thrust of a cylinder approximately 100 t, the maximum load each rod bears is about 50 t. The force diagram of "L-shaped" rod is shown in Fig. 15.3. Q345B is chosen as the material of "L-shaped" rod in order to maintain the fine ductility, welding, and mechanical properties.

Fig. 15.3 Force diagram of “L-shaped” rod



1. Stress analysis of “L-shaped” rod

The anti-force F_1 produced by bosses makes the “L-shaped” rods tend to rotate around the hinge pin counterclockwise. Meanwhile, the baffle would give the “L-shaped” rod corresponding anti-force F_2 . According to the equilibrium condition, Function (15.1) is obtained.

$$F_2 = F_1 \cdot I_{12} \tag{15.1}$$

In this paper, the “L-shaped” rod mainly withstands moment which can be equivalent to the combination of two plates (Fig. 15.4).

Taking the force characteristics of the “L-shaped” rod into account, the sectional dimension of cross A is calculated firstly. Then, based on the dimension, the stress of the other plate is judged whether it satisfies the allowable stress or not.

2. Allowable stress [2]

- (a) Allowable stress of tension, compression, and bending (i.e., basic allowable stress) σ due to (Table 15.1)

$$\begin{aligned} \sigma S \sigma b &\leq 275,470 \approx 0.585 < 0.7, \\ \sigma = \sigma S n &= 2,751.48 \approx 185.8 \text{ MPa} \end{aligned} \tag{15.2}$$

Fig. 15.4 Equivalent force diagram of “L-shaped” rod

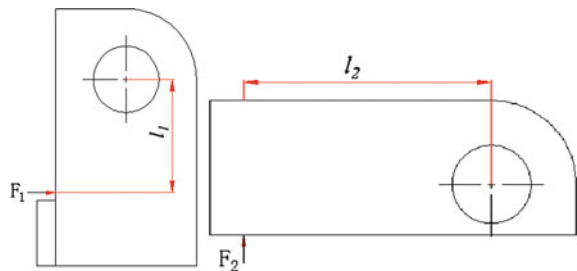


Table 15.1 Chemical composition and mechanical properties of low-alloy structural steel Q345B

Sign	Quality grade	Thickness/mm	Yield point σ_s /MPa	Tensile strength σ_b
Q345	B	>50–100	275	470–630

(b) Shearing allowable stress $[\tau]$

$$\tau = [\sigma]3 \approx 107.28 \text{ MPa} \tag{15.3}$$

According to the boss dimension, taking $b = 100 \text{ mm}$.

$$\begin{aligned} \sigma_{\max} &= M_{\max} W_z = 50 \times 103 \times 9.806 \div I1100 \times 10^{-3} \times h26 \\ &\leq [\sigma] \tau_{\max} = FSb \times h = 50 \times 103 \times 9.806h \times 100 \times 10^{-3} \leq [\tau] \end{aligned} \tag{15.4}$$

The solution is given below based on simultaneous Eqs. (15.1)–(15.4)

$$I1 \leq 6.3158h2h \geq 45.7 \text{ mm}$$

Taking the dimensions of the anti-force support into account, $l_1 = 120 \text{ mm}$, $h = 150 \text{ mm}$ is finally defined. That is to say, the cross-dimension is defined. In order to reduce the anti-force received by the upper end, $l_2 = 250 \text{ mm}$ is taken. The model of “L-shaped” rod and anti-force support are shown in Fig. 15.5.

3. Strength check of anti-force support

Anti-force support, which is used to install the cylinder and detection equipment, is the important component of the hydraulic pushing device. It is also used to transfer the force. When designing the support structure, in addition to consider the relative position of relevant parts and the overall layout, the key components should also be checked to have sufficient rigidity and strength.

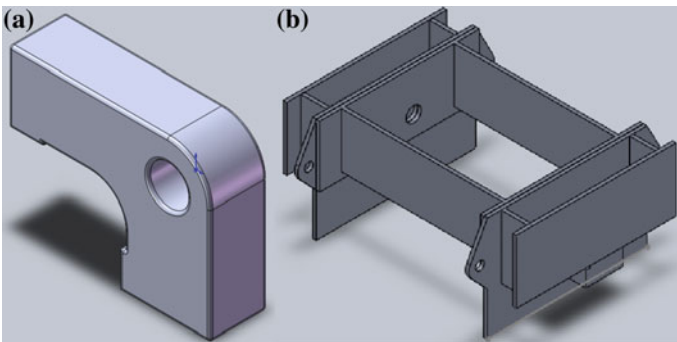


Fig. 15.5 Model of “L-shaped” rod and anti-force support. **a** “L-shaped” rod. **b** Anti-force support

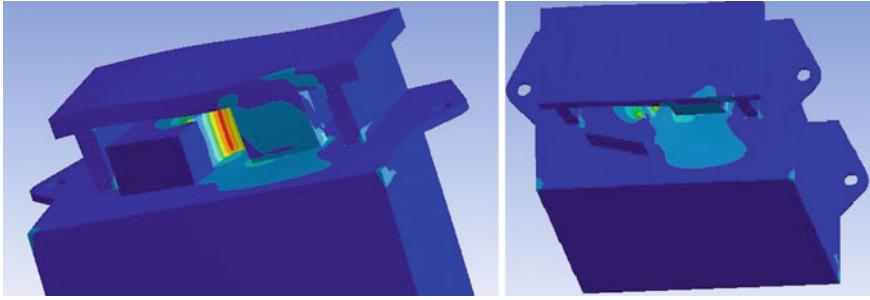


Fig. 15.6 Calculation of anti-force support

Strength analysis is to ensure that the anti-force support has enough bearing capacity when working; moreover, it can also ensure its safety and reliability. At the same time, the device should be minimized its weight and the bearing capacity should be played sufficiently.

The pushing device provides cylinder anti-force intermittently during walking operation; additionally, the velocity is relatively low, and thus, the anti-force support can be checked in accordance with the static strength. Evaluation method of static strength: Under normal operating load, the largest Von Mises stress is not greater than the allowable stress, i.e., $\sigma_{\max} \leq [\sigma]$, and the maximum shear stress is not greater than the allowable shear stress, i.e., $\tau_{\max} \leq [\tau]$ [3]. Firstly, the anti-force support and “L-shaped” rod are analyzed in ANSYS, and the stress distribution is shown in Fig. 15.6.

According to the results, it is easy to find the maximum stress concentrated in the “L-shaped” rod, and the rod would be checked in detail.

Building the rod finite element model in ANSYS, applying load according to load cases and solving the Von Mises stress value and stress pattern is the main aim of rod strength analysis. For the stress-concentrated area, the static strength should be assessed by the static strength theory [4]. Stress calculation results of “L-shaped” rod are shown in Fig. 15.7.

According to the analysis results, the largest Von Mises stress is $\sigma_{\max} = 170 \text{ MPa} < [\sigma]$ and the maximum shear stress is $\tau_{\max} = 71.4 \text{ MPa} < [\tau]$. Therefore, the key components of this device meet the strength requirements.

15.4 Application Prospect

The most common hydraulic pushing device in domestic market is stationary hydraulic cylinder, which is generally used for short-range translation or temporary construction. But it is difficult to achieve long-range translation. Stationary hydraulic cylinder, installed easily, is used in some cases in order to achieve continuous pushing. But its maintainability is inconvenient and expensive.

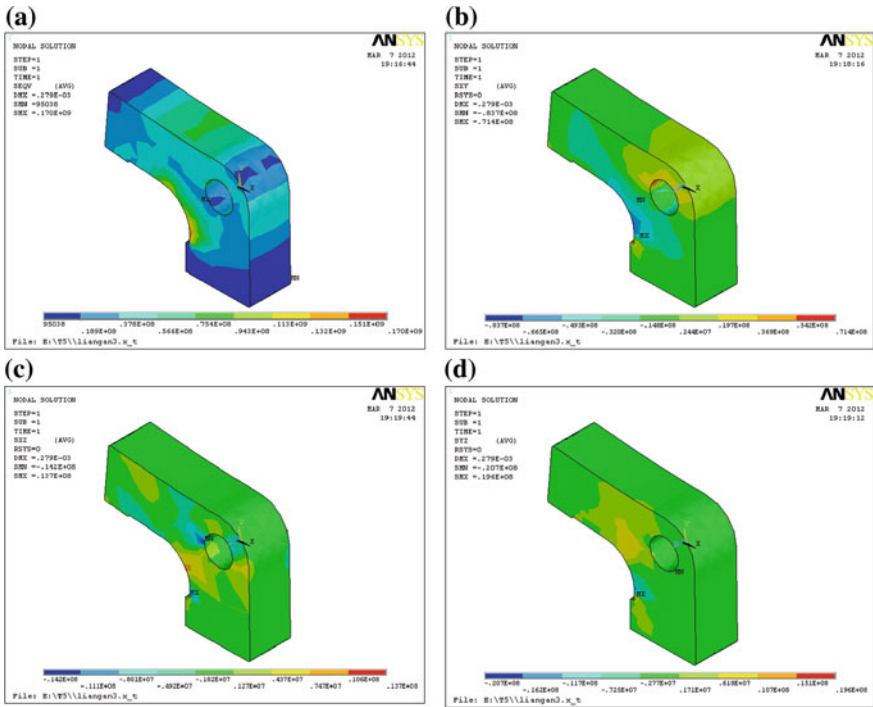


Fig. 15.7 Stress calculation result of rod. **a** Von Mises distribution. **b** Shear stress distribution in plane XY. **c** Shear stress distribution in plane YZ. **d** Shear stress distribution in plane XZ

Stationary cylinder’s cost is relatively high, and what is more, it is difficult to maintain because of so many fault points [5].

The development of new hydraulic device lays foundation for the horizontal movement and is conducive to the large-scale structure and buildings’ translation. So this device can be used in areas such as municipal construction. Compared with fixed-pushing device, the new hydraulic pushing device as continuous pushing device has incomparable superiority in long-range translation. The new hydraulic pushing device, with characteristics such as small size, low cost, easy installation and removal, fewer fault points, and infrequent changes, has strong market competitiveness. This device can be applied not only in ring crane to push trolley, but also in the translation of steel truss girder cable-stayed bridge.

15.5 Conclusion

The new hydraulic pushing device is developed for the translation of super-heavy equipment and structures and has great use value in fields such as construction, lifting, and metallurgy. The device in this paper can work without external

clamping pressure, and the structure is simple. Besides, it is easy to be clamped and to assembly. The device can be widely used in the movement of roads, bridges, buildings, railways, metallurgy, and petrochemical and other areas, but the installation of bosses on both sides of the track is complicated. The device, which is a strong representation in the installation and construction of similar equipment, has broad application prospects.

References

1. Chen J (2008) Key process improvement of incremental launching method construction. *Road Mach Constr Mech* (3)
2. Wang J, Zhang Q, Shen X (2011) Steel structure design of hoisting machinery. Chemistry Industry Press, Beijing
3. Li B, Chen X, Zhuo J (2010) ANSYS engineering application. Tsinghua University Press, Beijing
4. Ding Y (2011) ANSYS 12.0 finite element analysis manual. Electronic Industry Press, Beijing
5. Research and application of mechanical hydraulic pushing device. *Constr Technol* (2008)

Chapter 16

The Improvement of Running Condition on the Crane with the Wheel Flange

Jigui Kuang, Dabao Liu, Xuequan Xiao and Hao Wu

Abstract There is always snaking phenomenon while the crane running. Associated with the snaking phenomenon, the flange wear and the boring noise will emerge. The flange wear has greatly cut down the service life of the wheels, and the noise has an adverse effect upon the stuffs on site. After conducting the analysis of forces, a new kind of structure has been argued through theory analysis and actual test, and the wheel flange lubrication has been introduced. The running condition is improved greatly.

Keywords Snaking phenomenon · Wheel flange lubrication · The structure

16.1 Introduction

Because of the fabricate and the assembly, there will be snaking phenomenon in 70–80 % of the running, and the flange abrasion will come about directly. The wheel flange restrains the transverse movement, so the flange abrasion is worse than the wheel tread. According to statistics, the service life of the flange is about 0.5–1 year, while the wheel tread is about 2–3 years. So the flange abrasion restricts the service life of the wheel. Besides, there may be the regular structure snaking and the greater noise on the crane in the higher classification group. That can have an adverse effect on not only the crane operating conditions and the field staff and can cause hidden trouble to safety.

J. Kuang (✉) · D. Liu · X. Xiao · H. Wu
Shandong Special Equipment Inspection and Research Academy, Jinan,
People's Republic of China
e-mail: kuangjigui@126.com

© Springer-Verlag Berlin Heidelberg 2015
Logistics Engineering Institution, CMES (ed.),
Proceedings of China Modern Logistics Engineering,
Lecture Notes in Electrical Engineering 286, DOI 10.1007/978-3-662-44674-4_16

16.2 Theory Analysis

When there can be an offset angle between the center line of the wheel and the one of the rail, it will appear that the sliding friction between the wheel tread and the rail, and the lateral resistance come into being. The component of the friction in the running direction forms the additional running resistance, and the one in the vertical direction forms the side pressure of the wheel. The side pressure is born by either the horizontal control roller or the wheel flange. Then, the phenomenon of gnawing track emerges, resulting in flange wear (Figs. 16.1 and 16.2).

The speed of the spindle is just the crane running speed v , and it is v_h , that is, the speed of the wheel contact points relative to the crane in the circumferential direction, and the angle is β between v and v_h . So the sheer speed of the contact points is just the sliding speed between the wheel and the rail, the v_h , the vectorial sum of the two.

$$v_h = v + v_{2h}$$

The friction between the wheel and the rail is in the opposite direction to v_h . If it ignore the friction in the bearing, the friction could be in the same direction with the spindle that means v_h could be in the direction. The figure shows:

$$v_h = v \sin \beta \approx v\beta$$

This says: the wider the offset angle is, the higher the sliding speed is, the worse the wear.

Fig. 16.1 The mechanical analysis

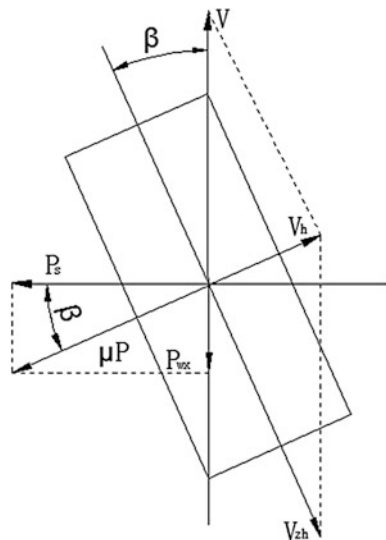
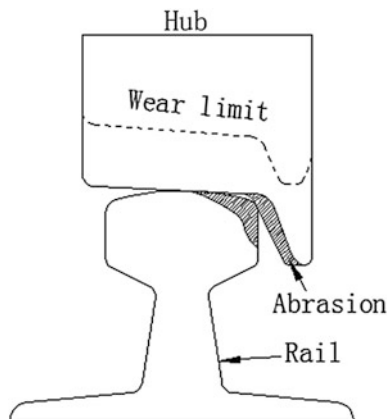


Fig. 16.2 The abrasion

It is P_{wk} , which is the component in the running direction of the friction, and the additional resistance for the wheel askew. The component in vertical direction is the side pressure P_s .

$$P_{wk} = \mu p \sin \beta \approx \mu p \beta$$

$$P_s = \mu p \cos \beta \approx \mu p$$

In theory, when there should be a tiny offset angle, the same size side pressure P_s should emerge. So the side pressure is unavoidable in running.

When the metal constructions rigidity is not enough, there will be cyclical springing phenomenon and noise sometimes. For the metal constructions rigidity, there is the elastic displacement in the side direction at first, not the sliding. The lateral pressure increases with the magnitude of displacement proportionally, and when P_s increases to $\mu_0 p$ (μ_0 is the static friction coefficient between the wheel and the rail, greater than dynamic friction coefficient), the wheel starts to slid, and the friction drops to μp . For the friction smaller than the resilience, the wheel will rebound suddenly, and the strong noise will appear [1].

16.3 Technology on the Wheel Flange Lubrication

The active impacts have been recognized by the continuous improvement, the technology brings which emerged in the western countries firstly. The engineers of original German federal railways had concluded that the distance could grow by 400 % at most between two copings [2]. (Figs. 16.3 and 16.4)

According to the lubricating material, it can be divided into three kinds: solid lubrication, liquid lubrication, and mixed lubrication. The main solid lubricating material is the graphite mixed with other materials in general. The reason of reducing friction is that the molecules of surface adsorption are formed on the

Fig. 16.3 The liquid lubrication

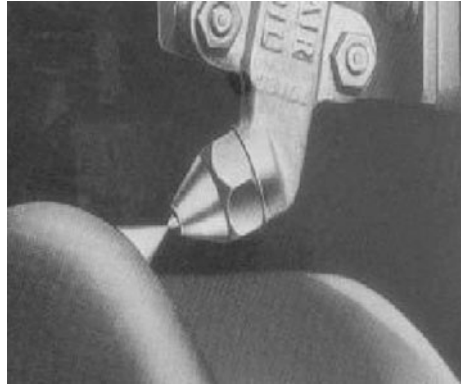


Fig. 16.4 The solid lubrication



lubricant contact, whose role is the same as the additive molecules of the liquid friction under the state of boundary lubrication. When accelerating the friction surface running-in, the graphite forms a veneer of solid lubricant at the friction sector in the running-in period rapidly and improves surface quality effectively. The lubricants are the main liquid lubricating material now, but the early is mostly mineral thin oil. Under the pressure supplied by pneumatic pumps, according to certain proportion mixed with the air, the lubricant forms a layer of coating at the wheel flange after accelerating ejection by the nozzle. If the jet velocity matches well with the speed of the wheels in optimal system, the lubricant should not drip, but can guarantee the lubrication effect [3]. After the actual tested, the best lubricant is viscid which is mixed with higher rates of the solid particles at present, for example, the graphite and the aluminum powder. Just for the best lubricant, the wear is close to zero between the wheel flange and the rail, and the wear of the wheel flange is better than the one of the tread, so the mixed lubrication is. The flange wear is more serious, for the cranes at the higher classification group, for instance, the metallurgical crane. After adopting the wheel flange lubrication, the

life of the wheels increases obviously, and the operating condition is improved greatly, for reducing drag and the noise. But there are some questions on the wheel flange.

1. The special work environment. The edge of rail will be used by the rail clamping device, for the wind-proof cranes. But it is just coated with the lubricating film in the lubrication on the wheel flange, impacting the rail clamping device. So it does not apply.
2. The specificity of the crane. In the liquid lubrication, the cost is higher for the aerodynamic force and the oil delivery, but the work is less in the routine maintenance. In the solid lubrication, the cost is lower, and the routine maintenance is easier, but more frequent. The solid lubrication is more suitable, when no air power source and strict cost requirements. And there are some appearance requirements, avoiding the bulge of partial structure, and the cost requirement is looser. So the liquid lubrication is more suitable at the moment.

16.4 The Improvement of the Structure

In our country, there is a fillet R1 in the transition region of the flange and the tread, and there is also a fillet R on the top of the rail, $R1 < R$ [4]. But in Western Europe, it is the type showed in Fig. 16.5. Just for the new type, it emerges that the phenomenon of the flange growing, because of the flange wear reducing and the working life increasing in the project. The wheels can work for more distances before grinding, and cutting quantity is much fewer, so there are more copings before replace (Fig. 16.6).

In solidworks, the physical model is built, the wheel diameter is 700 mm, wheel pressure is 540 Mpa, and side pressure is 81 Mpa. There is an analysis of the stress distribution, the strains, and the fatigue damage, in the simulation.

Fig. 16.5 The internal type

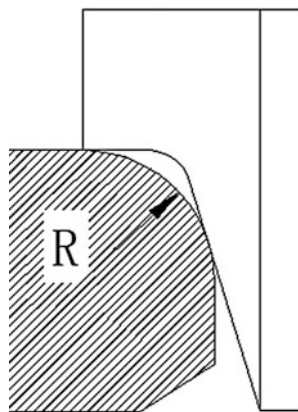
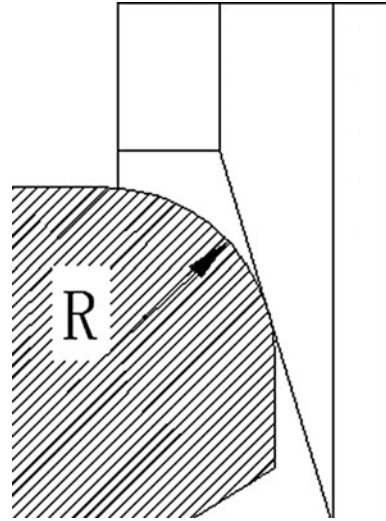


Fig. 16.6 The abroad type

Because the safe factor is bigger in practice, the differences are not obvious in the fatigue analysis.

The stress distributions are little changed by watching, but the maximum stress reduces by 7.5 %. The stresses reduce accordingly at each range, so the new structure is superior to the old.

16.5 Conclusions

With the development of manufacturing in China, the manufacturing techniques have changed greatly. It has stepped off the rough, cumbersome and heavy stage. The running conditions are improved after introducing the new type of the structure and the wheel flange lubrication, resulted in improving the loading conditions, reducing the flange wear, and extending the service life of the wheels.

References

1. Design rule for cranes, GB/T3811-2008
2. Cao E (2007) REBS wheel flange lubrication system, Urban Mass Transit, 2007
3. Rail wheels for crane, JB/T6392-2008
4. Otte R (2006) Reduce the rail wear by the flange lubrication device. Urban Mass Transit, 2006

Chapter 17

Lightweight Design for the Combinatorial Jib

Jiong Zhao, Qicai Zhou, Wenjun Li and Zailei Zhou

Abstract To realize the lightweight design of the combinatorial jib, the design theory of the combinatorial jib was analyzed, and the sectional dimensions and the limb spacing were taken as design variables. Based on the rigidity, strength, and stability of the combinatorial jib, the mathematical model of lightweight design of the combinatorial jib was established. Then, a practical problem was studied. Moreover, the mathematical model was solved, and its lightweight design solution was obtained. The results demonstrated the validity of the solution, and it provided a certain way to realize the lightweight design of the combinatorial jib in engineering.

Keywords Combinatorial jib · Lightweight design · Stability

With the demand of engineering construction and the development of the hoisting technology, some super-tonnage jib cranes emerged, and the crawler crane that over 3000 tons has appeared both at home and overseas [1–3]. Most cranes of this kind use high-strength combinatorial jib as bearing structure and change the total length of the jib by means of the combination of different numbers of standard jib segments, to adapt to different lifting tasks and environments.

Jib structures have occupied an important role in the working process of cranes. In the classical design method, to ensure the safety of crane jib, the designer usually took an excessive safety factor. So, the structures designed in this way were always too ponderous, and obviously, they would consume more steel than they really need, and it was contradicting to the lightweight design of cranes. In recent years, with the development of computer technologies and the improvement of design theories, through the optimization design of the jib structures, it has been a new development trend that to reduce the weight of structures and the power of the mechanism, but to ensure the safety and fulfill the performance requirements at the same time [4–6].

J. Zhao (✉) · Q. Zhou · W. Li · Z. Zhou
College of Mechanical Engineering, Tongji University, Shanghai 201804, China
e-mail: jiong.zhao@tongji.edu.cn

© Springer-Verlag Berlin Heidelberg 2015
Logistics Engineering Institution, CMES (ed.),
Proceedings of China Modern Logistics Engineering,
Lecture Notes in Electrical Engineering 286, DOI 10.1007/978-3-662-44674-4_17

179

Compared with other structures, truss structure has a smaller deadweight, a better resistance to buckling, and a greater load capacity. So, it had been widely used in jib cranes, especially in super-tonnage jib cranes. With the combination of several standard jib segments, the jib could expand the working range. Therefore, this article made a design and research on combinatorial jib, established its mathematical model of lightweight design. Then, this method was applied to a practical problem and obtained the corresponding lightweight design solution.

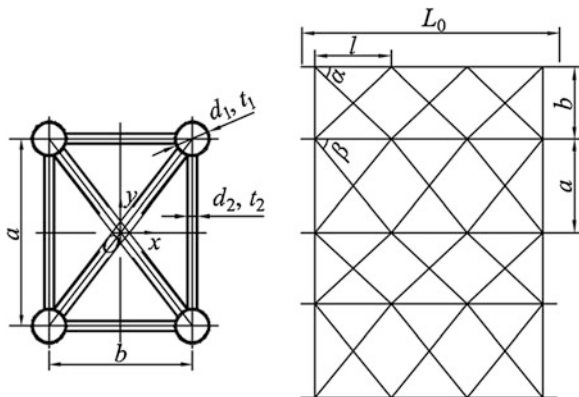
17.1 Lightweight Mathematical Model

Figure 17.1 shows the section of a 4-limb standard jib segment and the unfolded drawing of the truss structure. It uses cross-shaped web member architecture. Refer to this figure, suppose n is the number of standard jib segment, L_0 is the length of standard jib segment, a and b are limb spacing, l is the distance between two adjacent nodal points, d_1 and t_1 are, respectively, the outer diameter and wall thickness of the chord members, d_2 and t_2 are the outer diameter and wall thickness of the web members, α is the angle between the tilted web member and the chord member in the truss plane that parallel to x -axis, β is the angle between the tilted web member and the chord member in the truss plane that parallel to y -axis. In the most dangerous working condition, suppose the axial force of the dangerous section is N , the moments in x and y directions are, respectively, M_x and M_y ; the maximum shear force is Q . The yield strength of the material of the jib is σ_s , and the allowable strength is $[\sigma]$.

17.1.1 Selection of Design Variables

Generally, the jibs of super-tonnage crane are lattice structures that compressed eccentrically. Previously, many researchers had researched the optimal design

Fig. 17.1 Standard jib segment



method about the structures of this type, but they mainly selected the wall thicknesses of the chord members and web members as design variables and established non-linear programming to solve it. For example, reference [7] selected the wall thickness of the chord members of different jib segments as design variables, and the design variables of reference [8] are the coordinates of the nodal points and the sectional area of members, to conduct the layout optimization of members. But, the design variables are all of the same type.

Practically, for the lattice structure that compressed eccentrically, compared with the lattice structure that compressed axially, when influenced by the same external load, with the spacing between chord members increasing, the internal force of them would decrease, and the sectional area would also decrease. However, the shear force of web members keeps invariant, so the length of web members would increase rapidly, and it would consume more steel consequently [9]. To sum up, to determine the spacing between chord members reasonably, is the key factors of lightweight design of lattice structures in cranes. In reference [10], although the spacing between chord members were taken into account in the optimal design of crane jibs, the writer did not researched the effect of shear force to web members.

In conclusion, this paper elected the spacing between chord members, a , b , and the wall thicknesses of chord members and web members, t_1 , t_2 , as the design variables.

$$x = [a, b, t_1, t_2]^T = [x_1, x_2, x_3, x_4]^T \quad (1)$$

17.1.2 Objective Function

In this paper, the weight of the crane jib was taken as the optimization objective, so the objective function is

$$w(x) = \pi\rho L_0 \left[d_1^2 - (d_1 - 2x_3)^2 \right] + 3\pi\rho \left(\sqrt{l^2 + x_1^2} + \sqrt{l^2 + x_2^2} \right) \left[d_2^2 - (d_2 - 2x_4)^2 \right] \quad (2)$$

17.1.3 Constraint Conditions

Based on the design requirements and design theories, and combined with engineering practice, the constraint conditions consist of: the overall rigidity, strength, and stability of the jib, the rigidity, strength, and stability of components, etc. Specially, when analyzing the internal force of the structure, section method was applied and researched the effect of shear force to web members.

(1) Overall Rigidity and Stability Condition

$$\lambda_{hx} - \lambda_0 \approx \left(\frac{2nL}{x_1} \right) + \frac{40^2}{3n} \cdot \frac{d_1^2 - (d_1 - 2x_3)^2}{d_2^2 - (d_2 - 2x_4)^2} - [\lambda_0] \leq 0 \quad (3)$$

$$\lambda_{hy} - [\lambda_0] \approx \left(\frac{2nL}{x_2} \right)^2 + \frac{40}{3n} \cdot \frac{d_1^2 - (d_1 - 2x_3)^2}{d_2^2 - (d_2 - 2x_4)^2} - [\lambda_0] \leq 0 \quad (4)$$

$$\begin{aligned} \frac{N}{\varphi_0 A} + \frac{M_x}{W_x} + \frac{M_y}{W_y} - [\sigma] &\approx \frac{N}{\varphi_0 \pi [d_1^2 - (d_1^2 - 2x_3)^2]} \\ &+ \frac{M_x}{\frac{\pi x_1}{2} [d_1^2 - (d_1^2 - 2x_3)^2]} + \frac{M_y}{\frac{\pi x_2}{2} [d_1^2 - (d_1 - 2x_3)^2]} - [\sigma] \leq 0 \end{aligned} \quad (5)$$

where, λ_{hx} and λ_{hy} are, respectively, the equivalent slenderness ratio of the jib in the x - x and y - y plane; $[\lambda_0]$ is the overall allowable slenderness ratio of the jib; L is the equivalent length of the jib; φ_0 is the overall stability coefficient of the jib.

(2) Component Rigidity Conditions and Diameter–thickness ratio Conditions [11]

$$\lambda_1 - [\lambda_1] = \frac{4L}{\sqrt{d_1^2 + (d_1 - 2x_3)^2}} - [\lambda_1] \leq 0 \quad (6)$$

$$\lambda_2 - [\lambda_2] = \frac{4\sqrt{x_1^2 + l^2}}{\sqrt{d_2^2 + (d_2 - 2x_4)^2}} - [\lambda_2] \leq 0 \quad (7)$$

$$\lambda_2 - [\lambda_2] = \frac{4x_1^2 + l^2}{\sqrt{d_2^2 + (d_2 - 2x_4)^2}} - [\lambda_2] \leq 0 \quad \frac{d_1}{x_3} - 100 \cdot \frac{235}{\sigma_s} \leq 0 \quad (8)$$

$$\frac{d_2}{x_4} - 100 \cdot \frac{235}{\sigma_s} \leq 0 \quad (9)$$

where, λ_1 and λ_2 are, respectively, the slenderness ratio of chord members and web members; $[\lambda_1]$ and $[\lambda_2]$ are the allowable slenderness ratio of the corresponding components.

(3) Stability Conditions of Components

$$\frac{\frac{N}{4} + \frac{M_x}{2x_2} + \frac{M_y}{2x_1}}{\frac{\pi}{4} \varphi_1 [d_1^2 - (d_1 - 2x_3)^2]} - [\sigma] \leq 0 \tag{10}$$

$$\frac{Q}{\varphi_2 \pi \sin \beta [d_2^2 - (d_2 - 2x_4)^2]} - [\sigma] \leq 0 \tag{11}$$

where, φ_1 and φ_2 are the stability coefficients of chord members and web members; $\sin \beta = \frac{x_1}{x_1^2 + l^2}$. Compared with the axial force and moments, the effect on the stability of chord members that derived from the shear force is rather small, so the shear force is not taken into account in Formula (10). But, this situation must be checked after optimal design.

17.2 Practical Computing Example

One super-tonnage jib crane, it adopts double jib structure, as shown in Fig. 17.2. When the jib is the shortest, and the range is 10 meters, the maximum lifting capacity is up to 2,500 tons. This paper studied a single jib, and its two ends are both box structures, as shown in Fig. 17.2. On condition of the shortest jib, it is made up of 6 standard jib segments, that is $n = 6$, the length of a standard jib segment is $L_0 = 5.7(m)$, and the total weight of the jib is 41,202(kg). In the jib, the section of chord member is $\phi 406 \times 22(mm)$, and the section of web member is

Fig. 17.2 The jib structure and overall dimensions of one super crane

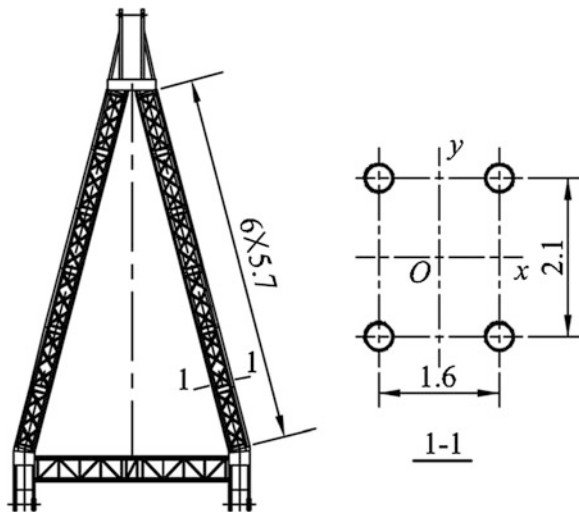
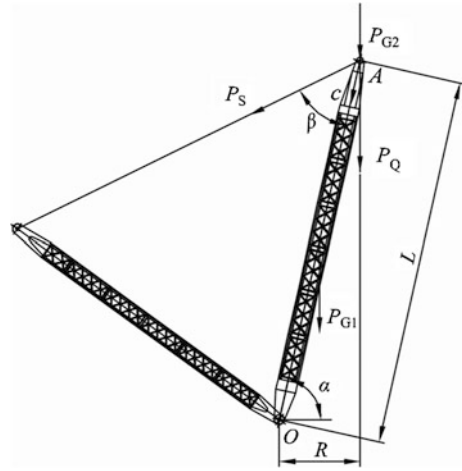


Fig. 17.3 Force analysis in the luffing plane



$\phi 152 \times 10(\text{mm})$. The overall dimensions of the standard jib segment are $a = 2.1(\text{m})$, $b = 1.6(\text{m})$. The material of jib is Q345, and the yield strength is $\sigma_s = 345(\text{MPa})$. According to the reference [12], the strength safety factor of load combination B is 1.34, so $[\sigma] = \sigma_s/1.34 = 257.5(\text{MPa})$.

17.2.1 Load Analysis

The worst working condition of the crane is that the wind flowing from side direction and the hoisting mechanism is still working. At the moment, the jib would bear lateral loads. In the luffing plane, the jib can be simplified as a beam that simply supported at both ends, and the force diagram is shown in Fig. 17.3. While in the rotary plane, the jib can be simplified as a cantilever beam that fixed at the root of the jib but free at the upper end, and the force diagram is shown in Fig. 17.4.

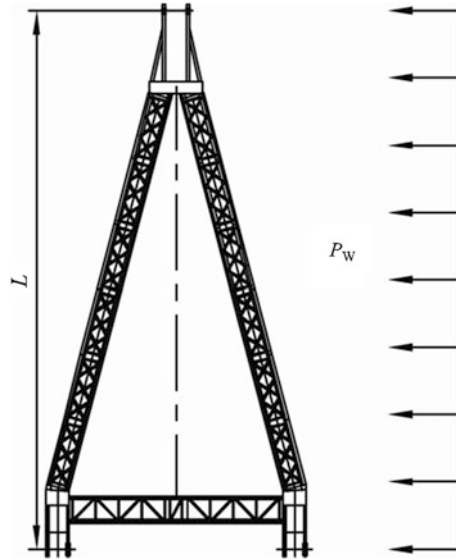
Where, P_Q is the hoisting load and imposed at the top end point A, it consists of the lifting weight and the deadweight of spreader and steel strand, (N); ϕ_2 is the dynamic hoisting load coefficient, $\phi_2 = 1.05$; P_{G1} is the deadweight of the jib structure and uniformly distributed on the jib, (N); the impact coefficient of hoisting load ϕ_1 can be neglected; P_{G2} is the vertical load imposed at the top end point A, (N); P_W is the lateral wind load that uniformly distributed on the jib, (N); P_S is the luffing force that imposed at the top end point A, N; L is the length of the jib, (m); R is the working range of the crane, (m).

The luffing plane :

At the boot hinge point O, list the moment equilibrium equation, that is :

$$P_S \cdot L \sin \beta - (\phi_2 P_Q + P_{G2})L \cos \alpha - P_{G1} \cdot \frac{L \cos \alpha}{2} = 0 \quad (12)$$

Fig. 17.4 Force analysis in the rotary plane



So, the luffing force is:

$$P_s = \frac{(\emptyset_2 P_Q + P_{G2}) \cos \alpha + P_{G1} \cdot \frac{\cos \alpha}{2}}{\sin \beta} \quad (13)$$

According to Fig. 17.3, analyze the forces and get the formulas below. The axial force of any cross section of the jib is:

$$N_c = (\emptyset_2 P_Q) \sin \alpha + P_s \cos \beta + \frac{c}{L} P_{G1} \sin \alpha \quad (14)$$

The shear force of any cross section of the jib is:

$$Q_c = P_{G1} \left(\frac{1}{2} - \frac{c}{L} \right) \cos \alpha \quad (15)$$

The moment of any cross section of the jib is:

$$M_{cx} = \frac{P_{G1} \cos \alpha}{2} \left(c - \frac{c^2}{L} \right) \quad (16)$$

where, c is the distance between the cross section to the upper hinge point A of the jib, m.

The rotary plane:

The moment of any cross section of the jib is:

$$M_{cy} = \frac{P_w}{2L} c^2 \quad (17)$$

According to Formulas (14)—(17), it is easily gotten that the maximum axial force and the maximum shear force appear at the boot of the jib, the maximum moment of X -axis appears at the middle cross section of the jib, and the maximum moment of y -axis appear at the boot cross section. Therefore, the middle and root cross sections are dangerous sections that should be analyzed and checked. Generally, the load capacity of crane jibs depends on its overall stability condition [13]. For the jib structure in this practical example, the overall stability of the boot cross section is more important. So, this paper selected the load of the boot cross section as the lightweight design load.

17.2.2 Lightweight Design Solution

Based on the analysis above and the practical data of the crane, this paper calculated and converted the result to a single jib, got the load of the root cross section:

$$N = 17,667,909 \text{ N}, \quad M_x = 388,283 \text{ N} \cdot \text{m}, \quad M_y = 307,406 \text{ N} \cdot \text{m},$$

The maximum shear force was $Q_c = 86,994 \text{ N}$.

According to the data, the lightweight mathematical model was established.

The outer diameters of chord members and web members are constant values, which are: $d_1 = 0.406 \text{ m}$, $d_2 = 0.152 \text{ m}$; According to the lightweight requirements and practical engineering, the top and bottom limitations of limb spacing, respectively, are: $1.6(\text{m}) \leq x_1 \leq 2.1(\text{m})$, $1.2(\text{m}) \leq x_2 \leq 1.6(\text{m})$; the diameter-thickness ratio conditions could be transformed to the state variables of the design variables, which determined the top and bottom limitations of wall thickness of the chord members and web members, to increase the computation speed. Reference the standard of seamless steel tube [14], the bounds of x_3 , and x_4 are: $0.009(\text{m}) \leq x_3 \leq 0.022(\text{m})$, $0.003(\text{m}) \leq x_4 \leq 0.01(\text{m})$.

Obviously, it is a non-linear optimization problem to solve the lightweight mathematical model. Therefore, the non-linear programming algorithm in the MATLAB optimization toolbox was applied for optimization design in this paper. Based on the discussion above, the top and bottom limitations of 4 design variables were defined in two matrixes vlb and vub :

$$vlb = [1.6; 1.2; 0.009; 0.003]$$

$$vub = [2.1; 1.6; 0.022; 0.01]$$

Wrote the MATLAB program of the lightweight mathematical model, solved it by calling the optimization algorithm.

And, the results are:

$$x^* = [1.9836, 1.5213, 0.0192, 0.0094]^T.$$

Because the results are all precise values, before adopting the results, the data should be rounded and processed based on practical engineering and relevant standards [14]. So, the final lightweight design solution is $x_{\text{opt}} = [1.985, 1.525, 0.02, 0.0095]^T$ and the weight after optimization of the jib is $W_{(x_{\text{opt}})} = 37,816.2$ kg. Obviously, the total weight of the optimal design solution has reduced about 8.22 % than before, and it shows an evident effect on weight reduction of truss structures.

17.3 Conclusions

For the super-tonnage jib cranes, their jibs always consume large quantities of steel. Specially in consideration of the interchangeability and generality of standard jib segments of different cranes, to design the combinatorial jib reasonably, is beneficial to realize the lightweight of jib structure of cranes. In this paper, a kind of jib structure was analyzed and researched. Based on the rigidity, strength, and stability conditions of the jib structure, the lightweight design mathematical model was established. Then, combined with a practical example, made an optimal design to reduce the weight of the jib and achieved a good result.

To sum up, the lightweight design method proposed in this paper is based on the design theories of the lattice compression-bending members and integrated with the practical constraint conditions in engineering, met the safety requirements of jib structures, and closed to engineering practices. It could provide a certain basis and reference to the lightweight design of jib structures.

References

1. Huikun Zhai (2011) SANY group of China creates the world first [J]. *Constr Mach* 4:58–59
2. Xia W (2010) Super-tonnage cranes lead the development of technology[J]. *Constr Mach Technol Manage* 12:42–47
3. Xuewei Xue (2011) The way of crawler cranes of “made in China” took the top [J]. *Constr Mach Technol Manage* 24(6):50–52
4. Wenming Cheng, Yamin Li, Zeqiang Zhang (2012) Criteria on lightweight design for gantry and overhead cranes [J]. *Chinese J Constr Mach* 10(1):41–49
5. Martinez P, Marti P, Querin OM (2007) Growth method for size, topology, and geometry optimization of truss structures [J]. *Struct Multidisc Optim* 33:13–26

6. Shin YS, Park JH, Ha DH (2009) Optimal design of a steel box girder bridge considering life cycle cost [J]. *J Civil Eng* 13(6):433–440
7. Chaoyun Z, Lihua Y (2005) Optimal design of crane booms that made of chord members of different thicknesses [J]. *Hoisting Conveying Mach* 12:37–40
8. Yixiao Q, Feng T (1995) Layout optimal design of truss Jib structure [J]. *Port Oper* 5:1–5
9. Wang J , Zhang Q, Shen X et al. (2011) Steel structure design of hoisting machinery [M]. Chemistry Industry Press, Beijing
10. Huan Z, Changsheng X. Optimized design for the structure of truss crane Jib based on MATLAB and parameterized model [J]. *J Wuhan Univ Technol (Transport Sci Eng)* 35 (1):201–204
11. GB/T 50017—2011 (2011) Code for design of steel structures [S]. China Standard Press, Beijing
12. GB/T 3811—2008 (2008) Design rules for cranes [S]. China Standard Press, Beijing
13. Dashan D (2011) Metal structure of hoisting machinery [M]. Shanghai Jiaotong University Press, Shanghai
14. GB/T 17395—2008 (2008) Dimensions, shapes, masses and tolerances of seamless steel tubes [S]. China Standard Press, Beijing

Chapter 18

Research on the Overload Protection System of Knuckle Boom Crane

Kun Song, Yaofeng Xue, Lei Xu and Bo Zhang

Abstract Due to the particularity of the knuckle boom truck-mounted crane structure, it is difficult to express the rated operating capacity at various states simply with the rated lifting load curve. The operator cannot get an intuitive understanding of the operational capacity of the crane. Therefore, there is a big security risk. According to the GB 6067–2010 “Safety rules for lifting appliances,” the overload protection system must be installed on the knuckle boom crane. In this paper, studying on the structural characteristics of the knuckle boom crane, a torque limit method is proposed based on programmable controller, weight sensor, angle sensors, length sensor, and electromagnetic unloading valves. And it is introduced from the system structure, establishment of a mathematical model, and so on. The overload protection system based on this method is now applied to a knuckle boom crane, and the method can dynamically and accurately reflect the rated lifting load, lifting load, and operating range and also achieve the crane overload warning and action limits in any conditions, providing a guarantee for safe operation, and the system can also be programmed to expand vertical lifting function, with a very good application prospect.

Keywords Knuckle boom crane · Truck-mounted crane · Overload protection system · Vertical lifting

18.1 Introduction

Truck-mounted crane is a kind of crane which was placed on a truck to lift goods [1]. It was divided into two types: knuckle boom crane and stiff boom crane. Compared with stiff boom crane, knuckle boom crane has compact structure and

K. Song (✉) · Y. Xue · L. Xu · B. Zhang
General Logistics Department, Construction Engineering Research Institute, Xi'an 710032,
People's Republic of China
e-mail: sk62026@126.com

© Springer-Verlag Berlin Heidelberg 2015
Logistics Engineering Institution, CMES (ed.),
Proceedings of China Modern Logistics Engineering,
Lecture Notes in Electrical Engineering 286, DOI 10.1007/978-3-662-44674-4_18

obvious advantages in operability, functionality, security, and maintainability. Because of its unique structure, it is difficult to show the rated operating capacity of the various states with the rated load curve; the operator cannot get an intuitive understanding of the operational capacity of the crane, so there is a big security risk. As the GB 6067–2010 “Safety rules for lifting appliances” is issued, it is really necessary to install the overload protection system on the mobile crane [2], and the knuckle boom crane is also asked to be with overload limit mandatory requirements.

To make sure the operations on knuckle boom crane are safe, some study puts forward a method using a moment-limiting valve [3]. This method still has some shortcomings because sometimes the moment decays as operating range increases. Another study puts forward a way using pressure sensors, angle sensors, and length sensor [4], but the zero drift and hysteresis will increase the calculation error. This paper presents a method using angle sensors, length sensor, and weight sensor, which can be useful in any conditions to warn and limit overloading operation.

18.2 Knuckle Boom Crane

18.2.1 Figures

As shown in Fig. 18.1, generally, a knuckle boom crane is constituted by outriggers, base, turntable, main boom, telescopic boom, lifting hook, cylinder, and so on.

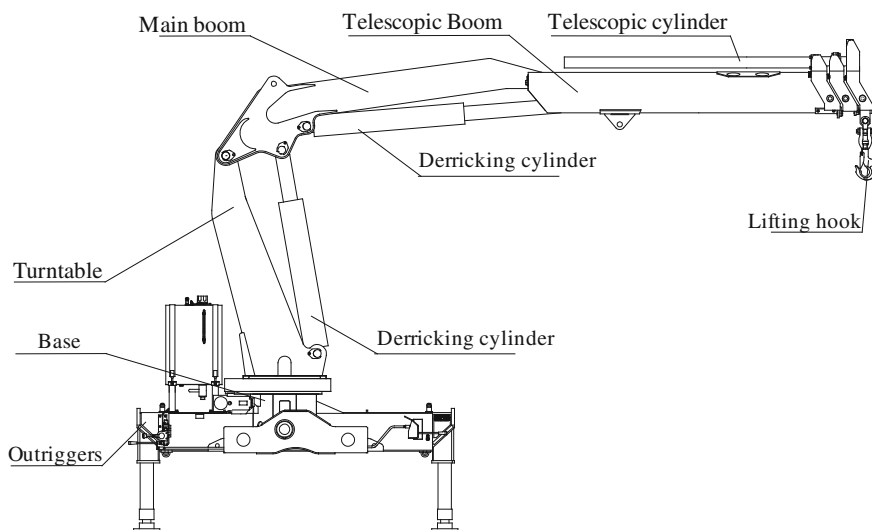
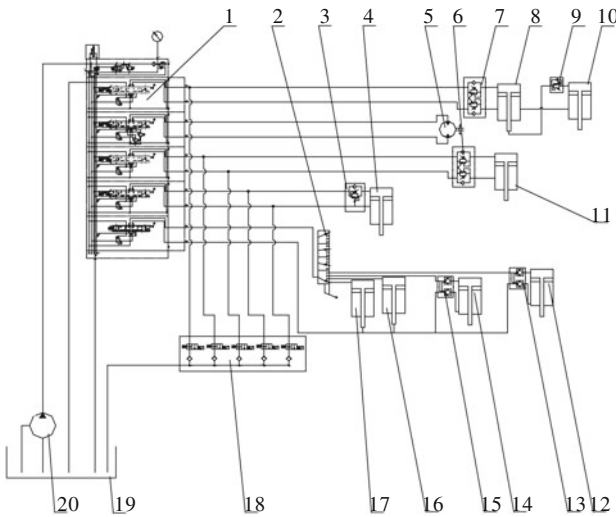


Fig. 18.1 The structure composing of a knuckle boom crane

18.2.2 Hydraulic System

Figure 18.2 is the hydraulic system diagram of some knuckle boom crane which has a two section telescopic arm. In this system, there are five electromagnetic unloading valves to make sure that the overload protection system can limit overloading operation. Electromagnetic unloading valve is a kind of relief valve supplemented with an electromagnetic change valve. It is closed when it is not electrified. When the crane is overloaded, it will be electrified, and the valve port will open, and the oil will go back to the tank directly. In this way, the dangerous operations will be avoided. The five valves correspond successively to prevent main boom rising and decreasing, telescopic boom rising and decreasing, and telescopic boom extending.



1-multi-way direction valve;2- selector valve;3- unidirectional balance valve;4- derricking cylinder 1; 5- gyration motor ;6,7-bidirectional balance valve;8-telescopic cylinder 1;9- sequence valve;10- telescopic cylinder 2;11- derricking cylinder 2;12,14- vertical outrigger cylinder;13,15- double-direction hydraulic lock;16,17- horizontal outrigger cylinder;18- electromagnetic unloading valves;19- tank;20- piston pump

Fig. 18.2 Hydraulic system diagram of some knuckle boom crane. 1 multi-way direction valve; 2 selector valve; 3 unidirectional balance valve; 4 derricking cylinder 1; 5 gyration motor ; 6, 7 bidirectional balance valve; 8 telescopic cylinder 1; 9 sequence valve; 10 telescopic cylinder 2; 11 derricking cylinder 2; 12, 14 vertical outrigger cylinder; 13, 15 double-direction hydraulic lock; 16, 17 horizontal outrigger cylinder; 18 electromagnetic unloading valves; 19 tank; 20 piston pump

18.3 Mathematical Model

18.3.1 Parameter Setting

Figure 18.3 shows the force analysis diagram for a certain type of truck-mounted crane operations. To simplify the calculation process, it is assumed here that the center of gravity of each boom approximate overlaps at the midpoint of the line between twisted points.

Figure 18.3a, b, d, and e are the distances between the twisted points; α_1, α_2 , and α_3 are angles between connection of twisted points and the horizontal direction or booms; L_1 and L_2 are the length of the main boom and basic telescopic boom; L_3 is the distance from twist point C to the rotation center; and m_1, m_2 and m_3 stand for the quality of the main boom, basic telescopic boom and inner telescopic boom respectively. These parameters are known as structural parameters of the crane.

There are four variables measured by the sensors: amplitude angle of the main boom, amplitude angle of the telescopic boom, telescopic boom extension length, and lifting load. Other variables such as force arm h_1 and force arm h_2 can be solved using the above parameters. To solve the rated lifting load, the force F_1 and F_2 can be solved by the rated pressure and area of cylinders.

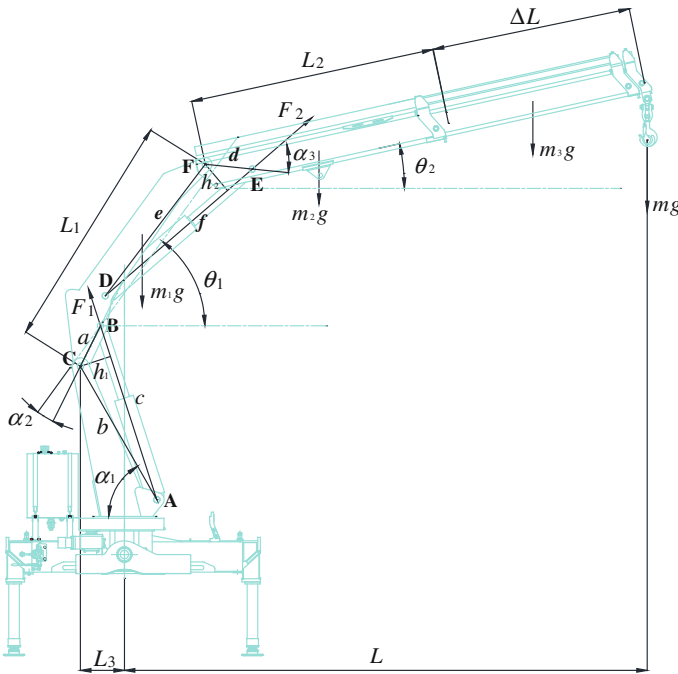


Fig. 18.3 The force analysis diagram of a knuckle boom crane

18.3.2 Modeling

In the process of knuckle boom crane operations, the rated moment is mainly determined by the pressure of the derricking cylinders, the overturning moment of the vehicle, and the allowable stress of the steel structure. According to the rated load curve characteristics of a product, the rated pressure of both derricking cylinders and the calibrated rated load curve to model is selected to model.

(1) Moment model based on the derricking cylinder 1

In the triangle ABC:

$$\begin{cases} \angle C = \theta_1 + \alpha_1 + \alpha_2 \\ h_1 = \frac{2s}{c} \\ s = \frac{1}{2}ab \sin \angle C \\ c^2 = a^2 + b^2 - 2ab \cos \angle C \end{cases}$$

So the force arm h_1 can be solved.

$$h_1 = \frac{ab \sin(\theta_1 + \alpha_1 + \alpha_2)}{a^2 + b^2 - 2ab \cos(\theta_1 + \alpha_1 + \alpha_2)}$$

Therefore, the moment of derricking cylinder 1 on the twist point C is as follows:

$$M_1 = F_1 h_1 = \frac{p\pi r_1^2 ab \sin(\theta_1 + \alpha_1 + \alpha_2)}{\sqrt{a^2 + b^2 - 2ab \cos(\theta_1 + \alpha_1 + \alpha_2)}}$$

The moment of booms and lifting load on the twist point C is as follows:

$$\begin{aligned} M'_1 &= \frac{m_1 g L_1 \cos \theta_1}{2} + m_2 g \left(L_1 \cos \theta_1 + \frac{L_2 \cos \theta_2}{2} \right) + m_2 g \left(L_1 \cos \theta_1 + \frac{L_2 \cos \theta_2}{2} \right) \\ &+ m_3 g \left(L_1 \cos \theta_1 + \frac{L_2 \cos \theta_2}{2} \right) + mg(L_1 \cos \theta_1 + L_2 \cos \theta_2 + \Delta L \cos \theta_2) \end{aligned}$$

The rated lifting load m_{r1} can be solved by the moment equilibrium equation.

$$m_{r1} = \left[\begin{aligned} &\frac{p\pi r_1^2 ab \sin(\theta_1 + \alpha_1 + \alpha_2)}{\sqrt{a^2 + b^2 - 2ab \cos(\theta_1 + \alpha_1 + \alpha_2)}} - \frac{m_1 g L_1 \cos \theta_1}{2} - m_2 g \left(L_1 \cos \theta_1 + \frac{L_2 \cos \theta_2}{2} \right) \\ &- m_3 g \left(L_1 \cos \theta_1 + \frac{L_2 \cos \theta_2}{2} \right) \end{aligned} \right] \div [mg(L_1 \cos \theta_1 + L_2 \cos \theta_2 + \Delta L \cos \theta_2)]$$

In the equation, P is the rated pressure of the hydraulic system; r_1 is the radius of derricking cylinder 1.

(2) Moment model based on the derricking cylinder 1

Similarly, according to the moment of derricking cylinder 2 on the twist point F and the moment equilibrium equation, the rated lifting load $m_{r,2}$ can be solved.

$$m_{r,2} = \left[\begin{array}{l} \frac{p\pi r^2 de \sin(\pi + \theta_2 - \theta_1 - \alpha_3)}{\sqrt{d^2 + e^2 - 2de \cos(\pi + \theta_2 - \theta_1 - \alpha_3)}} - \frac{m_2 g L_2 \cos \theta_2}{2} \\ - m_3 g \left(\Delta L + \frac{L_2}{2} \right) \cos \theta_2 \end{array} \right] \div [g(L_2 + \Delta L) \cos \theta_2]$$

In the equation, r_2 is the radius of derricking cylinder 2.

(3) Moment model based on calibrated rated lifting load curve or overturning moment of the vehicle

The crane's calibrated rated lifting load curve has been verified through the most dangerous conditions of structure stress. According to the calibrated rated lifting load curve or the overturning moment of the vehicle, it can be modeled as follows.

$$T(1 - K/\Delta L) = \frac{m_1 g(L_1 \cos \theta_1 - L_3)}{2} + m_2 g \left(L_1 \cos \theta_1 + \frac{L_2 \cos \theta_2}{2} - L_3 \right) + m_3 g \left(L_1 \cos \theta_1 + \frac{L_2 \cos \theta_2}{2} - L_3 \right) + mg(L_1 \cos \theta_1 + L_2 \cos \theta_2 + \Delta L \cos \theta_2 - L_3)$$

The rated lifting load $m_{r,3}$ can be solved.

$$m_r = \left[\begin{array}{l} T(1 - K/\Delta L) - \frac{m_1 g(L_1 \cos \theta_1 - L_3)}{2} - m_2 g \left(L_1 \cos \theta_1 + \frac{L_2 \cos \theta_2}{2} - L_3 \right) \\ - m_3 g \left(L_1 \cos \theta_1 + \frac{L_2 \cos \theta_2}{2} - L_3 \right) \end{array} \right] \div (L_1 \cos \theta_1 + L_2 \cos \theta_2 + \Delta L \cos \theta_2 - L_3)$$

In the equation, T is the calibrated rated hoisting moment of the crane, and $1 - k/\Delta L$ is the attenuation coefficient of the moment of non-constant moment crane.

(4) The current rated lifting load

The current rated weight is the minimum of $m_{r,1}$, $m_{r,2}$, and $m_{r,3}$.

According to the measured parameters, the current operating range can be calculated by measured parameters.

$$L = L_1 \cos \theta_1 + L_2 \cos \theta_2 + \Delta L \cos \theta_2 - L_3$$

When the lifting load equals to the rated lifting load, add a given step to the angle of main boom or telescopic boom to calculate the rated lifting load of each action, and it can be determined that which valves should be unloaded to restrict dangerous operations.

18.4 Composition and Principle of the Overload Protection System

Figure 18.4 shows the installation location diagram of the overload protection system installed on the crane. The overload protection system is mainly composed of PLC, input circuit and output circuit, angle sensor 1, angle sensor 2, length sensor, weight sensor, and actuators (buzzer and electromagnetic unloading valves, etc.). The function of the overload protection system is that when the lifting load reaches 90 % of the rated lifting load, the buzzer alarms, and when the lifting load reaches 100 % of the rated lifting load, the corresponding unloading valve ports are

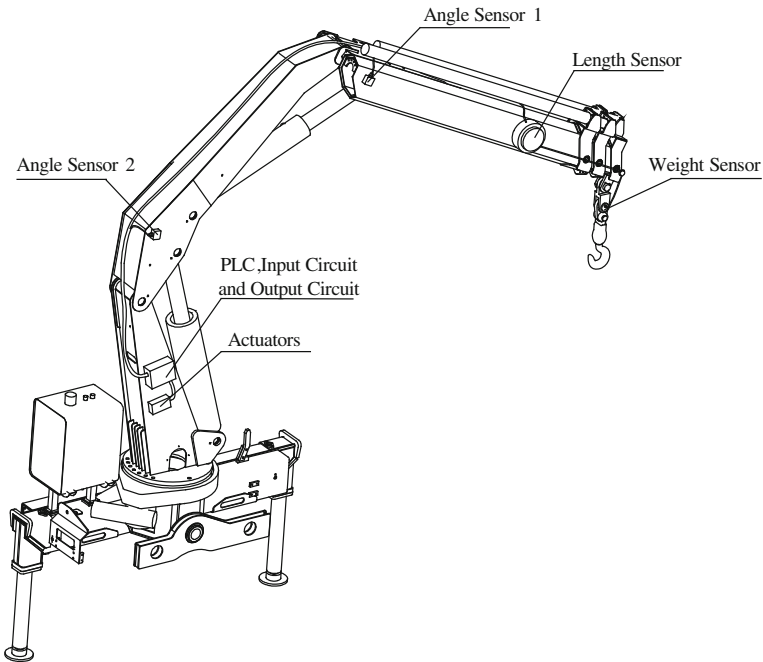
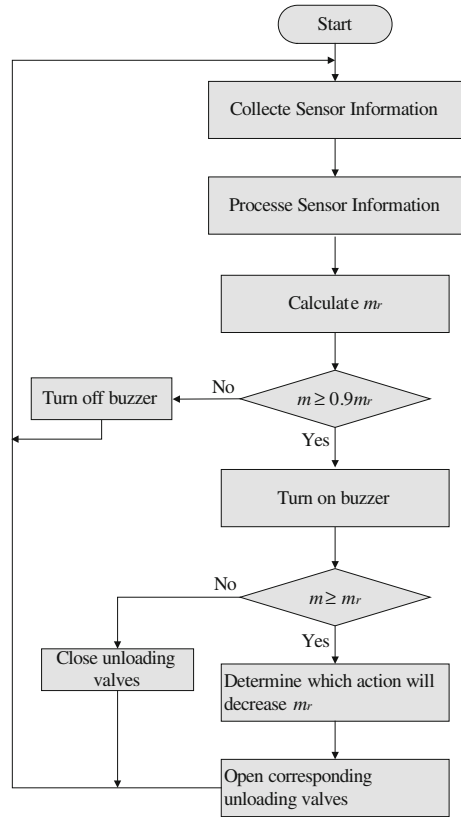


Fig. 18.4 Location diagram of the overload protection system

Fig. 18.5 System flowchart of the overload protection system



open to prevent the operations to the unsafe direction, while allow the operations to the safe direction.

Figure 18.5 is the system flowchart of this overload protection system.

18.5 Features

The overload protection system has the following characteristics:

- (1) Rated lifting load is calculated based on data collected in real time to avoid the inconvenience of inputting the rated lifting load curve and the imperfection of the curve.
- (2) The system can be useful in any working conditions as a full-featured overload protection system.
- (3) Calculating from the system pressure, structural stress, stability, and so on, it has a good safety performance, and it can adapt to a variety of knuckle boom crane by modifying the parameters according to the actual situation.

- (4) The system has a high precision using a weight sensor measuring the lifting load directly, which avoids the calculation error brought by the zero drift and hysteresis of pressure sensors.
- (5) The system uses a programmable controller, so it is convenient to expand the function.

18.6 Conclusion

The overload protection system developed on the basis of this method has been used in a certain knuckle boom crane. That crane uses a operation mode of wired remote control. It has set up a display screen on the wired remote control, which can dynamically show the rated lifting load, lifting load, operating range, angle, and other parameters, so the operator can have an intuitive understanding of the operational status of the crane. The system provided a safety guarantee by alarming and restricting dangerous operations, and the overload operations can be inquired. On the basis of the overload protection system, it can be expand in the program to achieve vertical lifting. This function can be used in some special places requiring more precise operation, which can reduce manually adjusting operation and improve efficiency.

References

1. Wang FP, Sun Y, Zheng Y (2004) Chinese J Constr Mach Equip 2:33
2. GB 6067-2010 (2010) Safety rules for lifting appliances, Chinese S. Standards Press of China, Beijing
3. Li XR (2012) Chinese J Hoisting Conveying Mach 1:75
4. MAO HY (2011) Chinese J Dev Innov Mach Electr Prod 24:117

Chapter 19

Research on Energy Consumption of Variable Frequency Control for Portal or Overhead Crane

Lili Ma and Wenming Cheng

Abstract In order to make research on the hoisting mechanism, motor's energy consumption during the motor's starting period and smooth running period for the portal crane or overhead crane, the rotational inertia, and load torque of the hoisting mechanism are converted to the rotor side; an equivalent uniaxial motor driving system is derived according to motor driving system of the hoisting mechanism; and the variable frequency control system is designed based on the slip frequency between stator's synchronous angular speed and rotor's electric angular speed and it made comparative research about energy consumption with the direct running synchronous motor. The research results showed the following: The variable frequency running motor could rapidly reach the given rotational speed within 0.2 s and could rapidly track the load torque; the frequency and amplitude of the stator's 3-phase variable frequency modulation voltage would be gradually increasing during the motor's starting period, and the 3-phase variable frequency modulation voltage would be constant during the motor's smooth running period; start energy consumption would not exceed 2×10^4 J when variable frequency running motor's load did not exceed heavy load and the load torque's effect on the energy consumption wave was small; the motor's energy saving was obvious during starting period and smooth running period if the variable frequency running motor's load exceeded medium load.

Keywords Portal or overhead crane · Hoisting synchronous motor · Variable frequency · Slip frequency · Energy consumption

L. Ma (✉)

Equipment Engineering College, Engineering University of Chinese Armed Police Force, Xi'an 710086, China

e-mail: malilichina@163.com

W. Cheng

Research Institute of Mechanical Engineering, Southwest Jiaotong University, Chengdu 610031, People's Republic of China

© Springer-Verlag Berlin Heidelberg 2015

Logistics Engineering Institution, CMES (ed.),

Proceedings of China Modern Logistics Engineering,

Lecture Notes in Electrical Engineering 286, DOI 10.1007/978-3-662-44674-4_19

19.1 Introduction

Synchronous motor is portal or overhead crane's (hereinafter referred to as crane) power plant and used to hoisting load. Though these modern control methods such as adaptive inverse control, passive control, adaptive backstepping control can regulate the synchronous motor's speed, and these modern control methods can adapt to situation that demand good speed adjusting performance for synchronous, energy consumption is usually hoisting motor's control emphasis on the motor's starting period, smooth running period, and braking period, for the portal crane or overhead crane whose hoisting mechanism can hoisting load according to designed hoisting speed. Generally, the motor's variable frequency control system can realize motor's speed adjusting through changing the motor's power frequency. Some experts made series of researches and obtained achievements. But, their researches' emphasis was mainly on the motor's speed adjusting, and the energy consumption of motor's variable motor's variable frequency control system was not studied, especially, the motor's energy consumption on the motor's starting period and smooth running period even was not studied. The reference [1] put forward the energy saving method of motor's regulation voltage aiming at crane's motor's hoisting mechanism with the characteristic of constant torque load and variable working condition load. This method took the motor's electric total loss as objective function. This method's characteristic is to make the motor's slip power to be consumed in the motor's rotor circuit, and the motor's rotor will be heated [2–3]. So, the motor's energy saving is obvious if crane is running with no load, but the energy saving is not obvious when crane is running with medium load or above medium load. So, it is necessary to improve this motor's energy saving method of regulation voltage [4–6]. In this paper, the variable frequency control system is designed based on the slip frequency between the motor's stator and rotor. The control system can fast respond motor's load torque and given rotational speed and energy saving will be realized. Comparative research will be made for motor's starting time and starting energy consumption and smooth running power consumption through motor's direct running mode and variable frequency running mode on various load conditions.

19.2 Equivalent Calculating of Hoisting Load Torque

Generally, the hoisting mechanism's motor driving system may be as shown in Fig. 19.1a [7]. In order to conveniently calculate, we give Fig. 19.1a's equivalent uniaxial motor driving system as shown in Fig. 19.1b. The motor rotor's equivalent rotational inertia is expressed as

$$J = J_e + J_1 \frac{1}{f_1^2} + J_2 \frac{1}{f_2^2} + J_r \frac{1}{f_r^2} + m \left(\frac{v_L}{n} \right)^2 + \frac{W_{fd}}{n^2} \quad (19.1)$$

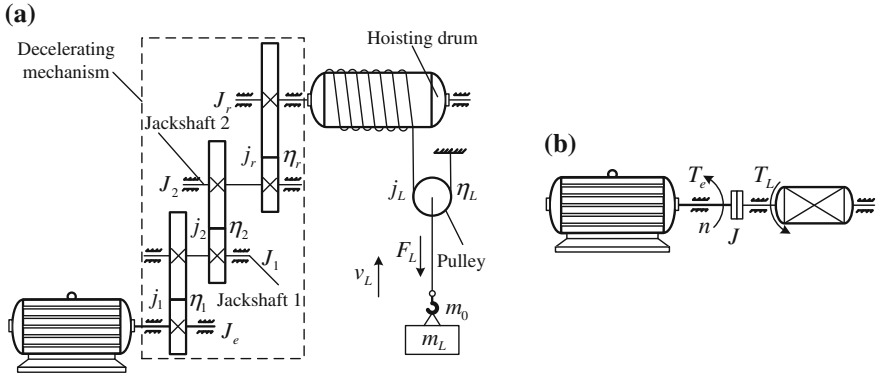


Fig. 19.1 Crane's hoisting mechanism and its equivalent uniaxial motor driving system. **a** Hoisting mechanism, **b** equivalent uniaxial driving system

where: J_e is motor rotor's rotational inertia, and its unit is kg m^2 . J_1 is the jackshaft 1's rotational inertia, J_2 is the jackshaft 2's rotational inertia, and J_r is the drum's rotational inertia. $j_1 = \frac{n}{n_1}$, $j_2 = \frac{n}{n_2}$, and $j_r = \frac{n}{n_r}$ are, respectively, reduction gear ratio of the jackshafts 1 and 2 and the drum. n is the motor's rotational speed, and its unit is r/min . n_1 , n_2 , and n_r are, respectively, the jackshafts 1, 2 and drum's rotational speed. $m = \left(\frac{30}{\pi}\right)^2 (m_0 + m_L)$ is equivalent quality, and its unit is kg . m_0 and m_L are, respectively, the spreader's quality and hoisting quality. $W_{fd} = 2 \times \left(\frac{30}{\pi}\right)^2 W_f$ is equivalent loss, and its unit is J , and W_f is the loss because of these factors such as friction.

Generally, $j_1^2, j_2^2, j_r^2 \gg 1$, and $\frac{1}{n^2} \approx 0$, it is known from expression (19.1) that the transmission mechanism's equivalent rotational inertia J is only determined by the motor rotor's rotational inertia J_e . So, often takes $J \approx J_e$ in engineering calculation [8].

The motor rotor's equivalent load torque (hereinafter referred to as load torque, its unit is Nm) can be expressed as

$$T_L = \frac{DF_L}{2j_1j_2j_rj_L\eta_1\eta_2\eta_r\eta_L} \tag{19.2}$$

where: D is the drum's diameter, its unit is m . $j_L = \frac{n}{n_L}$ is the pulleys' reduction ratio. $F_L = (m_0 + m_L)g$ is the steer wire rope's static tension, and its unit is N . g is gravity acceleration, and its unit is m/s^2 . η_1 and η_2 are transmission efficiencies of the jackshafts 1 and 2, respectively. η_r is the drum's transmission efficiency. And η_L is the pulley's transmission efficiency.

19.3 Motor's Variable Frequency Control System's Design Based on Slip Frequency

Seeing motor's two-phase static orthogonal coordinate system $\alpha\beta$ and two-phase rotating orthogonal coordinate system dq whose angular velocity of rotation is the stator's synchronous angular velocity ω_1 as shown in Fig. 19.2a, the angle between axis d and axis α is φ , φ 's unit is rad. $d\varphi/dt = \omega_1$, and O is coordinate axis' origin [9]. i_{sd} and i_{sq} are the stator winding's current on the axis d and axis q , respectively. i_{rd} and i_{rq} are the rotor winding's current on the axis d and axis q , respectively. u_{sd} and u_{sq} are stator's voltage. The unit of u_{sd} and u_{sq} is V u_{rd} and u_{rq} are rotor's voltages. The unit of u_{rd} and u_{rq} is V. The direction of i_{sd} , i_{sq} , i_{rd} , i_{rq} , u_{sd} , u_{sq} , u_{rd} , and u_{rq} is shown in Fig. 19.2. The state equations can be expressed as the following:

$$\left. \begin{aligned} \dot{\omega} &= k \left(i_{sq} \psi_{rd} - i_{sd} \psi_{rq} \right) - \frac{n_p}{J} T_L \\ \dot{i}_{sd} &= a \psi_{rd} + b \omega \psi_{rq} - c i_{sd} + \omega_1 i_{sq} + d u_{sd} \\ \dot{i}_{sq} &= a \psi_{rq} - b \omega \psi_{rd} - c i_{sq} - \omega_1 i_{sd} + d u_{sq} \\ \dot{\psi}_{rd} &= -e \psi_{rd} + (\omega_1 - \omega) \psi_{rq} + f i_{sd} \\ \dot{\psi}_{rq} &= -e \psi_{rq} - (\omega_1 - \omega) \psi_{rd} + f i_{sq} \end{aligned} \right\} \quad (19.3)$$

where: $\omega = n_p \omega_r$ is rotor's electricity angular velocity, n_p is the motor's pole-pair number, and $\omega_r = \frac{\pi}{30} n$ is the motor rotor's mechanical angular velocity, namely rotor's mechanical angular frequency or rotor's angular velocity. Coefficients $k = \frac{n_p^2 L_m}{J L_r}$, $a = \frac{L_m}{\delta L_s L_r T_r} \psi_{rd}$, $b = \frac{L_m}{\delta L_s L_r}$, $c = \frac{R_s L_r^2 + R_r L_m^2}{\delta L_s L_r^2}$, $d = \frac{1}{\delta L_s}$, $e = \frac{1}{T_r}$, $f = \frac{L_m}{T_r}$. And R_s is the motor stator's resistance, R_r is the motor rotor's resistance. Resistance's unit is Ω . L_s is stator's self-inductance. L_r is rotor's self-inductance. L_m is mutual inductance between stator and rotor. Inductance's unit is H. $T_r = \frac{L_r}{R_r}$ is called as rotor's electromagnetic time constant. T_r 's unit is S. $\delta = 1 - \frac{L_m^2}{L_s L_r}$ is called as motor's magnetic leakage factor.

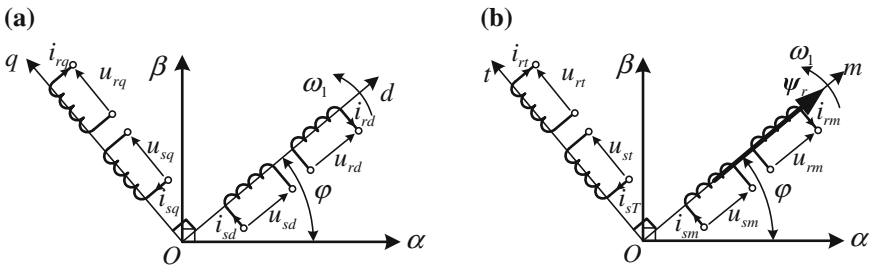


Fig. 19.2 Motor's static orthogonal coordinate system $\alpha\beta$ and rotating orthogonal coordinate system dq

Now, let axis d coincide with flux linkage vector ψ_r . So, synchronous rotation orthogonal coordinate system mt may be established according to rotor flux linkage orientation. We change axis d into axis m , and change axis t as shown in Fig. 19.2b. Because axis d always coincides with rotor flux linkage vector, $\psi_{rm} = \psi_{rd} = \psi_r$, $\psi_{rt} = \psi_{rq} = 0$, and $\dot{\psi}_{rd} = \dot{\psi}_{rq} = 0$. According to the expression (19.3), when the subscript d is changed into m and q is changed into t , we may obtain the following motor's state equations base on coordinate system.

$$\left. \begin{aligned} \dot{\omega} &= ki_{st}\psi_r - \frac{n_p}{J}T_L \\ \dot{i}_{sm} &= a\psi_r - ci_{sm} + \omega_1 i_{st} + du_{sm} \\ \dot{i}_{st} &= -b\omega\psi_r - ci_{st} - \omega_1 i_{sm} + du_{st} \\ \dot{\psi}_r &= -e\psi_r + fi_{sm} \end{aligned} \right\} \quad (19.4)$$

Motor's electromagnetic torque is

$$T_e = ki_{st}\psi_r \quad (19.5)$$

Rotor's flux linkage is

$$\psi_r = L_m i_{sm}^* \left(1 - e^{-\frac{1}{T_r}t}\right) \quad (19.6)$$

Let $\dot{\psi}_{rq} = 0$ and $\psi_{rd} = \psi_r$, we have

$$\omega_1 - \omega = \frac{L_m}{T_r} \frac{\dot{i}_{st}}{\psi_r} \quad (19.7)$$

In expression (19.7), let $\omega_s = \omega_1 - \omega$. And we call ω_s as slip frequency. The hoisting motor's variable frequency control system is designed based on slip frequency ω_s as shown in Fig. 19.3. Energy consumption is shown in Fig. 19.3 variable frequency control system.

19.4 Running Motor and Variable Frequency Running Motor Comparative Research for Direct

Suppose motor's parameters: 380 V, 50 Hz, nominal power 37 kw, nominal torque $T_N = 235$ N m, $R_s = 0.435 \Omega$, $R_r = 0.816 \Omega$, $L_s = L_r = 0.071$ H, $L_m = 0.069$ H, $n_p = 2$, $J_e = 0.189$ kg m², crane's working parameters: $v_L = 16.5$ m/min, $D = 0.5$ m, $j_1 = 11$, $j_2 = 10$, $j_r = 3$, $j_L = 2$, $\eta_1 = \eta_2 = \eta_r = \eta_L = 0.95$, $W_f = 0$, $m_0 = 500$ kg. Maximum hoisting load is $m = 50 \times 10^3$ kg. For variable frequency control system: motor's reference rotational speed is $n^* = 800$ r/min, and reference

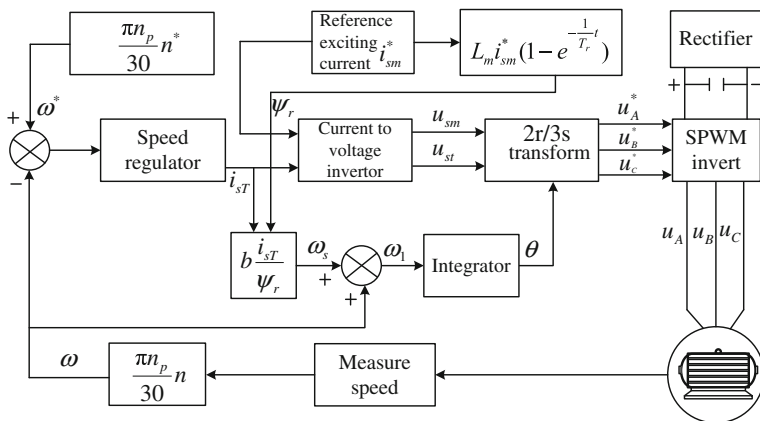


Fig. 19.3 Motor's variable frequency control system

excitation current is $i_{sm}^* = 8.5$ A. So, maximum load torque is $T_L = 230$ N m according to the expression (19.2).

The dynamic response simulation results of motor's speed and electromagnetic torque for variable frequency control system are shown in Fig. 19.4. From Fig. 19.4, we know that motor's speed fast reaches the reference speed when time is $t_s = 0.147$ s; at the same time, the electromagnetic torque is equal to load torque.

When the motor is working with full load ($100\%T_L$), heavy load ($90\%T_L \leq T_L < 100\%T_L$), middle heavy load ($50\%T_L < T_L < 90\%T_L$), moderate load ($50\%T_L$), and light load ($T_L < 30\%T_L$), the columnar comparative graph about starting time and about starting energy consumption are shown in Figs. 19.5 and 19.6, respectively. From Fig. 19.5, we know that the starting time is less than 0.2 s for the variable frequency running motor when the motor is working with full load and heavy load, the starting time is more than 0.3 s for the direct running motor

Fig. 19.4 Motor's speed and electromagnetic ($T_L = 80$ N m)

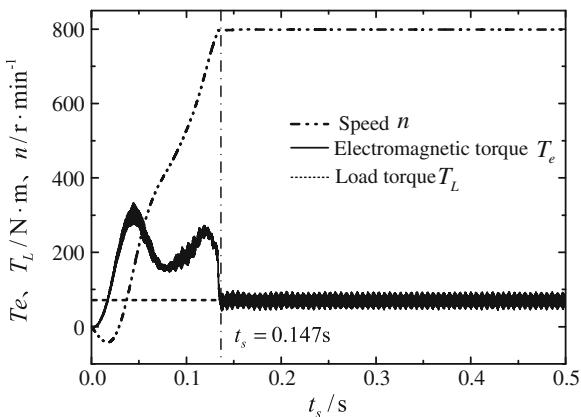


Fig. 19.5 Comparison of starting time

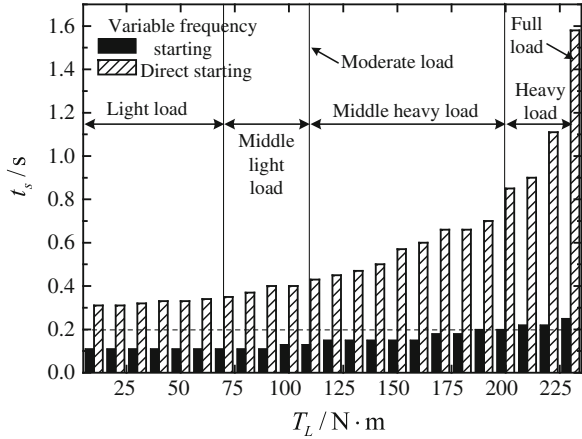
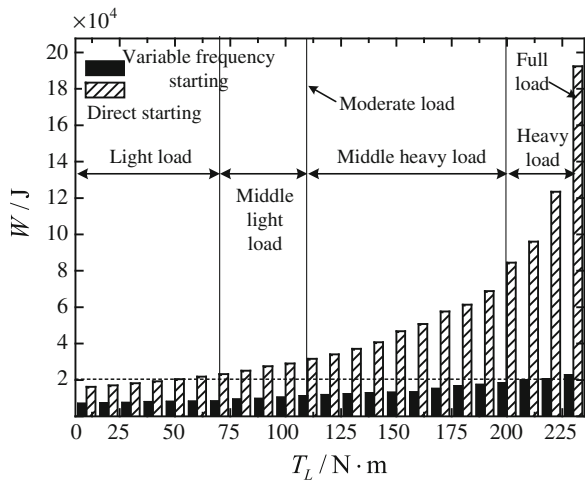


Fig. 19.6 Comparison of starting energy consumption



when the motor is working with all kinds of working conditions, especially starting time is more than 0.5 s for the moderate load or above. So, the variable frequency running motor has better dynamic performance. From Fig. 19.6, we know that starting energy consumption is less than 2.0×10^4 J for the variable frequency running motor when the motor is working with heavy load or below, and energy consumption fluctuation is smaller for load torque's change; the direct running motor's starting energy consumption is obviously more than the variable frequency sunning motor's starting energy consumption. So, when the variable frequency running motor is working with moderate load or above, the effect of energy saving is obvious.

Power consumption comparison is shown in Fig. 19.7 when the motor is smoothly running. From Fig. 19.7, we know that variable frequency running motor

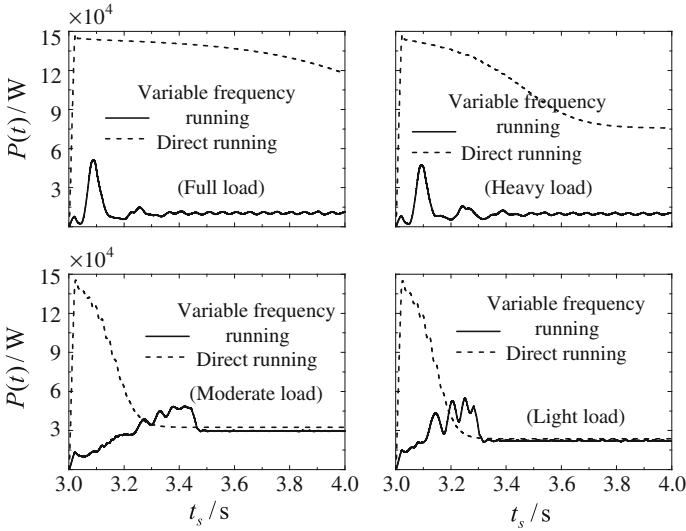


Fig. 19.7 Results of power consumption comparison

has obvious effect of energy saving when motor's load is moderate load or above. But when motor's load is below moderate load, power consumption of variable frequency running motor is nearly equal to power consumption of direct running motor.

19.5 Conclusion

In this paper, the variable frequency control system was designed based on crane's hoisting motor's slip frequency. Comparative research was made about motor's starting time, energy consumption, and power consumption for the variable frequency running motor and the direct running motor. We have the following conclusions:

- (1) The variable frequency running motor's speed can reach the reference speed in 0.2 s, and at the same time, the motor's electromagnetic torque is equal to load torque.
- (2) When the variable frequency running motor is working with heavy load or below, the starting energy consumption is less than 2.0×10^4 J, and energy consumption fluctuation is smaller.
- (3) The variable frequency running motor has obvious effect of energy saving when motor's load is moderate load or above

Acknowledgements This research and work is funded by the National Natural Science Foundation of China (51175442).

References

1. Ma LL, Cheng WM, Zhang ZQ (2012) Research on energy saving method of optimal regulation voltage for the railway container crane's asynchronous motor. *China Railway Sci* 33 (1):126–132
2. Zhang XH, Dai XZ (2002) Speed control system of induction motor based on inverse system method. *Control Decis* 15(6):708–711
3. Zhang XH, Dai XZ (2001) Torque and speed control of induction motor based on passivity. *Trans China Electrotechnical Soc* 16(4):34–38
4. Zhang CP, Lin F, Song WC et al (2004) Backstepping design for robust controller of induction motor. *Control Decis* 19(3):267–271 289
5. Liu JY, Shi S, Han XH, Liu J (2010) Based on the energy consumption of the smallest three-phase asynchronous motor optimize control of energy saving. In: *Proceedings of the Asia-Pacific Power and Energy Engineering Conference*. IEEE Press, Chengdu, pp 1–4
6. Petrushina V, Petrushina NS, Kalenik B (2010) Designing of asynchronous induction machines for adjustable speed asynchronous electric drive systems. In: *Proceedings of the International Conference on Modern Problems of Radio Engineering, Telecommunications and Computer Science*. IEEE Press, Lviv-Slavsko, pp 203–206
7. Xu XZ, Qin Y (2002) Adaptive control and parameter identification for vector-controlled induction motor. *Electr Mach Control* 6(2):111–113 114
8. Cui NX, Zhang CH, Du CS (2004) Advances in efficiency optimization control of inverter-fed induction motor drives. *Trans China Electrotechnical Soc* 19(5):36–42
9. Kang ZJ, Chen XY (2001) A design method of nonlinear extension state observer. *Electr Mach Control* 5(3):199–203

Chapter 20

User-Oriented and Visualized Optimization for Crane Design

Yuanfang Tao and Chaofei Hong

Abstract Traditional optimization methods suffer from hardness to inspect and control during the process. To solve the problem, the paper discussed a user-oriented and visualized optimization, which shows the result in drawing form by emulation and can control the process by the operator. This technique has been used in overhead crane CAD software as a post-process for traditional optimization and leads to a good result of what you see is what you get. So, the design focused on specialized machine, user-oriented, automation, visualization will be the tendency for the optimization design software.

Keywords Optimization design · Visualization · Overhead crane · CAD

20.1 Introduction

The optimization technology is one of the most important modern design methods, some of the classical theories and methods have been put into practical use with the development of the computer hardware and software. Optimization technology enjoyed a most rapid development and been widely adopted into practical use in 1980s–1990s. New methods in optimization are still undergoing development, such as the genetic algorithm, the particle swarm algorithm, the neural network, etc. And in the meantime, the optimization methods have also becoming more applicable. In the development of machinery specialized CAD software, the user-oriented and visualization technology is introduced to optimization software. The technology is focused on design of specified machinery. It aim is to achieve a user-oriented interaction mode, visualizing the optimization process and result.

Y. Tao (✉) · C. Hong
Taiyuan University of Science and Technology, Taiyuan 030024, People's Republic of China
e-mail: kdtao@126.com

© Springer-Verlag Berlin Heidelberg 2015
Logistics Engineering Institution, CMES (ed.),
Proceedings of China Modern Logistics Engineering,
Lecture Notes in Electrical Engineering 286, DOI 10.1007/978-3-662-44674-4_20

209

20.2 Specialized Optimization Software for Certain Kind of Machinery

20.2.1 To Do the Design Work

Except choosing the structure, a design procedure should at least include determining the dimensions, check the performance and the stress, and generate the engineering drawings. When the design work was done by hand, the designer often put the emphases on the drawing, draw something, than modify it a little, and check it at the same time. This process makes it looks like that drawing is design. But for all we know, design is not just drawing [1], and a good aided design software should be able to automatically determine the dimensions, check calculations, and also guide the design process.

The design work is not just checking the given product dimensions. It should be a creative work. Commonly, the dimensions of the product are not able to derive from a set of equations.

So, the design work is a complicated, repetitive, intelligent, and needs much of experience. How to improve the design functionality of the CAD software is the key part to convert the computer-aided drawing into computer-aided design. Some of the mechanical CAD software adopts the drawing library to offer the design function, but that is just a sorting and indexing to the existed drawings, not a real design. And for non-standard designs, there is nothing that can be done with the drawing library.

In a CAD system, using the optimization as the design function is a good choice, especially for certain kind of machine, such as overhead crane. The dimensions are taken as parameters to be optimized, the weight or the performance of the machine is considered to be the objective function, than the strain and stress, etc., are concerned to be the constraint function. Here, the emphasis is on the design, not on the optimization. The optimization algorithm is used just as the means to describe design process of the machine mathematically, and then, it can be dealt by computer. Optimization of the result is not the main goal of the process; generally, optimized result would be more reasonable, with less defection, at least a realizable one.

20.2.2 To Be the Parameter Generator for Parameter Drawing

As described above, drawing cannot take the place of design, but design cannot be done without drawing. The drawings are the ultimate description of the design. In the modern CAD software for specialized machinery, the parameter drawing technologies are widely used. Parameter drawing means drawing automatically, supported by the drawing support software, with the interface or interface file, according to the coordinates, derived from several main parameter of the certain

machine with fixed structure. The parameter drawing needs not only several parameters derived from optimization software, but whole geometry parameters of the drawing. So other than the object function and subject function, it will be necessary to compose a geometry parameter model.

20.2.3 Subdivisions of the Optimization Technology

There are many theories and methods of optimization, which each of them is suitable for a certain field, none of them are universal. There are specified physical and mathematics model for each practical project, which has special object and constraint function and needs specified optimization method. So, to develop optimization software for certain kind of machinery is necessary.

With a specifically optimization method, a given geometry dimension model, a specialized object and constraint function, and a set of initial values and limits, it forms a specialized optimization software for certain kind of machinery. Specialization is an inevitable tendency, when the optimization technology developed and widespread to certain level. It is the result of subdivisions of market needs.

20.3 The User-Oriented Optimization Software

20.3.1 Optimization Process Transparent to User

The common shortcoming for many traditional optimization theory or method, which is widely used, is that the operator cannot inspect the process of the optimization intuitively and also cannot control or influence it. One can only wait until the optimization is done. Designer's experience has not been well utilized.

20.3.2 To See the Result of the Optimization in a Graphics Mode

The user of the optimization software can only see the result in a numeric format in the past, which is unintuitive. Only those who have been through expertise training can know what that means from the numeric format. So, we should change the numeric format into a picture or a graphics mode by means of simulation. Only in that way can we judge the result conveniently, and then, the designer's sight and experience can do some thing about the products.

20.3.3 The Control or Influence to the Result of Optimization

The result of optimization is used to be unforeseen, unique, abstract, and it cannot be adjusted easily. The designer will be bewildered when the result of optimization is not consistent with the standard or special requirement, such as the dimensions need to be integer, standard or serial product requirement, production process requirement, has to fit with the existing product, or has to make a new product with different dimensions. In all those cases, the unchangeable result hindered the application of the optimization technology greatly. The result of the optimization should be adjustable. CAD means aid, not instead of designer. The decision should be made by designer with plenty of experience, not by computer, or software.

20.3.4 Make the Object of the Optimization Changeable Flexibly

In the real mechanical optimization design project, there are often multi-object and multi-constraint. The object function systems for a certain project are usually complex and often influenced by the user's opinion or requirements. Some result is good for a group of user, but not for others. Furthermore, the process of the optimization is a numerical cycle, the result is unforeseen, and actually useless some times. Getting a good result is something random or lucky. Designer's experience for certain machinery cannot help.

20.3.5 Make a Friendly Interface for the Optimization Software

Sometimes, optimization cannot get the best solution in overall dimension, because many factors need to set manually, such as the origin point, the step, the dimension limits, and other factors related to the optimization. Those interactive operations are in source file level, only for the programmer to do, which is not convenient for the user. If the optimization software has a friendly interface, which can guide the user conveniently, then the software can be a good tool for the designers to use and with commercial values.

User orientation is necessary for commercial software. The history of the development for software shows clearly that such as the windows with graphical user interface replace the DOS, the Visual Basic and Visual C++ replace the BASIC and C language.

The common interface should be adopted in the optimization software to be universal and to facilitate the user, such as the I/O interface, the data files, and database.

The optimization technology seems not fashionable and not friendly. But if those problems above solved properly, the optimization software will be the essential part in CAD system for specialized machinery.

20.4 The Visualized Optimization and the Visualized Design

The essential process of optimization design in computer is a kind of random test directed by optimization theory or method. In optimization process, taking advantage of computer's highly computational power, the function of optimization theory or method is to reduce the number of test, both help to find the best solution for design. The programmer develops the software by analysis the physical model, builds up the numerical relationship between dimensions and performance and strain and stress, and then adopts computer optimization for a certain kind of machinery.

20.4.1 The Visualization for the Process and Result of the Optimization

If there is a set of program that can calculate the performance, strain, and stress, then an interactive process can be carry out, which change the parameter and check the constraint function right afterward, until a satisfactory result to be found. Actually that is a kind of optimization, a computer-aided manual optimization [2]. That is: to change the parameters interactively, to calculate the performance the strain and stress by computer at the same time, to evaluate the result by human being, then change the parameters again, until find a satisfactory result. There are parameters to be optimized, performances to be object functions, strain and stress to be constraint functions. Necessary elements for optimization are all here. The only difference here is the method, all the process of the optimization such as adjustment and evaluation is made under the interactive manual control. The result is also depending on the user's opinion and decision.

In mechanical optimization design, the result of optimization means a set of dimensions for a machine to be manufactured. To make the result sensible, the simulation technology is adopted according to the situation, the sketch of the machine's associated part is put on the screen to scale. This process can be regarded as the post-treatment of the optimization result, such as in the finite element analysis (FEA).

20.4.2 The Control of the Visual Optimization

For the process of the visual optimization to be controlled, a set of buttons are arranged on the interface of the software, then the parameters can be adjusted easily. There are a set of buttons to change the parameters, a set of text column to display the numeric result, an area to show the picture of the structure. Interface forms of the software integrated with the calculation model forms the visual optimization software [1]. This software is convenient to use, sensible to the result, and what you see is what you get.

20.4.3 The Purpose of Visual Optimization

Of course, for a computer-aided manual optimization, the speed of visual optimization is slow. Due to the complex dimension system and the hidden relationship between parameters and functions, to determine all the parameters manually is difficult too. So, the visual optimization could be used as the post-treatment after the numerical optimization, to get rid of the shortcoming for traditional optimization. For the complex of the programming, the key to realize the visual optimization is that it limits the field to certain kind machine with fixed structure, and then, the problem can be reduced, the algorithm will be realized easily.

20.5 The Visual Optimization Used in CAD Software for Overhead Crane

When an overhead crane is to be designed, the main parameters are the height of the beam, the width of the beam, the thickness for every plate, etc. These parameters will affect the strain and stress of the crane. The total weight of the crane, the outline of the crane, the passage access, the manufacturability, is also related to those parameters.

For the further perfect result, an elementary result can be done by traditional optimization. Put this elementary result on the screen in a picture form according to scale, show the weight, strain and stress at the same time, and then the outline and performance of the crane are clear. Defining a set of buttons aside, the parameters of the crane can be changed easily by mouse, and the change can be reflected on the screen meanwhile. Thus, the designer can chose the model he likes easily. Figures 20.1 and 20.2 show the main beam section and checking interface in the software.

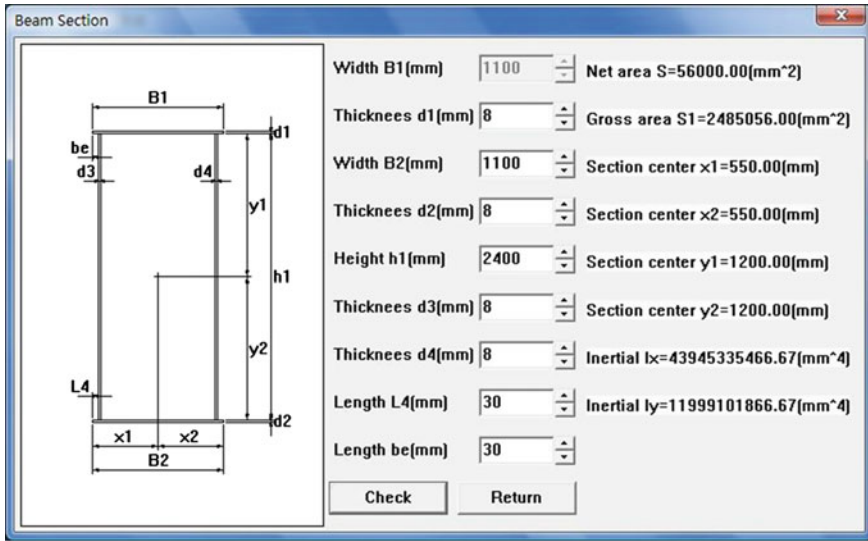
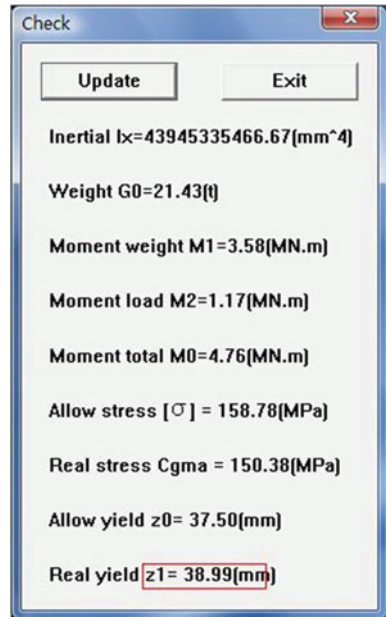


Fig. 20.1 Beam-section visual optimization

Fig. 20.2 Check interface



20.6 Conclusion

It will be the tendency for the optimization design software to be design focused, applied for specialized machinery, user-oriented, automatized, visualized. What user need is the kind of software, which can be easily used, adjustable and controllable. Only this kind of optimization software can give the designer the maximum free space for design, to make the design work go from “have to” to “want to.” This kind of demand can only be met by developing the specialized optimization software for certain kind of machinery. Visualization is a common tendency for software. Although the property of “what you see is what you get” appeared early in the filed of office automation, it is also needed in the field of computer-aided design. The visualization is concerned with the emulation, the simulation, and the modeling, is also the base of virtual design.

The adjustments and checking calculations have to be done and repeated all the time, so it is a hardwork to do the design by hand. The result of the traditional optimization is not sensible, cannot be controlled, and has nothing to do with the designer’s experience. With visualized optimization, experience of the designer can be fully considered. The process of the visualized optimization is similar to the design process by hand, so the dimension of existing serial product can be inherited, the environment of production, etc., can be think over, the process is used to the designer of the plant, it is a delightful technology, the potential of development is great [2].

The optimization plays an important part in the modern design methods. The potential application for visualized optimization in the specialized machinery is satisfactory. Only in this way, the optimization design technology can be the practical and useful methods and tools for engineer.

Acknowledgment This work is supported by the reform project for postgraduate student No. 20102034, from Shanxi Provincial Education Department.

References

1. Tao Y, Gao C, Zhai J (1999) The key-controlled optimization for the double beam gantry crane. ICMH/ICFP’99, Shanghai, p 227
2. Tao Y, Xie W (2007) Development of visualization CAD software for hoisting mechanism of crane. Hoisting Conveying Mach 12:35 (in Chinese)

Chapter 21

Design of the Special Spreader of Super-Tonnage Crane

Jiong Zhao, Xiaolei Xiong, Wenjun Li and Yujun Hu

Abstract A kind of special spreaders of super-tonnage crane are studied and designed, which are used for lifting large-scale tower equipments. As a very key component or bearing of the crane, the design of the special spreader is in the pursuit of the rationalization and the lightweight of the structure on the premise of ensuring high security. Studying and analyzing the mechanical characteristics and the actual working conditions of the tower equipment, using Solid Works to build the parametric model and importing the image into the ANSYS Workbench for the finite element analysis which is based on the traditional mechanical design, a comprehensive scheme combining the traditional design and the parametric modeling and finite element design is proposed. Finally, take the spreader of the 2,500-t ring crane as an example, which proves the feasibility of the design concept and the design process. Also, it provides a theoretical basis and design method for the design of similar projects.

Keywords The spreader of super-tonnage crane · Force analysis · Finite element analysis · Structural design

With the rapid development of China's oil refining and petrochemical industry, especially in the field of large-scale tower tanks used as the core petrochemical equipment of unit operation for stripping, distillation, extraction, absorption, flash [1], which is now trending toward large scale. The characteristics of these tower equipments are with large weight, high altitude, complex structure, high slenderness ratio, poor stability, and strict requirements for installation.

The early domestic lifting method of petrochemical equipment adopted the mast and hoist. However, in terms of overall lifting for oversized, overweight, and overtop petrochemical equipments, the capacity of early lifting is far from enough. The liter weight and the lifting height of hydraulic synchronization

J. Zhao (✉) · X. Xiong · W. Li · Y. Hu
College of Mechanical Engineering, Tongji University, Shanghai 201804, China
e-mail: jiong.zhao@tongji.edu.cn

© Springer-Verlag Berlin Heidelberg 2015
Logistics Engineering Institution, CMES (ed.),
Proceedings of China Modern Logistics Engineering,
Lecture Notes in Electrical Engineering 286, DOI 10.1007/978-3-662-44674-4_21

217

lifting technology are unrestricted. This technology is steady, safe, and reliable. Hydraulic synchronization lifting technology has a clearly advantage especially in overall lifting of huge equipment [2].

Spreader as a core component in one crane is used for connecting the lifting system and the liter heavy. The pros and cons of the design of spreader have impact on the security and economy of the entire crane directly [3]. Especially for large and high tower equipment, it is necessary to design spreader in specially according to the force analysis of lifted equipment during lifting process and the structural characteristics of lifted equipment. This paper aims at the design of the dedicated spreader, combining the traditional design and the finite element design concept, which provides a reference for similar engineering projects.

21.1 Design Process of Dedicated Spreader

The design process of the dedicated spreader for large tower equipment can draw on part of the structure of previous products and concepts. This paper presents a design process as Fig. 21.1. Firstly, analyze the force state of tower equipment accurately

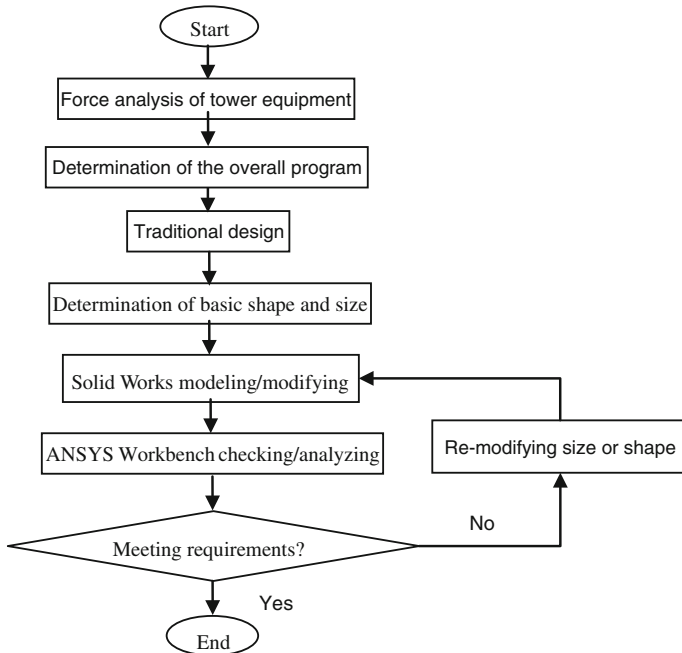


Fig. 21.1 Design process of dedicated spreader

and specifically during the lifting. Secondly, refer to the structure of traditional spreader and then determine the shape of the dedicated spreader, which provides clear design tasks and requirements for the following detailed design steps. This step is critical and essential. On the basis of the above, adapting traditional design methods, theoretical experience, and related manuals to complete the preliminary design of the various components and the corresponding structure size [4]. Then, apply Solid Works to do parametric modeling of the various components and import the model into ANSYS Workbench for finite element analysis. If the analysis result shows that the structure does not meet the requirements of stiffness or strength, the model will be returned back to Solid Works to re-modify the shape or size and then re-imported into ANSYS Workbench for another finite element analysis until the result meets the requirements. The design process combines the traditional design and the finite element analysis together, which not only double guarantees the components satisfy the design requirements such as strength and stiffness, but also make up the shortcoming that the traditional design cannot provide the accurate calculation of intensity or the stress of dangerous points of the components [5, 6]. At the same time, it gives a comprehensive understanding of the practical performance of the spreader at the design stage, reduces the production cycle, and improves production efficiency.

21.2 Force Analysis of the Lifting of Tower Equipment

As for lifting large tower equipment, if a crane is used as the main one and another two cranes are slipped at the tail of the tower equipment, it will occur to be instability when the gravity vertical line of the entire tower exceeds the vertical lifting slipped tail rope during the rise of the tower equipment. Therefore, usually choosing one main crane and one slipped crane is suitable as shown in Fig. 21.2.

Main crane is connected with the upper lifting lug of tower equipment, while another crane is slipped at the tail. In the following, it will analyze the theoretical force of the equipment from the horizontal position of the ground gradually rising to the vertical position. Figure 21.3 shows the force analysis of the tower in the lifting process.

Figure 21.3 shows as follows: F_Z : the main crane capacity force; F_L : the slipped crane capacity force; G : the weight of the tower; L_1 : the distance from main lug to the center of gravity; L_2 : the distance from slipped tail to the center of gravity; R : the radius of the equipment; α : the angle between the centerline and F_Z . Relationships are listed as follows according to the tower force balance and moment equilibrium.

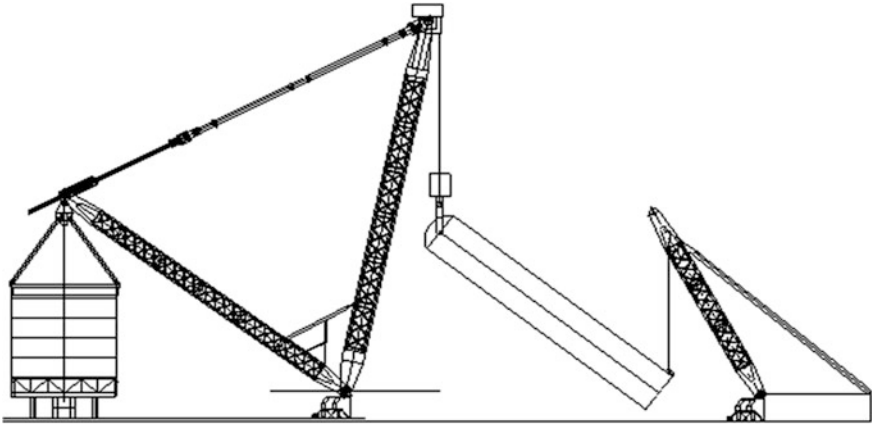


Fig. 21.2 Schematic diagram of lifting tower equipment

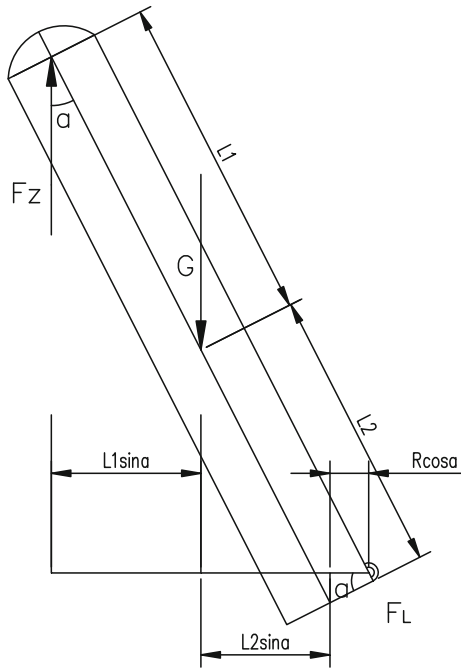


Fig. 21.3 Force analysis of tower equipment

$$F_Z + F_L = G \quad (21.1)$$

$$F_Z(L_1 \sin a + L_2 \sin a + R \cos a) = G(L_2 \sin a + R \cos a) \quad (21.2)$$

$$\Rightarrow F_Z = G \frac{L_2 \sin a + R \cos a}{L_1 \sin a + L_2 \sin a + R \cos a} = G \frac{L_2 \tan a + R}{(L_1 + L_2) \tan a + R} \quad (21.3)$$

$$\Rightarrow F_L = G \frac{L_1 \tan a}{(L_1 + L_2) \tan a + R} = G \frac{L_1}{(L_1 + L_2) + R \cot a}. \quad (21.4)$$

As $a \in [0 \pi/2]$, $y = \cot a$ is a monotonically decreasing function, while $F_L = GL_1/(L_1 + L_2 + R \cot a)$ is a monotonically increasing function. That means the slipped crane capacity force F_L will increase with a . On the contrary, $F_Z = G - F_L$ is a monotonically decreasing function, i.e., the main crane capacity force F_Z will decrease with a .

At the time $a = \pi/2$ when the tower equipment is in the horizontal lifting position and $F_Z = GL_2/(L_1 + L_2)$, $F_L = GL_1/(L_1 + L_2)$, the slipped crane capacity force F_L reaches the maximum. While at the time $a = 0$ when the tower equipment is in the vertical position, $F_Z = G$, $F_L = 0$, i.e., the slipped crane capacity force F_L is close to zero, and main crane capacity force F_Z is the maximum which is equal to the weight of the equipment.

21.3 Determination of the Overall Program

Strand through the upper part of the special spreader of tower equipment is connected with cluster hydraulic synchronization lifter. Thus, the form of the spreader's upper part is according to the layout design of hydraulic lifters on the platform. The lifters can be distributed in a row as Chinese word “—” or like a polygon such as four points. The design of the pattern of the through-holes for fixing strand can refer to the distribution of hydraulic lifters. The bottom of spreader is generally linked with the equipment-lifting lug instead of fixing the tower equipment directly. Equipment-lifting lug is a kind of special component made up of metal plates or fittings to be convenient for the easy connection of rigging or spreader. It is welded on containers, tower equipment, or other structural parts [7]. Therefore, the bottom can be designed into a through-hole and fix the equipment-lifting lug in pin roll method which is increasingly becoming one of the most preferred connection methods in large tonnage cranes. Spreader's middle part can be a triangulation twisted branch board or a U-shaped structure for connecting the upper and the bottom. And usually, pin connection is still the first choice of connecting among different parts. Compared to the structure of traditional hook, this kind of dedicated spreader' structure is not only more compact, simpler processing, but also carrying greater loads.

21.4 Analysis of an Example

Ring rail crane is one of new types of over large cranes, especially suitable for the overall lifting of overweight and ultrahigh tower equipment. Its superiority reflects on the aspects of the substantial increase of weight, the convenience of the container transitions, high stability, and low development cost. Next, take 2,500-t ring rail crane as the example to explore the research and development of the design of large tonnage crane's spreader.

21.4.1 Force Analysis

The force analysis of tower equipment can refer to Fig. 21.3. According to the derivation of the formula (21.3), when the equipment is close to the upright position at the time $a = 0$, $F_Z = G$ namely the main crane capacity force F_Z is equal to the weight of the equipment.

G includes the weight of the tower equipment and steel strands. Considering lifting dynamic load factor ϕ_2 and comprehensive working conditions, ϕ_2 is taken as 1.05 and the weight of tower equipment is taken as 2,564 t, steel strands as 44 t. As followings:

$$F_Z = \phi_2 G = 1.05 \times (2,564 + 44) \times 9.806 \times 1,000 = 2.6853 \times 10^7 \text{ N} \quad (21.5)$$

21.4.1.1 Determination of the Initial Program

The initial program is as shown in Fig. 21.4. 2,500-t ring rail crane has a total of four hydraulic lifters which correspond with the four small connectors with the steel strands. Four small connectors are arranged in parallel as Chinese word "one" type. Strands pass through the corresponding small connectors on the upper of the spreader with supporting anchorage fixing at the bottom of the small connector. Four small cutter support plates connect pin rolls and four small connectors. So pin rolls and large connectors are connected by two large cutter support plates. The ring spreader passes through the middle through-hole of large connector from the bottom to the up connected with a large nut, which is inserted with an aligning thrust bearing inside. Retaining rings are used at the shaft end of small connectors, pin rolls, and large connectors to prevent axial movement. The overall structure of this special spreader presents a gradual contraction from the up to the down, which is compact, smooth, and complying with the characteristics of the actual lifting force.

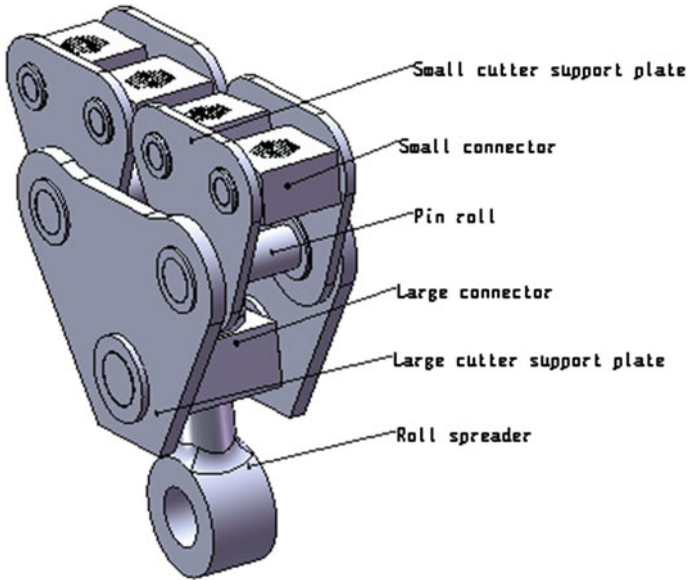


Fig. 21.4 The model diagram of the spreader of 2,500-t ring rail crane

21.4.1.2 Traditional Design and Finite Analysis

Design of Ring Spreader

The ring spreader selects forged steel DG34Cr2Ni2Mo with yield stress $\sigma_s = 687$ MPa [8]. The tentative size parameters are as follows: annual ring diameter $d = 550$ mm, outer diameter $D = 1,100$ mm, length $\delta = 800$ mm; boom diameter $d_1 = 545$ mm.

The check of boom’s tensile stress is as follows:

$$\sigma = \frac{F_z}{\frac{\pi}{4}d_1^2} = 115 \text{ MPa} \leq [\sigma] = \frac{\sigma_s}{5} = 137.4 \text{ MPa} \quad (21.6)$$

The horizontal section of annual ring is dangerous. The check of its maximum medial stress [9] is as follows: Including: $R = 412.5$ mm and $h = 275$ mm, K is a cross-sectional shape factor.

$$K = \frac{R}{h} \cdot \ln \frac{2R + h}{2r - h} - 1 = 0.0397 \quad (21.7)$$

The maximum medial stress of the horizontal section:

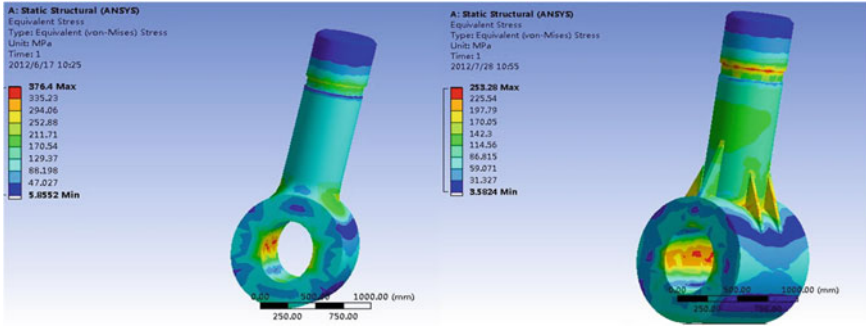


Fig. 21.5 The stress cloud diagram of initial program and of modified program

$$\begin{aligned}
 \sigma_n^b &= \frac{F_z}{h \cdot \delta} \left[0.405 + \frac{0.095}{K} \times \frac{h}{2R - h} \right] = \frac{2.6853 \times 10^7}{275 \times 800} \left(0.405 + \frac{0.095}{0.0397} \times \frac{275}{550} \right) \\
 &= 194.5 \text{ MPa} \langle [\sigma] \rangle = \frac{\sigma_s}{2.5} = 274.8 \text{ MPa}
 \end{aligned}
 \tag{21.8}$$

The check of the traditional design meets the requirements. In order to examine the overall security in the actual operating conditions, the finite element for specific analysis must be taken. Imposing loads and constraints on the model and selecting mesh element size of 100, the stress cloud result is shown as Fig. 21.5 on the left. The figure shows the distribution of the medial stress of the horizontal section is too concentrated, which is verified with the actual situation. But the maximum stress 376.4 MPa is greater than allowable stress 274.8 MPa. Therefore, the design of the structure does not satisfy with the requirements and has to be re-modified.

The fact is that the medial stress of the horizontal section is too concentrated, and the annual ring’s diameter and out diameter have already been great enough. It is not suitable to make the diameter or out diameter greater to let the maximum stress below the allowable stress. Also, the cross-sectional shape factor K should not be changed. Thus, the length δ is made to increase from 800 to 1,000 mm. At the same time, 40-mm-thick ribs boards are added on the connector between the boom and the annual ring to improve the local strength. Solid Works is applied to modify its structure and parametric dimensions for re-modeling. Then, the new model is imported into ANSYS Workbench for a new finite element analysis. The result is as shown in Fig. 21.5 on the right side. The maximum stress value is still on the predicted position and less than the allowable stress 274.8 MPa. The distribution of overall stress is almost uniform, and the change gradient of stress is not obvious, which means there is no large area of low stress region and the material utilization rate is high [10]. Thus, the new design of the structural is

reasonable. If only the traditional design method is adopted, each performance will be known until the trial is completed. When the structure of the trial is not qualified, the size parameters and shape have to be modified for a further optimization of the structure, which not only leads to a high cost, but also extends the design cycle.

Large and Small Connector

Large connector selects forged steel DG34Cr2Ni2Mo with yield stress $\sigma_s = 687$ MPa. There is a through-hole in the middle of it for connecting ring spreader with nut. The tentative size parameters are as follows: the axial end diameter $d = 450$ mm, the width of the rectangular section $B = 1,100$ mm, the height of intermediate section $h = 600$ mm, the distance from the axial end of the beam to the force point $l_1 = 1,370$ mm, and the distance from the square cross section to the force point $l_2 = 90$ mm.

The middle section is dangerous. The check of bending stress is as follows:

$$\left[\sigma = \frac{M}{W} = \frac{1.5F_Z l_1}{(B-d)h^2} \right] = \frac{1.5 \times 2.6853 \times 10^7 \times 1,370}{(1,100 - 450) \times 600^2} = 235 \text{ MPa} \leq [\sigma] \quad (21.9)$$

$$= \frac{\sigma_s}{2.5} = 274.8 \text{ MPa}$$

The check of the maximum bending stress of the axial end is as follows:

$$\sigma = \frac{M}{W} = \frac{\frac{F_z}{2} \times l_2}{\frac{\pi d^3}{32}} = \frac{\frac{2.6853 \times 10^7}{2} \times 90}{\frac{3.14 \times 450^3}{32}} = 135.2 \text{ MPa} \leq [\sigma] \quad (21.10)$$

$$= \frac{\sigma_s}{2.5} = 274.8 \text{ MPa}$$

Small connector selects forged steel DG34Cr2Ni2Mo with yield stress $\sigma_s = 687$ MPa. The tentative size parameters are as follows: the axial end diameter $d = 250$ mm, the width of the rectangular section $B = 700$ mm, the height of intermediate section $h = 500$ mm, the distance from the axial end of the beam to the force point is $l_1 = 940$ mm, and the distance from the square cross section to the force point is $l_2 = 75$ mm.

The middle section is dangerous. The check of bending stress is as follows:

$$\sigma = \frac{M}{W} = \frac{\frac{F_z}{8} \times \frac{l_1}{2}}{\frac{B}{6} h^2} = \frac{\frac{2.6853 \times 10^7}{8} \times \frac{940}{2}}{\frac{700}{6} \times 500^2} = 54 \text{ MPa} \leq [\sigma] = 274.8 \text{ MPa} \quad (21.11)$$

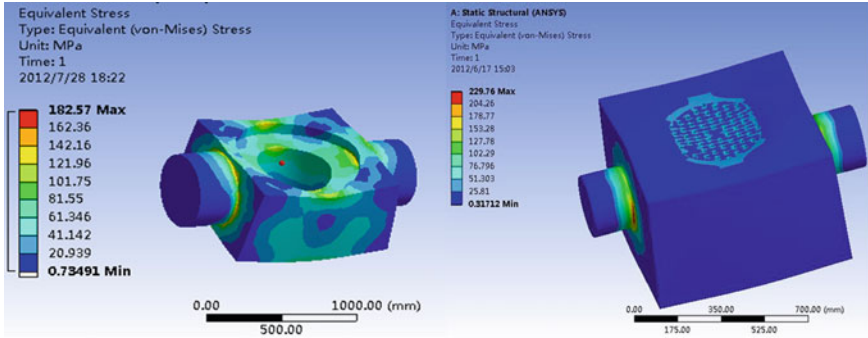


Fig. 21.6 The stress cloud diagram of large connector and small connector

The check of the maximum bending stress of the axial end is as follows:

$$\sigma = \frac{M}{W} = \frac{\frac{F_z}{8} \times l_2}{\frac{\pi d^3}{32}} = \frac{\frac{2.6853 \times 10^7}{8} \times 75}{\frac{3.14 \times 250^3}{32}} = 164.2 \text{ MPa} \leq [\sigma] = \frac{\sigma_s}{2.5} = 274.8 \text{ MPa} \tag{21.12}$$

The results of large connector and small connector can be seen in Fig. 21.6 which show both of their maximum stresses are less than allowable stresses. The designs are qualified.

Large and Small Cutter Support Plate

Large cutter support plate selects high-strength structural steel S690Q with yield stress $\sigma_s = 630 \text{ MPa}$. The tentative size parameters are as follows: the thickness of the plate $\delta = 150 \text{ mm}$, reinforcing earrings at two sides of the plate $\delta' = 65 \text{ mm}$, and the cross-sectional shape parameter $R = 412.5 \text{ mm}$ and $h = 375 \text{ mm}$.

$$K = \frac{R}{h} \cdot \ln \frac{2R + h}{2R - h} - 1 = 0.079 \tag{21.13}$$

The maximum medial stress of the horizontal section:

$$\begin{aligned} \sigma_n^b &= \frac{\frac{F_z}{2}}{h \cdot (\delta + 2\delta')} \left(0.405 + \frac{0.095}{K} \times \frac{h}{2R - h} \right) = 179.9 \text{ MPa} \langle [\sigma] \rangle = \frac{\sigma_s}{2.5} \\ &= 252 \text{ MPa} \end{aligned} \tag{21.14}$$

While small cutter support plate selects high-strength structural steel S690Q with yield stress $\sigma_s = 630 \text{ MPa}$. The tentative size parameters are as follows: the thickness of the plate $\delta = 100 \text{ mm}$, reinforcing earrings at two sides of the plate

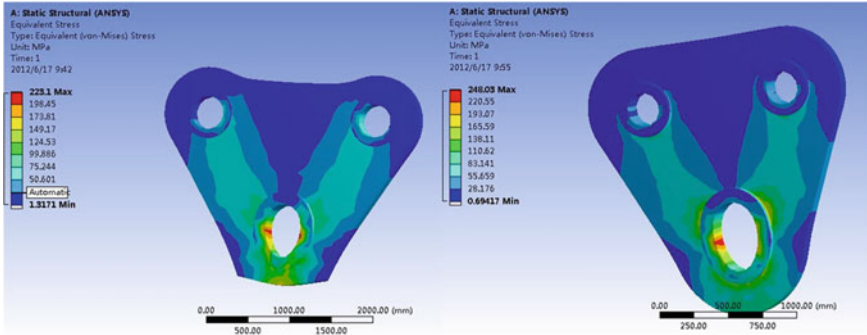


Fig. 21.7 The stress cloud diagram of large and small cutter support plate

$\delta' = 40$ mm, and the cross-sectional shape parameter $R = 312.5$ mm and $h = 275$ mm.

$$K = \frac{R}{h} \cdot \ln \frac{2R + h}{2R - h} - 1 = 0.073 \tag{21.15}$$

The maximum medial stress of the horizontal section:

$$\begin{aligned} \sigma_n^b &= \frac{\frac{F_z}{4}}{h \cdot (\delta + 2\delta')} \left(0.045 + \frac{0.095}{K} \times \frac{h}{2R - h} \right) = 193.6 \text{ MPa} \langle [\sigma] \rangle = \frac{\sigma_s}{2.5} \\ &= 252 \text{ MPa} \end{aligned} \tag{21.16}$$

The results of large and small cutter support plates are shown in Fig. 21.7. Both of their maximum stresses are less than allowable stresses. Thus, the design meets the requirement.

21.5 Conclusion

This paper proposes a set of design process of dedicated spreader of large-scale crane aiming at oversized tower equipment, including the research of actual mechanical characteristics of the equipment, the exploration of how to confirm the structure program of this kind of dedicated spreader, and the combination of traditional design and finite element analysis. Take this process as the reference and the spreader of 2500-t ring rail crane as the example. Explicitly the actual force situation and determine the structure of the spreader to undertake the traditional mechanics checking. Then, parametric modeling and finite element analysis of the structure of the various parts are taken. The structures that are not qualified with the strength or stiffness requirements have to be re-modified the shape or parameters until they meet the design requirements, which provide the basis for the security

and reliability. It completes the seamless connectivity of design, modeling, analysis, and improvement, which reduce the cycle time and improve productivity greatly. It is believed that the design method and process will get a wide range of applications and be learned by designers of other dedicated spreaders of large tower equipments.

References

1. Lin-jiang Yang (2011) Installation of tower equipment of large petrochemical plant. *Petrochemical Constr* 05:63–66
2. Sun AP, Yan YJ, Geng JT, Xei LQ (2007) Optimization and application of large-scale equipment installation plan. *Coal Technol* 24(5):155–158
3. Zhang CW, Lu GF (2010) Research on the optimization design of shaped hook. *Mech Res Appl* 5:15–18
4. Zhang H, He ZQ, Chen HY (2009) Parametric design and finite analysis of special spreader of large-scale equipment. *Hoisting Conveying Mach* 6:60–64
5. Bao JH, Pan ZW, Bao W (2007) Optimization design of HFCG120 roller press rack. *Mech Des* 24(5):63–65
6. Zhao WQ (2004) Stress analysis of several key points of large equipment lifting. In: 2004 seminar proceedings of national project construction industry and technology of large-scale lifting equipment market. Petrochemical Construction Publishing, Hebei, pp 54–58
7. Pan WJ (2009) The design and acceptance of the lug of heavy lifting equipment. *Petrol Eng Const* 35(3):49–51
8. Zhang ZW, Yu HQi, Wang JN (1998) Crane design manual. China Railway Press, Beijing
9. Wang JN, Yu LF (2002) The lifting transport aircraft metal structures. China Railway Press, Beijing
10. Zhang J, Zhou KS, Mao XD (2010) Vertical container support bearing design based on ANSYS. *Process Equip* 47(2):1–4

Chapter 22

Research of Crane Parametric Collaborative Design Platform

Zongyan Wang, Fen Yang, Jian Zhao, Jian Li
and Rongbin Zhai

Abstract Aim to figure out information exchange redundancy, centralized serial solving low-efficiency problems of the intricacy product design process, based on the intensive considering the mechanism of intricacy product task decomposition and communication mechanism of networked collaborative design, a distributed parallel-driven collaborative design way based on message information module was raised, the submission method of multi-user dynamic data, heterogeneous mechanism of network space, and time sequence was studied, a parametric collaborative design process platform based on multi-client single server multi-workstation (MCSSMW) for multi-user was set up. United with features of the high level of comparability of the large intricacy ladle crane structure, parametric variant design technology was introduced and the ladle crane parametric collaborative design system for multi-user was exploited. Finally, a trolley frame was taken as an example to be validated.

Keywords Ladle crane · Integrated designing platform · Parametric design · Trolley frame

22.1 Introduction

To compete in the increasingly fierce market development of mechanical products tend to be faster, better, updated design pattern. Currently promoted by rapid development technologies of 3D modeling information, network and database, traditional waterfall serial development mode of large-sized complex products transform to direction of parallel, digital, intelligent. Combined with inter-organization synergy, distributed collaborative team and design resources range charac-

Z. Wang (✉) · F. Yang · J. Zhao · J. Li · R. Zhai
School of Mechanical and Power Engineering, North University of China,
Taiyuan 030051, China
e-mail: iamwangzongyan@sina.com

teristics of the modern enterprise organization, the research of large-sized and complex product has become a product across time, space, the research focus in the field of multidisciplinary design. Introduce parametric design technology into high-degree structure-type curing and much similar products makes the design more feasible.

At present, domestic and foreign scholars have do many researches on the networked collaborative design and parametric design and made a lot of achievements.

Literature [1, 2] proposes a service-oriented, open cooperative design platform for solving the complex product design process information, resources sharing, and integration problems; literature [3, 4] puts forward a collaborative design system based on SORCER for complex products, and the structure of the system and engineering software tools package and integration for service method was given; literature [5] communicates design information based on product information model; literature [6] realizes the remote collaborative design based on parametric layout model based on parametric layout model; literature [7] describes structure model, process model, and integrated model of foreign heterogeneous distributed collaborative design structure model; literature [8] achieves multi-user real-time condition more collaborative design combining with parametric design technology through the user interaction forms; literature [9] studies product modeling and parameter transfer structure supporting variant design method; literature [10] realizes joint driving of the product three-dimensional parametric model based on hierarchical data table, combining hierarchical data table technology. However, on the whole, the study on networked collaborative design process research is not deep enough, problems are as follows:

1. Low-level design process information sharing, slow transfer speed, and many are static information;
2. Various network collaborative design platform and collaborative interaction types, hard to provide a general method to construct;
3. More single mode of operation and concentrated solution, less distributed and parallel driving solving-related research;
4. Network collaborative design and parametric design are not combined organically.

According to the deficiency, based on the developed ladle crane digital design platform oriented to multi-user, working mode “client /server /workstation” (multi-client single server multi-workstation, referred to as MCSSMW) was put forward, the real-time communication tools to assist the development of the Message information module was put forward, parametric collaborative design model based on distributed parallel drive solving method was constructed. Ladle crane trolley frames design process as an example, decompose it on the layer, divide the parameter class, submitted real-time design parameters, complete automated integrated design of parametric model driven, parametric finite element analysis, and product drawing generation.

22.2 Parametric Collaborative Design Process

Distributed modular design The different areas of expertise knowledge, which was related to different aspects of a complex product design problem, were not able to be mastered by a single designer. Therefore, it could be solved by people or institutions with the core competitiveness in different subjects. To definite a complex product design, according to the principle of Quality Function Deployment (QFD), product function could be decomposed into a series of modular subproblem under the driving of customers demand. For instance, metal structure, which was in different models, levels, weight, and in different span, has higher similarity, while each component of it has an independent function. According to the independence principle of the function and structure and “products—components—sub-components” model, it could be decomposed into bridge, accessory structure, small frame, and some other subproblems as shown in Fig. 22.1.

According to the principle that each module has similarity, module interface (interface sketch, interface size) of every subset problems was designed and was coded in accordance with the established encoding rules. Each module represented a part of the design problem; the common problem was solved through public programs, and the particular problem was solved by compiling a special program. The operation and the management to the internal data were conducted in an interactive method. Each design module was shared by a shared product information model, communication, and interaction of product information that were realized.

Parametric design Parametric design took the geometric relationship constraint, dimension constraint, structural feature constraint as technology foundation, including the 3D model that came from the updating of the series of three-dimensional model had similar, whose active size was modified directly, as well as

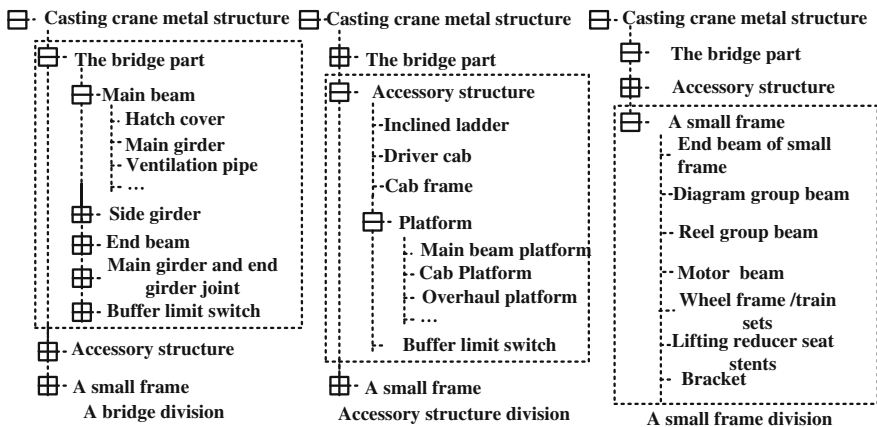


Fig. 22.1 Ladle crane metal structure module

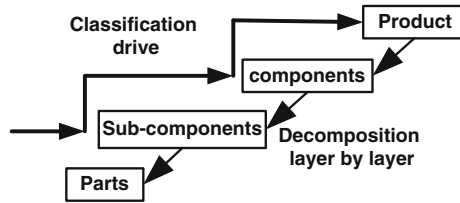


Fig. 22.2 Drive principle

the other driven dimension being modified indirectly, and the finite element analysis checking that had the same parameter with three-dimensional model, such as view scale, position, size, number, BOM notes, tables, and other related information of the engineering drawings updating automatically and optimized adjustment, was related to three-dimensional parametric model and process information statistics. Following step-by-step modeling, symmetrical modeling, template maximization principle, by using top-down and bottom-up combined layout sketch assembly method, established the holographic parametric template; all the geometric and non-geometric information were characterization dynamically by parameter. Based on decomposing layer-by-layer principle and classified driving principle, as shown in Fig. 22.2, namely according to product decomposition levels, with “part—sub-components—components—products” order, product-level parametric variant design was achieved.

Net-based Collaborative design platform Net-based collaborative design refers to that design personnel distributed in different place, in wide area network environment, based on the computer in virtual collaborative environment, orbiting a same product design task, assumed corresponding design tasks, completed the design task in a paralleled, interactive, collaborative method. The platform constructing was related to parallel working process of user, user access control, and conflict resolution solution, its topological structure as shown in Fig. 22.3. The paralleled and interactive work of multiple users was supported which relied on the platform; new products could be designed by user independently, parts parameter could be submitted, and the design tasks could be completed directly through the platform. The server stored the data, product documentation, kept real-time reception and data maintaining, and data could be updated synchronously, and well-arranged work everything in good order. Parametric model driven, finite element analysis, and optimization adjustment of engineering drawing checking process took longer, and had a large amount of calculation, was the bottleneck of the design process. In order to eliminate the bottleneck point, platform set multiple workstations to carrying the parallel calculation work based on the same database and the same electronic warehouse, to project as the unit, allocated the task to requesting workstation free. Then the workstation acquired the task in real time according to its operational capacity, once the task execution was completed, idle workstations

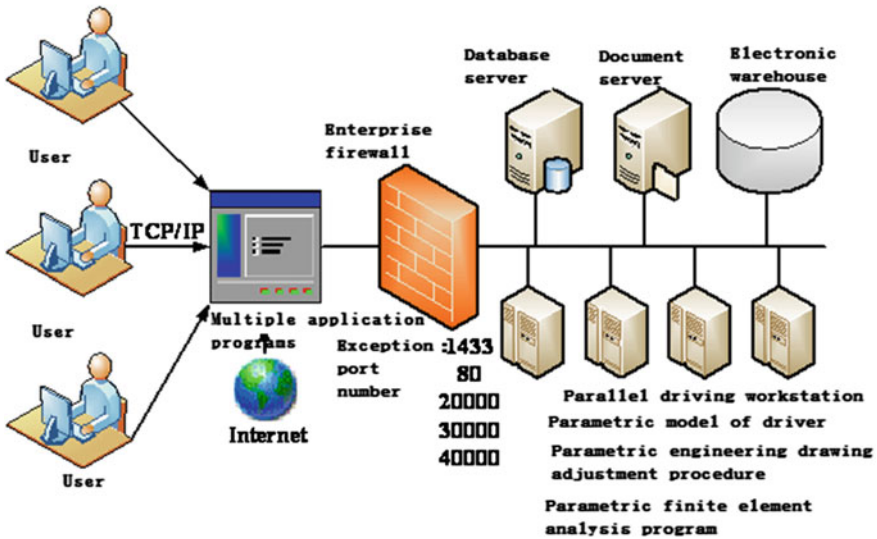


Fig. 22.3 Network collaborative design platform topology

might appear, then, reallocating the incomplete task automatically, multiple workstations real-time request and parallel driving working condition was realized. Finally, the product documentation was checked into the electronic warehouse.

22.3 Composition of the Distributed Parallel Driving Environment

The architecture of the operation environment Based on the client /server (Client/Server, C/S) architecture applications, with strong transaction processing and data processing capability, data consistency, integrity, and confidentiality is higher, but with the different hardware and the constant change of project members, the C/S network structure’s adaptability is poor, which cannot satisfy the requirement of this kind of change; the client is greatly simplified to a certain extent based on Browser /server (Browser/Server, B/S) network architecture; a Web browser can act as client’s role, but it has great difficulties in the completion of the project management, permission assignment, role enactment, task division, and other complex tasks. A three-layer system structure with hybrid network model is put forward as shown in Fig. 22.4 in combination with the respective advantages of B/S and C/S, which concludes a support layer, a functional layer, and user layer in turn.

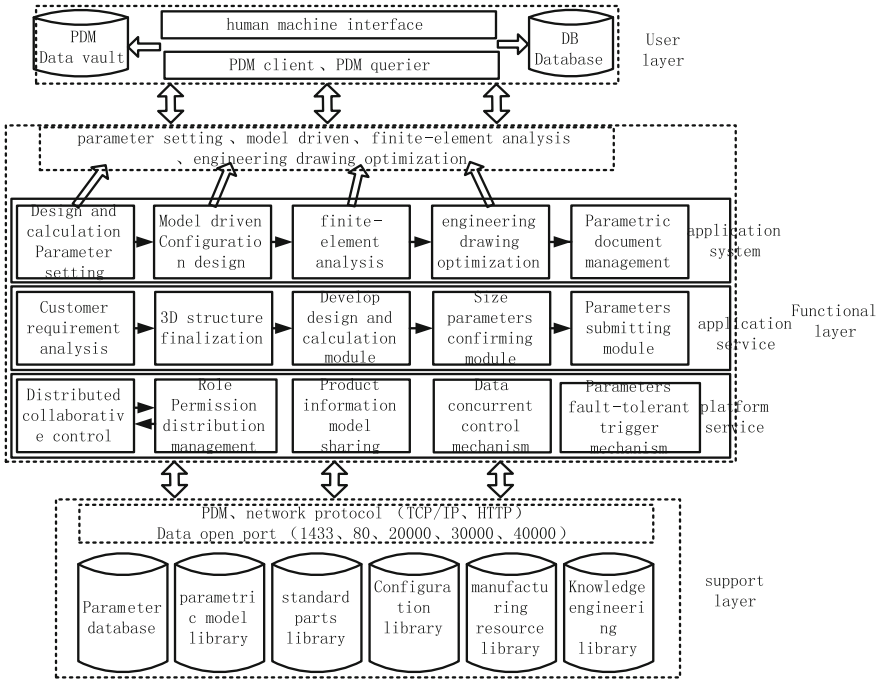


Fig. 22.4 The architecture of the operation environment

1. Supporting layer

Combin C/S and B/S two kinds of network architecture, base on PDM system, follow the TCP/IP, HTTP protocol, open SQL Server’s server port 1433 and PDM communication data interchange port 80,20000,30000,40000. Building integrated design platform bottom database, which including product data parameters database, parametric models library (model templates and the engineering drawing templates), standard parts and common parts library, modular configuration design library (similarity matching), the enterprise manufacturing resource library ,and the design standard and experience knowledge engineering library.

2. The functional layer

The functional layer is constituted by application service layer and application system layer. Taking platform service layer as foundation, distributed collaborative control mechanism is responsible for the customer communication and information interaction transmission, role rights management module assign roles and task to users, product information model sharing guarantee information synchronization for different users in the design process, data concurrency control mechanism confirm the consistency and effectiveness of parameter table data, and parameter fault-tolerant mechanism activate the rationality of the parameters submitted under

real-time monitoring. Taking the application service layer as the core, converting the parameters that customer needed to product model structural ones, confirming the product structure model reasonably, writing design and calculate program according to the existing codes, and standards to ensure the reliability of the parameters source, submitting the parameters to the data server by program. Taking application system layer as output terminal, interacting directly with user layer as its display form, design calculation and parameter setting module form the man-machine interactive platform, model driven and configuration design complete the update of new products model, finite element analysis module verify and evaluate the effectiveness of output results, drawing optimization and adjustment module complete the post-process of engineering drawing to ensure its standardization and practicality, parametric document management module take project as unit to manage document information based on PDM thought.

3. The user layer

User layer is the ultimate form of integrated design platform. User can submit design parameter to data server by man-machine interactive interface, which has good user information tips and can realize semi-automatic operation. Parametric design documents can be checked in data vault by Checkin module, which has established version scheme and total life cycle solution. User can review the document through the PDM client or PDM access device.

Information interaction based on the Message module Through the secondary development of Message information module, information sharing and mutual communication is realize, work instructions is delivered smoothly, instructions or information flow is shown in Fig. 22.5. Specific communication mechanism is as follows:

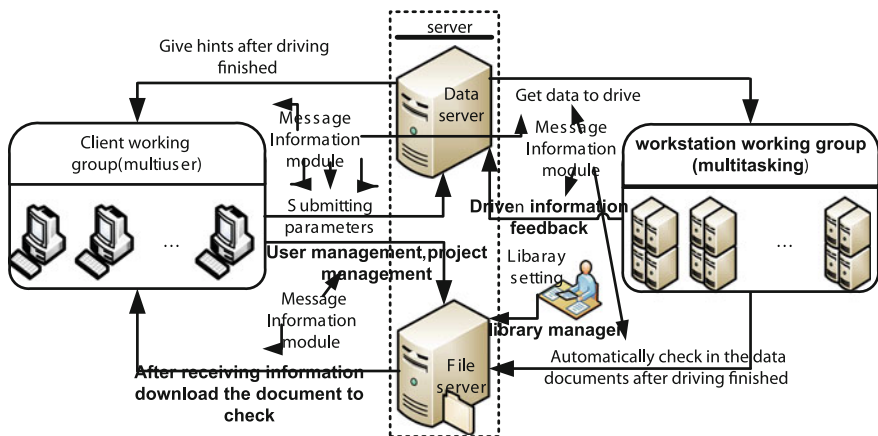


Fig. 22.5 Information communication mechanism based on Message module

Collaborative team members complete their components' parameter setting, design calculation, and finite element analysis setting in client working group through parameter setting program and submit design parameters to the database server; database server receives real-time data and updates the components reference table status value. Work group in workstation iterate through the change of project status table's characteristic value, activate program running according to the established condition to carry parametric model driven, parametric finite element analysis, engineering drawing adjustment and optimization, process information statistics, and other tasks such as generating product data files (3D model, engineering drawing, BOM, process information table, analysis report, etc.), which are checked in data vault of file server by Checkin module. Parameter table's information field values of the corresponding parts have changed at this time, and product data files have been generated and uploaded to the file server. Designer consult or checkout product data files which they have authority by PDMWW client, modify and update the files. Client working groups are responsible for the product data submission and document revision and review; the server is mainly in charge of product data storage and maintenance, product document management and transfer information and work instruction; workstations take charge of the parametric model driven, parametric finite element analysis and engineering drawing optimization and adjustment, generate required models and engineering drawings and check them in file server.

22.4 Parametric Collaborative Design Process Frame Model

Based on the above design ideas, to a certain type of four of the crane beam four rail casting metal structure for preliminary basis module, by use of object-oriented development tools Visual Basic 6.0, SolidWorks 2011 as three-dimensional design platform, MS Access2007, SQL Server 2000 as the database management software, three-layer architecture with a hybrid network model as a framework, built "multiple clients /single server /multi-workstation" (MCSSMW) into a working model of multi-user-oriented ladle crane parametric collaborative design model. Mainly it includes four functional modules: Role permissions distribution, structure design, parametric design, and database management, as shown in Fig. 22.6. Each of its introductions is as follows:

Role permission distribution module It supports multiple users of networked collaborative design platform and provides for the operation of the unit to project file access control—reading and writing; subprojects can obtain the appropriate permissions from the parent group, and users of the system have only one or some of the items as readable, writable, or read–write permissions; at the same time, they can have the same access to design the collaborative team with one-time operation privileges; all authorized operation is limited to a database administrator

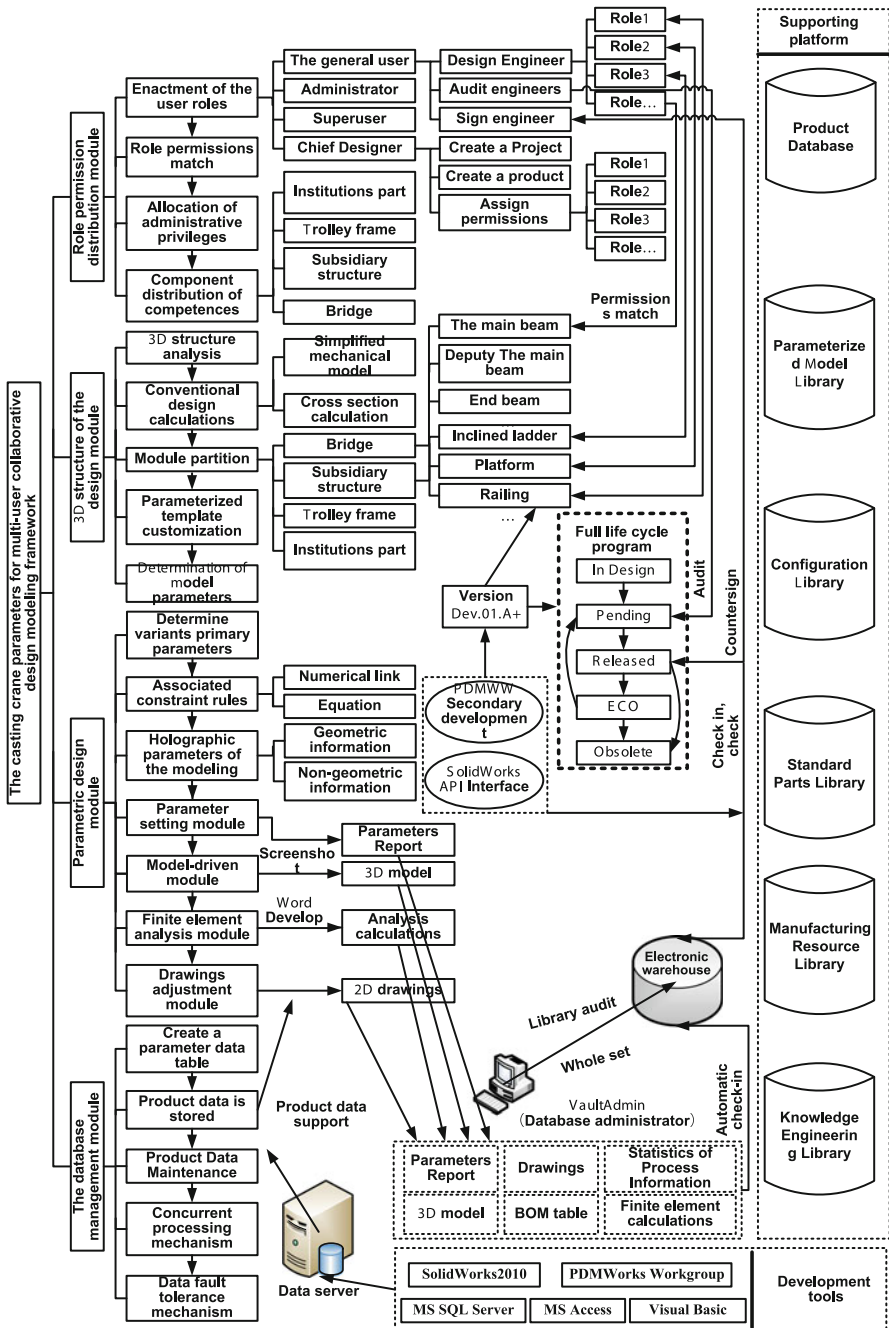


Fig. 22.6 Model framework of the ladle crane parameter collaborative design for multi-user

pdmwadmin. On this basis, the development of client-oriented group ladle crane design platform for users will be divided into general users, chief designer, system administrators, super users, and different user types with different permissions. According to the product, components are further subdivided collaborative team members design authority; according to the different icons to distinguish, the design engineer has the authority to operate. The different roles of users with different types of operating authority, director of the new project, with designers design personnel as the design task allocation of the starting point.

Three-dimensional structure design module Customer demand-driven basis, according to the industry's existing design standards and design experience, combined with the demand of enterprises, make detailed analysis of the product function modules. Functional modules to the product structure of the mapping based on the principle of quality function deployment (QFD); methods and principles in accordance with the module partition, ladle crane metal structure is divided into multi-level module, defined interfaces between modules; based on the template to the principle of maximizing, using the layout sketch assembly and dynamic holographic model to establish the parameters of the model templates and drawing template; preparation of key components designs calculation program (strength, stiffness calculation). In the Visual Basic 6.0, compiler environment establishes the calculating object man-machine interface, making the background design calculation procedure, the various calculation constants, formula, and some experience are the parameters characterizing and written to the design and calculation module. Collaborative team members according to the graphical interface to dynamically update the design parameters table (component parameters table, system data sheet, etc.), to issue commands to the workstation.

Parametric design module Based on the template drawings, rational division of parts of the parameter level (primary parameter, secondary parameters) as well as the master-slave relationship and determine the reasonable range of parameter variations and structural changes in space. Constraint relations between the whole and the parts associated with the size and dimensions of transmission direction; add a holographic model of the geometrical information and non-geometry information, and associated with drawings; customized parameter settings interface (man-machine interface) and add the two-dimensional, three-dimensional dynamic preview function, used to dynamically submit the design parameters; develop parametric program, parameterized finite element analysis program (command stream documentation, product data import, export the results of the analysis, generate calculations, etc.) and drawings optimal adjustment program (view position adjustment, view scale adjustment, dimensional position adjustment, part reference adjustment, annotation class adjustment, vacant content deletion, etc.) generate a new model and its finite element analysis check of the same parameters, check results to determine whether to proceed with the optimization and adjustment of engineering drawings, reasonable tuning plot, otherwise re-submit or modify the design parameters; product data documentation by Checkin module checks into the electronic warehouse, conduct version control, and lifecycle management.

Database management module With MS SQL Server 2000 and MS Access 2007 for database management software, all product data parameters, standard parts parameter table, process information statistics table, finite element analysis parameter table, and design knowledge are stored in the same server database HRCraneDB_2011 and are related to the functional modules of data connection such as create data tables, database backup and recovery, data concurrent processing, data fault tolerance, and disaster recovery. In order to avoid misunderstanding, misuse written, incomplete and inconsistent data, to take the transaction, and the lock mechanism to control, the user read and write access to the database.

22.5 Application of Engineering

Taking a certain type of four beams and four-railed ladle crane trolley frame design process as an example, briefly describe multi-user-oriented ladle crane parametric collaborative design system in mechanical product development application. The trolley frame runs on main beam rail of the bridge through the trolley or wheel frame. According to the weight coefficient organization project of task, distribution the team work, configure working environment, and hardware facilities, members communicate from each other through Message information module. Creating different projects and products in different basic parameters for boundaries, make project as unit organization design task, design task subdivide to the part assigns to team members through the role permission settings module, take an example, A is responsible for parameters of the trolley frame assembly, B is responsible for the design the end beam of trolley frame, C responsible for design the fixed pulley group beam, D for the drum group, E for the electrical beam, F for the operation mechanism bracket, a wheel frame, a lifting reducer base, G is responsible for vetting, H for the sign, and so on.

Dynamically, setting trolley frame's assembly size and each component's position size through the client group, each sub component reads the superior size according to the main parameter list and set their detailed size, then submits parameters to their respective lists, such as tb_Main_T, whose parameter setting interface is shown in Fig. 22.7. At the same time, define related parameters (material, unit type, mesh pattern, etc.) for the finite element analysis and store them in the corresponding lists. Traverse project status table and component parameter table real time give instructions to the idle workstations, assign tasks to each workstation reasonably, complete drive operation tasks concurrently including the generation of new 3D model, which is shown in Fig. 22.8, and conduct the finite element analysis, decide if it is necessary to optimize the engineering drawing and check product documentation in PDM data vault.

Fig. 22.7 Trolley frame assembly parameter setting interface

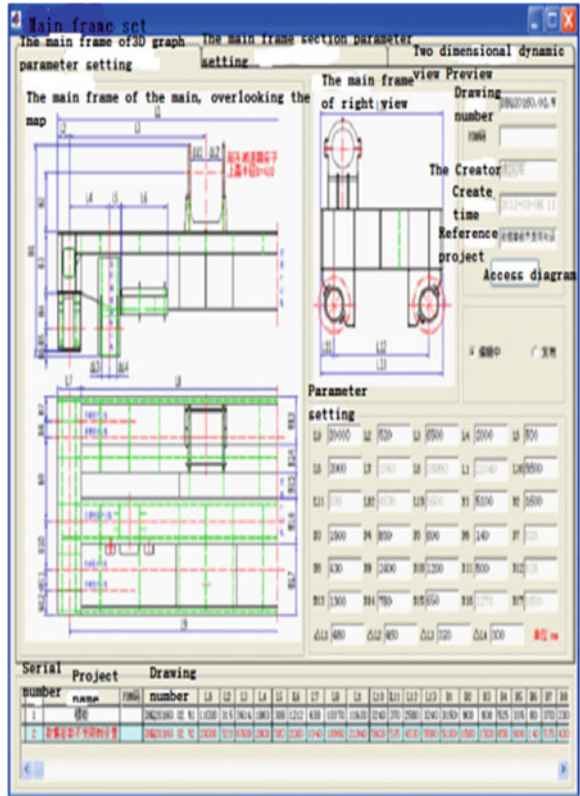
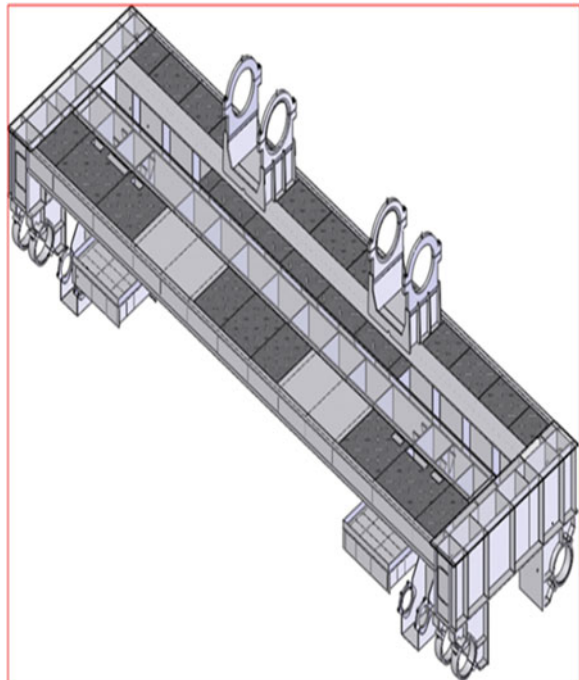


Fig. 22.8 Trolley frame assembly after driven



22.6 Conclusions

In this paper, distributed modular design and parametric design were combined with Net-based collaborative design methods; organically, it presented MCSSMW architecture, which is a hybrid network model. Based on Message information module, parametric collaborative design process model was built, which oriented multiple users and distributed parallel driving. According to the characteristics of the ladle crane structure having a higher solidifying degree is the development of the multiple user-oriented ladle crane parametric collaborative design system. Relying on the system, the “parameter—calculation and design—submitted model driven—finite element analysis check—drawings optimization adjustment” integrated design can be achieved. The application of this method can improve the crane product design efficiency more than three times significantly.

References

1. He DJ, Song X, Wang Q (2011) Method for complex product collaborative design based on cloud service. *Comput Integr Manuf Syst* 11(3):533–539 (in Chinese)
2. De-yu ZQQ (2011) Service-oriented collaborative design platform for cloud manufacturing. *J S Chin Univ Technol (Nat Sci Edn)* 39(11):75–81 (in Chinese)
3. Sobolewski M, Kolonay RM (2006) Federated grid computing with interactive service-oriented programming. *Int J Concurrent Eng: Res Appl* 14:55–66
4. Jia-qing YU, Jian-zhong CHA, Yi-ping LU et al (2010) Distributed collaborative design system for complex product. *J Central S Univ (Sci Technol)* 41(2):539–545 (in Chinese)
5. Hong-Chao X et al (2002) Collaborative designing method of distributed modularization. *J Mach Des* 05:7–10 (in Chinese)
6. Bai YW, Chen ZN, Bin HZ, Hua J (2005) Collaborative design based on product layout feature. *Univ Sci Tech (Nat Sci Edn)* 33(1):68–70
7. McDowell DL, Panchal HJ, Choi HJ et al (2010) Distributed collaborative design frameworks. *Integr Des Multiscale*, 313–349
8. Yong ZRZ (2005) Quick cooperative design with customized cad functions embedded in web pages. *J Comput Aided Des Comput Graph* 17(11):2570–2574
9. Wu Q, Zong C, Zhang Q et al (2008) Research on variant design and parameter transfer method for complicated products. *Chin Mech Eng* 19(22):2955–2960
10. Liang WWTRH et al (2005) Research and realization on the variant design of mechanical products based on parametric techniques. *Chin Mech Eng* 16(3):218–222

Chapter 23

Mechanical Performance of Crane's Main Girders with Corrugated Webs

Guo-qian Wei, Hai-tao Dong, Yue Li and Qin Fan

Abstract Girder with corrugated webs is a new form of structure with better performance and of high potential in crane's metal structure. Firstly, the mechanical performance of this kind of structure was investigated qualitatively by the conventional bending beam theory. It showed that the strength and stiffness of girders with corrugated webs is lower than those with flat webs which are of similar sizes. Due to the great advantage in the shear performance, the height of the girder with corrugated webs can be increased properly to make up the decrease of its strength and stiffness, and thus, the design requirements can be met. Then, FEA method was utilized to simulate the mechanical properties of both middle-rail and bias-rail box girder with corrugated webs, and the above conclusion was validated. The result of FEA also indicated that the flange's bending behavior of the box girder with corrugated webs was much more complicated. Hence, not only the overall bending stress but also the transverse bending stress should be considered in the design.

Keywords Corrugated web · Main girder · Crane · Mechanical performance

23.1 Introduction

Girder with corrugated webs is a new form of structure. Since its corrugated webs can only bear little bending moment and axial force, it seldom meets the instability problem under the pressure and the bending. This kind of structure can easily break the conventional limitation about the webs' wideness–thickness ratio to obtain components with better bending resistance, larger webs' height, and smaller webs' thickness [1]. From this point of view, it is feasible to employ this kind of structure in crane's main girders.

G. Wei (✉) · H. Dong · Y. Li · Q. Fan
Mechanical & Electronic Engineering Institute, WUST, Wuhan 430081, China
e-mail: weiguoqian@wust.edu.cn

In fact, this kind of component had been ever adopted as the crane's metal structure in our country in a small range in the last century. And in the early 1980, the former First Machinery Industry Department conducted a series of experiments on cranes with corrugated web structure [2]. The experiment object was a 2-t crane with corrugated web jib. The thickness of the corrugated webs was 3 mm instead of 6 mm which is the commonly used thickness in the flat webs structure. All the stiffened ribs to prevent webs losing their stability were canceled. Static loading test, dynamic loading test, and fatigue failure test were all included in the experiment. The result showed that the practical capacity of corrugated web girders was larger than the theoretical calculating value. The stability of the girder was also greatly improved. However, due to the limitations of manufacturing processing and its devices, corrugated web girders have not been recognized and utilized widely in crane's metal structure in China since then.

In the new century, manufacturing and processing technology of metal structure develops rapidly. There are some developed technologies and equipments such as mold pressing and rolling pressing which can be used to produce corrugated webs. Therefore, corrugated web girders have obtained attentions from the crane industry again. In 2005, Chi [3] utilized FEM to simulate the mechanical behavior of the main girder with corrugated webs under typical crane loads. The results showed that the box girder with one corrugated web and one flat web was a better form for crane's main girders. It was proposed in this literature that the Von Mises stress in the main girders with corrugated webs can be reduced 50 % to the structure with double flat webs under the same conditions. But the detailed mechanical performances of the corrugated webs and up- and low-cover plates did not mentioned in it. In order to promote the employment of the corrugated web structure in the crane's metal structure, mechanical performances of the main girders with corrugated webs for the overhead bridge crane were systematically investigated in this paper.

23.2 Comparison of the Basic Mechanical Performance

23.2.1 *Mechanical Model of the Overhead Bridge Crane's Main Girder*

Figure 23.1 shows the typical loads and the boundary conditions of the overhead bridge crane's main girders, where S is the span of overhead bridge crane, P is a movable concentrated force which describes the load-lifting capacity and the weight of the trolley, q is a distributed load which describes the weight of the main girder, G_S is a fixed concentrated force which describes the weight of the driver's cab, and other loads also can be simplified to these three types.

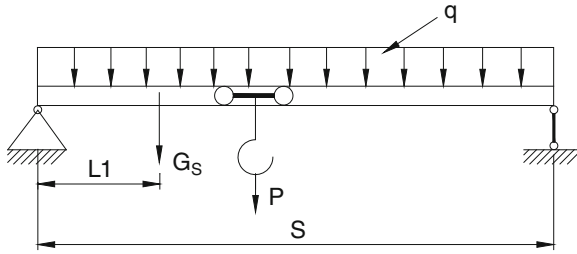


Fig. 23.1 Typical loads and boundary conditions of the overhead bridge crane's main girders

23.2.2 Basic Calculating Method

As a supporting structure, the crane's main girder mainly bears the bending moment and the shear force. Generally, it needs to satisfy the requirements of 3S (Strength, stiffness, and stability) in its design. Among them, the maximum bending normal stress is the main evaluation index of the strength. And the static stiffness, which is the vertical deflection of the mid-span section under the load-lifting capacity and the weight of the trolley, is the key parameter to describe the rigidity performance of the crane's main girders. Stability can be guaranteed by controlling the dimensions constraints and setting the internal stiffened plates, so it does not need special calculating.

According to the conventional bending beam theory, when P is located in the mid of the span, the bending moment at the middle cross section reaches the maximum, and the maximum bending normal stress appears on the outside surface of the cover plate. It can be expressed as,

$$\sigma_{\max} = \frac{M_{\max} \cdot h}{I} \tag{23.1}$$

where M_{\max} is the maximum bending moment, h is the distance from the neutral plane to the outside surface of the cover plate, and I is the inertia moment of the cross section.

Vertical static stiffness can be calculated by the following formula:

$$f_v = \frac{P \cdot S^3}{48EI} + \frac{5q \cdot S^4}{384EI} + \frac{P \cdot S}{4G'A_w} + \frac{q \cdot S^2}{8G'A_w} \tag{23.2}$$

Herein, G' is the shear modulus considered the influences of the corrugated webs, which is only about 10 % of the steel plate's shear modulus G .

23.2.3 3S Performance Analysis of the Girders with Corrugated Webs

As for the corrugated web girders, its corrugated web bears little bending moment, so the inertia moment of the webs can be neglected in formula (23.1). Thus, the inertia moment of the cross section of the corrugated web girder will be decreased, which will lead to the increase of the maximum bending normal stress. In formula (23.2), the first two parts are bending-induced deflection, while the other two parts are shear-induced deflection. Because it is thin webs that are commonly used as the corrugated webs, their shear deformation can not be neglected and their values will be more. So the corrugated web girders will have more vertical deflections than those of flat web girders under the same conditions. Based on this, the strength and stiffness performances of the corrugated web girders will actually be reduced under the same conditions.

However, present investigations show that the corrugated web girder has outstanding vertical stability, which will keep satisfying the girder's stability requirement while increasing its height. The inertia moment of the cross section will be increased with the increase of the height of girder. Then, the strength and stiffness performances of the girder will consequently be improved. From this point of view, corrugated web girders still have some degree of potentials in the design of the cranes' main girders.

23.3 Finite Element Method Analysis

23.3.1 Basic Parameters of Finite Element Model

According to the typical box main girder of a certain $32t \times 22.5$ m overhead bridge crane, three kinds of structure were designed. Some main parameters were chosen as followed: the height of the girder $H = 1,600$ mm, the thickness of the web $t = 6$ mm, the thickness of the upper and lower cover plate $\delta = 14$ mm, and the width of the upper and lower cover plate $B = 600$ mm. The detailed dimension parameters of the web's corrugated profile are referred to the No. 3 recommended profile in Technical Specification for Corrugated Web Steel Structure, as shown in Fig. 23.2. Three kinds of webs' configurations were listed in Table 23.1.

Quad elements were used to model the structure. The material is Q235, whose elasticity modulus $E = 2.06 \times 10^5$ MPa and Poisson's ratio $\mu = 0.3$. The boundary constraint was applied as the simply supported beam. A concentrated force $P = 20$ kN was applied in the middle of the span, which was under middle-rail form and bias-rail form, respectively. Figure 23.3 shows the typical finite element mesh of the three types.

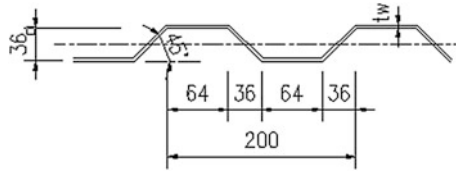


Fig. 23.2 Details of the corrugated profile

Table 23.1 Webs' configurations

Name	Description	Memo
G_FF	flat web + Flat web	Without internal stiffened plates
G_FFR	flat web + Flat web	With internal stiffened plates
G_FC	flat web + corrugated web	Without internal stiffened plates

23.3.2 The Bending Normal Stress Result and Its Analysis

23.3.2.1 Under Middle-Rail Form

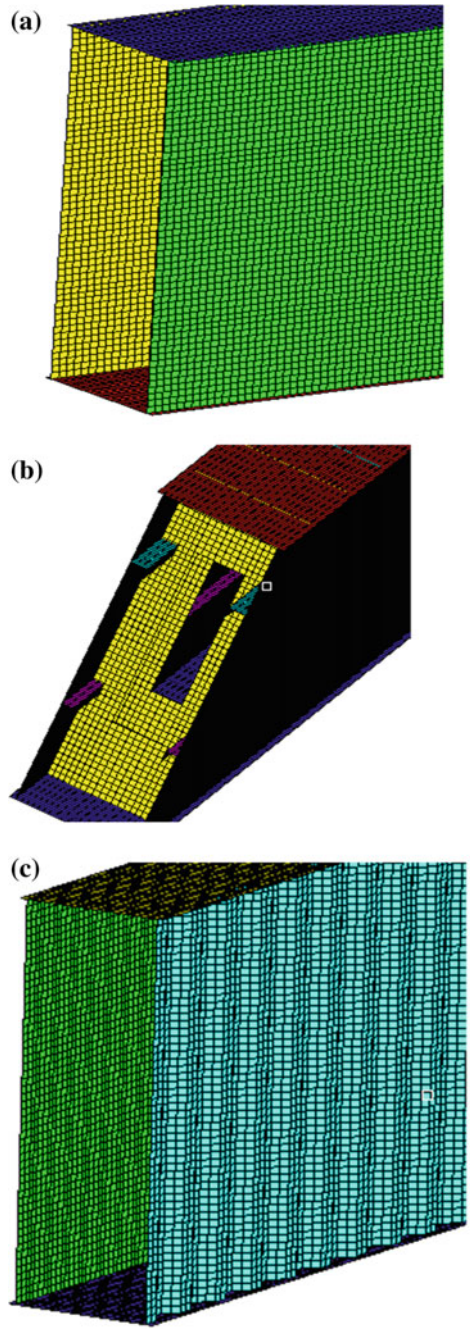
Figure 23.4 describes the distribution curves of the bending normal stress along three longitudinal lines on the lower cover plate under middle-rail form.

According to Fig. 23.4, when there are two flat webs in the main girder (G_FF Structure), the maximum bending normal stress about 60 MPa appears in the mid-span. The bending normal stress is uniform along the transverse direction, so three curves are essentially coincident. Whether using internal stiffened plates or not has a little influence on the value and distribution of the longitudinal bending normal stress on G_FF structure. Stress concentration phenomenon only happens in the small areas where stiffened plates set. In the middle of the span, bending normal stress reaches its maximum about 66 MPa.

When there are one flat web and one corrugated web in the main girder (G_FC Structure), the bending normal stress along the transverse direction varies obviously with the transverse location. On the side of the corrugated web, the bending normal stress increases greatly and appears obvious corrugated distribution form. Its maximum reaches 108 MPa. Bending normal stress also increases on the center line and its maximum reaches 74 MPa. On the side of the flat web, bending normal stress is approximately same as that of G_FF structure. The maximum is about 59 MPa with a larger affected area.

The above phenomena result from the property of corrugated webs barely bearing bending moment. So cover plate has to bear more bending moment on this side, which leads to bending normal stress increases obviously on this side.

Fig. 23.3 Typical finite element mesh **a** G_FF, **b** G_FFR, **c** G_FC



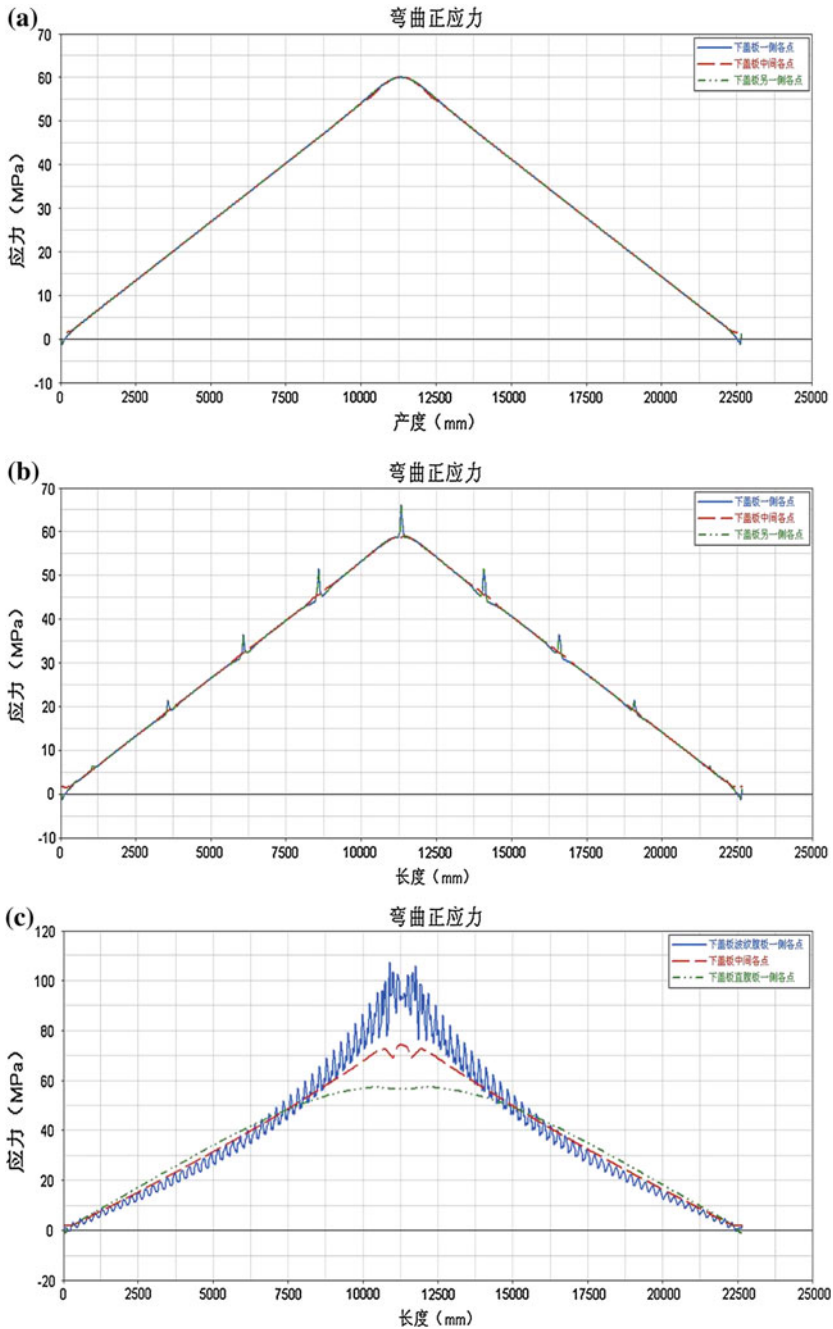


Fig. 23.4 Bending stress curves of the middle-rail box main girder along the lower cover plate's edge **a** G_FF, **b** G_FFR, **c** G_FC

23.3.2.2 Under Bias-Rail Form

Figure 23.5 describes the distribution curves of the bending normal stress along three longitudinal lines on the lower cover plate under bias-rail form. It is notable that the corrugated web in G_FC structure is the main web which bears the concentrated force.

From this figure, three bending normal stress curves along the longitudinal direction in G_FF structure are totally different. The maximum and minimum both appear on the side of the main web. The maximum reaches 94 MPa in the mid-span, while the minimum reaches -25 MPa at the end of the girder. Bending normal stress on the side of the auxiliary web varies a little gently and ranges from 22 to 30 MPa. On the center line, the bending normal stress has similar distribution to that under middle-rail form. And its value can be approximately looked as the mean value of that on both side curves. It means that the distribution of the bending normal stress along the transverse direction is linear and is mainly caused by the torsion of the girder.

In G_FFR structure, the bending normal stress distribution curve of the lower cover plate is similar to that under middle-rail form. It illustrates that internal stiffed plates have better effect on resisting the torsion. And box girders with internal stiffed plates can be suitable for both middle-rail form and bias-rail form.

In G_FC structure, three bending normal stress curves are also different, and its overall variation trend is similar to the G_FFR structure. The distribution curve on the center line is nearly same as that in the G_FFR structure. Bending normal stress on the side of the corrugated web is more than those in the other two lines and is also of corrugated distribution form. The maximum reaches 128 MPa. On the side of flat web, the bending normal stress decreases a little and is about 50 MPa in the middle of the span. The result shows that the corrugated web in G_FC structure can improve the torsion-resisting performance to some extent. However, it will lead to the decline of the bending-resisting performance.

23.3.3 Buckling Result and Its Analysis

The major advantage of corrugated webs lies in its higher compression-resisting performance. Web's stability can be guaranteed with increasing the girder's height. This paper employed eigenvalue method to verify this property. The buckling factors and their buckling modes were obtained. The buckling factors of the lowest order are shown in Table 23.2.

From Table 23.3, no matter middle-rail form or bias-rail form, the buckling factor of G_FF is the minimum, which means this kind of structure's stability is the worst. G_FFR structure has the best stability. It illustrates that the internal stiffed plates can greatly improve the stability of the box girder. The buckling factor of G_FC structure is between those of G_FF structure and G_FFR structure. It is worth noting that the buckling factors of G_FC structure are very close to those of

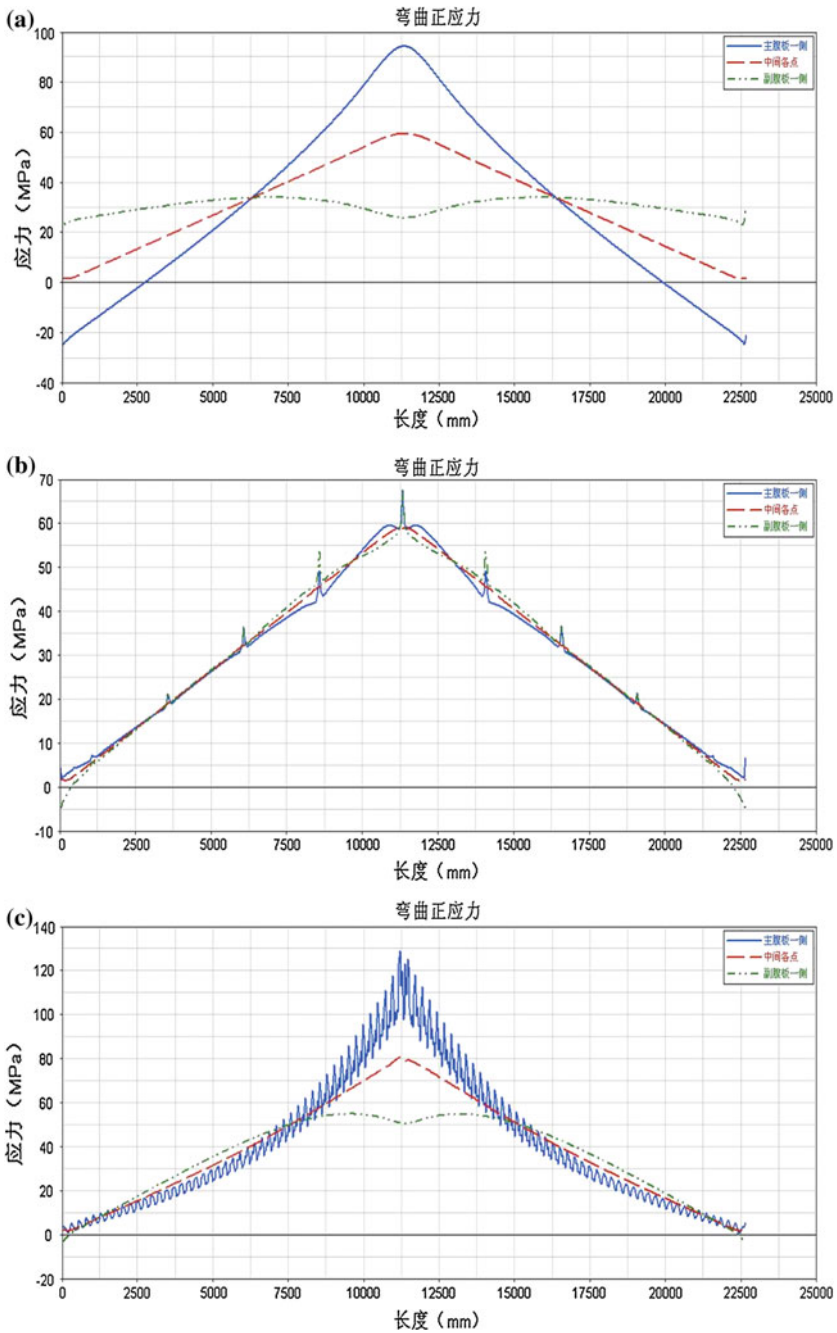


Fig. 23.5 Bending stress curves of the bias-rail box main girder along the lower cover plate's edge

Table 23.2 Buckling factor

Name	Middle-rail	Bias-rail
G_FF	1.2556	0.6895
G_FC	1.7148	1.8689
G_FFR	2.1863	1.9893

G_FFR structure under bias-rail form. It shows that they have very similar stability. In another word, the corrugated web can play a significant role in reinforcing the structures.

However, G_FC structure also has some other advantages. It can get rid of lots of internal stiffed plates and reduce some complicated welding process. The inner space of the girder can be enlarged so as to contain more components such as electrical cabinets. In addition, lots of internal stiffed plates in box girders are arranged crosswise. The stress concentration level of the attachment weld on these areas is rather higher. Getting rid of or decreasing these stiffed plates can change the weld joint detail and improve the corresponding stress concentration situation level. Then, the fatigue properties of the main girder will be effectively enhanced. From this point of view, main girders of corrugated webs have higher value.

23.4 Transverse Bending of the Cover Plate

The above FEA computation shows that corrugated webs can lead to obvious corrugated form for the bending normal stress along longitudinal direction of the box main girder's cover plate. The corrugated stress distribution will result in larger increment to the stress value. So, it cannot be ignored and has to be considered in the design.

Abbas proposed that this kind of stress increment was caused by cover plate's transverse bending. He took the I-shaped girder with corrugated web under in-plane load as the research object, carried on a systematic investigation on the flange's transverse bending problem [4, 5]. The results showed that the corrugated change of the web will lead to a local twist of the girder's cross section even if under the in-plane loads. This local twist makes flanges produce obvious transverse displacement, which will cause the flanges produce transverse bending moment and extra longitudinal normal stress. Based on this, Abbas put forward the following formula to calculate the bending strength for the corrugated structures.

$$\sigma_{\max} = \frac{M_{\max}}{W} + \frac{M_t}{W_t} \quad (23.3)$$

The first part in formula (23.3) is the girder's overall bending stress which can be solved by the conventional bending beam theory. The second part is the transverse bending normal stress which is caused by flange's transverse bending. It was discussed in detail in literature [4–6].

23.5 Conclusion

Based on above discussion, some conclusion can be drawn as follows:

1. According to the static strength and the static stiffness, corrugated web girders are no better than the traditional box girders with flat webs. Simply replacing flat web of the existing box girders to corrugated webs will only reduce their mechanical performance.
2. Box girder with one flat web and one corrugated web has advantages in its mechanical performance under the bias-rail form. However, the transverse bending of the cover plate should be considered in its design.
3. Box girder with corrugated webs has larger advantage in its material using efficiency, weld processing, and the fatigue behavior. These features are worth focusing on and deep research.

Acknowledgments This work is sponsored by the open fund of Research Center of Green Manufacturing and Energy-Saving and Emission Reduction Technology in Wuhan University of Science and Technology (B1003).

References

1. Guo Y, Zhang Q (2006) Design method of section bearing capacity of I-type member of corrugated web. *J Architect Civil Eng* 23(4):58–63
2. Crane's curve web girders research team of the First Machinery Industry Department (1972) Experiment study on the curve web girders of a 2t jib crane. *Hoisting Conveying Mach* 3 (3):35–63
3. Chi Y (2005) Research of corrugated-web structure and its finite element analysis. *Mach Des Manuf* 2(2):20–22
4. Abbas HH, Sause R, Driver RG (2006) Behavior of corrugated web I-girders under in-plane loads. *J Eng Mech* 132(8):806–814
5. Abbas HH, Sause R, Driver RG (2007) Analysis of flange transverse bending of corrugated web I-girders under in-plane loads. *J Struct Eng* 133(3):347–355
6. Wei G, Yu Z, Fan Q (2012) Research on flange transverse bending stress of corrugated web I-girders. *Mod Manuf Eng* 4(4):62–66

Chapter 24

The Electric Control Scheme of 2500t Ring Crane

Xiaolei Xiong, Jiong Zhao, Qicai Zhou and Li Zeng

Abstract This paper is based on the design of 2500t ring crane. Because of the high-reliability requirement of this crane, a design scheme of distributed control system based on CAN bus in huge crane is proposed. The author mainly introduces the composition and realization of the system, the design of data communications, and the design of monitoring and controlling function of host computer. This system can achieve coordinated distributed control in the actions of hosting, luffing, slewing, machine leveling, and tower head leveling of the crane. It can also collect and monitor the status information of the crane in real time.

Keywords Ring · Crane · Distributed control · CAN bus

24.1 Introduction

With the development of hoisting industry, the performance of crane, the efficiency of work, and transition and the benefits are required higher and higher. The ring crane is a new type of crane. Compared with traditional crawler cranes, the hoisting weight can be designed greatly large, the transition is convenient with containers, the cost can be controlled low, and the price is affordable. At present, some foreign hoisting companies have produced a series of such products, which have been used in engineering (Fig. 24.1).

The ring crane electric control system is composed by host computer and seven control subsystem constituting fieldbus network.

X. Xiong (✉) · J. Zhao · Q. Zhou · L. Zeng
College of Mechanical Engineering, Tongji University, Shanghai 201804, China
e-mail: gohigh@163.com

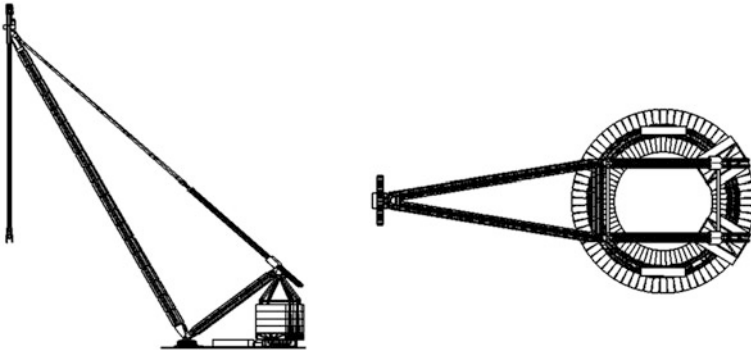


Fig. 24.1 Ring rail cranes diagram

24.2 System Composition

The ring crane is huge in scale, and the number of control mode is large. So, if the type of control system is centralization, the network will be too large, thereby reducing the real time and reliability of the control system. Distributed control network using CAN bus let subsystem perform their duties and produce its own control task, so that the host computer only needs to give the subsystem the command of handle and receive the status information from subsystem for the operator to know the crane working state.

CAN bus is short for control area network, which is a serial data communication protocol developed by Bosch corporation. CAN bus has the characteristics of low cost, far-distance transmission (up to 10 km), and high communication rate (up to 1 Mbps), which is widely used in the vehicle control system [1]. With CAN bus using in ring crane control system, the network can constitute a distributed control system and enhance the flexibility and reliability of the system.

As shown in Fig. 24.2, the host computer and seven subsystems constitute distributed CAN fieldbus network. The type of controllers is TTC60, which has two CAN2.0B interfaces [2] in which one is connected in the fieldbus and the other one is used as digital sensors and program downloading interface.

For ultra-large crane, the primary consideration of the lifting process must be safety and reliability, so the three major movements (hoisting, luffing, slewing) of the crane are designed interlocking. Interlocking information is sent to the fieldbus in the form of process data object (PDO). For example, when the hoisting system is lifting goods, the controller will send PDO, which includes interlock information to reset the luffing and slewing system so that the host computer cannot handle the luffing and slewing system.

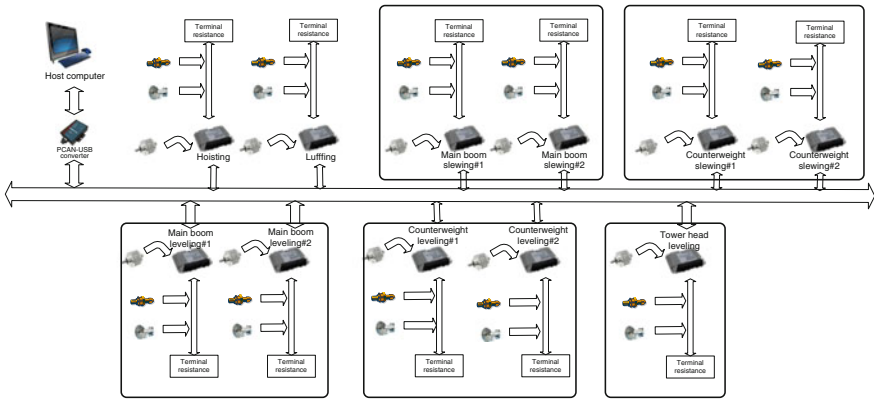


Fig. 24.2 Ring crane network frame

24.3 System Realization

Presently, take the main boom leveling system as an example of system realization process.

When the crane is working, the main boom needs to stand level to ensure the safety of the hoisting construction smooth, so the levelness needs to be adjusted in real time. Main boom leveling system is composed of eight hydraulic cylinder, hydraulic system, and control system, which are located at two walk sliders under the main boom. In each slider, one set of hydraulic pump station drives four hydraulic cylinders, supporting the main boom, and one controller drives four proportional directional valves, realizing the controlling of four hydraulic cylinders. In the two controllers, one is specified as the main controller. The host computer sends a leveling start data to the main controller, and then the function of leveling is completed by the cooperation between the two controllers of the main boom leveling system. When the crane produces certain tilt due to the uneven of foundation, the angle sensor on the intermediate balance beam and the walk sliders sends the angle values to controllers. Two controllers separately calculate their four hydraulic cylinders' height difference, and the main controller calculates the relative height difference of the two sliders. Then, the main controller judges the state of crane and selects the reference of leveling plane and reference cylinder. The proportional directional valve opening quantity is calculated through PI arithmetic and sent to the sub-controller through network by the main controller. Two controllers, respectively, output current to control proportional directional valve open, make leveling benchmark cylinder action, and other cylinders following until the crane returns even status. The process is completely finished by cooperation between the two controllers, and the host computer just sends start command and receives state messages from the bus (Fig. 24.3).

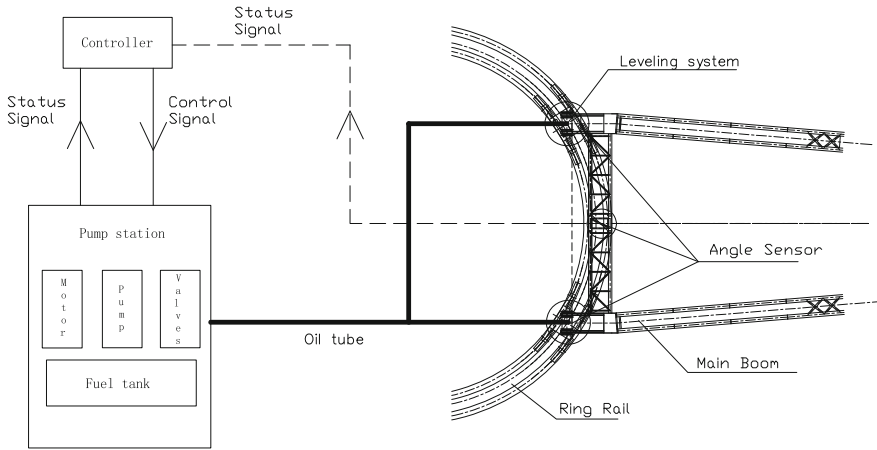


Fig. 24.3 Main boom leveling system schematic diagram

24.4 Communication Protocol Design

24.4.1 Standard Frame and Extended Frame Selection

CAN2.0B has two different frame formats: standard frame and the expansion frame, the former for 11 bits of identifier and the latter for 29 bits. Considering that overall control functions of the crane are not too much but as the real-time requirement is the higher, select standard frame in ring crane electric control system. The communication rate is relatively higher, which has less bytes so that it can better meet the requirement of real-time system [3] (Table 24.1).

Table 24.1 CAN 2.0B standard frame format

	7	6	5	4	3	2	1	0
Byte 1	FF	RTR	×	×	DLC (data length)			
Byte 2	(Identifier) ID.28-ID.21							
Byte 3	ID.20-ID.18			×	×	×	×	×
Byte 4	Data 1							
Byte 5	Data 2							
Byte 6	Data 3							
Byte 7	Data 4							
Byte 8	Data 5							
Byte 9	Data 6							
Byte 10	Data 7							
Byte 11	Data 8							

24.4.2 Identifier Assignment

The CAN2.0B standard frame specification only defines the frame structure, but undefined the meaning of the 11 bits of identifier, so users can define the 11 bits by themselves according to the real system. According to the definition of ID identifier definition rule in CANopen, the 11 bits of identifier in the ring crane control system can be defined in the way of 7 low bits for source node ID and 4 high bits for message function code. The message defined rules are shown in Table 24.2. The function code allocation is shown in Table 24.3.

24.4.3 Communication Table Establishment

To make the data on the bus identified by control nodes, a communication list that covers the meaning of each byte in the frame must be created. As shown in Table 24.4 for part communication list of slewing node, when host computer sends the message of ID 281H, each node will be testing the ID of message. If the ID is the same with setting ID, the node will accept the message so that realizing the communication among nodes.

24.4.4 CAN Communication Program

As shown in the code, firstly declare the variable `can_ret` to receive the return value of `can_read ()` function. Secondly, define `aRxCANFrames_0` as the type of `T_can_frame` that is a kind of data structure in the library. `Hr_00` is the handle of

Table 24.2 Message defined rules

	node ID 1	node ID 2	node ID 3	...	node ID 15
PDO 1(tx)	0 × 181	0 × 182	0 × 183	...	0 × 18E
PDO 2(tx)	0 × 281	0 × 282	0 × 283	...	0 × 28E
PDO 3(tx)	0 × 381	0 × 383	0 × 383	...	0 × 38E
PDO 4(tx)	0 × 481	0 × 482	0 × 483	...	0 × 48E

Table 24.3 Function code allocation

Function code	Frame type	4 high bits of ID
1	Failure warning	0001
2	Action command	0010
3	Parameter setting message	0011
4	Status message	0100

Table 24.4 Slewing node PDO-ID: 281

Byte	Data	Meaning	Unit	Comments
BYTE0	automatic/manual	Automatic/Manual	NC	0/1
BYTE1	steer	Slewing direction	NC	0/1
BYTE2	angle_rotate	Slewing angle low byte	°	
BYTE3	angle_rotate	Slewing angle high byte	°	
BYTE4	speed_rotate	Slewing rate	m/h	

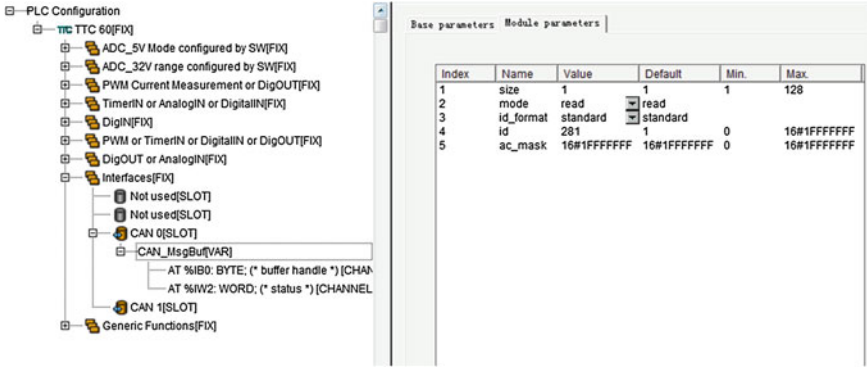


Fig. 24.4 Configuration of receiving message

CAN receiving frame. The PDO-ID is configured in software and downloaded into controller as Fig. 24.4 shows (Tables 24.5, 24.6).

24.5 Monitoring and Controlling Function Design

The host computer is located in the driver cab, which is 100 m far from the hoisting construction site. A PCAN-USB converter connects the host computer and the CAN network. The working process is: firstly opening the communication port,

Table 24.5 PDO receiving

VAR	Variable declaration: receiving data structures
can_ret:WORD;	
aRxCANFrames_0:t_can_frame;	
frames_received_0:BYTE;	
END_VAR	
can_ret:=can_read(hr_00,ADR(aRxCAN-Frames_0),1,ADR(frames_received_0));	Program part: resolve the slewing rate from data structure
speed_rotate:=BYTE_TO_UINT(aRxCANFrames_0.data[4]);	

Table 24.6 PDO sending

<pre>VAR can_ret: WORD; init_can_0_tx: BOOL; aTxCANFrames_0: t_can_frame; END_VAR</pre>	<p>Variable declaration:</p>
<pre>IF init_can_0_tx THEN aTxCANFrames_0.id_format :=0; aTxCANFrames_0.id:=16#483; aTxCANFrames_0.length:=8; init_can_0_tx:=FALSE; END_IF aTxCANFrames_0.data[0]:=hz_cylinder_pre_1_in; aTxCANFrames_0.data[1]:=hz_cylinder_pre_1_out; aTxCANFrames_0.data[2]:=hz_cylinder_pre_2_in; aTxCANFrames_0.data[3]:=hz_cylinder_pre_2_out; can_ret:= can_write(ht_01,ADR(aTxCANFrames_0), 1);</pre>	<p>Program part: Standard frame definition Define the ID as 483h Define the data length</p> <p>hz_cylinder_pre_1_in as the first byte hz_cylinder_pre_1_out as the second byte hz_cylinder_pre_2_in as the third byte hz_cylinder_pre_2_out as the fourth byte PDO sending function calling</p>

secondly, setting communication parameters, thirdly sending data to the network, and receiving data from the network. The monitor interface as shown in Fig. 24.5 shows, its realization features include:

1. System parameter setting, which can set the maximum working pressure of the hydraulic oil cylinders, the maximum working temperature of hydraulic system, and the working environment limitations.
2. Control parameter setting, which can set the operation speed, lifting height, slewing rate, etc.

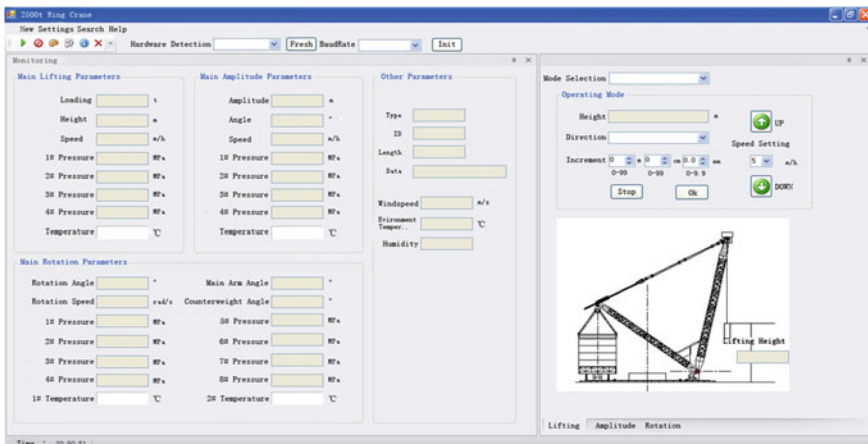


Fig. 24.5 Monitoring and controlling interface

3. Operation, which can control the action of the crane, such as promotion, drop, clockwise slewing, counterclockwise slewing, etc.
4. Status monitoring, which can display the status information in real time.
5. Alarm, which can warn the driver when the state data of crane is abnormal.
6. Database storage, which can store the data from sensors to SQL database in every two seconds and generate reports.

24.6 Conclusion

This paper introduces a design scheme of distributed control system based on CAN bus in huge crane, expounds the composition and realization of the system, and designs the communication protocol and the function of monitoring and controlling interface. As a kind of high performance and high reliability of fieldbus, CAN is very suitable for distributed control system in ring crane. As a scheme study, this paper has a certain reference significance to the design of distributed control system in ring crane.

References

1. Yong-ming BIAN, Ying-ming DAI, Xiao-lin JIN (2008) CAN-bus-based distributed control system for 900-ton pneumatic beam gantry cranes. *Chin J Constr Mach* 6(1):38–43
2. Shanghai Pal-Fin Auto Control Company. *Electrical Products Catalog*
3. Rao Y, Zou J (2003) *CAN Fieldbus Principles and Applications of Technology*. Beihang University Press, Beijing

Part III
Logistics Warehousing and Distribution
Technology Management (LWDT)

Chapter 25

Research on Picking Route Optimization for One Stacker in Multiple Aisles Automated Storage and Retrieval System

Ailan Feng, Zhanzhen Di and Wenying Ding

Abstract The paper analyzed the characteristic of the stacker about working mode and proposed a method to optimize the order picking path of one stacker in multiple aisles AS/RS. As developed transformation rules correspond to picking operations, the order picker routing problem was transferred into a TSP. Based on the return strategy picking model, a mathematical model was built with packing capacity constraints and improved ant colony algorithm is presented to solve the order picker routing problem. Experimental results show that the improved algorithm has better overall search ability and astringency, and it is an effective solution to the order picking problem.

Keywords Stacker · Ant colony algorithm · The optimization of picking route

25.1 Introduction

Automatic storage and retrieval system plays an important role in industrial production as a new storage pattern in the field of modern logistics technique. In certain range of inbound–outbound frequency, it has practical significance that the AS/RS under the control of one stacker not only saves company’s cost, but also has a high picking efficiency. Therefore, this system is used in the warehouse that has low storage frequency such as emergency supplies warehouse, spare parts warehouse, and so on. The crucial link to improve order picking process efficiency is the optimization the stackers’ picking route [1]. As a result, a study on it is extremely

A. Feng (✉) · W. Ding
School of Mechanical Engineering, University of Science and Technology Beijing,
Beijing 100083 China
e-mail: feng_ailan@sina.com

Z. Di
The International Logistics Company, Hebei Irons and Steel Group,
Shijiazhuang 05000 Hebei Province, China

© Springer-Verlag Berlin Heidelberg 2015
Logistics Engineering Institution, CMES (ed.),
Proceedings of China Modern Logistics Engineering,
Lecture Notes in Electrical Engineering 286, DOI 10.1007/978-3-662-44674-4_25

significant in both theoretical research and practical applications. MOB picking (man-on-board AS/RS) is one of the most popular modes of picking operation [2, 3]. The picking tasks are sent to the stacker through communication networks by management controlling system and showed on the touchable operation screen in cab before the operator starts picking. After finishing a picking, the operator needs to press a button to inform the system to show the next task, and then, the stacker will be moved to the position of new task. When all tasks are finished or the picking container is full, the controllable stacker will return to the I/O ports.

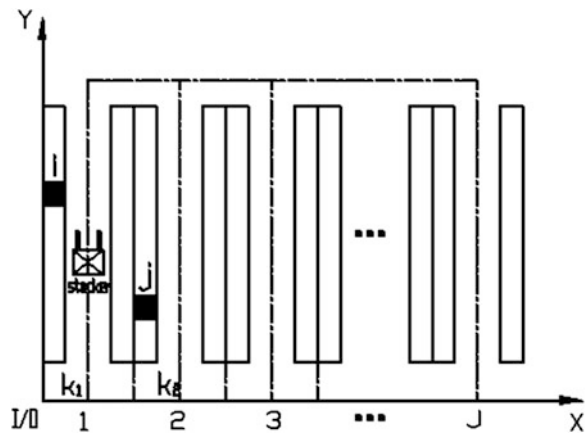
25.2 Stacker’s Picking Optimization Model

25.2.1 Descriptions

The optimization model of one stacker in multiple aisles automated storage and retrieval system is proposed bases on a lot of analyses about stacker’s picking processes and operating features.

The aisles that the stacker accesses goods in are between two adjacent racks, and an I/O platform is on the left side of the storage area. One stacker is responsible to picking goods from multiple aisles in this area. It starts from the I/O carrying a tote, passes several objective units, picks relevant goods, changes a new empty tote and picks again after the old one is full, stops operating till all picking tasks are finished. At the end, the tote is sent to conveyor system by stacker. The storage area plan view is shown in Fig. 25.1.

Fig. 25.1 Storage area plan view



25.2.2 Basic Assumptions

The basic assumptions about this research are listed as follows:

1. The storage unit's location could be shown as the coordinates (X, Y, Z) , and the aisle number is as $\{k_1, k_2 \in (1, 2, \dots, J)\}$. The coordinates of I/O platform are $(0, 0, 0)$, and it is also the additional unit in the whole operation. The spacing between each rack is expressed as d . The length, width, and height of each unit are a, b , and h , which are all constants. The lists are numbered as $\{1, 2, \dots, n\}$, to minimize the travel time used for finishing a picking list, finding the best sequence items on the picking list.
2. The types of goods on racks are given, and the storage state (empty or full) of the rack is certain. The speed of stacker is constant, not changed by the number of goods. The timings of start, stop, and shunt are also constant.
3. The stacker can move along the direction of x and z axes or of y and z axes while picking goods, but the direction of x and y axes is not available.
4. The stacker's pick time is not changed by different picking sequence. When we calculate travel time, the pick time could be ignored.

25.2.3 Mathematical Model

The stacker starts from I/O ports. The travel time of accessing goods is:

$$T_{i_k1j_k2} = \begin{cases} \max \left\{ \frac{|Y_i - Y_j|}{V_y}, \frac{|Z_i - Z_j|}{V_z} \right\} + B, k_1 = k_2 \\ \max \left\{ \frac{|X_i - X_j|}{V_x} + \frac{|Y_i + Y_j|}{V_y}, \frac{|Z_i - Z_j|}{V_z} \right\} + B + 2C, k_1 \neq k_2, |Y_i + Y_j| \leq Y \\ \max \left\{ \frac{|X_i - X_j|}{V_x} + \frac{|Y - Y_i - Y_j|}{V_y}, \frac{|Z_i - Z_j|}{V_z} \right\} + B + 2C, k_1 \neq k_2, |Y_i + Y_j| > Y \end{cases} \tag{25.1}$$

X_i, Y_i, Z_i are the coordinates of unit i . X_j, Y_j, Z_j are the coordinates of unit j . V_x, V_y, V_z are the stacker's average speeds of x, y , and z axes. B is stacker's start or stop time, C is the shunt time between x and y axes, and Y is the length of y axis. B, C , and Y are all constants.

The volume limits must be satisfied during one picking tour:

$$\sum_{k_1, k_2=1}^J \sum_{i, j=1}^n q_{i_k1j_k2} \leq Q$$

n is the number of picking units in one picking tour, $q_{i_k1j_k2}$ is the size of goods to be retrieved in pick unit (i, j) , and Q is the volume of a tote.

According to the analyses above, the optimization algorithm of this picking scheduling is described as follows:

On the premise that the amounts of picked goods every time are less than the tote's volume, how to arrange the picking order sequence to reduce stacker's travel time, meanwhile decrease operating times, and improve system's efficiency.

Introducing a decision variable $x_{i_k1j_k2}^l$, the range of this variable allowed is

$$x_{i_k1j_k2}^l \in \{0, 1\}, \quad i_{k1}, j_{k2} = 1, 2, \dots, n, i_{k1} \neq j_{k2}$$

l is the operating times, $l = 1, 2, \dots, m$

$$x_{i_k1j_k2}^l = \begin{cases} 0, & \text{the } l \text{ time that the stacker does not choose this path} \\ 1, & \text{the } l \text{ time that the stacker is going to aisle } k_2 \text{ accessing unit } j \text{ after aisle } k_1 \end{cases}$$

The constructed mathematical model is as follows:

$$\min \sum_{k_1, k_2=1}^J \sum_{i, j=1}^n \sum_{l=1}^m T_{i_k1j_k2} x_{i_k1j_k2}^l \tag{25.2}$$

$$\min m \tag{25.3}$$

The constraint conditions are:

$$\sum_{k_1, k_2=1}^J \sum_{i, j=1}^n \sum_{l=1}^m x_{i_k1j_k2}^l = \begin{cases} 1, & j_{k_2} = 1, 2, \dots, n \\ m, & j_{k_2} = 0 \end{cases} \tag{25.4}$$

$$\sum_{k_1, k_2=1}^J \sum_{i, j=1}^n q_{i_k1j_k2} \leq Q \tag{25.5}$$

Objective (2) indicates that the stacker's picking travel time is the shortest. Objective (3) minimizes the times of picking tour. Constraint (4) ensures that each unit is just accessed once and constraint (5) requires the amounts of picked goods every time are not more than the max volume of a tote.

25.2.4 Improved Ant Colony Algorithm Design for Picking Route

25.2.4.1 Symbol Description

From the view of artificial intelligence, the ant among ant colony algorithm is called as artificial ant. In this situation, each ant is an agent choosing the direction randomly based on the pheromone strength on each picking road. Each ant is set as $A_k = (F_k, E_k, V'_k)$. F_k is the objective function value of this case according to Formula (25.2) after the ant finishes an iteration and is also the picking travel time. E_k is the quantity of pheromone that the ant leaves on a road, and $E_k = Q_L/F_k$, Q_L is constant. v'_k is the set of vertices that the ant passed road.

In the research of picking route, set all unit position in picking list composing a directed graph expressed by graph $G = (V, R)$. Besides, $V = \{v_i | i = 0, 1, \dots, n\}$ is the set of vertices, v_0 is the I/O ports, others vertices are goods locations in the picking list, $R = \{r_{ij} | i \in [0, n], j \in [0, n]\}$ is the set of all roads among all vertices, t is the number of circulation, and N_{max} is the biggest iteration times.

Assuming as there are M ants moving in the graph, the transition probability for the k th ant moving from v_i to v_j at time t is

$$P_{ij}^k(t) = \begin{cases} \frac{\tau_{ij}^\alpha(t) \cdot \eta_{ij}^\beta(t)}{\sum_{s \in \text{allowed}_k} \tau_{is}^\alpha(t) \cdot \eta_{is}^\beta(t)}, & j \in \text{allowed}_k \\ 0, & \text{otherwise} \end{cases} \tag{25.6}$$

$\text{allowed}_k = V - V'_k$

From the above formula, you could know $\text{allowed}_k = V - V'_k$ means the next chosen vertex for the k th ant, and the allowed_k needs to be modified because the volume restriction of tote is added.

$$\text{allowed}_k = \left\{ V - V'_k - \left\{ j \mid \sum_{i=V'_k}^n q_i + q_j > Q, j \notin V'_k \right\} \right\}$$

α and β are the relative influence of the pheromone trails and the visibility values, $\tau_{ij}(t)$ means the pheromone density on road (v_i, v_j) in circulation t . After n periods, when ant finishes a circulation, the pheromone on each road could be modified referring the formula $\tau_{ij}(t+n) = \rho\tau_{ij}(t) + (1-\rho)\Delta\tau_{ij}(t)$, ρ is the speed of pheromone volatilization, $\Delta\tau_{ij}(t)$ is the pheromone increment on road (v_i, v_j) in this circulation. $\eta_{ij}^\beta(t)$ is the heuristic function:

$$\Delta\tau_{ij}(t) = \sum_{k=1}^m \Delta\tau_{ij}^k(t) \quad (25.6)$$

$$\Delta\tau_{ij}^k(t) = \begin{cases} E_k, & \text{ant } k \text{ passing road in circulation } t \\ 0, & \text{if not} \end{cases} \quad (25.7)$$

From the above, we could know $\Delta\tau_{ij}^k(t)$ is the pheromone increment on road (v_i, v_j) from the k -Thant.

25.2.4.2 Algorithm Improvement

1. Dynamically Inserting Point

The moving track of ants is a logic track, and it will become the real track after the inserting point, which is the real solution of this problem. For example, the moving track of an ant is $(v_0, v_1, v_3, v_5, v_4, v_2)$, and after the operation of inserting point, if the result becomes $(v_0, v_1, v_3, v_0, v_5, v_4, v_2, v_0)$, it means this picking operation is partitioned into two times. The first route is (v_0, v_1, v_3, v_0) , and the second one is $(v_0, v_5, v_4, v_2, v_0)$.

The choosing of inserting point needs to consider the volume constraint of a tote, which means the stacker's max volume Q cannot be exceeded while one picking tour.

2. Inserting Point Calculation

From the second point on moving track, set $i' = 1$, accumulate each picking volume on unit, when $\sum_{i=i'}^k q_i \leq Q$ and $\sum_{i=i'}^{k+1} q_i > Q$ insert the point v_0 between k and $k + 1$, then make $i' = k + 1$ from the point $k + 1$.

3. Description of Improved Algorithm

Step 1. Initialize parameters that $t = 0, n = 0, \tau_{ij}(0) = \tau_0, V'_k = \phi$ (Tabu table is empty) and set the value of $\rho_0, \rho_{\min}, \alpha, \beta, Q$.

Step 2. Put M ants at the starting position of I/O ports and then the start to searching route circularly. According to Formula (25.6), calculate the probability p_{ij}^k of the k th ant, choose the next picking unit v_j , record it, and put in V'_k .

Step 3. Estimate whether it satisfies $\sum_{i=i'}^k q_i \leq Q$ and $\sum_{i=i'}^{k+1} q_i > Q$, if yes, go ahead; if not, turn to Step 2.

Step 4. Calculate the inserting point, insert v_0 into V'_k , calculate G_k and E_k , and revise V_k and clear V'_k .

Step 5. Calculate pheromone volatilization speed parameter.

Step 6. Choose the best route of this iteration and record A^* .

Step 7. Update the pheromone density $\tau_{ij}(t + n)$ on the road.

Table 25.1 Before-and-after optimization performance indicators' comparison of picking operation

	<i>n</i> = 30		<i>n</i> = 50		<i>n</i> = 100	
	Before	After	Before	After	Before	After
Picking times	5	4	6	5	15	10
Travel time (s)	1,035.283	332.9274	1,285.379	344.3628	2,684.438	355.9362
Optimization rate of picking times (%)	20		16.67		33.33	
Optimization rate of travel time (%)	66.97		73.21		86.74	

Step 8. Estimate the routes that all ants passed by are same or not, if not, insert v_0 into V'_k , turn to Step 2. Otherwise, end the procedure.

25.3 Algorithm Experimental Comparison

The parameters of racks and stackers are $a = 1$ m, $b = 1$ m, $h = 1$ m, the racks have 10 rows, 20 columns, and 10 layers, the speed of stacker is $V_x = 1$ m/s, $V_y = 1$ m/s, $V_z = 0.3$ m/s, $B = 2$ s, $C = 10$ s. The numbers of picking lists are 30, 50, and 100, results are shown in Table 25.1.

Among the experiments of three different order picking numbers, the travel time and picking operation times after ant colony algorithm optimization are much better than before, and this algorithm has a better global optimum capability and fast convergence. In particular, after taking closed loop policy, the storage area has been used sufficiently, the circuitry has been avoided, and the stacker's travel time has been reduced significantly. As the chosen goods get more on a picking list, the optimization effect becomes more obvious. It means the optimization algorithm in this article is effective.

25.4 Conclusions

The picking route optimization for one stacker in multiple aisles automated storage and retrieval system is stated in this article. First of all, building a mathematical model of picking operation of one stacker in multiple aisles automated storage and retrieval system transforms the question of stacker's picking operation scheduling into the common TSP issue. Based on real situation, the tote constraint is added,

and the ant colony algorithm with a selection operator and inserting point operation is proposed. Experiments show that this algorithm has a better global optimum capability, fast convergence and is an effective algorithm of solving picking route optimization.

References

1. Yang H, Li X, Zhong M (2005) Optimal order picking operation allocation for AS/RS. *Hoisting Conveying Mach* 3:23–26
2. Wang G, Li M-J, Chen X-B (2008) Research on path planning problem for single aisle fixed storage rack. *Comput Eng Appl* 44(16):111–115
3. H-J Zhang (2008) Research on task scheduling in automated storage and retrieval system based on ant colony algorithm. Tianjin University of Technology

Chapter 26

A Cellular Ant Algorithm-Based Method for Solving Stereo Warehouse Slotting Optimization Problem

Meng Jin, Xihui Mu, Fengpo Du and Lei Luo

Abstract A new model for the ant colony optimization (ACO) method which is optimized by combining the cellular automata (CA) is proposed in this paper. The mathematic model of slotting optimization for stereo warehouse, together with the proposed ACO-based searching process is developed. Through the evolutionary mechanism of cellular and the redistribution of pheromones, the proposed ACO method is able to improve the searching effectiveness of solution space, and the case of getting into local optimums is avoided. Compared to the traditional ACO algorithm, the proposed ACO method can find the global optimal solution easily. The efficiency of the proposed method is demonstrated in the case study.

Keywords Slotting optimization · Cellular automata · Ant colony optimization

26.1 Introduction

Slotting optimization problem is to find a proper assignment of storage locations to cargos with the objective of minimizing the expected operational loss. How to maximize the operational effectiveness of warehouse system with limited resource and model the decision-making process of storage location assignment, become the important program of the modern logistics research. Slotting optimization problem is a NP-complete problem. The time to solve slotting optimization problem shows exponential growth as the dimensions growing. Ant colony optimization (ACO) algorithm is a heuristic algorithm to solve NP-complete problem. Comparing with other algorithms (i.e., simulated annealing, neural network, and genetic algorithm), it has the excellence of distributed, positive feedback, robustness and to combine

M. Jin (✉)

Ammunition Engineering Department, Mechanical Engineering College, Shijiazhuang, China
e-mail: mgfqxh@163.com

X. Mu · F. Du · L. Luo

Research Institute of Mechanical Technology, Shijiazhuang, China

© Springer-Verlag Berlin Heidelberg 2015

Logistics Engineering Institution, CMES (ed.),

Proceedings of China Modern Logistics Engineering,

Lecture Notes in Electrical Engineering 286, DOI 10.1007/978-3-662-44674-4_26

with other algorithms easily [1, 2]. It also has some shortcoming such as low convergence rate and to fall into local optimization easily. Cellular automata (CA) [3, 4], which was presented by J.von Neumann, is a math model which is time and spatial spreading. Combining ACO with CA, try to build the cellular ant model and solve the shortcoming of low convergence rate and to fall into local optimization easily used as slotting optimization problem [5].

26.2 The Slotting Optimization Problem

The slotting optimization problem for fixed rack and partition random accessing could be supposed as the following scenario. There are K picking areas and T cargos to store, the associated coefficient of cargo j to area k is p_{kj} . There are n_k cargos related to the area k , and the coefficient of access difficulty of the area is w_k . There are W slots in all areas to be filled, and there are m_k slots of the area k . The filling probability of slot i to cargo j is γ_{ij} , which decided by the cargo's properties such as mass bulk and slot's properties such as the distance from the entrance—the slotting optimization problem could be modeled as the following.

$$\min \sum_{k=1}^K w_k \prod_{j=1}^{n_k} [p_{kj} \prod_{i=1}^W (1 - \gamma_{ij} x_{ij})]. \quad (26.1)$$

$$\text{s.t. } \sum_{k=1}^K n_{kj} = T. \quad (26.2)$$

$$\sum_{i=1}^W x_{ij} = 1, i = 1, 2, \dots, W. \quad (26.3)$$

$$x_{ij} \in \{0, 1\}, i = 1, 2, \dots, W, j = 1, 2, \dots, T. \quad (26.4)$$

where x_{ij} is a Boolean value indicating whether the i th slot is assigned to the j th cargo. $x_{ij} = 1$ indicates that the i th slot is assigned to the j th cargo. The constraint (26.3) implies each slot can be assigned to only one cargo. The model is a simple and basic, and many slotting optimization problems could be extended from it.

26.3 Slotting Optimization Model Based on CAA

26.3.1 The Principle of ACO Algorithm

Scientists found that ant individual communicates with others through something called ectohormone, in searching of how the blind animals such as ants look for the best route from nest to food source. When an alone ant moves randomly, it can feel

the information element released by other ants, and move along the route, then release information elements itself, so the information elements on the route is enhanced [7, 8]. These form a positive feedback. The strength of information element on the best route becomes stronger, and the ones on other routes become weaker. Finally, the ant colony will find out the best route. The ant colony also can acclimatize oneself to the changing environment, so it can find the best route again rapidly when a roadblock is put on the route.

With TSP problem, the basic idea and principle of ACO is described below. The variables and constants in use are:

- m count of ants in the ant colony;
- η_{ij} visibility of edge (i, j) , value of $1/d_{ij}$;
- τ_{ij} route strength of edge (i, j) ;
- $\Delta\tau_{ij}^k$ amount of information element which is left by the k th ant on edge (i, j) per unit length;

$$\Delta\tau_{ij}^k = \begin{cases} Z_k/d_{ij}, & \text{if edge } (i, j) \text{ is on the best route,} \\ 0, & \text{other.} \end{cases}$$

Z_k is value of aim function

P_{ij}^k transfer probability of the k th ant which is proportional to $\tau_{ij}^\alpha \cdot \eta_{ij}^\beta$, j is node which has not accessed; the function of route strength is: $\tau_{ij}^{new} = \rho \cdot \tau_{ij}^{old} + \sum \Delta\tau_{ij}^k$. The meanings of parameters are:

- α the relative importance of route ($\alpha \geq 0$);
- β the relative importance of visibility ($\beta \geq 0$);
- ρ the lasting degree of information on route ($0 \leq \rho < 1$), and $1 - \rho$ is attenuation degree;
- Q a constant that can present the amount of information element left by ants.

So, the main steps of ACO are described:

- Step 1: $nc \leftarrow 0$ (nc is the number of iterative of search step); Initialize τ_{ij} and $\Delta\tau_{ij}$; Put the ant to the node;
- Step 2: Put the start node of ants to the current solution set; Move the k th ant to next node by probability of P_{ij}^k ; Put the node j to current solution set;
- Step 3: Compute the value of aim function of every ant; Record the current best solution;
- Step 4: Modify the route strength with update function;
- Step 5: For every edge (i, j) , $\Delta\tau_{ij} \leftarrow 0$; $nc \leftarrow nc + 1$;
- Step 6: If $nc <$ count of iterative steps, and no degradation appears, go to Step 2;
- Step 7: Print the current best solution.

26.3.2 The Principle of Cellular Automata

CA is a math model, which is time and spatial spreading. As far as set theory is concerned, the CA has an exacting mathematical description and definition. In the entire sequel, e denotes dimension of space. k stands for its cellular condition and achieves its parameters in limited collection T . Throughout this paper, δ stands for the neighborhood size parameter of the cellular. Z denotes an integer set. t stands for time. For simplicity, we let $e = 1$, and only consider the CA on one-dimensional space. So, we call the distribution of all cellular space, denoted by T^Z , i.e., the distribution of the condition set T on integer sets Z . The dynamic evolutionary of the CA is a variation of the state combination:

$$F : T_t^Z \rightarrow T_{t+1}^Z$$

It should be noted that the dynamic evolutionary is in control of each cellular's locally evolutionary regulation f . This locally function is usually called locally regulation. For one-dimensional space, the cellular and its neighbor can be marked by $T^{2\delta+1}$. Then, the locally function is denoted as follows:

$$f : T_t^{2\delta+1} \rightarrow T_{t+1}$$

For locally regulation f , the input sets and output sets of the function are all finite sets. As a matter of fact, it is a finite table of reference. We implement above locally function for the cellular of cellular space. Then, it yields the global CA evolutionary model:

$$F(d_{t+1}^j) = f(d_t^{j-\delta}, \dots, d_t^j, \dots, d_t^{j+\delta})$$

Here, d_t^j is a cellular, and its locality is in j .

The most basic structures of the CA include the cellular, cellular space, neighbor, and regulation. The normal CA is made up of four elements, and its mathematical symbols description is as follows:

$$S = (L_e, T, V, f)$$

where S is the CA system; L denotes the automata space; e is a positive integer and denotes the dimension of space in the CA system; T is a finite and discrete condition set of the cellular; V denotes a cellular's combination in all neighborhoods and includes the center cellular; $f: T^V \rightarrow T$ is a locally translation function. Each cellular locates on e -dimensional space, and its location can be determined by an e -dimensional integer matrix Z^e .

26.3.3 The Slotting Optimization Algorithm Based on CAA

The key of solving slotting optimization problem with cellular ant algorithm is to convert slotting optimization to ants net. Here, convert the process of slotting optimization problem to the one below: the slot W_i is a city C_i ; the cargo T_j is a route l_{ij} from city C_i to city C_{i+1} ; the process of slot W_i filled by cargo T_j is a process of choosing route from city C_i to city C_{i+1} ; so form a ants net as Fig. 26.1a. The result of slotting optimization problem corresponds to a route from city C_1 to city C_{m+1} as Fig. 26.1b.

With the conversion above, the slotting optimization problem is converted to ants net, and it can be solved with cellular ant algorithm. Firstly, there are some definitions of cellular ant algorithm (see details in 2.1 for meanings of the parameters).

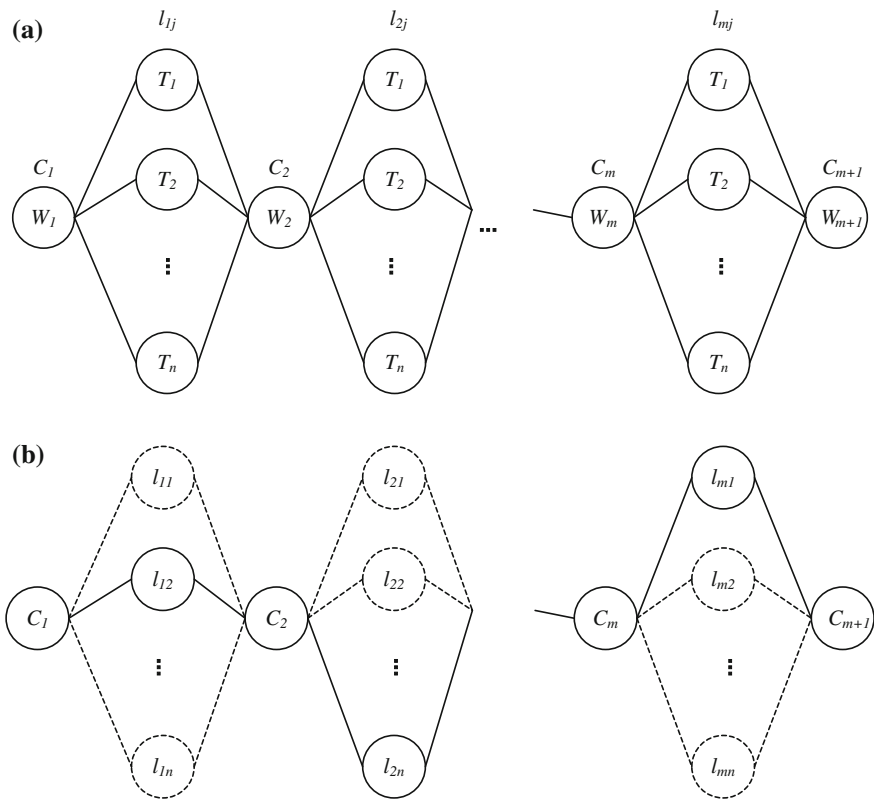
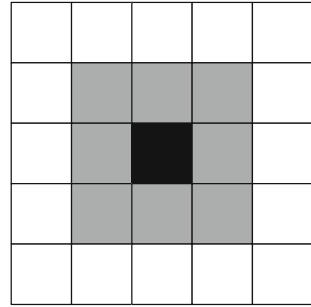


Fig. 26.1 Ants net figure of slotting optimization problem. **a** Convert slotting optimization to choosing route problem, **b** One route from city C_1 to city C_{m+1}

Fig. 26.2 Moore-type neighbor model



Definition 1 There is a set of city element $C = \{c_1, c_2, \dots, c_{m+1}\}$. The ants access the cities by the order of $1, 2, \dots, m + 1$. There are n routes to choose from city C_i to city C_{i+1} , and the length of the route is marked as $l_{ij}(i = 1, 2, \dots, m; j = 1, 2, \dots, n)$. When the ant move from city C_i to city C_{i+1} , if it chooses the j th route, the ant can choose the j th route any more in the later city. So the route set from city C_1 to city C_{m+1} is the cellular space, presented by $L = \{\text{cell}X = (l_{1j}, l_{2j}, \dots, l_{mj}) | j \in \{1, 2, 3, \dots, n\}\}$, where $j \in \{1, 2, 3, \dots, n\}$ means the element l_{ij} and l_{mn} in each cellX are satisfied with: when $i \neq m, j \neq n$.

Definition 2 The cellular neighbor adopts Moore-type neighbor as follows (Fig. 26.2):

$$N_{\text{moore}} = \{\text{cell}Y | \text{diff}(\text{cell}Y - \text{cell}X) \leq 1, \text{cell}X, \text{cell}Y \in L\}$$

Definition 3 The transfer probability of ant:

$$P_{ij}^k = \frac{\tau_{ij}^\alpha \cdot \eta_{ij}^\beta}{\sum_k \tau_{ik}^\alpha \cdot \eta_{ik}^\beta}, \eta_{ij} = 1/(1 - l_{ij})$$

Definition 4 The equation of aim function:

$$Z_k = \sum_{j=1}^n \prod_{i=1}^m (1 - l_{ij}x_{ij}), l_{ij} \in \text{cell}X$$

Definition 5 The equation of updating strength of information element:

$$\tau_{ij}^{\text{new}} = \rho \cdot \tau_{ij}^{\text{old}} + \sum_k \Delta \tau_{ij}^k$$

$$\Delta \tau_{ij}^k = \begin{cases} Z_k / (1 - l_{ij}), & \text{edge } (i, j) \text{ is on the best route,} \\ 0, & \text{other.} \end{cases}$$

Definition 6 The rule of the cellular evolutionary is defined as follows: Compute the aim functions of cellular neighbor based on the definition of cellular neighbor; then compare the cellular and its neighbor, and choose the best solution.

The implement steps of solving slotting optimization problem with cellular ant algorithm as follow:

- Step 1: $nc \leftarrow 0$ (nc is the number of iterative of search step); initialize τ_{ij} and $\Delta\tau_{ij}$; fix on the size of the zone by the number of ants and cellular space; put the ant to the city C_1 ;
- Step 2: Search the route for each ant; move the k th ant to next node by probability of P_{ij}^k ; put the city C_{j+1} to current solution set;
- Step 3: Compute the value Z_k of aim function of every ant; record the current best solution;
- Step 4: Evolve in area of neighbor base on the definition of cellular neighbor; record the current best solution;
- Step 5: Modify the route strength with update function;
- Step 6: For every edge (i,j) , $\Delta\tau_{ij} \leftarrow 0$; $nc \leftarrow nc + 1$;
- Step 7: If $nc < \text{count of iterative steps}$, and no degradation appears, go to step 2;
- Step 8: Print the current best solution.

Because the computing complexity of the CAA is related to the partition of cellular space, the model partitions the space equably [6]. To do this above can reduce the computing time. Every zone is formed by cellular and its neighbor. The center of the zone is cellular. Others are cellular's neighbor. The zone's life is decided by the states of cellular and its neighbor. In the zone search, the cellular randomly and computing the best solution. To avoid local optimization solution, we can enlarge the size of the zone. It is beneficial for global optimization.

26.4 Simulation Result

There are six cargos, T_1, T_2, T_3, T_4, T_5 and T_6 , and the slots are distributed on six areas, W_1, W_2, W_3, W_4, W_5 , and W_6 . The associated coefficient of area W_i -related cargo T_j is $P_{ij}(i = 1, 2, 3, 4, 5, 6; j = 1, 2, 3, 4, 5, 6)$ as in Table 26.1.

Adopting ACO and CAA, respectively, execute the simulation 100 times ($\alpha = 1, \beta = 5, \rho = 0.7, Q = 100$). The two plans both retrieve the best solution: Slot 1 filled by cargo 4, slot 2 filled by cargo 5, slot 3 filled by cargo 1, slot 4 filled by cargo 2, slot 5 filled by cargo 3, slot 6 filled by cargo 6, as in Table 26.2.

Table 26.3 gives the best solution, average solution, maximum iterative degree, minimum iterative degree, and average iterative degree. From the data, it is obvious that the average solution of CAA is better than ACO's one, and CAA's iterative degree is less, and its convergence speed is faster.

Figure 26.3 gives the compare the convergence of ACO and CAA, when each algorithm executes once. Both the two algorithms retrieve the best solution. But

Table 26.1 Probability table

Slots	Cargos					
	T_1	T_2	T_3	T_4	T_5	T_6
W_1	0.88	0.77	0.86	0.65	0.45	0.58
W_2	0.79	0.76	0.75	0.67	0.65	0.60
W_3	0.81	0.78	0.74	0.60	0.40	0.52
W_4	0.73	0.72	0.69	0.60	0.45	0.40
W_5	0.88	0.77	0.86	0.65	0.45	0.58
W_6	0.79	0.65	0.80	0.74	0.62	0.65

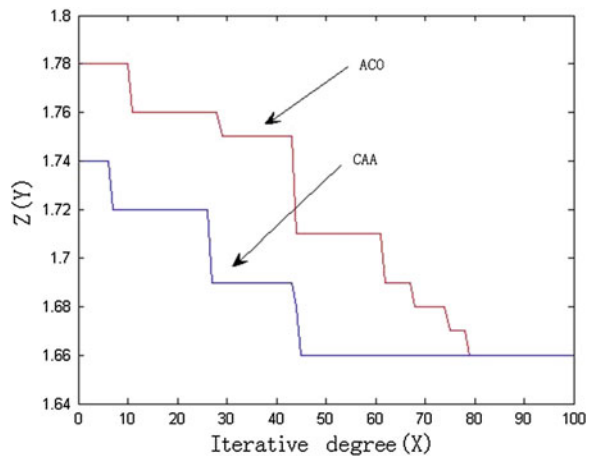
Table 26.2 The best solution of WTA

Cargo	T_1	T_2	T_3	T_4	T_5	T_6
Slot ID	3	4	5	1	2	6

Table 26.3 Simulation result comparison

Algorithm	Results				
	Best solution	Average solution	Max iterative degree	Min iterative degree	Average iterative degree
ACO	1.66	1.72	90	28	46.1
CAA	1.66	1.69	75	20	39.7

Fig. 26.3 Compare the convergence of ACO and CAA



from the figure, we can see that CAA's convergence speed is faster. This illuminates adequately that it is effective that using CA to improve the convergence speed of ACO.

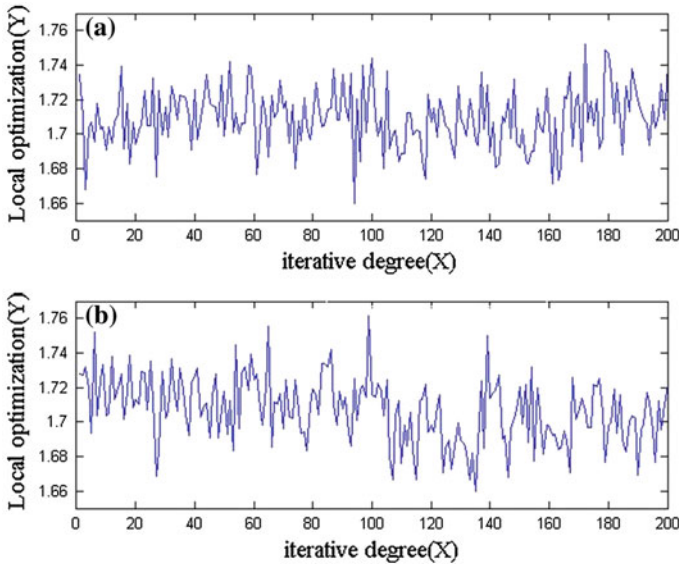


Fig. 26.4 Variety of ACO's and CAA's solution

Figure 26.4 gives the variety of ACO's and CAA's solution. The x -axis denotes the iterative degree, and the y -axis denotes the local optimization solution. From the figure, it is clear that the fluctuation of ACO's solution is less than CAA's solution, so using CAA, we can retrieve more various local optimization solution. This shows that CAA has good variety, and it can improve ACO, so the solution cannot fall into local optimization, and then retrieve better global optimization solution.

26.5 Conclusions

Cellular ant algorithm simulates the behavior for seeking food of ant colony in nature. Combining the principle of CA, the basic idea is simple, and the program is easy to implement. The algorithm which has good convergence can solve most nonlinear optimizing problem. Solving slotting optimization problem with CAA, the result shows that usability of CAA in solving slotting optimization problem, and there is a good foreground for using CAA in related to engineering optimizing problem. It can solve similar nonlinear integral optimizing problem.

Slotting optimization problem is a very complicated problem. When the dimension of the system grows fast using CAA to solve slotting optimization problem is truly available. The situation discussed in this article is simple, and there are many details which need to research, i.e., dynamic slotting optimization.

References

1. von Neumann J (1966) Theory of self reproducing cellular automata. University of Illinois Press, Urbana and London
2. Cai HP, Liu JX, Chen YW, Wang H (2006) Survey of the research on dynamic weapon-target assignment problem. *J Sys Eng Electron* 17(3):559–565
3. Ressler JL, Augusteijn MF (1992) Weapon target assignment accessibility using neural networks. *Intell Eng Sys Through Artif Neural Networks* 2:397–402
4. Li HR and MiaoY (2000) WTA with the maximum kill probability based on simulated annealing algorithms, the special committee of C2 and computer of the electronic technology academic committee of china, ship engineering society. *Academica conference*, pp 436–440
5. Lee ZJ, Lee CY, Su SF (2002) An immunity-based ant colony optimization algorithm for solving weapon-target assignment problem. *Appl Soft Comput J* 2(1):39–47
6. Guo P, Yan WJ (2007) The review of ant colony algorithm based on TSP. *J Comput Sci China* 34(10):181–184 194
7. Macro D, Maria GL (1997) Ant colony system: a cooperative learning approach to the traveling salesman problem. *IEEE Trans EC* 1(1):53–66
8. Dorigo M, Maniezzo V, Colomi A (1996) Ant system: optimization by a colony of cooperating agents. *IEEE Trans SMC* 26(1):29–41

Chapter 27

Research on Process Optimization of Automated Warehouse

Wei Yang, Dan Li, Chen Yan and Yuxiao Du

Abstract Automated warehouse, which is a new type in the field of modern logistics technology, is playing an increasingly important role in the industrial production. And the increasingly requirements of the logistics operation efficiency means that the requirements of operation efficiency in the warehouse system are increasingly high, while the optimization is an efficient way to improve the operation process efficiency. To improve the efficiency of automated warehouse, we introduce the integrated modeling ideas, which are based on the unified modeling language (UML) and polychromatic sets theory (PST), into the optimization study of warehouse process. This paper established the automated warehouse process model according to the research framework of manufacturing enterprise workflow process and an integrated workflow modeling method. By the analysis and optimization of the operation process model, it studies the instance migration technology that supporting the dynamic changes, to improve the automated warehouse operating efficiency, and increase the flexibility. This paper discusses the feasibility of application in automatic warehouse operations process optimization through the example.

Keywords Automated warehouse · The unified modeling language · Polychromatic sets · Operation process · Dynamic change

27.1 Introduction

Automated warehouse is also called automated storage or retrieval system [1]. And the increasing requirements of the logistics operation efficiency means that the requirements of operation efficiency in the warehouse system are increasingly high, while the optimization is an efficient way to improve the operation process efficiency.

W. Yang (✉) · D. Li · C. Yan · Y. Du
Mechanical and Electrical Engineering College, Shaanxi University of Science and Technology, Xi'an 710021, China
e-mail: yangwei613@126.com; 704344035@qq.com

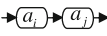
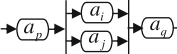
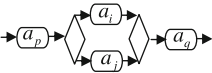
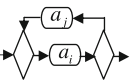
© Springer-Verlag Berlin Heidelberg 2015
Logistics Engineering Institution, CMES (ed.),
Proceedings of China Modern Logistics Engineering,
Lecture Notes in Electrical Engineering 286, DOI 10.1007/978-3-662-44674-4_27

For the optimization of automated warehouse process, there have been lots of researches focused on the loading and unloading scheduling problem, such as expert system [2], genetic algorithm (GA), and simulated annealing (SA). The integrated modeling method based on the unified modeling language (UML) and the polychromatic sets (PS) is widely used in the analysis and integration of optimizing enterprise workflow process. But, there is little literature involved it in application about the research on process optimization of automated warehouse. According to the integrated modeling method of UML and PS, this article chose the common automated warehouse to analyze and optimize the process, and to study the instance migration technology that supporting the dynamic changes, then the paper discussed the feasibilities of the application by the examples.

27.2 The Integrated Modeling Theory of the Unified Modeling Language and the Polychromatic Sets [3]

The integrated modeling framework of UML and PS includes two levels, one is the graphical modeling based on UML and the other is formalizing of UML model based on PS. Its basic modeling elements (node and connection relationship) constitute the four basic model structures and it is shown in Table 27.1. That is the sequence structure, parallel structure, selection structure, and iteration structure. And the corresponding four simplified rules are as follows: The sequence simplified rules, parallel simplified rules; selection simplified rules, and iteration simplified rules.

Table 27.1 The basic model structure

model structure	UML activity diagram model	models of PS relationship rules	structural mapping rules																								
Sequence structure		(a_i, a_j) <table border="1" style="display: inline-table; vertical-align: middle;"> <tr> <td></td> <td>F₁</td> <td>F₂</td> <td>F₃</td> <td>F₄</td> <td>F₅</td> </tr> <tr> <td></td> <td>•</td> <td></td> <td></td> <td></td> <td></td> </tr> </table>		F₁	F₂	F₃	F₄	F₅		•					$F_1(a_i, a_j) = 1$												
	F₁	F₂	F₃	F₄	F₅																						
	•																										
Parallel structure		(a_p, a_i) (a_i, a_q) (a_p, a_j) (a_j, a_q) <table border="1" style="display: inline-table; vertical-align: middle;"> <tr> <td></td> <td>F₁</td> <td>F₂</td> <td>F₃</td> <td>F₄</td> <td>F₅</td> </tr> <tr> <td></td> <td></td> <td>•</td> <td></td> <td></td> <td></td> </tr> <tr> <td></td> <td></td> <td></td> <td>•</td> <td></td> <td></td> </tr> <tr> <td></td> <td></td> <td></td> <td></td> <td>•</td> <td></td> </tr> </table>		F₁	F₂	F₃	F₄	F₅			•							•							•		$F_2(a_p, a_i) \wedge F_3(a_i, a_q) \wedge$ $F_2(a_p, a_j) \wedge F_3(a_j, a_q) = 1$
	F₁	F₂	F₃	F₄	F₅																						
		•																									
			•																								
				•																							
Selection structure		(a_p, a_i) (a_i, a_q) (a_p, a_j) (a_j, a_q) <table border="1" style="display: inline-table; vertical-align: middle;"> <tr> <td></td> <td>F₁</td> <td>F₂</td> <td>F₃</td> <td>F₄</td> <td>F₅</td> </tr> <tr> <td></td> <td></td> <td></td> <td></td> <td>•</td> <td></td> </tr> <tr> <td></td> <td></td> <td></td> <td></td> <td></td> <td>•</td> </tr> <tr> <td></td> <td></td> <td></td> <td></td> <td>•</td> <td></td> </tr> </table>		F₁	F₂	F₃	F₄	F₅					•							•					•		$F_4(a_p, a_i) \wedge F_5(a_i, a_q) \wedge$ $F_4(a_p, a_j) \wedge F_5(a_j, a_q) =$ 1
	F₁	F₂	F₃	F₄	F₅																						
				•																							
					•																						
				•																							
Iteration structure		(a_i, a_j) (a_j, a_i) <table border="1" style="display: inline-table; vertical-align: middle;"> <tr> <td></td> <td>F₁</td> <td>F₂</td> <td>F₃</td> <td>F₄</td> <td>F₅</td> </tr> <tr> <td></td> <td></td> <td></td> <td></td> <td>•</td> <td></td> </tr> <tr> <td></td> <td></td> <td></td> <td></td> <td></td> <td>•</td> </tr> </table>		F₁	F₂	F₃	F₄	F₅					•							•	$F_4(a_i, a_j) \wedge F_5(a_j, a_i) = 1$						
	F₁	F₂	F₃	F₄	F₅																						
				•																							
					•																						

27.3 Modeling of Automated Warehouse Operation Process and the Research on Optimization

This paper chose the automated warehouse with same side of loading and unloading as the research object, it includes five parts: Fixed shelf and stacker system, rotary shelf systems, transportation system, sorting system, and computer control system [4].

27.3.1 Modeling of Automated Warehouse Process and Structure Analysis

1. According to the automated warehouse structure and the process [4], we can build the UML activity diagram model of the automated warehouse as shown in Fig. 27.1.
2. Then according to the mapping rules of UML + PS-integrated modeling method, the models of PS relationship rules mapped from the UML activity diagram model is shown in Table 27.2a.
3. In order to find the possible structure conflicts in UML model, we should also simplify the model by the rules of simplifying basic model structure. In this paper, the origin and destination of this model can connect directly through a virtual node, which means that there is no structure conflict in the UML activity diagram model of the warehouse operation process.

27.3.2 The Dynamic Changes of Automated Warehouse Process Model

1. In order to make the AS/RS have higher flexibility to match the high efficiency of system, firstly, according to Fig. 27.1 and actual processing condition, we can set up a new UML activity diagram model by adding nodes and changing node structures. The specific detail of the changes is shown in Fig. 27.2 and the corresponding matrix of PS is also shown in Table 27.2b.
2. Secondly, when the dynamic change happened, we still need to decide to use what kind of instance migration strategy for the operation instances. So, we should use the recognition algorithms of workflow area to simplify the new process model from the inside to outside, analyze the relationship between various nodes and workflow region, and measure the inference relations between various nodes and workflow region to determine the instance migration.

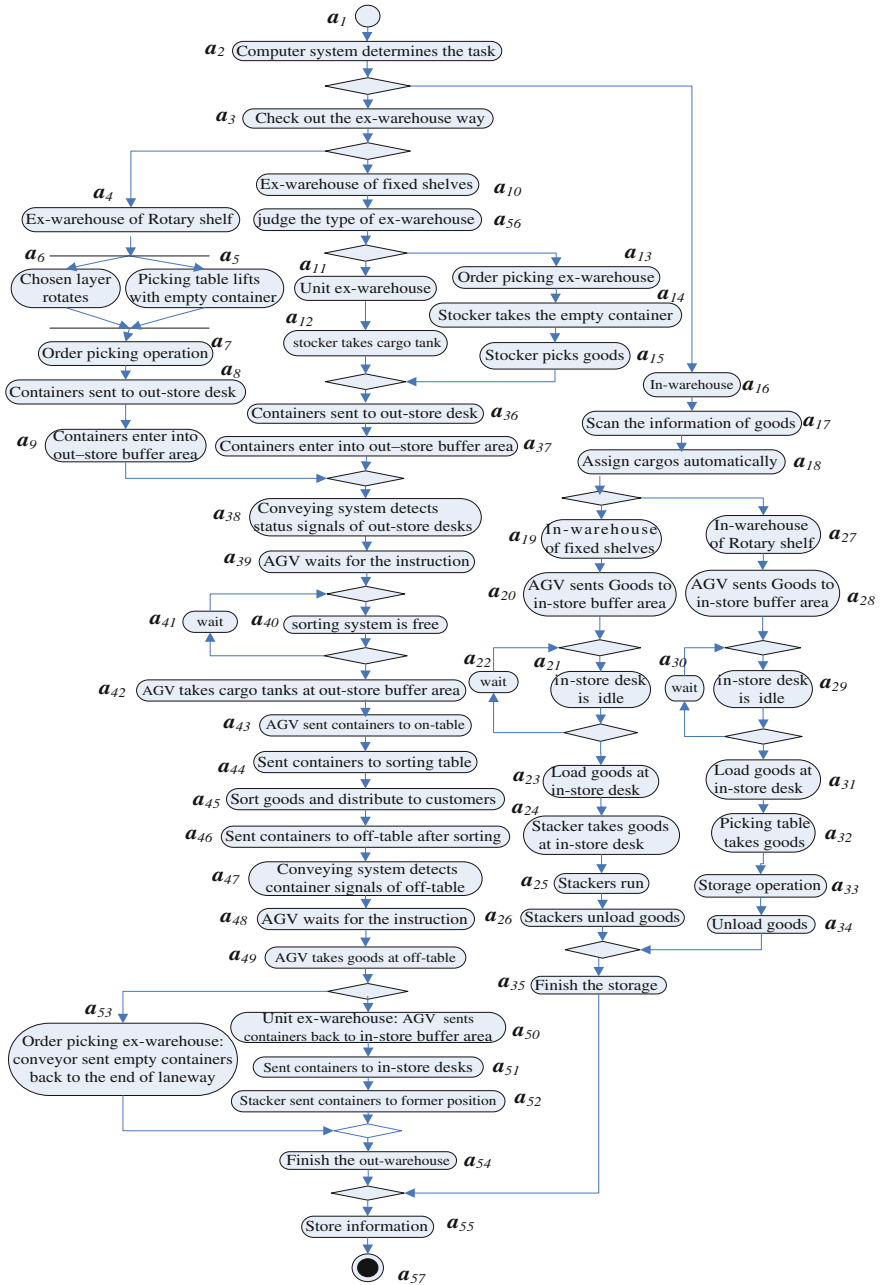


Fig. 27.1 The UML activity diagram model of warehouse (before the changes)

Table 27.2 Matrix of PS

	F ₁	F ₂	F ₃	F ₄	F ₅		F ₁	F ₂	F ₃	F ₄	F ₅
(a ₁ , a ₂)	•					(a ₁ , a ₂)	•				
(a ₂ , a ₃)				•		(a ₂ , a ₃)				•	
(a ₂ , a ₁₆)				•		(a ₂ , a ₁₆)				•	
(a ₁₇ , a ₁₈)	•					(a ₁₇ , a ₁₈)				•	
(a ₁₈ , a ₁₉)				•		(a ₁₈ , a ₅₉)					•
(a ₄₄ , a ₄₅)	•					(a ₄₄ , a ₄₅)		•			
(a ₄₆ , a ₄₇)	•					(a ₄₅ , a ₄₇)			•		
(a ₁₀ , a ₅₆)	•					(a ₁₀ , a ₅₆)		•			
(a ₅₆ , a ₁₁)				•		(a ₁₀ , a ₆₀)		•			
(a ₂₃ , a ₂₄)	•					(a ₆₀ , a ₃₇)			•		
(a ₁₈ , a ₂₇)				•		(a ₃₆ , a ₃₇)			•		
(a ₁₂ , a ₃₆)					•	(a ₁₂ , a ₃₆)					•
(a ₂₈ , a ₂₉)					•	(a ₂₈ , a ₂₉)					•
(a ₄₀ , a ₄₁)				•		(a ₄₀ , a ₄₁)				•	
(a ₄₀ , a ₄₂)				•		(a ₄₀ , a ₄₂)				•	
(a ₄₂ , a ₄₃)	•					(a ₄₂ , a ₄₃)	•				
(a ₅₀ , a ₅₁)	•					(a ₅₀ , a ₅₁)	•				
(a ₅₂ , a ₅₄)					•	(a ₅₂ , a ₅₄)					•
(2-a. Before the changes)						(2-b. After the changes)					

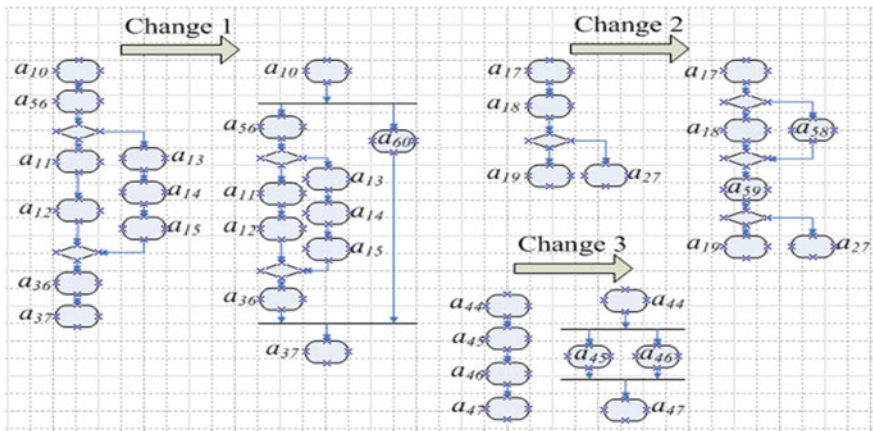


Fig. 27.2 The specific detail of the changes

27.4 The Result of Research on Warehouse Operations Process Optimization

27.4.1 The Specific Dynamic Change and the Instance Migration

1. For the research object in this paper, we make dynamic changes in three parts, and the specific results about dynamic changes were as follows: First, for the node a_{18} “distribute goods automatically,” considering the possible failure of management machine, we can add node a_{58} “inputting cargo space manually” [5] to form selection structure with node a_{18} , and add a empty node a_{59} to ensure that the structure is correct and smooth. Second, In order to shorten the time and improve the operation efficiency, we can change the node a_{45} and node a_{46} to parallel structure. Last, add the node a_{60} “other stackers which has the same goods” to form the parallel structure with $(a_{56}, ((a_{11}, a_{12}) \oplus (a_{13}, a_{14}, a_{15})), a_{36})$ that increased the information sharing between the stackers in different lane-ways, which means that if one stacker broke down, the system will dispatch other stackers to finish the task. So, it can ensure the accomplishment of warehouse operation.
2. AS/RS workflow instance migration that supporting dynamic changes
Here, we only choose parts of the path as the examples:

- (a) For the running instance with the execution path $P_1 = \{a_1, a_2, a_{16}, a_{17}\}$ before changes, we can see the currently running node $a_{17} \subset V_{20} \subset V_{31} \subset V_{32} \subset V_{34}$, and the positional order relationship between the nodes and changes is $V_{20} \geq V_{21}, V_{20} \geq a_{59}, V_{10} \subset V_{19}, V_{18} \subset V_{19}, V_{32} = (V_{19} \oplus V_{31}), a_{17} \neq a_{45}, a_{17} \neq a_{46}, a_{17} \neq a_{60}$, so, we can migrate running instances directly, and the actual execution path is $P_2 = \{a_1, a_2, a_{16}, a_{17}\}$.
- (b) For the instance with the execution path $P_1 = \{a_1, a_2, a_3, a_{10}, ((a_{56}, ((a_{11}, a_{12}) \oplus (a_{13}, a_{14}, a_{15})), a_{36}) \otimes a_{60}), a_{37}\}$, the inference relation is as follows: $a_{37} \subset V_9 \subset V_{10} \subset V_{19} \subset V_{32} \subset V_{34}, a_{37} \neq a_{58}, a_{37} \neq a_{59}, V_4 \geq a_{37}, V_9 \geq V_{35}$, we can see that it must return back first and the back path is $P_2 = \{a_{37}, ((a_{56}, ((a_{11}, a_{12}) \oplus (a_{13}, a_{14}, a_{15})), a_{36}) \otimes a_{60})', a'_{10}\}$, the actual execution path is $P_3 = \{a_1, a_2, a_3, a_{10}, ((a_{56}, ((a_{11}, a_{12}) \oplus (a_{13}, a_{14}, a_{15})), a_{36}) \otimes a_{60}), a_{37}, a_{37}((a_{56}, ((a_{11}, a_{12}) \oplus (a_{13}, a_{14}, a_{15})), a_{36}) \otimes a_{60}), a_{37}\}$,

27.4.2 The Result Analysis of Automated Warehouse Process Optimization

1. For the node a_{18} , adding the node a_{58} can ensure that the warehouse will not be influenced by possible failures of management machine.
2. For the node a_{45} and a_{46} that changing to parallel structure, we can assume that the time of node a_{45} is T_1 , the time of node a_{46} is T_2 , then the time between node a_{45} and node a_{46} is $T_1 + T_2$ before changes, but after the changes the time between node a_{45} and node a_{46} is T_1 (when $T_1 \geq T_2$) or T_2 (when $T_2 \geq T_1$), while $\max\{T_1, T_2\} \leq T_1 + T_2$, so the time becomes shorter.

27.5 Summary

This paper established the automated warehouse workflow model according to the research framework of manufacturing enterprise workflow process and an integrated workflow modeling method. And it is based on the research of the UML and the PS theory. By the analysis and optimization of the workflow process model, it studies the instance migration technology that supporting the dynamic changes, to improve the automated warehouse operating efficiency. It provides new ideas and methods for the optimization study of warehouse process.

Acknowledgment This work was supported by Special Grant of Shaanxi Provincial Education Department (Grant number: 12JK0516) and by National College Students' Innovative Business Plan Project.

References

1. Jie YS (2008) Optimization and Simulation of scheduling based on the automated warehouse. Beijing
2. Xu XL (2005) Research on storage scheduling based on expert system. Xi'an
3. Gao XG (2008) Research of manufacturing enterprise workflow process modeling methods and key technology based on UML and polychromatic sets. Xi'an
4. Tian GH (2005) Research on material storage and distribution system dispatching problem based on colored Petri net. J Mech 4(4):148-153
5. Zhu YM (2006) Research on optimal scheduling of automated warehouse. Shandong

Chapter 28

Research and Implementation of Condition-Based Maintenance System for Stack Crane in Automatic Storage and Retrieval System

Sixia Fan, Qicai Zhou, Jiong Zhao and Xiaolei Xiong

Abstract Aiming at solving the problem of excess or lack of maintenance which exists in traditional maintenance of stack crane in automatic storage and retrieval system, the stack-crane monitor and diagnostic system (SCMDS) based on the component module has been proposed, using the SCMDS as a research object, and utilizing the open-system architecture for condition-based maintenance (OSA-CBM) model and component technology theory for reference. First, this paper details the internal structure, functional modules, and interactive interface of the generic component module with the reconfigurable and scalable features in SCMDS. Second, it puts forward the six layers whole project of SCMDS which constituted by single and nested components. Finally, using the fault tree analysis model which established on the physical characteristics of the stack crane as an example, it describes the specific implementation of a single component and also provides the theoretical basis for application.

Keywords Stack crane · Condition-based maintenance · Component · Monitor and diagnostic

28.1 Introduction

Automated storage and retrieval system (AS/RS), as the core hub of production and storage in modern logistics design, is an integrated comprehensive system, consisting of high shelves, handling equipment, electrical control, programming, and

S. Fan (✉) · Q. Zhou · J. Zhao · X. Xiong
School of Mechanical and Engineering, Tongji University, Shanghai 201804,
People's Republic of China
e-mail: dongxia1249@163.com

© Springer-Verlag Berlin Heidelberg 2015
Logistics Engineering Institution, CMES (ed.),
Proceedings of China Modern Logistics Engineering,
Lecture Notes in Electrical Engineering 286, DOI 10.1007/978-3-662-44674-4_28

management [1]. For stack crane is the sign of AS/RS's features, it is the major machine for goods stockpiling in high-rise warehouse, and its performance status is directly related to the warehouse operations. With the AS/RS becoming more and more large scale, flexible, intelligent, and goods in and out per unit time more frequently, if the equipment have faults or shut down for repairing, it could affect the normal operation and security task, in warehouse, and also bring a huge loss to storage users. Therefore, condition monitor online, fault diagnosis, health prognosis, and maintenance decision optimization could be the important contents of equipment maintenance and supporting in AS/RS.

Currently, preventive maintenance and corrective maintenance are the two main modes in the warehouse, and the traditional maintenance brings some disadvantages such as excess or lack of maintenance. Condition-based maintenance (CBM) is a new way for supporting the equipment, and it programs the equipment maintenance according to the measured parameter values comprehensive assessment, through monitoring the system operating conditions online or off-line. This paper proposes the stack-crane monitor and diagnostic system (SCMDS), using the CBM as architecture, with condition detection, health assessment (HA), fault diagnosis, prognosis maintenance, and other functions. Reducing the complexity of SCMDS development, and increasing its reusability, according to open-system architecture for condition-based maintenance (OSA-CBM), the architecture of SCMDS based on the component has been proposed. This system could meet the requirements of standard, integration, generality, distribution, flexibility, and other specialty, and it provides the theoretical guidance and methods for practical application in SCMDS.

28.2 System Architecture

28.2.1 OSA-CBM Architecture

CBM is a new way of equipment maintenance. With artificial intelligence and other advanced computational methods, diagnostic and prognostic about the remaining useful life (RUL) could be made out timely, and the equipment maintenance scheduling time would be arranged reasonably, by the real-time monitoring of the state of equipment and the working environment [2]. The objective of CBM is to enable the equipment maintenance effectively and timely, to reduce the life cycle costs, to enhance devices reliably, and to avoid the risks and losses which due to the sudden failure of equipment.

OSA-CBM, funded by the US Navy, is formulated by a joint team of experts coming from some well-known companies such Boeing, Caterpillar, Rockwell Automation, Rockwell Science Center, Newport News Shipbuilding, and Oceana Sensor Technologies, issued and managed by Machinery Information Management Open Standards Alliance (MIMOSA). This standardization develops an open-system architecture for CBM, and it is the guidance to achieve the standard

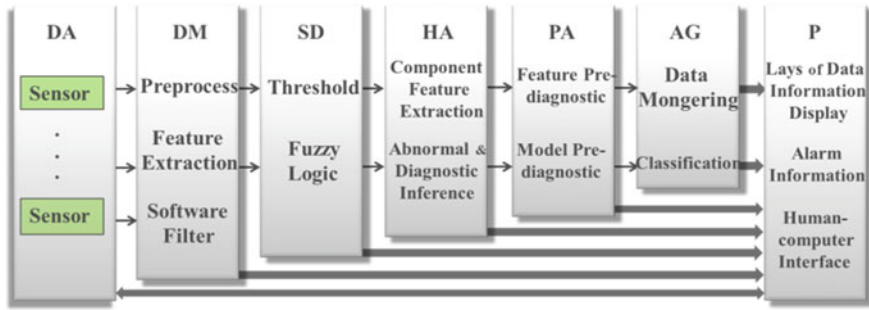


Fig. 28.1 OSA-CBM general framework

framework of CBM system. OSA-CBM system is used to monitor the operation of complex mechanical systems and provide accurate assessment of the system’s current health status to the operators. The goal is that the standardization would drive the CBM supplier to produce interchangeable and interoperable hardware and software components for enhancing system-integration capability.

OSA-CBM consists of 7-layer distributed modules as the Fig. 28.1 showed below. They are data acquisition (DA), data manipulation (DM), state detection (SD), health assessment (HS), prognostics assessment (PS), advisory generation (AG), and presentation (P). OSA-CBM focuses on the description of information and interface specification of each functional layer [3], and provides a reference standard for the formation of SCMDS system architecture. For it lacked of the definition of modules implementation in different layers, thus the SCMDS design based on components has been proposed, referring to the compatible and reconfigurable concepts in OSA-CBM, with adaptability and scalability characteristics.

28.2.2 Component Module System

The Components package specifies a set of constructs that can be used to define software systems of arbitrary size and complexity [4], and they are the modular system which can be released and are replaceable. Component encapsulates the implementation section and provides a set of interfaces, one or more classes of them determining the uses. The most basic goal of component is to develop the system collaborative, and the function is to be the adhesive between multiple modules. System development based on component technology has a high degree of integration, user transparency, openness, reusability, and ease of scalability.

With enough flexible, numbers of different functions of subsystems composed of a distributed monitoring and diagnosis system, through collaboration between the sub-monitoring system, and it can adapt to different devices and various monitoring requirements for giving a comprehensive diagnostic. It is benefit to achieve the

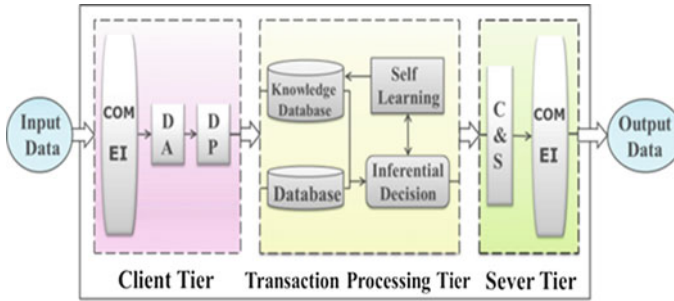


Fig. 28.2 The structure of component module

function of plug and play, using the component module method to build the system. With dynamic configuration and flexible adjustment based on the detection of the AS/RS equipment, SCMDS can form a loose coupling decentralized structure between functional layers, by invoking the various functional components, during the system operation.

Each component has the functional module of DA, data processing (DP), data storage, self-learning, inferential decision, communication, and transmission in SCMDS. Meanwhile, the system exists collaboration and information exchange between the components which could act as a server-side or a client-side. The internal of component could be divided into 3 tier as shown in Fig. 28.2. (1) Client tier, this tier consists of DA and DP modules and supplies the external interfaces (COM EI) for invoking by the other components as the server-side. DA module is responsible for collecting the real-time data uploaded by the data collectors and other modules. DP module is responsible for dealing with the huge amounts of data, in data-level fusion, ensuring the reliability of data. (2) Transaction-processing tier, knowledge database, inferential decision, self-learning, data storage, and other modules compose this tier. Information, uploaded by the client tier, will be processed in feature-level fusion, after data-level fusion processing. Applying the appropriate reasoning mechanism, the target results requested by clients can be figured out, on the basis of rules and methods setting in knowledge database. Data after two levels fusion will be stored in database, meanwhile, improve and expand the knowledge base through self-learning module. (3) Server tier, this tier provides the external interfaces of the component for communication and transmission module (C&S), and its ability is to transmit the data after processing by transaction-processing tier to client-side, or to act as the communication interfaces of client-side to be invoked by the other components. According to the actual situation, component modules can enable all or parts of the functions owned by the internal structure, or insert the relevant functional module based on the actual application requirements. All these make contribution to increasing the reconfigurability and scalability of components.

Client and server (C/S) mode will be used to communicate and transmit between components. Each component can act as a server-side or client-side, calling and transferring target information by invoking the external interfaces. As a

EntryPoint	EntryPointSink
<pre> +epRequestConnection() +epRequestStatus() +epRequestDataSet() +epRequestConfig() +epRequestExplanationDataSet() +epRequestExplanationDataRefSet() +epNotifyControl() +epRequestControl() +epNotifyApp() +epRequestApp() +epRequestErr() </pre>	<pre> +sinkNotifyConnection() +sinkNotifyStatus() +sinkNotifyDataSet() +sinkNotifyConfig() +sinkNotifyExplanation() +sinkNotifyControl() +sinkNotifyApp() +sinkNotifyErr() </pre>

Fig. 28.3 The specific method of EntryPoint and EntryPointSink interfaces representing based on UML

service-side, component provides services to client-side through the EntryPoint interface [5]. Figure 28.3 showed the specific methods. It includes request data connection, request status information, request data sets, request configuration, request explanation, and other methods. EntryPoint interface can be implemented in client tier of component module. As a client-side, EntryPointSink interface of the component would be the data interface for receiving information from the server-side. As the figure displayed below, it contains notify connection, notify status, notify the data sets, notify configuration, and other methods.

Communication between the various components uses simple object access protocol (SOAP) access mode and utilizes Web service for receiving different types of requests. SOAP, relied on Extensible Markup Language(XML), is a protocol specification for exchanging structured information in the implementation of Web services in computer networks [6]. SOAP, based on TCP/IP, is compatible with existing network communication protocol maximally in application layer. Reference to OSA-CBM, communication between the components could use four modes, such as synchronous, asynchronous, service, and subscription, according to the actual situation.

28.3 Design and Implementation of SCMDS

28.3.1 Architecture of SCMDS Based on Components

By using the stack-crane condition information which collected by the DA installed in AS/RS, SCMDS makes prognostic about condition trend and RUL of the system and components, and provides alarm information to the users timely, after data fusion, feature vector extraction, threshold comparison, and other processes. Depending on the HA results and decision support module, reasonable maintenance would be made out, and monitoring and diagnostic function based on condition of stack crane could also be implemented.

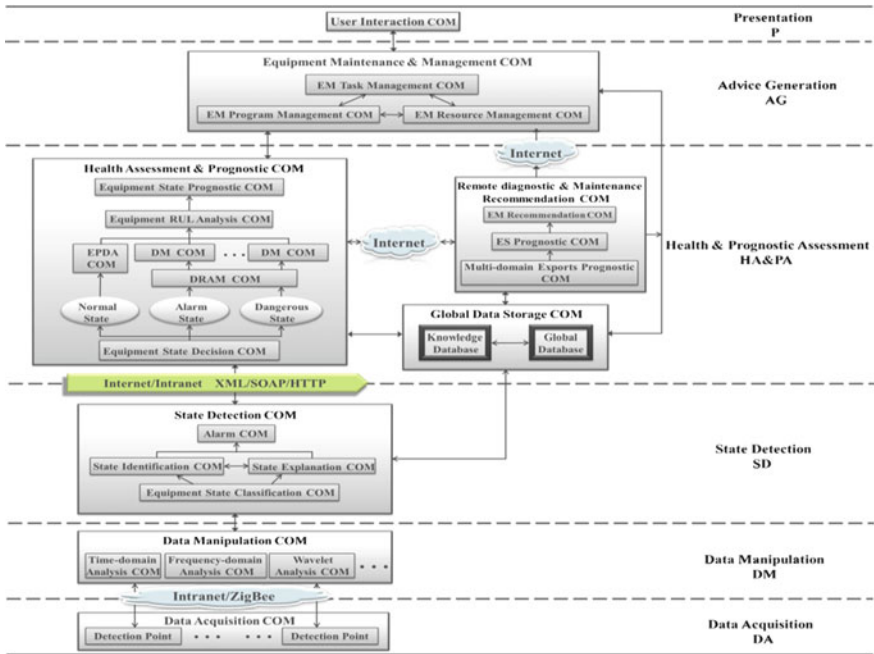


Fig. 28.4 The overall structure of SCMDS. *Note* DRAM COM: diagnostic resource allocation and management components, EPRA COM: equipment performance decline assessment component

Reference to the functional requirements of OSA-CBM system, SCMDS, based on condition, is constituted by data acquisition com (component), data manipulation com, state detection com, HA and prognostic com, remote diagnostic and maintenance recommendation com, global data storage com, equipment maintenance and management com, and user interaction com. Figure 28.4 showed the structure of SCMDS.

Each monitoring point component is contained in data acquisition com. Condition data, collected from a variety of sensors, can be transferred to data manipulation com, via Intranet, Zigbee, or other network transmission. Data acquisition com consists of time domain, frequency domain, Wavelet, and multiple of DP functional components. In accordance with the signal category collected by each sensor, first, selects the corresponding processing component; second, processes the information in global data-level fusion; and third, extracts the feature vectors. In state detection com, equipment state classification component can process the data uploaded from below in feature-level fusion, compare with the relevant threshold, and alarm the over-limit data timely, with the mutual cooperation between state identification component and explanation component.

HA and prognostic component is a multi-component-nested module. Firstly, the monitoring information will be classified into 3 classes: normal, alarm, and danger. Secondly, equipment and components' performance will be assessed by different

processing model, judging whether the system or sub-system is under the performance decline phase. Thirdly, by using many diagnostic model components (DM COM), the health of system will be assessed. Finally, with analyzing the faults that may occur or has occurred, the RUL and operation trend will be prognosed. Fault tree analysis (FTA) method is the usual diagnostic model; choosing this model could not only locate the equipment exception quickly, but also expand the equipment fault knowledge base timely with self-learning function. At meanwhile, it can provide theoretical guidance for the production pre-design and post-maintenance. The following will detail the implementation of diagnostic component in SCMDS, using FTA as an example.

When the local HA and prognostic component cannot meet the diagnostic capabilities of the system, the remote diagnostic and maintenance recommendation component would be invoked via the Internet, diagnosing the system and components of stack crane in detail, with the multi-expert systems provided by professional organizations. In equipment maintenance and management component, combining the diagnostic information supplied by HA and prognostic component and remote maintenance recommendation, the maintenance can be made out according to the optimized plan that system provided, after processing the data in decision-level fusion. Equipment maintenance task will be arranged depending on the inventory of maintenance resource, and the final plan will be submitted to the user interaction component for displaying. User interaction component is used to display all the information of the other six-layer modules in the SCMDS. Operators can invoke any layer module in accordance with the interfaces that components provided, and choose the optimal project from a variety of maintenance programs to be implied, through the way of human-computer interaction. User interaction component includes user authority component and equipment ledger component. The former provides the corresponding monitoring information to the different managers, and the latter establishes the management log and gives the reference to the decision-maker for managing and procuring the devices, during the life cycle. As the center data storage for the entire system, global data storage component updates the system database timely and improves knowledge database, using the target results, history records, and maintenance logs, in order to enhance reliability and practicality of SCMDS. Because of favorable to increase the compatibility and normalization for DP and invoking, all messages storage format will be regulated in XML format in global data storage component.

28.3.2 Implementation of SCMDS Based on Components

28.3.2.1 Implementation of Diagnostic Model Component

Health diagnostic module is the core component of SCMDS, the stability, security, and economic maintenance of operational stack crane will be impacted directly by the timeliness and accuracy of health diagnostic. Choosing diagnostic model is a

complex job in HA and prognostic component. By selecting single or combining different diagnostic models, the work of ascertaining and identifying the hidden danger and initial abnormality, locating fault rootstock and prognosing RUL of stack crane can be accomplished, as providing a theoretical basis for the formulation of maintenance. FTA model component, as a single instance of the diagnostic model component in HA and prognostic component of SCMDS, would be introduced in detail.

FTA model component used the general component of SCMDS. With the connection and invocation with other components, information of diagnostic or provided by management component can be processed, fused, and transferred to the transaction-processing tier, in client tier. In transaction-processing tier, through analyzing the operational control principle of stack crane, stack-crane faults figure could be constructed by using FTA method [7], with combination of equipment common faults [8]. After putting up the knowledge database in this tier, the minimum cutsets of stack-crane's faults can be found out and be used as a basis to diagnose equipment.

The system is divided into two parts according to the working and control principle of stack crane, and these are mechanical system and electrical control system. Mechanical system consists of rack, traveling mechanism, lifting mechanism, telescoping fork mechanism, object stage, and accessing cargo mechanism. Electrical control system is composed by main circuit, electric traction, control detection, security protection, and other mechanism. As Fig. 28.5 showed, a fault tree with '*stacker-crane fault*' as the top event first branched into '*mechanical system fault*' and '*electrical control system fault*.' Then, the node '*mechanical system fault*' further split into three branches: '*traveling mechanism fault*,' '*lifting mechanism fault*,' and '*fork mechanism fault*.' Meanwhile, the mother node '*electrical control system fault*' forked into two branches: '*main circuit fault*' and '*control mechanism fault*.' Finally, the fault tree continued to develop to the bottom events from the five branches.

In the fault tree of stack crane, E represents composite parts, and X represents minimum cutsets. Minimum cutsets are all possible unique combinations of component failures that cause a system failure (top event). The minimum cutsets of stack crane are {X1}, {X2}, ... {X39}.

Using FTA knowledge database to diagnose the hidden danger and abnormality of stack crane in transaction-processing tier, then submit diagnostic result to server tier, meanwhile, stores them in database. When FTA model in knowledge could not diagnose the faults, it should invoke other diagnostic model components or remote diagnostic component to completing diagnostic function, and update knowledge database by self-learning function in transaction-processing tier for expanding fault tree of stack crane and consummating FTA diagnostic model component.

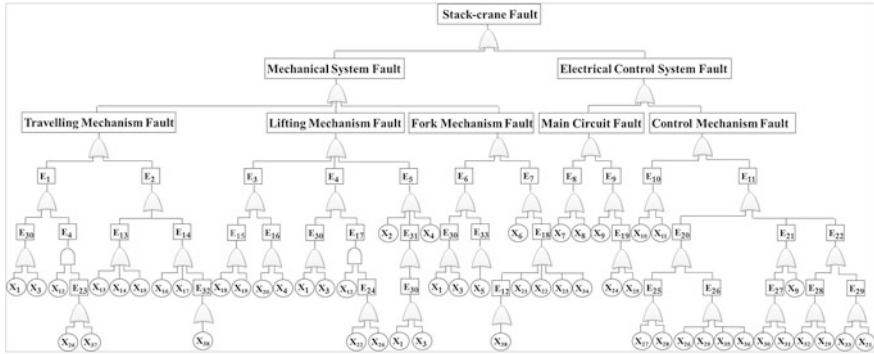


Fig. 28.5 Stack-crane fault tree diagram. *Note* E1 driving system of traveling mechanism fault; E2 mechanical system of traveling mechanism fault; E3 loading shelf fault; E4 speed changer mechanism of lifting mechanism fault; E5 lifting mechanism fault; E6 driving system of fork mechanism fault; E7 fork failed to stretch; E8 open phase; E9 no voltage at both ends of the motor; E10 software fault; E11 hardware fault; E12 Fork-stretched overrun; E13 skew traveling of crane’s running gears; E14 stacker-crane running unstable; E15 loading shelf running unstable; E16 loading shelf falling; E17 transmission fault; E18 obstruction in the movement of fork; E19 electric transmission line fault; E20 unable to locate accurately; E21 frequency conversion fault; E22 fork is out of control; E23 reduction gear fault; E24 speed changer box fault; E25 error positioning; E26 positioning in the wrong location; E27 no variable speed control signal; E28 location failed to store cargo; E29 fork failed to moving; E30 motor fault; E31 reel destruction; E32 traveling mechanism only forward and backward; E33 gearbox failure; X1 motor bearings fault; X2 tilt wheel; X3 excessive load; X4 wire rope breaking; X5 cycloid fault; X6 clutch fault; X7 capacitor failure; X8 power failure; X9 frequency converter fault; X10 human error in operation; X11 faulty data communication; X12 motor running normally; X13 track installation error; X14 traveling wheel deviation; X15 track under poor maintenance; X16 track existing a certain slope; X17 brake fault; X18 columns deformation; X19 track supporting wheels wearing down; X20 fall-proof machine fault; X21 fork failed to stretch; X22 pinion and rack fault; X23 chain and sprockets fault; X24 cable fault; X25 sliding contact device fault; X26 coupling fault; X27 address identification device fault; X28 identification bar loosen or migrated; X29 other failures; X30 arithmetic unit of control system fault; X31 counter fault; X32 sensor faults; X33 fork stretching out overtime; X34 fork buffer spring loose; X35 high-level photoelectric switch loose or damaged; X36 forward photoelectric switch loose or damaged; X37 decelerating bearing fault; X38 limit switches loose

28.4 Conclusions

CBM is a new way for equipment maintenance, making up, and solving the problem of excess or lack of maintenance. Based on the framework of OSA-CBM, using stack crane in AS/RS as an example, this paper has introduced the structure and implementation of SCMDS based on components. Utilizing OSA-CBM standardization, it is benefit to improving the system’s generality and standards. The distribution of system with collaboration functions will be realized by adopting the component technology, and it makes contribute to accommodating to the heterogeneity and loose coupling environment in SCMDS, therefore increasing self-adaptive ability of the system. The implementation of single component module has

been detailed by using FTA diagnostic model component as an instance. The uniform interfaces provided by the system for achieving plug-and-play functionality, with integrating the core part of each component into transaction-processing tier, through consummating component knowledge database by self-learning module, would enhance the reconstruction and scalability of components and system. The proposed SCMDS based on components has provided the theoretical guidance for the practical application of the system in development and implementation stage.

References

1. Zhou QC (2002) Study on control and management techniques of automated storage and retrieval system (AS/RS) basing on modern logistics. Southwest Jiaotong University (in Chinese)
2. Guo QJ, Xu AD, Yu HB (2005) Research on open standards for condition—based maintenance. Shandong Univ (Eng Sci) 6:213–217 (in Chinese)
3. Thurston MG (2001). An open standard for Web-based condition-based maintenance systems. In: IEEE systems readiness technology conference autotestcon proceedings, pp 401–415
4. OMG Unified Modeling Language Specification (Version2.4.1), August 2011
5. MIMOSA OSA-CBM 3.3.1, Post date: 20 Aug 10. www.mimosa.org
6. Jing B, Tan Z, Li JL (2006) Design and implementation of embedded web sensor network communication module. Comput Eng 2:215–219 (in Chinese)
7. Vesely WE, Roberts NH, Hassl DF (1987) Fault tree handbook. Government Printing Office, Washington
8. Xiong XL, Zhao J, Zhou QC (2002) Research on abnormality detection and self-recovery ability of automated storage/retrieval machine. Hoisting Conveying Mach 9:1–4 (in Chinese)

Part IV
Conveying Machinery Technology
Research (CMTR)

Chapter 29

The Research of Integrated Supply Chain Model Rested on Joint Ordering

Wenxue Ran and Yang Yu

Abstract The integrated supply chain is to integrate positive sources and distribute them in order to maximize the benefits of supply chain and utilize these advantages. The essay is based on the actual optimization cost on warehouse inventory of joint ordering model and the test of cases that will resolve the practical issues, so as to optimize inventory, reduce costs, and improve the efficiency.

Keywords Combined purchase · Supply chain integration · Model

29.1 Introduction

Supply chain management (SCM) is one of management theories, which was raised in the early 1980s. At first, the theory referred to the coordination and management among internal market, sales, planning, purchasing, and manufacturing within a firm. Then, it evolved toward the supply and demand management between enterprises and their suppliers, and the chain management from resource suppliers, manufacturers, and retailers to clients. Modern SCM emphasizes on a network-type management, which is a functional network management model including planning, coordinating, and controlling from resources supplying, through producing process to selling network, then to combine the suppliers, manufacturers, distributors and retailers, and finally to the customers, which can make sure to transfer the right products to right clients in right time and places [1, 2].

Integrated supply chain is designed based on supply chain operations reference model (SCOR) developed by International Supply Chain Council [3, 4] in which integrated supply chain is a network structure, which consists of members of

W. Ran
School of Logistics, Yunnan University of Finance and Economics, Kunming, China

Y. Yu (✉)
ZHONGHUA Vocational College, Yunnan University of Finance and Economics,
Kunming, China
e-mail: yy0309@yeah.com

suppliers, manufacturers, distributors, retailers, and customers. Members supply resources, components, products, and services mutually; via redesigning, planning, and controlling of the distributions, information flows and fund flows, it can guarantee to transfer right products or services in right amount or standard to right places in appropriate time, thereby, to improve the customers' satisfaction level and lessen the total cost of supply chain [5].

Integrated supply chain can achieve the optimal allocation of resources firstly. It uses the resources efficiently by allocating employers, funds, information, and materials. When resources are limited, the rational and optimal utilization of resources among enterprises will be achieved. Secondly, it can improve the service level. The existence and development of supply chain focus on meeting customer needs, and the integrated supply chain is to pursue more efficient service and take advantages to raise customer satisfaction and loyalty. Thirdly, it can maximize the core competitiveness of related enterprises. In SCM theory, all the enterprises should collect energy and resources to improve the core competitiveness. As a result, this will not only improve the core competitiveness of cooperative enterprises but also achieve integration of the whole supply chain and improvement of competitive capacity.

Many domestic scholars conducted a number of in-depth researches and exploration of supply chain, which are based on the combined purchase. Xu Xin proved that the joint order of a variety of products has certain effect on SCM and coordination; Qin Junxue have studied the financial constraints on the optimization model, which includes multi-commodity order in order to minimize inventory cost [6]; Liu Bin, studied a class of short-life cycle products in terms of the order- and price-united deciding system in stochastic demands price-dependent circumstances; the research showed that "the system performance is mainly from sales of the first stage, the operator should focus more on making profits on this stage" [7].

The essay will rest on the joint ordering model in order to research the integration of supply chain. It will get the solution of integrated model and will be verified with examples to improve the market competitiveness of the enterprise.

29.2 The Integrated Supply Chain Model of the Joint Ordering

In order to ensure continuous production in the producing process, it must set a certain amount of inventory, of which the essential stocks can be optimized by the joint ordering. For solving problems by the joint ordering more conveniently, assume that:

1. The demand of each product is fixed;
2. The replenishment quantity of products may appear the decimal;
3. Shortages will not be allowed;
4. Instant delivery of ordered goods, the lead time is zero.

Letters are defined as follows:

1. K —the subscription fee for ordering products only related to order number, not species;
2. f_i —additional costs, which the I product need to pay;
3. Q_i —market demand rate of the I product;
4. d_i —unit cost of the i product;
5. n —the number of product categories;
6. h —the percentage of inventory holding cost per unit in purchasing cost per unit.

29.2.1 The Model of Ordering All Products at the Same Time

There is a need to prepare goods and materials for projects of the company, which enjoys the same order cycle time. When ordered, each product needs to be ordered once. It can be assumed that the order cycle time of products is T , and there are N kinds of products prepared to order; therefore, the average inventory level for the I product is:

$$\bar{I}_i = \frac{D_i}{2} = \frac{Q_i T}{2} \tag{29.1}$$

The average total cost per unit time is:

$$C = \left(\frac{K + \sum_{i=1}^n f_i}{T} + \sum_{i=1}^n \frac{Q_i T h d_i}{2} \right) \tag{29.2}$$

To make cost C of the average cost per unit time minimum, it is required to determine the optimal order cycle time T' .

Let $\frac{\partial C}{\partial T} = 0$, then the optimal order cycle time is:

$$\frac{\partial C}{\partial T} = \left(\frac{K + \sum_{i=1}^n f_i}{T} + \sum_{i=1}^n \frac{Q_i T h d_i}{2} \right) = 0$$

And it can be obtained the equation:

$$\frac{K + \sum_{i=1}^n f_i}{T^2} = \sum_{i=1}^n \frac{Q_i T h d_i}{2} \tag{29.3}$$

If set $T^2 = R$, so

$$R = \frac{K + \sum_{i=1}^n f_i}{\sum_{i=1}^n Q_i d_i} \times \frac{2}{h} \tag{29.4}$$

and it can be obtained T' :

$$T' = \left(\frac{K + \sum_{i=1}^n f_i}{\sum_{i=1}^n Q_i d_i} \times \frac{2}{h} \right)^{\frac{1}{2}} \tag{29.5}$$

Putting Formula (29.5) into Formula (29.2), the minimum cost per unit can be worked out C' :

$$\begin{aligned} C' &= \sqrt{\frac{(K + \sum_{i=1}^n f_i)^2 \times h \times \sum_{i=1}^n Q_i d_i}{2(K + \sum_{i=1}^n f_i)}} + \sqrt{\frac{2(K + \sum_{i=1}^n f_i) \times h^2 \times (\sum_{i=1}^n Q_i d_i)^2}{4 \times h \sum_{i=1}^n Q_i d_i}} \\ &= \sqrt{2 \left(K + \sum_{i=1}^n f_i \right) h \sum_{i=1}^n Q_i d_i} \end{aligned} \tag{29.6}$$

The optimal order batch of the i product is:

$$D_i = Q_i * T' \tag{29.7}$$

And the optimal average inventory level of the I product is:

$$\bar{I}_i = \frac{D_i}{2} = \frac{Q_i T'}{2} \tag{29.8}$$

29.2.2 The Model of Some Products Joint Ordering

As the frequency of ordering various products is different, when the prepared goods are out of stock, it will be more favorable to use joint ordering method for a part of goods. Assume m_i to mean the order cycle time of the various products is m_i times of the basic order cycle time. So, the average inventory level of the I product is $\bar{I}_i = \frac{D_i}{2} = \frac{Q_i m_i T}{2}$. Thus, when n kinds of products joint ordering, the average total cost per unit time is:

$$C^* = \frac{K + \sum_{i=1}^n \frac{f_i}{m_i}}{T} + \sum_{i=1}^n \frac{Q_i m_i T h d_i}{2} \tag{29.9}$$

Set $\frac{\partial C}{\partial T} = 0$, then the optimal order cycle time is: (with the same derivation step of all products ordered)

$$T' = \left(\frac{K + \sum_{i=1}^n \frac{f_i}{m_i}}{\sum_{i=1}^n Q_i d_i} \times \frac{2}{h} \right)^{\frac{1}{2}} \tag{29.10}$$

Putting Formula (29.10) into Formula (29.9), the result is:

$$C' = \sqrt{2} \times \sqrt{\left(K + \sum_{i=1}^n \frac{f_i}{m_i} \right) h \sum_{i=1}^n Q_i d_i} \tag{29.11}$$

29.2.3 The Optimal Strategy of Joint Ordering

To work out the lowest average total cost C^* of the system, it has to make optimal order multiplier m_i best. To make the C^* minimum, it should work out the

$$F(m_1, \dots, m_n) = \left(K + \sum_{i=1}^n \frac{f_i}{m_i} \right) h \sum_{i=1}^n m_i Q_i d_i$$

Make $F(m_1, \dots, m_n)$ on the partial derivative m_i to zero, the derivation process:

First assume $n = 2$, then

$$F(m_1, m_2) = \left(K + \frac{f_1}{m_1} + \frac{f_2}{m_2} \right) h (m_1 Q_1 d_1 + m_2 Q_2 d_2) \tag{29.12}$$

Find the partial derivatives:

$$-\left(\frac{f_1}{m_1^2} \right) (h m_1 Q_1 d_1 + h m_2 Q_2 d_2) + \left(K + \frac{f_1}{m_1} + \frac{f_2}{m_2} \right) h Q_1 d_1 = 0$$

then:

$$-f_1 (m_1 Q_1 d_1 + m_2 Q_2 d_2) + m_1^2 Q_1 d_1 \left(K + \frac{f_1}{m_1} + \frac{f_2}{m_2} \right) = 0$$

Solution obtained:

$$m_1^2 = \frac{f_1 \sum_{i=1}^2 m_i Q_i d_i}{Q_1 d_1 \left(K + \sum_{i=1}^2 \frac{f_i}{m_i} \right)} \tag{29.13}$$

Similarly,

$$m_2^2 = \frac{f_2 \sum_{i=1}^2 m_i Q_i d_i}{Q_2 d_2 \left(K + \sum_{i=1}^2 \frac{f_i}{m_i} \right)} \tag{29.14}$$

Generally, the derivative of the variable is m_i , from

$$F(m_1, \dots, m_n) = \left(K + \sum_{i=1}^n \frac{f_i}{m_i} \right) h \sum_{i=1}^n m_i Q_i d_i = K \sum_{i=1}^n m_i Q_i d_i + \sum_{i=1}^n \frac{f_i}{m_i} \sum_{i=1}^n m_i Q_i d_i. \tag{29.15}$$

Make the derivation of the formula above equal to zero, then can find

$$m_i^2 = \frac{f_i \sum_{i=1}^n m_i Q_i d_i}{Q_i d_i (K + \sum_{i=1}^n \frac{f_i}{m_i})} \tag{29.16}$$

By comparison with $n = 1$ and $n = 2$, the results $\sum_{i=1}^n m_i Q_i d_i$ and $\sum_{i=1}^n \frac{f_i}{m_i}$ are unchanged. But the $\frac{f_i}{Q_i d_i}$ part changes with the change of n . Therefore, the following re-introduction of a variable j changes the Formula (29.16) to:

$$m_j^2 = \frac{f_j \sum_{i=1}^n m_i Q_i d_i}{Q_j d_j (K + \sum_{i=1}^n \frac{f_i}{m_i})}, \quad j = 1, 2, \dots, n. \tag{29.17}$$

To minimize value of the $\frac{f_j}{Q_j d_j}$, then $m_1 = 1$ when the corresponding product is the first product, then by Formula (29.17):

$$m_j = \sqrt{\frac{f_j}{Q_j d_j}} \times \sqrt{\frac{\sum_{i=1}^n m_i Q_i d_i}{K + \sum_{i=1}^n \frac{f_i}{m_i}}}$$

make

$$\Phi = \sqrt{\frac{\sum_{i=1}^n m_i Q_i d_i}{K + \sum_{i=1}^n \frac{f_i}{m_i}}} \tag{29.18}$$

Then,

$$m_j = \Phi \times \sqrt{\frac{f_j}{Q_j d_j}}, \quad j = 1, 2, \dots, n \tag{29.19}$$

The result:

$$\begin{aligned} \sum_{i=1}^n m_i Q_i d_i &= m_1 Q_1 d_1 + m_2 Q_2 d_2 + \dots + m_n Q_n d_n = Q_1 d_1 \\ &+ \sum_{i=2}^n \Phi \sqrt{\frac{f_i}{Q_i d_i}} \times Q_i d_i = Q_1 d_1 + \Phi \sum_{i=2}^n \sqrt{f_i Q_i d_i} \end{aligned} \tag{29.20}$$

It can be concluded:

$$\sum_{i=1}^n \frac{f_i}{m_i} = f_1 + \frac{1}{\Phi} \sum_{i=2}^n \sqrt{f_i Q_i d_i} \tag{29.21}$$

Putting Formula (29.20) and Formula (29.21) into Formula (29.18), we get:

$$\frac{Q_1 d_1 + \Phi \sum_{i=2}^n \sqrt{f_i Q_i d_i}}{K + f_1 + \frac{1}{\Phi} \sum_{i=2}^n \sqrt{f_i Q_i d_i}} = \Phi^2 \tag{29.22}$$

be simplified:

$$\Phi = \sqrt{\frac{Q_1 d_1}{K + f_1}}. \tag{29.23}$$

Putting Formula (29.13) into Formula (29.10), we get

$$m_j = \sqrt{\frac{Q_1 d_1}{K + f_1} \frac{f_j}{Q_j d_j}}, \quad j = 1, 2, \dots, n \tag{29.24}$$

Therefore, we get the following optimal algorithm of the joint ordering strategy:

1. Make the product whose $\frac{f_i}{Q_i d_i}$ value is minimum as the first product, note $m_1 = 1$;
2. To calculate $m_i = \sqrt{\frac{Q_1 d_1}{K + f_1} \frac{f_i}{Q_i d_i}}$, and make m_i close to integer;
3. Use Formula (29.10) to calculate T' ;
4. Calculate the optimal order quantity $D_i = m_i Q_i T', i = 1, 2, \dots, n$.

29.3 Case Analysis

Assume that a company needs to order 5 kinds of goods, the fixed cost of each ordering is $K = 60$ Yuan, the annual year inventory carrying cost per unit account for the purchase cost $h = 20\%$. The ordering cost of components and parts is f_i , the cost of product per unit is d_i , and the annual demand rate is Q_i (see Table 29.1).

1. If under the previous method of one-time procurement of all goods, the total cost is:

$$\begin{aligned} C'_1 &= K + \sum_{i=1}^5 f_i + \sum_{i=1}^5 Q_i h d_i = 60 + 10 \times 5 + (25 \times 20\% \times 300 + 40 \times 20\% \times 200 \\ &\quad + 100 \times 20\% \times 50 + 200 \times 20\% \times 10 + 30 \times 20\% \times 150) = 5,510 \text{ Yuan} \end{aligned}$$

Table 29.1 The related parameter values of five materials

Product i	1	2	3	4	5
f_i	10	10	10	10	10
d_i	300	200	50	10	150
Q_i	25	40	100	200	30

2. If you use “the model of ordering all products at the same time,” known by Formula (29.2), the optimal order cycle $T' = 0.202$ year ≈ 11 weeks; putting T' into Formula (29.3), we can calculate the optimal average cost as follows:

$$C' = \sqrt{2} \times \sqrt{(K + \sum_{i=1}^n \frac{f_i}{m_i})h \sum_{i=1}^n Q_i d_i} = 1,089.95 \text{ Yuan}$$

The total cost is: $C'_2 = C' \times 365/7/T' = 1,089.95 \times 365/7/11 = 5,166.67$ Yuan

The order batch of each kind of material is: $D_1 = Q_1 \times T = 25 \times 0.128 \approx 3$ units and can be calculated in the same way that $D_2 \approx 5$ units, $D_3 \approx 13$ units, $D_4 \approx 26$ units, and $D_5 \approx 4$ units.

3. If you use “the model of some products joint ordering,” $m_1 = 1$, and use Formula (29.14) to calculate:

$$m_2 = \Phi \sqrt{\frac{f_i}{Q_i d_i}} = \sqrt{\frac{Q_1 d_1}{K + a_1}} \times \sqrt{\frac{f_2}{Q_2 d_2}} = \sqrt{\frac{25 \times 300}{70}} \times \frac{10}{200 \times 40} = 0.37 \rightarrow 1$$

$$m_3 = \sqrt{\frac{25 \times 300}{70}} \times \frac{10}{100 \times 50} = 0.46 \rightarrow 1$$

$$m_4 = \sqrt{\frac{25 \times 300}{70}} \times \frac{10}{200 \times 10} = 0.732 \rightarrow 1$$

$$m_5 = \sqrt{\frac{25 \times 300}{70}} \times \frac{10}{150 \times 30} = 0.488 \rightarrow 1$$

The basic order cycle is:

$$\begin{aligned}
 T' &= \sqrt{\frac{K + \sum_{i=1}^n \frac{f_i}{m_i}}{\sum_{i=1}^n m_i Q_i d_i}} \times \frac{2}{h} \\
 &= \sqrt{\frac{2 \times (60 + \frac{10}{1} + \frac{10}{1} + \frac{10}{1} + \frac{10}{1} + \frac{10}{1})}{0.2 \times 1 \times (300 \times 25 + 200 \times 40 + 50 \times 100 + 10 \times 200 + 150 \times 30)}} \\
 &= 0.202 \text{ year} \approx 11 \text{ weeks}
 \end{aligned}$$

Table 29.2 The total cost of the three ordering methods comparison chart

	Method 1	Method 2	Method 3
Total cost (Yuan)	5,510.00	5,166.67	5,166.67

The order batch of each kind of product is:

$$\begin{aligned}
 D_1 &= 1 \times 300 \times 0.143 \approx 50; & D_2 &= 1 \times 200 \times 0.143 \approx 29; \\
 D_3 &= 1 \times 50 \times 0.143 \approx 7; & D_4 &= 1 \times 10 \times 0.143 \approx 1; \\
 D_5 &= 1 \times 150 \times 0.143 \approx 21
 \end{aligned}$$

Putting the above results into Formula (29.5), one can get the optimal average total cost as:

$$\begin{aligned}
 C' &= \sqrt{2} \times \sqrt{\left(K + \sum_{i=1}^n \frac{f_i}{m_i}\right) h \sum_{i=1}^n m_i Q_i d_i} \\
 &= \sqrt{\left(60 + \frac{10}{1} \times 5\right) \times 0.2 \times (300 \times 25 + 200 \times 40 + 50 \times 100 + 10 \times 200 + 150 \times 30)} \times \sqrt{2} \\
 &= 1089.95 \text{ Yuan}
 \end{aligned}$$

The total cost is:

$$C'_3 = C' \times 365/7/T' = 1,089.95 \times 365/7/11 = 5,166.67 \text{ Yuan}$$

According to the calculation results of the specific circumstances of the case above in three different ways, the cost of one-time purchase of several products is much higher than the joint ordering model cost. And from reasonable storage, the use of joint ordering model can significantly reduce the maximum inventory levels, which will achieve storage rationalization (Table 29.2).

29.3.1 Closing

In this paper, the joint ordering model is utilized in the integrated supply chain to solve the optimization of inventory and supply chain costs, and applied to practical business to resolve practical problems.

Joint ordering model analyzes the materials needed, tested by two different models and to compare the costs of three different methods. The model shows the advantages and the cost saving, and also reflects the conception of optimization of reducing inventories. After the case analysis, we can see the advantages of the joint ordering model and the effectiveness in the applying process.

The method in the essay—joint ordering model—is based on the corresponding assumptions. But, the assumption will not affect the non-specific industry. Therefore, it has a universal adaptability.

References

1. Cox JF, Blackstone JH, Spencer MS (eds) (1995) APICS Dictionary, 8th ed. American Production And Inventory Control Society, Falls Church, VA
2. Li Y, Ran W, Xie K (2008) Introduction to logistics management. Science Press
3. Wu X (2007) Supply chain integration. China Bus Mark (02)
4. Wiesner, Li Y (2006) Balanced approach to supply chain management principles. Tsinghua University Press
5. Christopher, Mingke HE (2006) Logistics and supply chain management. Publishing House of Electronic Industry
6. Qin J, Dai G (2008) A multi item ordering model with incremental quantity discount and fund constraint. J Qingdao Univ (03):79–81
7. Liu B, Liu S, Qiu G (2007) Jointed decision model on ordering and pricing for short-life-cycle product. J Nanjing Univ Aeronaut Astronaut 39(5):69–69

Chapter 30

The Necessity of Construction of the Three Gorges Emergency Logistics Base and Its Measures

Juan Wang, Weijun He and Yasan Fu

Abstract The passage investigated natural hazard, which occurred in the Three Gorges and periphery area. The major hazards include drought, heavy rain, and floods; in addition, there are geological hazards, which include landslide, rock fall, debris flow, earthquake, and so on. What is more, the passage has collected a lot of related data about natural hazards that took place in Yichang City of Hubei Province, the city of Chongqing, and the Hubei Province as a whole from 2004 to 2010. This passage analyzed the data. The natural hazard that occurred in Hubei Province and the city of Chongqing has become extremely serious. The number of such hazard events is on a rising trend from 2009. As the natural hazard that occurred in the Three Gorges is uncertain and unexpected, it is important to build an emergency logistics base in the Three Gorges. Such base can provide vigorous rear rescue activity quickly to avoid the natural hazard. Based on the investigation on the variety of natural hazards in this area, the time of such hazards, and frequency, this passage provided several measures.

Keywords Three Gorges area · Natural hazard · Emergency logistics base

30.1 Introduction

The three gorges region stretches across two provinces; they are Hubei and Chongqing. From east to west, there are: Xiling Gorge, Wu Gorge, and Qutang Gorge. The three gorges dam, which is located in the middle of Xiling Gorge of Yichang City in Hubei Province, is the world's largest hydropower project in the world. Due to its complex geological structure, natural disasters of the three gorges region include drought and heavy rains flooding, along with geological disasters,

J. Wang (✉) · W. He (✉) · Y. Fu
Economic and Management College, China Three Gorges University,
Yichang 443002, Hubei, China
e-mail: 804499808@qq.com

© Springer-Verlag Berlin Heidelberg 2015
Logistics Engineering Institution, CMES (ed.),
Proceedings of China Modern Logistics Engineering,
Lecture Notes in Electrical Engineering 286, DOI 10.1007/978-3-662-44674-4_30

such as landslides, avalanches, landslides, ground subsidence, which are triggered by heavy rain floods.¹ In recent years, with the risen water level of the three gorges reservoir, a large number of low-lying mountains are being flooded, causing the reservoir bank to be collapsed and the occurrence of landslides; this has caused the natural disaster occurred increasingly frequent. In particular, in 2009, since the three gorges project conducted 3 times 175 m of pilot water, the losses of two provinces of Hubei and Chongqing have made natural disasters grow exponentially.

Facing with the frequency of such disaster occurred in three gorges area, government departments have taken some measures, such as monitoring, early warning, relocation, and construction management; there is still a lack of awareness of the necessity to construct the three gorges emergency logistics base. However, the government departments still did not realize the importance of constructing the three gorges base. At least, the following three aspects are to be noted.

30.2 The Necessity of Construction of the Three Gorges Emergency Logistics Base

30.2.1 The Natural Disasters of the Three Gorges Occur with High Frequency

The three gorges region stretches across two provinces, Hubei and Chongqing. And the three gorges dam sited in Zigui county of Yichang City. Due to the natural conditions and geological condition are complex in the Three Gorges, there are more and more rainstorm, the flood, and geologic hazard. In recent years, with the engineering construction of the three gorges continue advancing, the natural disasters of the three gorges area occurred more and more frequent. This article collected data of natural disaster in Yichang City, Hubei Province, and Chongqing City in order to make a full analysis.

30.2.1.1 The natural disasters of Yichang City, Hubei Province

(1) The natural disasters of Hubei Province

Hubei Province is located in China's south-central, which is a part of the three gorges region. Due to complex geological condition, abundant amount of rainfall, and human engineering activities, there is a high frequency of occurrence of geological disasters in this region. As can be seen from Fig. 30.1, in the period 2002–2010, the natural disaster losses of Hubei remain at 1,000,000 ha; however, it

¹ See Ref. [1].

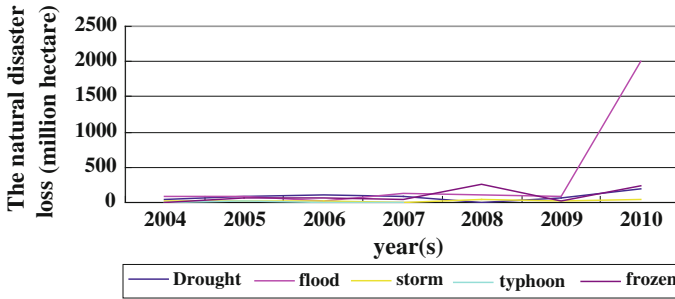


Fig. 30.1 2004–2010 Hubei Province natural disaster losses

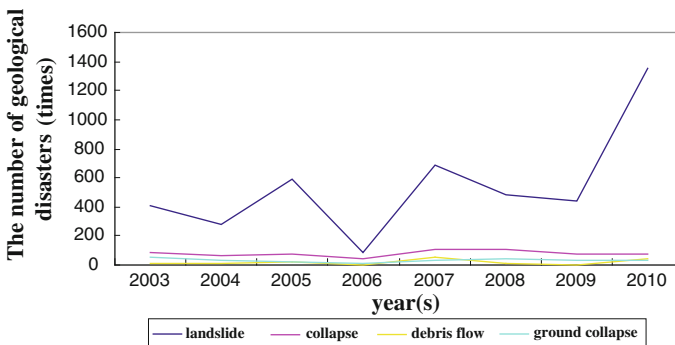


Fig. 30.2 2003–2010 Hubei Province, the main geological disasters

rises substantially in 2010, reached to 19,989,000 ha and rose nearly 20 times.² The reason for this phenomenon lies in the fact that there are three water storage experiments that caused the water level rising up to 175 m in the three gorges dam in 2009; another reason is that the number of geological disasters occurrence is still increasing. From Figs. 30.1 and 30.2, we can see that the natural disaster types of Hubei Province are drought, flood, and waterlogging followed by geological disasters, such as landslides, avalanches, landslides, ground subsidence. Landslide is the most serious.

According to the article «Geological disaster prevention and control planning in Hubei Province during 2003 to 2015», there are more than 5,657 geological disasters in Hubei Province, among which there are 267 major geological disaster points. These disasters mainly occurred in three gorges area and western area of Hubei Province from Badong to Xintan.³ Natural disasters in three gorges area take mainly place of the disaster of Hubei Province (Fig. 30.3).

² See Ref. [2].

³ See Ref. [3].



Fig. 30.3 Hubei Province natural disaster-prone areas topographic maps

Table 30.1 Geological disaster type and frequency

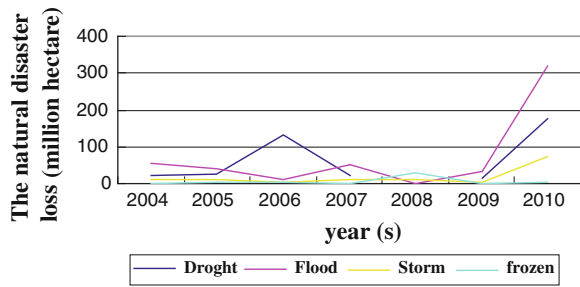
Geological Disaster type	Landslide	Collapse	Earth’s surface sinking	Debris flow	Ground fissure
Frequency	1,709	523	94	19	17

(2) The natural disaster in Yichang city

Yichang City, located in southwest of Hubei province, builds its connection with upper and middle Yangtze River and is the site of three gorges dam. Due to its complex geological condition and high-frequency rainstorm, Yichang City is one of the heaviest natural disaster areas in China. These disasters mainly located in three gorges area, Qingjiang River, and phosphate rock and along the roads area. According to the article <Geological disaster prevention and control planning in Yichang City during 2010–2020>, there are more than 284 significant levels of geological disaster in Yichang, among which there are 106 super level. After China was established in 1949, the geological disaster has so far caused 446 people death in Yichang.⁴ If we look at Table 30.1, the geological disaster in Yichang is mainly landslide, which located in three gorges area and Qingjiang area act.

⁴ See Ref. [4].

Fig. 30.4 Chongqing natural disaster situations from 2004 to 2010



30.2.1.2 The Natural Disaster in Chongqing Province

Chongqing Province, the economic center of the upper Yangtze River, is located in the west-south of China as a part of three gorges area. Due to its complex geological condition and high-frequency rainstorm, Chongqing City is one of the heaviest natural disaster areas in China. If we look at Fig. 30.4, the major type of its natural disasters are drought and flood; followed by that we can see the geological disasters such as landslides, avalanches, landslides, ground subsidence landslide, which is the most serious. The disaster loss fluctuates around 100 million from 2004 to 2009 while the loss reaches 320.5 million in 2010, which is a 3 times growth compared to 2004. The reasons for these damages are the same as Hubei Province.

According to <Geological disaster prevention and control planning of Chongqing City in 2004–2015>, there are more than 8,301 geological disaster risks hidden in Chongqing by the end of 2003, within 2,480 natural disaster in the three gorges reservoir area and 5,821 outside of it. Its geological disaster types are as follows (Table 30.2).⁵

Judging from the geological disaster occurring in these two areas, we can make the following conclusion:

- (1) In three gorges area, Yichang Province and Chongqing Province are world famous for three gorges dam. Due to its complex geological features, three gorges area’s natural disasters are mainly drought and flood; the following are geological disasters that include landslide, collapse, debris flow, ground subsidence act.
- (2) From Figs. 30.1, 30.2, and 30.3, the natural disasters that occurred at three gorges area have low frequencies from 2004 to 2009. However, with water storage achieves 175 m in three gorges dam, events of geological disaster have also risen sharply, especially the most serious disaster—landslide. Water storage not only resulted in some old landslide and collapse recurrence but also led to new landslide, collapse, and bank collapse. In future, geological

⁵ See Ref. [5].

Table 30.2 Geological disaster type and frequency

Geological Disaster type	Landslide	Collapse	Earth's surface sinking	Debris flow	Ground fissure
Frequency	6,954	1,073	120	110	44

disasters in Yichang City are estimated to be along the mining area, the three gorges reservoir area, railway sections, and human activities frequent zone.⁶

- (3) The common characteristics that these geological disasters share are their types, wide range, the degree of deterioration; most of these occurred in the rainy season when the three gorges reservoir volume changes.

In conclusion, there is a high rate of natural disaster in the three gorges area. The government should not only make monitoring and warning of the geological hazards and the project management of prevention and control measures, they should also be prepared to emergency rescue and preparation, and timely, they should deal with the possibility of natural disasters that occurred to this area and try their best to reduce personal injury and economic loss. Therefore, we are in urgent need of an emergency logistics base that can provide timely, effective rear rescue activities.

30.2.2 National Emergency Materials Reserve Point Cannot Meet the Demand of the Three Gorges Area Emergencies Now

There is a proverb: An army marches on its stomach. It means when faced with emergency events, it is important to make good preparation for good materials and equipment. The ministry of finance issued «The Central Disaster Relief Management Approach»,⁷ clearly suggesting about setting-up Tianjin, Wuhan, Changsha, Chengdu, and Xi'an and about 10 central disaster relief materials store and reserve points (as shown Fig. 30.5).

From Fig. 30.5, the central disaster relief materials store and reserve point in China mainly located in eastern and central regions while there are relatively few in western region. There is only one central disaster relief material store and reserve point in Wuhan, which is far and it cannot meet the needs of three gorges area. What is more, there is long distance from other reserve points to three gorges area. Once the relief supplies cannot reach the site in time, it can lead to more serious personal injuries and economic loss. Considering the current central reserve points and three gorges region, which cannot meet the needs of natural disaster, it is urgent

⁶ See Ref. [4].

⁷ See Ref. [6].



Fig. 30.5 10 central disaster relief materials store and reserve point

to setup 1–2 local materials reserve center in three gorges area to reduce loss and save life.

30.3 Measures of the Construction of Three Gorges Emergency Logistic Base

The construction of three gorges emergency base should be considered from two aspects, micro and macro, based on the consideration of the speciality of three gorges region. From the macro-aspect, what should be considered is its policy, economy, construction, etc. From micro-aspect, the variety, location, season, and level of disasters are needed to think about so as to make sure what is needed for the construction of the base, such as the kinds of goods and materials, the inner structure of the base itself, the location and layout of the base, the design of emergency command center, and staff training.

30.3.1 The Macro-aspect

30.3.1.1 Gain Government Support in Policy Making

In these years, the center government has paid much attention on the development of logistic service and successively made out many laws and policies that are relevant to logistic emergency. For instance, the state council issued ‘The logistics

industry adjustment and revitalization,' which clearly put forward the building of emergency production, circulation, transportation, and logistical company information system in case of the occurrence of emergency events. But there are three shortages in the laws: (1) most of the policies are temporary regulation, and its enforcement cannot reach what the real word requires. (2) The existing legal provisions are too rough and have loopholes; especially when the emergency events happened, problems cannot get settled as soon as possible. (3) The issued laws not really be implemented as it was supposed to be. The situation requires governments of all levels to increase their support to emergency logistic; the efforts must be majorly put into the following three aspects: firstly, issuing available laws. Organizing professional team to collect and systemize the basic information about the natural disasters in the three gorges region, then inviting experts to discuss the existing problems. Secondly, forming the general public supervision mechanism. In the process of carrying out the emergency policies, if the complementation cannot be carried out, the general public can supervise, complain, or report by email, phone, and text message, etc., in order to make sure every policy has been complemented effectively and appropriately. Thirdly, forming the information feedback mechanism. Organizing special information feedback team. After the measures have been carried out, the team will pay a return visit and inquire whether or not the policies have been well complemented and the team will draw on these experience and lessons from these visits, and then adjust the polices to better serve people.

30.3.1.2 Increase Emergency Funds

Every year, the governments of all levers will fund the people who have suffered from the disaster so that every county level can afford the relief goods and material. But, there exists two problems: firstly, the insufficient emergency capital. Taking Yichang, for example: In 2010, central natural disasters subsidies have reached 15.28 million yuan; in 2011, central natural disasters subsidies are only 5.19 million yuan. But in 2010 and 2011, the direct economic losses of the flood disaster singly are 1.39 billion yuan and 639 million yuan, respectively. Therefore, there is a big gap between aid fund and direct economic loss, which totally cannot make the end meet. The purchase of the emergency materials is comparatively dispersed. Taking Yichang City as an example, every year its government will allocate emergency funds directly into each county, city, and district, and these authorities will purchase from material and goods, respectively, which will lead to dispersion of material purchasing; furthermore, this will lead to comparatively higher purchasing price, resulting in waste of money. Therefore, the government should not only increase the emergency fund input, but also should take centralized bidding procurement, and other ways to save money. In addition, basic infrastructure construction is very important to emergency logistics base; the fund of building highway, railway and service facilities construction should be increased, which will be prepared for the prevention of the emergency events.

30.3.1.3 Putting More Efforts into the Construction of the Emergency Logistic Base

The Contingency Plan for the Natural Disasters of Yichang, 2011, said that we need to integrate the existed emergency supplies and repository plans and manage them in classified way. At the same time, the municipal government should establish 3–5 repositories, and counties should establish several small repositories or depots. All of the repositories should be equipped with emergency supplies.

However, since the repositories construction belong to the commonwealth construction, not involved in commercial activities, so they are poor in profitability and weak in the goods circulation; their social and economic benefits cannot be measured by the commercial profit model. That is why no emergency logistic base has ever been established in the three gorges area.

Therefore, the government should adopt the mode of combining the government and enterprise, to attract enterprises with policies such as budget expenditure, subsidies, subsidized loan, or tax exemptions. The government can sign agreement with enterprises, under the condition that the enterprise ensured the production, processing, storage, handling, loading, and unloading of the emergency supplies smoothly; in this way, they can manage the emergency repositories reasonable. For example, they can recruit scattered small-and-medium-sized suppliers charging them at cheaper rent fees. So that emergency repositories will not be wasted, they can be utilized reasonable and effectively.

30.3.2 Micro-aspects

30.3.2.1 The Location and Layout of the Three Gorges Emergency Logistics Base

The three gorges area includes Yichang in Hubei Province and most areas of Chongqing Province; the purpose of the construction of the three gorges emergency logistic base is to prevent and resolve the emergency problems of the three gorges area. Historical data show that the highest losses of natural disasters in Hubei covered an area of 19.989 million hectares; however, the highest losses of natural disasters in Chongqing province are up to 3.205 million ha, and we can conclude that the highest losses of natural disasters in Hubei Province are about six times that of Chongqing Province.

According to the Hubei Province Geological Disaster Prevention Plan, the main geological disaster areas in Hubei Province are distributed in the three gorges reservoir area and the mountainous area of EnShi, especially the districts ranging from the Badong of three gorges reservoir to the XinTan landslides area and the west YangZhouQiao Town landslides area in ZiGui. Badong is near Yichang, and ZiGui belongs to Yichang; furthermore, the three gorges dam is located in ZiGui

Town of Yichang.⁸ Therefore, we can locate the three gorges emergency logistics base in Yichang, Hubei Province, in order to make close investigation and design the layout.

30.3.2.2 The Procurement Strategies for the Three Gorges Emergency Supplies

We can determine the types and cardinal numbers of emergency supplies in the construction of the three gorges emergency logistics base based on its types, places, times, and degrees of natural disasters occurred in previous years. (1) To determine the type of emergency supplies according to the types of natural disasters. The main natural disasters in the three gorges area are droughts and floods, followed by geological disasters, which include landslides, avalanches, landslides, and ground subsidence. Therefore, the main supplies needed should be living materials (such as food, tents, camping vehicles, mobile homes, cotton-padded clothes, quilts) and emergency supplies (such as mobile pump truck, excavator, aggregate, standby generators, shovels, cable, wire, etc.). (2) To determine the procurement number of supplies according to the time of natural disasters. Taking Yichang, for example, the flood disaster usually happened in August; so at that time, we should integrate and fully use the existing emergency information from all the industries and departments. For example, organizing rescuing formulation and relief plans from every department and, making summary of the last year's disaster relief work, centralizing experts to analyze the data of natural disasters in the region, forecasting the coming year's natural disasters preliminarily according to the professional information, including meteorological and climate information, making analysis on last year's relief supplies, to check whether those supplies are lacking or sufficient. Taking relief and rescue plans, supplies and the required standards of all the industries and departments are taken into account, to formulate the disaster and relief plans, supplies required and deployment plan for the next year and, finally, purchasing emergency supplies through ways of project tender or government procurement.

Taking the flood control and drought relief work of Yichang, for example, according to the summary of the flood control and drought relief work in Yichang, 2008–2011, we can sum up relevant supplies and recorded numbers, we can select three kinds of supplies to compare, and they are woven cloth, sack bags, and aggregates (Table 30.3). From the table, we can see that there was a big gap between the procurement number in 2009 compared with 2008, 2010, and 2011, which dues to the information collected were not comprehensively. However, the number of procurement in 2008, 2010, and 2011 was generally kept in a horizontal line; we can calculate the required procurement number in the coming year according to the empirical method and the projection method.

⁸ See Ref. [4].

Table 30.3 The table for the number of the related supplies in Yichang, 2008–2011

Year (years)	2008	2009	2010	2011
Relief supplies				
Woven cloth (square meters)	89,000	151,500	89,000	127,900
Sack bags (Article)	1,170,000	1,606,400	1,170,000	1,710,000
Aggregate (cubic meters)	71,800	93,400	71,800	83,900

Source the summery of the flood control and drought relief work in Yichang

30.3.2.3 The Setting-up of the Three Gorges Emergency Command Center

We can also take into account the case of Yichang; Yichang has the Emergency Management Office and the Emergency Response Headquarters Office, which are located in the Municipal Civil Affairs Bureau; it is responsible for directing the daily work. However, due to the little communication among the department, various functional departments, and enterprises, the emergency supplies cannot be allocated at the first time. Therefore, we can set up the Emergency Response Headquarters Office in the emergency logistics base, to build an emergency logistics leadership and command team that government led, and the relevant departments (such as Municipal Development and Reform Commission, Municipal Civil Affairs Bureau, the Municipal Bureau of Commerce, City Land Resources Bureau, the Municipal Environmental Protection Bureau, the city lived Construction Committee, Municipal Transportation Bureau) and enterprises (manufacturers, logistics companies, transport enterprises) should also be involved in. At the same time, we have to train the members of the leading group regularly, so as to provide appropriate organizational and technical security for emergency.

30.3.2.4 Strengthen the Professional Training for Relief Workers

The famous economist Adam Smith believed that nationals' useful capacity should be seen as a part of the capital; people should clear up the value of human capital. Therefore, relief workers played an important role in the process of disaster-relieving process. Taking the flood control and drought relief work of Yichang, for example, according to the summery of the flood control and drought relief work in Yichang between 2008 and 2011, the relief workers from 2008 to 2011 can be generally divided into the following four stages: The first-line persons involved in flood control and rescue were 28,000–29,000 persons; the second-line persons involved in rescue were 72,800–75,000 persons; the third-line persons involved in rescue were 154,300–160,000 persons; the rescue commandos of the city were 74,855–100,000 persons (Table 30.4).

From the table, we recognized that Yichang was not lacking of relief workers, but the city is lacking the professional training and practical exercises for them. Therefore, we can take the structure of the production–learning–researching, open a

Table 30.4 The table for the number of persons involved in the flood control and drought relief in Yichang, 2008–2011

Year (years)	2008	2009	2010	2011
Persons involved in rescue				
The first-line persons involved in flood control and rescue	28,000	/	28,000	29,000
The second-line persons involved in rescue	75,000	/	75,000	72,800
The third-line persons involved in rescue	160,000	/	160,000	154,300
The rescue commandos of the city	100,000	/	100,000	74,855

public safety professional course in the Three Gorges University of Yichang, and give them theoretical training regularly. Certainly, we should not forget to hold practical drills in the emergency logistics base, combing the theory and practice, thus making better preparations for the rescue work.

30.4 Conclusion

The three gorges region is prone to have drought, floods, and geological disasters, and geological disasters include landslides, avalanches, landslides, earthquakes, etc. In particular, the landslide has the highest frequency. In 2009, with the gradual increase of the storage capacity of the three gorges dam, the incidence of the three gorges region natural disasters also rise. In the face of sudden natural disasters in the three gorges region, there is an urgent need in the construction of the three gorges region into individual emergency logistics base, and quick and agile for the occurrence of natural disasters to provide a strong rear rescue activities. According to the types of the three gorges region, natural disasters' time and frequency are the reason for the proposed construction of the three gorges emergency logistics base in Yichang City, Hubei Province.

References

1. Zhang H (2008) The Three Gorges reservoir area (Chongqing) natural disaster risk comprehensive evaluation. Chongqing Normal University (Natural Science), China Environment Statistical Yearbook, 2008.01
2. National Bureau of Statistics (2009) Ministry of environmental protection. China Statistics Press
3. Hubei Provincial Department (2003) Geological Disaster Prevention Plan of Hubei Province (2003–2015), 2003.10
4. Yichang City Land and Resources Bureau (2010) Geological disaster prevention plan of Yichang City, Hubei Province (2010–2020), 2010.6

5. Chongqing Municipal Land Resources, Housing Authority Website (2010) Chongqing geological disaster prevention plan (2004–2015)
6. The Ministry of Civil Affairs, The Ministry of Finance (2010) The Central Disaster Relief Material Reserves Management Measures

Chapter 31

Resistance Analysis for Bulk Materials in the Vertical Section of Pipe Scraper Conveyor

Yanping Yao, Wenjun Meng, Ziming Kou and Zhicheng Liao

Abstract The conveying mechanism of the pipe scraper conveyor's vertical section is researched in detail by using the theory of granular media mechanics. It mainly analyses the packing and moving state, stress condition of the bulk materials in the vertical pipe, and deduces the relationship among the parameters of pressure distribution, running resistance of the bulk materials and structure, space and area of the scraper, deduces the calculation formula of running resistance in the vertical section of pipe scraper conveyor, then illustrates the effect of each parameter on the running resistance of bulk materials with living examples, whose purpose is to provide an effective reference for the design of such a pipe scraper conveyor.

Keywords Pipe scraper conveyor · Bulk materials · Pressure · Running resistance

31.1 Introduction

In 1920s, the British flour supplier REDLER invented Buried Scraper Conveyor, on this basis, The FLOVEYOR Cable Pipe Scraper Conveyor was invented in the year of 1960. The Pipe Scraper Conveyor was used as an economical peanuts transmit device originally, and now has been popularized and applied in over 30 countries, involving food processing, medicine, chemical, and other industries, mainly suitable for the

Y. Yao (✉) · Z. Kou
Taiyuan University of Technology, Taiyuan 030024, China
e-mail: yyping13@sina.com

Z. Kou
e-mail: zmkou@163.com

Y. Yao · W. Meng
Taiyuan University of Science and Technology, Taiyuan 030024, China
e-mail: tyustmwj@126.com

Z. Liao
Guangxi Baise Mining Machinery Factory Co. Ltd., Guangxi 533000, China
e-mail: lzhchbs@163.com

transmission of powdery and bulk materials [1, 2]. With an increasing number of users and expansion of usable range, a higher demand of its structure and technical characteristic was put forward. The key factor to accelerate the advancement of our country's scraper conveyor technical level is to study its structure and technical performance and master the new foreign develop trend timely. So far, the analysis of principle aspects pipeline scraper conveyor in materials handling principle aspects is still in the blank, a continuous study and complement is still needed: For instance, the influencing factors to convey bulk materials include the inner pressure of bulk materials, compaction factors, the factor of friction, bays section, traction components dimension, and other factors outside such as the scraper area and adjacent scraper spacing.

The pipeline scraper conveyor is composed by chains, scrapers which were fixed in the chain and closed pipe, bulk materials can be conveyed continuously by chains, and scrapers within the pipeline. Due to chains' flexibility, the transmission lines can be more flexible, both in horizontal and vertical directions.

31.2 Some Assumptions

1. The pipeline scraper conveyor is fed in the horizontal segment, and the compaction factors was never took into account in the horizontal feeding segment, furthermore, assume that the effective volume between the scraper is completely filled with bulk materials;
2. The dynamic compaction factors among bulk materials is only considered in vertical conveying section, and assume that internal friction factor is invariable within bulk materials;
3. The friction factor between bulk materials and the trough is invariable when bulk materials is compacted;
4. In the vertical lifting, assume the per unit area pressure that scraper act on bulk materials is uniformly distributed in the scraper surface;
5. Bulk material's movement without considering the impact of air power.

31.3 The Analysis of Convey Mechanism When Materials in the Vertical Section

31.3.1 *Compaction Factor*

The packing density of bulk materials [3] is related to the composition characteristics of granular materials in a large extent. Bulk density of bulk materials will both increase when the static and dynamic load compact on granular materials. When

granular media is under the static loading and the particles generate the plastic deformation, the particles move little distance, so the compacted bulk density of bulk materials change a little; but when under the vibration pressure, the directions of friction in granular media change severely and with complex features, which results in regrouping the granular media and compacting very densely, so that the density of the bulk materials increase.

Compaction factor of bulk material is calculated as follows:

$$k_y = \frac{G_y}{G}$$

K_y compacting factor;

G_y the quality when the same volume of bulk materials after compaction, kg;

G the quality when the same volume of bulk materials before compaction, kg;

$$\text{Similarly: } \gamma_y = k_y \gamma \quad (31.1)$$

$$v_y = \frac{v}{k_y} \quad (31.2)$$

γ_y packing density of compacted bulk materials, N/m^3 ;

γ packing density of bulk materials, N/m^3 ;

v_y the occupied volume that the same quality of bulk materials after compaction, m^3 ;

v the occupied volume that the same quality of bulk materials before compaction, m^3 .

31.3.2 Lateral Pressure Calculation

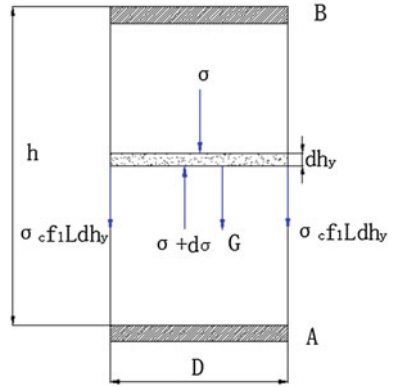
Ignoring the materials column in the gap around the scraper and bays, the vertical section materials will suffer:

The downward friction of the groove wall, the materials self weight, the upward shored force of scraper.

Taking the materials between adjacent scraper A and B as a monomer, the force's regularity of distribution is consistent of each pair of adjacent scraper in the vertical section.

Using two infinitely thin horizontal levels to intercept a materials layer whose thickness is dh_y (Fig. 31.1) and analyze the force of the layer and write differential equations of various vertical forces in the selected unit body. Meanwhile, write the vertical force's differential equations that impact on the unit cell been taken [4]:

Fig. 31.1 Calculation model for vertical conveying



$$\omega \cdot \sigma + G = (\sigma + d\sigma)\omega - \sigma_c f_1 L dh_y$$

That is:

$$\begin{aligned} \omega \cdot \sigma + r_y \cdot \omega dh_y &= \sigma\omega + d\sigma \cdot \omega - \sigma_c f_1 L dh_y \\ r_y \omega dh_y &= \omega \cdot d\sigma - \sigma_c f_1 L dh_y \\ \therefore n &= \frac{\sigma_c}{\sigma} \quad \therefore \sigma = \frac{\sigma_c}{n} \end{aligned}$$

Substituting it to the above formula and arrange:

$$dh_y = \frac{d(r_y \cdot n + a\sigma_c)}{a(r_y n + a\sigma_c)}$$

After integral:

$$\begin{aligned} h_y &= \frac{1}{a} \int_0^{\sigma_c} \frac{d(r_y n + a\sigma_c)}{r_y n + a\sigma_c} = \frac{1}{a} \cdot \ln \frac{r_y n + a\sigma_c}{r_y n} \\ \sigma_c &= \frac{r_y n}{a} (e^{ah_y} - 1) \end{aligned} \tag{31.3}$$

where

$$a = \frac{f_1 L \cdot n}{\omega} \tag{31.4}$$

- ω cross-sectional area of trough, m^2 ;
- L the circumference of trough cross section, m ;
- σ the average vertical pressure on an area of ω , N/m^2 ;
- G the gravity of bulk materials, N ;

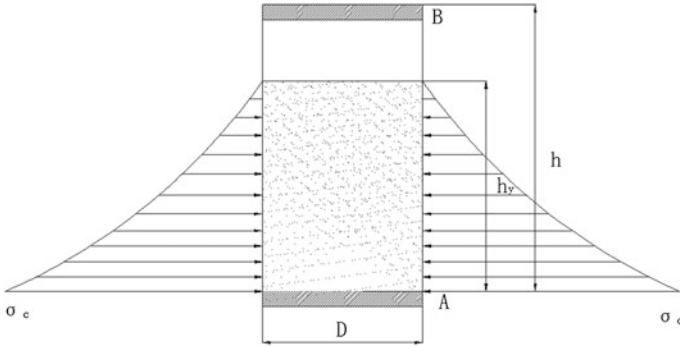


Fig. 31.2 The lateral pressure distribution curve

- f_1 the friction factor between bulk materials and trough;
- σ_c lateral pressure of bulk materials, N/m^2 ;
- n lateral pressure factor.

With Formula (31.3), we can get that the pressure distribution on groove walls fit the regular pattern of exponential distribution (Fig. 31.2), with the height increases of stock column, the lateral pressure increases sharply, and the running resistance in materials increases too.

31.3.3 Running Resistance Calculation

When the materials is hoisted to the height $H(m)$, the frictional resistance between materials and trough is as follows:

$$\begin{aligned}
 W &= \left[\int_0^{h_y} \sigma_c \cdot dh_y \right] \cdot \frac{H}{h} \cdot Lf_1 \\
 &= \frac{H}{h} Lf_1 \int_0^{h_y} \frac{r_y n}{a} (e^{ah_y} - 1) dh_y \\
 &= \frac{H}{h} L \cdot f_1 \cdot \frac{r_y n}{a} \left(\frac{e^{ah_y}}{a} - h_y \right)
 \end{aligned}
 \tag{31.5}$$

Substituting Formulas (31.1) (31.2) into (31.5) gives:

$$W = \frac{H}{h} L \cdot f_1 \cdot \frac{k_y r n}{a} \left(\frac{e^{ah/k_y}}{a} - \frac{h}{k_y} \right) \quad (31.6)$$

$$\therefore a = \frac{f_1 L \cdot n}{\omega} \quad \omega = \frac{\pi D^2}{4} \quad L = \pi D$$

$\therefore a = \frac{4f_1 n}{D}$, substituting to the Formula (31.6) and we can get a common type:

$$\begin{aligned} W &= \frac{H}{h} L \cdot f_1 \cdot \frac{k_y r n}{a} \left(\frac{e^{ah/k_y}}{a} - \frac{h}{k_y} \right) \\ &= \frac{H}{h} k_y r \cdot \frac{\pi D^2}{4} \left[\frac{e^{\frac{4f_1 n h}{D k_y}}}{\frac{4f_1 n}{D}} - \frac{h}{k_y} \right] = q_M \cdot \frac{H}{h} \cdot k_y \cdot \frac{D}{4f_1 n} \cdot \left[e^{\frac{4f_1 n h}{D k_y}} - \frac{4f_1 n h}{D k_y} \right] \end{aligned} \quad (31.7)$$

q_M Bulk materials per unit length of line load, N/m make $k = \frac{h}{D}$

k The scraper pitch factor

Then Formula (31.7) transforms into:

$$W = q_M \cdot H \cdot \frac{k_y}{4f_1 n k} \cdot \left(e^{4f_1 n k / k_y} - \frac{4f_1 n k}{k_y} \right) = q_M \cdot H \left(\frac{k_y e^{4f_1 n k / k_y}}{4f_1 n k} - 1 \right) \quad (31.8)$$

f_1 the friction factor between bulk materials and trough;

f the friction factor within the materials;

Make frictional resistance W minimum, the W 's derivative value is zero. After derivation to W can obtain:

$$W' = \left[q_M \cdot H \left(\frac{k_y e^{4f_1 n k / k_y}}{4f_1 n k} - 1 \right) \right]' = q_M \cdot H \cdot \frac{k_y}{4f_1 n} \cdot e^{4f_1 n k / k_y} \left(\frac{4f_1 n}{k \cdot k_y} - \frac{1}{k^2} \right) \quad (31.9)$$

Make $W' = 0$, that is: $\frac{4f_1 n}{k \cdot k_y} - \frac{1}{k^2} = 0$

Obtained $k = \frac{k_y}{4f_1 n}$

That is:

$$k = \frac{1 + 2f^2 + \sqrt{1 + 2f^2}(f + \sqrt{f^2 - f_1^2})}{4f_1} \cdot k_y \quad (31.10)$$

So, when the K number is calculated by the Formula (31.10), frictional resistance W is minimum.

In the vertical segment, the total dynamic resistance caused by traction components and materials has been conveyed as:

$$W_z = g \left[(q_0 + q_M) + q_M \left(\frac{k_y e^{4f_1 nk/k_y}}{4f_1 nk} - 1 \right) \right] \cdot H \quad (31.11)$$

where

q_0 The unit length quality of traction components (kg/m)

31.3.4 Case Study

Take buckwheat for example, assume $f_1 = 0.5, f = 0.7, k_y = 1.15,$

So the lateral pressure factor:

$$\begin{aligned} n &= \frac{1}{1 + 2f^2 + \sqrt{1 + f^2}(f + \sqrt{f^2 - f_1^2})} \\ &= \frac{1}{1 + 2 \times 0.7^2 + \sqrt{1 + 0.7^2}(0.7 + \sqrt{0.7^2 - 0.5^2})} \\ &= 0.29 \\ W &= q_M \cdot H \cdot \left(\frac{1.15 e^{0.504k}}{0.58k} - 1 \right) \end{aligned}$$

When

$$k = \frac{h}{D} = 0.8, \quad W = 2.71q_M H$$

$$k = 1, \quad W = 2.28q_M H$$

$$k = 1.5, \quad W = 1.82q_M H$$

$$k = 2, \quad W = 1.72q_M H$$

$$k = 2.5, \quad W = 1.80q_M H$$

Thus, it is clear that the running resistance W reduces in pace with the k number increasing, but not a linear relationship, when the k number increases to a certain value, the W number increases on the contrary.

About buckwheat, when $k = 1.97,$ the running resistance W is minimum, and now $W = 1.71q_M H.$

Table 31.1 The scraper pitch factor numbers when the running resistance is minimum for different bulk materials

Materials	Factor of internal friction f	Factor of external friction f_1	Dynamic compaction factor k_y	Scraper pitch factor k' when the compaction factor is out of consideration	The scraper pitch factor k
Millet	0.41	0.31	1.08	1.67	1.8
Buckwheat	0.7	0.5	1.15	1.72	1.97
Sunflower	0.8	0.49	1.1	2.01	2.3
Rye	0.6	0.5	1.05	1.4	1.47
Power stone	0.75	0.5	0.75	1.88	1.41
Sawdust	1.0	0.7	1.30	1.94	2.52
Agglomerate	1.0	0.6	1.07	2.31	2.47
Powdered phosphate rock materials	0.60	0.58	1.2	1.12	1.34

For different kinds of bulk materials, and trough with different materials quality, the k can take different numbers, the common bulk materials is listed in Table 31.1.

31.4 Conclusion

1. Using the mechanics of granular media, make a force analysis of the bulk materials in vertical segment of the pipeline scraper conveyor to deduce the exponential distribution situation of lateral compression when bulk materials are running in vertical tube;
2. Considering the impact of the bulk materials compaction factor, deduce the resistance computational formula when the bulk materials are running in the vertical segment of the pipeline scraper conveyor;
3. In order to make the running resistance minimum, we have deduced the relationship between the scraper spacing and area parameters, and combined with an example to explain description scraper pitch factor's affection to running resistance of bulk materials, and this conclusion breaking the traditional selection of scraper pitch factor. Thus, it can provide the basis theory for the design of pipeline scraper conveyor.

References

1. Usov KA (1960) ТРУЦЫ ВНИИПТ МАШ. Xiubao Kang, translated, the Soviet Union
2. Wu W, Ruan J (2011) FLOVEYOR The cable pipe scraper conveyor. Food and fodder industries
3. Jiang Q et al (1991) translated. [The Soviet Union] P. Л. ЗЕНКОВ. Bulk-cargo mechanical. Harbour Handling Publishing House «Harbour Handling» Supplement
4. Krein ГК-g (1983) Structural mechanics bulk materials. China Railway Publishing House, Beijing

Chapter 32

Material Uninterrupted Feeding Technology and Feeding Speed Control Research of Large Electroslag Remelting Furnace

C.Z. Wang and J.C. Song

Abstract Electroslag remelting is one of the most important special metallurgy technologies. To obtain electroslag remelting steel with characters of high purity, dense organization, and good mechanical properties, the temperature field and remelting speed of the electroslag molten bath must be constant, which means material's uninterrupted feeding and feeding speed must be controlled. In this paper, based on soft-detection technique, electrohydraulic proportional control technique, modern detecting technique, and intelligence control technique, the material uninterrupted feeding system of the electroslag remelting furnace was designed; the system's three-dimensional model was established; the mathematical model of the surplus-ingot length soft-sensing detecting system was established; the S-style position control curve of the ingot was designed. The research results were applied to an experimental electroslag remelting furnace, and dissection research of the experimental product was made, and system control curves and the experimental production dissection results were obtained. It was found that the material uninterrupted feeding system and the feeding speed control system introduced in this paper meet the production process and technique requirements of large electroslag remelting furnace and provide references for design and application of new-style electroslag remelting furnaces.

Keywords Electroslag remelting · Material uninterrupted feeding · Feeding speed control · Experiment research

C.Z. Wang (✉) · J.C. Song
School of Mechanical Engineering and Automation, Northeastern University,
Shenyang 110819, People's Republic of China
e-mail: chzhwang@mail.neu.edu.cn

© Springer-Verlag Berlin Heidelberg 2015
Logistics Engineering Institution, CMES (ed.),
Proceedings of China Modern Logistics Engineering,
Lecture Notes in Electrical Engineering 286, DOI 10.1007/978-3-662-44674-4_32

337

32.1 Introduction

Electroslag remelting (ESR) is one of the most important special metallurgy technologies of purifying metal and obtaining electroslag ingot with characters of high purity, dense organization, and good mechanical properties. Material (electrode) uninterrupted feeding control is of most importance in the electroslag remelting process. In the production process, space between the electrode and the molten metal determines electric resistance and input power of the slag bath. To keep the space and then to keep the remelting speed, it is necessary to control the electrode's position according to its melting speed. On the other hand, large ESR furnaces, 120t level, for example, usually need scores of electrodes to product one electroslag ingot, and the electrodes should be replaced continually. If the process of electrode replacement and feeding is not continuous, the balance of the power short-net system and the interior temperature uniformity of the crystallizer will be destroyed, and then, the production quality will be defective. To solve the problems discussed above, scientific researches on the material uninterrupted feeding and feeding speed control technique of large ESR furnace were studied in this paper.

32.2 Electroslag Remelting Principle

The basic principle of electroslag remelting is as shown in Fig. 32.1 [1]. In the beginning of remelting process, molten slag is poured into a coppery water-cooling crystallizer, and then, the electrode being carried by an electric-conducting cross-arm is inserted into the slag bath. When large current goes through the conducting loop made up of electrode, slag, bottom water box, transformer, and short-net system, great voltage drop will be caused, which will then generate a mass of heat and then

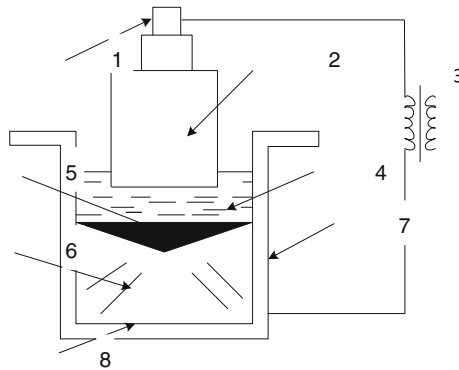


Fig. 32.1 Electroslag remelting principle draft. 1 false electrode; 2 electrode; 3 transformer; 4 slag bath; 5 molten metal bath; 6 electroslag ingot; 7 crystallizer; 8 bottom water box

melt the inserted electrode gradually. The molten metal will form a molten bath below the slag bath. The molten metal bath, being cooled by the water-cooling crystallizer, transforms into electroslag ingot gradually. The molten metal bath's cooling and solidification process is from bottom to top, and a slag shell will be generated between the ingot and the crystallizer wall in the solidification process. The slag shell is good for the ingot's sequence crystallization and makes the ingot to be compact and without ingot pipes. In the whole process, to replenish the vacant volume of the solidification metal bath, the electrode should be fed into the slag bath at certain speed according to its melting speed. A series of physical chemical reaction will happen to the molten metal and slag in the process of metal drop's forming and dropping; then, the nonmetal impurities and pernicious can be detached.

32.3 Material Uninterrupted Feeding System

The material feeding system mainly consists of rotating pillar, electro-conducting cross-arm, and lifting equipment, which is traditionally made up of variable frequency motor and ball screw. The limiting factors of the traditional cross-arm lifting equipments are as follows [2, 3]:

- (1) Stringent manufacture specifications of the ball screw make the ball screw production mainly depend on import;
- (2) High cost of manufacture, assemble, and maintaining;
- (3) The transformation of rotation motion to linear motion usually causes mechanical wear and efficiency droop, and then leads control accuracy to be lower and lower.

Innovation design of ESR material feeding system was made [4]. 3D solid model and the hydraulic system principle of the innovated system are, respectively, shown in Figs. 32.2 and 32.3.

Large-scale hydraulic cylinder and magnetic scale are applied to the improved cross-arm lifting equipment. The cylinder's motion is controlled by an electro-hydraulic proportional speed control valve and detected by a magnetic scale, and then, the closed loop control of the cross-arm and the electrode can be obtained. This kind of driving and control type avoided motion mode transmission and owns the characters of large stiffness and high frequency response. Agility control and accurate control of the electrode position control system can then be obtained.

32.4 Soft Detection of Electrode Surplus-Ingot Length

In the ESR process, the space between the electrode and the molten steel determines electric resistance and input power of the slag bath. With the electrode's continuous melting, its length keeps shortening, and the liquid steel level keeps rising. To

Fig. 32.2 3D solid model of the material feeding system. 1 support bay; 2 rotating pillar; 3 cross-arm; 4 cylinder with magnetic scale; 5 electrode

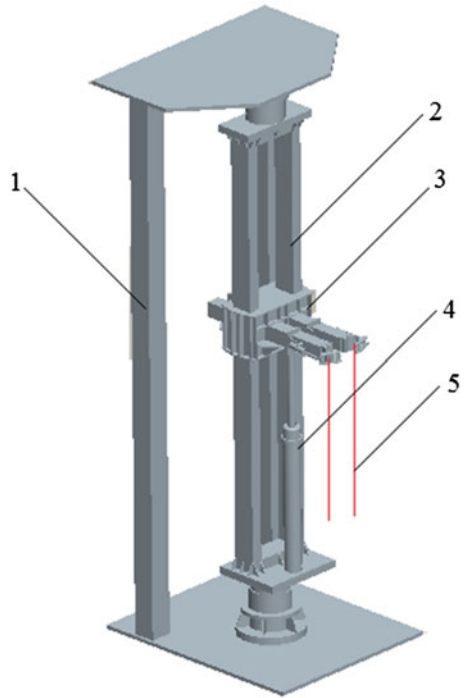
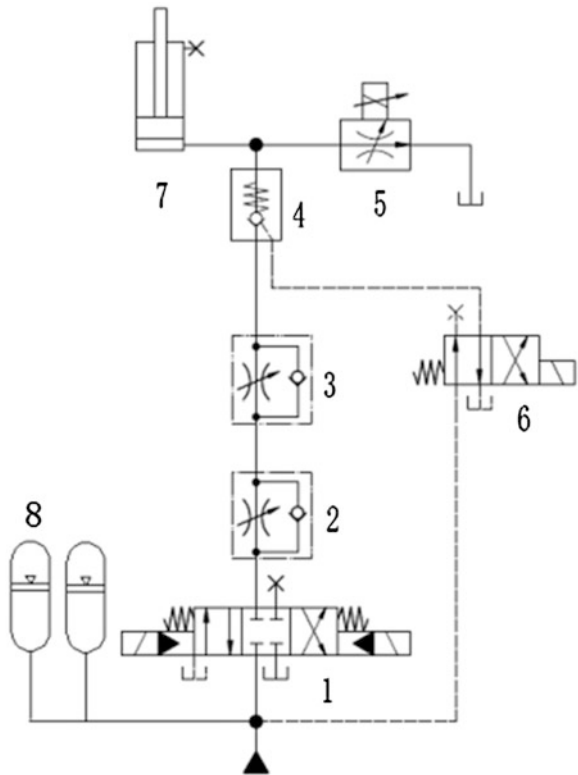


Fig. 32.3 Hydraulic principle draft of the cross-arm lifting equipment. 1 electro-hydraulic direction valve; 2, 3 check throttle valve; 4 pilot operated check valve; 5 electro-hydraulic proportional speed control valve; 6 direction valve; 7 hydraulic cylinder; 8 accumulator



maintain the space between the electrode and the liquid steel and then maintain the melting current, real-time detection and control of the electrode position are needed. While considering the high melting temperature and vast exhaust gas, direct length detection of the electrode is difficult. In this paper, a method of soft detection is proposed and applied to acquire length detection of the melting electrode. As the soft-detection method, the electrode's position is detected by a magnetic scale, and the electrode's weight is detected by a weighing sensor; and finally, the electrode's surplus-ingot length can be obtained by data fusion technique using the detection results. Position relationships of the electrode, slag bath, and electroslag ingot are shown in Fig. 32.4.

According to melting-crystallization theory and Fig. 32.4, the electrode surplus-ingot length can be obtained:

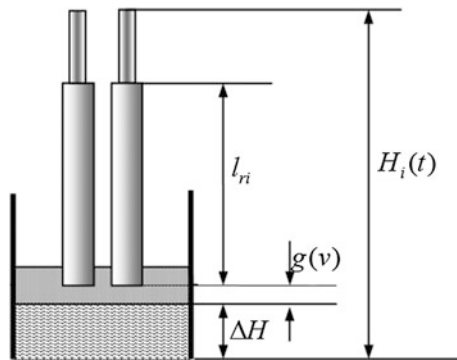
$$\begin{cases} l_{ri} = l_{0i} - l_i \\ H_i(t) = H_i(0) - l_i + f(l_1, l_2, l_3) + g(v) \end{cases} \quad i = 1, 2, 3$$

where, l_{ri} is electrode's surplus length; l_{0i} is electrode's initial length; l_i is electrode's consumed length; $H_i(t)$ is electrode's effective melting position; $H_i(0)$ is electrode's initial steady arcing position, which should be renewed every time; $\Delta H = f(l_1, l_2, l_3)$ is ingot's melting-crystallization model; $g(v)$ is slag-replenishing model.

In reality, since the electrode's density, the crystallizer's conical degree, and the electroslag's replenishing volume are all of uncertainties, the cross-correlation between the electrode melting-crystallization model and the slag-replenishing model would cause detection errors.

To improve the detection accuracy, the following control methods were applied: (1) To combine the data of all sensors, merge together Gaussian probability density functions of all soft-detection sensors to generate a new Gaussian probability density function; and (2) to get each model's combined weighting coefficient, apply the single decision-making output of fuzzy logical construction model and make the batch output variable and error of each model to be the decision-making variable of fuzzy logical control strategy.

Fig. 32.4 Position relationship draft of the electrode, slag bath, and electroslag ingot



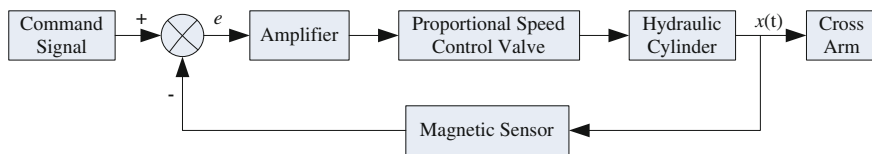


Fig. 32.5 Control block diagram of the material uninterrupted feeding system

32.5 Material Uninterrupted Feeding Speed Control

Remelting speed is the key parameter of electroslag remelting process control system, and it is an important standard of production quality, energy consumption, and throughput [5]. Since for large ESR furnaces, the crystallizer measurement is usually bigger and the remelting time is longer, along with the remelting process, the ingot's cooling intensity becomes lower and lower. So to keep the molten bath's shape, it is necessary to control the remelting speed at every remelting phase according to the steel types. Constant current control and constant voltage control usually lead to temperature field change and then cause the ingot structure change. While, constant remelting control, which means control the remelting power according to actual remelting speed feedback, can guarantee the ingot's crystallization quality to be unanimous and, thus, guarantee the production quality.

Material uninterrupted feeding speed control is the core technique of constant remelting speed control. And according to Figs. 32.2 and 32.3, the material uninterrupted feeding system is, in practice, an electro-hydraulic proportional control system, and its control principle can be illustrated as in Fig. 32.5.

32.6 Electrode Auto-Replace System

For large electroslag remelting furnace, 120t level, for example, usually scores of electrodes are needed to get one electroslag ingot, and the electrodes should be replaced continually. If the process of electrode replacement and feeding is not continuous, the balance of the short-net system and the interior temperature uniformity of the crystallizer will be destroyed, and then, the production quality will be defective. In this paper, the electrode auto-replace system was designed, and its mechanism is as shown in Fig. 32.2.

Working principle of the electrode auto-replace system: The system uses hydraulic cylinders as the cross-arm's lifting and clamping device, and also as the rotating pillar's driving device; uses magnetic scale as the cross-arm's and the crystallizer's position detection device; uses an encoder as the rotating pillar's angle detection device; and uses electrode surplus-ingot length soft-detection method and self-optimizing fuzzy control method to realize electrode auto-replace control. The system's working process is shown in Fig. 32.6.

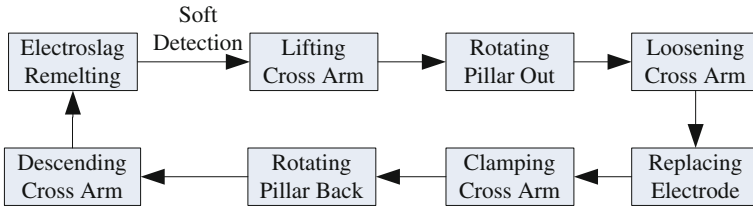


Fig. 32.6 Flow chart of the electrode auto-replace system

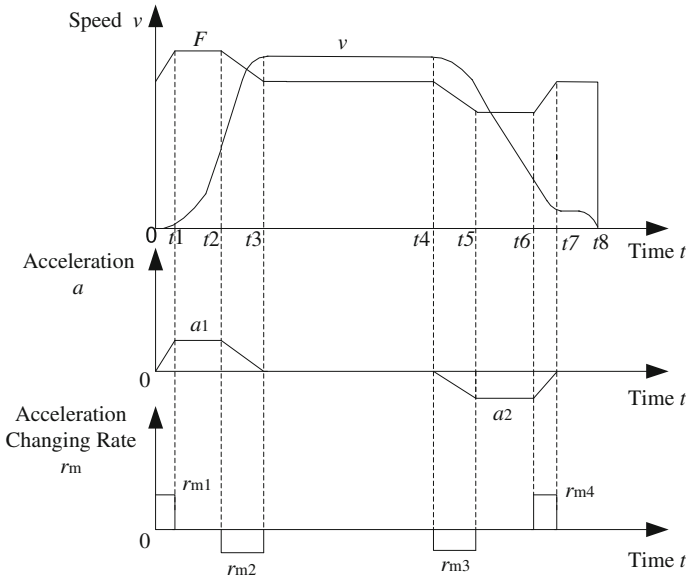


Fig. 32.7 S-style speed control curve

To realize fast and accurate auto-replace, reduce vibration and impact, and extend the equipment’s service life, the speed control strategies were researched; and the S-style speed control curve, as shown in Fig. 32.7, was designed to achieve the electrode’s acceleration and deceleration control [6–8].

32.7 Experiment Research

Experiment researches were carried out with a 120t-level ESR furnace in a heavy machinery work. And it was found that the control accuracy and stability of the material feeding system meet the technical demands very well; and the electrode feeding speed, remelting current, and voltage is relatively stable, as shown in

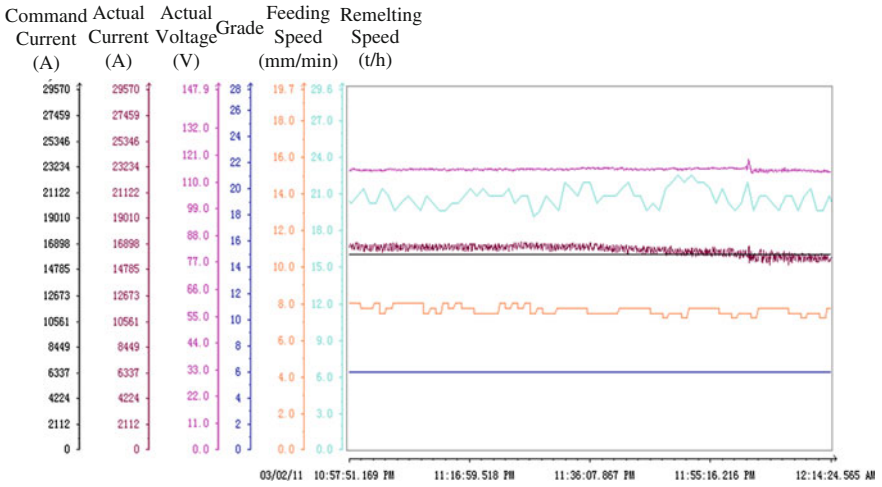


Fig. 32.8 Material feeding speed, remelting current and voltage experimental curves

Fig. 32.9 Experimental ingot dissection structure



Fig. 32.10 Microscopic metallographic structure

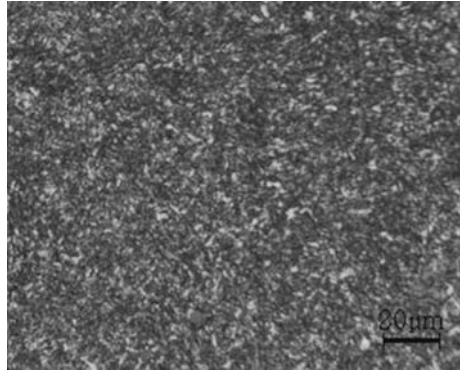


Fig. 32.8; the electrode replacement time is commendably shortened to nearly 3 min; the dissection results, as shown in Figs. 32.9 and 32.10, show that the production has the metallographic structure characters of high purity and dense organization.

32.8 Conclusions

In this paper, the material uninterrupted feeding system for large ESR furnace was studied based on research strategies of principle analysis, modeling, control curve design, simulation, and experiment. It was found that the material uninterrupted feeding system and speed control strategy studied in this paper meet the craft and technical requirements very well. And the following conclusions can be drawn:

- (1) The material uninterrupted feeding system and the matched detection system were designed; the electrode auto-replace requirement was fulfilled, and the replacement time was shortened to nearly 3 min; the balance of the short-net system and the interior temperature uniformity of the crystallizer were perfectly guaranteed.
- (2) The electrode surplus-ingot length soft-detection system and the S-style electrode speed control curve were designed, and commendable control effect was acquired.
- (3) Experiment researches were carried out; the production dissection result shows that the system control effect and production quality meet the ESR craft and technical requirements very well.

Acknowledgments This paper roots in a China 11th Five-Year national sponsored significant research project. Project number: 2009ZX04006-032.

References

1. Li ZB (1996) Electroslag metallurgy principle and application[M]. Metallurgical Industry Press, Beijing, pp 104–120
2. Hotzgruber W (1982) New ESR technology for new improved products[A]. In: Proceeding of 7th international conference on vacuum metallurgy. Tokyo, Japan, pp 1452–1458
3. Ernet C (1982) International european conference on tooling materials[C]. Schweiz
4. Stein G (1989) Industrial manufacture of massively nitrogen alloyed steels in a pressure ESR furnace[J]. Steel Times 217(3):3
5. Modovar BI, Demchenko VF, Bogachenko AG et al (1977) Temperature fields of large ESR slab ingots [A]. Mechanical Engineering Transactions-Institution of Engineers, Australia, pp 153–156
6. Deb K, Pratap A (2002) A fast and elitist multiobjective genetic algorithm: NSGAI II [J]. IEEE Trans Evol Comput 6(2):182–197
7. Julier SJ, Uhlmann JK (2004) Unscented filtering and nonlinear estimation[J], IEEE Proc Aerosp Electron Syst 92(3):401–422
8. Kushner HJ (1967) Dynamical equations for optimum nonlinear filtering[J]. J Differ Equat 26 (3):179–190

Chapter 33

Structure Weight Reduction of Ship Unloader Based on the Orthogonal Experiment Method

Suiran Yu, Jingxing Qian and Jianguo Zhang

Abstract As a bulk cargo handling equipment, ship unloader plays a very important role in port bulk material handling. As the international bulk cargo ship is becoming increasingly larger, the ship unloader is becoming larger as well. This paper builds the finite element model of the ship unloader, proposes a structure optimization method based on the orthogonal experimental method and a parametric modeling method, and develops software based on the two methods introduced above. The research includes the following: a new method to ship unloader's structure optimization based on the orthogonal experimental method; the finite element model and the parametric modeling method of the ship unloader; and the parametric modeling and structure optimization software of the ship unloader. The software provides two functions: One is the parametric modeling function, and people can realize the ship unloader's modeling by input parameters on the interface. The other is the structure optimization function, which can realize the weight reduction target of ship unloader by the structure optimization method based on the orthogonal experimental method.

Keywords Weight reduction · Orthogonal experiment · Structure optimization · Parametric modeling · Ship unloader

33.1 Introduction

As the most common bulk cargo handling equipment in China's port, grab ship unloaders (hereinafter referred to as the ship unloader) are widely used, mainly for handling coal, ore, grain, fertilizer, and other bulk cargo handling [1]. Larger scale

S. Yu (✉) · J. Qian

School of Mechanical and Power Engineering, Shanghai Jiao Tong University,
800 Dongchuan Road, Shanghai 200240, People's Republic of China
e-mail: sryu<sryu@sjtu.edu.cn>

J. Zhang

Shanghai Zhenhua Heavy Industry Co., Ltd. (ZPMC), 3261 Dong Fang-Lu,
Shanghai 200125, People's Republic of China

© Springer-Verlag Berlin Heidelberg 2015

Logistics Engineering Institution, CMES (ed.),

Proceedings of China Modern Logistics Engineering,

Lecture Notes in Electrical Engineering 286, DOI 10.1007/978-3-662-44674-4_33

of the ship unloader means heavier weight of the structure; therefore, for ship unloader, weight reduction design has become a major issue for ship unloader manufacturers.

Weight reduction is a common trend of domestic and foreign ship unloader design. Weight reduction includes the steel structure, equipment, and walking module. There are three reasons for weight reduction of the ship unloader:

1. Cost: A large ship unloader costs tens of millions, and the whole weight is always thousands of tons. The ship unloader's structure and the devices are mainly made of steel. But the high price of the steel leads to the high cost of ship unloaders. Reducing the use of steel can greatly reduce the manufacturing costs of the ship unloader, which is very important for the manufacturers.
2. Wheel pressure: The ship unloader is working on its track, so the wheels on the track have to withstand the total weight. Weight reduction can reduce the wheel pressure and lower the design standard of the wheel and the track.
3. Traction energy consumption: Ship unloader's intermittent motions on the cart track require energy. The heavier the ship unloader is, the higher the energy consumption it causes. Therefore, weight reduction can lower traction energy consumption.

At present time, the design of ship unloader is still mainly based on the traditional design experience. The traditional way is to design the structure with experience and then use the finite element method to check the strength, the stiffness, and the modes of the structure. Even there is weight reduction in the design, it is a few modifications of some parameters based on experience and then uses finite element method to confirm the security of the design [2]. However, it is difficult to get the optimized results just with the experience. For this reason, a reasonable and effective to optimize the structure of ship structure is greatly needed.

The weight of the structure can be reduced by using lighter material or making a better structural design. This paper will focus on the discussion of the later one, because those new and lighter materials usually mean higher price [3], and optimized structural design can more effectively reduce the cost.

33.2 Methods

33.2.1 Purpose and Object

The purpose of the ship unloader's structural optimization is weight reduction, so the target function for the optimization of the structure can be expressed as follows:

$$W = \sum_{i=1}^n \rho_i L_i A_i \quad (33.1)$$

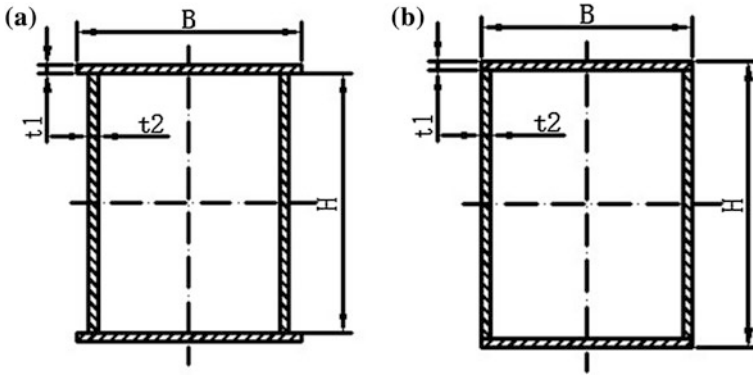


Fig. 33.1 Section parameter of the beam and column. **a** Original section parameter. **b** Simplify section parameter

W is the total weight of the structure; ρ_i , L_i , and A_i ($i = 1, \dots, n$), respectively, refer to the density, length, and cross-sectional area of the i th beam.

During the optimization, the length and position of each beam are defined as parameters. The parameters of each beam's cross-sectional are regarded as variables in the optimization.

According to the simplification of the cross-sectional area in Fig. 33.1b, a single cross-sectional area can be expressed as follows:

$$A_i = 2B^i t_1^i + 2H^i t_2^i - 4t_1^i t_2^i \tag{33.2}$$

Then, the target function turns into

$$W = \sum_{i=1}^n \rho_i L_i A_i = \sum_{i=1}^n \rho_i L_i (2B^i t_1^i + 2H^i t_2^i - 4t_1^i t_2^i) \tag{33.3}$$

In the structural optimization of the ship unloader, the constraints such as strength and stiffness need to be considered. Each variable has its own range; for example, the plate thickness, which cannot be arbitrarily selected, can only take the standardized values. Therefore, the mathematical model of the ship unloader's optimization problem can be summarized as follows:

$$\left\{ \begin{array}{l} \min \quad W = \sum_{i=1}^n \rho_i L_i A_i = \sum_{i=1}^n \rho_i L_i (2B^i t_1^i + 2H^i t_2^i - 4t_1^i t_2^i) \\ \text{s.t.} \quad |\sigma| \leq [\sigma] \\ \quad \quad |u| \leq [u] \\ \quad \quad X \leq l, \quad (i = 1, 2, \dots, n) \\ \quad \quad X \geq m, \quad (i = 1, 2, \dots, n) \end{array} \right. \tag{33.4}$$

B^i , H^i , t_1^i , and t_2^i , respectively, refer to width, height, wing plate's thickness, and web thickness of the i th beam; σ and $[\sigma]$ refer to maximum stress and allowable stress of the ship unloader's structure, respectively; u and $[u]$ refer to maximum displacement and allowable displacement, respectively; l_i and m_i are upper and lower limits, respectively, for each beam.

33.2.2 Parametric Finite Element Modeling

In the process of ship unloader's entire finite element analysis [4], modeling costs a large percentage of time. Therefore shortening the time of modeling plays an important role in improving the efficiency in the optimization.

Parametric modeling method [5] contains two aspects. On the one hand, the finite element model parameterization of the ship unloader makes it possible to change the finite element model when the values of these parameters are updated. It is needed for structural optimization, because the process of structural optimization is to constantly change design parameters and then get through the different combinations of parameter calculation to determine the pros and cons of the program and finally achieve the optimization of the design. On the other hand, in the parametric modeling, it is needed to give the most basic locating dimensions, since other related locating dimensions can be calculated in the background of the software, according to the relation among these parameters; for example, the software only needs to get one point's Z coordinate on front and back main beams to calculate all the key points of the Z coordinate on front and back main beams. Therefore, parametric modeling method reduces the amount of modeling's input data, improving the efficiency of the modeling.

Parametric modeling needs to input four kinds of parameters, namely modeling parameters, the cross-sectional parameters, the allocation of linear property, and load parameters. Modeling parameters are these critical dimensions of the structure of the ship unloader, as shown in Fig. 33.2. Cross-sectional parameters are pre-defined property parameters of cross sections. The allocation of linear property defines the element type, material type, cross section's type, and direction. The load parameters are the values of loads on load positions.

Parametric modeling's task [6] is the establishment of the finite element model for the ship unloader based on these input parameters. So these input parameters are used to form the ANSYS software command file [7], which automatically establishes the finite element model of the ship unloader.

In finite element modeling [8], except locating dimensions, the loads and constraints in the structure in the different working conditions should be considered.

According to the working conditions of the ship unloader, most of the load changes in the life cycle of the ship unloader are caused by the following factors:

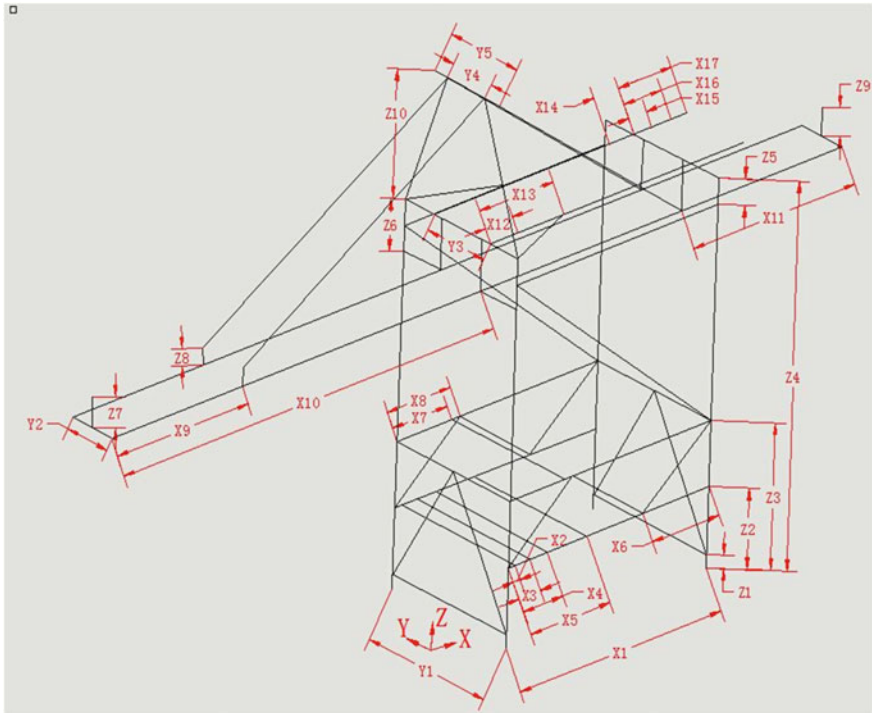


Fig. 33.2 Key dimension parameters of ship unloader's structure

- (a) Gravity load of the car at different locations,
- (b) Wind or no wind load,
- (c) Normal wind or extreme wind loads,
- (d) Impact load of the car buffer.

Moving loads (car) at the four positions in the finite element model are mainly considered:

- (a) The main car at the maximal front distance (Case 1),
- (b) The main car at the position between the front tension rod pin and pin linking front and back main beams (Case 2),
- (c) The main car at hopper unloading section (Case 3),
- (d) The main car at the maximal front distance (Case 4).

According to different combinations of these factors, we can get the load combinations of work status and non-working status of the ship unloader and then analyze the working status of the ship unloader under different conditions. The finite element model and ship unloader's stress and deformation calculation results in Case 1 condition before optimization are as shown in Fig. 33.3.

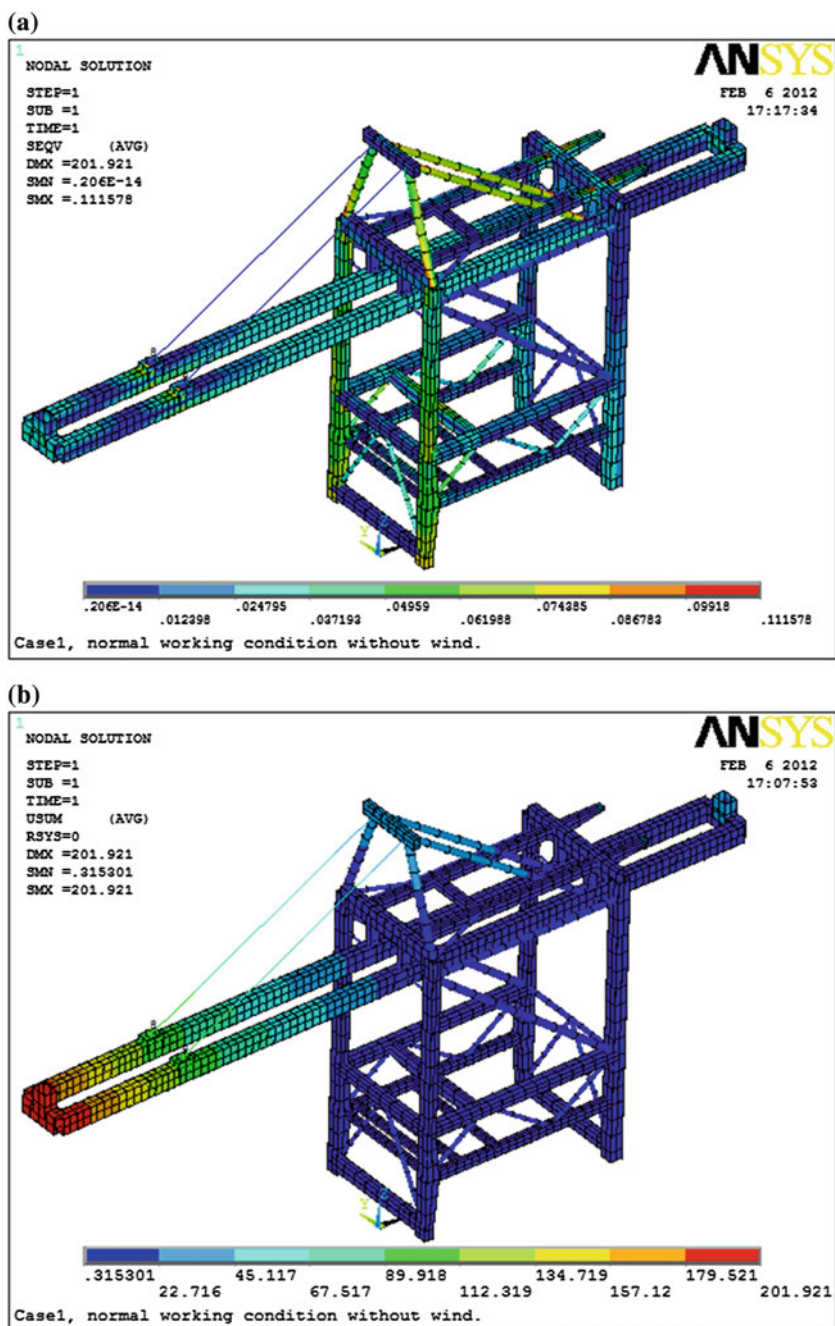


Fig. 33.3 Stress and deformation graph under Case 1. **a** Stress graph. **b** Deformation graph

33.2.3 Optimization Algorithm

After the establishment of mathematical model for structural optimization, orthogonal experiment method is used in optimization for cross-sectional area. The process is as follows (Fig. 33.4).

- Step 1: Define the design variables, the level and convergence factor k ($0 < k < 1$), and the number of iteration times N ($N \geq 1$);
- Step 2: Build a suitable three-level orthogonal experiment design Table [9], according to the selected design variables and the level number;
- Step 3: Start the n th iteration. When $n = 1$, the factor values are initial values. When $n > 1$, the factor values are determined by the optimal combination in the last orthogonal experiment and the convergence factor k (suppose there are two experimental factors A and B in three-level orthogonal experimental design). In the n th iteration, the levels are $A_1^n, A_2^n, A_3^n, B_1^n, B_3^n$. If the optimal combination is $A_2^n B_1^n$, in the next iteration, let $A_1^{n+1} = A_1^n - (A_1^n - A_2^n) \times k$, $A_2^{n+1} = A_2^n$, $A_3^{n+1} = A_3^n - (A_3^n - A_2^n) \times k$;
- Step 4: Do orthogonal experiment, and calculate the whole weight under different combinations of experimental factors;
- Step 5: Use ANSYS to calculate the maximum stress and deformation of the structure under each experimental scheme;
- Step 6: Select the combinations of experimental factors, which satisfy the required constraints, and choose the one that has the minimum weight to be the optimal solution in this iteration [10];
- Step 7: Output the optimal solution in Step 6, and judge whether n equals N . If $n = N$, turn to Step 8; if not, then let $n = n + 1$, and go back to Step 3;
- Step 8: Output the final solution and end the process.

33.3 Results and Discussions

33.3.1 Case Analysis

In this study, the original program structure, a 2,500-t/h bridge-type grab ship unloader [11], is optimized for the weight reduction design, using the optimization software. Before the optimization design, the values of the parameters in the original program are given. This original program is a relatively reasonable design, so an original value can be set as a basic point, and a range extended to both sides of the basic point is the domain of each variable in the optimization process.

According to the level's changing interval, we can set the value of convergence factor and the iteration times. Take parameter No. 1 for example. The change

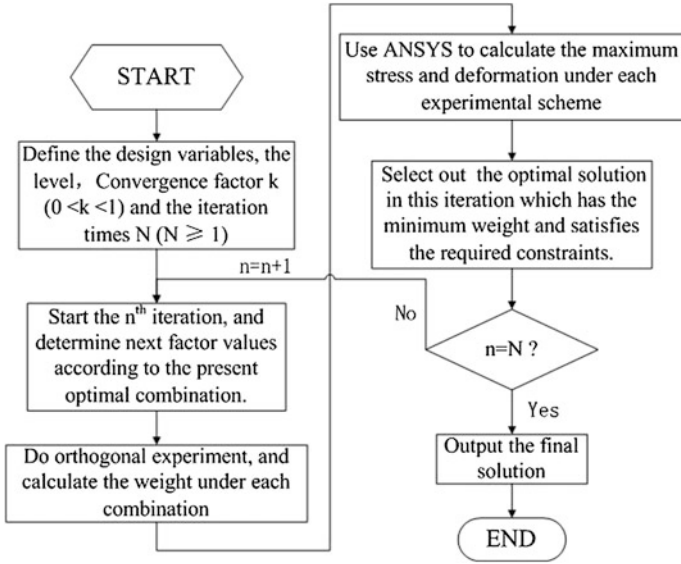
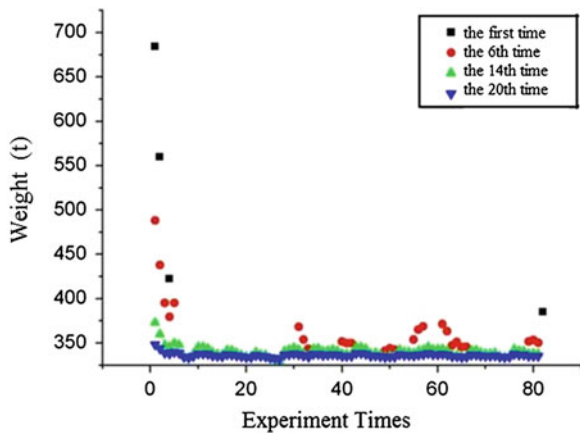


Fig. 33.4 Flowchart of structure optimization

interval is 800 mm, but the interval to less than 50 mm is finally wanted. So the convergence factor and the iteration times should be able to let the interval converge from 800 to 50 mm. Let the convergence factor be $k = 0.15$ and the iteration times $N = 20$. In this optimization, the allowable stress is 160 MPa, and the maximum allowable deformation is 200 mm. Input the original parameters into the software to initialize the database, and then follow the optimization process.

Through 20 times of iterations, as the number of iterations grows, the number of results satisfying the constraints increases and the weight of the structure in the optimal combination declines, as shown in Fig. 33.5.

Fig. 33.5 Distribution feasible solution



According to Fig. 33.5, after the first iteration, only four combinations of factors satisfy the constraints, ranging from 350 to 750 mm; after the 6th iteration, the feasible interval turns to [300, 500]; what is more, after the 14th and 20th iterations, almost all the combinations satisfy the constraints and the feasible interval becomes even smaller.

33.3.2 Evaluation of Optimal Results

Evaluation comes from two aspects. Firstly, compare the weight of the optimized design with the original one to see how much weight it can decline. Secondly, compare optimization method based on the orthogonal experiment with genetic algorithm optimization, figuring out the pros and cons.

Values of the parameter of each cross section can be obtained from the optimized results of the software. The comparison of the beam width, flange thickness, height, and web thickness of these four parameters between before optimization and after optimization of the structure is shown in Table 33.1 (optimized results have been rounded), and structural weight comparison of before optimization and after optimization is shown in Table 33.2.

From Table 33.2, it can be seen that the final result of the orthogonal experiment method makes reduction of 53.66 tons, 2.8 % of the original weight, which is 1,900 tons.

33.3.3 Calculation Time Comparison

The biggest advantage of the structural optimization method based on the orthogonal experiment is the efficiency of the finite element calculation times and makes it possible to optimize the structure of the ship unloader in an acceptable time. The comparison of proposed method in this paper with other methods shows that the proposed one is less time-consuming.

In the optimization process, each iteration has to calculate for four different working conditions. Each condition has to calculate 81 times, and each calculation needs the analysis in ANSYS. So for 20 times of iterations, it needs to do $8 \times 14 \times 20 = 6,480$ times of calculations in ANSYS in total. Each calculation in ANSYS needs about 4 s. Then, it takes approximately 7.2 h on a computer with 2.13 GHz dual-core CPU.

If the traditional genetic algorithm is taken in this case, 18.5 days is needed on the same computer (The initial number of individuals in a population is 100, and the number of iteration times is 1,000, hypothetically).

Table 33.1 Parameter comparison before and after optimization (mm)

No.	1	2	3	4	5	6	7	8
Before	1,800	14	2,500	12	1,800	14	2,500	12
After	1,760	9	2,760	12	1,570	10	2,440	11
Parameter	B	t_1	H	t_2	B	t_1	H	t_2
Component	Front main beam				Back main beam			
No.	9	10	11	12	13	14	15	16
Before	1,850	12	1,300	14	1,300	18	2,500	14
After	1,700	12	1,450	13	1,420	13	2,670	12
Parameter	B	t_1	H	t_2	B	t_1	H	t_2
Component	Land-sea side column				Land-sea upper crossbeam			
No.	17	18	19	20	21	22	23	24
Before	1,000	16	2,000	10	1,000	16	1,600	14
After	850	10	2,170	17	1,150	13	1,700	12
Parameter	B	t_1	H	t_2	B	t_1	H	t_2
Component	Hopper back beam				Ladder top crossbeam			
No.	25	26	27	28	29	30	31	32
Before	1,000	10	1,400	10	1,300	12	1,450	10
After	1,080	12	1,350	12	1,450	14	1,250	14
Parameter	B	t_1	H	t_2	B	t_1	H	t_2
Component	Engine room classis beam				Hopper front beam			
No.	33	34	35	36	37	38	39	40
Before	1,850	10	1,400	10	1,000	10	1,400	10
After	1,800	12	1,230	7	660	10	1,650	14
Parameter	B	t_1	H	t_2	B	t_1	H	t_2
Component	Land-sea contact beam (middle)				Land-sea contact beam (down)			

Thus, the optimization method based on orthogonal experiment can not only get optimal result, satisfying the constraints, but also greatly save the calculation time, which makes it convenient to call analysis in ANSYS.

Table 33.2 Weight comparison before and after optimization

No.	Component	Before (<i>t</i>)	After (<i>t</i>)	Reduction (<i>t</i>)	Reduction (%)
1	Front main beam	100.62	81.81	18.81	18.7
2	Back main beam	102.94	75.83	27.1	26.33
3	Land–sea side column	51.63	49.15	2.48	4.8
4	Land–sea upper crossbeam	35.44	29.07	6.36	17.96
5	Hopper back beam	11.78	10.12	1.66	14.08
6	Ladder top crossbeam	6.41	5.83	0.58	9.1
7	Engine room classis beam	21.31	25.85	−4.54	−21.31
8	Hopper front beam	8.52	10.57	−2.05	−24.03
9	Land–sea contact beam (middle)	30.43	25.61	4.81	15.81
10	Land–sea contact beam (down)	22.42	23.98	−1.56	−6.97
Total		391.5	337.84	53.66	13.7

33.4 Conclusion and Future Work

For the study in ship unloader's weight reduction, this paper presents an optimization method based on orthogonal test structure. The entire process of the optimization design is as follows: Define the structure of the ship unloader's optimization objective function and design variables; build parametric finite element model, which can be changed by modifying the parameters, for calculating stress and deformation of the structure in each iteration with various factor combinations, avoiding wasting time in re-establishing different models; develop ship unloader's beam cross section optimization process with the orthogonal experiment method; finally, use advanced language and finite element analysis software to develop the software for optimization. Compared with the traditional genetic algorithm, the optimization method based on the orthogonal experiment improves the efficiency of the ship unloader's structural optimization for weight reduction. The final optimized results satisfy the constraints and reduce the weight of the structure and the cost for manufacturing. Meanwhile, for the structural optimization method and the software, there are still some aspects to be improved. The future work is to generate orthogonal table automatically, find a better way to deal with the structural constraints in optimization, and improve the design of the ship unloader's parametric modeling software's interface and the way to input data for improving the efficiency.

Acknowledgments This research is financially supported by Natural Science Foundation of China (Project Nos. 51075275 and 51135004).

References

1. Meng Q (2007) Grab ship unloader parametric design method and the programming. Dalian Technology University, Dalian, p 6
2. Tao D (2010) Modern design methods. China Petrochemical Press, Beijing, p 1
3. Coello CA, Christiansen AD (2000) Multiobjective optimization of trusses using genetic algorithms. *Comput Struct* 75:647–660
4. Xu T (2009) Orthogonal experiment design based on object-oriented finite element program and its research in structural optimization. Jilin University, Jilin, p 6
5. Barrios Hernandez CR (2006) Thinking parametric design: introducing parametric Gaudi. *Des Stud* 27(3):309–324
6. Montgomery DC (2007) Experimental design and analysis. People Posts and Telecommunications Press, Beijing, pp 1–22
7. Li Y, Hu C (2008) Experimental design and data processing. Chemical Industry Press, Beijing, pp 124–161
8. Wang M (2003) Finite element method. Qinghua University Press, Beijing
9. Pang S (2004) Orthogonal table construction method and its application. Electronic Science and Technology University Press, Sichuan, pp 1–67
10. Fredricson H (2005) Topology optimization of frame structures-joint penalty and material selection. *Struct Multidisc Optim* 30:193–200
11. Zhang J (2000) 2500 t/h Grab ship unloader. To meet the new development of materials handling technology in the 21st century—Chinese Mechanical Engineering Society sixth annual meeting of material handling branch, pp 194–198

Part V
Enterprise Logistics (EL)

Chapter 34

Given Target Position Path Planning of Concrete Pump Vehicle

Xin Wang, Hui Jin, Xuyang Cao, Shunde Gao and Shujun Ming

Abstract In order to solve the problem of given target position path planning of concrete pump vehicle (GTPPPCPV problem), first of all, this paper sets up the mathematic model, which includes defining the problem for concrete pump vehicle's path planning, describing the concrete pump vehicle's state, and the path length in configuration space. Then put forward an improved rapidly exploring random tree (RRT) algorithm, Muti-RRTs base on target restriction, by the manner of bi-directional and multi-step to extend the RRTs, (GoalRestMutiConConRRT), to solve the GTPPPCPV problem, and then a path optimization method is given to optimize the path. Finally, the GoalRestMutiConConRRT algorithm and the optimization method are applied to two cases, pouring in the window of high building and changing the pouring windows. The result verified the feasibility and validity to solve the problem of GTPPPCPV using GoalRestMutiConConRRT algorithm.

Keywords Concrete pump vehicle · Path planning · RRT · Given target position

34.1 Introduction

It is a very common task of the concrete pump vehicle that makes the end hose reach the pouring location from current state. The control of the concrete pump vehicle mainly relies on the control handle in cab or the remote in venues, to adjust the angle of each boom and the slewing table, so that the end hose can reach the specified location. It is a complicated work for the operator to get a collision free and lowest cost path [1–3]. So, this study aims to provide a motion plan to guide the concrete pump operator to make the corresponding operation, so that the efficiency and the safety can be improved. In addition, the foundation for the fully automatic concrete pump vehicle operation in the future is laid in this paper.

X. Wang · H. Jin · X. Cao · S. Gao · S. Ming (✉)
School of Mechanical Engineering, Dalian University of Technology, Dalian
Liaoning, People's Republic of China
e-mail: wangxbd21@163.com

© Springer-Verlag Berlin Heidelberg 2015
Logistics Engineering Institution, CMES (ed.),
Proceedings of China Modern Logistics Engineering,
Lecture Notes in Electrical Engineering 286, DOI 10.1007/978-3-662-44674-4_34

Rapidly exploring random tree (RRT) [4–9] is a very popular algorithm which is based on random sampling. Because of outstanding performance in high-dimensional space, RRT has been widely used in many path planning problems. Concrete pump vehicle path planning is considered as a typical high-dimensional path planning problem, so RRT is very applicable to solve concrete pump vehicle path planning problem.

In order to solve the problem of concrete pump vehicle path planning, first we attempt to use an advanced RRT algorithm, Muti-RRTs based on target restriction, by the manner of bi-directional and multi-step to extend the RRTs (Goal-RestMutiConConRRT) in this paper, and then the path optimization method will optimize the path which has been found before. Finally, through experiments, this method is verified a good way to solve GTPPPCPV problem.

34.2 Set up the Mathematic Model

34.2.1 *The Definition of the Problem of Concrete Pump Vehicle's Path Planning*

The problem of concrete pump vehicle's path planning is to search a motion sequence from current state and make the end hose reach the pouring location in C space. In this sequence, concrete pump vehicle with environment and itself collision free, the motion of each boom and slewing table in limited scope is required.

34.2.2 *The Description of Concrete Pump Vehicle State*

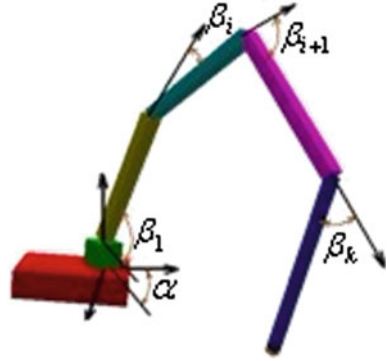
Concrete pump vehicle can be seen as a single arm robot with chassis, slewing table, and k sections boom (With the end hose not considered). This is a kind of typical open chain structure and we can describe its state by a C space which is composed of $k + 1$ DOFs. Here, we use $X = (\alpha, \beta_1, \dots, \beta_i, \beta_{i+1}, \dots, \beta_k)$ to describe the state of concrete pump vehicle at any time, as shown in Fig. 34.1.

Here,

- α Rotating angle of the slewing table relative to chassis;
- β_1 Rotating angle of the first section boom relative to horizontal plane;
- β_i Rotating angle of the i th section boom relative to $(i - 1)$ th section boom ($i \in [2, \dots, k]$)

Using this state space which is composed of $k + 1$ DOFs, we can transform GTPPPCPV problem of concrete pump vehicle path planning to the problem for finding a security motion sequence in C space.

Fig. 34.1 The state of concrete pump vehicle



34.2.3 Denote of Path Length

According to the motion feature of concrete pump vehicle, the revolving of slewing table will make the entire boom rotate together, and the angle change of the i th section boom will cause the boom from $(i + 1)$ th to k th section change their corresponding angles. It can be seen that the motion cost of each part increasing from top to bottom. So, this study describes concrete pump vehicle's path length with the sum of the slewing table and each boom's angles, and each angle should consider its corresponding cost.

If $X_j = (\alpha^j, \beta_1^j, \dots, \beta_i^j, \beta_{i+1}^j, \dots, \beta_k^j)$ and $X_{j+1} = (\alpha^{j+1}, \beta_1^{j+1}, \dots, \beta_i^{j+1}, \beta_{i+1}^{j+1}, \dots, \beta_k^{j+1})$ are the any two states of concrete pump vehicle, then:

$$d(X_j, X_{j+1}) = \left| (r_1 \times (\alpha^{j+1} - \alpha^j)) \right| + \left| (r_2 \times (\beta_1^{j+1} - \beta_1^j)) \right| + \dots + \left| (r_m \times (\beta_i^{j+1} - \beta_i^j)) \right| + \left| (r_{m+1} \times (\beta_{i+1}^{j+1} - \beta_{i+1}^j)) \right| + \dots + \left| (r_{k+1} \times (\beta_k^{j+1} - \beta_k^j)) \right| \quad (30.1)$$

Here,

- $d(X_j, X_{j+1})$ The distance from state X_j to state X_{j+1} ;
- r_1 The motion cost of the slewing table, $r_1 = 1$;
- r_m The motion cost of the i th section boom $r_m = 0.5 + \frac{0.5}{k+1} \times (k - i)$ ($m \in [2, 3, \dots, k + 1], m = i + 1$);

So, the entire length of the path L can be expressed as $L = \sum_{i=0}^{n-1} d(X_j, X_{j+1})$, n is the number of the state nodes in the path.

34.3 GoalRestMutiConConRRT Algorithm and Path Optimized Method

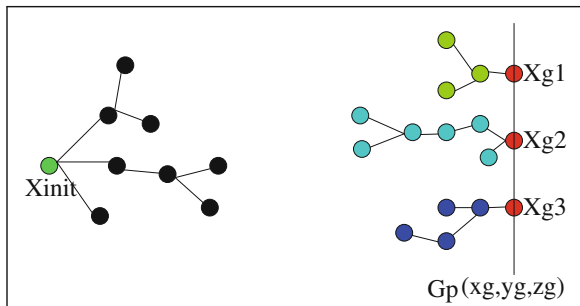
34.3.1 GoalRestMutiConConRRT Algorithm

In order to solve GTPPPCPV problem, this paper proposes GoalRestMutiConConRRT algorithm. As shown in Fig. 34.2, this algorithm first builds an initial tree, the root of which is at initial state and the tree extends in forward direction. Then a target tree set is built, states of these tree roots all are mapped with the target position of the end-effector, and the target trees extend in reverse direction (In Fig. 34.2, the line denotes the target position, the points on the line are the states which mapped with the target position, and other points are the states in C space. GoalRestMutiConConRRT algorithm will take into account both the tree's extension and new tree's creation.

34.3.1.1 GoalRestMutiConConRRT Algorithm Main Function

As shown in Fig. 34.3, X_{init} is the initial state of the concrete pump vehicle, Gp denotes the target position of the end-effector, T_{num} is the ceiling of target tree number, listGTRoot is used to save state points which are mapped with Gp . Firstly, the main function builds an initial tree, the root of which is at initial state, uses inverse kinematics function, GetInvKinState(), to get a target states X_{goal} mapped with Gp , then adds X_{goal} into listGTRoot and uses X_{goal} as root to build a target tree. Secondly, the main function enters into the big circle phase, the terminal condition of the function is the number of sample points reaching limit K or the initial tree and one of the target trees meeting with each other. If the number of target trees does not reach T_{max} , the main function executes ExtendTree() function to extend existing trees in p probability, or uses BuildTargetTree() function to build a new target tree in $1-p$ probability. On the other hand, it only uses ExtendTree() function to extend existing trees.

Fig. 34.2 Extend manner of GoalRestMutiConConRRT trees



```

GoalRestMutiConConRRT( $X_{init}$ ,  $C_p$ ,  $T_{min}$ )
1  BuildInitTree( $X_{init}$ ) ;
2   $X_{goal} = \text{GetInvKinState}(C_p(x,y,z))$ ;
3  listGTRoot.add_vertex( $X_{goal}$ ) ;
4  BuildtargetTree( $X_{goal}$ ) ;
5  While ( $i < K$ ) and (! connected)
6    If  $T_{min} < T_{max}$ 
7      Do ExtendTree() by  $p\%$  ;
8      Do BuildTargetTree( $C_p(x,y,z)$ ) by  $(1-p)\%$  ;
9    else
10     ExtendTree() ;

```

Fig. 34.3 GoalRestMutiConConRRT algorithm main function

34.3.1.2 Extend Tree

Function `ExtendTree()` is used to extend existing trees. This function executes the first 6 rows to let the initial tree extend by a step and get a new configuration $X_{i_{new}}$ in p probability, rows 2 to 6 are used to get a tree from target trees, the root configuration of which is nearest to $X_{i_{new}}$, or executes rows 7 and 8 to select a target tree randomly in $1-p$ probability. Finally, this function uses RRTConCon algorithm which is mentioned in [10] and [11] to extend initial tree and the selected target tree bidirectionally, as shown in Fig. 34.4.

Fig. 34.4 Extend tree function

```

ExtendTree()
//Do row 1 to 6 by  $q\%$ .
1   $X_{i_{new}} = \text{Extend}(T_{init})$  ;
2  for  $k = 1$  to listGTRoot.size()
3     $\text{StateDis2} = \text{Metric}(X_{i_{new}}, \text{listGTRoot}[k])$  ;
4    If ( $\text{StateDis2} < \text{minStateDis2}$ )
5       $\text{minStateDis2} = \text{StateDis2}$  ;
6       $T_{sel} = T_i[k]$  ;
// Do row 7, 8 by  $1-q\%$ .
10  $k = \text{rand}(\text{listGTRoot.size})$  ;
11  $T_{sel} = T_i[k]$  ;
12 RRTConCon( $T_{init}$ ,  $T_{sel}$ ) ;

```

34.3.1.3 Build New Target Tree

As shown in Fig. 34.5, BuildTargetTree() is used to build a new target tree. This function enters into the big circle phase in m probability. In this circle, the function uses GetInvKinState() to get a target configuration X_{temp} which is mapped with Gp firstly. Rows 3 to 7 are used to let the distance between X_{temp} and the configuration in listGTRoot which has the smallest distance from X_{temp} , greater than threshold d . A target configuration X_{goal} will be got through rows 8 and 9, and the distance between X_{goal} and the new configuration of initial tree is smallest. And then 11–14 rows make sure that the distance between X_{temp} and the configuration in listGTRoot which is nearest from X_{temp} , greater than threshold d . Rows 15 and 16 are used to build a new target tree with the root X_{goal} , which is added into listGTRoot. Finally, the count of tree number T_{num} adds one.

Fig. 34.5 BuildTargetTree function

```

BuildTargetTree()
//Do the follow loop by m%.
1  While j < N
2     $X_{temp} = \text{GetInvKinState}(Gp(x,y,z)) ;$ 
3    StateDis = min(Metric( $X_{temp}$ , listGTRoot));
4    While (StateDis < d)
5       $X_{temp} = \text{GetInvKinState}(Gp(x,y,z)) ;$ 
6      StateDis = min(Metric( $X_{temp}$ , listGTRoot));
7    StateDis1 = Metric( $X_{temp}$ ,  $X_{i_{new}}$ );
8    If (StateDis1 < minStateDis1)
9      minStateDis1 = StateDis1
10    $X_{goal} = X_{temp} ;$ 
//Do row 11 to 14 by 1-m%.
11   $X_{goal} = \text{GetInvKinState}(Gp(x,y,z)) ;$ 
12  StateDis = min(Metric( $X_{goal}$ , listGTRoot));
13  While (StateDis < d)
14     $X_{goal} = \text{GetInvKinState}(Gp(x,y,z)) ;$ 
15  Ti[ $T_{num}$ ] = new Tree( $X_{goal}$ );
16  listGTRoot.add_vertex( $X_{goal}$ );
17   $T_{num} ++ ;$ 

```

34.3.2 Path Optimized Method

Using GoalRestMutiConConRRT algorithm can rapidly find a path in C space, but the quality of the path is not high, so a method to optimize this path is introduced in this paper. The method is described as follows:

1. Set the iteration number N . This paper takes $N = 2000$;
2. Select two state nodes in the path randomly and then connect this two state nodes using RRT-connect method;
3. If the new path is better than the saved one, then replace it with the new path. Otherwise end this iterate;
4. Repeat steps (2) and (3) until the number of iterations is equal to N .

34.4 Cases Study

34.4.1 Parameter Setting

- The construction parameter of the concrete pump vehicle

In this experiment, the concrete pump vehicle with four sections booms whose folded form is winding was selected as the object of study. The main parameter can be seen in Table 34.1.

- The rotation scope of each part

According to the limitation of the construction and folded form, the rotation scope of slewing table and each boom can be seen in Table 34.2.

34.4.2 Two Typical Cases

The first case shown in Fig. 34.6 requires concrete pump vehicle's boom to enter the window to pour. The location of the window that is colored with yellow, with the world coordinate $(-6.6, 32, 8)$ can be seen in picture. Concrete pump vehicle will change the state from $X_{init}(1.57, 1.0, -0.5, -0.3, -0.8)$ as shown in Fig. 34.6 over high voltage to get the pouring position. During the whole motion process, the concrete pump vehicle cannot collide with itself or environment, and the threat of high voltage should be considered.

The second case in Fig. 34.7 is a usual case. In order to pour each room in turn, when a window has been poured, the end-effector changes its position to pour into another window. This case uses the first case's target state as its initial state. Then change end-effector's position to pour another window which is painted with yellow in Fig. 34.7 and its world coordinate is $(-7.3, 27.0, 22.5)$. It is required as same

Table 34.1 Construction parameter

First boom		Second boom		Third boom		Fourth boom		Rotating angle of slewing table	Horizon length of boom	Vertical height of boom
Length	Angle	Length	Angle	Length	Angle	Length	Angle			
10,250 mm	92°	9,180 mm	180°	9,240 mm	180°	9,330 mm	260°	360°	38 m	42 m

Table 34.2 The rotating scope of each part

Rotating scope of the slewing table (rad)	Rotating scope of the first boom (rad)	Rotating scope of the second boom (rad)	Rotating scope of the third boom (rad)	Rotating scope of the fourth boom (rad)
$[-3.14, 3.14]$	$[0, 1.60]$	$[-3.14, 0]$	$[-3.14, 0]$	$[-3.14, 1.39]$

Note The angle between slewing table and chassis turning counterclockwise is positive; the angle of first boom in lifting direction is positive; the angle of other booms relative to the last boom lifting direction is positive

Fig. 34.6 Pouring inside the window of the tall building

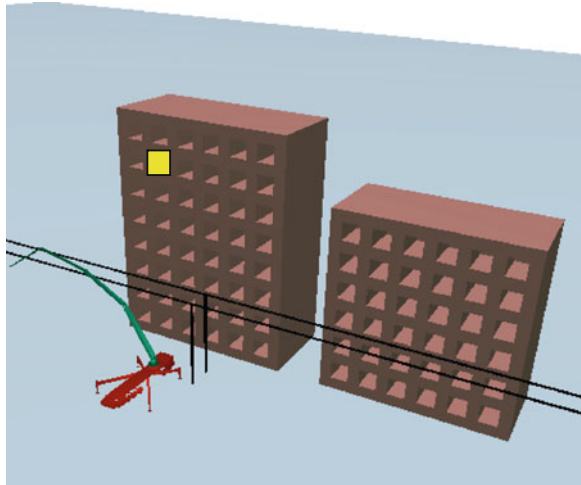
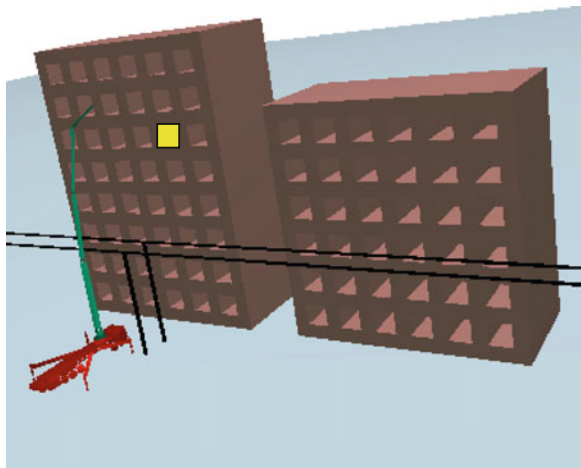


Fig. 34.7 Changing pouring window



as the first case that the concrete pump vehicle cannot collide with itself neither with environment, and the threat of high voltage should be considered.

34.4.3 Planning Result

- Planning effect of pouring inside the window of the tall building
- Planning effect of changing pouring window

The correlative data of two cases which are executed 100 times, respectively, can be seen in Table 34.3. From Figs. 34.8, 34.9 and Table 34.3, we can see that using the method mentioned in this paper, a good path can be found in short time.

Table 34.3 The performance of the method in the two cases

working conditions	Success number	Avg. find path time (s)	Avg. path length before optimizing (rad)	Avg. optimized time (s)	Avg. path length after optimizing (rad)
Case 1	100	1.26	10.62	3.54	4.88
Case 2	100	0.79	10.30	1.37	3.04

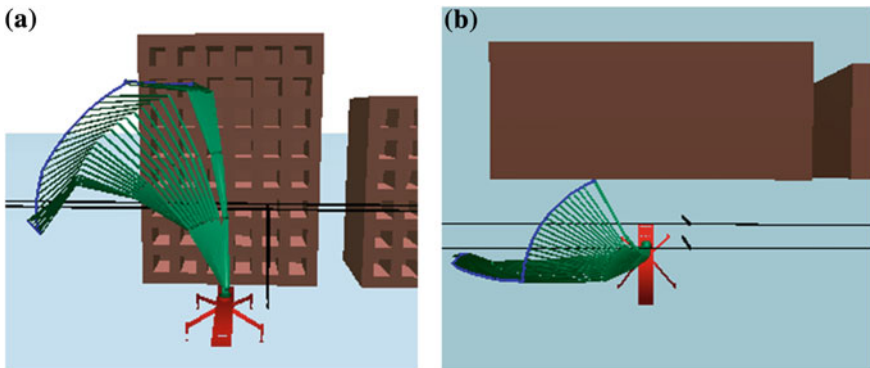


Fig. 34.8 Planning effect of pouring inside the window of the tall building: **a** front view **b** top view

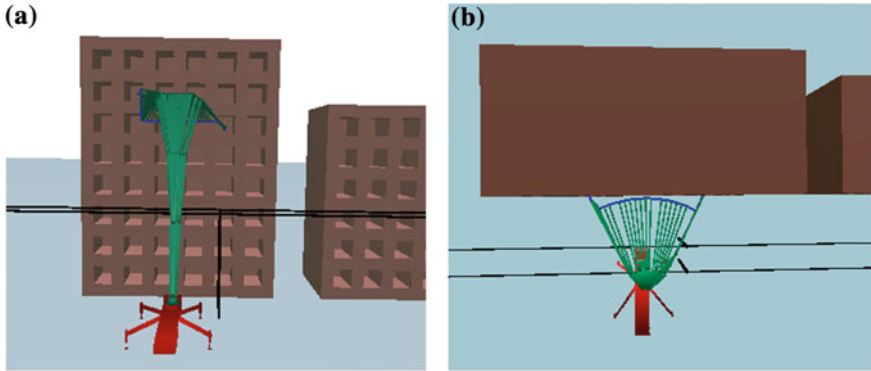


Fig. 34.9 Planning effect of changing pouring window: **a** front view **b** top view

34.5 Conclusions

In this paper, an improved RRT algorithm (GoalRestMutiConConRRT) and a path optimization method is used to solve GTPPPCPV problem. By using this method in two cases, this paper verified that using this method can rapidly find a safe and available path in complicated environment. The method presented in this paper can provide a motion plan to direct the operator do the corresponding actions. If this motion plan is adopted, the efficiency and safety of the operation can be greatly improved and the requirement of the operator's experience can be reduced.

References

1. Wang T, Wang Gm Liu K (2009) Simulation control of concrete pump truck boom based on PSO and adaptive robust PD. In: Chinese control and decision conference, Guilin, China, 17–19 June 2009
2. Tang XJ, Wu ZY, Shi PK, Liu HM (2008) Kinematical simulation and control on intelligent booms of concrete pump vehicles. *Chin J Constr Mach* 6
3. Guo DM, Ou GH, Li YG, Liu K (2011) Simulation applying to planning tracks of concrete pump truck arms. *J Syst Simul* 6
4. LaValle SM (1998) Rapidly-exploring random trees: a new tool for path planning. Iowa State University, Iowa
5. LaValle SM, Kuffner J (2000) Rapidly-exploring random trees: progress and prospects. In: Proceedings of the 4th international workshop on algorithmic foundations of robotics (WAFR), Journal of Robotics Research, Dartmouth
6. LaValle SM, Kuffner J (2001) Randomized kinodynamic planning. *Int J Robot Res* 20:5
7. Wang W, Li Y (2009) A multi-RRTs framework for robot path planning in high-dimensional configuration space with narrow passages. In: 2009 IEEE international conference on mechatronics and automation, Changchun, China, 9–12 Aug 2009

8. Wang W, Li Y, Xu X, Yang SX (2010) An adaptive roadmap guided Multi-RRTs strategy for single query path planning. In: 2010 IEEE international conference on robotics and automation, Alaska, USA, 3–7 May 2010
9. Wang W, Xu X, Li Y, Song J, He H (2010) Triple rrts: An effective method for path planning in narrow passages. *Adv Robot* 24:7
10. Kuffner JJ Jr., LaValle SM (2000) RRT-connect: an efficient approach to single-query path planning. In: Proceedings of ICRA '00. IEEE international conference on robotics and automation, San Francisco, CA, USA
11. Song JZ, Dai B, Shan EZ, He HG (2010) An improved RRT path planning algorithm. *Dianzi Xuebao (Acta Electronica Sinica)* 38:2

Chapter 35

A New Hybrid Topology Optimization Method Coupling ESO and SIMP Method

Hongyu Jiao, Qicai Zhou, Sixia Fan and Ying Li

Abstract In this paper, a new hybrid topology optimization named ESO–SIMP which couples evolutionary structural optimization (ESO) and SIMP is proposed. In ESO–SIMP method, the relative densities of elements are taken as the design variables, and the mean compliance is selected as the objective function. The mathematical model of topology optimization is built, and the iterative formula based on optimization criteria is obtained. A filtering function using strain energy as sensitivity number is introduced to prevent checkerboards and to eliminate mesh independency. In the process of each iteration, elements whose relative densities are less than or equal to rejection ratio are removed from the design domain and all remained elements are entered into the next iteration. The ESO method and the SIMP method are merged together perfectly in this paper. It is found that the new ESO–SIMP method has many advantages over the ESO method and the SIMP method in terms of efficiency and robustness.

Keywords Topology optimization · SIMP · ESO · ESO–SIMP

35.1 Introduction

Topology optimization of structures has been extensively researched in the past two decades, and many optimization methods have been developed such as evolutionary structural optimization (ESO) [1, 2], variable density method [3, 4], level set method [5, 6], and so on.

H. Jiao (✉) · Q. Zhou · S. Fan · Y. Li
College of Mechanical Engineering, Tongji University, Shanghai 201804, China
e-mail: cslgjhy@163.com

H. Jiao · Y. Li
College of Mechanical Engineering, Changshu Institute of Technology, Suzhou
215500, China

© Springer-Verlag Berlin Heidelberg 2015
Logistics Engineering Institution, CMES (ed.),
Proceedings of China Modern Logistics Engineering,
Lecture Notes in Electrical Engineering 286, DOI 10.1007/978-3-662-44674-4_35

The ESO method, developed by Xie and Steven, gradually removed underutilized material to achieve an optimal design. The amount of removed material is controlled by two parameters: rejection ratio (RR) and evolutionary rate (ER) [7]. These two parameters must be small. If the rejection ratio and evolutionary rate are too large, it will lead to deletion of too many elements in the process of iterations. Consequently, it results in numerical instabilities and the optimization result's differences.

The SIMP method originally introduced by Bendsoe and Sigmund is extensively used on the topology optimization of continuum structures as a kind of variable density method due to its advantages of fewer design variables and higher efficiency. However, one of SIMP's mayor drawbacks is that resulting topologies do not converge to fully black-and-white designs, exhibiting areas of intermediate densities that do not have physical meaning.

This paper presents a new hybrid topology optimization which couples ESO and SIMP under given boundary and loading conditions. Firstly, the SIMP method and the ESO method are described briefly. Secondly, the proposed algorithm named ESO-SIMP is introduced in more detail. Finally, an example is presented and analyzed.

35.2 ESO-SIMP Algorithm

35.2.1 The SIMP Method

The SIMP method has been widely accepted and applied. It considers material density as the design variable. An optimal structural topology is gotten by redistributing material within a reference domain, based on an optimality criteria or a mathematical programming method.

In SIMP method, the design domain Ω is discretized with finite elements. The material properties are constant in each of these elements and depend on the relative density x_i . The relative density should be either 1 or 0 in the design domain Ω after the optimization. To avoid the intermediate relative density, the penalization factor p is used to punish the intermediate density.

The relationship between elastic modulus and the relative density is written as

$$E(x_i) = E_{\min} + (x_i)^p(E_0 - E_{\min}) \quad (35.1)$$

where E_0 is the elastic modulus of material. E_{\min} is taken as $E_0/1000$ for the numerical stability. x_i is the relative density of the i th element. p is the penalization factor.

The relative densities of elements are taken as the design variables, and the mean compliance is selected as the objective function. Then, the topology optimization problem for minimum compliance can be written as

$$\text{Find: } X = \{x_1, x_2, x_3, \dots, x_i\}^T, \quad i = 1, 2, \dots, n \quad (35.2)$$

$$\text{Minimize: } C(X) = F^T U = U^T K U = \sum_{i=1}^n u_i^T k_i u_i = \sum_{i=1}^n (x_i)^p u_i^T k_0 u_i$$

$$\text{Subject to: } K U = F, \quad V = f_0 \cdot V_0 = \sum_{i=1}^n x_i v_i$$

$$0 < x_{\min} \leq x_i \leq x_{\max} \leq 1$$

where the objective function C is defined as the mean compliance. X is the vector of design variables; x_{\min} and x_{\max} are the minimum and maximum relative density of elements, respectively. The purpose of introducing x_{\min} is it must be nonzero to avoid singularity. F is the global load vector, and U is the displacement vector. K is the global stiffness matrix. k_i and u_i are the stiffness matrix and the nodal displacement vector of elements. V is the material volume, and V_0 is the initial volume of the design domain. f_0 is the prescribed volume ratio.

35.2.2 The ESO Method

The ESO process begins with a full design domain and gradually removes under-utilized elements. The amount of removed elements is controlled by

$$RR_{k+1} = RR_k + ER \quad (35.3)$$

where RR is rejection ratio and ER is evolutionary rate. k is the current iteration number.

35.2.3 A New Hybrid Method Coupling ESO and SIMP Method

A new hybrid topology optimization method in this paper, named ESO–SIMP, aims at coupling ESO and SIMP. By doing so, it is possible to obtain a clear profile of topology with no “gray” area. In ESO–SIMP method, the relative densities of elements are taken as the design variables, and the mean compliance is selected as the objective function. Then, the optimization problem for minimum mean compliance based on ESO–SIMP algorithm can be written as

$$\text{Find: } X = \{x_1, x_2, x_3, \dots, x_i\}^T, \quad i = 1, 2, \dots, n \quad (35.4)$$

$$\text{Minimize: } C(X) = U^T K U = \sum_{i=1}^n u_i^T k_i u_i = \sum_{i=1}^n (x_i)^p u_i^T k_0 u_i$$

$$\text{Subject to: } K U = F, \quad V = \sum_{i=1}^m x_i v_i \leq f_0 \cdot V_0$$

$$0 < x_{\min} \leq x_i \leq x_{\max} \leq 1$$

The difference between ESO–SIMP and SIMP methods is volume constraint. In process of optimization, elements whose relative densities are less than or equal to rejection ratio are removed from the design domain. The total volume of all remained elements V should satisfy

$$V = \sum_{i=1}^m x_i v_i \leq f_0 \cdot V_0 \quad (35.5)$$

where m is the number of all remained elements.

However, V is not the real total volume of remained elements V' which is expressed as

$$V' = \sum_{i=1}^m v_i \quad (35.6)$$

When volume constraint is satisfied, the real total volume of all remained elements V' is greater than V because of intermediate relative density. It is not beneficial to topology optimization for volume constraint. So during the process of optimization, the real total volume of all remained elements V' must be monitored.

35.2.4 Numerical Instabilities and Filtering

Topology optimization can often exhibit an instability for which the resulting topology contains a checkerboard pattern of active and removed elements. A popular heuristic treatment for preventing checkerboards is filtering or local smoothing of sensitivities similar to low-pass filtering in signal and image processing. This filtering technique works by smoothing local sensitivities after analysis, and these smooth sensitivities are used to modify and optimize the design.

First, the strain energy of elements, which are defined by averaging the sensitivity numbers of connected elements, is calculated as

$$s_i = \frac{1}{2} u_i^T k_i u_i \quad (35.7)$$

The defined filter functions are based on a length scale r_{\min} . The primary role of the scale parameter r_{\min} in the filter scheme is to identify the elements that influence the sensitivity of i th element. This can be visualized by drawing a circle of radius r_{\min} centered at the center of the i th element, thus generating the circular subdomain Ω_i . Elements located inside Ω_i contribute to the computation of the improved sensitivity number of i th element as

$$s'_i = \frac{\sum_{i=1}^M d_{ij} s_i}{\sum_{i=1}^M d_{ij}} \quad (35.8)$$

where s'_i denotes the sensitivity number after filtering, M is the total number of elements in the subdomain Ω_i , and d_{ij} is the linear weight factor defined by where r_{ij} is the distance between the center of the i th element and the element j th.

$$d_{ij} = r_{\min} - r_{ij} \quad (35.9)$$

35.2.5 Optimization Criteria and Iterative Formula

The optimization criteria can be derived by Lagrange function that consists of objective function and constraint conditions. The optimization criteria can be written as

$$B_i^k = \frac{p(x_i)^p u_i^T k_0 u_i}{\lambda_1 v_i} = \frac{2p}{\lambda_1 v_1 x_i} \times \frac{1}{2} u_i^T k_i u_i = \frac{2ps_i}{\lambda_1 v_i x_i} \quad (35.10)$$

The Eq. 35.8 is substituted to Eq. 35.10, and then, the optimization criteria after filtering can be written as

$$B_i^k = \frac{2ps'_i}{\lambda_1 v_i x_i} \quad (35.11)$$

The iterative formula based on optimization criteria can be written as

$$\begin{aligned} x_i^{k+1} &= (B_i^k)^\eta x_i^k & \text{if } x_{\min} < (B_i^k)^\eta x_i^k < x_{\max} \\ x_i^{k+1} &= x_{\min} & \text{if } (B_i^k)^\eta x_i^k \leq x_{\min} \\ x_i^{k+1} &= x_{\max} & \text{if } (B_i^k)^\eta x_i^k \geq x_{\max} \end{aligned} \quad (35.12)$$

Elements are removed from the design domain if they satisfy

$$x_i^{k+1} \leq RR \quad (35.13)$$

35.3 Topology Optimization Procedure Based on ESO–SIMP Method

To explain better how ESO–SIMP can be implemented into a computer program, a step-by-step algorithm is given as follows:

- Step 1: The maximum design domain is discretized with a densely finite element mesh.
- Step 2: Define all boundary constraints and apply load.
- Step 3: Assign design variables the initial values ($x_i^1 = 1$).
- Step 4: Form the relationship between elastic modulus and design variables as Eq. 35.1.
- Step 5: Carry out a linear finite element analysis of the structure.
- Step 6: Calculate the strain energy for all existed elements as Eq. 35.7.
- Step 7: Calculate the sensitivity number for all existed element as Eq. 35.8.
- Step 8: Calculate optimization criteria as Eq. 35.11 and update the design variables as Eq. 35.12.
- Step 9: Elements are removed if they satisfy Eq. 35.13.
- Step 10: If the total volume of all remained elements V satisfies volume constraint as Eq. 35.5, an optimum is reached. Otherwise, go to Step 4.

Flowchart depicting logical steps of ESO–SIMP is shown in Fig. 35.1.

35.4 Example and Discussion

An example [8] considers the stiffness optimization design of a cantilever beam under a concentrated loading as shown in Fig. 35.2. The design domain has length 80 mm, height 50 mm, and thickness 1 mm. The force is applied downward at the center of the free end with the magnitude of 100 N. The material has elastic modulus of 100 GPa and Poisson's ratio of 0.3. ESO–SIMP starts from the full design which is subdivided using a regular mesh of size 1×1 , tolling 4,000 four-node quadrilateral elements. The ESO–SIMP parameters are $RR = 0.1$, $r_{\min} = 2$ mm, $f_0 = 0.3$.

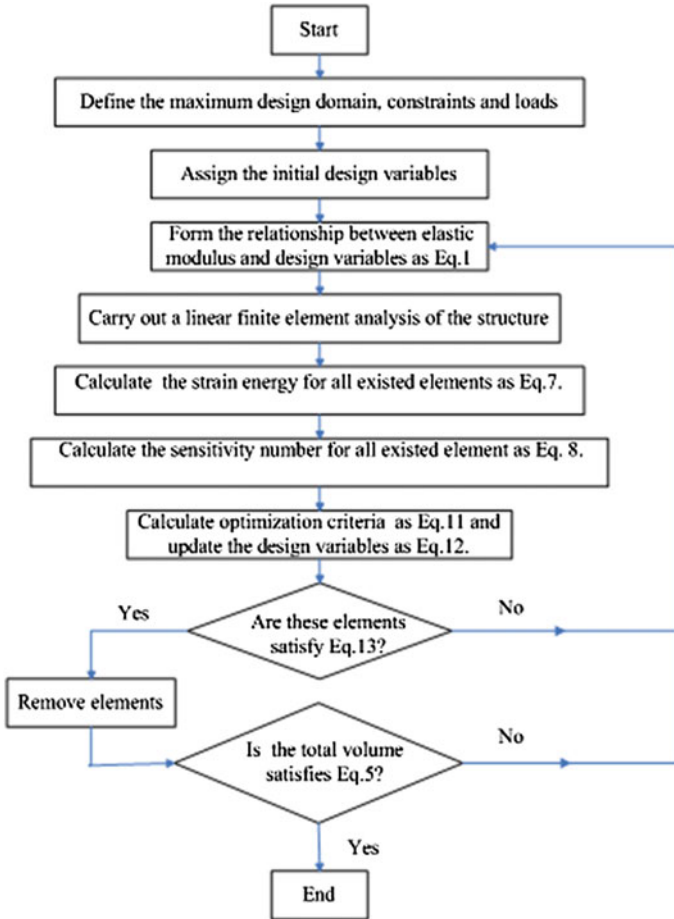
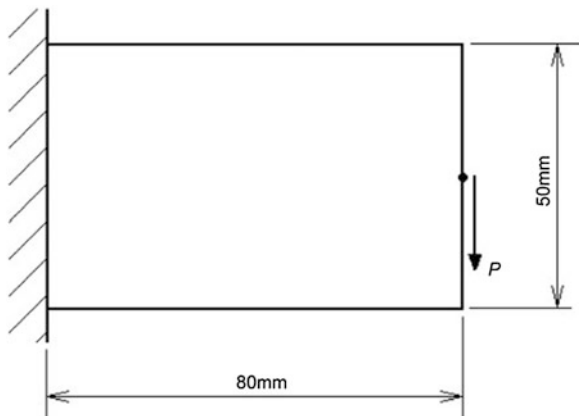


Fig. 35.1 Flowchart depicting logical steps of ESO-SIMP

Fig. 35.2 Dimensions of the design domain and boundary and loading conditions



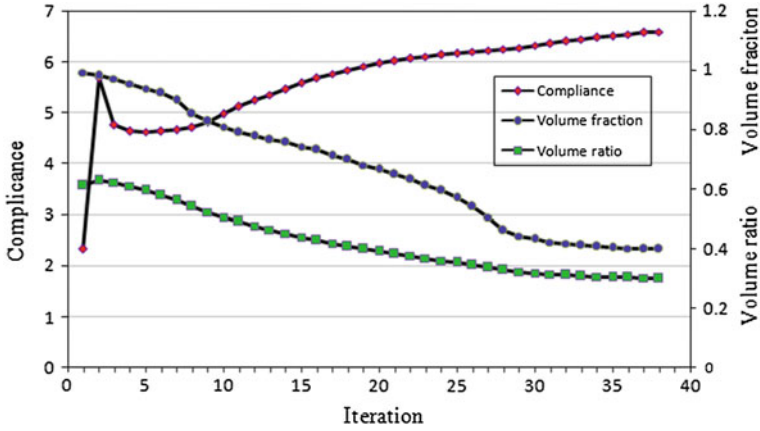


Fig. 35.3 The evolution histories of mean compliance C , volume ratio f , and volume fraction V_f

Figure 35.3 shows the evolution histories of mean compliance C , volume ratio f , and volume fraction V_f which is real total volume of remained elements to the initial volume. The mean compliance increases as the material is gradually removed from the design domain. After the total volume of remained elements reaches the objective volume, mean compliance reaches 6.589 N mm which is higher than that of the BESO method. This difference may be attributed to the overestimated strain energy of the intermediate-density elements.

The ESO-SIMP method reached 30 % of the initial volume ($f_0 = 0.3$) in 38th iteration, and volume fraction V_f is 0.3995. When V_f is equal to 0.5, the ESO-SIMP method only needs 27 iterations which is less than the BESO method which requires about 80 iterations [1, 8].

Figure 35.4 shows the history of topology where the final topology is shown in Fig. 35.4f. All remained elements are displayed on each topological graph. Each topological graph has a clear outline which is superior to the SIMP method. Simultaneously, the relative densities of all remained elements for final topology can be displayed as shown in Fig. 35.5.

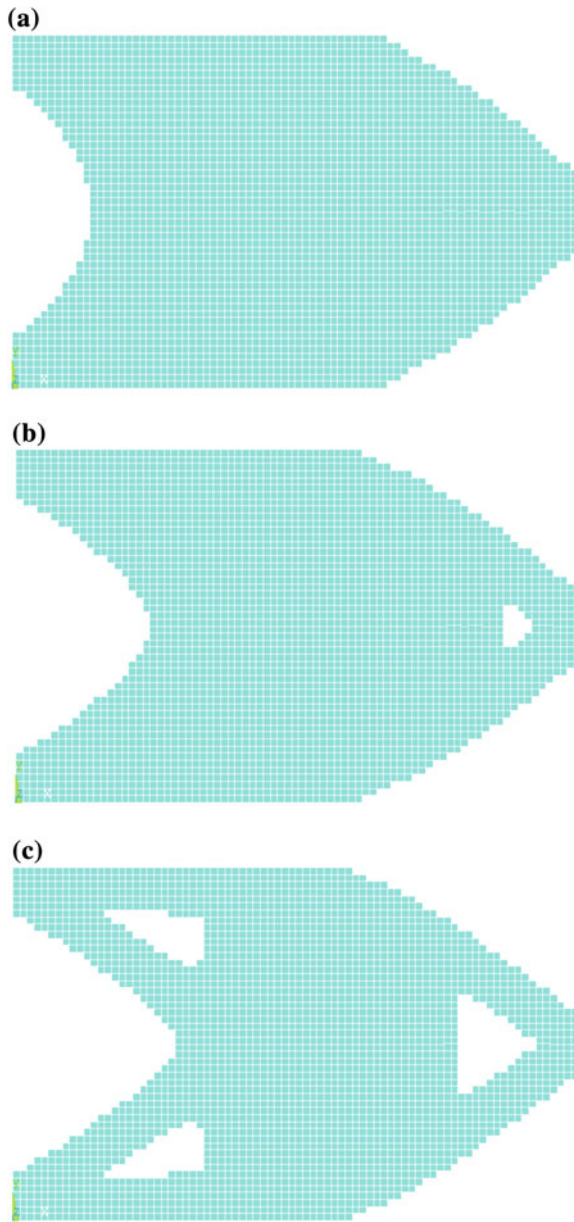


Fig. 35.4 The history of topology. **a** Iteration = 10. **b** Iteration = 15. **c** Iteration = 20. **d** Iteration = 25. **e** Iteration = 30. **f** Final topology

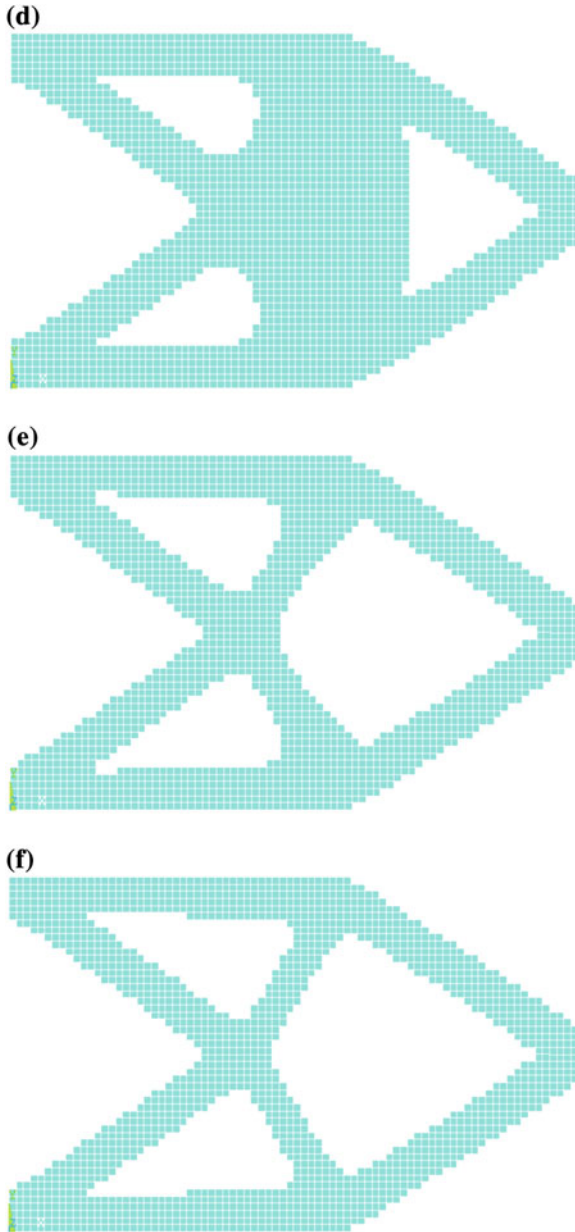
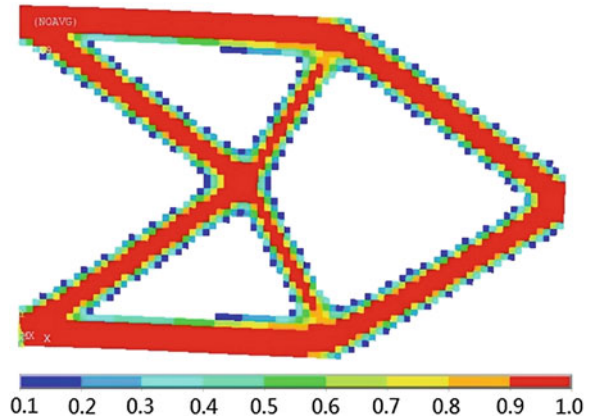


Fig. 35.4 (continued)

Fig. 35.5 The relative densities of all remained elements



35.5 Conclusions

This paper presents a new hybrid topology optimization which couples ESO and SIMP under given boundary and loading conditions. In ESO–SIMP method, the relative densities of elements are taken as the design variables, and the mean compliance is selected as the objective function. The mathematical model of topology optimization for minimum compliance based on the ESO–SIMP is built. A filtering function using strain energy as sensitivity numbers is introduced to prevent checkerboards and to eliminate mesh independency. The iterative formula based on optimization criteria can be obtained. In the process of each iteration, elements whose relative densities are less than or equal to rejection ratio can be removed from the design domain and all remained elements enter the next iteration. The ESO–SIMP method has higher computational efficiency and is more robust over the SIMP method and the ESO method.

References

1. Xie YM, Steven GP (1993) A simple evolutionary procedure for structural optimization. *Comput Struct* 49:885–896
2. Yang XY, Xie YM, Steven GP, Querin, OM (1999) Bidirectional evolutionary method for stiffness optimization. *AIAA J* 37(11):1483–1488
3. Bendsøe MP (1989) Optimal shape design as a material distribution problem. *Struct Optim* 1:193–202
4. Zhou M (1991) Rozvany Gin, the COC algorithm, part II: topological, geometry and generalized shape optimization. *Comp Methods Appl Mesh Eng* 89:197–224
5. Sethian JA (1999) *Level set methods and fast marching methods: evolving interfaces in computational geometry, fluid mechanics, computer vision, and materials Science*. Cambridge University Press

6. Osher S, Fedkiw R (2003) Level set methods and dynamic implicit surfaces. Springer, New York
7. Querin QM, Steven GP (1998) Evolutionary structural optimization (ESO) using a bidirectional algorithm. *Eng Comput* 15:1031–1048
8. Huang X, Xie YM (2007) Convergent and mesh-independent solutions for the bi-directional evolutionary structural optimization method. *Finite Elem Anal Des* 43:1039–1049

Chapter 36

An Integrated Conceptual Design Calculation Method for Logistics Machinery Based on Working Condition and Load Combination

Zhiyi Pan, Shunde Gao, Xin Wang and Xuyang Cao

Abstract Aiming at changeable market demands, it is difficult to obtain a reasonable and optimized design project efficiently and intelligently by theoretic calculation, which needs to be solved emergently. The character of calculation in logistics machinery product conceptual design includes lots of working condition (WC) and load combination (LC). An integrated strategy is applied to the logistics machinery product conceptual design, and an integrated conceptual design calculation method for logistics machinery based on WC and LC is presented in the paper. By solving the worst work condition and LC, resolving and clustering coupling in product parameters, and synchronization evolution of calculation model and geometry model, uniform and standardized calculation model for the logistics machinery product conceptual design is established, and clustering of project design and loose coupling between calculations is realized. Therefore, software framework is easy to accomplish. Conceptual design calculation software for straight-arm self-propelled high-altitude working platform is developed and applied in the GTBZ serial products. The software can improve the efficiency of conceptual design greatly and used in parameters optimization.

Keywords Conceptual design · Working condition · Load combination · Logistics machinery

With the complicated product design process, lots of uncertain factors and inevitable repeated modification, the design cycle is long and design quality is poor. However, with the fierce market competition, the requirement for enterprise to respond to customers demands quickly and to develop once to succeed is increasingly urgent. The important position and function of the conceptual design during the development process of the product full life cycle is widely taken

Z. Pan (✉) · S. Gao · X. Wang · X. Cao
School of Mechanical Engineering, Dalian University of Technology, Dalian 116024, China
e-mail: panzhiyi@dlut.edu.cn

seriously and has become one of the research hotspot in the design field. Though the actual input expenses of design phase only account for 5 % of the total cost of the product, it has determined about 70 % cost of product [1].

The logistics machinery product conceptual design is a cyclic iteration process of calculation, cut and try, and validation, etc. While the type of design knowledge is complicated, requirements change frequently, design cycle is short, and workload is heavy. Aiming at changeable market demands, it is difficult to obtain a reasonable and optimized design conceptual efficiently and intelligently by theoretic calculation, which needs to be solved emergently. With lots of uncertain factors during the conceptual design phase, frequent transfer of the input–output and other relevant parameters of the calculation model, and lots of complicated items of the conceptual design calculation, every designer usually takes charge of different calculation items in order to accomplish the design assignment in time, which brings the follow problems:

1. Usually, it is not accurate and easy to make mistakes to choose some of the working condition (WC) and load combination (LC) of logistics machinery, which is in a large number by experience.
2. Every index needs to be recalculated when the design is changed, which leads to the heavy workload and a long conceptual calculation period.
3. The calculation item is accomplished by multiple people, which leads to the coordination problem and the calculation mistake that is made by data inconsistency.
4. The management of the design process, the record of the calculation's gradual progress, and the writing and repeated modification of the calculation description are difficult.
5. Many important design indexes are difficult to be obtained. And the indexes are difficult to be optimized quickly through modifying the related parameters in general terms. Therefore, the resulting project is usually possible, but not optimized.

Therefore, the character of calculation in logistics machinery product conceptual design is lots of WC and LC. An integrated strategy is applied to the logistics machinery product conceptual design, and an integrated conceptual design calculation method for logistics machinery based on WC and LC is presented and adopted to develop the conceptual design calculation software for straight-arm self-propelled high-altitude working platform in the paper.

36.1 The Working Condition and Load Combination of Logistics Machinery Product

WC is the abbreviation of the working condition. LC is the combination of various types of force and torque loaded in the logistics machinery operating mechanism, which can be expressed by the letters LC. The important calculation basis for

logistics machinery conceptual design consists of WC and LC. The diversity of the logistics machinery operation in the form and the complexity of the mechanism lead to a large number of WC. It is difficult to choose the most dangerous WC and LC for an index from the large number of WC and LC. With the complexity of logistics machinery product WC and LC, it is not accurate to obtain the most dangerous WC by traditional theoretical analysis and experience, which is easy to make mistakes due to miscalculation and omission.

36.1.1 Working Condition and Working Conditional Parameters

Geometric parameters of the product WC are called WC parameters, which usually correspond to the motive mechanism of logistics machinery product. Taking the straight-arm self-propelled high-altitude working platform, for example, WC parameters include telescopic cylinder stroke, telescopic boom luffing angle, rotation angle, leveling angle, swing angle, and fly jib luffing angle. A WC set of WC, which consists of finite or infinite WC_i is established. Therefore, the WC_i can be synthetically characterized by a group of its WC parameters P_{ij}^C .

$$WC = \{WC_1, WC_2, \dots, WC_i, \dots\} \quad (36.1)$$

$$WC_i = \{P_{i1}^C, P_{i2}^C, \dots, P_{ij}^C, \dots\} \quad (36.2)$$

Every index in different WC can be calculated by WC parameters, which are the important parameters of theoretical calculation during the conceptual design process. For the finite WC, the WC parameters of pair-wise interaction coverage are placed into formula to calculate one by one to obtain the index in different WC by exhaustive combinatory method. For the infinite WC, discrete combinatory method is adopted. By this way, the finite value set is formed by each continuous WC parameter that is dispersed according to a certain size; then, the index in different WC is calculated based on exhaustive combinatory method, the calculation accuracy depends on the discrete size.

36.1.2 Load Combination and Load Combination Parameters

There are many types of loads that need to be considered during the calculation process of logistic machinery product design, such as self-weight, operating load, wind load, and special load.

1. Self-weight is the gravity of the various components of the product, which includes the gravity of metal structures, machinery, and electrical equipments.

At the beginning of the design calculation, the self-weight is unknown and needs to be estimated based on the similar products.

2. Operating load, which is an important performance index, is the external load during the logistics machinery product operating. It includes the lifting weight of crane, the weight of people, and tools on the high-altitude working platform.
3. Wind load is the maximum calculation wind power in WC and not-WC. The wind load can be expressed as the product of the wind factor, the calculation pressure, and frontal area.
4. Special load is temperature load, test load, slope load, etc.

P^L , P_K^L , and A_K are defined as the set of load parameters, the K th load parameter, nonzero value; then:

$$P^L = \{P_1^L, P_2^L, \dots, P_k^L, \dots / P_k^L = 0, A_k\} \tag{36.3}$$

These loads constitute the load parameters. Every load parameter of nonzero value consists of load size v , coefficient, and direction d , then:

$$A_k = (v_k, \varphi_k, d_k) \tag{36.4}$$

The load parameters are “nonzero” and “zero” two options. Then, the LC consists of parts of the load parameters’ two options. LC set of the LC is defined, then:

$$\begin{aligned} LC &\in \{P_1^L \otimes P_1^L \otimes \dots \otimes P_k^L \otimes \dots\} \\ &\in \left\{ \begin{pmatrix} A_1 \\ 0 \end{pmatrix} \otimes \begin{pmatrix} A_2 \\ 0 \end{pmatrix} \otimes \dots \otimes \begin{pmatrix} A_k \\ 0 \end{pmatrix} \otimes \dots \right\} \\ &= \{LC_1, LC_2, \dots, LC_j, \dots\} \end{aligned} \tag{36.5}$$

The sign \otimes is combination operator, and LC is the parts of LCs that are selected from the combination set based on the design requirements. Usually, an extreme LC should be determined as the basis for the calculation. Due to the complexity of the index calculation, it is difficult to determine the extreme LC accurately. Therefore, the whole indexes that are determined by LC need to be calculated to be compared and selected.

36.1.3 The Solving of the Most Dangerous Working Condition and Load Combination

The traditional solving of the most dangerous WC and LC is to solve several dangerous conditions that are selected with experience, which makes it easy to make design troubles on the relatively complicated products. The most dangerous

WC and LC is solved by the method of going through the whole WC and LC. The input parameters of index calculation consist of WC and LC, and the $WC \otimes LC$ set is formed by the collocation of WC and LC, then:

$$\begin{aligned} WC \otimes LC &= \{WC_1, WC_2, \dots, WC_j, \dots\} \otimes \{LC_1, LC_2, \dots, LC_j, \dots\} \\ &= \{WC_i, LC_j\} \quad (i = 1, 2, \dots, m, j = 1, 2, \dots, n) \end{aligned} \quad (36.6)$$

By the method of computer programming, the parameters of the $WC \otimes LC$ set is placed to the index calculation formula to obtain a group of index solutions, and the most dangerous WC and LC is obtained by comparison and selection of the group of the index solutions.

36.2 The Calculation Model of Logistics Machinery Product Conceptual Design

Logistics machinery product conceptual design includes the determination of project and technology parameters, the determination of the key pivot point's position, stability analysis of the whole machine, the determination of the whole machine operating performance and the force calculation of the component, and preliminary design of the typical component. And the theoretical calculation is the key and important basis of the conceptual design. After the determination of the mechanism form, whether the project can meet the requirement of the product function and performance, the mechanism and structure are reasonable, and every index and parameter is optimized or not is estimated by theoretical calculation.

36.2.1 Resolving and Clustering Coupling in Product Parameters

The input parameters of the conceptual design calculation include WC parameters and structure parameters. The structure parameters P^M set that includes the whole machine size, the quality of counter weight, the length of lifting arm, and the position of key pivot point is a group of main parameters of the product structures and the basis of establishing the product design model. It is usually obtained from function parameters, design standards and handbook, and other related experience. WC parameters are the parameters of the position relation of the structures that correspond to the motion mechanisms. Therefore, the WC parameters and the structure parameters are uncoupled. In order to realize the integration of the conceptual design calculation, a parameter set is formed by resolving and clustering coupling the structure parameters that the index calculation required. The datum that all of index calculations required is obtained from the parameter set.

Fig. 36.1 The coupling relation of the parameters in the middle set

	$P_1^{M^*}$	$P_2^{M^*}$	$P_3^{M^*}$	$P_4^{M^*}$	$P_5^{M^*}$	$P_6^{M^*}$	$P_7^{M^*}$	$P_8^{M^*}$	$P_9^{M^*}$	
$P_1^{M^*}$	0	1	0	0	0	0	0	0	1	...
$P_2^{M^*}$			0	0	0	0	0	0	0	...
$P_3^{M^*}$				1	0	1	0	0	0	...
$P_4^{M^*}$					0	0	1	0	0	...
$P_5^{M^*}$						0	0	0	1	...
$P_6^{M^*}$							0	1	0	...
$P_7^{M^*}$								0	1	...
$P_8^{M^*}$									0	...
$P_9^{M^*}$...
...										...

Reference of the representation method of information that is applied to the design structure matrix and the method of resolving the structure parameters are as follows:

1. P_i^M is defined as i th design index parameter, and the middle set P^{M^*} is obtained by combining all the index parameters and removing the repeated parameters.

$$P^{M^*} = U P_i^M \tag{36.7}$$

2. The coupling relation of the parameters in the middle set P^{M^*} is represented by the design structure matrix. The two parameters are regarded as coupling if one depends on the other one to be obtained. A matrix is formed from all the parameters in the set P^{M^*} with the lateral and vertical arrangements. The parameter P_{ij} is 1 if there is the coupling relation between P_i^M and P_j^M ; otherwise, it is 0. Therefore, the coupling relation can be represented as an upper triangular matrix, as shown in Fig. 36.1.
3. The design structure matrix $A = [P_{ij}]_{n \times n}$ is established; then, one of P_i^M and P_j^M is removed or replaced with other parameter. The second step is repeated until the upper triangular matrix of DSM is a zero matrix, namely $A = [0]_{n \times n}$. If it is difficult to obtain zero DSM in special condition, the treatment of the parameters is realized by interactive operation. The coupling resolving operator is represented as Γ ; then:

$$P^{M^*} \frac{\Gamma}{\text{DSM}} \rightarrow P^M \tag{36.8}$$

The parameters are encapsulated in different type in order to convenient for the later object-oriented programming, which is called the coupling in the structure parameters of logistics machinery product. The structure parameters of logistics

machinery product can be divided to the solid element, the key point, the hydraulic cylinder, the coefficient, and the others.

Due to the large number of WC of logistics machinery product, the key pivot point and mass abundance centric coordinates, etc., in structure parameters change with the conditions, which need to be paid attention to. In order to be convenient for software programming, a standard WC being used as the input for the structure parameters is provided. Taking the high-altitude working platform, for example, the condition that the telescopic boom is level and in the shortest condition, the turntable turns 90° , and fly jib is level is selected as the standard condition.

36.2.2 The Content of Conceptual Design Calculation

The logistics machinery product design index is an important basis for estimating whether the conceptual design can meet the requirement of the function and performance and ordering all kinds of the corollary parts. The purpose of the conceptual design calculation is to obtain every index to estimate the feasibility and optimal extent. The content of logistics machinery product conceptual design can be divided to 5 types. They are operating performance check, mental structure check, the whole machine stability check, dynamic, and driving calculation. Each of which includes several indexes.

36.2.3 The Synchronization Evolution of Calculation Model and Geometry Model

Actually, the logistics machinery product conceptual design is the process of the synchronization evolution of calculation model and geometry model. That is to feed back the design parameters and index that are obtained from the calculation model and geometry model, respectively, to verify in the conceptual design model until the proper solution is obtained. The geometry model that can be used to all the conceptual calculation instead of the detailed one is formed from assembling the simplified structure of each subsystem by simplifying and abstracting the real and complete model and getting rid of the tiny structure during the process of design. The logistics machinery product conceptual geometry model can be represented by logic component [2]. The logic component that is the abstract of the real product structure only emphasizes the information that is related to the design phase and ignores the others [2]. It has the ability of representing the requirement of special function formally during composing the product and includes a certain semantic of design function. It is also highly abstractive. To abstract the logistics machinery product by using logic component is to extract the key information that is related to product conceptual design to establish the abstract model and ignore the concrete

component information of product. The logic component can be established by the parametric and modular sketch function of 3D-CAD system [3]. The logic component of typical product is synthetically represented by the components of its main function elements, as the logic component of straight-arm self-propelled high-altitude working platform can be represented by the logic component of main arm, turntable, base structure, platform, etc.

36.3 The Integrated Calculation and Software Frame of Conceptual Design for Logistics Machinery

On the basis of the process and method of conceptual design being arranged by summarizing logistics machinery product WC and LC, an integrated conceptual design calculation method for logistics machinery based on WC and LC is put forward. That is to combine the integrated concept with conceptual design calculation, by solving the worst WC and LC, and resolving and clustering coupling in product parameters, extract the input parameters that conceptual design calculation requires, input to every type of calculation model uniformly to solve each index synchronously [4]. At the same time, the calculation model and geometry model evolve synchronously to realize the fast iteration of conceptual design calculation by modifying design parameters and resolving. The design calculation method that has certain universality is encapsulated by conceptual design software [5]. The software can show the performance curve of each index in task intervals quickly, record the calculation process automatically, and form the calculation description automatically, which increase the reliability of calculation, reduce workload, and create condition for design optimization. Due to the difficult problems like WC and LC, parameters coupling, etc., are treated efficiently; the frame of the software is simple and easy to be realized, as shown in Fig. 36.2.

The indexes of the content of logistics machinery product conceptual design calculation are different in different WC and LC. Actually, only the extreme index

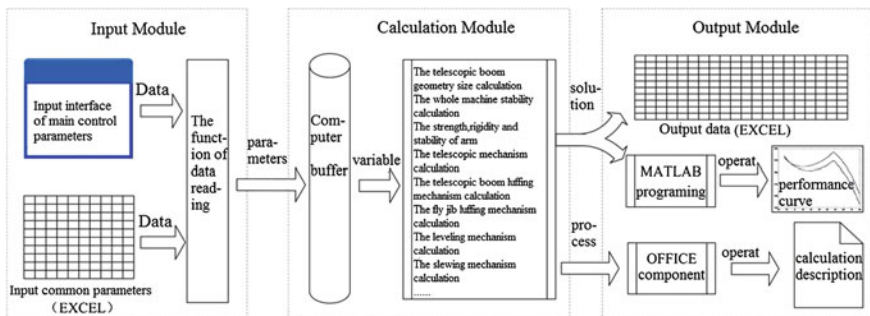


Fig. 36.2 The software frame of conceptual design calculation

that is in the most dangerous WC and LC is meaningful for evaluating the project, such as the ultimate strength of telescopic boom, the maximum wheel pressure, minimum stability coefficient, etc. Therefore, WC and LC set $WC \otimes LC$ and structure parameters P^M are placed to index calculation formula for cyclic solving after they are combined. And the extreme value is the index one that is required. S_i is defined as the i th index, EXTREME, which is the maximum value, or the minimum value based on the actual requirements is defined as the function that is to solve the extreme value, and $f_{(x)}$ is defined as the calculation method. Then:

$$S_i = \text{EXTREME}(f(WC \otimes LC) \cup P^M) \quad (36.9)$$

The implementing steps of the integrated calculation and software development of conceptual design for logistics machinery are as follows:

1. The design standard is the basis of product design. Therefore, to begin with the design standard, find out the difference of WC and LC, the difference of safety coefficient, and the difference of the calculation method. Allocate different calculation method and coefficient parameter based on different standard;
2. Aiming at the content of conceptual design calculation, sort out the uniform and reasonable method based on the related design standard;
3. Analyze the structure form of each system of product and establish the mapping relation between calculation method and structure form;
4. Depurate and optimize the conceptual design process, analyze the mutual restriction and the important degree of each calculation step, fully excavate and cure the parameters that restrict the efficiency of product design, and the later software design depends on this process [4];
5. Establish the conceptual geometry model that can evolve synchronously with calculation model;
6. Develop the conceptual design calculation software. The environment of VC++ and the object-oriented frame are applied to software, which is open and can be allocated and extended dynamically. The software with the generality and real time of calculation can complete the input and calculation that is repeated and tedious instead of people.
7. Verify the application of software. The software prototype system is verified to test the correctness and reliability by being applied to the conceptual design of straight-arm self-propelled and mixed arm high-altitude working platform.

By the method that is put forward, conceptual design calculation software for straight-arm self-propelled high-altitude working platform is developed and applied in the GTBZ serial products. The software can improve the efficiency of conceptual design greatly and used in parameters optimization.

36.4 Conclusion

The characteristics of the integrated conceptual design calculation method for logistics machinery based on WC and LC are as follows: ① The reasonable solving method of the most dangerous WC and LC in logistics machinery product is put forward, which makes the solution more accurate and reduces the workload greatly; ② The knowledge elements of conceptual design calculation is clustered, and the loose coupling type is applied to establish the connection between each calculation step, which makes the product design process oriented and simple; ③ The conceptual geometry model and calculation model are integrated; the method of synchronization evolution of calculation model and geometry model is applied, and the conceptual geometry model is represented as logic component.

References

1. Wei Z, Tan J, Feng Y (2008) Method of conceptual design of mechanic product driven by generalized performance. *Chin J Mech Eng* 44(5):2–10
2. Tang D-B, Li Z, Li Z-Z (2001) Research on computer aided die conceptual design system. *Comput Integr Manufact Syst* 7(4):52–57
3. Wang Y, Xing Y, Ruan X-Y (2002) Information modeling and re-engineering for design process. *Comput Integr Manufact Syst* 8(2):112–114
4. Tang D, Liu Z (2008) Execution sequence planning of computational models based on incidence matrix and design structure matrix. *Chin J Mech Eng* 44(12): 173–179
5. Pan Z, Li Y, Huang X (2008) A novel concurrent design process planning method and application. In: *Proceeding of IEEE 12th international conference on computer supported cooperative work in design*, pp 204–209. Xi'an, China, April 2008

Chapter 37

Improved Heuristic Procedure for Mixed-Model U-line Balancing Problem with Fuzzy Times

Zeqiang Zhang and Wenming Cheng

Abstract Facing the increasingly competitive market environment, variety of customer needs, and rapidly changing market, more and more assembly lines are switching to U-line and mixed model produced due to the use of just-in-time production principles. Considering that some uncertainties are existing in practical problem, this paper focuses on the mixed-model U-line balancing problem (MMULBP) with processing time and cycle time as fuzzy numbers. An improved heuristic procedure is proposed to solve the problem. The procedures are based on the traditional ranked positional weight method, and some improvements are made on fuzzy number operation and two-direction search for U-line layout, in order to solve the complex practical problem. The results of an experimental study indicate that the proposed procedure is effective.

Keywords Mixed-model U-line balancing problem · Position weight method · Heuristic · Fuzzy

37.1 Introduction

Facing the increasingly competitive market environment, variety of customer needs, and rapidly changing market, the traditional straight assembly line cannot meet the demands of the modern society. More and more assembly lines are switching to

Z. Zhang (✉) · W. Cheng
School of Mechanical Engineering, Southwest Jiaotong University,
Chengdu 610031, China
e-mail: zhangzeqiang@gmail.com

W. Cheng
e-mail: wmcheng@swjtu.cn

U-line and mixed model produced due to the use of just-in-time production principles [1, 2].

For the importance of the simple assembly line balancing problem (ALBP), there are numerous researches on ALBP [3–5], but only few literatures focus on mixed-model U-line balancing problem (MMULBP). Sparling and Miltenburg [6] first presented MMULBP and the formulation for the problem, and an approximate solution algorithm for the MMULBP is also proposed. And then, some researches about exact algorithms are also conducted [7, 8], such as goal programming [9], mixed integer linear programming [10], and branch-and-bound algorithms [11]. The simple ALBP falls into the NP hard class of combinatorial optimization problems, and MMULBP is more complex for with larger search space. So, heuristics is an effective way to solve the problem [12].

There are numerous literatures for ALBP, and most of them assume constant and deterministic operation times, but only few studies are reported for solving the fuzzy line balancing problem. Nguyen Van [13] developed a heuristic solution for fuzzy mixed-model line balancing problem. Fonseca et al. [14] proposed modified COMSOAL and ranked positional weighting technique to solve the straight line balancing problem with a fuzzy representation of the time variables. Zhang et al. [15] proposed an effective heuristic for solving type 1 of the fuzzy ULBP. Tsujimura et al. [16] presented a genetic algorithm to solve the traditional straight ALBP with fuzzy operation time. Zacharia and Nearchou [17] presented a new multi-objective genetic algorithm for solving the fuzzy extension of the simple ALBP of type 2.

This paper presents a heuristic for the type 1 mixed-model U-shaped line balancing problem with fuzzy processing times. The rest of the paper is as follows. In Sect. 37.2, the fuzzy MMULBP-1 is discussed and mathematical model is presented. Next, Sect. 37.3 will develop the heuristic solution for fuzzy MMULBP-1. Then, an example problem is solved using the proposed method in Sect. 37.4. Finally, some conclusions are presented in Sect. 37.5.

37.2 Problem Statement and Formulation

37.2.1 Problem Statement

In order to reduce the production cost and provide customers with a variety of products in a timely manner, different products or models should be produced on the same line. Mixed-model assembly line balancing problem (MMALBP) can be described as follows: Given P models, the set of tasks associated with each model, the processing time of each task, and the set of precedence relations of tasks for each model, the problem is to assign the tasks to an ordered sequence of stations such that some constraints are satisfied and some performance measures are

optimized. The mixed-model U-shaped line balancing problem is an extension of MMALBP with respect to U-shaped line instead of straight line. Three versions of the problem can be divided as follows:

- (I) MMULBP-1 consists of assigning tasks to work stations such that the number of stations is minimized for a given cycle time.
- (II) MMULBP-2 is to minimize the cycle time for a given number of stations.
- (III) MMULBP-E is obtained by maximizing the line efficiency for varying production rates and numbers of stations.

37.2.2 Assumptions

1. Task processing time of each model is given and is a fuzzy number.
2. Precedence diagrams for each model are given and can be accumulated into a single combined precedence diagram.
3. WIP inventory buffer is not allowed between workstation.
4. Parallel workstation is not allowed.
5. Common tasks exist between models that must be assigned to the same workstation.

37.2.3 Combined Precedence Diagram

Different models in mixed-model assembly line usually exists some similar tasks; precedence relations of same tasks in different models are usually similar. According to this character, transform different models into an equivalent single model by taking the union of the nodes and the precedence relations of the diagrams of all the models.

Let G_p be the precedence diagram of model p . G_p has a set of nodes $N(p)$ and of arcs $L(p)$ where

$$N(p) = \{n(p)_1, n(p)_2, \dots\} \quad (37.1)$$

$$L(p) = \{l(p)_1, l(p)_2, \dots\} \quad (37.2)$$

The nodes and arcs represent tasks and precedence relations, respectively. If an arc $l(p)_h$ has initial node $n(p)_i$ and terminal node $n(p)_j$, then the task represented by $n(p)_i$ must be completed before the task $n(p)_j$.

Precedence relations for a set of models $\hat{P} = \{1, 2, \dots, P\}$ are represented by directed graphs G_1, G_2, \dots, G_P . Then, we can define a single graph $G_{\hat{P}}$ with nodes $N(\hat{P})$ and arcs $L(\hat{P})$ where

$$N(\hat{P}) = \{N(1) \cup N(2) \cup \dots \cup N(P)\} \tag{37.3}$$

$$L(\hat{P}) = \{L(1) \cup L(2) \cup \dots \cup L(P)\} \tag{37.4}$$

For different models, a task may be included in some models and not included in others, so define δ_{ip} as follows:

$$\delta_{ip} = \begin{cases} 1 & \text{if task } n(p)_i \text{ is part of model } p \\ 0 & \text{otherwise} \end{cases} \tag{37.5}$$

Then, the weighted average processing time of task i (\tilde{t}_i) in the planning horizon (\tilde{T}) is computed as follows:

$$\tilde{t}_i = \frac{\sum_{p=1}^P Q_p \delta_{ip} \tilde{t}_{ip}}{\sum_{p=1}^P Q_p} \tag{37.6}$$

where \tilde{t}_{ip} denotes the fuzzy processing time of task i for model p , $i = 1, \dots, N$, $p = 1, \dots, P$, where N and P are the total number of tasks and models in the problem, respectively. Q_p is the production quantity of model p in the planning horizon.

The cycle time is calculated as follows:

$$\tilde{C} = \frac{\tilde{T}}{\sum_{p=1}^P Q_p} \tag{37.7}$$

So if we use \tilde{t}_i as the processing of task i in combined precedence diagram, then we can use the method of single-model assembly line balancing to solve the problem.

37.2.4 Constraints

1. All tasks must be assigned to one workstation.
2. Each task is assigned only once, i.e., a task cannot be split among two or more stations.
3. The work content in any workstation for any model cannot exceed the cycle time of that model.
4. The precedence constraints are not violated on the U-line.

37.2.5 Problem Formulation

Based on the above assumptions, the MMULBP with fuzzy times of type 1 (MMULBP-1) is formulated as follows:

$$\min \sum_{p=1}^P \sum_{k=1}^K \left(\tilde{C}_p - \sum_{i=1}^N v_{ipk} \tilde{t}_{ip} \right) \tag{37.8}$$

subject to

$$\bigcup_{k=1}^K S_k = E \tag{37.9}$$

$$S_i \cap S_j = \phi \quad i, j = 1, \dots, K \quad i \neq j \tag{37.10}$$

$$\sum_{i=1}^N v_{ipk} \tilde{t}_{ip} \leq \tilde{C}_p \quad p = 1, 2, \dots, P \quad k = 1, 2, \dots, K \tag{37.11}$$

$$\begin{aligned} \forall x \in S_i, y \in S_j, \quad & \text{if } p_{xy} = 1, \text{ then } i \leq j; \text{ or} \\ \forall y \in S_j, z \in S_k, \quad & \text{if } p_{yz} = 1, \text{ then } k \leq j. \end{aligned} \tag{37.12}$$

where

E the set of tasks in the line, $E = \{1, 2, \dots, N\}$.

K the number of workstations.

S_k the set of tasks assigned to workstation k , $S_k = \{i | \text{task } i \text{ is assigned to workstation } k\}$.

\tilde{C}_p cycle time of model p .

$$v_{ipk} = \begin{cases} 1 & \text{if task } i \text{ of model } p \text{ is assigned to station } k \\ 0 & \text{otherwise} \end{cases} \tag{37.13}$$

$$p_{ij} = \begin{cases} 1 & \text{if task } i \text{ is performed before task } j \\ 0 & \text{otherwise} \end{cases} \tag{37.14}$$

37.2.6 The Character of U-Shaped Layout

U-shaped layouts with the straight line are mainly distinct in that the entrance and exit are located in the same direction. So we can add or remove workers in assembly line according to the demands. Taking the following problem as example [8], the problem has seven tasks and the precedence diagram is given in Fig. 37.1a. The numbers within and above the nodes represent tasks and the associated task

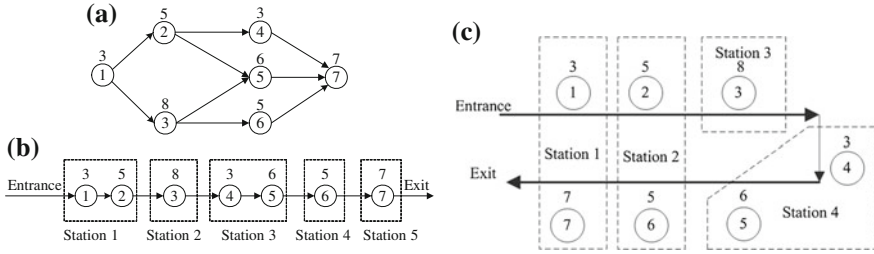


Fig. 37.1 Precedence diagram (a), traditional (b) and U-shaped (c) line balancing results

times, respectively. The directed arrow connecting the nodes specifies the precedence relations. When assuming a cycle time of 10, it can be seen that all tasks are performed at five workstations (shown in Fig. 37.1b, the idle time is 13 and the efficiency is 74 %) in traditional assembly line, whereas all tasks are performed at four workstations (shown in Fig. 37.1c, the idle time is 3 and the efficiency is 92.5 %) in U-shaped assembly line. We can see that U-shaped layout can eliminate excess idle time and achieve more balancing situation in this example. Taking tasks 1 and 7 in Fig. 37.1c as example, although tasks 1 and 7 are located at the beginning and end of the line, respectively, they have been processed by the same workstation (workstation 1). This means that the U-shaped layout has great assignment flexibility and balancing efficiency.

According to the character of U-shaped assembly line, the main difference in assigning the tasks compared to the traditional line is as follows: Straight line only allows assigning tasks according to the arcs direction in the precedence diagram. However, U-shaped line permits assigning tasks according to the arcs direction, or reverse direction, or both arcs direction and reverse direction. So, the U-shaped line balancing problem is much more complicated than the traditional line balancing problem due to the increased search space.

37.3 The Heuristic Procedure for MMULBP

For the content about arithmetics and ranking fuzzy numbers, the readers can refer to the paper [18].

37.3.1 Nomenclature

Notation for fuzzy RPWT procedure is given below:

- $\tilde{t}(i)$ fuzzy processing time of task $i(i = 1, \dots, n)$, defined as a triplet (a_1, a_2, a_3)
- \tilde{W}_i fuzzy ranked positional weight of task i

- $\tilde{t}(S_k)$ fuzzy time required to complete all tasks assigned to workstation S_k ($k = 1, \dots, m$)
- \tilde{c} fuzzy cycle time after assignments
- \tilde{I}_k fuzzy idle time for workstation S_k , ($k = 1, \dots, m$)
- \tilde{t}_{sum} total processing time in all workstations
- \tilde{C}_{max} permitted fuzzy cycle time
- $\tilde{\eta}$ fuzzy balance efficiency

According to the characters of the problem, we can have the following result:

$$\tilde{c} = \max\{\tilde{t}(S_k)\}. \tag{37.15}$$

$$\tilde{t}(S_k) = \sum_{j \in S_k} \tilde{t}(j), \quad k = 1, \dots, m. \tag{37.16}$$

$$\tilde{I}_k = \tilde{C}_{\text{max}} - \tilde{t}(S_k). \tag{37.17}$$

$$\tilde{t}_{\text{sum}} = \sum_{k=1}^m \tilde{t}(S_k), \quad k = 1, \dots, m. \tag{37.18}$$

$$\tilde{\eta} = \frac{\tilde{t}_{\text{sum}}}{m \times \tilde{c}}. \tag{37.19}$$

37.3.2 Fuzzification of RPWT for MMULBP

The proposed procedure for fuzzy MMULBP-1 is based on the RPWT method, and some modifications should be made. We should translate the MMULBP-1 to ULBP-1 based on the methods given in Sect. 37.2.3. Then, we can use the methods for single model to solve the problem. And the fuzzy positional weight for each task, \tilde{W}_i , can be calculated by summing the processing time of the current task with the processing times of all its successors or predecessors.

$$\tilde{W}_i = \max \left\{ \tilde{t}(k) + \sum_{i \in U_s(k)} \tilde{t}(i), \tilde{t}(k) + \sum_{j \in U_p(k)} \tilde{t}(j) \right\}. \tag{37.20}$$

where $U_p(k)$ [or $U_s(k)$] be the set of tasks which must precede (or succeed) task k , respectively.

The fuzzy operator will be utilized in this calculation for the processing times is fuzzy numbers. And the mean comparison method is used for the comparison [19].

The ranking of tasks based on their positional weights is also very important for the RPWT method in which the tasks are ranked in a decreasing order. And the average height method [18] is used for ranking of triangular fuzzy numbers. Compute the value H for tasks \tilde{A} and \tilde{B} where $H(\tilde{A}) = (a_1 + a_2 + a_3)/3$ and $H(\tilde{B}) = (b_1 + b_2 + b_3)/3$; if $H(\tilde{A}) > H(\tilde{B})$, then $\tilde{A} > \tilde{B}$.

Whenever a new task is added to a workstation, fuzzy processing times are accumulated using the fuzzy addition operator. And the mean comparison method is used to check whether the station time violates the permitted cycle time or not. If $\tilde{t}(S_k) + \tilde{t}(i) \leq \tilde{C}_{\max}$, then task i can be added to the current workstation. If $\tilde{t}(S_k) + \tilde{t}(i) > \tilde{C}_{\max}$ and task i cannot be assigned to the current workstation and a new workstation must be opened to accommodate the task.

37.3.3 Steps involved in the Procedure

The procedure of the proposed heuristic for MMULBP-1 is presented as follows.

- Step 1: Convert the mixed-model U-line balancing problem into the single-model U-line balancing problem (including the processing time, cycle time, and precedence diagrams) according to Sect. 37.2.3;
- Step 2: Based on the combined precedence diagram, establish each task's processing time given the cycle time as TFNs;
- Step 3: Establish combined precedence relationships for the problem;
- Step 4: Aggregate fuzzy cycle time and processing time;
- Step 5: Compute the positional weight for each task in the new combined precedence diagram according to Eq. (37.20);
- Step 6: Rank positional weight into List A, and an initial task assignment sequence is obtained. We use the average height method to rank the tasks in a descending order;
- Step 7: Assign aggregated tasks in List A to workstation 1 based on the precedence relations and their positional weight rank, and the fuzzy process times will be accumulated;
- Step 8: Continue to assign the next succeeding ranked task to the workstation, as long as the task fits the precedence relationships and the station times do not exceed the cycle time;
- Step 9: If the station times exceed cycle time with the addition of new task i , then create a new workstation;
- Step 10: Repeat steps 8–9 until all tasks are assigned;

Step 11: Determine the number of workstations and calculate idle time for each station after final assignment according to Eq. (37.17); compute fuzzy balance efficiency according to Eq. (37.19).

37.4 Numerical Example and Experiment

A numerical example is used to illustrate the proposed heuristic procedure. Three models, A, B, and C, with demand of $Q_1 = 400$, $Q_2 = 200$, and $Q_3 = 200$, respectively, each day, are simultaneously assembled in a line. For one day, the production time is fuzzy number $\tilde{T} = (480\ 493\ 507)$ min. There are 20 tasks in the production, and the precedence diagram for each model is given in Fig. 37.2. The task processing times for the three models are shown in Table 37.1.

According to Sect. 1.3, we can obtain the combined precedence diagram as shown in Fig. 37.3. By using Eq. (37.6), the weighted average processing time for each task i can be calculated; refer to the column \hat{t}_i in Table 37.2. And we also can calculate the fuzzy cycle time, $\tilde{C}_{max} = (36, 37, 38)$, according to the Eq. (37.7).

The fuzzy positional weight for the problem can be calculated by Eq. (37.20). The average height of the triangular fuzzy number also can be obtained according to the average height method, and the results are shown in Table 37.2.

Based on the above data, the solution can be found by using the algorithm proposed in Sect. 37.3.3, and the best solution is obtained for 6 workstations. The proposed procedure has the advantages of quick search by using positional weight ranking. For the detailed results, we can refer the readers to Table 37.3. After calculations, the practical fuzzy cycle is $\tilde{c} = (33, 36, 39)$, the total processing time in all workstations is $\tilde{t}_{sum} = (184.25, 199, 213.75)$ by Eq. (37.18), and the line efficiency is $(0.787, 0.921, 1)$ by Eq. (37.19). And we can see that this assembly line with high production rate can meet the demands of the production.

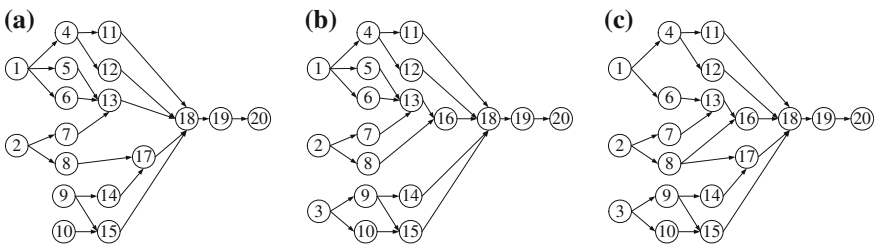


Fig. 37.2 Precedence diagram for models A (a), B (b), and C (c)

Table 37.1 Fuzzy processing time of every task in each model

Task no.	Processing time (s)			Task no.	Processing time (s)		
	\tilde{t}_{i1}	\tilde{t}_{i2}	\tilde{t}_{i3}		\tilde{t}_{i1}	\tilde{t}_{i2}	\tilde{t}_{i3}
1	(15 16 17)	(15 16 17)	(15 16 17)	11	(15 16 17)	(15 16 17)	(15 16 17)
2	(6.5 7 7.5)	(6.5 7 7.5)	(6.5 7 7.5)	12	(8.5 9 9.5)	(8.5 9 9.5)	(8.5 9 9.5)
3	(0 0 0)	(11 12 13)	(11 12 13)	13	(12 13 14)	(12 13 14)	(12 13 14)
4	(8.5 9 9.5)	(8.5 9 9.5)	(8.5 9 9.5)	14	(11 12 13)	(11 12 13)	(11 12 13)
5	(11 12 13)	(11 12 13)	(0 0 0)	15	(14 15 16)	(14 15 16)	(14 15 16)
6	(14 15 16)	(14 15 16)	(14 15 16)	16	(0 0 0)	(9 10 11)	(9 10 11)
7	(5.5 6 6.5)	(5.5 6 6.5)	(5.5 6 6.5)	17	(8.5 9 9.5)	(0 0 0)	(9 10 11)
8	(13 14 15)	(13 14 15)	(13 14 15)	18	(10 11 12)	(10 11 12)	(10 11 12)
9	(5.5 6 6.5)	(5.5 6 6.5)	(5.5 6 6.5)	19	(3.5 4 4.5)	(3.5 4 4.5)	(3.5 4 4.5)
10	(4.5 5 5.5)	(4.5 5 5.5)	(4.5 5 5.5)	20	(13 14 15)	(13 14 15)	(13 14 15)

Fig. 37.3 Combined precedence diagram for three models

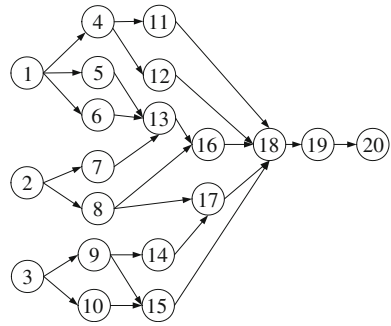


Table 37.2 Positional weight for the problem

Task no.	\tilde{W}_i	$H(\tilde{W}_i)$	Task no.	\tilde{W}_i	$H(\tilde{W}_i)$
1	(112.25 121 129.75)	121	11	(41.5 45 48.5)	45
2	(74.5 81 87.5)	81	12	(35 38 41)	38
3	(73.5 80 86.5)	80	13	(49.25 53 56.75)	53
4	(58.5 63 67.5)	63	14	(44 48 52)	48
5	(51.25 56 60.75)	56	15	(40.5 44 47.5)	44
6	(57 62 67)	62	16	(66.75 72 77.25)	72
7	(48.5 53 57.5)	53	17	(48 52 56)	52
8	(50.5 55 59.5)	55	18	(167.75 181 194.25)	181
9	(63.5 69 74.5)	69	19	(171.25 185 198.75)	185
10	(45 49 53)	49	20	(184.25 199 213.75)	199

Table 37.3 Results for the problem

Station no.	Assigned tasks	$\tilde{t}(S_k)$	\tilde{I}_k
1	20, 19, 18, 2	(33 36 39)	(0 1 5)
2	1, 3, 16, 9	(30.5 33 35.5)	(0.5 4 7.5)
3	6, 5, 4	(30.75 33 35.25)	(0.75 4 7.25)
4	8, 7, 13	(30.5 33 35.5)	(0.5 4 7.5)
5	17, 10, 14, 12	(30.5 33 35.5)	(0.5 4 7.5)
6	11, 15	(29 31 33)	(3 6 9)
Line efficiency = (0.787, 0.921, 1)			

37.5 Conclusion

In this paper, an improved heuristic for MMULBP with fuzzy times is constructed. Computational experiments demonstrated the validity of the proposed procedure. In future studies, we hope to apply the improved heuristic method to extensions of the

MMULBP, such as fuzzy MMULBP with multiple objectives. The integration of intelligent methods, for example, heuristic method and ACO algorithms, to MMULBP is also an interesting topic in the future.

Acknowledgement This work was partially supported by the National Natural Science Foundation of China (No. 51205328), the Youth Foundation for Humanities and Social Sciences of Ministry of Education of China (No. 12YJCZH296), the PhD Programs Foundation of Ministry of Education of China (No. 200806131014), and the Research Center of Sichuan Province for Circular Economy (No. XHJJ-1205).

References

1. Cheng CH et al (2000) The effect of straight- and U-shaped lines on quality. *IEEE Trans Eng Manage* 47:321–334
2. Aase GR et al (2004) U-shaped assembly line layouts and their impact on labor productivity: an experimental study. *Eur J Oper Res* 156:698–711
3. Scholl A, Becker C (2006) State-of-the-art exact and heuristic solution procedures for simple assembly line balancing. *Eur J Oper Res* 168:666–693
4. Peeters M, Degraeve Z (2006) An linear programming based lower bound for the simple assembly line balancing problem. *Eur J Oper Res* 168:716–731
5. Zhang Z-Q et al (2007) Improved ant colony optimization for assembly line balancing problem. *Comput Integr Manuf Syst CIMS* 13:1632–1638
6. Sparling D, Miltenburg J (1998) The mixed-model U-line balancing problem. *Int J Prod Res* 36:485–501
7. Aase GR et al (2003) U-OPT: an analysis of exact U-shaped line balancing procedures. *Int J Prod Res* 41:4185–4210
8. Gokcen H et al (2005) A shortest route formulation of simple U-type assembly line balancing problem. *Appl Math Model* 29:373–380
9. Gokcen H, Agpak K (2006) A goal programming approach to simple U-line balancing problem. *Eur J Oper Res* 171:577–585
10. Kara Y, Tekin M (2009) A mixed integer linear programming formulation for optimal balancing of mixed-model U-lines. *Int J Prod Res* 47:4201–4233
11. Scholl A, Klein R (1999) ULINO: optimally balancing U-shaped JIT assembly lines. *Int J Prod Res* 37:721–736
12. Chiang W-C, Urban TL (2006) The stochastic U-line balancing problem: a heuristic procedure. *Eur J Oper Res* 175:1767–1781
13. Nguyen Van H (2006) A heuristic solution for fuzzy mixed-model line balancing problem. *Eur J Oper Res* 168:798–810
14. Fonseca DJ et al (2005) A fuzzy logic approach to assembly line balancing. *Mathware Soft Comput* 12:57–74
15. Zhang Z et al (2009) A heuristic approach for fuzzy U-shaped line balancing problem. In: 6th international conference on fuzzy systems and knowledge discovery, Tianjin, pp 228–232
16. Tsujimura Y et al (1995) Solving fuzzy assembly-line balancing problem with genetic algorithms. *Comput Ind Eng* 29:543–547
17. Zacharia PT, Nearchou AC (2012) Multi-objective fuzzy assembly line balancing using genetic algorithms. *J Intell Manuf* 23:615–627
18. Hong TP, Chuang TN (1999) A new triangular fuzzy Johnson algorithm. *Comput Ind Eng* 36:179–200
19. Gen M et al (1996) Fuzzy assembly line balancing using genetic algorithms. *Comput Ind Eng* 31:631–634

Chapter 38

Research and Building of Database Model of Logistics Business Platform

Li Li, Gaoyuan Meng, Xiaoping Liao and Wengui Su

Abstract This paper aims to provide guidance toward the design of the logistics business platform (LBP) database. In this paper, the structure of the database model of LBP was analyzed and a method of building database model based on the UML was put forward. Building the database model of LBP, four steps must be included, which demanded the characteristics such as complexity of the service object, diversification of the deal mode, standardization of the business process, normalization of the transaction data, and diversity of the data format. First, business trading model was achieved in the stage of requirements collection and analysis toward the application entity. Second, use case diagram and activity diagram which reflects the relationships of the use cases were acquired according to the business trading model. Thirdly, the static structure model was achieved with the obtention of class model via the analysis of entity classes and their relationships. Finally, the database model of LBP was completed on the basis of the mapping rules which can convert the class model to the database model.

Keywords Logistics business platform · UML method · Planning · Database model

38.1 Introduction

The unified modeling language (UML) is being used as the de facto standard in the software industry [1]. UML owns abundant modeling symbols which are used to create all sorts of models for the software system and can be applied to the requirements, analysis, and design in the whole process of a software project [2]. With the adoption of UML, the business rules can be described easily and the mapping of a database can be realized clearly. Then, the dynamic behavior model

L. Li (✉) · G. Meng (✉) · X. Liao · W. Su
College of Mechanical Engineering, Guangxi University, Nanning 530004, Guangxi, China
e-mail: liligxu@gxu.edu.cn

© Springer-Verlag Berlin Heidelberg 2015
Logistics Engineering Institution, CMES (ed.),
Proceedings of China Modern Logistics Engineering,
Lecture Notes in Electrical Engineering 286, DOI 10.1007/978-3-662-44674-4_38

and the static structure model can be achieved [3]. All the benefits will promote the maintainability, maneuverability, and scalability of a system [4]. So in this paper, we put forward a method of building database model based on the UML and analyze the structure of the database model of LBP.

38.2 Business Modeling

Business modeling is the foundation work. In the LBP, the characteristics such as complexity of the service object, diversification of the deal mode, standardization of the business process, normalization of the transaction data, and diversity of the data format are demanded, and the core activities including the handling of inquiry list, the management of negotiation forms, contracts, orders, and accounts payable are analyzed. By the business modeling, the functional requirements and data needs of both sides in the business transaction will be acquired [5].

In the LBP, the users can select the needed logistics supply information in two ways: One is that they can search the information satisfied themselves manually in the trading center. In the other way, they will discover the logistics supply information in their management backgrounds which display all the information matched with the published logistics demand information. Then they can order directly or negotiate with the logistics supplier on the Internet toward the matching scheme decided. Based on the functional requirements represented above, the business trading model is achieved. The transaction flow diagram of LBP is depicted in Fig. 38.1.

38.3 Demand Modeling

Through the analysis of the transaction flow diagram of LBP, the functional requirements are finished, the participants such as starting role and support role are isolated, and a variety of activities and functions are abstracted. The demand modeling will be built [6].

The actors can be divided into two kinds such as the main actors and the actors who support the operation of the system [2]. On the basis of the business modeling of LBP, the main actors include logistics supplier, logistics demander, and intelligent matching system of the platform. The China UnionPay system, through which the logistics demanders can pay for the suppliers with the credit cards, is auxiliary actor for the platform.

Use cases are also obtained through the analysis of the business flow chart, including searching the logistics supply information, ordering directly, generating contract orders, and handling the bills. The use case diagram of LBP is depicted in Fig. 38.2.

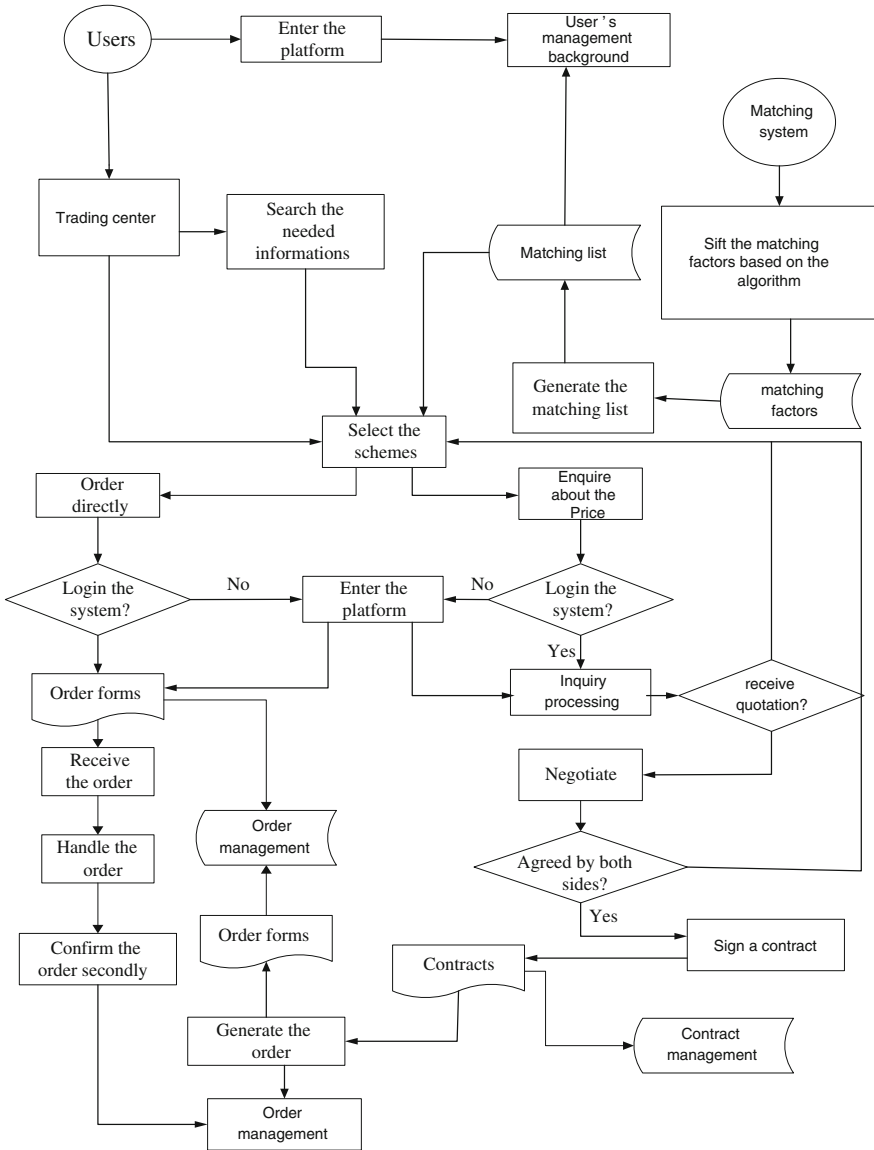


Fig. 38.1 Transaction flow diagram

Activity diagram is used to express the complex relationships among use cases by the method of integrating use cases and use case narratives and can reflect the business function requirements of LBP. At the beginning, logistics demanders search the requisite supply information manually or select the scheme with the help of intelligent matching system. And then, they make an order directly on the

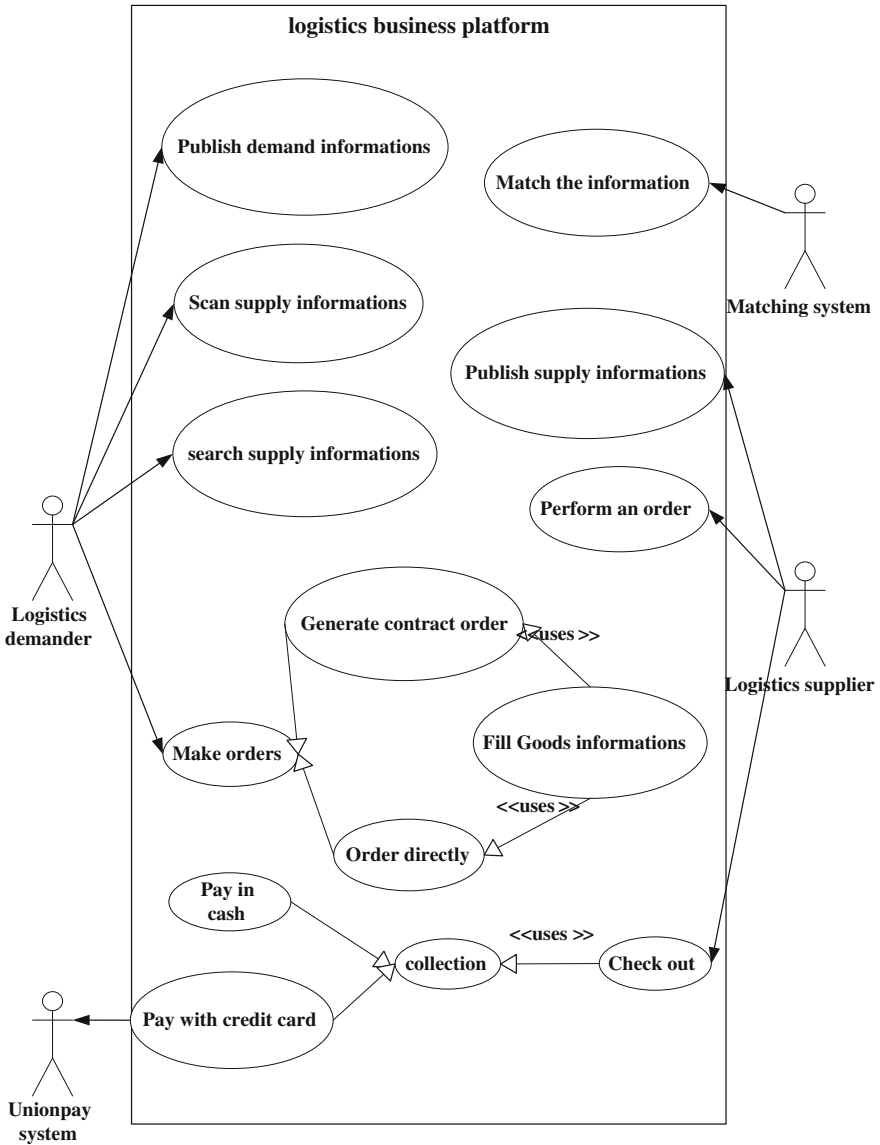


Fig. 38.2 Use case diagram of LBP

Internet or inquiry to logistics supplier. After a series of business process, an online order or order from a contract which will be performed by the supplier is formed, with the checkout executed, the whole business flow reaches the end. The activity diagram of the platform is shown in Fig. 38.3.

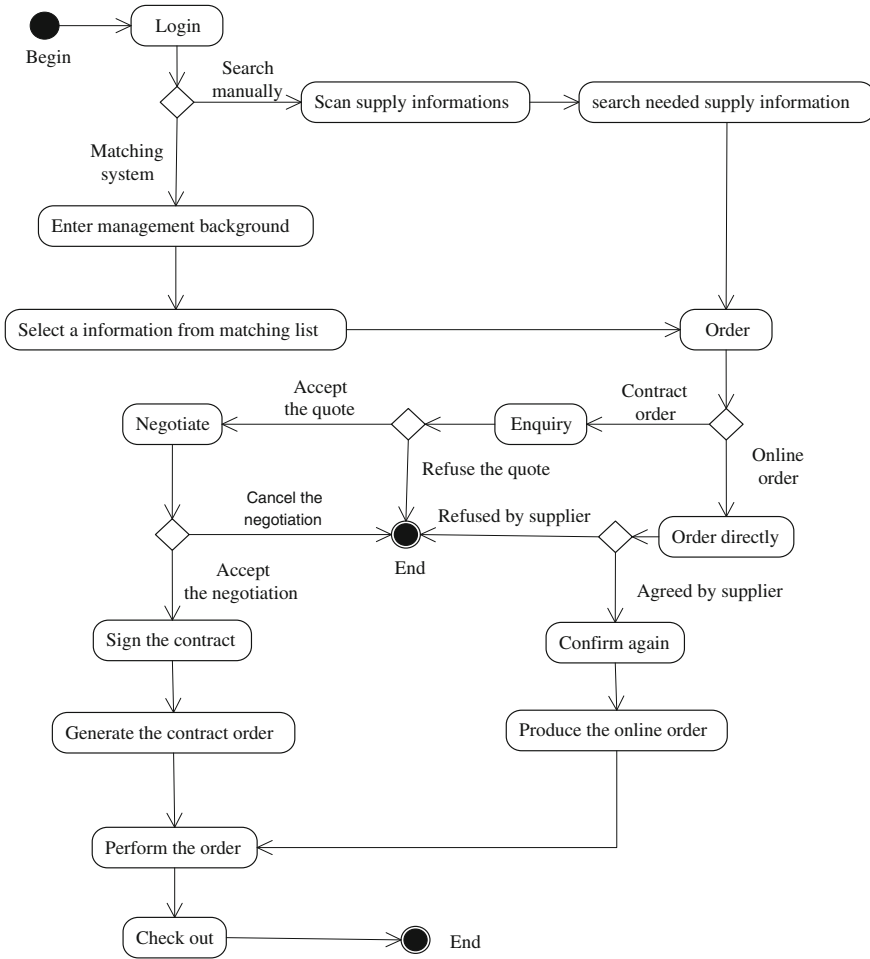


Fig. 38.3 Activity diagram of the platform

38.4 Static Structure Modeling

The objects of LBP are achieved after extracting use cases and actors from the business flow chart of LBP. And then, every object in the system should be modeled toward their static structures. For example, class diagram, object diagram, and package diagram are applied to construct the static structure in accordance with the particular analysis of use case diagram.

Class diagram is particularly important, by which the class model and their internal structures in the system can be defined and all kinds of contacts among them can be described [7].

The definition of every object class is listed as follows.

Supplier: Publishing the logistics supply information and performing the work of checkout. Attributes (SupplierID, UserName, Password, CompanyName). Methods (GetSupplierInfoBySupplierID, GetSupplierID). Each supplier can publish many supply information.

SupplyInfo: Providing logistics supply information to the demanders and displayed in the page of logistics business center. Attributes (ServeInfoID, PublishTime, VehicleType, Price). Methods (AddSupplyInfoDetails, GetSupplyInfoBySupplyInfoID, SearchSupplyInfo). Each supply information can be used to create many inquiry sheets and online orders.

Demander: Publishing the logistics demand information and making orders related to supply information. Attributes (DemanderID, UserName, Password, CompanyName). Methods (GetDemanderInfoByDemanderID, GetDemanderID). Each demander can publish many demand information and input the data of products.

DemandInfo: Providing logistics demand information to the suppliers and showed in the page of logistics business center. Attributes (DemandInfoID, PublishTime, GoodsName, Price, DemandVehicle). Methods (AddDemandInfoDetails, GetDemandInfoByDemandInfoID, GetDemandInfoID). Demand information is used to be matched with supply information by intelligent matching system. Each demand information can be matched with many supply information and vice versa.

Product: Used to reveal the data of products to the supplier. Attributes (ProductID, GoodsName, GoodsNum, GoodsWeight, GoodsVol). Methods (GenerateProductID, AddProductDetails, GetProductInfoByProductID, GetProductID). One product can be filled in one or more inquiry sheets or online orders.

OnlineOrder: An order placed by demander without negotiation with supplier. Attributes (OnlineOrderID, OrderTime, Remark, Status). Methods (GenerteOnlineOrderID, AddOnlineOrderDetails, GetOnlineOrderInfoByOnlineOrderID, GetOnlineOrderID, ChangeOnlineOrderStatus).

Query: A document produced by demander to inquiry to suppliers. Attributes (QueryID, QueryTime, Status). Methods (GenerateQueryID, AddQuery, GetQueryInfoByQueryID, GetQueryID, ChangeQueryStatus). Each inquiry sheet can produce many negotiation forms.

Negotiation: A file generated by an inquiry sheet if demander is satisfied with the offer from supplier. Attributes (NegotiationID, Status). Methods (GenerateNegotiationID, AddNegotiationDetails, GetNegotiationByNegotiationID, GetNegotiationID, ChangeNegotiationStatus).

Contract: An agreement reached by both sides in the business. Attributes (ContractID, Status, ContractTime). Methods (GenetateContractID, AddContractDetails, GetContractDetailsByContractID, GetContractID, ChangeContractStatus). The association between Negotiation and Contract is one to one.

ContractOrder: An order from a contract accepted by both sides. Attributes (ContractOrderID, Status). Methods (GenerateContractOrderID, AddContractOrderDetails, GetContractOrderInfo, GetContractOrderID, ChangeContractOrderStatus).

BillDetails: Providing the bill of an order for the demander. Attributes (BillID, OrderID, Price). Methods (GenerateBillID, AddBillDetails, GetBillInfoByBillID, GetBillID).

After the deep analysis of the relationships (association, generalization, inheritance) between entity classes, the entity classes are extracted from use case diagram and the multiplicity of every two associate classes is confirmed based on the definition of each class [8]. The class model of LBP is depicted in Fig. 38.4.

38.5 Database Modeling

Database model is completed on the basis of the mapping rules which can convert the class model to the database model [9].

38.5.1 *The Implementation Rules for Classes*

A class is mapped to a table, and the attributes of the class are converted to the fields of the table. The primary key should be confirmed based on the table structure. According to this rules and the class model, 11 tables are created and the primary key of each table is defined in the LBP, including Supplier, SupplyInfo, Demander, DemandInfo, OnlineOrder, Products, QuerySheets, NegotiationSheets, ContractSheets, ContractOrder, and Bills. The primary keys corresponding to every table listed above are SupplierID, SupplyInfoID, DemanderID, DemandInfoID, OnlineOrderID, ProductID, QueryID, NegotiationID, ContractID, ContractOrderID, and BillID.

38.5.2 *The Implementation Rules for Associations*

The rules depend on the multiplicity. For many-to-many associations, the association is implemented with a table and its primary key is the combination of the classes' primary key. If the association has attributes, they become additional columns. In the LBP, each supply information can be matched with many demand information by intelligent matching system and vice versa. So the association is many to many. MatchLists is generated as a single table whose primary key consists of SupplyInfoID and DemandInfoID on the basis of the implementation rules.

For one-to-many associations, each one becomes a foreign key buried in the table for the "many" class. For the platform, each logistics supplier can publish one or more supply information; therefore, the association existed between Supplier and SupplyInfo is one to many, and the primary key of Supplier becomes a foreign key appended to the table of SupplyInfo.

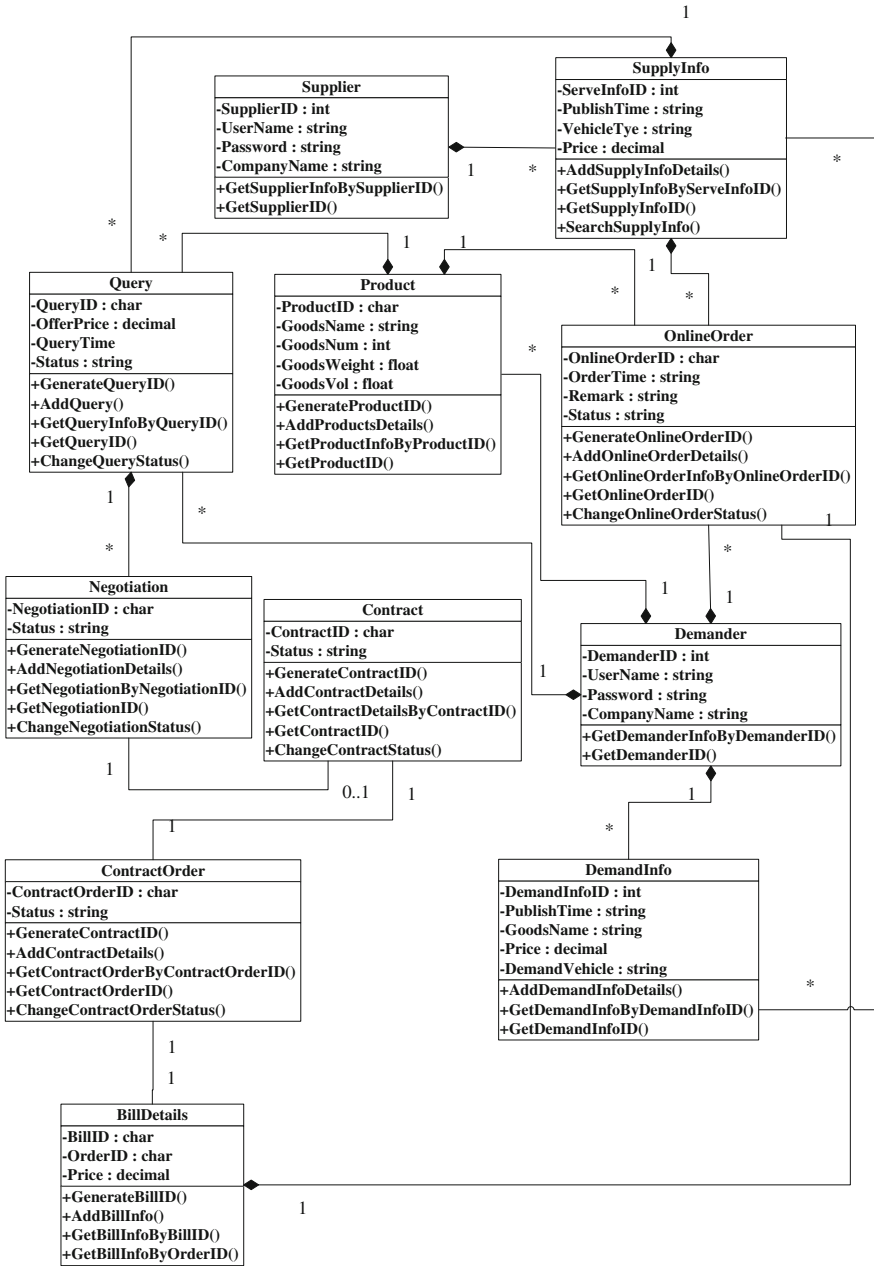


Fig. 38.4 Class model of LBP

For one-to-one associations, it can be handled by burying a foreign key in either class table. Required by the LBP, each contract can just result in the only contract order, so the primary key of Contract can become the foreign key of ContractOrder, or ContractOrderID may as well be added to Contract as a foreign key. Similarly, the bill for a contract order is also sole.

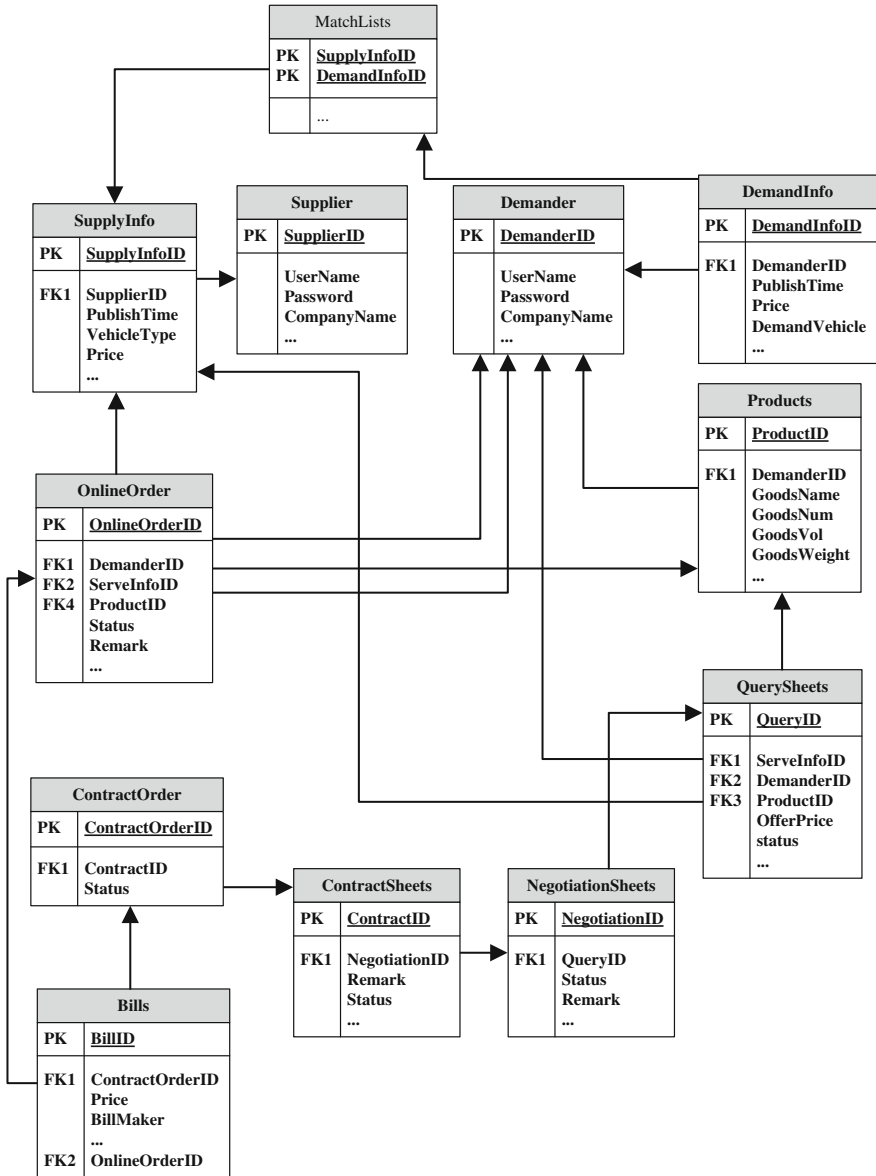


Fig. 38.5 Database model of LBP

The database model is achieved finally based on the implementation rules described above. The database model of LBP is depicted in Fig. 38.5.

38.6 Conclusion

The construction of LBP will promote the efficiency of logistics transactions and make the information flow run more fluently among all the nodes of the whole logistics supply chain. The design of the database plays a great role in the whole process of building the platform. As the data management background, the quality of the database influences the performance of the system directly. The paper introduces a method of database modeling based on UML. With the adoption of it, the transaction flow diagram, use case diagram, activity diagram which integrates use cases and use case narratives, class model, and database model are achieved, respectively, in different phases of designing a database. It can be seen that UML can describe the business rules without ambiguity during the procedure of modeling, promoting the maintainability, maneuverability, and scalability of a system [10].

Acknowledgments The work in this paper is partly supported by Director of topics of Guangxi Key Laboratory for advanced Manufacturing Systems (Nos. 11-031-12S04) and Guangxi (China) Science Technology Fund under grant (Nos. 201106LX010). The authors would like to thank the research group that took part in the study for their generous cooperation.

References

1. Song E, Yin S, Ray I (2006) Using UML to model relational database operations. *Comput Stans Interfaces* 5:343–354
2. Han L, Shi H (2012) Research of UML-based theme selection system for undergraduate graduation design. *Mod Electron Tech* 2:33–35
3. Qiang W, Zhang X (2004) Research of integrating use cases with activity diagram. *Comput Eng* 3:80–81
4. Juwei Y, Kunpeng Y, Hui-juan Z (2012) Modeling college teaching management system with unified modeling language. *Microcomput Inf* 4:98–99
5. Xia K, Li X, Zhang X (2009) Research on electronic commerce system modeling based on UML. *Comput Mod* 6:30–33
6. Yang B (2003) Modeling and development of material management system for power company base on UML. *Cent China Electr Power* 3:67–70
7. Blaha M, Rumbaugh J (2006) Object-oriented modeling and design with UML, Posts & Telecom Press, Beijing
8. Chen S, Zhu C (2012) Design and modeling for mission plan simulation system based on UML. *Sci Technol West China* 270:1–3
9. Naibmg EJ, Maksimchuk RA (2002) UML for database design. Posts & Telecom Press, Beijing
10. Qin lu (2011) Information system software architecture: a UML—based description. *J Eastern Liaoning Univ (Natural Science)* 4:311–314

Chapter 39

Research on Multi-service Demand Path Planning Based on Continuous Hopfield Neural Network

Yitong Zhang and Gang Zhao

Abstract In this paper, we focus on multi-vehicle and multiple types of dynamic vehicle routing problems. The introduction of dynamic traveling salesman problem (TSP) is to consider user's needs in many aspects. This paper uses the Hopfield neural network for solving the vehicle routing problem of "advanced request" to shorten the delivery path length and reduce the logistics cost. For "immediate request," we build the analytic hierarchy process model to analyze the final delivery order under a number of factors; use multi-type corresponds to multi-vehicles mixed queuing system model to obtain service indicators of the system, so as to improve the system efficiency compared with the single-delivery vehicle system. The combination of AHP and the Hopfield neural network algorithm is superior to the application of BP neural network classification and the Hopfield neural network.

Keywords Neural network · Analytical hierarchy process · Priority · Optimization · Queuing theory

39.1 Introduction

Multi-demand type of service routing problem is characterized by the division of service priority level. For immediate requests and advanced requests, there are two types of vehicles to service to ensure the principle of high delivery speed. Advanced service's goal is to shorten the access path length and get the order.

There is a wide range of application of the traveling salesman problem, such as the laying of gas pipelines, car navigation path planning, warehouse picking zoning, pharmaceutical distribution, and the robot moving path planning.

BP neural network can be applied to solve classification problems. The type of service is divided into many types, but the BP neural network has a slow rate of

Y. Zhang (✉) · G. Zhao
Beijing Information Science and Technology University, Beijing 100192, China
e-mail: zhangyitonggood@126.com

convergence. It is easy to fall into the shortcomings of local minimum, and considering the immediate requests is not comprehensive enough.

The use of minimum flow Dijkstra algorithm in operation research to obtain the shortest path for the logistics and transport is a simple calculation. In the weight matrix, mark the value of the element and its position in the final matrix. You can get the source to the other points of the shortest circuit length [1]. However, this method cannot guarantee that all the delivery sites in the network have been visited.

Genetic algorithms are global optimization algorithm. It has strong global search performance. In general, it has following steps: encoded, evaluation, selection, cross, re-evaluation and selecting the number of iterations [2]. In practical application, the selection of the evaluation function has a certain degree of difficulty and prone to the problem of premature convergence.

39.2 Mathematical Model Establishment and Optimization

39.2.1 TSP Description

The traveling salesman problem can be described as follows: There is a system of supply and demand relationship. There are several cars, a number of distribution centers and customers, requiring reasonable arrangements for the vehicle routing, which send the customer demand for the goods under the given constraints to the customer and the objective function to obtain the optimization [3].

N delivery locations finds a through to get the shortest distance. Without regard to direction and periodic, in the conditions of a given N , there may be a closed path for $\frac{1}{2}(N - 1)!$ [4]. When N is big, the workload of enumeration method of calculation is huge. Fast and comprehensively access of the order of all delivery locations is very important. In order to avoid the time delay, human and material resources waste in the goods delivery process, and consider expedited shipping needs, a better optimize the path selection is particularly important.

39.2.2 Multiple Types of Service Demand

We have to serve two types of requests in the application of dynamic vehicle routing vehicles: advanced request and immediate request. The former is the demand that static clients on the path of the process having before the start of the customer's requirements. The latter demand is obtained from the dynamic customers and arrives in real time in the day of operation. Putting immediate request into the planned route is usually a complex task. It may lead to partial or full replanning of routes. Complexity of the path directly affects the insertion of dynamic client. For example, the time window usually increases the difficulty of insertion. This may lead to the immediate request to be a denial of service.

Therefore, in this paper, we have two types of cars to serve immediate request and advanced request.

39.2.3 Poisson's Distribution

Set $N(t)$ as the number of customers to reach the system between $[0, t]$, if the following three conditions are met:

1. Smooth: The probability of customers arriving between $[t, t + \Delta t]$ is $\lambda t + o(\Delta t)$.
2. Independence: Any two disjoint independent customers arrive in the interval;
3. Generality: The probability of more than one customer arrives between $[t, t + \Delta t]$ is $o(\Delta t)$, called $\{N(t), t \geq 0\}$ is Poisson's distribution [5].

39.2.4 Path Planning Problem Solution Architecture

Continuous Hopfield neural network has an optimization feature. The energy function corresponds to the objective function of the TSP. The delivery location order corresponds to the state of neurons. Known by the stability theory of continuous Hopfield neural network, when the network energy function tends to the minimum, the state of neurons reaches equilibrium point. At the moment, the corresponding delivery order is the best route.

Two important factors affecting the queuing theory are system service rate and arrival rate per unit time. Factors affecting arrival rate per unit time are as follows: weekends, business promotion, and traffic. Factors affecting the service rate per unit time: the level of business familiar, the number of spare vehicles, and the degree of information.

Using MATLAB, randomly generated priority coefficient in turn corresponds to the delivery location. According to the paper, there are three "immediate request" delivery locations, and they are No. 5, No. 6, and No. 11 locations, respectively. In the weekend, business promotion, traffic, business familiar level, the number of vehicles, vehicle spare, and the degree of information all have different advantages and disadvantages to choose from. We need to take several indicators into consider in order to get a comprehensive evaluation of the sort.

In order to consider the choice of priority of delivery sites, the impact factor is divided into three layers: The first layer is the target layer, which determines the priority of delivery; the second layer is criteria layer, including weather and traffic; and the third layer is program layer. From top to bottom, it will directly affect the relationship between various factors. Arranged the factors at different levels, it constitutes the following hierarchy diagram (Fig. 39.1).

The type of service in this paper is divided into two categories, and we use multi-vehicle hybrid delivery vehicles queuing system model.

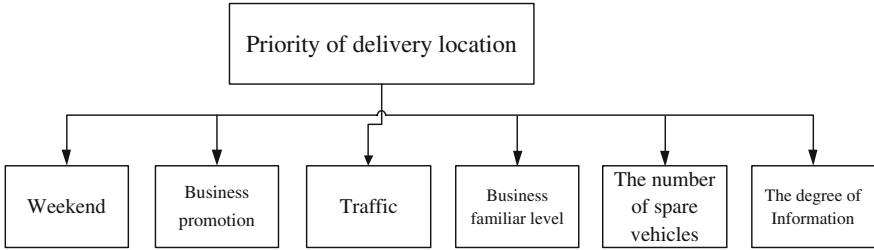


Fig. 39.1 Analytic hierarchy process model establishment

Customers waiting for service cannot wait indefinitely, so let us assume that the system capacity is limited and the number of customers waiting for serving is no more than three. Hence, there is customer loss rate. The calculation of the parameters in the queuing system is significantly better than the single-delivery vehicle system.

39.3 Continuous Hopfield Neural Network Solves TSP

39.3.1 Hopfield Neural Network

J. J. Hopfield took use of analog circuit to achieve a description of the neurons on the network. Assume that neuron j ($j = 1, 2, \dots, n$) internal membrane potential is U . Membrane input capacitance is C . The cell membrane transfer resistance is R . The output voltage is V . The external input current is I . which, R and C in parallel to simulate the time constant of the biological neurons. ω simulates the synaptic characteristic of neurons. I is equivalent to the threshold [6].

39.3.2 Network Stability Analysis

J. J. Hopfield defined the energy function to reflect the network’s stability. The more flatten of the image of the energy function indicated, the more close we can achieve the optimal outcome of the visit.

Energy function $E(t)$ is defined as follows:

$$E(t) = -\frac{1}{2} \sum_{j=1}^n \sum_{i=1}^n \omega_{ij} V_i(t) V_j(t) - \sum_{j=1}^n V_j(t) I_j + \sum_{j=1}^n \frac{1}{R_j} \int_0^{V_j(t)} g^{-1}(V) dV \quad (39.1)$$

where $g^{-1}(V)$ is the inverse function of $V_j(t) = g_j(U_j(t))$.

Take derivatives of energy function with time $dE(t)/dt$

$$\begin{aligned}
 \frac{dE(t)}{dt} &= - \sum_{j=1}^n \frac{dV_j(t)}{dt} \times C_j \frac{d[g_j^{-1}(V_j(t))]}{dt} \\
 &= - \sum_{j=1}^n \frac{dV_j(t)}{dt} \times C_j \frac{d[g_j^{-1}(V_j(t))]}{dV_j(t)} \times \frac{dV_j(t)}{dt} \\
 &= - \sum_{j=1}^n \left[\frac{dV_j(t)}{dt} \right]^2 \times C_j \times [g_j^{-1}(V_j(t))]'
 \end{aligned} \tag{39.2}$$

Transfer function $g(u)$ is monotonically increasing continuous bounded function, and then, its inverse function is monotonically increasing function. Therefore, we can see that its derivative is greater than 0, that is, $[g^{-1}(V_j(t))]' > 0$. At the same time, we know that $C_j > 0, \frac{dV_j(t)}{dt} \geq 0$; therefore, $\frac{dE(t)}{dt} \leq 0$, and only if $\frac{dV_j(t)}{dt} = 0, \frac{dE(t)}{dt} = 0$

It can be seen from the above proof process. If and only if the output of the neuron no longer changes with time, energy of the network will remain unchanged. In formula (39.1), the first two parts are constraints of the problem, and the third part is the goal to be optimized.

The dynamic equations of the network are as follows:

$$\frac{dU_{xi}}{dt} = - \frac{\partial E}{\partial V_{xi}} = -A \left(\sum_{i=1}^N V_{xi} - 1 \right) - A \left(\sum_{y=1}^N V_{yi} - 1 \right) - D \sum_{y=1}^N d_{xy} V_{y,i+1} \tag{39.3}$$

Transformed energy function expression is as follows:

$$E = \frac{A}{2} \sum_{x=1}^N \left(\sum_{i=1}^N V_{xi} - 1 \right)^2 + \frac{A}{2} \sum_{i=1}^N \left(\sum_{x=1}^N V_{xi} - 1 \right)^2 + \frac{D}{2} \sum_{x=1}^N \sum_{y=1}^N \sum_{i=1}^N V_{xi} d_{xy} V_{y,i+1} \tag{39.4}$$

according to the experience, where $A = 200, D = 100$ [7].

39.4 Quantitative Analysis of the Priority of Delivery Sites

39.4.1 Analytical Hierarchy Process

Analytical hierarchy process is a new system analysis method in the late 1970s [10]. This method is suitable to apply to the complicated structure and difficult to quantify problem.

If noted B_k as the weight vector in the layer of the matrix by column of all factors in the k th level relative to the relevant factors, the k th level's combination of the weight coefficient vector W^k to meet is

$$W^k = B_k \cdot B_{k-1} \dots B_2 \cdot B_1$$

where $B_1 = (1)$.

39.4.2 BP Areas of the Network Classifier Contrast

BP neural network model is a typical type of neural network. It has a good self-learning, adaptive, associative memory, parallel processing, and the ability of nonlinear conversion. It is currently the most widely used neural network model.

A three-layer BP network classifier contains the n -dimensional inputs, p hidden layer nodes, and m categories. Its structure is shown in Fig. 39.2. Among them, the activation function of hidden layer nodes is tansig. Output layer node's activation function is logsig. The output of the output layer adds a threshold function which will constitute a classifier. Using the advantage of BP neural network in the classification, we distributed the distribution center within the scope of the distribution site for division.

In a regional breakdown of the distribution points using the BP neural network, the number of nodes in the hidden layer and training times have an essential impact

Fig. 39.2 BP neural network structure

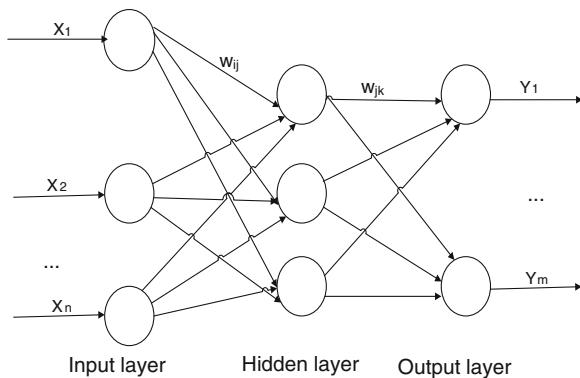
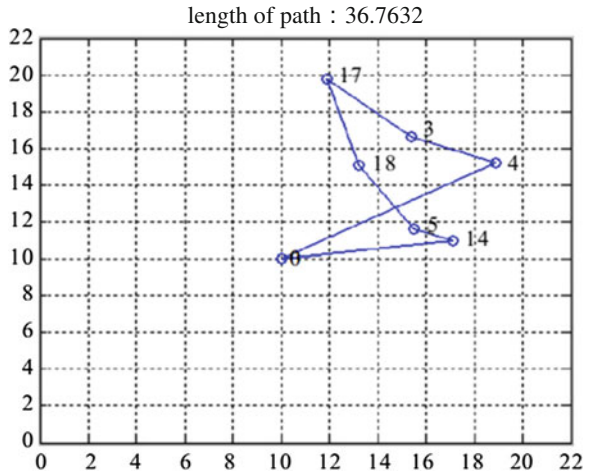


Fig. 39.3 Optimized figure using BP neural network classifier



on the result of division. This article simply distributed the shipping area into two parts, and we can use two cars to serve.

As shown in Fig. 39.3, in reference [8], the path planning after dividing the delivery area may have contributed to the phenomenon of the optimized one. The using of AHP and the combination with Hopfield network can effectively avoid this kind of circumstance. The introduction of analytic hierarchy process can make us consider the problem from a more comprehensive view of various factors.

Reference [8] does not consider the important parameters that impact the queuing theory: the arrival rate and service rate per unit time. They are the key affective factor of various indicators. This paper establishes analytical hierarchy process to focus on them to judge the delivery order. So this paper considers more fully and avoids the disadvantage of premature convergence of the BP network.

39.5 Application of Queuing Theory in Path Planning

Queuing is a frequently encountered phenomenon. That is waiting in line in order to obtain certain services, such problems are called overcrowding. Tangible queue is that the server is people, such as go to the hospital. Invisible queue is that the server is an object, such as the call telephone switch received. This paper is an invisible queue.

39.5.1 Multi-delivery Vehicle Hybrid System

In the multi-delivery vehicle hybrid system, M/M/s/K refers to the following: Customers were arriving in time to depend on the parameter λ for the negative exponential distribution (i.e., the customer arrival process is Poisson's stream). The number of delivery vehicles is s . The service time V depends on the parameter μ for the negative exponential distribution. The space of the system is K .

39.5.2 Steady-State and Waiting Service Mechanism

In steady state, inflow rate is equal to the outflow rate [9]. Thus, the steady-state equation is

$$C_n = \frac{\lambda_{n-1}\lambda_{n-2}\dots\lambda_0}{\mu_n\mu_{n-1}\dots\mu_1}, n = 1, 2, \dots, C_0 = 1$$

$$\rho = \frac{\lambda}{\mu}$$

- ρ is service intensity
- p_n the probability of state n

Average queuing length L : the number of customers in system (the number of customers waiting in line and the number of customers being serviced).

Average waiting length L_q : the number of customers waiting for service in system.

First, get the distribution of queue length in the steady state $p_n = P\{N = n\}$, $n = 0, 1, 2, \dots$. Queuing system can only accommodate a maximum of K customers, so

$$\lambda_n = \begin{cases} \lambda, & n = 0, 1, 2, \dots, K - 1 \\ 0, & n \geq K \end{cases}$$

$$\mu_n = \begin{cases} n\mu, & 0 \leq n < s \\ s\mu, & s \leq n \leq K \end{cases}$$

$$P_0 = \left(\sum_{n=0}^{s-1} \frac{\rho^n}{n!} + \frac{\rho^s(1 - \rho^{K-s+1})}{s!(1 - \rho_s)} \right)^{-1}, \rho_s \neq 1$$

As stationary distribution p_n , $n = 0, 1, 2, \dots, K$, we can get the average queue length:

$$L_q = \sum_{n=0}^K (n-s)p_n = \frac{\rho_0 \rho_s^s \rho_s}{s!(1-\rho_s)^2} [1 - \rho_s^{K-s+1} - (1-\rho_s)(K-s+1)\rho_s^{K-s}], \rho_s / = 1$$

Therefore, $p_n = \rho^n p_0, n = 1, 2, \dots, K$

$$p_0 = \left(\sum_{n=0}^{s-1} \frac{\rho^{n-1}}{n!} + \frac{\rho^s(1 + \rho^{K-s+1})}{s!(1-\rho_s)} \right)^{-1}, \rho_s \neq 1.$$

Due to the limited capacity of the queuing system, when the system space is filled, the customer’s demand will be a denial of service. Suppose the customer arrival rate (the average number of customers came to the system in unit time) is λ . When the system is in state of K , the customer can not enter the system, so the probability of customers entering the system is $1-p_K$. Therefore, the actually average number of customers entering the system in unit time is

$$\lambda_e = \lambda(1 - p_K), \text{ where } \rho_K = \frac{\rho^K}{S!S^{K-s}} \rho_0$$

λ_e is called the effective arrival rate. p_K is also called customer loss rate, which indicates that the proportion of customers cannot enter the system.

Average queue length: $L = L_q + s + p_0 \sum_{n=0}^{s-1} \frac{(n-s)\rho^n}{n!}$

Average waiting length: $L_q = \sum_{n=0}^K (n-1)p_n = L - \sum_{n=0}^{s-1} (n-s)\rho_n - s$

According to Little formula, we can see

Average length of stay: $W = \frac{L}{\lambda_e} = \frac{L}{\lambda(1-p_K)}$;

Average waiting time:

$$W_q = \frac{L_q}{\lambda_e} W - \frac{1}{\mu}$$

The average number of occupied delivery vehicles:

$$\bar{S} = \sum_{n=0}^{s-1} np_n + s \sum_{n=s}^K \rho_n = \rho(1 - \rho_K)$$

39.6 Simulation

Input the coordinates of each delivery location in the Hopfield neural network, as shown in Table 39.1.

Table 39.1 The coordinates of each delivery sites

The order of delivery sites	Abscissa	Ordinate
1	0.1	0.6
2	0.2	0.3
3	0.4	0.1
4	0.5	0.5
5	0.7	0.2
6	0.8	0.4
7	0.2	0.8
8	0.5	0.9
9	0.7	0.6
10	0.9	0.8
11	0.65	0.56
12	0.85	0.95
13	0.77	0.89
14	0.56	0.45
15	0.34	0.23
16	0.15	0.29
17	0.94	0.27
18	0.48	0.37
19	0.36	0.42
20	0.39	0.55

Using Matlab randomly generates priority: 0.7425, 0.7579, 0.3891, 0.4293, 0.9563, 0.5730, 0.8497, 0.2763, 0.6223, 0.5884, 0.9635, 0.0859, 0.5005, 0.5216, 0.0902, 0.9047, 0.8844, 0.4390, 0.5124, 0.2345, 0.7443, 0.2453, 0.5366. Assign these 23 values to the corresponding delivery sites. It is shown that delivery point No. 5, No. 11 and No. 16 is the highest three priority of all the delivery locations. The remaining 20 delivery sites can apply the Hopfield network for route planning (Fig. 39.4).

From Fig. 39.5, we can learn that the optimized delivery order is as follows: 17, 6, 18, 4, 11, 9, 10, 12, 13, 8, 7, 1, 20, 19, 16, 2, 15, 3, 5. Before optimization, the length of the path is 9.8236. The optimized path length is 3.8719. The optimization effect is very obvious.

Six factors that affect the delivery location of priority are the weekend, business promotion, traffic, business familiar level, the number of spare vehicles, and the degree of information, respectively. These six factors are pairwise-compared, and we can get judgment matrix A as follows:

Fig. 39.4 Random access road map

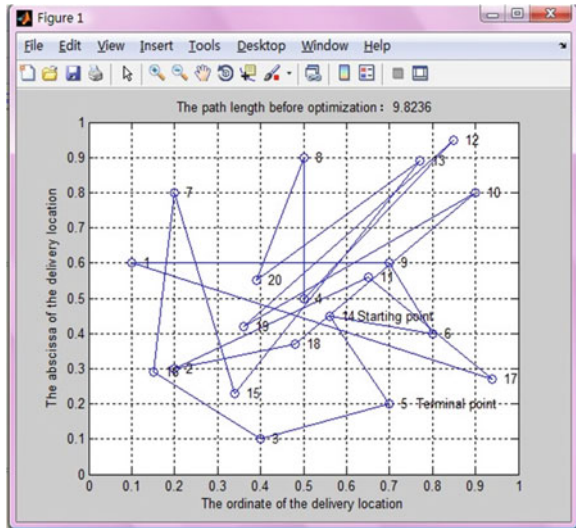
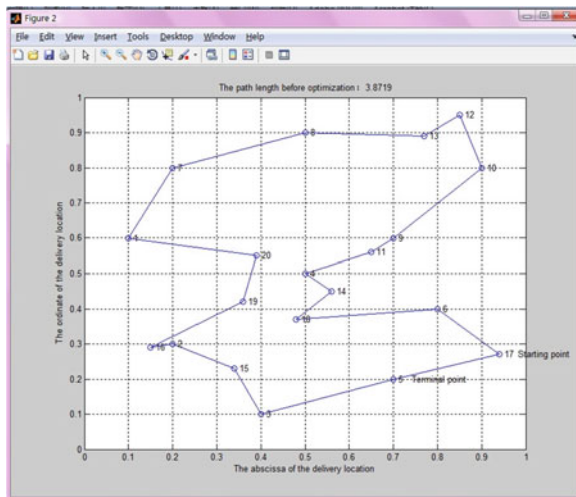


Fig. 39.5 Optimized road map



$$A = \begin{matrix} \text{Weekend} \\ \text{Business Promotion} \\ \text{Traffic} \\ \text{Business Familiar Level} \\ \text{Number of Spare Vehicles} \\ \text{Degree of Information} \end{matrix} \begin{bmatrix} 1 & 1 & 1 & 4 & 1 & 1/2 \\ 1 & 1 & 2 & 4 & 1 & 1/2 \\ 1 & 1/2 & 1 & 5 & 3 & 1/2 \\ 1/4 & 1/4 & 1/5 & 1 & 1/3 & 1/3 \\ 1 & 1 & 1/3 & 3 & 1 & 1 \\ 2 & 2 & 2 & 3 & 1 & 1 \end{bmatrix}$$

The largest eigenvalue of A is 6.35. The corresponding eigenvector is

$$B_2 = (0.16, 0.19, 0.19, 0.05, 0.12, 0.30)^T$$

Use eigenvector method to get the six factors for each of the weight coefficients. It has the largest eigenvalues and corresponding eigenvectors of each attribute, according to the column matrix B_3 .

$$B_3 = \begin{matrix} A \\ B \\ C \end{matrix} \begin{bmatrix} 0.14 & 0.10 & 0.32 & 0.28 & 0.47 & 0.77 \\ 0.68 & 0.33 & 0.22 & 0.65 & 0.47 & 0.17 \\ 0.24 & 0.57 & 0.46 & 0.07 & 0.07 & 0.05 \end{bmatrix}$$

Thus, $W^3 = B_3 B_2 = (0.40, 0.34, 0.26)^T$

The final order of immediate service request is 5, 11, 6.

The maximum of waiting customers is 3. Averagely, it takes one minute to reach an object. Service time depends on negative exponential distribution. Averagely, 1.25 min can service a delivery location. We can calculate relevant indicators of the system.

The system can be seen as a M/M/2/3 queuing system, which

$$\lambda = 1, \mu = \frac{1}{1.25} = 0.8, \rho = \frac{\lambda}{\mu} = \frac{1}{0.8} = 1.25, K = 3, s = 2$$

By the formula, we have

$$p_0 = \left(\sum_{n=0}^{s-1} \frac{\rho^n}{n!} + \frac{\rho^s(1 + \rho^{K-s+1})}{s!(1 - \rho_s)} \right)^{-1} = 0.2841$$

$$L_q = \frac{p_0 \rho^s \rho_s}{s!(1 - \rho_s)^2} [1 - \rho_s^{K-s+1} - (1 - \rho_s)(K - s + 1)\rho_s^{K-s}] = 0.4816$$

Customer loss rate: $P_K = 0.0677$

Effective arrival rate: $\lambda_e = \lambda(1 - p_3) = \mu(1 - p_0) = 1 \times (1 - 0.1387) = 0.8613$

Average queue length: $L = L_q + s + p_0 = \sum_{n=0}^{s-1} \frac{(n-s)\rho^n}{n!} = 1.5582$

Expected value of sojourn time: $W = \frac{L}{\lambda_e} = 1.8091$

Expected value of waiting time: $W_q = W - \frac{1}{\mu} = 0.5591$

The average occupancy number of delivery vehicles:

$$\bar{s} = \sum_{n=0}^{s-1} np_n + s \sum_{n=s}^K \rho_n = \rho(1 - \rho_K) = 1.0766$$

The index contrast in hybrid vehicles queuing system with single delivery under the same conditions is shown as follows:

	Index	λ_e	L	W	W_q
Delivery vehicles					
Single		0.6613	1.7751	2.6843	2.1474
Multiple		0.8613	1.5582	1.8091	0.5591

Therefore, multi-delivery vehicles can significantly improve the effective arrival rate of customers, but delivery of the average vehicle occupancy rate is only 1.0766. Thus, when an extremely urgent service is in need, multiple delivery of the vehicle system is relatively good. Or, it may cause waste of resources.

39.7 Conclusion

This paper uses continuous Hopfield neural network to optimize random access path. When the energy function changes very small, the neurons of the network reach equilibrium. At the moment, the corresponding order is the optimal path. The order is as follows: 17, 6, 18, 4, 11, 9, 10, 12, 13, 8, 7, 1, 20, 19, 16, 2, 15, 3, 5. This model made the length of path become significantly short.

On this basis, we introduce a new method of multi-level requirements of the delivery destination. We use the analytic hierarchy process from the weekend, business promotion, traffic, business familiar level, the number of spare vehicles, and the degree of information. Six factors evaluate the priority of sorting on the all indicators for each delivery location dominated by different factors, and you can have a quantitative selection basis.

Customers waiting for service in the system cannot be infinitely. When the capacity exceeds a certain level, they will lose customers. Take use of hybrid queuing model in the queuing theory. Set multiple vehicles for the two types of services. Each index is obviously better than single-delivery vehicle system. But at the same condition, delivery vehicles' utilization rate is not very high. When the system space is K , we can get average queue length, expected value of sojourn time, and other indicators.

This paper uses the Hopfield neural network to overcome the shortcoming that the random access of the delivery destination path is too long. Take into consideration the priority of delivery sites from the terms of arrival rate and service rate per unit time. In this paper, the model considers more comprehensively to overcome the drawback of the combination of BP neural network classifier and Hopfield network. Because the use of BP neural network may cause the path is not the best, two service vehicles serve for immediate request and advanced request, respectively. It is able to shorten the waiting time and reduce the rate of customer loss. The method is simple and practical. It can be used for real-time logistics path planning.

Acknowledgement This research is supported by the Funding Project for Academic Human Resources Development in Institutions of Higher Learning Under the Jurisdiction of Beijing Municipality PHR 201106133.

References

1. Xiong D, Hu Y (2011) A matrix method of solving shortest path using Dijkstra algorithm. *J Henan Polytech Univ (Nat Sci)* 30(5):608–612
2. Yu Y (2001) Hopfield neural network and genetic algorithm in solving travelling salesman problem: experimental comparison and analysis. *J Central Chin Normal Univ (Nat Sci)* 35(2):157–161
3. Smith SL, Pavone M, Bullo F, Frazzoli E (2008) Dynamic vehicle routing with heterogeneous demands. In: *Proceedings of CDC, Cancun, Mexico, Dec 2008*
4. Laren A (2000) The dynamic vehicle routing problem. Printer by IMM, DTU Bookbinder Hans Meyer, Denmark
5. Pavone M, Frazzoli E, Bullo F (2007) Decentralized algorithms for stochastic and dynamic vehicle routing with general target distribution. In: *Proceedings of CDC, New Orleans, LA*, pp 4869–4874
6. Zhou X, Liu W, Chen Y (2011) Surface mount technology optimization based on Hopfield neural network. *J Soochow Univ (Eng Sci Edn)* 31(6):25–29
7. Zhang Y, Cheng P (2003) The parameters analysis in using Hopfield NN to Solve the TSP. *Microelectron Comput* 2003(5):8–10
8. Yu B, Meng W (2011) Research on vehicle routing model based on hybrid neural networks. *Comput Eng Des* 32(11):3861–3864
9. Bertsimas D, Paschalidis IC, Tsitsiklis JN (1994) Optimization of multiclass queueing networks : polyhedral and nonlinear characterizations of achievable performance. *Ann Appl Probab* 4(1):43–75
10. Sun H, Geng L (2007) The application of AHP in logistics network planning in the environment of communication. *Electron Packag* 2007(2):41–44

Chapter 40

A Graded Optimization-Based Approach to Remanufacturing Production Decision

Yiwei Mo, Zhili Huang and Wei Huang

Abstract As a new kind of manufacturing method by recycling valuable part of used products, remanufacturing reduces production cost and environment pollution, so has received more and more attentions. The key problem in remanufacturing is making production decision. At present, such a problem is usually solved by converting it into an optimization problem, most of which use static models or simple dynamical models. Since both demand rate of new products and recycle rate of used products are dynamic, static models or even most simple dynamic models may not adequately describe such dynamic issues in remanufacturing production decision. For this case, in this paper, a complex dynamic optimization model is presented to describe the dynamic remanufacturing production decision problem. To solve this model, a new constraint-preferred graded optimization strategy-based genetic algorithm (CGGA) is given. Experiment example analysis demonstrates the proposed approach's feasibility.

Keywords Remanufacturing · Production decision · Graded optimization · Dynamical optimization

40.1 Introduction

As reduction of natural resources and the increasing of pollution, living environment of human suffers greater and greater stress. As a result, traditional way of manufacturing cannot meet the requirement of the social development. More and more attention is paid to recycling and reusing used production. As a new kind of manufacturing method by recycling valuable part of used products, remanufacturing plays more and more important role in products manufacture [1]. Unlike

Y. Mo (✉) · Z. Huang · W. Huang
Department of Mechanical Electronic Engineering, School of Mechanical Engineering,
Guangxi University, Nanning, Guangxi, People's Republic of China
e-mail: moyw@gxu.edu.cn

traditional manufacturing methods, remanufacturing process includes not only manufacturing part but also remanufacturing part, so how to coordinate the both of them becomes a key problem in remanufacturing. Deng and Yao study pricing joint decision and production decision problems for single-product manufacturers who are price-sensitive and capacity constrained [2]. Li et al. [3] optimize remanufacturing production plan and control strategy by combining hybrid cell genetic algorithm and DES model. Shi et al. [4] present a way to decide the best quantities of manufacturing and remanufacturing products, as well as price strategy, to obtain the best benefit when demand and recycling rates are both uncertain. Necati et al. [5] establish a new frame for comparing manufacturing primary strategy and remanufacturing primary strategy. They point out that remanufacturing primary strategy is more economic when recycle rate is up to certain level.

At present, most researches prefer to building static or simple dynamical models for remanufacturing problems [6, 7]. These models are relatively easy to analyze and many good results are obtained. However, since recycling rate and market demand are usually dynamically changing over time, static or simple dynamical models might not describe such dynamical process well, especially when dynamical production plans are required. For this problem, in this paper, a new approach for remanufacturing production decision is presented based on dynamical optimization. A complex dynamic optimization model is established, in which differential equations are employed to describe the dynamic relations among products, recoverable inventory, and demanding and recycling rates that perform as constraints.

General algorithms such as genetic algorithm (GA) are able to solve dynamical constraint optimization models theoretically using penalty functions. However, when dealing with complex models, the choice of penalty factors plays critical role: Too small penalty factors cannot meet the constraints and too large ones may lead to ill-posed problem that is difficult to converge. As a result, it is difficult to solve complex dynamical model by general optimization algorithms in practice, so we employ a new graded optimization-based GA, which considers the constraints and the cost function, respectively, in two different grades. Based on this algorithm, numerical examples show that this graded strategy is efficient, by which the optimal production decision for corresponding dynamical demanding and recycling rates is obtained, including the optimal quantities of manufacturing, remanufacturing, and disposing products.

40.2 Model Formulation

The general remanufacturing process is shown in Fig. 40.1. Firstly, used products have to be bought back from product holders. By preliminary cleaning and screening, recoverable ones of these used products are sent to the recoverable inventory and stocked there. The used products stored in the recoverable inventory are sent to remanufacturing process when needed, and then, they are disassembled and inspected there. Components in good condition are reused directly, while the

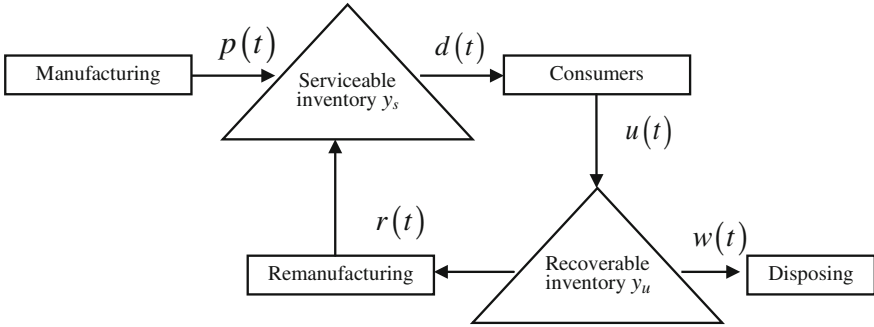


Fig. 40.1 The flow diagram of remanufacturing production

other are repaired or replaced to achieve using standard before reused. All these components are then remanufactured into new products and stored in the serviceable inventory. As a result, the products satisfying demands are actually produced in two ways, manufacture and remanufacture.

To describe the above remanufacturing production decision problem, we firstly present some general assumptions for remanufacturing:

- A1.** Manufacturing and remanufacturing products have no difference to consumers.
- A2.** At the end of production period, the serviceable inventory and recoverable inventory should be zero.
- A3.** The demands of products can be described by a determined function $d(t)$.
- A4.** The quantity of recycling used products can be described by recycling rate.

$$u(t) = \lambda d(t - b)$$

where $\lambda \in [0, 1]$ when $b > 0$ is time delay.

All these assumptions are general assumptions when studying remanufacturing decision problem, based on which we present the following remanufacturing production cost model:

$$\min \text{cos } T = \int_0^T \{c_p p(t) + c_r r(t) + c_u u(t) + c_w w(t) + h_s y_s(t)\} dt \tag{40.1}$$

$$\text{s.t. } y_s(t) = p(t) + r(t) - d(t) \tag{40.2}$$

$$y_u(t) = u(t) - r(t) - w(t) \tag{40.3}$$

$$y_s(t) \geq 0, y_s(0) = 0 \tag{40.4}$$

$$y_u(t) \geq 0, y_u(0) = 0 \tag{40.5}$$

$$p(t) \geq 0, r(t) \geq 0, w(t) \geq 0 \tag{40.6}$$

In this optimization model, the objective function is the cost function of production, where $p(t)$, $r(t)$, and $w(t)$ are control variables which are manufacturing production rate, remanufacturing production rate, and disposing rate, respectively. c_p and c_r are unit manufacturing and remanufacturing production costs, respectively. c_u and c_w are unit recycling and disposing costs, respectively. h_s and h_u are unit serviceable and recoverable inventory costs.

Two differential Eqs. (40.2) and (40.3) are employed in the constraints of model (40.1)–(40.6), to describe the dynamical relations among the serviceable inventory y_s , the recoverable inventory y_u , the manufacturing rate $p(t)$, remanufacturing rate $r(t)$, the demands rate $d(t)$, and disposing rate $w(t)$. Comparing with traditional model, such items can describe the impacts on inventories by the changes of demand rate, recycle rates, and production strategy. Constraints (40.2)–(40.6) are natural constraints.

Model (40.1)–(40.6) considers all production costs over a period as a whole. By solving it, the best production strategy that minimizes the cost function can be obtained, including the production strategy at every time point during the production period, which cannot be done by traditional static models.

40.3 Algorithm and Numeric Example

Model (40.1)–(40.6) is a kind of complex dynamical optimization model with constraints, which is more difficult to solve than traditional ones. A general way for solving it is using variation approach with penalty functions, where the selection of penalty factors is critical for performance. However, since the different orders between objective function and constraints, the selection of penalty factors is difficult that depends on experience and may lead to ill-posed problem [8].

Since proposed model is a complex dynamical optimization model, classic GA cannot solve it effectively. For this problem, we employ constraint-preferred graded optimization strategy-based genetic algorithm (CGGA).

In CGGA, we consider two parts. The first part is for constraints (40.2)–(40.6):

$$\min \int_0^T (y_s^-(t) + y_u^-(t)) dt \tag{40.7}$$

$$\text{s.t. } \bar{y}_s(t) = p(t) + r(t) - d(t) \tag{40.8}$$

$$\bar{y}(t) = u(t) - r(t) - w(t) \tag{40.9}$$

$$y_s(0) = 0 \tag{40.10}$$

$$y_u(0) = 0 \tag{40.11}$$

$$p(t) \geq 0, r(t) \geq 0, w(t) \geq 0 \tag{40.12}$$

where

$$y_s^- = -\min\{y_s(t), 0\} \tag{40.13}$$

$$y_u^- = -\min\{y_u(t), 0\} \tag{40.14}$$

The objective function (40.7) is established for constraints (40.4)–(40.5), which indicates that the serviceable inventory and recoverable inventory are nonnegative. It is easy to see that the above optimization problem is theoretically solvable. In [8], the authors use gradient method in this step. But our problem is difficult to define gradient of objective function and has much more complex constraints, so we use the classic genetic algorithm to find a group of feasible solutions $\{(p_f(t), r_f(t), w_f(t))\}$ instead.

The second part is the objective function of model (40.1)–(40.6):

$$\text{COST} = \int_0^T \{C_p p(t) + c_r r(t) + c_u u(t) + c_w w(t) + h_s y_s(t) + h_u y_u(t)\} dt \tag{40.15}$$

which is used to compute the fitness of $\{(p_f(t), r_f(t), w_f(t))\}$.

Based on the two parts, the diagram of CGGA is given as follows (Fig. 40.2).

CGGA simplifies the complex optimization problem (40.1)–(40.6) by converting it into two relatively simple parts, so it has better computing performance classic GA and avoids parameter selection problems as well. To specify the feasibility of our model and solving algorithm, we give an example as follows.

Example Assume that the demand rate is

$$d(t) = 1 + 0.5 \sin(t/\pi)$$

and the recycling rate is

$$u(t) = 0.7d(t + 0.5\pi^2)$$

Case 1 We suppose that production cost and inventory cost are on the same order of magnitude and let $c_p = 10$, $c_r = 5$, $c_u = 2$, $c_w = 0.5$, $h_s = 2.5$, and $h_u = 1.5$.

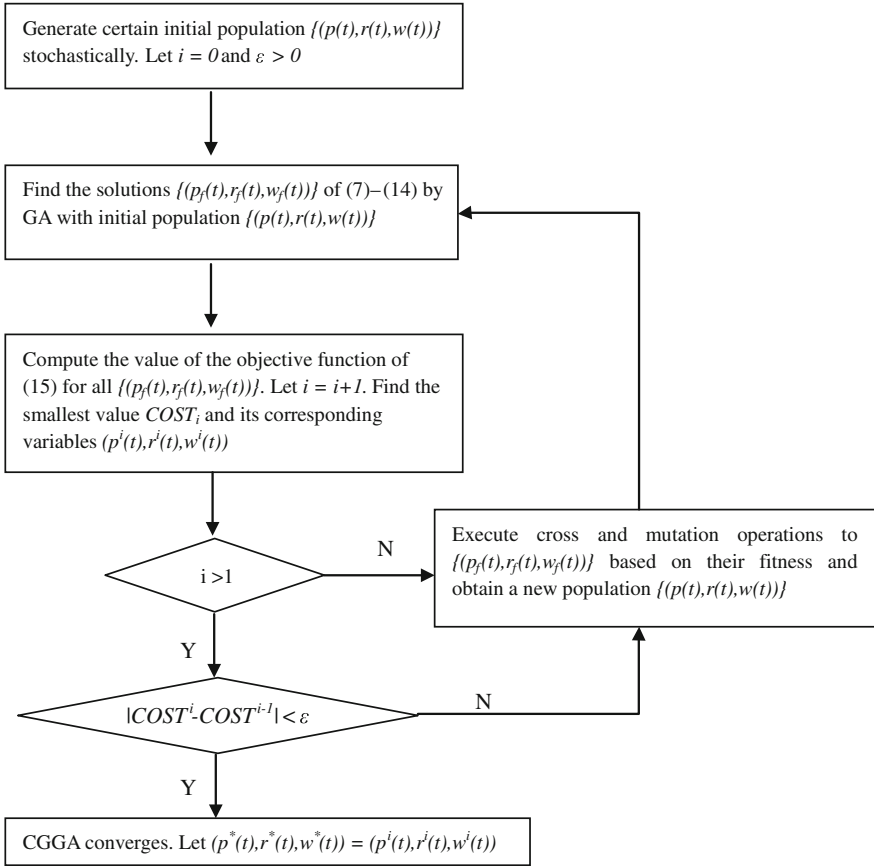


Fig. 40.2 CGGA diagram

Then, the remanufacturing production decision by coordinating manufacturing, remanufacturing, and disposing quantities is illustrated in Fig. 40.3.

Using CGGA, the best production strategy $p(t)$, $r(t)$, and $w(t)$ is obtained. At the beginning, when $d(t) > u(t)$, remanufacturing production rate $r(t)$ is almost equal to $u(t)$, while manufacturing production rate $p(t)$ is the difference between demand rate $d(t)$ and remanufacturing production rate $r(t)$. It implicates that all available are used to remanufacture and manufacturing process is started to meet the needs, when remanufacturing products is not enough to supply the demands. When $d(t) < u(t)$, remanufacturing production rate $r(t)$ is around $u(t)$ while manufacturing production rate $p(t)$ decreases to about zero and disposing rate $w(t)$ increases. It is coincident with theoretical result, showing that our model is feasible, and CGGA is efficient in solving these problems.

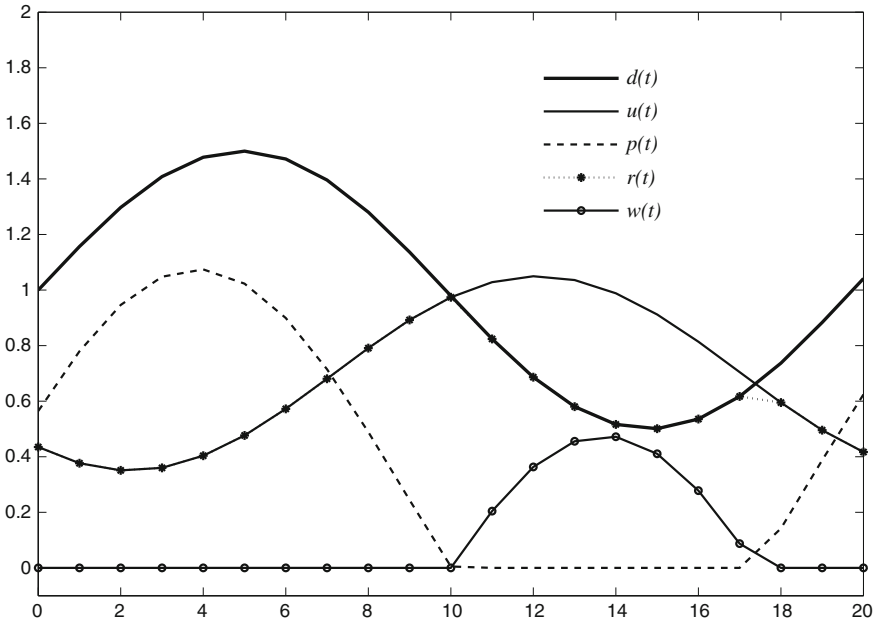


Fig. 40.3 Production decision

Case 2 When production cost is much larger than inventory cost, we get some different results in production strategy. By increasing manufacturing and remanufacturing production costs to $c_p = 1,000$, $c_r = 500$, and $c_u = 200$, while other parameters keep the same, we obtain the result shown in Fig. 40.4.

As shown in Fig. 40.4, $d(t) > u(t)$ before $t = 10$, the $p(t)$, $r(t)$, and $w(t)$ are similar with Fig. 40.3. When $d(t) < u(t)$ after $t = 10$, the disposing rate $w(t)$ increases. It indicates that some recycled used products are disposed. After $t = 17$, $d(t)$ is larger than $u(t)$ again. The remanufacturing production rate $r(t)$ increases even beyond $u(t)$, and it indicates that some recycled used products in inventory are used to remanufacturing process.

Comparing Figs. 40.3 and 40.4, it is easy to see an interesting result that difference of manufacturing and remanufacturing production costs respect to inventory costs may lead to different production strategies: When they are not too larger than inventory costs, there are few advantages to reserve recycled used products in inventory; and when they are much larger than inventory costs, reserving recycled used products in inventory is much more meaningful. This result is obviously coincident with general understandings.

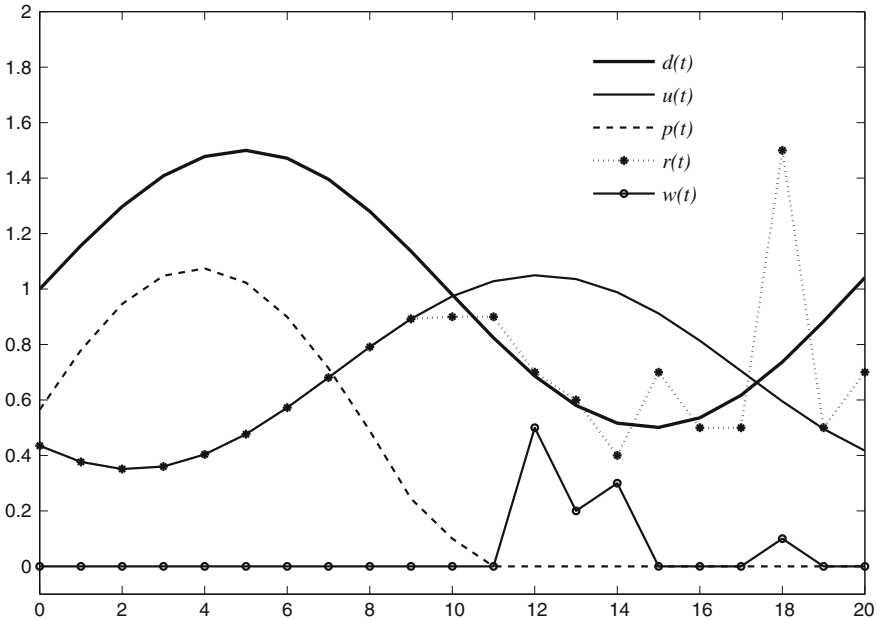


Fig. 40.4 Production decision

40.4 Conclusion

This paper investigates the remanufacturing production decision problem by coordinating manufacturing, remanufacturing, and disposing quantities. A new model for production decision is presented, which is a kind of complex dynamical optimization model that is more precisely and directly describes the impact that introduced by demands and recycles on production decision.

Since the proposed model is very complex, general computing algorithms, including classic GA, cannot solve it efficiently. As a result, a new CGGA is employed. CGGA reduces the complexity of the proposed model by converting it into two relatively simple parts and avoids the ill-pose problem introduced by penalty terms as well, showing good performance. Experiment example analysis demonstrates the proposed approach’s feasibility, and some interesting results are obtained.

A significant advantage of our approach is that time-dependent feasible production plans can be obtained. It is practically significant for actual production planning, since most of other investigations on remanufacturing production decision problem only present qualitative principles but not specific production plans.

Acknowledgments This study was supported by the National Key Technology R&D Program of China (Grant No. 2012BAF02B02)

References

1. Lu HJ, Guo W, Shao HW (2011) Research on remanufacturing production mode based on game theory. *J Mech Eng* 47:18
2. Daniel R, Guide J (2000) Production planning and control for remanufacturing: industry practice and research needs. *J Oper Manage* 18:467
3. Li J, Gonzalez M, Zhu Y (2009) A hybrid simulation optimization method for production planning of dedicated remanufacturing. *Int J Prod Econ* 117:286
4. Shi J, Zhang G, Sha J (2011) Optimal production planning for a multi-product closed loop system with uncertain demand and return. *Comput Oper Res* 38:641
5. Aras N, Boyacı T, Verter V (2006) Coordination and priority decisions in hybrid manufacturing/remanufacturing systems. *Prod Oper Manage* 15:528
6. Zhao P (2010) Investigation on remanufacturing production planning in reserve logistics. Master Thesis of Xi'an Electronic and Engineering University
7. Kleber R (2006) Dynamic inventory management in reverse logistics. Springer, Berlin, Heidelberg
8. Zhang B, Chen DZ, Wu XH (2005) Graded optimization strategy and its application to chemical dynamic optimization with fixed boundary. *J Chem Ind Eng* 56:1276 (China)

Chapter 41

Research About Slider Nonlinear Contact Analysis of the Telescopic Boom with Cylinder Supporting

Shilin Shen, Zhongpeng Zhang and Bin Gu

Abstract How to simulate the actual contact situation between the telescopic boom and slider has been the problem urgently to be solved for crane industry because of the complicated nonlinear contact. Took the new large tonnage railway crane as the research object, with the help of the international advanced nonlinear finite element analysis software ABAQUS, cylinder model was established, hinged relationship between the cylinder and telescopic boom was built by defining coupling constraints and connectors, sliding friction was taken into account, and the contact mechanics model was successfully acquired convergence after 103 times iterative calculation eventually. Contact stress response of the contact region was ascertained during the process of sliding contact with cylinder supporting which has filled the blank of the slider nonlinear contact analysis.

Keywords Nonlinear contact · Slider · ABAQUS · Telescopic boom · Cylinder

41.1 Introduction

Contact problems are inherently nonlinear since the contact area is a priori unknown, and the associated hybrid force/displacement boundary conditions are part of the solution [1]. The contact area and pressure distribution between the telescopic boom and sliders where the presence of sliding friction exists simultaneously always change during the contact process that makes the slider contact situation extremely complex. Some scholars have done related researches using the MPC multi-point constraints method to simulate the contact behavior [2]. But in the process of lifting goods, there has the tendency toward sliding existing between the telescopic boom and slider, so the freedom of the nodes belong to contact surfaces

S. Shen (✉) · Z. Zhang · B. Gu

Research Institute of Mechanical Engineering, Southwest Jiaotong University, Chengdu 610031, Sichuan, People's Republic of China
e-mail: goodboy2455@163.com

© Springer-Verlag Berlin Heidelberg 2015

Logistics Engineering Institution, CMES (ed.),

Proceedings of China Modern Logistics Engineering,

Lecture Notes in Electrical Engineering 286, DOI 10.1007/978-3-662-44674-4_41

should be released [3, 4]. Apparently, it will generate a big difference between the results of the slider contact simulation acquired on the basis of the coupling method and its actual contact behavior. On the other hand, the axial force is mainly shared by the cylinders while the telescopic boom is primarily subjected to the bending moment. The cylinders are usually replaced through applying an equivalent force in the hinged place currently, however, that will ignore the cylinders' weight as well as their boundary constraint function of the finite element model [5]. How to simulate the real role the cylinders play in reality when the crane is working is also the subject of one of the important contents of the study.

41.2 Nonlinear Problem-Solving Methods

The nonlinear models generally involve from a few to thousands of variables which need a lot of iteration to solve it that makes it more complex, higher costs, and more unpredictability than the linear problems. Newton–Raphson iterative method is widely used in which the tangential stiffness is calculated [6]. In terms of its variables, the equilibrium equations obtained by discretizing the virtual work equation can be written symbolically as:

$$F^N(u^M) = 0 \quad (41.1)$$

where F^N is the force component conjugate to the N th variable in the problem and u^M is the value of the M th variable.

Take Newton's method as a numerical technique for solving the nonlinear equilibrium equations, after iteration i , an approximation u_i^M to the solution has been obtained and let c_{i+1}^M be the difference between this solution and the exact solution to the discrete equilibrium equation (41.1) what means that:

$$F^N(u_i^M + c_{i+1}^M) = 0 \quad (41.2)$$

Expanding the left-hand side of Eq. (41.2) in a Taylor series about the approximate solution u_i^M , then gives:

$$F^N(u_i^M) + \frac{\partial F^N}{\partial u}(u_i^M)c_{i+1}^M + \frac{\partial^2 F^N}{\partial u^2}(u_i^M)c_{i+1}^2 + \dots = 0 \quad (41.3)$$

If u_i^M is a close approximation to the solution, the magnitude of each c_{i+1}^M will be small, and so all but the first two terms above can be neglected giving a linear system of equations:

$$K_i^N c_{i+1}^M = -F_i^N \tag{41.4}$$

where $K_i^N = \frac{\partial F_i^N}{\partial u} (u_i^M)$ is the Jacobian matrix and $F_i^N = F^N(u_i^M)$.

Convergence criteria of Newton’s method are best measured by ensuring that all entries in F_i^N and all entries in c_{i+1}^M are sufficiently small, or the iteration continues and the next approximation to the solution is then:

$$u_{i+1}^M = u_i^M + c_{i+1}^M \tag{41.5}$$

41.3 Finite Element Model

Taking the new telescopic boom of 160 t large tonnage and double-revolving railway crane as the research object, analyze the worst working condition the sliders bear of when the telescopic boom stretch out totally, as shown in Fig. 41.1. With the help of the powerful nonlinear finite element analysis software ABAQUS, take advantage of its seamless interfaces of the functional modules to accomplish the slider nonlinear contact analysis of the telescopic boom where the analysis process is presented in Fig. 41.2 [7].

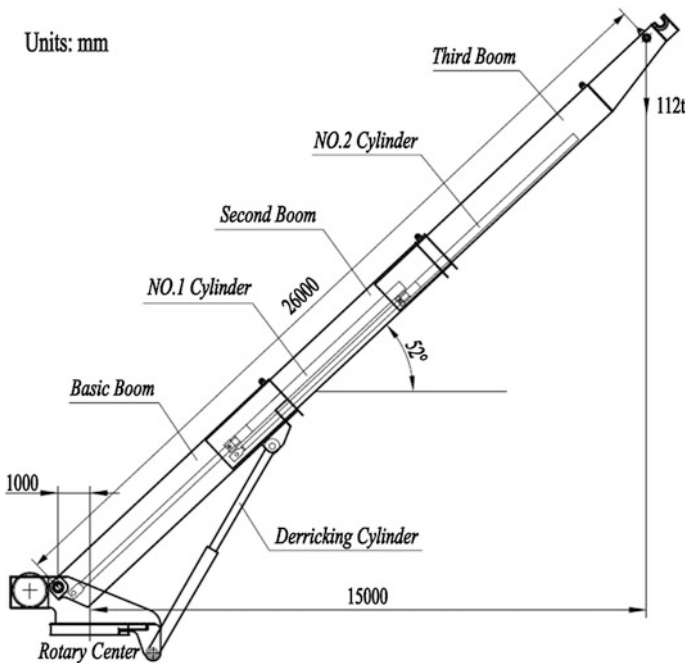
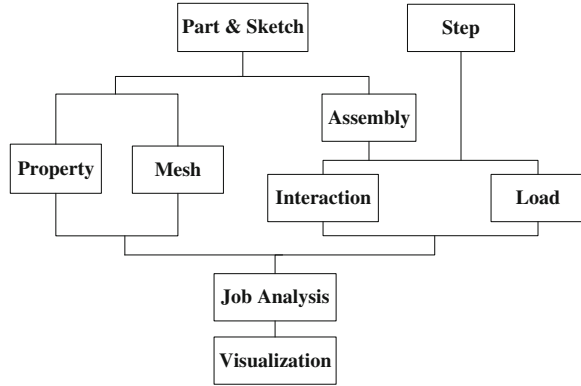


Fig. 41.1 Schematic diagram of telescopic boom in amplitude plane

Fig. 41.2 Nonlinear contact analysis process of telescopic boom



41.3.1 Geometric Model and Material Selection

The cross section of the telescopic boom is a new similar oval shape as shown in Fig. 41.3, and the top frange plate is an orthodrome trough slab, while the bottom frange plate is a semicircle trough slab that has the advantages of resistance to torsion as well as the special stability against elastic buckling. Effects of the force among the crane booms when the crane is working are transferred by means of the contact effect between the sliders and telescopic booms. Therefore, reasonable arrangement of the slider plays an important role in stress the telescopic booms bore [8]. On the lips of the basic boom and the second boom, there are 6 sliders which are eudipleural, and at the tail of the second boom and the third boom, there are four sliders which are also eudipleural. There are 20 sliders and 40 contact surfaces in the aggregate shown in Fig. 41.2.

Make use of the Sketch module and Part module in ABAQUS to build the three telescopic booms, two cylinders, and the twenty sliders as well as independent parts assembly with the help of the Assembly module. Cutaway view of the assembly is shown in Fig. 41.4.

Define materials property in the Property module. As the arm of the crane, the telescopic boom's bearing capacity is the key factor determines the overall hoisting capacity. The material of the telescopic boom mainly adopts the high-strength structural steel plate WELDOX 1100 made in Swiss which is a general structural steel with a minimum yield strength of 1,100 MPa except the sliders and cylinders. The metal welds and some subsidiary parts are ignored in the geometric model, so in order to guarantee the reliability of contact analysis, suitable enlargement of density is taken into consideration.

At present, the materials of crane sliders mainly adopt MC nylon or bronze. The maximum lifting torque of the railway crane achieves 1,700 t*m, and the crane demands its telescopic boom which can stretch out and draw back with relevant load; although nylon sliders have the advantages of better capacities with self-lubricating, impact resistance, fatigue resistance, and so on, its carrying capacity is

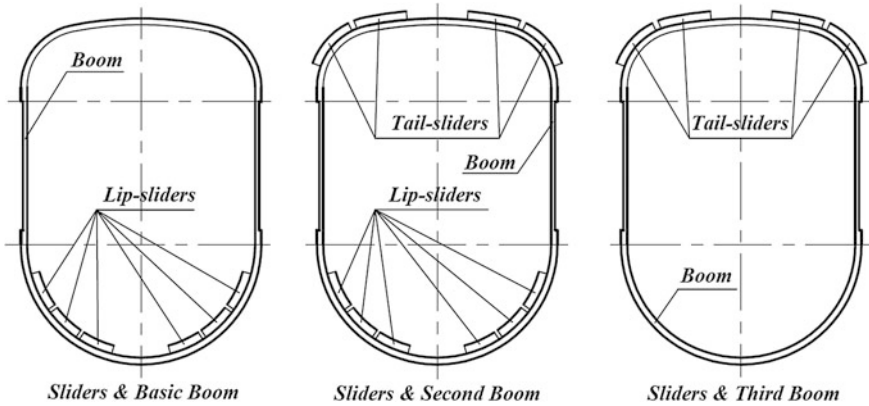


Fig. 41.3 Arrangement representation of sliders on telescopic boom

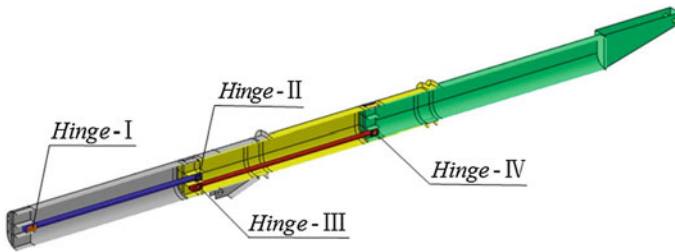


Fig. 41.4 Part cutaway view of telescopic boom assembly

worse, because they are likely to fail more easily in heavy case due to continuous friction heat which can probably cause immeasurable loss, while the bronze sliders have good elastoplasticity so that there does not exist crushing problems. All in all, bronze is still the first selection of the sliders' material.

41.3.2 Load Step and Contact Interaction

Telescopic boom withstands the loads on a variety of directions when the crane is working that complicates the load condition, in order to apply specific load and boundary conditions in different periods of time so as to improve the stability of the convergence, divided the loading history into several analysis steps in Step module.

Define the contact interaction and kinematic constraints between the various components in the Interaction module. The contact surfaces between the basic boom and the sliders on its lip, the second boom and the sliders on its lip and tail end, and the third boom and the sliders on its tail end are connected through tie

constraints to simulate actual contact behaviors. The contact surfaces between the sliders on the lip of basic boom and the second boom, the sliders on the tail end of the second boom and the basic boom, the sliders on the lip of second boom and the third boom, and the sliders on the tail end of the third boom and the second boom are defined by the surface-to-surface contact method with the augmented Lagrange method to strengthen the contact constraints while the friction between the telescopic boom and slider is defined by the penalty function method [9]. Assign the contact surfaces of the telescopic boom whose stiffness is larger than sliders as the master surfaces when setting the contact surface of the slider as the slave surfaces. As a result, it can ensure the nodes of the slave surfaces are always in coverage of the master surfaces during the contact analysis, namely that successfully avoid the difficult convergence that can appear when the nodes of the slave surface “drop” out of the coverage of the master surfaces [10].

The premise of how to simulate the function of the cylinder to sustain the motion of telescopic boom veritably is creating a correct hinged relationship between the cylinders and telescopic boom appropriately. Establish four rigid regions between the control points in the axes of hinge pins which belong to the No.1 Cylinder and No.2 Cylinder and the corresponding reference points through kinematic coupling method severally. Pinholes of the telescopic boom are dealt similarly as above. Then, build the four hinged relationships between the eight rigid regions from I to IV as shown in Fig. 41.4 with the help of the connector, constraint all translational degrees of freedom U1 & U2 & U3 and two rotational degrees of freedom UR2 & UR3, and release the degree of freedom UR1 the telescopic boom turn around the hinge pin which is used to connect the telescopic boom and derricking cylinder [8].

41.3.3 Mesh and Load and Boundary Conditions Applying

Mesh generation of contact area in the Mesh module is an important part of determining the accuracy of analysis. Partitioning contact surfaces of the telescopic boom and the cell of the sliders through geometric partition in order to refine the mesh of the master surfaces and slave surfaces as to make sure the nodes of the contact surfaces exactly one-to-one corresponding as shown in Fig. 41.5, other regions have noncontact and relatively lesser stresses are divided into rough mesh, and by doing so, it can acquire higher analysis precision and make contact analysis of the convergence more easier [8]. The sliders are given the 8-node solid element “C3D8R”, and telescopic booms which are the typical “thin-shell” are given the 4-node shell element “S4R”, and the rest parts are given default element of the ABAQUS system.

Define the boundary conditions and apply the load in the Load module. In the hinged place where the basic boom and revolving platform are connected, constraint all of the three translational degrees of freedom U1 & U2 & U3 and two rotational degrees of freedom UR2 & UR3, so as the same where derricking cylinder and the telescopic boom are connected. For the purpose of establishing the

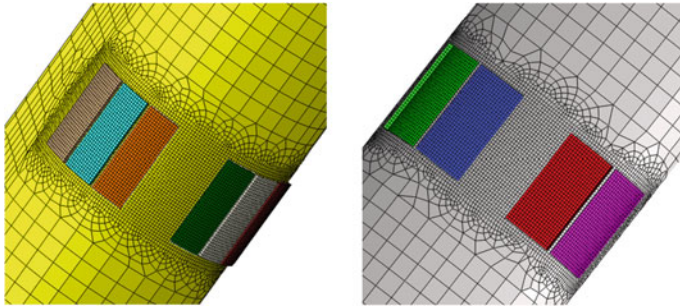


Fig. 41.5 Local mesh of sliders on lip of basic boom and tail end of second boom

Table 41.1 Load step applying history

Step	1	2	3	4	5	6	7
Load	G	(S + Q)/5	(S + Q)/5	(S + Q)/5	(S + Q)/5	(S + Q)/5	P

contact relationships steady, only apply the gravity G of the finite element analysis model in the first step and then gradually apply the lifting load and rope pull S in the amplitude plane homogeneously from step 2 to step 6, and lateral load P is applied in the final step, as shown in Table 41.1 [11].

41.3.4 Calculation of Nonlinear Contact

Execute an integral nonlinear contact calculation of the telescopic boom FEM model in the Job Analysis module. Accordingly, the general solution algorithm of a contact problem is depicted in Fig. 41.6 where P represents the contact pressure on slave surface nodes and h represents the distance measuring how much the slave surface nodes sinking into the master surface [12].

In the iterative procedure, firstly, the contact statuses of the candidate contact pairs are assumed, and the contact stiffness matrix is modified according to the assumed contact status. Secondly, the equilibrium equations are solved to determine the new contact forces and displacements. Thirdly, the assumed contact status is checked based on the computed contact forces and displacements. Once the assumption is found to be correct, the iterative procedure is terminated, otherwise proceed with a new iteration [13]. On the other hand, according to the iteration convergence, the system divides every analysis step into a series of small increment and adjusts the magnitude of the load increment during the iterative procedure which can help to solve the convergence difficulties of the highly nonlinear contact problems. Submit the task and get a convergence successfully appeared after 103 times' iteration.

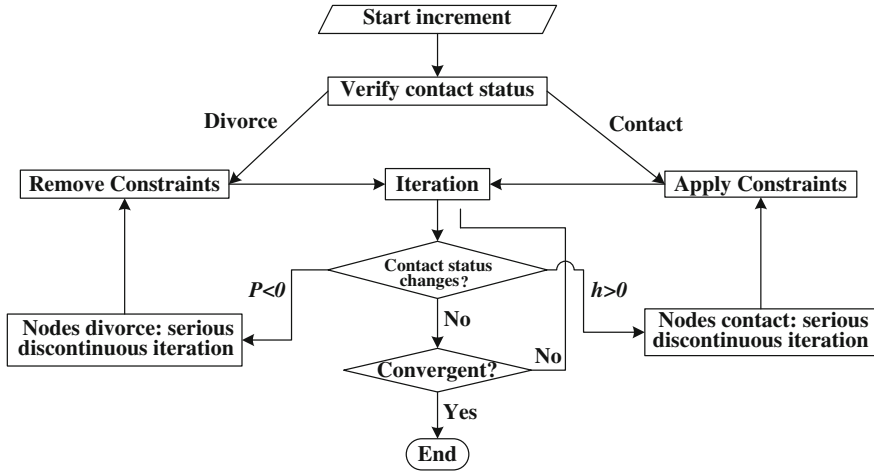


Fig. 41.6 Logical iterative procedure of the contact solution algorithm implemented in the ABAQUS/standard

41.4 Numerical Results and Discussion

Check the strength and stiffness according to the design rules for cranes national standards of People's Republic of China GB/T3811–2008. For high-strength structural steel, calculate the allowable stress according to Eq. (41.6) and calculate the allowable stiffness in the amplitude and rotation plane according to Eqs. (41.7) and (41.8).

$$[\sigma] = (0.35\sigma_b + 0.5\sigma_s)/n = 597 \text{ Mpa} \quad (41.6)$$

$$[f_L] = 0.1(L_c/100)^2 = 6,760 \text{ mm} \quad (41.7)$$

$$[Z_L] = 0.07(L_c/100)^2 = 4,730 \text{ mm} \quad (41.8)$$

where $[\sigma]$ is the allowable stress 597 MPa; σ_b is the yield strength, 830 MPa; σ_s is the tensile strength, 1,100 MPa; n is the safety factor, 1.34; $[f_L]$ is the allowable static stiffness in the amplitude plane, 6,760 mm; $[Z_L]$ is the allowable static stiffness t in the rotation plane, 4,730 mm; and L_c is the length of the static displacement of the telescopic boom, 26 m.

Extract the Von Mises stress cloud figure in the Visualization module, as shown in Fig. 41.7. The largest stress appeared on the second boom which is in accordance with reality [14] and located on the junction boundary where the second boom and sliders on the lip of the basic boom contact with each other. The maximum displacement in the amplitude plane is 680.65 mm, and the maximum displacement in

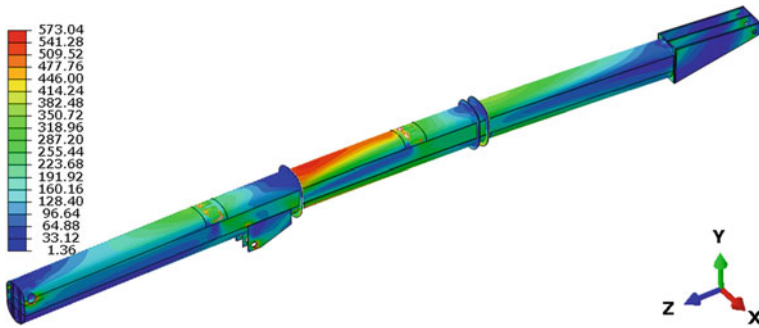


Fig. 41.7 Von Mises stress nephogram of the telescopic boom model

the rotation plane is 352.46 mm. Obviously, both the strength and stiffness of the analysis model can meet the requirements of GB/T3811–2008 [8].

In the situation of the local coordinate system is coincident with the global coordinate system, with the increase of the analysis step, extract the relative rotation “CUR1” of the connector element revolving the X axis and the counterforce “CRF3” along the Z axial direction of the four hinge joints I to IV (as shown in Fig. 41.4) of the No.1 Cylinder and No.2 Cylinder. The changing curves are shown in Figs. 41.8 and 41.9.

According to Fig. 41.8, the rotation value increases with load addition in the previous six steps. In last step 7, only lateral force is loaded; as a result, the rotation value revolving X axis just has a small change. For the NO.1 Cylinder, the directions of rotation of the hinge joint I and II are opposite, and rotation value of the joint II is larger. Both I and II share the same changing trend. For the NO.2 Cylinder, its tendency is as same as the NO.1 Cylinder. Besides, the reactive rotation revolving Y axis CUR2 and Z axis CUR3 are both zero. Therefore, the simulation of the function of the cylinder is successful.

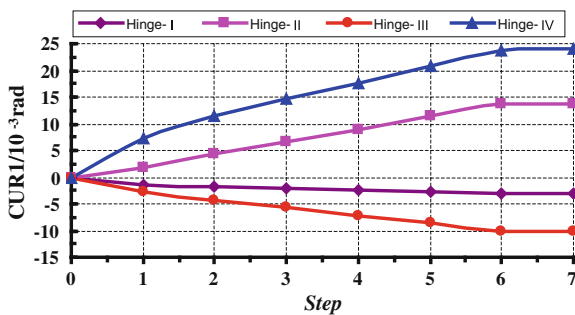


Fig. 41.8 Connector element reactive rotation revolving X axis CUR1 of the cylinder under the local coordinate system

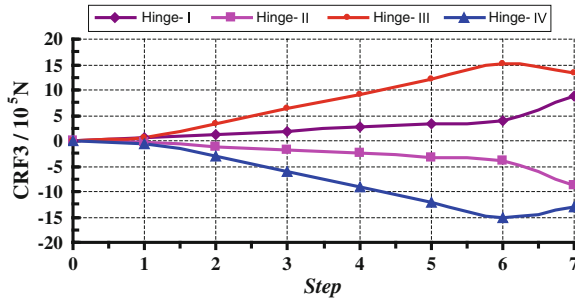


Fig. 41.9 Connector element reaction force CRF1 of the cylinder in axial direction Z under the local coordinate system

As can be seen from the Fig. 41.9, the cylinder burdens a symmetrical loading on the front and back joint. In the previous six steps, the axial force grows large with the load increasing; the NO.1 Cylinder is pressed in axis direction Z as well as the NO.2 Cylinder. In the 7th step, the force of the NO.1 Cylinder keeps growing, while the force of the NO.2 Cylinder appears undergoing decrease. It is because of the lateral force function which leads to a quite large torsion turn around local Z axis, and the influence of force superposition decreases the reaction force at joint III at the end of the NO.2 Cylinder; both joint II and joint III are located at the end of the second boom to resist torsion deformation that makes the axial reaction force in joint II keep increasing. The maximum axial force reaches $1.5 \times 10^6 \text{ N}$. The telescopic cylinder endured most of the total axial force of the mechanical model [15].

Extract the local stress nephogram of the sliders on the basic boom lip from analysis step 2–7, as shown in Fig. 41.10. The mesh of the local_① (shown in Fig. 41.10) in step 2 and local_② (shown in Fig. 41.10) in step 6 are magnified as shown in Figs. 41.11 and 41.12.

It can be obviously seen how the contact stress changes with the load increasing as shown in Fig. 41.10. Forces are only applied in the amplitude plane from step 1 to 6, so the contact stress distributions are symmetrical after convergence. In the last step, lateral force is applied, so the contact stress distributions asymmetrical on the left and right contact pairs. In the process of load applying, the front ends of the sliders touch the second boom earliest and have the larger contact stress. There is seriously stress concentration in the sharp corner of the sliders which can be avoided through replacing the sharp edges by smooth fillet in the actual manufacturing process. According to the stress nephogram of the last step 7, it can be concluded that parts of sliders near the lips of the basic boom bear heavier stress. As a result, selecting proper length of the sliders can give full play to the mechanical behavior of sliders [2].

Take the front edge of the slider shown in the Figs. 41.11 and 41.12 as the reference line. In the process of slider nonlinear contact analysis, there is an obvious sliding between the second boom and the sliders. From step 2 to step 6, the displacement of the relative slippage between the second boom and the sliders

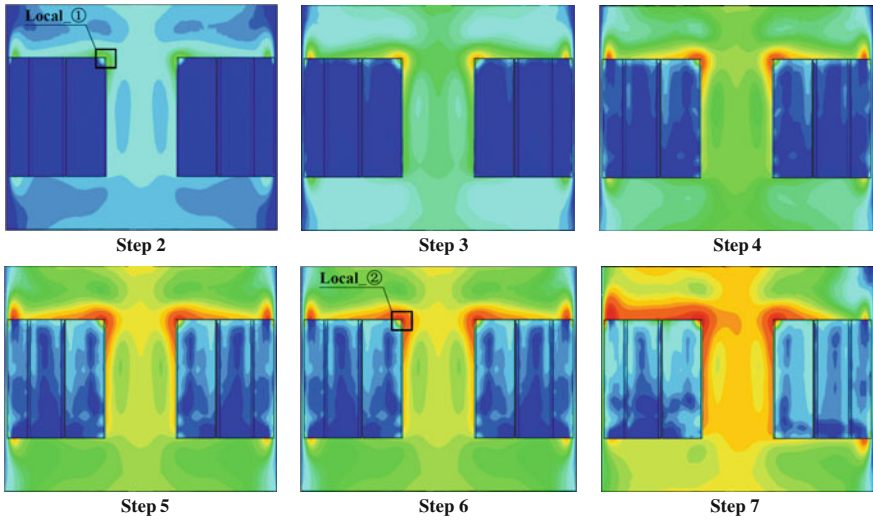
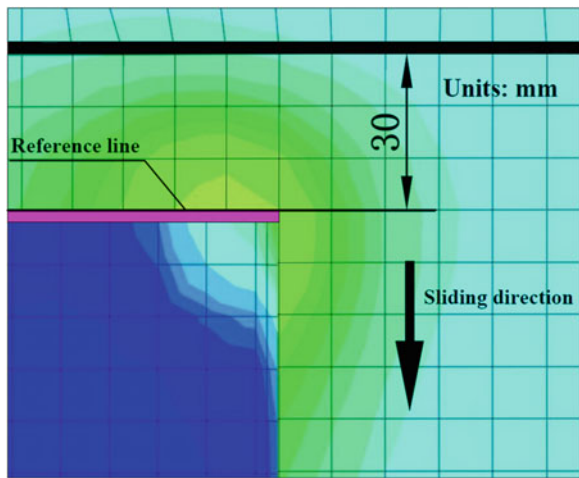


Fig. 41.10 Local stress nephogram of the sliders on basic boom

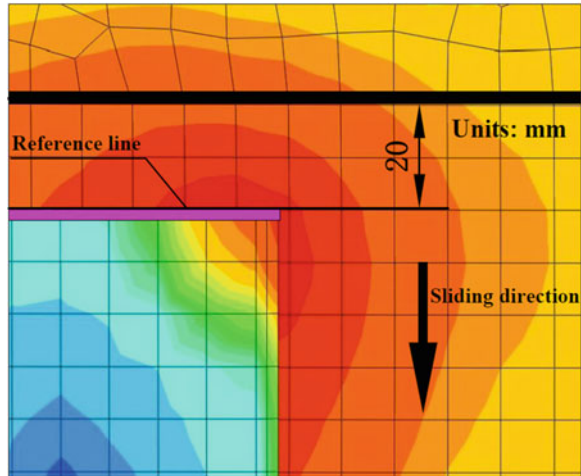
Fig. 41.11 Magnified mesh of the local_(1) in step 2



achieves about 10 mm in the axial direction which has exceeded the typical element size 8 mm. Therefore, adopting the finite sliding formula to slider nonlinear contact analysis is more reasonable. It states clearly that there exists the friction sliding between the sliders and telescopic booms meanwhile. Releasing the node degrees of the freedom on the contact pairs is more consistent with the actual working condition.

The average stress of all the 20 sliders is $200 \text{ MPa} < [\sigma] = 254 \text{ MPa}$, and the strength requirement is satisfied where the $[\sigma]$ is the allowable stress of the sliders. Because of the existence of the lateral force, the most right sliders on the lips of

Fig. 41.12 Magnified mesh of the local_(2) in step 6



basic boom and the second boom have the largest stresses in the negative direction along Z axis as well as the most left sliders on the end of the second boom and the third boom, and the stresses on the homologous contact pairs of the telescopic boom are also large that fits the actual situations.

41.5 Concluding Remarks

The research about slider nonlinear contact analysis of the telescopic boom with cylinder supporting has studied with the help of the powerful nonlinear finite element analysis software. The study reveals the following:

1. The system needs to form a new contact stiffness matrix and solve the equilibrium equations when it experiences a new iteration in the process of nonlinear contact analysis. Therefore, a large amount of iterations are needed in dealing with the nonlinear contact problem of the telescopic boom slider, and the cost is much higher than that of linear analysis.
2. The similar oval section possesses strong structural stability and fortissimo capacity to against elastic buckling. It will be developed as a popular and new type telescopic boom in the future.
3. The telescopic boom sustains various loads in multi-direction during the working time. It is advantageous to improve the stability of the calculation convergence by multi-step analysis. Refine the mesh in the contact zone and roughening the mesh in the zone which has non-contact and low stress can also reduce the difficulties of convergence and improve the analysis accuracy and efficiency. This method has provided the reference in dealing with the contact analysis of the complex model.

4. The cylinder sustains the most axial load and possesses an important role in the resistance to mechanical deformation and the special function of boundary constraint of the telescopic boom. The result indicates that the found of the model about slider nonlinear contact analysis of the telescopic boom with cylinder supporting is successful and most important of all it had laid a foundation for deeper researches for the large tonnage crane boom.

References

1. Batailly A, Magnain B, Chevaugon N (2012) A comparative study between two smoothing strategies for the simulation of contact with large sliding. *Comput Mech (Online First™)*
2. Li ZM, Zhang ZP, Zeng XY (2010) Local stress calculation and support position optimization of the slider on telescopic boom. *Hoisting Conveying Mach* 2:7–9
3. Goryacheva IG (1998) *Contact mechanics in tribology*. Kluwer Academic Publishers, Dordrecht
4. Johnson KL (1985) *Contact mechanics*, 1st edn. Cambridge University Press, New York
5. Wei SF, Wang SM, Zheng YQ (2011) Finite element analysis and experimental confirmation of telescopic boom on a truck crane. *J Mach Des* 28(6):92–96
6. Zmitrowicz A (2010) Contact stresses: a short survey of models and methods of computations. *Arch Appl Mech* 80(12):1407–1428
7. Liu Z, Zu JP, Qian YL (2008) *ABAQUS 6.6 basic course and detailed examples*. WaterPower Press, Beijing, China
8. Shen SL, Zhang ZP, Chen R (2012) Lightweight design and research for a new type crane arm. *Mach Des Manuf* 6:42–44
9. Popov VL (2010) *Contact mechanics and friction physical principles and applications*. Springer, Berlin, Germany
10. Jelenić G, Muñoz JJ (2007) Modelling multi-body systems using the master-slave approach. *Comput Methods Appl Sci* 4:1–22
11. Wang JN, Yu LF (2002) *Metal structure of cranes and transporters*. Railway Press, Beijing, China
12. Zhuang Z, Zhang F, Ceng S (2005) *ABAQUS nonlinear finite elements analysis and examples*, 1st edn. Science Press, Beijing, China
13. Hu ZQ, Soh A-K, Chen WJ (2006) Non-smooth nonlinear equations methods for solving 3D elastoplastic frictional contact problems. *Comput Mech* 39(6):849–858
14. Shen YF, Meng QH, Jing SH (2001) The calculating method of telescopic crane booms with hexagon section. *J Shandong Inst Technol* 15(3):23–27
15. Liu SM, Lu NL, Wang B (2010) Comparison of three calculation models on overall stability analysis of telescopic boom with built-in cylinder. In: *International conference on digital manufacturing and automation*, vol 1. pp 400–404

Chapter 42

Research on Automatic Layout Planning and Performance Analysis System of Production Line Based on Simulation

Lv Chao, Liu Shuang, Shiming Wang and bei Cai

Abstract The automatic layout planning and performance analysis of production system is important and key technology to manufacturing enterprise to response market demand. The factors of system configuration, production mode, WIP, and buffer configuration are considered in this paper to solve the lack of the automatic layout planning and performance analysis system with operation factors of production line. Based on the performance analysis of existing configuration, the layout configuration is stated in detail, the suffer allocation principle is studied by simulation, the dynamic mathematical model of system configuration and WIP is presented. The design integration frame of multi-product and variable batch product line automatic layout and performance is presented based on these proposed models and key technologies. The software system is developed and the effectiveness is verified; this platform has high practical reference and application value to the automatic layout planning and performance analysis of enterprise production line.

Keywords Production line · Automatic layout planning · Dynamic performance analysis · Simulation

42.1 Introduction

Along with the competition in the market, manufacturers need a modern production system to respond to market demand for customized, the required of production lines and systems for modern manufacturing are becoming increasingly reflect the adjust of intelligent dynamic, the superior of system configuration, adapt to the varieties to variable volume and the agile response characteristics, so the research on production line layout planning cannot be divorced from the goal of the factors

L. Chao (✉) · L. Shuang · S. Wang · b. Cai
College of Engineering Science and Technology, Shanghai Ocean University,
Shanghai, China
e-mail: dblvchao@163.com

of production, it should be research on multi-factor index, such as integrated production mode, the system configuration, buffer configuration, dynamically adjustable and the amount of product and so on. Analysis of existing domestic and foreign literatures, Solimanpur and other scholars study the impact of different layout on manufacturing system [1, 2]. Renzhong Jiang proposed hybrid array structure and Holon structure, the establishment of a mathematical programming model based on matroids [3, 4]. Zhong and other scholars studied the impact principle of a different layout structure and performance of manufacturing system and provided the thinking framework for performance analysis method.

Design of normal layout of manufacturing systems often used the corresponding algorithm to solve the optimal or suboptimal solutions of the model under constraints of the portfolio objectives; goals used in the layout design include the cost targets, the utilization target, logistics objectives, the convenience target, and so on; in this area, domestic and foreign scholars conducted in-depth study, the optimization method summed up in operations research methods, nonlinear programming methods, genetic algorithms, simulated annealing algorithm, and particle swarm and have achieved good results within a certain range [5, 6]. Wang, Hui, Suo using the method based on the classification of the device and manufacturing systems function to research the layout of the production line [7–9]. Above for the research of layout design of the production line is based on the conditions of the specific constraints and objectives, use corresponding algorithm analysis and solving a layout problem, and made some achievements. But, the literature is mostly focused on sorting, and comparison of the algorithm leads to the results of the practical application that has a big gap to practical application. Lack of configuration based on the production line with production mode, buffer configuration, WIP, and many other factors of production, this paper study the problem of dynamic layout of the production line.

42.2 Configuration and Performance of Production Line System

Research on layout planning of production line should be based on production line configuration; production line configuration has a direct impact on system performance indicators, different configurations lead to different production line performance, general production line system configurations, including three forms which are series, parallel and hybrid, series, and parallel are basic configuration, the hybrid structure is then evolution of the basic configuration. Commonly used production line system configurations that include the following as shown in Fig. 42.1a, b are the basic configuration in figure, c, d, and e are evolved from the basic configuration, c1 and d1 are conversion from c and d. The most widely used system configurations in manufacturing now is mixed structure which comes from basic string and parallel structure.

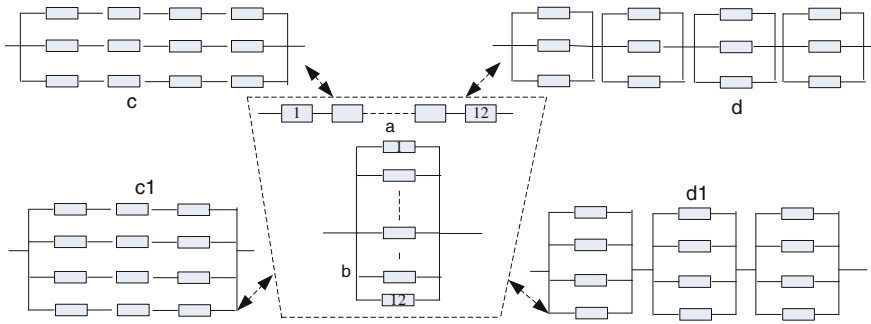


Fig. 42.1 Normal system configuration of production line

The production line performance is depended on its reliability, productivity, quality, cost, and scalability. Following the production line configuration topology, the reliability of the formula is given below:

$$R_a = \prod_{i=1}^n R_i \text{ (a Conformation);}$$

$$R_b = 1 - \prod_{i=1}^n (1 - R_i) \text{ (b Conformation);}$$

$$R_c = 1 - [1 - \prod_{i=1}^n R_i]^m \text{ (c Conformation);}$$

$$R_d = \prod_{i=1}^n [1 - (1 - R_i)^m] \text{ (d Conformation);}$$

where R_i is the reliability of the equipment or components of the system, n representative of series, m representative of the number of devices in each level. The reliability of different configuration can be calculated according to these formulas.

Based on the reliability of system equipment and set up equipment normal and failure state, to study the relationship between the different configurations and productivity, the system productivity can take advantage of the statistical formulas:

$$P_s = \sum_{i=1 \dots n} Ca_i R_i \cdot R_h \cdots R_n;$$

where $R_i \cdot R_h \cdots R_n$ is value of possible states of system running, Ca_i means production capacity of the system is in this state, and productivity is the product of all possible states. It can be seen in this formula, not only the higher of reliability the higher productivity, but also the increase productivity of hybrid form of the structure which accompany with parallel extension also increased, d configuration is better than c.

It is a better way to the use of variable flow theory to analytical processing based on the configuration structure in quality and performance analysis of the production line system. The quality error accumulation of hybrid configuration relative to other structure is larger; this is the reason why hybrid configuration of system should add the corresponding fault diagnosis equipment [10]. For the cost, scalability, and interrelated of the production line system configurations, based on incremental principles method can know that d configuration of the hybrid structure is better than c conformation.

For the above analysis, to meet the market demand which varieties variable volume, fast customized d configuration of the hybrid structure of the system configuration of the production line is the system structure and is chosen in this article.

42.3 Buffer Configuration Principle of Production Line

Buffer configuration of the production system is an effective measure to improve the production system balance and to improve production and profits, the buffer configuration principle of the existing studies have focused on optimizing the algorithm, but ignored the product of the actual processing time. Based on different processing time, the simulation method is used with the same number of machines. The result of simulation is shown in Fig. 42.2. The principle can be presented by simulation:

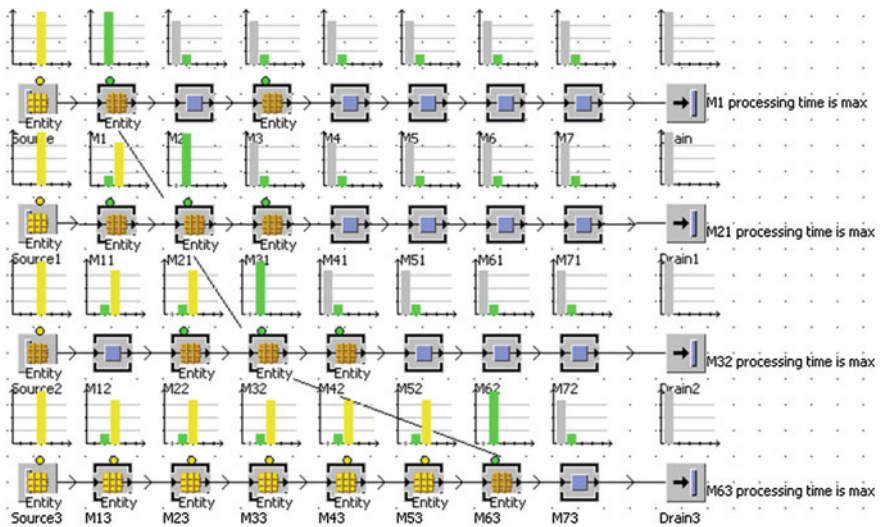


Fig. 42.2 The simulation result of buffer principle

- (1) According to processing time to find the bottleneck process, add a new configuration or equipment to deal with bottleneck processes;
- (2) System does not need to add buffer if the maxi processing time (MPT) is in first place of this system, or buffer should be added;
- (3) Thereafter without considering buffer, if need to add, judge before MPT;
- (4) Each of the local rows is checked to find the MPT value, if WIP is greater than 10, consider adding or delineated buffer reserve area.
- (5) If WIP is less than zero and the absolute value is greater than 10, consider adding or delineated buffer reserve area.

42.4 The System Dynamic Machine Layout Spacing Model

As per the actual production process, except the system configuration, modes of production, and buffer configuration, the system WIP is also an important factor to affect the performance of production lines. The buffer configuration is related to the WIP. And the WIP impacts on the dynamic distance between the individual equipments of the system layout. For the production line system of many varieties and various batch mode, the production line layout has dynamic scalability. The dynamics of the system layout can improve system responsiveness and is an effective measure to meet the multi-species, variable volume. and customized market demand. In the actual process, because of the size and weight of the equipment, the device spacing is difficult to achieve through constantly adjusting the physical device. Based on the principles of production management and organization, rely on the adjustment of the production planning and scheduling and the logistics transmission and transmission time between the equipment, through the implementation of the system, it can be achieved.

Based on the researched system configurations, in order to reflect the dynamic nature of the system layout, in a given space constraints, assuming that each equipment line is in a parallel state and the devices are shaped in accordance with a rectangular, each working ground is indicated as a rectangular and has the necessary ideal function. The dynamic machine spacing model of the system layout can be established:

$$W_T = \text{Pro} \times \partial \left(\frac{t_j - t_i}{t_i t_j} \right);$$

$$M_{d1} = W_T \times G_p; 0 < W_T < a;$$

$$M_{d2} = (W_T - m) \times G_p; a \leq W_T \leq b;$$

$$M_{d3} = K \times G_p; b < W_T \text{ 或 } W_T < 0;$$

where

W_T is the number of WIP between the adjacent processes and operation places, G_p refers to the standard length of the part geometry value for the products of the

same family, Pr_o refers to production capacity of bulk value, $\hat{\sigma}$ refers to the influence coefficient of the work area (empirical reference value), and the t_i is the processing time of the No i places. a, b is the number of WIP based on different processing time and different work piece. m, K is the characteristic parameter of work piece. Based on the optimized configuration of the system and the above model, combined with the existing production system layout principles, system which includes variable mass production mode, the buffer configuration, and dynamic layout planning for the production line in WIP can be established.

42.5 The System Integration Design

Based on the above analysis of principle, establish computer-aided automatic production line layout planning and performance analysis system, the spatial extent of the system layout can realize parametric design and enter the adjustments. Each module of the system based on a unified database platform (SQL Server 2000), the data sheet as the media to achieve seamless integration between the various modules. In each module, resource management module is responsible for the management of basic information of the production tasks, process, and manufacturing resource. In support of basic information, mode of production, distribution planning, and performance analysis and simulation optimization module, coordinate with each other and generate different results the program reports. These programs are stored in a unified database.

The main features of computer-aided automatic production line layout planning and performance analysis system is agility, timely and accurate access to required information is the premise to ensure the dynamic layout of the production line quickly analyze and design. At present, most companies are using product data management (PDM) and enterprise resource planning systems, such as ERP for manufacturing integrated platform, through the establishment of interfaces with other systems, information can be shared enterprise-wide. In the specific implementation process, the public database integrates with other systems, namely establish an independent shared data tables and data area. The shared data area stores the share data between different systems in a consistent data model.

42.6 Examples

In this paper, based on the integrated design thinking above, a computer-aided automatic production line layout planning and analysis system is developed. Using the secondary language SimTALK provided by the simulation software Plant Simulation, the SQL Server 2000 and VC ++ 6.0 software environment combined with the modular modeling idea, and the development is completed. There is an example of 14 machines, the integration system is shown. System interface shown

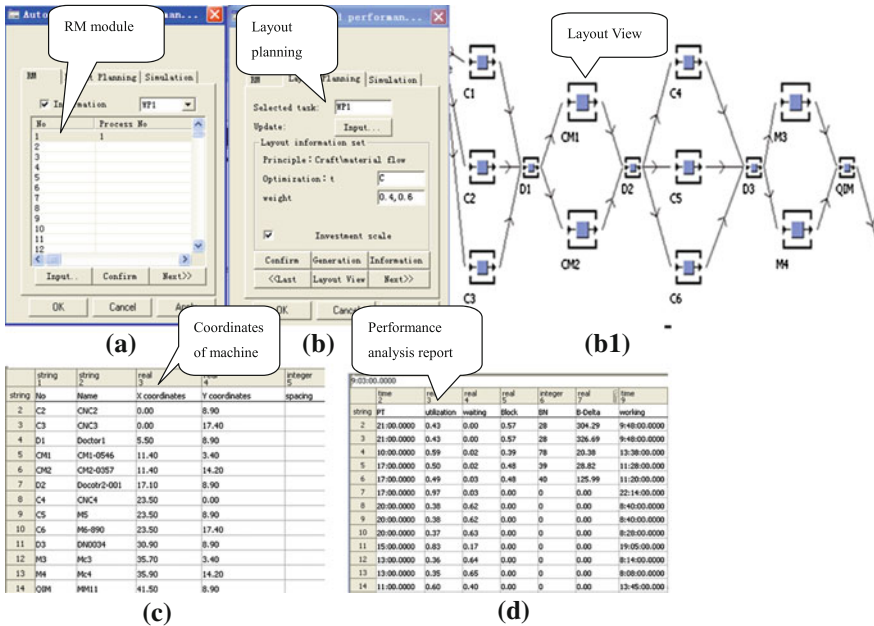


Fig. 42.3 The layout planning and performance integration simulation system

in Fig. 42.3. Resource management module (Fig. 42.3a) connects with the database to provide the basic information needed. Layout model bases on multiple factors of production generated by the layout planning module (Fig. 42.3b) layout program and can control the scheduling policy of interrelated input and output. The layout configuration coordinates information (Fig. 42.3c) according to the generated layout program that analyzes system layout, performance, planning and scheduling, equipment failure, scheduling plans, and other information associated. Reporting module (Fig. 42.3d), according to the planning results, production information, simulation and optimization results, formulates appropriate performance analysis reports, which can be referred and shared in LAN.

42.7 Conclusion

The work of this paper is supported by Shanghai Ocean University initial funding (No. 860610000113) and Shanghai Ocean University curriculum reform funding (No.2400110205). In this paper, a computer-aided automatic production line layout planning and performance analysis system is presented, and including of basic information, layout planning, and performance analysis and simulation optimization. And use the appropriate software environment to make the system development. The current layout configuration of production line system is studied. Based

on multi-processing time and simulation methods, the principles of the buffer configuration, the ways and means to achieve dynamic layout of the production line, production mode, the buffer configuration, and amount of the WIP are given. The system integration is stated. The system completes the layout planning and performance analysis and provides help and reference for the corporate workshop management solutions, planning strategy, and scheduling formulation. The system uses simulation modeling techniques to develop the program more scientific and reasonable and builds the connecting bridge of the planning department and the production workshop. Currently, the system has been applied to layout planning of a car seat production line. It can provide solutions and support tools for the layout planning of multi-species variable mass and mixed production in enterprises.

References

1. Solimanpur M, Vrat P, Shankar R (2005) An ant algorithm for the single row layout problem in flexible manufacturing systems. *Comput Oper Res* 32(3):583–598
2. Noaker PM (1994) The search for agile manufacturing. *Manuf Eng* 13:34–40
3. Koren Y (2005) What is a reconfigurable manufacturing system? CIRP-Sponsored 3rd international conference on reconfigurable manufacturing systems, keynote paper report
4. Corry P, Kozan E (2004) Antcolony optimisation for machine layout problems. *C Optim Appl* 28(3):287–310
5. Baykasogly A, Derlei T, Sabuncu I (2006) An ant colony algorithm for solving budget constrained and unconstrained dynamic facility layout problems. *Int J Manag Sci* 34(4):385–396
6. Sha DY, Chen CW (2001) A new approach to the multiple objective facility layout problem. *Integr Manuf Syst* 12(1):59–66
7. Wang L, Xiao T, Fan L (2004) Research on clustering planning of machine cell for product family. *Comput Integr Manuf Syst* 10(10):1257–1262
8. Hui L, Qiuyin Z, Xiumin F (2002) Productline plant layout based on facilities classification. *Mach Tool Hydraulics* 3:197–201
9. X Suo, Z Yang, Y Yang (2008) Feasibility of layout in axiomatic design based on manufacturing system functionality. *Tool Eng* 42:27–31
10. Agrawal R, Lawless JF, Mackay RJ (1999) Analysis of variation transmission in manufacturing processes-part II. *J Qual Technol* 31(2):143–154

Chapter 43

Optimization Study Based on Lean Logistics in Manufacturing Enterprises

Xiaoyan Wang

Abstract When manufacturing is the main economic activities in an industry, changes in production patterns pose a challenge to the logistics system, forcing manufacturers to optimize the logistics system. Based on the manufacturing status and problems of logistics management analysis, this article constructs a three-level logistic model using a lean manufacturing logistics optimization system, then from logistics system planning and design, logistics process, logistics organization, logistics operation, logistics standardization and logistics management technology, logistics professionals, logistics cost management, and logistics performance evaluation system proposes specific strategies for optimizing manufacturing logistics system.

Keywords Lean logistics · Manufacturing enterprise · Enterprise logistics · Three-level optimization model

43.1 Introduction

Since the founding of New China, China's manufacturing industry has made great achievements, laying a solid foundation for nationwide industrialization and modernization. Today, China's manufacturing industry has developed a large-scale and highly technical industrial system with a wide range of production categories. With the rapid development of China's manufacturing industry, the manufacturing sector continues its rapid logistical growth and becomes the largest portion of total social logistics. In 2010, industrial logistics amounted to 113.1 trillion Chinese yuan (an annual increase of 14.6 %), accounting for 90.2 % of the total social logistics that year. Manufacturing is the main industry in China's economy, and manufacturing logistics is the foundation and a strong driving force of industry [1].

X. Wang (✉)
Hefei University, Hefei 230601, People's Republic of China
e-mail: wxy274@126.com

In response to globalization and China's own rapid development, China's manufacturing enterprises have been restructuring to a make-to-order (MTO) production system to increase their competitiveness and to better meet customer demand [2]. These changes in production patterns pose a challenge to the logistics system, forcing optimization.

Lean logistics originated in lean manufacturing, which applies lean thinking to manage logistics activities. Lean thinking is the core of "the elimination of all waste, at the right time, right place, providing the right amount of product." Lean logistics, a recent management approach, emphasizes customers first; timely, accurate, overall optimization; continuous improvement; and innovative ideas—it is consistent with the developing trend of manufacturing logistics [3]. In this paper, the author studies existing problems in current manufacturing logistics operations, applies lean logistics management thinking to optimize the logistics system, and proposes a three-level optimization model and strategic plans.

43.2 Analysis of Current Logistics Management in China

In recent years, the market-oriented economy has been increasingly important to China's overall economy. The email industrial structure has been upgrading gradually, with manufacturing logistics standards also improving. But because of old thinking that "the flow of commerce is more important than the logistics," there is an inadequate understanding of logistics in manufacturing industries. The analysis of logistics operations is as follows:

The proportion of logistics subcontracting in manufacturing logistics increased annually. It reached 57.64 % in 2008, an increase of 7.24 % from 2007. Manufacturing companies have come to understand that logistics subcontracting can reduce costs, allowing enterprises to focus on core businesses. The enterprises also pay more attention to speed rather than lower logistics costs [4]. More and more manufacturing companies are taking a timely, flexible strategy as the speed of logistics services has become increasingly critical.

The proportion of logistics system design and logistics information management has increased, indicating that the manufacturers require more professional, integrated, informative, and systematic logistic services.

The average utilization rate of manufacturing continues to increase. The segments of 30 % or less, 30–50 %, and 50–70 % have significantly decreased. The remaining segments all show increased utilization, which indicates that inventory management level has been improving [5].

Sophisticated and professional logistics management trends began to appear. Research shows that manufacturing logistics management is becoming more precise. The professional management trend is clearly accelerating, and the development of the logistics industry is becoming more and more obvious.

Applying enterprises' logistics facility to general social services is not widely observed, primarily because of resistance from inside enterprises.

Modern logistics technologies and products have begun to be applied in logistics operations.

Although some manufacturers are at the forefront in design, renovation, and application of modern logistics management, most Chinese manufacturers cannot establish an efficient and competitive logistics supply chain because of many problems in their operation and management of logistics, including

- Lack of awareness of modern logistics;
- Inefficient logistics operations;
- Lagging in logistics standardization;
- Low use of internal logistics facilities;
- Lack of professional logistics personnel.

In general, logistics management is still fragmented and at the very preliminary phase of development. All of the problems can damage a company's core competitiveness. They constrain the enterprise's just-in-time production and rapid response to customer needs, and they create high management costs and logistical costs. Therefore, initiating change in the integration and optimization in an enterprise's logistics system is essential for success.

43.3 Building Manufacturing Enterprise Logistics System Optimization Model

In lean logistics systems, customer demand is the starting point of the value stream, which drives production. To apply lean logistics, enterprises should first take full advantage of modern information technology to integrate logistics information into all aspects of their manufacturing systems. They should also work closely with upstream and downstream enterprises to enable quick responses to market changes. Under the guidance of an overall logistics development strategy paired with customer demand, enterprises should apply lean thinking throughout the entire process of production, management, procurement, and marketing. In addition, they should fully employ waste logistics and recycling logistics management. Figure 43.1 shows the three-level optimization model based on lean logistics for manufacture enterprises.

As shown in the optimization model, optimization of manufacturing logistics system consists of three levels (operations, control, and support) and nine sublevels. The operations' level includes four optimization sublevels: logistics system planning and design, logistics process, logistics organization, and operation. At the control level, the two optimization sublevels are logistics cost management and the logistics performance evaluation system. At the support level, the three optimization sublevels are logistics professionals, logistics standardization, and logistics management technology.

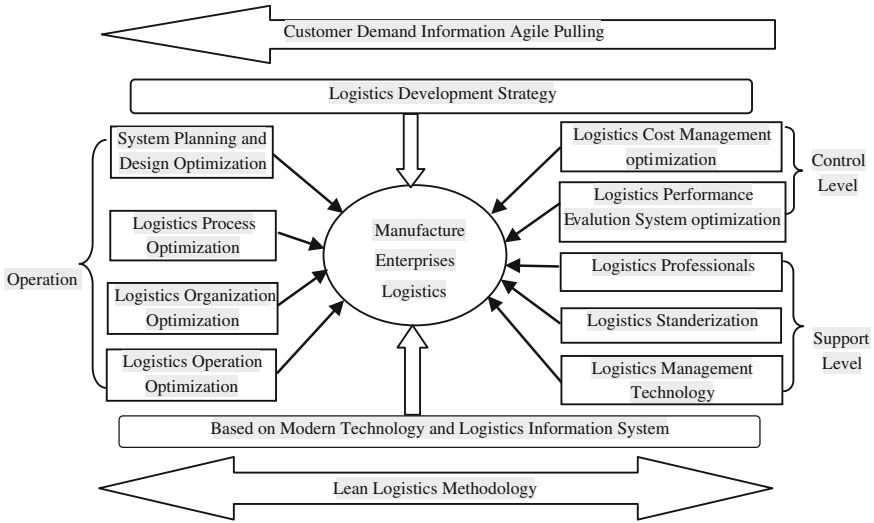


Fig. 43.1 Manufacturing logistics optimization model based on lean logistics

43.4 Manufacturing Enterprise Logistics System Optimization Strategies

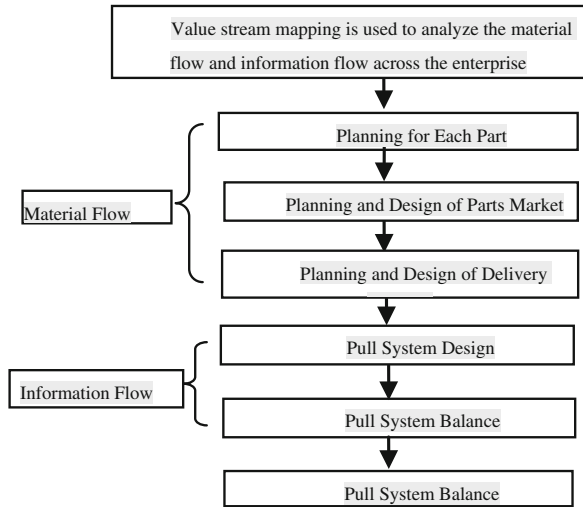
43.4.1 Logistics System Planning and Design Optimization Strategies

Although many manufacturing logistics problems seem external, they develop from inherent problems embedded at the very beginning of the system, so it is essential for enterprises to begin improving their logistics systems with optimizing planning and designing. Manufacturing logistics for equipment and facilities layout requires a large, long-term, and focused investment of money and energy, as well as a long-term, strategic perspective. The first step is data collection and analysis, which is the basis for planning the logistics system. Valid and accurate data are critical for rational planning; without solid data, an enterprise cannot develop a highly efficient, lean logistics system. The second step is concept planning, including scenario analysis, matching investment analysis, and operating cost analysis. To make the best decision most suitable to the enterprise, the last step is technical designing, which converts concept planning into specific operating plans and details.

Lean logistics system planning and design can be divided into two submodules: material flow and information flow, as shown in Fig. 43.2.

Value stream mapping (VSM) is a powerful tool that can model the entire value stream flow by generating a visual status map and highlighting the value flow problems, which allows more effective elimination of waste. Planning at every step includes developing a parts database. The parts market is the final storage of

Fig. 43.2 Lean logistics system planning and design framework of manufacturing enterprise



preproduction parts, equivalent to parts distribution centers. The pull system precisely controls quantity, time, and location during parts delivery; it can be balanced to meet customer needs effectively and to optimize the entire value stream from all aspects: inventory, investment, human resources, and product delivery. One of the essences of lean thinking is to never stop the “improvement.” As a dynamic management theory, lean logistics requires continuous improvement of logistics activities supported by an atmosphere of innovation. Using this approach, the enterprises can leap forward in its development.

43.4.2 Logistics Process Optimization Strategies

Process optimization reconstructs the business processes based on lean thinking. The enterprise must focus on customer demand, analyzing the customer value stream to eliminate all non-value-added logistics activities, thereby establishing systematic work standards and process specifications. Based on the principal of “simply and streamline,” the logistics management process workflow diagrams can be used to build a parallel, flat organization process, simultaneously breaking regional barriers and emphasizing team spirit. Value stream mapping can also be useful in logistics operation process analysis. Through business process reengineering, the material flow can be separated from the business flow. Enterprises can cancel, simplify, and rearrange to minimize unnecessary, non-value-added business areas, enhancing the value-added services. High-tech communication helps eliminate barriers between departments/organizations, connecting them to improve logistics system in terms of speed, quality, cost, and customer service.

43.4.3 Logistics Organization Structure Optimization Strategies

Manufacturing enterprises in China are falling behind in logistics organizational innovation. Most manufacturers still use the “functional,” “decentralized” logistics organization, which is inefficient, costly, and has poor sensitivity. This obsolete organizational approach severely weakens the competitiveness of enterprises, which must establish a customer-centric, process-oriented, flat logistics organization [6]. Within the enterprise, reintegration means merging numerous logistics-related departments such as order processing, customer service, inventory, procurement, delivery, storage, and distribution. This integrated logistics system unifies the entire management system process, promoting coordination among logistics department, production department, and sales department, which in turn improves overall service levels by enhancing their competitiveness and profitability. Outside the enterprise, the integrated organization links the upstream and downstream enterprises in the supply chain, synchronizes the supply chain logistics operations, and enhances supply and demand coordination.

43.4.4 Logistics Operation Optimization Strategies

Production logistics is the core of the enterprise’s logistics; therefore, we pay close attention to optimization strategy. Applying lean logistics to the production logistics system involves stringent requirements: The production logistics must have flexibility, environmental adaptability, agility, high reliability, rapid response to the market, reduced inventory costs, and ability to achieve on-time delivery. Therefore, the manufacturers need to change traditional “push” logistics operations into a lean “pull” production logistics business model, as shown in Fig. 43.3. The lean pull production logistics business model is a customer demand-driven model. The data flow from demand to production and logistics. In the production process, each

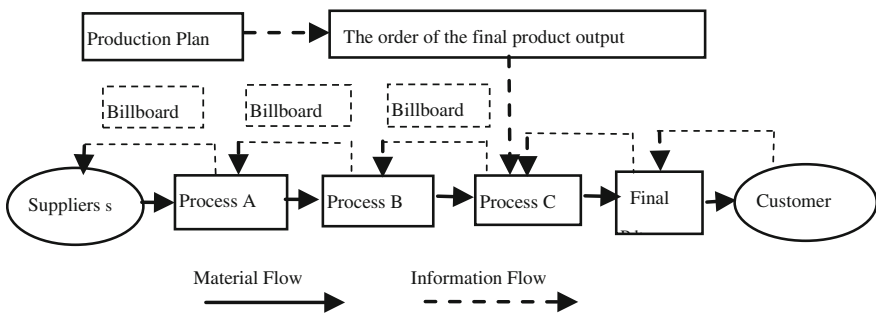


Fig. 43.3 Lean pull production operation model

process treats the next process as customers, where the production and order supplies are determined by the demand for the next process. The pull logistics model must follow the JIT principle, which is manufacturing according to customer demanded location, quantity, quality, and price, and must achieve zero inventory, zero defects, and zero failure.

43.4.5 Standardization and Logistics Management Optimization Strategies

Logistics standardization is the basis for promoting lean logistics. It is also a strong foundation for the globalization of China's logistics industry. Enterprises should actively cooperate with the development of standards and conscientiously implement the national standards. Enterprises should accelerate the development and implementation of standardization of shipping and handling, storage containers, a documentation system for logistics, a product information coding system and cost accounting system, a logistics infrastructure, and logistics safety management systems. Not only the sizes but also operating procedures and methods should be standardized as much as possible, and logistics performance evaluation system should also be standardized. An effective information system is very important to support the logistics system and is also a prerequisite for the implementation of lean logistics. To develop a user-friendly and efficient logistics information system, we must first optimize and standardize logistics process and then introduce an advanced software system. Manufacturing enterprises should vigorously use the high-tech logistics facilities and equipment based on their own needs. They should speed up the implementation of approaches such as automated warehouses, integrated logistics centers, dedicated vehicles, advanced handling, storage equipment, and use of EDI, GPS, RFID, and other information technologies.

43.4.6 Logistics Professional Personnel's Optimization Strategies

The human factor plays a vital role in the implementation of the lean logistics process. Advanced logistics facilities depend on professionals to complete their logistics systems. Differences in various logistics systems coupled with individual customer's requirements result in increasingly high reliance on logistics professionals.

43.4.7 Logistics Cost Management Optimization Strategies

From the lean logistics perspective, optimization cost management strategies include developing solid logistics operation management and information management, as well as strengthening the implementation of logistics cost accounting management. To accurately calculate the cost of logistics, the first step is base data collection, followed by the definition of the composition of logistics cost. After that, one must analyze logistics costs, manufacturing costs, and other expenses, as well as the relationships within the logistics system. Effective control over logistics systems requires clear understanding of resource allocation and establishment of a logistics costs database.

43.4.8 Logistics Performance Evolution Optimization Strategies

Logistics performance evaluation plays an important role in reducing logistics costs. Therefore, enterprises should focus on strengthening the enterprise culture so that all employees have a comprehensive understanding of the importance of logistics performance management and apply this understanding to practical work. The logistics performance evaluation results should be reflected in employee incentive. In addition, enterprises should use the “system theory” in logistics for both global control and local control to strengthen logistics cost management and risk management.

Optimization of logistics systems is a continuous process; excellence comes from continuously working to improve.

43.5 Conclusion

For modern manufacturing enterprises, logistics is a core process. This paper emphasizes lean logistics thinking: customers first; timely, accurate, overall optimization; continuous improvement; and innovative thinking. The paper also constructs a three-level optimization model based on lean logistics. Finally, the paper proposes specific logistics system optimization strategies to reduce logistics costs and enhance competitiveness.

Effective implementation of lean logistics will help change our current extensive management concepts in manufacturing enterprises and will help improve core competitiveness of enterprises, which will have a profound impact on the development of China’s manufacturing industry and the national economy.

References

1. Harland C (1997) Supply chain operational performance roles. *Integr Manufact Syst* 18 (2):70–78
2. Liu D (2010) Conduct business based on production of value-added logistics services to enterprises. *China Logistics China Logistics Purchasing* 20:76–77
3. Research Group (2007) China logistics industry situation and policy suggestions. *Anal Chin Manufact Enterp Logistics* 6:31–36
4. Shen J, Liu H, Liu C (2006) Thinking of establish lean logistics system in China enterprises. *Logistics Technol* 6:71–74
5. Zhou Q, Cong L (2008) To achieve sustained logistics engineering and scientific development. China Railway Publishing House, Beijing
6. Fan X (2007) Modern manufacturing production logistics cost management. *Reformation Strategy* 3:104–106

Chapter 44

Power Assembly and Monitoring Management System of Lithium Ion Battery in Mine

Zhihao Yu, Chuanyu Sun, Jiancheng Fang and Linjing Xiao

Abstract According to “Power security technology manual of the mining explode-proof (or Essence safety) type lithium ion battery”, the paper puts forward a kind solution of the power assembly and monitoring management system used in coal mine lithium ion (Li^+) battery. Based on CAN bus communication, the paper adopts layer modular structure design, comes out with the hardware circuit and the software flow chart based on the finite state machine, achieves the comprehensive detection of Li^+ battery temperature, voltage, and current, solves the problem of Li^+ battery equilibrium management during grouping process, improves the performance and lifetime of Li^+ battery, establishes the Li^+ battery state observation matrix, through the nonlinear curve fitting, estimates the Li^+ battery state of charge (SOC), and improves the accuracy and reliability of calculating the battery capacity. The system can be used as momentum power supply, start power supply, and reserved power supply to coal mine equipment and has good development prospect and broad application market.

Keywords Lithium ion battery · Power supply assembly · Battery equilibrium management · State observation matrix

The pollution of lead–acid battery has attracted people’s great concern. Ministry of Environmental Protection issued a notice on strengthening the pollution prevention and control work of the lead–acid batteries and the regeneration of the aluminum industry, and ministry of Industry and Information Technology issued the comprehensive prevention programs of the heavy metal pollution of the battery industry in order to rectify the lead–acid battery industry and eliminate backward production capacity. Before 2013, the lead–acid battery whose cadmium content is greater than 0.002 % and lead–acid battery manufacturers whose scale is under 200,000 KVA/year should be obsoleted. Lead–acid battery production project whose scale is under 500,000 KVA/year (excluding advanced new lead–acid batteries) should be

Z. Yu (✉) · C. Sun · J. Fang · L. Xiao

College of Mechanical and Electronic Engineering, Shandong University of Science and Technology, Qingdao 266590, Shandong, People’s Republic of China
e-mail: azhihaoa@163.com

© Springer-Verlag Berlin Heidelberg 2015

Logistics Engineering Institution, CMES (ed.),

Proceedings of China Modern Logistics Engineering,

Lecture Notes in Electrical Engineering 286, DOI 10.1007/978-3-662-44674-4_44

limited [1, 2]. Jingzhong Wang, the vice chairman of China battery industry association said “It means that the lead-acid battery companies whose annual output value is less than 100 million will have to be discontinued after 2 or 3 years, then the number of country’s lead-acid battery companies will be reduced from two thousand to sever hundred, which means the vast majority of enterprises will be obsoleted” [3]. Lead–acid battery industry is shrinking, while the Li⁺ battery is a new efficient and environmentally friendly battery which meets the requirements of the times. This paper practices the Li⁺ battery in underground coal mine and studies the assembly structure and monitoring management system.

44.1 The Power Assembly Used in Coal Mine Li⁺ Battery

According to *Power security technology manual of the mining explode-proof (or Essence safety) type lithium ion battery*, the power assembly used in coal mine Li⁺ battery includes two parts: explosion-proof battery box and explosion-proof assembly control box, as shown in Fig. 44.1.

The explosion-proof battery box is divided into three explosion-proof cavities: the battery cavity, the control cavity, and the wiring cavity. The battery cavity stores Li⁺ battery module, including Li⁺ batteries, fuses, temperature sensor, wire, and nothing else; the control cavity stores Li⁺ battery module management system; wiring cavity stores the external connection wires. Explosion-proof assembly control box is divided into two explosion-proof cavities: control cavity and wiring cavity. The control cavity stores the assembly control management system only; wiring cavity stores the external connection wires only.

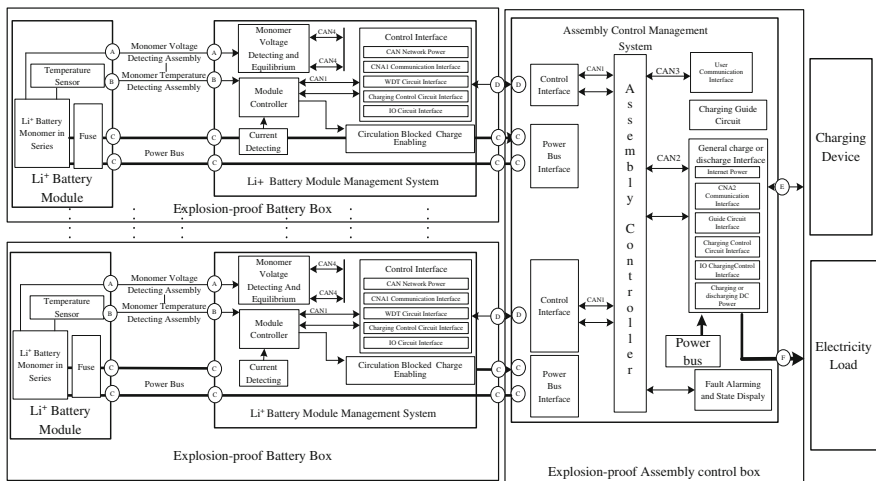


Fig. 44.1 Power supply assembly of mining Li⁺ battery

The interfaces between the explosion-proof battery box and explosion-proof assembly control box including the D-type control line and the C-type power line have explosion protection requirements. Each explosion-proof battery box can be connected to any group of C-type interfaces and D-type interfaces; these interfaces cannot be connected to each other inside, and its states are controlled by the assembly controller. Through D-type interface, assembly control and management system can obtain the running information of any monomer Li^+ battery module, detect the state of each Li^+ battery module, and achieve the function of state display and data storage. It can alarm and cut off the connection between the module and the bus line at the same time. The interface between the Li^+ battery module and the Li^+ battery module management system, including A-type monomers voltage detection signal line, B-type monomer temperature detection signal line, and C-type power line, is located in the explosion-proof battery box, and the connection interfaces have no explosion protection requirements, while E-type between the explosion-proof assembly control box and the charging device and F-type interface between the explosion-proof assembly control box and electricity load both require explosion protection.

44.2 Monitoring and Management System of Mining Li^+ Battery

44.2.1 Circuit Design of Modular Control System

44.2.1.1 Circuit Design of Li^+ Battery Monomer Control

Li^+ battery monomer control circuit belongs to Li^+ battery module management system. The nominal voltage value controlled by Li^+ batteries monomer is 3.2 V, and monomer capacity is not more than 100 Ah. Moreover, each explosion-proof cavity allows only in series but not in parallel. The control mode, each Li^+ battery is collocated with one MCU, is adopted, in order to solve the problems during the detecting process, including the high total voltage, many selector switches, and big differential-mode interference. As shown in Fig. 44.2, the Li^+ battery is not only the supply power to the circuit board but also the object which is measured. If N batteries are in series, the number of monomer voltage detection line is $N + 1$. Temperature detection adopts digital temperature sensor with 3 buses, and the number of output power bus is 2. The CAN bus sends the detected data to the Li^+ battery module management system and in the meanwhile receives the instruction sent from Li^+ battery module management system. Li^+ battery monomer control circuit, working as an actuator, completes the voltage detection of monomer battery, management of monomer battery equilibrium, temperature detection of monomer battery, and various functions of fault protection.

In photoelectric isolation CAN communication circuit [4, 5], PCA82C250 chip, the interface of MCU and CAN physical bus, is adopted to provide the differential receiving and sending functions to the bus, and photoelectric isolation is achieved

detector, which can complete the compensation function of temperature, current, and voltage, and its transmission speed can be up to 10 M Bit/S. LED D11 is used as receiving data indicator lights, and LED D12 is used as sending data indicator lights. And when there is data communication, they will effulge.

44.2.1.2 Design of Li⁺ Battery Module Control Circuit

Each Li⁺ battery module is consisted of a group of series batteries, whose module control circuit is also a part of the Li⁺ battery module management system. It uses high-performance RISC CPU STM32F107 whose structure is optimized by 32-bit ARM Cortex-M3 as a core controller [6, 7], whose standard peripherals include ten timers; two 12-bit 1 M sample/s AD converter; two 12-bit DA converter; two I2C interfaces; five USART interfaces; three SPI ports and high-quality digital audio interface IIS; full-speed USB (OTG) interface; CAN2.0 interface; 10/100 M ethernet interface; and so on. As shown in Fig. 44.4, 1-wire sensor DS18B20 is adopted to detect temperature; Hall current sensor CS3B401B4C is adopted to detect the output current of the module; 2-way CAN bus signal is adopted, one of which is connected to the Li⁺ battery monomer control circuit, and the other is connected to Li⁺ battery assembly control circuit. USART interface is connected to the computer serial port to transfer the data to the Li⁺ battery management software for display on human-computer interface. The system is also equipped with two settings button and one LED digital tube display in explosion-proof battery box.

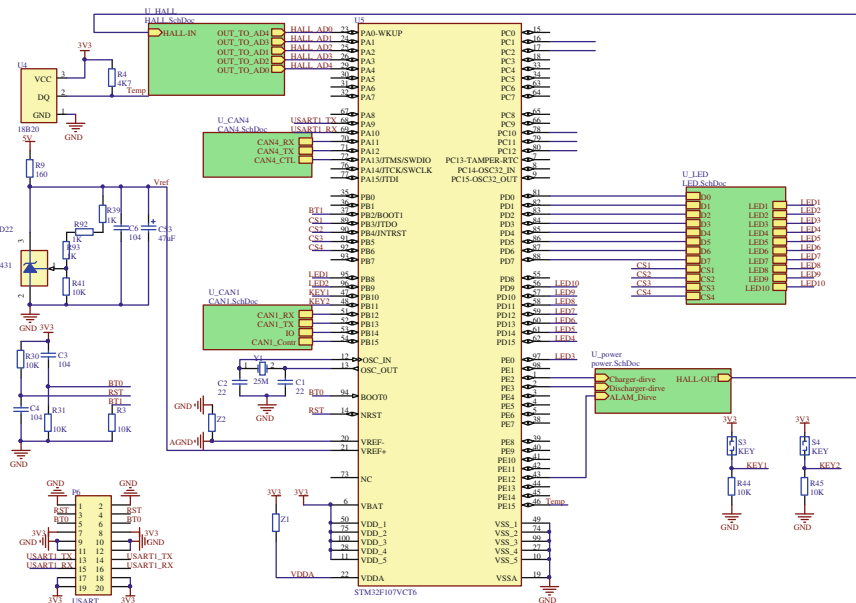


Fig. 44.4 Control circuit of Li⁺ battery module

Failure alarm and status display unit adopt LCD display ILI9481 which is 3.5 “480 × 320 dot matrix. It is placed in assembly control box and displays the status and information of the Li⁺ battery through the tempered glass. ILI9481 LCD controller completes communication with Li⁺ battery assembly controller through the control bus and data bus, in which the control bus is used to transfer, read, and write signals of RAM, chip select signals, and command and data conversion signal inside the LCD display, and the data bus is used to transmit display data. In order to improve the operating efficiency of the CPU, ILI9481 controller, as peripheral, is mapped to the static memory controller (FSMC) of Li⁺ battery assembly controller. It adopts 16 bits display mode, which means that the distribution form of the RGB color mode is 5:6:5 [8]. FSMC is configured for NOR flash memory access, and the NE [1] signal, the NOE signal, NWE signal, and the A16 signal are adopted as chip select signal, the read strobe, write strobe, and command and data conversion signal of ILI9481 controller. The data signal D[15:0] corresponds with low 16 bits of ILI9481 controller, and the command word and data are mapped to the address of 0X60000000 and 0X60020000 of the Li⁺ battery assembly controller. Display circuit interface is shown in Fig. 44.6.

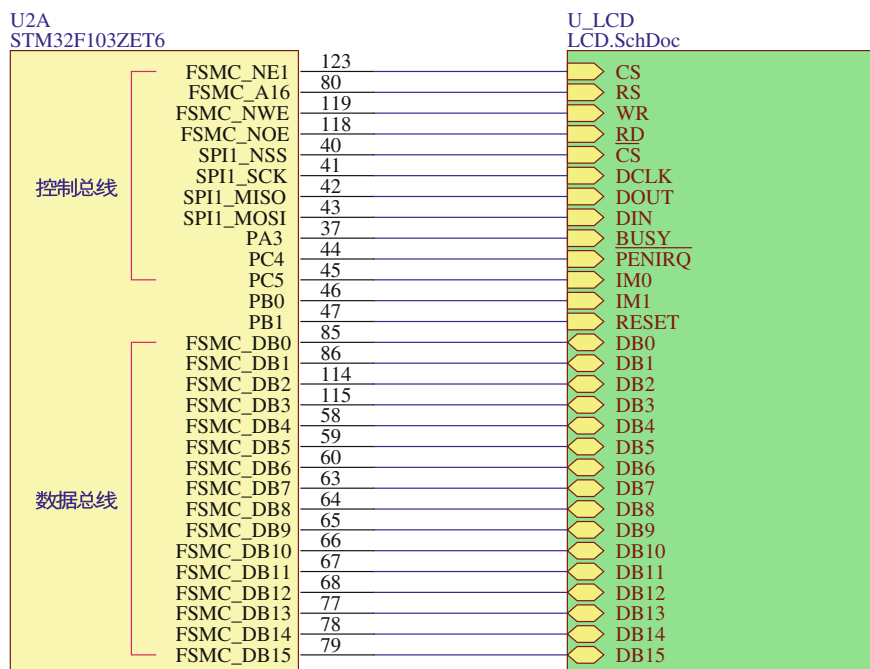


Fig. 44.6 Circuit interface of Li⁺ battery assembly display

44.2.2 Control Flow Switch Based on State Machine

Sequence process is the control structure of most traditional application, which follows the logic set in advanced. Process executes from the start to the end, while interrupt can break the current execution and allow interrupt nesting, but it must return to the state before the interrupt after the completion of interrupt. Based on different control program of state machine’s switching, it adopts event-driven way and uses directed graph to show their work status. It is constituted with state, event, transformation, and activities. Each state has action of enter and exit. Each transformation has one source state, one target state, and one event associated [9]. During the source state, if an event occurs and guard condition of the conversion triggered is true, it will execute the following action in order: the exit action of source state; transition actions; and the entry action of target state.

Li⁺ battery module management system state machine is shown in Fig. 44.7. The module will be in the default discharge state [only discharge no charge] after a reduction with a delay of 10 s, and each module has a discharge flow event and discharge undervoltage event. The module neither discharge nor charge after entering overcurrent protection state or undervoltage protection state, and assembly controller will send commands to it make it enter the default state in 10 s. If assembly controller or communication circuit breaks down, it will be automatically switched to the default state by the module controller after 10-s countdown. Module can also manage the performance of the Li⁺ battery in charging state [both charge and discharge], can program and debug the Li⁺ battery monomer controller in a state of charging protection [only discharge no charge.], and can number and debug the DS18B20 in waiting state [neither discharge nor charge].

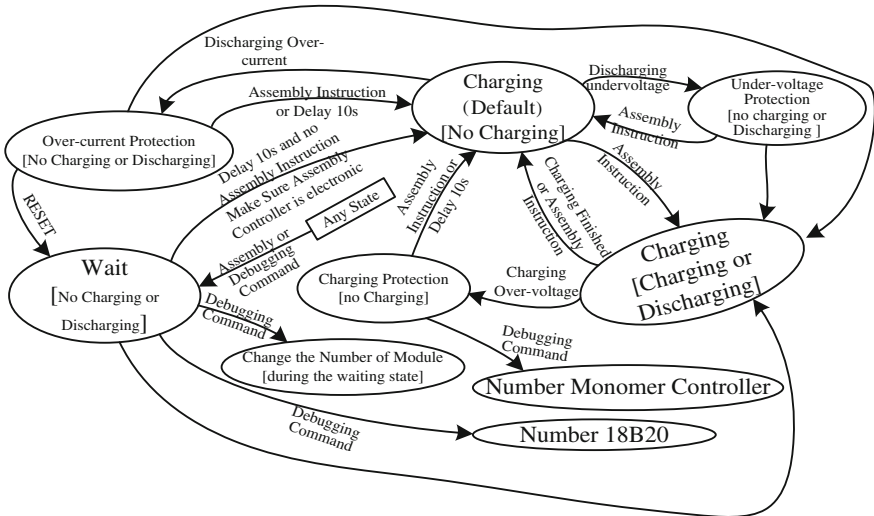


Fig. 44.7 State machine of Li⁺ battery module management system

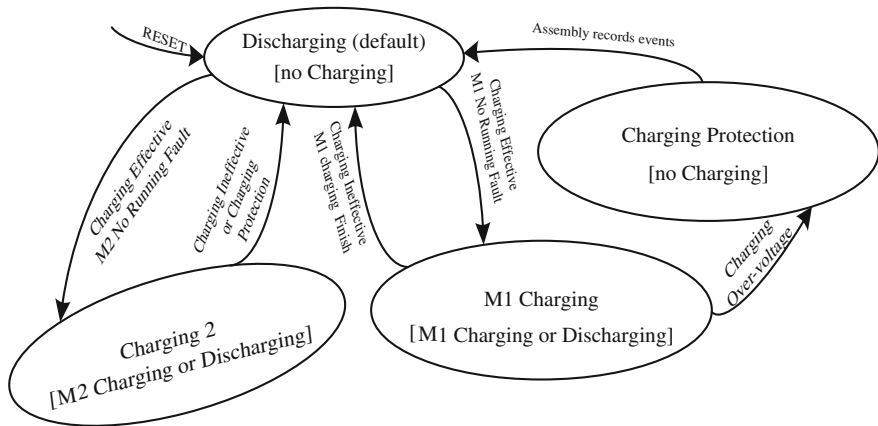


Fig. 44.8 Assembly control management system state machine

Assembly discharge status is the output of each Li^+ battery module in parallel, and assembly charge state is also the input of Li^+ battery module in parallel. The running state machine is shown in Fig. 44.8. If assembly controller detects the charging marker ineffective, it will send instructions to each module management system in order to make each module in discharging state [only discharge no charge], namely default state. If assembly controller detects the charging mark effective, each charging module M1, M2, etc., will be controlled together, so module without running fault will be set in charging state [both charge and discharge], and the broken module will be cut off [neither charge nor discharge]. When the voltage of module is full or charging is ineffective, assembly controller issues instruction to module management system to order modules in discharging state. If any module is charging overvoltage, it enters charging protection state [only discharge no charge], and assembly controller enters default discharge state after recording the events.

44.2.3 Multivariate Nonlinear Regression SOC Algorithm

State of charger (SOC) is a physical quantity that describes the remaining battery capacity, which is a significant parameter in studying the change of battery performance. Detecting changes in the SOC accurately and effectively is the premise of completing the management of high-performance Li^+ battery. There are several methods to estimate battery SOC: ① Internal resistance method is a method to estimate the battery capacity through determining the internal resistance. The smaller internal resistance is, the bigger battery capacity is, and the bigger internal resistance is, the smaller battery capacity is. It can be used in determining whether the battery is good or bad; ② ampere-hour metering method is to estimate the

battery capacity through the integral of the charge and discharge current, which can be used to calculate the SOC under all situations but may be affected by temperature, resistance, current, and so on; ③ Kalman filter method is to acquire each state parameters based on minimum variance, which is an optimal estimation method with a high requirement of controller and be complex to achieve; ④ open circuit voltage method is to estimate the SOC of the Li⁺ battery by measuring the open circuit voltage, which is the easiest way but has a poor linearity [10]; therefore, multivariate nonlinear regression algorithm is popularly adopted to improve accuracy of estimating the SOC.

Suppose variable x represents the open circuit voltage of Li⁺ battery, variable y represents the capacity of the Li⁺ battery, and \hat{y} represents the estimated value (including the data error) of the capacity of the Li⁺ battery. An element nonlinear regression mathematical model is established as follows:

$$\hat{y} = b_0 + b_1x + b_2x^2 + \dots + b_px^p \tag{44.1}$$

Ordering $x_1 = x, x_2 = x^2, \dots, x_p = x^p$, the mathematical model of multivariate nonlinear regression is obtained:

$$\hat{y} = b_0 + b_1x_1 + b_2x_2 + \dots + b_px \tag{44.2}$$

One Li⁺ battery multifunctional parameter measuring instrument is used to measure groups of data points (x_n, y_n) , and the quantity of measurement points is no less than that of unknown quantities, namely $n \geq p$, at the same time, calculates the value of $x_1x_2 \dots x_p$ measured each time. The state observer matrix can be written based on these

$$Y = \begin{pmatrix} y_1 \\ y_2 \\ \vdots \\ y_n \end{pmatrix} \quad X = \begin{pmatrix} 1 & x_{11} & x_{12} & \dots & x_{1p} \\ 1 & x_{21} & x_{22} & \dots & x_{2p} \\ \vdots & & & & \\ 1 & x_{n1} & x_{n2} & \dots & x_{np} \end{pmatrix} \tag{44.3}$$

In the formula, X_{ij} stands for the j th calculated value of X from the i th measurement.

According to the normal system of equation [11] based on least squares method, the coefficient matrix B which is the unitary nonlinear regression mathematical model is obtained:

$$B = \begin{pmatrix} b_0 \\ b_1 \\ \vdots \\ b_p \end{pmatrix} = (X^T X)^{-1} X^T Y \tag{44.4}$$

Each section of the Li^+ battery is tested and analyzed through Li battery multifunctional parameter measuring instrument. The data show that the experimental values of the SOC are close to the theoretical values when the quantity of measurement points $n \geq 13$ and the order of regression curve $P \geq 3$, in which the maximum error is 5.79 % [12]. In order to further reduce the error, the system samples 30 points and takes 6 steps in the fitting curves during the SOC off-line modeling.

44.3 Application Analysis of the Power Supply Assembly and the Monitoring Management System

44.3.1 Used in the Coal Mine Electric Locomotive as Power Supply

In order to improve energy utilization, the drive mode adopts a DC motor + IGBT chopper, instead of the AC motor + inverter. Power-driven system with twin motor and dual power is shown in Fig. 44.9. There are two sets of Li^+ explosion-proof power supply (with explosion-proof assembly control box) and two DC series motors, motor M1 drives the two front wheels of mine electric locomotive and is controlled by IGBT1, motor M2 drive the two rear wheels of mine electric locomotive and it controlled by IGBT2. Motor M1 and motor M2 can work separately or simultaneously. Contact switches K1, K12, and K2 are mainly used to select battery that drives motor. Normally, Li^+ power 1 is used as a dedicated power supply of motor M1, and Li power 2 is used as a dedicated power supply of motor M2 when contactor K12 is disconnection. Li^+ power 1 is used as a standby power

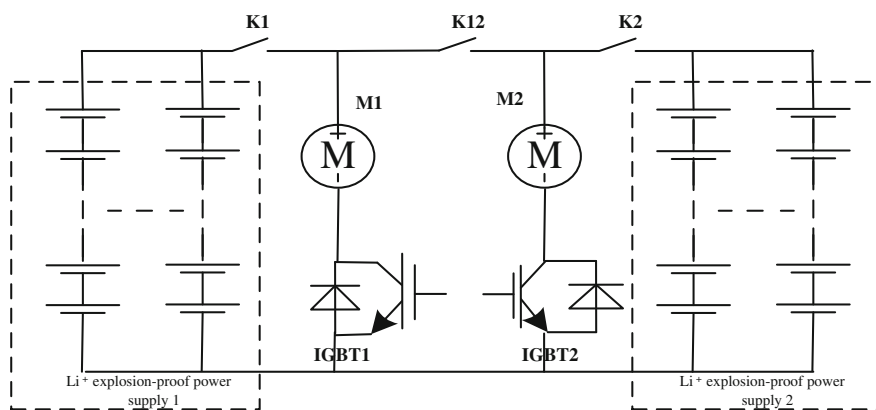


Fig. 44.9 Power drive systems with twin motor and dual power

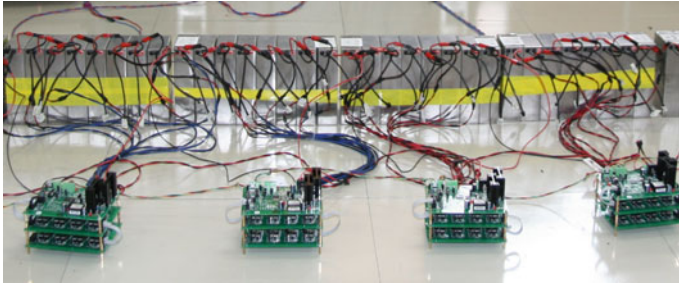


Fig. 44.10 Backup power supply of refuge chamber (without explosion-proof)

supply of motor M2, and Li power 2 is used as a standby power supply of motor M1 under the situation of failure or maintenance. Compared with the same specification old-fashioned lead–acid battery locomotive, the service life of Li^+ battery electrical locomotive can be increased 2–4 times; cruising ability of it can be increased 1–3 times, and charging time of it can be reduced $\frac{1}{4}$ – $\frac{1}{2}$.

44.3.2 Used in the Coal Mine Refuge Chamber as a Backup Power

Refuge chamber can resist high temperature and flue gas, can cut off the toxic and harmful gases, can provide oxygen, food, and water to the trapped miners, and can create conditions and gain time for the emergency rescue. As shown in the Fig. 44.10, mining Li^+ battery is used as backup power supply and applied to the coal mine refuge chamber, to provide a continuous 96-h power supply to the various environmental monitoring sensors underground, communication base stations, oxygen control valve, lights, and so on. The safe and reliable operation of the refuge chamber can be ensured by long Li^+ battery life, good battery performance, comprehensive and reliable monitoring and management system, intelligent battery maintenance, and friendly display interface.

44.4 Conclusions

Li^+ battery power supply assembly and monitoring management system with a design of layer modular structure achieve the comprehensive monitoring and management of the status of Li^+ battery. Reliable hardware circuit and flexible state machine procedures improves the performance and lifespan of Li^+ batteries. The nonlinear curve fitting based on state observation matrix improves the accuracy of the battery SOC calculation. The fact shows that this system has a broad market

prospect. It can be used as both dynamical power and start power supply in mine electric locomotive, monorail, and trackless tyred vehicle. It can also be applied to refuge chamber or control-based station.

Acknowledgements This work was financially supported by Science & Technology Development Plan Project of Shandong Province (2012GSF11606).

References

1. Liu F (2011) Alternative opportunities for lithium batteries industry and stop of lead-acid batteries industry. Consumption Daily. 06 Sept 2011
2. Qianqian L, Yue Z. Chose hundreds of lithium batteries companies after the blood lead event. Economic information daily. 24 May 2011
3. Wu Y, Wang H, Wang J (2005) The controller area network interface chip 82C250 and its application. J Guizhou Univ Technol 34(3):76–79
4. Zhou H (2011) Rectify and reform of the lead-acid batteries and the coming of lithium batteries. China United Commercial Daily. 11 July 2011
5. Jiang Z, Liu L, Li P (2003) A design of hybrid electric locomotive control system based on can bus. Mach Dev 32(5):63–65
6. Wang Y, Xu W, Hao L (2008) STM32 series ARM cortex-M3 micro controller principle and practice. Beijing Aerospace University Press, Beijing
7. Li J (2010) Power measurement and data transmission based on STM32 chip. Autom Instrum 3:137–139
8. Zhou L (2008) Simply ARM7-LPC2400. Guangzhou Zhi Yuan Electronics Company, Guangzhou
9. Xu X, Wang L, Zhou H (2003) Implementation framework of finite state machines. J Eng Des 10(5):251–255
10. Cai Z, Gui C (2007) Relationship between open-circuit voltage and discharge capacity of VRLA batteries for electric bicycles. Chin Battery Ind 12(6):366–369
11. Yetai F (2010) Error theory and data processing. Mechanical Industry Press, Beijing
12. Zeng J, Bu F (2011) Study of SOC estimation and measurement of Li-ion battery based on polynomial regression algorithm. J Dalian Jiaotong Univ 32(4):70–74